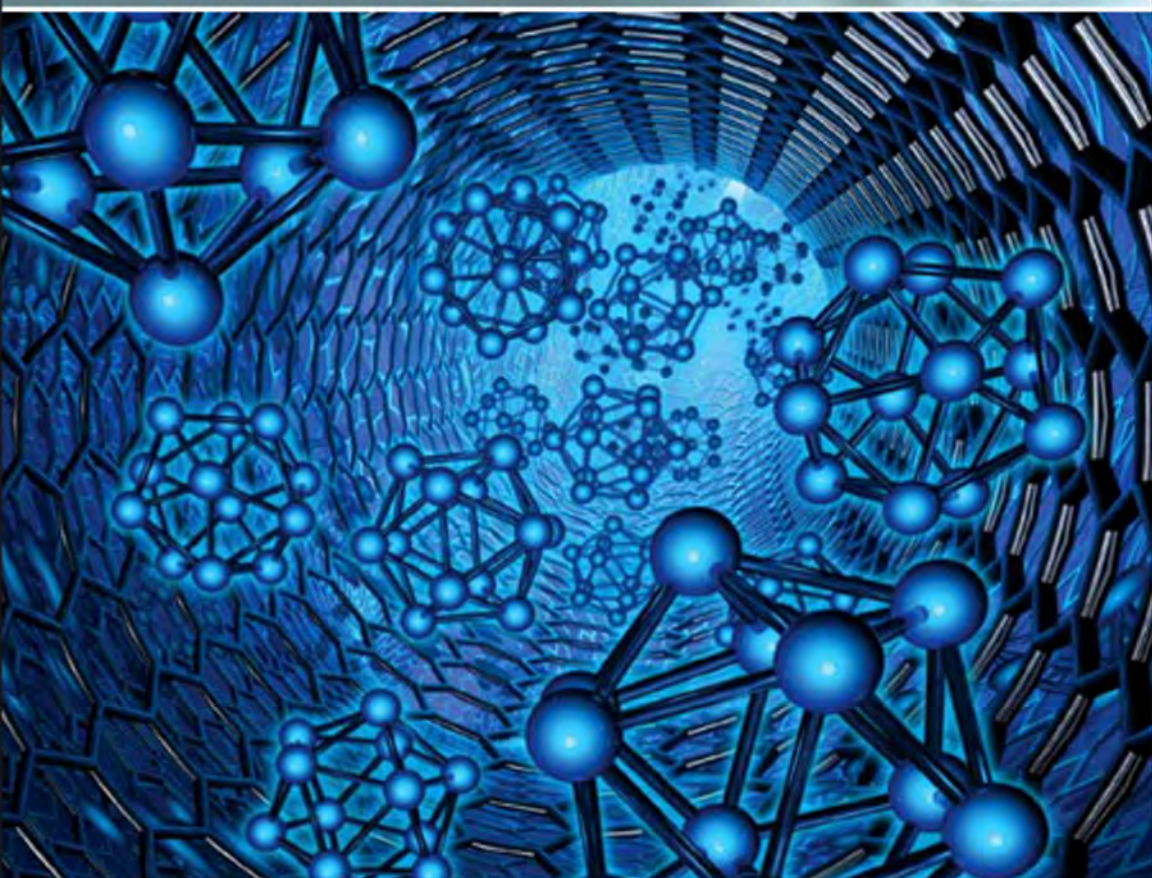




**ELSEVIER INSIGHTS**



# INTRODUCTION TO PRACTICE OF MOLECULAR SIMULATION

MOLECULAR DYNAMICS, MONTE CARLO, BROWNIAN DYNAMICS,  
LATTICE BOLTZMANN AND DISSIPATIVE PARTICLE DYNAMICS

AKIRA SATOH

# **Introduction to Practice of Molecular Simulation**

This page intentionally left blank

# **Introduction to Practice of Molecular Simulation**

## **Molecular Dynamics, Monte Carlo, Brownian Dynamics, Lattice Boltzmann, Dissipative Particle Dynamics**

***Akira Sato***

*Akita Prefectural University  
Japan*



**ELSEVIER**

AMSTERDAM • BOSTON • HEIDELBERG • LONDON • NEW YORK • OXFORD  
PARIS • SAN DIEGO • SAN FRANCISCO • SINGAPORE • SYDNEY • TOKYO

Elsevier  
32 Jamestown Road London NW1 7BY  
30 Corporate Drive, Suite 400, Burlington, MA 01803, USA

First published 2011

Copyright © 2011 Elsevier Inc. All rights reserved

No part of this publication may be reproduced or transmitted in any form or by any means, electronic or mechanical, including photocopying, recording, or any information storage and retrieval system, without permission in writing from the publisher. Details on how to seek permission, further information about the Publisher's permissions policies and our arrangement with organizations such as the Copyright Clearance Center and the Copyright Licensing Agency, can be found at our website: [www.elsevier.com/permissions](http://www.elsevier.com/permissions)

This book and the individual contributions contained in it are protected under copyright by the Publisher (other than as may be noted herein).

### Notices

Knowledge and best practice in this field are constantly changing. As new research and experience broaden our understanding, changes in research methods, professional practices, or medical treatment may become necessary.

Practitioners and researchers must always rely on their own experience and knowledge in evaluating and using any information, methods, compounds, or experiments described herein. In using such information or methods they should be mindful of their own safety and the safety of others, including parties for whom they have a professional responsibility.

To the fullest extent of the law, neither the Publisher nor the authors, contributors, or editors, assume any liability for any injury and/or damage to persons or property as a matter of products liability, negligence or otherwise, or from any use or operation of any methods, products, instructions, or ideas contained in the material herein.

### British Library Cataloguing-in-Publication Data

A catalogue record for this book is available from the British Library

### Library of Congress Cataloguing-in-Publication Data

A catalog record for this book is available from the Library of Congress

ISBN: 978-0-12-385148-2

For information on all Elsevier publications  
visit our website at [www.elsevierdirect.com](http://www.elsevierdirect.com)

This book has been manufactured using Print On Demand technology. Each copy is produced to order and is limited to black ink. The online version of this book will show color figures where appropriate.

Working together to grow  
libraries in developing countries

[www.elsevier.com](http://www.elsevier.com) | [www.bookaid.org](http://www.bookaid.org) | [www.sabre.org](http://www.sabre.org)

ELSEVIER BOOK AID International Sabre Foundation

# Contents

Preface	ix
<b>1 Outline of Molecular Simulation and Microsimulation Methods</b>	<b>1</b>
1.1 Molecular Dynamics Method	1
1.1.1 Spherical Particle Systems	2
1.1.2 Nonspherical Particle Systems	5
1.2 Monte Carlo Method	11
1.3 Brownian Dynamics Method	15
1.4 Dissipative Particle Dynamics Method	19
1.5 Lattice Boltzmann Method	24
<b>2 Outline of Methodology of Simulations</b>	<b>29</b>
2.1 Initial Positions	29
2.1.1 Spherical Particle Systems	29
2.1.2 Nonspherical Particle Systems	32
2.2 Initial Velocities	35
2.2.1 Spherical Particle Systems	35
2.2.2 Nonspherical Particle Systems	37
2.3 Reduction Methods of Computation Time	39
2.3.1 Cutoff Distance	39
2.3.2 Cell Index Method	41
2.3.3 Verlet Neighbor List Method	42
2.4 Boundary Conditions	43
2.4.1 Periodic Boundary Condition	43
2.4.2 Lees–Edwards Boundary Condition	45
<b>3 Practice of Molecular Dynamics Simulations</b>	<b>49</b>
3.1 Diffusion Phenomena in a System of Light and Heavy Molecules	49
3.1.1 Physical Phenomena of Interest	50
3.1.2 Specification of Problems in Equations	50
3.1.3 Verlet Algorithm	51
3.1.4 Parameters for Simulations	52
3.1.5 Results of Simulations	54
3.1.6 Simulation Program	55

3.2	Behavior of Rod-like Particles in a Simple Shear Flow	63
3.2.1	Physical Phenomena of Interest	64
3.2.2	Particle Model	64
3.2.3	Equation of Motion and Molecular Dynamics Algorithm	66
3.2.4	Modeling of Steric Repulsive Interaction	69
3.2.5	Nondimensionalization of Basic Equations	72
3.2.6	Treatment of the Criteria for Particle Overlap in Simulations	74
3.2.7	Parameters for Simulations	75
3.2.8	Results of Simulations	77
3.2.9	Simulation Program	81
<b>4</b>	<b>Practice of Monte Carlo Simulations</b>	<b>105</b>
4.1	Orientational Phenomena of Rod-like Particles in an Applied Magnetic Field	105
4.1.1	Physical Phenomena of Interest	105
4.1.2	Specification of Problems in Equations	106
4.1.3	Canonical Monte Carlo Algorithm	111
4.1.4	Parameters for Simulations	115
4.1.5	Results of Simulations	116
4.1.6	Simulation Program	118
4.2	Aggregation Phenomena in a Dispersion of Plate-like Particles	134
4.2.1	Physical Phenomena of Interest	134
4.2.2	Particle Model	134
4.2.3	Criterion of the Particle Overlap	136
4.2.4	Canonical Monte Carlo Algorithm	143
4.2.5	Treatment of the Criterion of the Particle Overlap in Simulations	143
4.2.6	Particle-Fixed Coordinate System and the Absolute Coordinate System	144
4.2.7	Attempt of Small Angular Changes in the Particle Axis and the Magnetic Moment	145
4.2.8	Parameters for Simulations	146
4.2.9	Results of Simulations	147
4.2.10	Simulation Program	150
<b>5</b>	<b>Practice of Brownian Dynamics Simulations</b>	<b>173</b>
5.1	Sedimentation Phenomena of Lennard-Jones Particles	173
5.2	Specification of Problems in Equations	173
5.3	Brownian Dynamics Algorithm	174
5.4	Parameters for Simulations	176
5.5	Results of Simulations	176
5.6	Simulation Program	179

<b>6 Practice of Dissipative Particle Dynamics Simulations</b>	<b>187</b>
6.1 Aggregation Phenomena of Magnetic Particles	187
6.2 Specification of Problems in Equations	187
6.2.1 Kinetic Equation of Dissipative Particles	187
6.2.2 Model of Particles	189
6.2.3 Model Potential for Interactions Between Dissipative and Magnetic Particles	190
6.2.4 Nondimensionalization of the Equation of Motion and Related Quantities	191
6.3 Parameters for Simulations	193
6.4 Results of Simulations	194
6.5 Simulation Program	197
<b>7 Practice of Lattice Boltzmann Simulations</b>	<b>219</b>
7.1 Uniform Flow Around a Two-Dimensional Circular Cylinder	219
7.2 Specification of Problems in Equations	220
7.3 Boundary Conditions	221
7.4 Various Treatments in the Simulation Program	223
7.4.1 Definition and Evaluation of the Drag Coefficient	223
7.4.2 Choice of the Procedures by Coloring Lattice Sites	224
7.4.3 Treatment of Interactions on the Cylinder Surface	225
7.4.4 Evaluation of the Velocity and Density	225
7.5 Nondimensionalization of the Basic Equations	226
7.6 Conditions for Simulations	227
7.6.1 Initial Distribution	227
7.6.2 Parameters for Simulations	227
7.7 Results of Simulations	227
7.8 Simulation Program	231
<b>8 Theoretical Background of Lattice Boltzmann Method</b>	<b>255</b>
8.1 Equilibrium Distribution	255
8.1.1 D2Q9 Model	257
8.1.2 D3Q19 Model	264
8.2 Navier–Stokes Equation	271
8.3 Body Force	275
8.4 Boundary Conditions	277
8.4.1 Bounce-back Rule	277
8.4.2 BFL Method	279
8.4.3 YMLS Method	281
8.4.4 Other Methods	282
8.5 Force and Torque Acting on Particles	282
8.6 Nondimensionalization	283

<b>Appendix 1: Chapman–Enskog Expansion</b>	<b>285</b>
<b>Appendix 2: Generation of Random Numbers According to Gaussian Distribution</b>	<b>291</b>
<b>Appendix 3: Outline of Basic Grammars of FORTRAN and C Languages</b>	<b>293</b>
<b>Appendix 4: Unit Systems of Magnetic Materials</b>	<b>317</b>
<b>How to Acquire Simulation Programs</b>	<b>319</b>
<b>References</b>	<b>321</b>

# Preface

The control of internal structure during the fabrication of materials on the nanoscale may enable us to develop a new generation of materials. A deeper understanding of phenomena on the microscopic scale may lead to completely new fields of application. As a tool for microscopic analysis, molecular simulation methods—such as the molecular dynamics and the Monte Carlo methods—have currently been playing an extremely important role in numerous fields, ranging from pure science and engineering to the medical, pharmaceutical, and agricultural sciences. The importance of these methods is expected to increase significantly with the advance of science and technology.

Many physics textbooks address the molecular simulation method for pure liquid or solid systems. In contrast, textbooks concerning the simulation method for suspensions or dispersions are less common; this fact provided the motivation for my previous textbook. Moreover, students or nonexperts needing to apply the molecular simulation method to a physical problem have few tools for cultivating the skill of developing a simulation program that do not require training under a supervisor with expertise in simulation techniques. It became clear that students and nonexpert researchers would find useful a textbook that taught the important concepts of the simulation technique and honed programming skills by tackling practical physical problems with guidance from sample simulation programs. This book would need to be written carefully; it would not simply explain a sample simulation program, but also explains the analysis procedures and include the essence of the theory, the specification of the basic equations, the method of nondimensionalization, and appropriate discussion of results. A brief explanation of the essence of the grammar of programming languages also would be useful.

In order to apply the simulation methods to more complex systems, such as carbon-nanotubes, polymeric liquids, and DNA/protein systems, the present book addresses a range of practical methods, including molecular dynamics and Monte Carlo, for simulations of practical systems such as the spherocylinder and the disk-like particle suspension. Moreover, this book discusses the dissipative particle dynamics method and the lattice Boltzmann method, both currently being developed as simulation techniques for taking into account the multibody hydrodynamic interaction among dispersed particles in a particle suspension or among polymers in a polymeric liquid.

The resulting characteristics of the present book are as follows. The important and essential background relating to the theory of each simulation technique is explained, avoiding complex mathematical manipulation as much as possible. The equations that are included herein are all important expressions; an understanding

of them is key to reading a specialized textbook that treats the more theoretical aspects of the simulation methods. Much of the methodology, such as the assignment of the initial position and velocity of particles, is explained in detail in order to be useful to the reader developing a practical simulation program.

In the chapters dedicated to advancing the reader's practical skill for developing a simulation program, the following methodology is adopted. First, the sample physical phenomenon is described in order to discuss the simulation method that will be addressed in the chapter. This is followed by a series of analyses (including the theoretical backgrounds) that are conducted mainly from the viewpoint of developing a simulation program. Then, the assignment of the important parameters and the assumptions that are required for conducting the simulation of the physical problem are described. Finally, results that have been obtained from the simulation are shown and discussed, with emphasis on the visualization of the results by snapshots. Each example is conducted with a sample copy of the simulation program from which the results were obtained, together with sufficient explanatory descriptions of the important features in the simulation program to aid to the reader's understanding.

Most of the sample simulation programs are written in the FORTRAN language, excepting the simulation program for the Brownian dynamics method. We take into account that some readers may be unfamiliar with programming languages, that is, the FORTRAN or the C language; therefore, an appendix explains the important features of these programming languages from the viewpoint of developing a scientific simulation program. These explanations are expected to significantly reduce the reader's effort of understanding the grammar of the programming languages when referring to a textbook of the FORTRAN or the C language.

The present book has been written in a self-learning mode as much as possible, and therefore readers are expected to derive the important expressions for themselves—that is the essence of each simulation demonstration. This approach should appeal to the reader who is more interested in the theoretical aspects of the simulation methods.

Finally, the author strongly hopes that this book will interest many students in molecular and microsimulation methods and direct them to the growing number of research fields in which these simulation methods are indispensable, and that one day they will be the preeminent researchers in those fields.

The author deeply acknowledges contribution of Dr. Geoff N. Coverdale, who volunteered valuable assistance during the development of the manuscript. The author also wishes to express his thanks to Ms. Aya Saitoh for her dedication and patience during the preparation of so many digital files derived from the handwritten manuscripts.

Akira Satoh  
*Kisarazu City, Chiba Prefecture, Japan*  
December 2010

# 1 Outline of Molecular Simulation and Microsimulation Methods

In the modern nanotechnology age, microscopic analysis methods are indispensable in order to generate new functional materials and investigate physical phenomena on a molecular level. These methods treat the constituent species of a system, such as molecules and fine particles. Macroscopic and microscopic quantities of interest are derived from analyzing the behavior of these species.

These approaches, called “molecular simulation methods,” are represented by the Monte Carlo (MC) and molecular dynamics (MD) methods [1–3]. MC methods exhibit a powerful ability to analyze thermodynamic equilibrium, but are unsuitable for investigating dynamic phenomena. MD methods are useful for thermodynamic equilibrium but are more advantageous for investigating the dynamic properties of a system in a nonequilibrium situation. This book examines MD and MC methods of a nonspherical particle dispersion in a three-dimensional system, which may be directly applicable to such complicated dispersions as DNA and polymeric liquids. This book also addresses Brownian dynamics (BD) methods [1,4], which can simulate the Brownian motion of dispersed particles; dissipative particle dynamics (DPD) [5–8]; and lattice Boltzmann methods [9–12], in which a liquid system is regarded as composed of virtual fluid particles. Simulation methods using the concept of virtual fluid particles are generally used for pure liquid systems, but are useful for simulating particle dispersions.

## 1.1 Molecular Dynamics Method

A spherical particle dispersion can be treated straightforwardly in simulations because only the translational motion of particles is important, and the treatment of the rotational motion is basically unnecessary. In contrast, since the translational and rotational motion has to be simulated for an axisymmetric particle dispersion, MD simulations become much more complicated in comparison with the spherical particle system. Simulation techniques for a dispersion composed of nonspherical particles with a general shape may be obtained by generalizing the methods employed to an axisymmetric particle dispersion. It is, therefore, very important to understand the MD method for the axisymmetric particle system.

### 1.1.1 Spherical Particle Systems

The concept of the MD method is rather straightforward and logical. The motion of molecules is generally governed by Newton's equations of motion in classical theory. In MD simulations, particle motion is simulated on a computer according to the equations of motion. If one molecule moves solely on a classical mechanics level, a computer is unnecessary because mathematical calculation with pencil and paper is sufficient to solve the motion of the molecule. However, since molecules in a real system are numerous and interact with each other, such mathematical analysis is impracticable. In this situation, therefore, computer simulations become a powerful tool for a microscopic analysis.

If the mass of molecule  $i$  is denoted by  $m_i$ , and the force acting on molecule  $i$  by the ambient molecules and an external field denoted by  $\mathbf{f}_i$ , then the motion of a particle is described by Newton's equation of motion:

$$m_i \frac{d^2 \mathbf{r}_i}{dt^2} = \mathbf{f}_i \quad (1.1)$$

If a system is composed of  $N$  molecules, there are  $N$  sets of similar equations, and the motion of  $N$  molecules interacts through forces acting among the molecules.

Differential equations such as Eq. (1.1) are unsuitable for solving the set of  $N$  equations of motion on a computer. Computers readily solve simple equations, such as algebraic ones, but are quite poor at intuitive solving procedures such as a trial-and-error approach to find solutions. Hence, Eq. (1.1) will be transformed into an algebraic equation. To do so, the second-order differential term in Eq. (1.1) must be expressed as an algebraic expression, using the following Taylor series expansion:

$$x(t+h) = x(t) + h \frac{dx(t)}{dt} + \frac{1}{2!} h^2 \frac{d^2 x(t)}{dt^2} + \frac{1}{3!} h^3 \frac{d^3 x(t)}{dt^3} + \dots \quad (1.2)$$

Equation (1.2) implies that  $x$  at time  $(t+h)$  can be expressed as the sum of  $x$  itself, the first-order differential, the second-order differential, and so on, multiplied by a constant for each term. If  $x$  does not significantly change with time, the higher-order differential terms can be neglected for a sufficiently small value of the time interval  $h$ . In order to approximate the second-order differential term in Eq. (1.1) as an algebraic expression, another form of the Taylor series expansion is necessary:

$$x(t-h) = x(t) - h \frac{dx(t)}{dt} + \frac{1}{2!} h^2 \frac{d^2 x(t)}{dt^2} - \frac{1}{3!} h^3 \frac{d^3 x(t)}{dt^3} + \dots \quad (1.3)$$

If the first-order differential term is eliminated from Eqs. (1.2) and (1.3), the second-order differential term can be solved as

$$\frac{d^2 x(t)}{dt^2} = \frac{x(t+h) - 2x(t) + x(t-h)}{h^2} + O(h^2) \quad (1.4)$$

The last term on the right-hand side of this equation implies the accuracy of the approximation, and, in this case, terms higher than  $h^2$  are neglected. If the second-order differential is approximated as

$$\frac{d^2x(t)}{dt^2} = \frac{x(t+h) - 2x(t) + x(t-h)}{h^2} \quad (1.5)$$

This expression is called the “central difference approximation.” With this approximation and the notation  $\mathbf{r}_i = (x_i, y_i, z_i)$  for the molecular position and  $\mathbf{f}_i = (f_{xi}, f_{yi}, f_{zi})$  for the force acting on particle  $i$ , the equation of the  $x$ -component of Newton’s equation of motion can be written as

$$x_i(t+h) = 2x_i(t) - x_i(t-h) + \frac{h^2}{m_i} f_{xi}(t) \quad (1.6)$$

Similar equations are satisfied for the other components. Since Eq. (1.6) is a simple algebraic equation, the molecular position at the next time step can be evaluated using the present and previous positions and the present force. If a system is composed of  $N$  molecules, there are  $3N$  algebraic equations for specifying the motion of molecules; these numerous equations are solved on a computer, where the motion of the molecules in a system can be pursued with the time variable. Eq. (1.6) does not require the velocity terms for determining the molecular position at the next time step. This scheme is called the “Verlet method” [13]. The velocity, if required, can be evaluated from the central difference approximation as

$$\mathbf{v}_i(t) = \frac{\mathbf{r}_i(t+h) - \mathbf{r}_i(t-h)}{2h} \quad (1.7)$$

This approximation can be derived by eliminating the second-order differential terms in Eqs. (1.2) and (1.3). It has already been noted that the velocities are unnecessary for evaluating the position at the next time step; however, a scheme using the positions and velocities simultaneously may be more desirable in order to keep the system temperature constant. We show such a method in the following paragraphs.

If we take into account that the first- and second-order differentials of the position are equal to the velocity and acceleration, respectively, the neglect of differential terms equal to or higher than third-order in Eq. (1.2) leads to the following equation:

$$\mathbf{r}_i(t+h) = \mathbf{r}_i(t) + h\mathbf{v}_i(t) + \frac{h^2}{2m_i} \mathbf{f}_i(t) \quad (1.8)$$

This equation determines the position of the molecules, but the velocity term arises on the right-hand side, so that another equation is necessary for specifying

the velocity. The first-order differential of the velocity is equal to the acceleration:

$$\mathbf{v}_i(t+h) = \mathbf{v}_i(t) + \frac{h}{m_i} \mathbf{f}_i(t) \quad (1.9)$$

In order to improve accuracy, the force term in Eq. (1.9) is slightly modified and the following equation obtained:

$$\mathbf{v}_i(t+h) = \mathbf{v}_i(t) + \frac{h}{2m_i} (\mathbf{f}_i(t) + \mathbf{f}_i(t+h)) \quad (1.10)$$

The scheme of using Eqs. (1.8) and (1.10) for determining the motion of molecules is called the “velocity Verlet method” [14]. It is well known that the velocity Verlet method is significantly superior in regard to the stability and accuracy of a simulation.

Consider another representative scheme. Noting that the first-order differential of the position is the velocity and that of the velocity is the acceleration, the application of the central difference approximation to these first-order differentials leads to the following equations:

$$\mathbf{r}_i(t+h) = \mathbf{r}_i(t) + h\mathbf{v}_i(t+h/2) \quad (1.11)$$

$$\mathbf{v}_i(t+h/2) = \mathbf{v}_i(t-h/2) + \frac{h}{m_i} \mathbf{f}_i(t) \quad (1.12)$$

The scheme of pursuing the positions and velocities of the molecules with Eqs. (1.11) and (1.12) is called the “leapfrog method” [15]. This name arises from the evaluation of the positions and forces, and then the velocities, by using time steps in a leapfrog manner. This method is also a significantly superior scheme in regard to stability and accuracy, comparable to the velocity Verlet method.

The MD method is applicable to both equilibrium and nonequilibrium physical phenomena, which makes it a powerful computational tool that can be used to simulate many physical phenomena (if computing power is sufficient).

We show the main procedure for conducting the MD simulation using the velocity Verlet method in the following steps:

1. Specify the initial position and velocity of all molecules.
2. Calculate the forces acting on molecules.
3. Evaluate the positions of all molecules at the next time step from Eq. (1.8).
4. Evaluate the velocities of all molecules at the next time step from Eq. (1.10).
5. Repeat the procedures from step 2.

In the above procedure, the positions and velocities will be evaluated at every time interval  $h$  in the MD simulation. The method of specifying the initial positions and velocities will be shown in Chapter 2.

Finally, we show the method of evaluating the system averages, which are necessary to make a comparison with experimental or theoretical values. Since

microscopic quantities such as positions and velocities are evaluated at every time interval in MD simulations, a quantity evaluated from such microscopic values—for example, the pressure—will differ from that measured experimentally. In order to compare with experimental data, instant pressure is sampled at each time step, and these values are averaged during a short sampling time to yield a macroscopic pressure. This average can be expressed as

$$\bar{A} = \frac{1}{N} \sum_{n=1}^N A_n / N \quad (1.13)$$

in which  $A_n$  is the  $n$ th sampled value of an arbitrary physical quantity  $A$ , and  $\bar{A}$ , called the “time average,” is the mathematical average of  $N$  sampling data.

## 1.1.2 Nonspherical Particle Systems

### 1.1.2.1 Case of Taking into Account the Inertia Terms

For the case of nonspherical particles, we need to consider the translational motion of the center of mass of a particle and also the rotational motion about an axis through the center of mass. Axisymmetric particles are very useful as a particle model for simulations, so we will focus on the axisymmetric particle model in this section. As shown in Figure 1.1, the important rotational motion is to be treated about the short axis line. If the particle mass is denoted by  $m$ , the inertia moment by  $I$ , the position and velocity vectors of the center of mass of particle  $i$  by  $\mathbf{r}_i$  and  $\mathbf{v}_i$ , respectively, the angular velocity vector about the short axis by  $\omega_i$ , and the force and torque acting on the particle by  $\mathbf{f}_i$  and  $\mathbf{T}_i$ , respectively, then the equations of motion concerning the translational and rotational motion can be written as

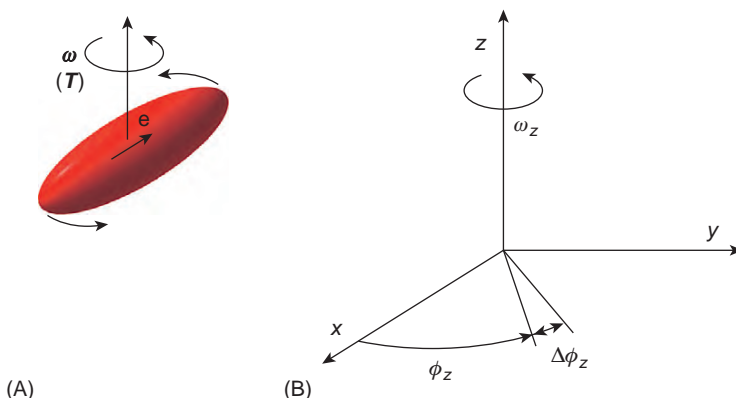


**Figure 1.1** Linear particle and angular velocity: (A) the axisymmetric particle and (B) the coordinate system.

$$m \frac{d^2 \mathbf{r}_i}{dt^2} = \mathbf{f}_i \quad (1.14)$$

$$I \frac{d\omega_i}{dt} = \mathbf{T}_i \quad (1.15)$$

Since the translational velocity  $\mathbf{v}_i$  is related to the position vector  $\mathbf{r}_i$  as  $\mathbf{v}_i = d\mathbf{r}_i/dt$ , we now consider the meaning of a quantity  $\phi_i$ , which is related to the angular velocity  $\omega_i$  as  $\omega_i = d\phi_i/dt$ . It is assumed that during a short time interval  $\Delta t$ ,  $\phi_i$  changes into  $(\phi_i + \Delta\phi_i)$  where  $\Delta\phi_i$  is expressed as  $\Delta\phi_i = (\Delta\phi_{ix}, \Delta\phi_{iy}, \Delta\phi_{iz})$ . As shown in Figure 1.1B,  $\omega_z$  is related to the rotational angle in the  $xy$ -plane about the  $z$ -axis,  $\Delta\phi_z$ . The other components have the same meanings, so that  $\phi_i$  and  $\omega_i$  for particle  $i$  can be related in the following expression:

$$\Delta\phi_i = \phi_i(t + \Delta t) - \phi_i(t) = \Delta t \omega_i(t) \quad (1.16)$$

Is the use of the quantity  $\phi_i$ , corresponding to  $\mathbf{r}_i$ , general? It seems to be more direct and more intuitive to use the unit vector  $\mathbf{e}_i$  denoting the particle direction rather than the quantity  $\phi_i$ . The change in  $\mathbf{e}_i$  during an infinitesimal time interval,  $\Delta\mathbf{e}_i$ , can be written using the angular velocity  $\omega_i$  as

$$\Delta\mathbf{e}_i(t) = \mathbf{e}_i(t + \Delta t) - \mathbf{e}_i(t) = \Delta t \omega_i(t) \times \mathbf{e}_i(t) \quad (1.17)$$

From Eqs. (1.16) and (1.17),  $\mathbf{e}_i$  can be related to  $\phi_i$  as

$$\Delta\mathbf{e}_i(t) = \Delta\phi_i(t) \times \mathbf{e}_i(t) \quad (1.18)$$

Equation (1.17) leads to the governing equation specifying the change of the particle direction:

$$\frac{d\mathbf{e}_i(t)}{dt} = \omega_i(t) \times \mathbf{e}_i(t) \quad (1.19)$$

Hence, Eq. (1.15) for the angular velocity and Eq. (1.19) for the particle direction govern the rotational motion of an axisymmetric particle.

In order to solve Eqs. (1.15) and (1.19) for the rotational motion on a computer, these equations have to be translated into finite difference equations. To do so, as already explained, the first- and second-order differentials have to be expressed as algebraic expressions using the finite difference approximations based on Taylor series expansions. General finite difference expressions are as follows:

$$\left. \begin{aligned} \frac{dx(t)}{dt} &= \frac{x(t + \Delta t) - x(t)}{\Delta t} + O(\Delta t), & \frac{dx(t)}{dt} &= \frac{x(t) - x(t - \Delta t)}{\Delta t} + O(\Delta t) \\ \frac{dx(t)}{dt} &= \frac{x(t + \Delta t) - x(t - \Delta t)}{2\Delta t} + O((\Delta t)^2) \end{aligned} \right\} \quad (1.20)$$

$$\frac{d^2x(t)}{dt^2} = \frac{x(t + \Delta t) - 2x(t) + x(t - \Delta t)}{(\Delta t)^2} + O((\Delta t)^2) \quad (1.21)$$

The simplest algorithm can be obtained using the forward finite difference approximation in Eq. (1.20) as

$$\left. \begin{aligned} \mathbf{e}_i(t + \Delta t) &= \mathbf{e}_i(t) + \Delta t \omega_i(t) \times \mathbf{e}_i(t) \\ \omega_i(t + \Delta t) &= \omega_i(t) + \Delta t \frac{\mathbf{T}_i(t)}{I} \end{aligned} \right\} \quad (1.22)$$

This algorithm is quite straightforward and understandable, but in practice does not have sufficient accuracy, since the error of the forward finite difference approximation is of the order of  $\Delta t$ . In order to improve the accuracy, the following algorithm has already been presented.

If the new vector function  $\mathbf{u}_i(t)$  such as  $\mathbf{u}_i(t) = \omega_i(t) \times \mathbf{e}_i(t)$  is introduced, Eq. (1.19) can be written as

$$\frac{d\mathbf{e}_i(t)}{dt} = \mathbf{u}_i(t) \quad (1.23)$$

By conducting the operator  $\times \mathbf{e}$  from the right side on the both sides of Eq. (1.15), the following equation is obtained:

$$\frac{d\omega_i(t)}{dt} \times \mathbf{e}_i(t) = \frac{1}{I} \mathbf{T}_i(t) \times \mathbf{e}_i(t) \quad (1.24)$$

The left-hand side of this equation leads to

$$\frac{d\omega_i}{dt} \times \mathbf{e}_i = \frac{d(\omega_i \times \mathbf{e}_i)}{dt} - \omega_i \times \frac{d\mathbf{e}_i}{dt} = \frac{d\mathbf{u}_i}{dt} - \omega_i \times \mathbf{u}_i \quad (1.25)$$

By substituting this equation into Eq. (1.24), the following equation can be obtained:

$$\begin{aligned} \frac{d\mathbf{u}_i(t)}{dt} &= \frac{1}{I} \mathbf{T}_i(t) \times \mathbf{e}_i(t) + \omega_i(t) \times \mathbf{u}_i(t) = \frac{1}{I} \mathbf{T}_i(t) \times \mathbf{e}_i(t) - |\omega_i(t)|^2 \mathbf{e}_i(t) \\ &= \frac{1}{I} \mathbf{T}_i(t) \times \mathbf{e}_i(t) + \lambda_i(t) \mathbf{e}_i(t) \end{aligned} \quad (1.26)$$

In the transformation from the first to the second expressions on the right-hand side, we have used the identity  $\mathbf{a} \times (\mathbf{b} \times \mathbf{c}) = (\mathbf{a} \cdot \mathbf{c})\mathbf{b} - (\mathbf{a} \cdot \mathbf{b})\mathbf{c}$  in evaluating  $\omega \times (\omega \times \mathbf{e})$ . The quantity  $\lambda_i(t)$  in the third expression has been introduced in order to satisfy the following relationship:

$$\mathbf{e}_i \cdot \mathbf{u}_i = \mathbf{e}_i \cdot (\omega_i \times \mathbf{e}_i) = 0 \quad (1.27)$$

We have now completed the transformation of the variables from  $\mathbf{e}_i$  and  $\omega_i$  to  $\mathbf{e}_i$  and  $\mathbf{u}_i$  for solving the rotational motion of particles.

According to the leapfrog algorithm [15], Eqs. (1.23) and (1.26) reduce to the following algebraic equations:

$$\mathbf{e}_i(t + \Delta t) = \mathbf{e}_i(t) + \Delta t \mathbf{u}_i(t + \Delta t/2) \quad (1.28)$$

$$\mathbf{u}_i(t + \Delta t/2) = \mathbf{u}_i(t - \Delta t/2) + \Delta t \frac{\mathbf{T}_i(t) \times \mathbf{e}_i(t)}{I} + \Delta t \lambda_i(t) \mathbf{e}_i(t) \quad (1.29)$$

Another equation is necessary for determining the value of  $\lambda_i(t)$ . The velocity  $\mathbf{u}_i(t)$  can be evaluated from the arithmetic average of  $\mathbf{u}_i(t + \Delta t/2)$  and  $\mathbf{u}_i(t - \Delta t/2)$ , and the expression is finally written using Eq. (1.29) as

$$\begin{aligned} \mathbf{u}_i(t) &= \frac{\mathbf{u}_i(t + \Delta t/2) + \mathbf{u}_i(t - \Delta t/2)}{2} \\ &= \mathbf{u}_i(t - \Delta t/2) + \frac{\Delta t}{2} \cdot \frac{\mathbf{T}_i(t) \times \mathbf{e}_i(t)}{I} + \frac{\Delta t}{2} \lambda_i(t) \mathbf{e}_i(t) \end{aligned} \quad (1.30)$$

Since  $\mathbf{u}_i(t)$  has to satisfy the orthogonality condition shown in Eq. (1.27), the substitution of Eq. (1.30) into Eq. (1.27) leads to the equation of  $\lambda_i(t)$  as

$$\lambda_i(t) = -\frac{2}{\Delta t} \cdot \mathbf{e}_i(t) \cdot \mathbf{u}_i(t - \Delta t/2) \quad (1.31)$$

In obtaining this expression, the identity  $\mathbf{a} \cdot (\mathbf{b} \times \mathbf{a}) = 0$  has been used to evaluate  $\mathbf{e}_i \cdot (\mathbf{T} \times \mathbf{e}_i)$ .

Now all the equations have been derived for determining the rotational motion of axisymmetric particles. With the value  $\lambda_i(t)$  in Eq. (1.31),  $\mathbf{u}_i$  at  $(t + \Delta t/2)$  is first evaluated from Eq. (1.29), and then  $\mathbf{e}_i$  at  $(t + \Delta t)$  is obtained from Eq. (1.28). This procedure shows that the solution of  $\mathbf{u}_i(t + \Delta t/2)$  gives rise to the values of  $\mathbf{e}_i(t + \Delta t)$  and  $\mathbf{T}_i(t + \Delta t)$ , and these solutions lead to  $\mathbf{u}_i(t + 3\Delta t/2)$ , and so forth. This algorithm is therefore another example of a leapfrog algorithm.

For the translational motion, the velocity Verlet algorithm may be used, and the particle position  $\mathbf{r}_i(t + \Delta t)$  and velocity  $\mathbf{v}_i(t + \Delta t)$  can be evaluated as

$$\left. \begin{aligned} \mathbf{r}_i(t + \Delta t) &= \mathbf{r}_i(t) + \Delta t \mathbf{v}_i(t) + \frac{(\Delta t)^2}{2m} \mathbf{f}_i(t) \\ \mathbf{v}_i(t + \Delta t) &= \mathbf{v}_i(t) + \frac{\Delta t}{2m} \left\{ \mathbf{f}_i(t) + \mathbf{f}_i(t + \Delta t) \right\} \end{aligned} \right\} \quad (1.32)$$

These equations can be derived in a straightforward manner from the finite difference approximations in Eqs. (1.20) and (1.21).

We have shown all the equations for specifying the translational and rotational motion of axisymmetric particles for the case of taking into account the inertia terms. The main procedure for conducting the MD simulation is as follows:

1. Specify the initial configuration and velocity of the axisymmetric particles for the translational and rotational motion.
2. Calculate the forces and torques acting on particles.
3. Evaluate the positions and velocities of the translational motion at  $(t + \Delta t)$  from Eq. (1.32).
4. Evaluate  $\lambda_i(t)$  ( $i = 1, 2, \dots, N$ ) from Eq. (1.31).
5. Evaluate  $\mathbf{u}_i$  ( $i = 1, 2, \dots, N$ ) at  $(t + \Delta t/2)$  from Eq. (1.29).
6. Evaluate the unit vectors  $\mathbf{e}_i$  ( $i = 1, 2, \dots, N$ ) at  $(t + \Delta t)$  from Eq. (1.28).
7. Advance one time step to repeat the procedures from step 2.

By following this procedure, the MD method for axisymmetric particles with the inertia terms can simulate the positions and velocities, and the directions and angular velocities, at every time interval  $\Delta t$ .

### 1.1.2.2 Case of Neglected Inertia Terms

When treating a colloidal dispersion or a polymeric solution, the Stokesian dynamics and BD methods are usually employed as a microscopic or mesoscopic analysis tool. In these methods, dispersed particles or polymers are modeled as idealized spherical or dumbbell particles, but the base liquid is usually assumed to be a continuum medium and its effect is included in the equations of motion of the particles or the polymers only as friction terms. If particle size approximates to or is smaller than micron-order, the inertia terms may be considered as negligible. In this section, we treat this type of small particles and neglect the inertia terms. For the case of axisymmetric particles moving in a quiescent fluid, the translational and angular velocities of particle  $i$ ,  $\mathbf{v}_i$  and  $\boldsymbol{\omega}_i$ , are written as

$$\mathbf{v}_i = \frac{1}{\eta} \left\{ \frac{1}{X^A} \mathbf{e}_i \mathbf{e}_i + \frac{1}{Y^A} (\mathbf{I} - \mathbf{e}_i \mathbf{e}_i) \right\} \cdot \mathbf{F}_i \quad (1.33)$$

$$\boldsymbol{\omega}_i = \frac{1}{\eta} \left\{ \frac{1}{X^C} \mathbf{e}_i \mathbf{e}_i + \frac{1}{Y^C} (\mathbf{I} - \mathbf{e}_i \mathbf{e}_i) \right\} \cdot \mathbf{T}_i \quad (1.34)$$

in which  $X^A$ ,  $X^C$ ,  $Y^A$ , and  $Y^C$  are the resistance functions specifying the particle shape. If the long- and short-axis lengths are denoted by  $2a$  and  $2b$ , respectively, and the eccentricity is denoted by  $s$  ( $= (a^2 - b^2)^{1/2}/a$ ), the resistance functions for the spheroidal particle are written as [16–18]

$$X^A = 6\pi a \cdot \frac{8}{3} \cdot \frac{s^3}{-2s + (1 + s^2)L}, \quad Y^A = 6\pi a \cdot \frac{16}{3} \cdot \frac{s^3}{2s + (3s^2 - 1)L} \quad (1.35)$$

$$X^C = 8\pi a^3 \cdot \frac{4}{3} \cdot \frac{s^3(1-s^2)}{2s-(1-s^2)L}, \quad Y^C = 8\pi a^3 \cdot \frac{4}{3} \cdot \frac{s^3(2-s^2)}{-2s+(1+s^2)L} \quad (1.36)$$

in which  $L$  is a function of the eccentricity and is expressed as

$$L = L(s) = \ln \frac{1+s}{1-s} \quad (1.37)$$

For the case of  $s \ll 1$ , Eqs. (1.35) and (1.36) are approximated using Taylor series expansions as

$$X^A = 6\pi a \left( 1 - \frac{2}{5}s^2 + \dots \right), \quad Y^A = 6\pi a \left( 1 - \frac{3}{10}s^2 + \dots \right) \quad (1.38)$$

$$X^C = 8\pi a^3 \left( 1 - \frac{6}{5}s^2 + \dots \right), \quad Y^C = 8\pi a^3 \left( 1 - \frac{9}{10}s^2 + \dots \right) \quad (1.39)$$

In the limit of  $s \rightarrow 0$ , the well-known Stokes drag formula for a spherical particle in a quiescent fluid can be obtained from Eqs. (1.33), (1.34), (1.38), and (1.39):

$$\mathbf{v}_i = \frac{1}{6\pi\eta a} \mathbf{F}_i, \quad \boldsymbol{\omega}_i = \frac{1}{8\pi\eta a^3} \mathbf{T}_i \quad (1.40)$$

It is possible to pursue the motion of an axisymmetric particle using Eqs. (1.33) and (1.34), but further simplified equations can be used for the present axisymmetric particle. For an axisymmetric particle, the translational motion can be decomposed into the motion in the long axis direction and that in a direction normal to the particle axis. Similarly, the rotational motion can be decomposed into the rotation about the particle axis and that about a line normal to the particle axis through the mass center. If the force  $\mathbf{F}_i$  acting on the particle is expressed as the sum of the force  $\mathbf{F}_i^{\parallel}$  parallel to the particle axis and the force  $\mathbf{F}_i^{\perp}$  normal to that axis, then these forces can be expressed using the particle direction vector  $\mathbf{e}_i$  as

$$\mathbf{F}_i^{\parallel} = \mathbf{e}_i(\mathbf{e}_i \cdot \mathbf{F}_i) = \mathbf{e}_i \mathbf{e}_i \cdot \mathbf{F}_i, \quad \mathbf{F}_i^{\perp} = \mathbf{F}_i - \mathbf{F}_i^{\parallel} = (\mathbf{I} - \mathbf{e}_i \mathbf{e}_i) \cdot \mathbf{F}_i \quad (1.41)$$

With these expressions, the velocities  $\mathbf{v}_i^{\parallel}$  and  $\mathbf{v}_i^{\perp}$  parallel and normal to the particle axis, respectively, can be written from Eq. (1.33) as

$$\mathbf{v}_i^{\parallel} = \frac{1}{\eta X^A} \mathbf{F}_i^{\parallel}, \quad \mathbf{v}_i^{\perp} = \frac{1}{\eta Y^A} \mathbf{F}_i^{\perp} \quad (1.42)$$

Similarly, the angular velocities  $\omega_i^{\parallel}$  and  $\omega_i^{\perp}$  about the long and short axes, respectively, are written from Eq. (1.34) as

$$\omega_i^{\parallel} = \frac{1}{\eta X^C} \mathbf{T}_i^{\parallel}, \quad \omega_i^{\perp} = \frac{1}{\eta Y^C} \mathbf{T}_i^{\perp} \quad (1.43)$$

According to Eqs. (1.42) and (1.43),  $\mathbf{v}_i^{\parallel}$ ,  $\mathbf{v}_i^{\perp}$ ,  $\omega_i^{\parallel}$ , and  $\omega_i^{\perp}$  can be evaluated from values of  $\mathbf{F}_i^{\parallel}$ ,  $\mathbf{F}_i^{\perp}$ ,  $\mathbf{T}_i^{\parallel}$ , and  $\mathbf{T}_i^{\perp}$ . The translational velocity  $\mathbf{v}_i$  and angular velocity  $\omega_i$  are then obtained as

$$\mathbf{v}_i = \mathbf{v}_i^{\parallel} + \mathbf{v}_i^{\perp}, \quad \omega_i = \omega_i^{\parallel} + \omega_i^{\perp} \quad (1.44)$$

With the solutions of the translational and angular velocities at the time step  $t$  shown in Eq. (1.44), the position vector  $\mathbf{r}_i$  and the particle direction vector  $\mathbf{e}_i$  at the next time step ( $t + \Delta t$ ) can finally be obtained as

$$\mathbf{r}_i(t + \Delta t) = \mathbf{r}_i(t) + \Delta t \mathbf{v}_i(t) \quad (1.45)$$

$$\mathbf{e}_i(t + \Delta t) = \mathbf{e}_i(t) + \Delta t \omega_i(t) \times \mathbf{e}_i(t) \quad (1.46)$$

Lastly, we show the main procedure for the simulation in the following steps:

1. Specify the initial configuration and velocity of all axisymmetric particles for the translational and rotational motion.
2. Calculate all the forces and torques acting on particles.
3. Evaluate  $\mathbf{F}_i^{\parallel}$ ,  $\mathbf{F}_i^{\perp}$ ,  $\mathbf{T}_i^{\parallel}$ , and  $\mathbf{T}_i^{\perp}$  ( $i = 1, 2, \dots, N$ ) from Eq. (1.41) and similar equations for the torques.
4. Calculate  $\mathbf{v}_i^{\parallel}$ ,  $\mathbf{v}_i^{\perp}$ ,  $\omega_i^{\parallel}$ , and  $\omega_i^{\perp}$  ( $i = 1, 2, \dots, N$ ) from Eqs. (1.42) and (1.43).
5. Calculate  $\mathbf{v}_i$  and  $\omega_i$  ( $i = 1, 2, \dots, N$ ) from Eq. (1.44).
6. Calculate  $\mathbf{r}_i$  and  $\mathbf{e}_i$  ( $i = 1, 2, \dots, N$ ) at the next time step ( $t + \Delta t$ ) from Eqs. (1.45) and (1.46).
7. Advance one time step and repeat the procedures from step 2.

## 1.2 Monte Carlo Method

In the MD method, the motion of molecules (particles) is simulated according to the equations of motion and therefore it is applicable to both thermodynamic equilibrium and nonequilibrium phenomena. In contrast, the MC method generates a series of microscopic states under a certain stochastic law, irrespective of the equations of motion of particles. Since the MC method does not use the equations of motion, it cannot include the concept of explicit time, and thus is only a simulation technique for phenomena in thermodynamic equilibrium. Hence, it is unsuitable for the MC method to deal with the dynamic properties of a system, which are dependent on time. In the following paragraphs, we explain important points of the concept of the MC method.



**Figure 1.2** Typical energy situations for a two particle system.

How do microscopic states arise for thermodynamic equilibrium in a practical situation? We discuss this problem by considering a two-particle attractive system using Figure 1.2. As shown in Figure 1.2A, if the two particles overlap, then a repulsive force or a significant interaction energy arises. As shown in Figure 1.2B, for the case of close proximity, the interaction energy becomes low and an attractive force acts on the particles. If the two particles are sufficiently distant, as shown in Figure 1.2C, the interactive force is negligible and the interaction energy can be regarded as zero. In actual phenomena, microscopic states which induce a significantly high energy, as shown in Figure 1.2A, seldom appear, but microscopic states which give rise to a low-energy system, as shown in Figure 1.2B, frequently arise. However, this does not mean that only microscopic states that induce a minimum-energy system appear. Consider the fact that oxygen and nitrogen molecules do not gather in a limited area, but distribute uniformly in a room. It is seen from this discussion that, for thermodynamic equilibrium, microscopic states do not give rise to a minimum of the total system energy, but to a minimum free energy of a system. For example, in the case of a system specified by the number of particles  $N$ , temperature  $T$ , and volume of the system  $V$ , microscopic states arise such that the following Helmholtz free energy  $F$  becomes a minimum:

$$F = E - TS \quad (1.47)$$

in which  $E$  is the potential energy of the system, and  $S$  is the entropy. In the preceding example, the reason why oxygen or nitrogen molecules do not gather in a limited area can be explained by taking into account the entropy term on the right-hand side in Eq. (1.47). That is, the situation in which molecules do not gather together and form flocks but expand to fill a room gives rise to a large value of the entropy. Hence, according to the counterbalance relationship of the energy and the entropy, real microscopic states arise such that the free energy of a system is at minimum.

Next, we consider how microscopic states arise stochastically. We here treat a system composed of  $N$  interacting spherical particles with temperature  $T$  and volume  $V$  of the system; these quantities are given values and assumed to be constant. If the position vector of an arbitrary particle  $i$  ( $i = 1, 2, \dots, N$ ) is denoted by  $\mathbf{r}_i$ , then the total interaction energy  $U$  of the system can be expressed as a function of the particle positions; that is, it can be expressed as  $U = U(\mathbf{r}_1, \mathbf{r}_2, \dots, \mathbf{r}_N)$ . For the present system specified by given values of  $N$ ,  $T$ , and  $V$ , the appearance of a microscopic state that the particle  $i$  ( $i = 1, 2, \dots, N$ ) exists within the small range

of  $\mathbf{r}_i \sim (\mathbf{r}_i + \Delta\mathbf{r}_i)$  is governed by the probability density function  $\rho(\mathbf{r}_1, \mathbf{r}_2, \dots, \mathbf{r}_N)$ . This can be expressed from statistical mechanics [19,20] as

$$\rho(\mathbf{r}_1, \mathbf{r}_2, \dots, \mathbf{r}_N) = \frac{\exp\{-U(\mathbf{r}_1, \mathbf{r}_2, \dots, \mathbf{r}_N)/kT\}}{\int_V \dots \int_V \exp\{-U(\mathbf{r}_1, \mathbf{r}_2, \dots, \mathbf{r}_N)/kT\} d\mathbf{r}_1 d\mathbf{r}_2 \dots d\mathbf{r}_N} \quad (1.48)$$

If a series of microscopic states is generated with an occurrence according to this probability, a simulation may have physical meaning. However, this approach is impracticable, as it is extraordinarily difficult and almost impossible to evaluate analytically the definite integral of the denominator in Eq. (1.48). In fact, if we were able to evaluate this integral term analytically, we would not need a computer simulation because it would be possible to evaluate almost all physical quantities analytically.

The “Metropolis method” [21] overcomes this difficulty for MC simulations. In the Metropolis method, the transition probability from microscopic states  $i$  to  $j$ ,  $p_{ij}$ , is expressed as

$$p_{ij} = \begin{cases} 1 & (\text{for } \rho_j/\rho_i \geq 1) \\ \frac{\rho_j}{\rho_i} & (\text{for } \rho_j/\rho_i < 1) \end{cases} \quad (1.49)$$

in which  $\rho_j$  and  $\rho_i$  are the probability density functions for microscopic states  $j$  and  $i$  appearing, respectively. The ratio of  $\rho_j/\rho_i$  is obtained from Eq. (1.48) as

$$\begin{aligned} \frac{\rho_j}{\rho_i} &= \exp \left\{ -\frac{1}{kT} (U_j - U_i) \right\} \\ &= \exp \left[ -\frac{1}{kT} \{ U(\mathbf{r}_1^j, \mathbf{r}_2^j, \dots, \mathbf{r}_N^j) - U(\mathbf{r}_1^i, \mathbf{r}_2^i, \dots, \mathbf{r}_N^i) \} \right] \end{aligned} \quad (1.50)$$

In the above equations,  $U_i$  and  $U_j$  are the interaction energies of microscopic states  $i$  and  $j$ , respectively. The superscripts attached to the position vectors denote the same meanings concerning microscopic states. Eq. (1.49) implies that, in the transition from microscopic states  $i$  to  $j$ , new microscopic state  $j$  is adopted if the system energy decreases, with the probability  $\rho_j/\rho_i (< 1)$  if the energy increases. As clearly demonstrated by Eq. (1.50), for  $\rho_j/\rho_i$  the denominator in Eq. (1.48) is not required in Eq. (1.50), because  $\rho_j$  is divided by  $\rho_i$  and the term is canceled through this operation. This is the main reason for the great success of the Metropolis method for MC simulations. That a new microscopic state is adopted with the probability  $\rho_j/\rho_i$ , even in the case of the increase in the interaction energy, verifies the accomplishment of the minimum free-energy condition for the system. In other words, the adoption of microscopic states, yielding an increase in the system energy, corresponds to an increase in the entropy.

The above discussion is directly applicable to a system composed of nonspherical particles. The situation of nonspherical particles in thermodynamic equilibrium can be specified by the particle position of the mass center,  $\mathbf{r}_i(i=1, 2, \dots, N)$ , and the unit vector  $\mathbf{e}_i(i=1, 2, \dots, N)$  denoting the particle direction. The transition probability from microscopic states  $i$  to  $j$ ,  $p_{ij}$  can be written in similar form to Eq. (1.49). The exact expression of  $\rho_j/\rho_i$  becomes

$$\frac{\rho_j}{\rho_i} = \exp \left\{ -\frac{1}{kT} (U_j - U_i) \right\} = \exp \left[ -\frac{1}{kT} \left\{ U(\mathbf{r}_1^j, \mathbf{r}_2^j, \mathbf{r}_N^j, \mathbf{e}_1^j, \mathbf{e}_2^j, \dots, \mathbf{e}_N^j) - U(\mathbf{r}_1^i, \mathbf{r}_2^i, \mathbf{r}_N^i, \mathbf{e}_1^i, \mathbf{e}_2^i, \dots, \mathbf{e}_N^i) \right\} \right] \quad (1.51)$$

The main procedure for the MC simulation of a nonspherical particle system is as follows:

1. Specify the initial position and direction of all particles.
2. Regard this state as microscopic state  $i$ , and calculate the interaction energy  $U_i$ .
3. Choose an arbitrary particle in order or randomly and call this particle “particle  $\alpha$ .”
4. Make particle  $\alpha$  move translationally using random numbers and calculate the interaction energy  $U_j$  for this new configuration.
5. Adopt this new microscopic state for the case of  $U_j \leq U_i$  and go to step 7.
6. Calculate  $\rho_j/\rho_i$  in Eq. (1.51) for the case of  $U_j > U_i$  and take a random number  $R_1$  from a uniform random number sequence distributed from zero to unity.
  - 6.1. If  $R_1 \leq \rho_j/\rho_i$ , adopt this microscopic state  $j$  and go to step 7.
  - 6.2. If  $R_1 > \rho_j/\rho_i$ , reject this microscopic state, regard previous state  $i$  as new microscopic state  $j$ , and go to step 7.
7. Change the direction of particle  $\alpha$  using random numbers and calculate the interaction energy  $U_k$  for this new state.
8. If  $U_k \leq U_j$ , adopt this new microscopic state and repeat from step 2.
9. If  $U_k > U_j$ , calculate  $\rho_k/\rho_j$  in Eq. (1.51) and take a random number  $R_2$  from the uniform random number sequence.
  - 9.1. If  $R_2 \leq \rho_k/\rho_j$ , adopt this new microscopic state  $k$  and repeat from step 2.
  - 9.2. If  $R_2 > \rho_k/\rho_j$ , reject this new state, regard previous state  $j$  as new microscopic state  $k$ , and repeat from step 2.

Although the treatment of the translational and rotational changes is carried out separately in the above algorithm, a simultaneous procedure is also possible in such a way that the position and direction of an arbitrary particle are simultaneously changed, and the new microscopic state is adopted according to the condition in Eq. (1.49). However, for a strongly interacting system, the separate treatment may be found to be more effective in many cases.

We will now briefly explain how the translational move is made using random numbers during a simulation. If the position vector of an arbitrary particle  $\alpha$  in microscopic state  $i$  is denoted by  $\mathbf{r}_\alpha = (x_\alpha, y_\alpha, z_\alpha)$ , this particle is moved to a new position  $\mathbf{r}'_\alpha = (x'_\alpha, y'_\alpha, z'_\alpha)$  by the following equations using random

numbers  $R_1$ ,  $R_2$ , and  $R_3$ , taken from a random number sequence ranged from zero to unity:

$$\left. \begin{aligned} x'_\alpha &= x_\alpha + R_1 \delta r_{\max} \\ y'_\alpha &= y_\alpha + R_2 \delta r_{\max} \\ z'_\alpha &= z_\alpha + R_3 \delta r_{\max} \end{aligned} \right\} \quad (1.52)$$

These equations imply that the particle is moved to an arbitrary position, determined by random numbers, within a cube centered at the particle center with side length of  $2\delta r_{\max}$ . A series of microscopic states is generated by moving the particles according to the above-mentioned procedure.

Finally, we show the method of evaluating the average of a physical quantity in MC simulations. These averages, called “ensemble averages,” are different from the time averages that are obtained from MD simulations. If a physical quantity  $A$  is a function of the microscopic states of a system, and  $A_n$  is the  $n$ th sampled value of this quantity in an MC simulation, then the ensemble average  $\langle A \rangle$  can be evaluated from the equation

$$\langle A \rangle = \sum_{n=1}^M A_n / M \quad (1.53)$$

in which  $M$  is the total sampling number. In actual simulations, the sampling procedure is not conducted at each time step but at regular intervals. This may be more efficient because if the data have significant correlations they are less likely to be sampled by taking a longer interval for the sampling time. The ensemble averages obtained in this way may be compared with experimental data.

### 1.3 Brownian Dynamics Method

A dispersion or suspension composed of fine particles dispersed in a base liquid is a difficult case to be treated by simulations in terms of the MD method, because the characteristic time of the motion of the solvent molecules is considerably different from that of the dispersed particles. Simply speaking, if we observe such a dispersion based on the characteristic time of the solvent molecules, we can see only the active motion of solvent molecules around the quiescent dispersed particles. Clearly the MD method is quite unrealistic as a simulation technique for particle dispersions. One approach to overcome this difficulty is to not focus on the motion of each solvent molecule, but regard the solvent molecules as a continuum medium and consider the motion of dispersed particles in such a medium. In this approach, the influence of the solvent molecules is included into the equations of motion of the particles as random forces. We can observe such random motion when pollen moves at a liquid surface or when dispersed particles move in a functional fluid such as a ferrofluid. The BD method simulates the random motion of dispersed particles

that is induced by the solvent molecules; thus, such particles are called “Brownian particles.”

If a particle dispersion is so significantly dilute that each particle can be regarded as moving independently, the motion of this Brownian particle is governed by the following Langevin equation [22]:

$$m \frac{d\mathbf{v}}{dt} = \mathbf{f} - \xi \mathbf{v} + \mathbf{f}^B \quad (1.54)$$

This equation is valid for a spherical particle dispersion. In Eq. (1.54),  $m$  is the mass of a spherical particle,  $\mathbf{v}$  is the velocity vector,  $\xi$  is the friction coefficient and is expressed as  $\xi = 3\pi\eta d$  for the particle diameter  $d$  with the viscosity  $\eta$  of a base liquid,  $\mathbf{f}$  is the force exerted by an external field, and  $\mathbf{f}^B (= (f_x^B, f_y^B, f_z^B))$  is the random force due to the motion of solvent molecules. This random force has the following stochastic properties:

$$\langle f_x^B(t) \rangle = \langle f_y^B(t) \rangle = \langle f_z^B(t) \rangle = 0 \quad (1.55)$$

$$\left\langle \{f_x^B(t)\}^2 \right\rangle = \left\langle \{f_y^B(t)\}^2 \right\rangle = \left\langle \{f_z^B(t)\}^2 \right\rangle = 2\xi kT \delta(t - t') \quad (1.56)$$

in which  $\delta(t - t')$  is the Dirac delta function. In Eq. (1.56) larger random forces act on Brownian particles at a higher temperature because the mean square average of each component of the random force is in proportion to the system temperature. At a higher temperature the solvent molecules move more actively and induce larger random forces.

In order to simulate the Brownian motion of particles, the basic equation in Eq. (1.54) has to be transformed into an algebraic equation, as in the MD method. If the time interval  $h$  is sufficiently short such that the change in the forces is negligible, Eq. (1.54) can be regarded as a simple first-order differential equation. Hence, Eq. (1.54) can be solved by standard textbook methods of differential equations [23], and algebraic equations can finally be obtained as

$$\begin{aligned} \mathbf{r}(t+h) &= \mathbf{r}(t) + \frac{m}{\xi} \mathbf{v}(t) \left\{ 1 - \exp\left(-\frac{\xi}{m} h\right) \right\} \\ &\quad + \frac{1}{\xi} \mathbf{f}(t) \left\{ h - \frac{m}{\xi} \left( 1 - \exp\left(-\frac{\xi}{m} h\right) \right) \right\} + \Delta\mathbf{r}^B \end{aligned} \quad (1.57)$$

$$\mathbf{v}(t+h) = \mathbf{v}(t) \exp\left(-\frac{\xi}{m} h\right) + \frac{1}{\xi} \mathbf{f}(t) \left( 1 - \exp\left(-\frac{\xi}{m} h\right) \right) + \Delta\mathbf{v}^B \quad (1.58)$$

in which  $\Delta\mathbf{r}^B$  and  $\Delta\mathbf{v}^B$  are a random displacement and velocity due to the motion of solvent molecules. The relationship of the  $x$ -components of  $\Delta\mathbf{r}^B$  and  $\Delta\mathbf{v}^B$  can

be expressed as a two-dimensional normal distribution (similarly for the other components). We do not show such an expression here [4], but instead consider a method that is superior in regard to the extension of the BD method to the case with multibody hydrodynamic interactions. The BD method based on Eqs. (1.57) and (1.58) is applicable to physical phenomena in which the inertia term is a governing factor.

Since the BD method with multibody hydrodynamic interactions among the particles is very complicated, we here focus on an alternative method that treats the friction forces between the particles and a base liquid, and the nonhydrodynamic interactions between the particles. This simpler type of simulation method is sometimes used as a first-order approximation because of the complexity of treating hydrodynamic interactions. A representative nonhydrodynamic force is the magnetic force influencing the magnetic particles in a ferrofluid.

Although the BD method based on the Ermak–McCammon analysis [24] takes into account multibody hydrodynamic interactions among particles, we apply this analysis method to the present dilute dispersion without hydrodynamic interactions, and can derive the basic equation of the position vector  $\mathbf{r}_i(i = 1, 2, \dots, N)$  of Brownian particle  $i$  as

$$\mathbf{r}_i(t + h) = \mathbf{r}_i(t) + \frac{1}{\xi} h \mathbf{f}_i(t) + \Delta \mathbf{r}_i^B \quad (1.59)$$

in which the components  $(\Delta x_i^B, \Delta y_i^B, \Delta z_i^B)$  of the random displacement  $\Delta \mathbf{r}_i^B$  have to satisfy the following stochastic properties:

$$\langle \Delta x_i^B \rangle = \langle \Delta y_i^B \rangle = \langle \Delta z_i^B \rangle = 0 \quad (1.60)$$

$$\left\langle (\Delta x_i^B)^2 \right\rangle = \left\langle (\Delta y_i^B)^2 \right\rangle = \left\langle (\Delta z_i^B)^2 \right\rangle = \frac{2kT}{\xi} h \quad (1.61)$$

Equations similar to Eq. (1.59) hold for every particle in the system. Interactions among particles arise through the force  $\mathbf{f}_i(i = 1, 2, \dots, N)$  acting on them.

If a Brownian particle exhibits magnetic properties and has, for example, a magnetic dipole moment at the particle center, it will have a tendency to incline in the direction of an applied magnetic field. Hence, even in the case of spherical particles, the rotational motion is influenced by an external field, so that both the translational and the rotational motion of a particle are treated simultaneously in simulations.

If the unit vector of the particle direction is denoted by  $\mathbf{n}_i$ , the equation of the change in  $\mathbf{n}_i$  can be derived under the same conditions assumed in deriving Eq. (1.59) as

$$\mathbf{n}_i(t + h) = \mathbf{n}_i(t) + \frac{1}{\xi_R} h \mathbf{T}_i(t) \times \mathbf{n}_i(t) + \Delta \mathbf{n}_i^B \quad (1.62)$$

in which  $\xi_R$  is the friction coefficient of the rotational motion, expressed as  $\xi_R = \pi\eta d^3$ , and  $T_i$  is the torque acting on particle  $i$  by nonhydrodynamic forces. Also,  $\Delta n_i^B$  is the rotational displacement due to random forces, expressed as

$$\Delta n_i^B = \Delta\phi_{\perp 1}^B \mathbf{n}_{\perp 1} + \Delta\phi_{\perp 2}^B \mathbf{n}_{\perp 2} \quad (1.63)$$

in which  $\mathbf{n}_{\perp 1}$  and  $\mathbf{n}_{\perp 2}$  are a set of unit vectors normal to the direction of particle  $i$ , and  $\Delta\phi_{\perp 1}^B$  and  $\Delta\phi_{\perp 2}^B$  have the following stochastic properties:

$$\langle \Delta\phi_{\perp 1}^B \rangle = \langle \Delta\phi_{\perp 2}^B \rangle = 0 \quad (1.64)$$

$$\langle (\Delta\phi_{\perp 1}^B)^2 \rangle = \langle (\Delta\phi_{\perp 2}^B)^2 \rangle = \frac{2kT}{\xi_R} h \quad (1.65)$$

Now consider the correspondence of quantities in the translational and rotational motion. The velocity  $v_i$  in the translational motion corresponds to the angular velocity  $\omega_i$  in the rotational motion, and the position vector  $r_i$  corresponds to the quantity  $\phi_i$  defined as  $d\phi/dt = \omega_i$ . Obviously, due to the similarity of Eqs. (1.64) and (1.65) to Eqs. (1.60) and (1.61), the components  $\Delta\phi_{\perp 1}^B$  and  $\Delta\phi_{\perp 2}^B$  of the vector  $\Delta\phi^B$  have to satisfy Eqs. (1.64) and (1.65).

The basic Eqs. (1.59) and (1.62) for governing the translational and rotational motion of particles have been derived under the assumptions that the momentum of particles is sufficiently relaxed during the time interval  $h$  and that the force acting on the particles is substantially constant during this infinitesimally short time. This is the essence of the Ermak–McCammon method for BD simulations.

Next, we show the method of generating random displacements according to Eqs. (1.60) and (1.61), but, before that, the normal probability distribution needs to be briefly described. If the behavior of a stochastic variable is described by the normal distribution  $\rho_{\text{normal}}(x)$  with variance  $\sigma^2$ ,  $\rho_{\text{normal}}(x)$  is written as

$$\rho_{\text{normal}}(x) = \frac{1}{(2\pi\sigma^2)^{1/2}} \exp(-x^2/2\sigma^2) \quad (1.66)$$

in which the variance  $\sigma^2$  is a measure of how wide the stochastic variable  $x$  is distributed around the mean value  $\langle x \rangle$ , which is taken as zero for this discussion. The variance  $\sigma^2$  is mathematically defined as

$$\sigma^2 = \langle (x - \langle x \rangle)^2 \rangle = \langle x^2 \rangle - \langle \langle x \rangle \rangle^2 \quad (1.67)$$

If Eq. (1.66) is applied to Eqs. (1.60) and (1.61), the random displacement  $\Delta x_i^B$  in the  $x$ -direction can be written in normal distribution form as

$$\rho_{\text{normal}}(\Delta x_i^B) = \left( \frac{\xi}{4\pi k Th} \right)^{1/2} \exp \left\{ -\frac{\xi}{4kTh} (\Delta x_i^B)^2 \right\} \quad (1.68)$$

The other components also obey a normal distribution. As seen in Eq. (1.68), larger random displacements tend to arise at a higher system temperature, which makes sense given that solvent molecules move more actively in the higher temperature case. The random displacements can therefore be generated by sampling according to the normal distributions shown in Eq. (1.68). An example of generating random displacements is shown in Appendix A2.

The main procedure for conducting the BD simulation based on Eqs. (1.59), (1.60), and (1.61) is:

1. Specify the initial position of all particles.
2. Calculate the forces acting on each particle.
3. Generate the random displacements  $\Delta\mathbf{r}_i^B = (\Delta x_i^B, \Delta y_i^B, \Delta z_i^B)$  ( $i = 1, 2, \dots, N$ ) using uniform random numbers: for example,  $\Delta x_i^B$  is sampled according to Eq. (1.68).
4. Calculate all the particle positions at the next time step from Eq. (1.59).
5. Return to step 2 and repeat.

The physical quantities of interest are evaluated by the time average, similar to the molecular dynamics method.

## 1.4 Dissipative Particle Dynamics Method

As already pointed out, it is not realistic to use the MD method to simulate the motion of solvent molecules and dispersed particles simultaneously, since the characteristic time of solvent molecules is much shorter than that of dispersed particles. Hence, in the BD method, the motion of solvent molecules is not treated, but a fluid is regarded as a continuum medium. The influence of the molecular motion is combined into the equations of motion of dispersed particles as stochastic random forces. Are there any simulation methods to simulate the motion of both the solvent molecules and the dispersed particles? As far as we treat the motion of real solvent molecules, the development of such simulation methods may be impractical. However, if groups or clusters of solvent molecules are regarded as virtual fluid particles, such that the characteristic time of the motion of such fluid particles is not so different from that of dispersed particles, then it is possible to simulate the motion of the dispersed and the fluid particles simultaneously. These virtual fluid particles are expected to exchange their momentum, exhibit a random motion similar to Brownian particles, and interact with each other by particle–particle potentials. We call these virtual fluid particles “dissipative particles,” and the simulation technique of treating the motion of dissipative particles instead of the solvent molecules is called the “dissipative particle dynamics (DPD) method” [4–8].

The DPD method is principally applicable to simulations of colloidal dispersions that take into account the multibody hydrodynamic interactions among particles. For colloidal dispersions, the combination of the flow field solutions for a three- or four-particle system into a simulation technique enables us to address the physical situation of multibody hydrodynamic interactions as accurately as possible. However, it is extraordinarily difficult to solve analytically the flow field even for

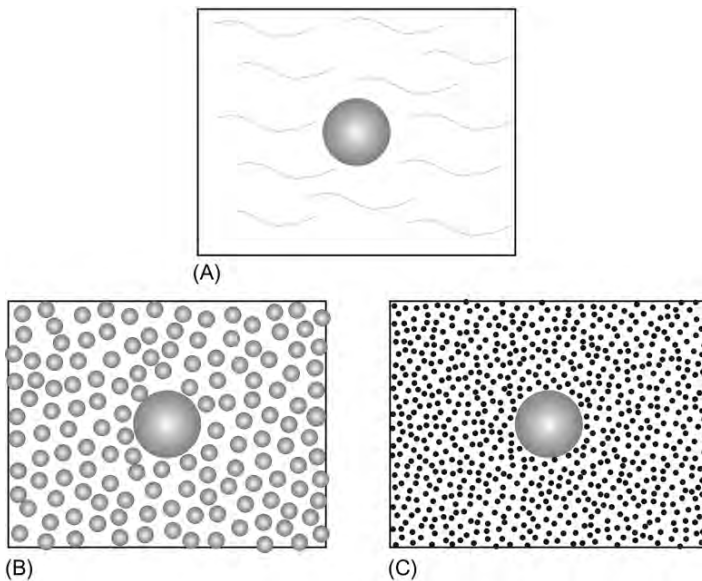


**Figure 1.3** Modeling of a fluid: (A) the macroscopic model, (B) the mesoscopic model, and (C) the microscopic model.

a three-particle system, so a solution for a nonspherical particle system is futile to attempt. In contrast, the DPD method does not require this type of solution of the flow field in conducting simulations of colloidal dispersions that take into account multibody hydrodynamic effects. This is because they are automatically reproduced from consideration of the interactions between the dissipative and the colloidal particles. This approach to the hydrodynamic interactions is a great advantage of the DPD method. In addition, this method is applicable to nonspherical particle dispersions, and a good simulation technique for colloidal dispersions.

We will show the general categories of models employed in the modeling of a fluid for numerical simulations before proceeding to the explanation of the DPD method. Figure 1.3 schematically shows the classification of the modeling of a fluid. Figure 1.3A shows a continuum medium model for a fluid. In this case, a solution of a flow field can be obtained by solving the Navier–Stokes equations, which are the governing equations of the motion of a fluid. Figure 1.3C shows a microscopic model in which the solvent molecules are treated and a solution of the flow field can be obtained by pursuing the motion of the solvent molecules: this is the MD approach. Figure 1.3B shows a mesoscopic model in which a fluid is assumed to be composed of virtual fluid particles: the DPD method is classified within this category.

In the following paragraphs, we discuss the equations of motion of the dissipative particles for a system composed of dissipative particles alone, without colloidal

particles. For simplification's sake, dissipative particles are simply called "particles" unless specifically identified.

In order that the solution of a flow field obtained from the particle motion agrees with that of the Navier–Stokes equations, the equations of motion of the particles have to be formalized in physically viable form. For example, as a physical restriction on the system behavior, the total momentum of a system should be conserved. The forces acting on particle  $i$  possibly seem to be a conservative force  $\mathbf{F}_{ij}^C$ , exerted by other particles (particle  $j$  in this case); a dissipative force  $\mathbf{F}_{ij}^D$ , due to the exchange of momentum; and a random force  $\mathbf{F}_{ij}^R$ , inducing the random motion of particles. With the particle mass  $m$  and the particle velocity  $\mathbf{v}_i$ , the equation of motion can be written as

$$m \frac{d\mathbf{v}_i}{dt} = \sum_{j \neq i} \mathbf{F}_{ij}^C + \sum_{j \neq i} \mathbf{F}_{ij}^D + \sum_{j \neq i} \mathbf{F}_{ij}^R \quad (1.69)$$

The subscripts in Eq. (1.69), for example in  $\mathbf{F}_{ij}^C$ , represent the force acting on particle  $i$  by particle  $j$ . Now, we embody specific expressions for each force. Since  $\mathbf{F}_{ij}^C$  is a conservative force between particles  $i$  and  $j$ , it is assumed to be dependent on the relative position  $\mathbf{r}_{ij}$  ( $=\mathbf{r}_i - \mathbf{r}_j$ ) alone, not on velocities. This specific expression will be shown later.  $\mathbf{F}_{ij}^D$  and  $\mathbf{F}_{ij}^R$  have to be conserved under a Galilean transformation (refer to a textbook of mechanics); thus, they must be independent of  $\mathbf{r}_i$  and  $\mathbf{v}_i$  in a given reference frame (quantities dependent on  $\mathbf{r}_i$  and  $\mathbf{v}_i$  are not conserved), but should be functions of the relative position vector  $\mathbf{r}_{ij}$  and relative velocity vector  $\mathbf{v}_{ij}$  ( $=\mathbf{v}_i - \mathbf{v}_j$ ). Furthermore, it is physically reasonable to assume that  $\mathbf{F}_{ij}^R$  is dependent only on the relative position  $\mathbf{r}_{ij}$ , and not on the relative velocity  $\mathbf{v}_{ij}$ . We also have to take into account that the particle motion is isotropic and the forces between particles decrease with the particle–particle separation. The following expressions for  $\mathbf{F}_{ij}^D$  and  $\mathbf{F}_{ij}^R$  satisfy all the above-mentioned requirements:

$$\mathbf{F}_{ij}^D = -\gamma w_D(r_{ij})(\mathbf{e}_{ij} \cdot \mathbf{v}_{ij})\mathbf{e}_{ij} \quad (1.70)$$

$$\mathbf{F}_{ij}^R = \sigma w_R(r_{ij})\mathbf{e}_{ij}\zeta_{ij} \quad (1.71)$$

in which  $r_{ij} = |\mathbf{r}_{ij}|$ , and  $\mathbf{e}_{ij}$  is the unit vector denoting the direction of a line drawn from particles  $j$  to  $i$ , expressed as  $\mathbf{e}_{ij} = \mathbf{r}_{ij}/r_{ij}$ . The  $\zeta_{ij}$  is the stochastic variable inducing the random motion of particles and has the following characteristics:

$$\langle \zeta_{ij} \rangle = 0, \quad \langle \zeta_{ij}(t)\zeta_{ij}(t') \rangle = (\delta_{ii'}\delta_{jj'} + \delta_{ij'}\delta_{ji'})\delta(t - t') \quad (1.72)$$

in which  $\delta_{ij}$  is the Kronecker delta, and  $\delta_{ij} = 1$  for  $i = j$  and  $\delta_{ij} = 0$  for the other cases. Since this variable satisfies the equation of  $\zeta_{ij} = \zeta_{ji}$ , the total momentum of a system is conserved. The  $w_D(r_{ij})$  and  $w_R(r_{ij})$  are weighting functions representing the characteristics of forces decreasing with the particle–particle separation, and  $\gamma$  and  $\sigma$  are constants specifying the strengths of the corresponding forces. As shown

later, these constants are related to the system temperature and friction coefficients. The  $\mathbf{F}_{ij}^D$  acts such that the relative motion of particles  $i$  and  $j$  relaxes, and  $\mathbf{F}_{ij}^R$  functions such that the thermal motion is activated. Since the action–reaction law is satisfied by  $\mathbf{F}_{ij}^R$ , the conservation of the total momentum is not violated by  $\mathbf{F}_{ij}^R$ .

By substituting Eqs. (1.70) and (1.71) into Eq. (1.69), the equation of motion of particles can be written as

$$m \frac{d\mathbf{v}_i}{dt} = \sum_{j(\neq i)} \mathbf{F}_{ij}^C(\mathbf{r}_{ij}) - \sum_{j(\neq i)} \gamma w_D(r_{ij})(\mathbf{e}_{ij} \cdot \mathbf{v}_{ij})\mathbf{e}_{ij} + \sum_{j(\neq i)} \sigma w_R(r_{ij})\mathbf{e}_{ij}\zeta_{ij} \quad (1.73)$$

The integral of this equation with respect to the time from  $t$  to  $(t + \Delta t)$  leads to the finite difference equations specifying the motion of the simulation particles:

$$\Delta\mathbf{r}_i = \mathbf{v}_i \Delta t \quad (1.74)$$

$$\Delta\mathbf{v}_i = \frac{1}{m} \left( \sum_{j(\neq i)} \mathbf{F}_{ij}^C(\mathbf{r}_{ij}) - \sum_{j(\neq i)} \gamma w_D(r_{ij})(\mathbf{e}_{ij} \cdot \mathbf{v}_{ij})\mathbf{e}_{ij} \right) \Delta t + \frac{1}{m} \sum_{j(\neq i)} \sigma w_R(r_{ij})\mathbf{e}_{ij} \Delta W_{ij} \quad (1.75)$$

The  $\Delta W_{ij}$  has to satisfy the following stochastic properties, which can be obtained from Eq. (1.72):

$$\left. \begin{aligned} \langle \Delta W_{ij} \rangle &= 0 \\ \langle \Delta W_{ij} \Delta W_{i'j'} \rangle &= (\delta_{ii'}\delta_{jj'} + \delta_{ij'}\delta_{ji'})\Delta t \end{aligned} \right\} \quad (1.76)$$

If a new stochastic variable  $\theta_{ij}$  is introduced from  $\Delta W_{ij} = \theta_{ij}(\Delta t)^{1/2}$ , the third term in Eq. (1.75) can be written as

$$\frac{1}{m} \sum_{j(\neq i)} \sigma w_R(r_{ij})\mathbf{e}_{ij}\theta_{ij}\sqrt{\Delta t} \quad (1.77)$$

in which  $\theta_{ij}$  has to satisfy the following stochastic characteristics:

$$\left. \begin{aligned} \langle \theta_{ij} \rangle &= 0 \\ \langle \theta_{ij} \theta_{i'j'} \rangle &= (\delta_{ii'}\delta_{jj'} + \delta_{ij'}\delta_{ji'}) \end{aligned} \right\} \quad (1.78)$$

In simulations, values of the stochastic variable are sampled from a normal distribution with zero-mean value and unit variance or from a uniform distribution.

The constants  $\gamma$  and  $\sigma$  and the weighting functions  $w_D(r_{ij})$  and  $w_R(r_{ij})$ , which appeared in Eq. (1.75), must satisfy the following relationships:

$$\left. \begin{aligned} w_D(r_{ij}) &= w_R^2(r_{ij}) \\ \sigma^2 &= 2\gamma kT \end{aligned} \right\} \quad (1.79)$$

The second equation is called the “fluctuation–dissipation theorem.” These relationships ensure a valid equilibrium distribution of particle velocities for thermodynamic equilibrium.

Next, we show expressions for the conservative force  $\mathbf{F}_{ij}^C$  and the weighting function  $w_R(r_{ij})$ . The  $\mathbf{F}_{ij}^C$  functions as a tool for preventing particles from significantly overlapping, so that the value of  $w_R(r_{ij})$  has to increase with particles  $i$  and  $j$  approaching each other. Given this consideration, these expressions may be written as

$$\mathbf{F}_{ij}^C = \alpha w_R(r_{ij}) \mathbf{e}_{ij} \quad (1.80)$$

$$w_R(r_{ij}) = \begin{cases} 1 - \frac{r_{ij}}{r_c} & \text{for } r_{ij} \leq r_c \\ 0 & \text{for } r_{ij} > r_c \end{cases} \quad (1.81)$$

in which  $\alpha$  is a constant representing the strength of a repulsive force. By substituting the above-mentioned expressions into Eq. (1.75) and taking into account Eq. (1.77), the final expressions for the equations of motion of particles can be obtained as

$$\Delta \mathbf{r}_i = \mathbf{v}_i \Delta t \quad (1.82)$$

$$\begin{aligned} \Delta \mathbf{v}_i = & \frac{\alpha}{m} \sum_{j \neq i} w_R(r_{ij}) \mathbf{e}_{ij} \Delta t - \frac{\gamma}{m} \sum_{j \neq i} w_R^2(r_{ij}) (\mathbf{e}_{ij} \cdot \mathbf{v}_{ij}) \mathbf{e}_{ij} \Delta t \\ & + \frac{(2\gamma kT)^{1/2}}{m} \sum_{j \neq i} w_R(r_{ij}) \mathbf{e}_{ij} \theta_{ij} \sqrt{\Delta t} \end{aligned} \quad (1.83)$$

As previously indicated,  $\theta_{ij}$  satisfies the stochastic characteristics in Eq. (1.78) and is sampled from a normal distribution or from a uniform distribution. The DPD dynamics method simulates the motion of the dissipative particles according to Eqs. (1.82) and (1.83).

For actual simulations, we show the method of nondimensionalizing quantities. The following representative values are used for nondimensionalization:  $(kT/m)^{1/2}$  for velocities,  $r_c$  for distances,  $r_c(m/kT)^{1/2}$  for time,  $(1/r_c^3)$  for number densities. Using these representative values, Eqs. (1.82) and (1.83) are nondimensionalized as

$$\Delta \mathbf{r}_i^* = \mathbf{v}_i^* \Delta t^* \quad (1.84)$$

$$\begin{aligned} \Delta \mathbf{v}_i^* = & \alpha^* \sum_{j \neq i} w_R(r_{ij}^*) \mathbf{e}_{ij} \Delta t^* - \gamma^* \sum_{j \neq i} w_R^2(r_{ij}^*) (\mathbf{e}_{ij} \cdot \mathbf{v}_{ij}^*) \mathbf{e}_{ij} \Delta t^* \\ & + (2\gamma^*)^{1/2} \sum_{j \neq i} w_R(r_{ij}^*) \mathbf{e}_{ij} \theta_{ij} \sqrt{\Delta t^*} \end{aligned} \quad (1.85)$$

in which

$$w_R(r_{ij}^*) = \begin{cases} 1 - r_{ij}^* & \text{for } r_{ij}^* \leq 1 \\ 0 & \text{for } r_{ij}^* > 1 \end{cases} \quad (1.86)$$

$$\alpha^* = \alpha \frac{r_c}{kT}, \quad \gamma^* = \gamma \frac{r_c}{(mkT)^{1/2}} \quad (1.87)$$

Nondimensionalized quantities are distinguished by the superscript \*. As seen in Eq. (1.85), the specification of the number density  $n^*$  ( $=nr_c^3$ ) and the number  $N$  of particles with appropriate values of  $\alpha^*$ ,  $\gamma^*$ , and  $\Delta t^*$  enables us to conduct DPD simulations. If we take into account that the time is nondimensionalized by the representative time based on the average velocity  $\bar{v}$  ( $\approx (kT/m)^{1/2}$ ) and distance  $r_c$ , the nondimensionalized time interval  $\Delta t^*$  has to be taken as  $\Delta t^* \ll 1$ .

The above-mentioned equations of motion retain a flexibility and are determined by our approach rather than the mathematical manipulation of certain basic key equations. These equations of motion are the revised version of the original equations, which were derived in order that the velocity distribution function of the particles converges to an equilibrium distribution for thermodynamic equilibrium. Hence, they are not the only valid equations of motion for the DPD method, and a new equation of motion may be proposed in order to enable us to conduct more accurate simulations.

The main procedure for conducting the DPD simulation is quite similar to the one we employed for BD simulations, so it is unnecessary to repeat the details here.

## 1.5 Lattice Boltzmann Method

Whether or not the lattice Boltzmann method is classified into the category of molecular simulation methods may depend on the researcher, but this method is expected to have a sufficient feasibility as a simulation technique for polymeric liquids and particle dispersions. We will therefore treat it in detail in this book. In the lattice Boltzmann method [4, 9–12], a fluid is assumed to be composed of virtual fluid particles, and such fluid particles move and collide with other fluid particles in a simulation region. A simulation area is regarded as a lattice system, and fluid particles move from site to site; that is, they do not move freely in a region. The most significant difference of this method in relation to the MD method is that the lattice Boltzmann method treats the particle distribution function of velocities rather than the positions and the velocities of the fluid particles.

Figure 1.4 illustrates the lattice Boltzmann method for a two-dimensional system. Figure 1.4A shows that a simulation region is divided into a lattice system. Figure 1.4B is a magnification of a unit square lattice cell. Virtual fluid particles, which are regarded as groups or clusters of solvent molecules, are permitted to move only to their neighboring sites, not to other, more distant sites. That is, the fluid particles at site 0 are permitted to stay there or to move to sites 1, 2, ..., 8 at the next time step. This implies that fluid particles for moving to sites 1, 2, 3, and 4 have the velocity  $c = (\Delta x / \Delta t)$ , and those for moving to sites 5, 6, 7, and 8 have

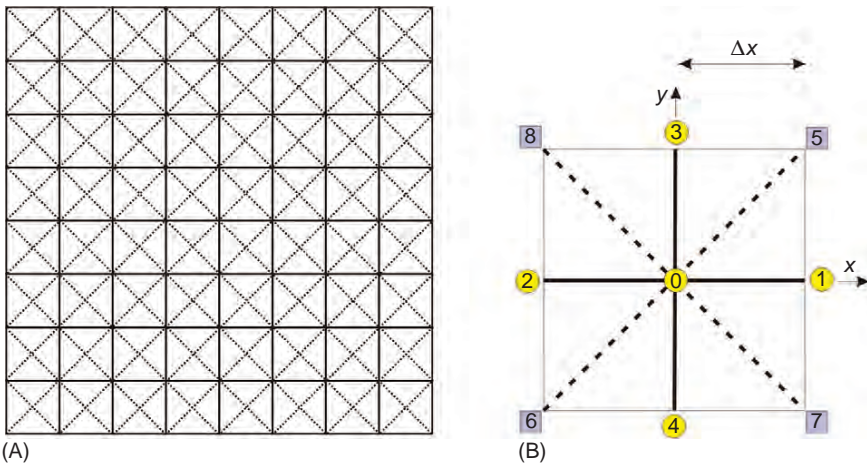


**Figure 1.4** Two-dimensional lattice model for the lattice Boltzmann method (D2Q9 model).

the velocity  $\sqrt{2}c$ , in which  $\Delta x$  is the lattice separation of the nearest two sites and  $\Delta t$  is the time interval for simulations. Since the movement speeds of fluid particles are known as  $c$  or  $\sqrt{2}c$ , macroscopic velocities of a fluid can be calculated by evaluating the number of particles moving to each neighboring lattice site. In the usual lattice Boltzmann method, we treat the particle distribution function, which is defined as a quantity such that the above-mentioned number is divided by the volume and multiplied by the mass occupied by each lattice site. This is the concept of the lattice Boltzmann method. The two-dimensional lattice model shown in Figure 1.4 is called the “D2Q9” model because fluid particles have nine possibilities of velocities, including the quiescent state (staying at the original site).

Next, we explain the basic equations of the particle distribution function and the method of solving these equations. The detailed explanation will be shown in Chapter 8; here we outline the essence of the method. The velocity vector for fluid particles moving to their neighboring site is usually denoted by  $\mathbf{c}_\alpha$  and, for the case of the D2Q9 model, there are nine possibilities, such as  $\mathbf{c}_0, \mathbf{c}_1, \mathbf{c}_2, \dots, \mathbf{c}_8$ . For example, the velocity of the movement in the left direction in Figure 1.4B is denoted by  $\mathbf{c}_2$ , and  $\mathbf{c}_0$  is zero vector for the quiescent state ( $\mathbf{c}_0 = \mathbf{0}$ ). We consider the particle distribution function  $f_\alpha(\mathbf{r}, t)$  at the position  $\mathbf{r}$  (at point 0 in Figure 1.4B) at time  $t$  in the  $\alpha$ -direction. Since  $f_\alpha(\mathbf{r}, t)$  is equal to the number density of fluid particles moving in the  $\alpha$ -direction, multiplied by the mass of a fluid particle, the summation of the particle distribution function concerning all the directions ( $\alpha = 0, 1, \dots, 8$ ) leads to the macroscopic density  $\rho(\mathbf{r}, t)$ :

$$\rho(\mathbf{r}, t) = \sum_{\alpha=0}^8 f_\alpha(\mathbf{r}, t) \quad (1.88)$$

Similarly, the macroscopic velocity  $\mathbf{u}(\mathbf{r},t)$  can be evaluated from the following relationship of the momentum per unit volume at the position  $\mathbf{r}$ :

$$\rho(\mathbf{r},t)\mathbf{u}(\mathbf{r},t) = \sum_{\alpha=0}^8 f_{\alpha}(\mathbf{r},t) \mathbf{c}_{\alpha} \quad (1.89)$$

In Eqs. (1.88) and (1.89), the macroscopic density  $\rho(\mathbf{r},t)$  and velocity  $\mathbf{u}(\mathbf{r},t)$  can be evaluated if the particle distribution function is known. Since fluid particles collide with the other fluid particles at each site, the rate of the number of particles moving to their neighboring sites changes. In the rarefied gas dynamics, the well-known Boltzmann equation is the basic equation specifying the velocity distribution function while taking into account the collision term due to the interactions of gaseous molecules; this collision term is a complicated integral expression. The Boltzmann equation is quite difficult to solve analytically, so an attempt has been made to simplify the collision term. One such simplified model is the Bhatnagar-Gross-Krook (BGK) collision model. It is well known that the BGK Boltzmann method gives rise to reasonably accurate solutions, although this collision model is expressed in quite simple form. We here show the lattice Boltzmann equation based on the BGK model. According to this model, the particle distribution function  $f_{\alpha}(\mathbf{r} + \mathbf{c}_{\alpha}\Delta t, t + \Delta t)$  in the  $\alpha$ -direction at the position  $(\mathbf{r} + \mathbf{c}_{\alpha}\Delta t)$  at time  $(t + \Delta t)$  can be evaluated by the following equation:

$$f_{\alpha}(\mathbf{r} + \mathbf{c}_{\alpha}\Delta t, t + \Delta t) = f_{\alpha}(\mathbf{r}, t) + \frac{1}{\tau} \{f_{\alpha}^{(0)}(\mathbf{r}, t) - f_{\alpha}(\mathbf{r}, t)\} \quad (1.90)$$

This equation is sometimes expressed in separate expressions indicating explicitly the two different processes of collision and transformation:

$$\left. \begin{aligned} f_{\alpha}(\mathbf{r} + \mathbf{c}_{\alpha}\Delta t, t + \Delta t) &= \tilde{f}_{\alpha}(\mathbf{r}, t) \\ \tilde{f}_{\alpha}(\mathbf{r}, t) &= f_{\alpha}(\mathbf{r}, t) + \frac{1}{\tau} \{f_{\alpha}^{(0)}(\mathbf{r}, t) - f_{\alpha}(\mathbf{r}, t)\} \end{aligned} \right\} \quad (1.91)$$

in which  $\tau$  is the relaxation time (dimensionless) and  $f_{\alpha}^{(0)}$  is the equilibrium distribution, expressed for the D2Q9 model as

$$f_{\alpha}^{(0)} = \rho w_{\alpha} \left\{ 1 + 3 \frac{\mathbf{c}_{\alpha} \cdot \mathbf{u}}{c^2} - \frac{3u^2}{2c^2} + \frac{9}{2} \cdot \frac{(\mathbf{c}_{\alpha} \cdot \mathbf{u})^2}{c^4} \right\} \quad (1.92)$$

$$w_{\alpha} = \begin{cases} 4/9 & \text{for } \alpha = 0 \\ 1/9 & \text{for } \alpha = 1, 2, 3, 4 \\ 1/36 & \text{for } \alpha = 5, 6, 7, 8 \end{cases} \quad |\mathbf{c}_{\alpha}| = \begin{cases} 0 & \text{for } \alpha = 0 \\ c & \text{for } \alpha = 1, 2, 3, 4 \\ \sqrt{2c} & \text{for } \alpha = 5, 6, 7, 8 \end{cases} \quad (1.93)$$

In these equations  $\rho$  is the local density at the position of interest,  $\mathbf{u}$  is the fluid velocity ( $u = |\mathbf{u}|$ ),  $c = \Delta x / \Delta t$ , and  $w_\alpha$  is the weighting constant.

The important feature of the BGK model shown in Eq. (1.91) is that the particle distribution function in the  $\alpha$ -direction is independent of the other directions. The particle distributions in the other directions indirectly influence  $f_\alpha(\mathbf{r} + \mathbf{c}_\alpha \Delta t, t + \Delta t)$  through the fluid velocity  $\mathbf{u}$  and the density  $\rho$ . The second expression in Eq. (1.91) implies that the particle distribution  $f_\alpha(\mathbf{r}, t)$  at the position  $\mathbf{r}$  changes into  $\tilde{f}_\alpha(\mathbf{r}, t)$  after the collision at the site at time  $t$ , and the first expression implies that  $\tilde{f}_\alpha(\mathbf{r}, t)$  becomes the distribution  $f_\alpha(\mathbf{r} + \mathbf{c}_\alpha \Delta t, t + \Delta t)$  at  $(\mathbf{r} + \mathbf{c}_\alpha \Delta t)$  after the time interval  $\Delta t$ .

The main procedure of the simulation is as follows:

1. Set appropriate fluid velocities and densities at each lattice site.
2. Calculate equilibrium particle densities  $f_\alpha^{(0)}$  ( $\alpha = 0, 1, \dots, 8$ ) at each lattice site from Eq. (1.92) and regard these distributions as the initial distributions,  $f_\alpha = f_\alpha^{(0)}$  ( $\alpha = 0, 1, \dots, 8$ ).
3. Calculate the collision terms  $\tilde{f}_\alpha(\mathbf{r}, t)$  ( $\alpha = 0, 1, \dots, 8$ ) at all sites from the second expression of Eq. (1.91).
4. Evaluate the distribution at the neighboring site in the  $\alpha$ -direction  $f_\alpha(\mathbf{r} + \mathbf{c}_\alpha \Delta t, t + \Delta t)$  from the first expression in Eq. (1.91).
5. Calculate the macroscopic velocities and densities from Eqs. (1.88) and (1.89), and repeat the procedures from step 3.

In addition to the above-mentioned procedures, we need to handle the treatment at the boundaries of the simulation region. These procedures are relatively complex and are explained in detail in Chapter 8. For example, the periodic boundary condition, which is usually used in MD simulations, may be applicable.

For the D3Q19 model shown in figure 8.3, which is applicable for three-dimensional simulations, the equilibrium distribution function is written in the same expression of Eq. (1.92), but the weighting constants are different from Eq. (1.93) and are expressed in Eq. (8.69). The basic equations for  $f_\alpha(\mathbf{r} + \mathbf{c}_\alpha \Delta t, t + \Delta t)$  are the same as Eq. (1.90) or (1.91), and the above-mentioned simulation procedure is also directly applicable to the D3Q19 model.

This page intentionally left blank

# 2 Outline of Methodology of Simulations

In order to develop a simulation program, it is necessary to have an overview of the general methodology, which should include the assignment of the initial configuration and velocities, the treatment of boundary conditions, and techniques for reducing computation time. An appropriate initial configuration has to be set with careful consideration given to the physical property of interest, so that the essential phenomena can be grasped. For example, if nonspherical molecules or particles are known to incline in a preferred direction, there may be some advantages to using a parallelepiped rectangular simulation region rather than a cubic one. The periodic boundary condition is a representative model to manage the boundary of a simulation region. It is almost always used for systems in thermodynamic equilibrium. On the other hand, for investigating the dynamic properties of a system, the simple shear flow is frequently treated and in this case the Lees–Edwards boundary condition is available. Techniques for reducing computation time become very important in large-scale three-dimensional simulations, and methods of tracking particle neighbors, such as the cell index method, are indispensable. The more important methods frequently employed in simulations are described in this chapter.

## 2.1 Initial Positions

### 2.1.1 *Spherical Particle Systems*

Setting an initial configuration of particles is an indispensable procedure for both MD and MC methods. Although it is possible to assign randomly the initial position of particles in a simulation region, a regular configuration, such as a simple cubic lattice or a face-centered cubic lattice, is handled in a more straightforward manner. The random allocation suffers from the problem of the undesirable overlap of particles and from possible difficulties in achieving high packing fractions. Lattice assignments are almost free from the overlap problem and can achieve high packing fractions. However, as will be shown later, the lattice packing may be too perfect for some simulations, requiring the adjustment of a small random perturbation. In the following paragraphs, we consider a system composed of spherical particles as an example to explain the method of setting the initial configuration in a

regular lattice formation for a two-dimensional configuration. We then proceed to a three-dimensional configuration.

Figure 2.1 shows several lattice systems that may be used to assign an initial configuration for a two-dimensional system. A basic lattice form is expanded to fill the whole simulation region, and the particles are then located at each lattice point. Figure 2.1A, the simplest lattice model, may be suitable for a gaseous system. However, even if the particle–particle distance  $a$  is equal to the particle diameter, a high packing fraction cannot be obtained by using this simple lattice model. Hence, it is inappropriate for the simulations of a liquid or solid system. Since there is only one particle in the unit cell shown in Figure 2.1A, a system with total particle number  $N (=Q^2)$  can be generated by replicating the unit cell ( $Q - 1$ ) times in each direction to make a square simulation region of side length  $L = Qa$ . So for the use of this lattice system as the initial configuration, the particle number  $N$  has to

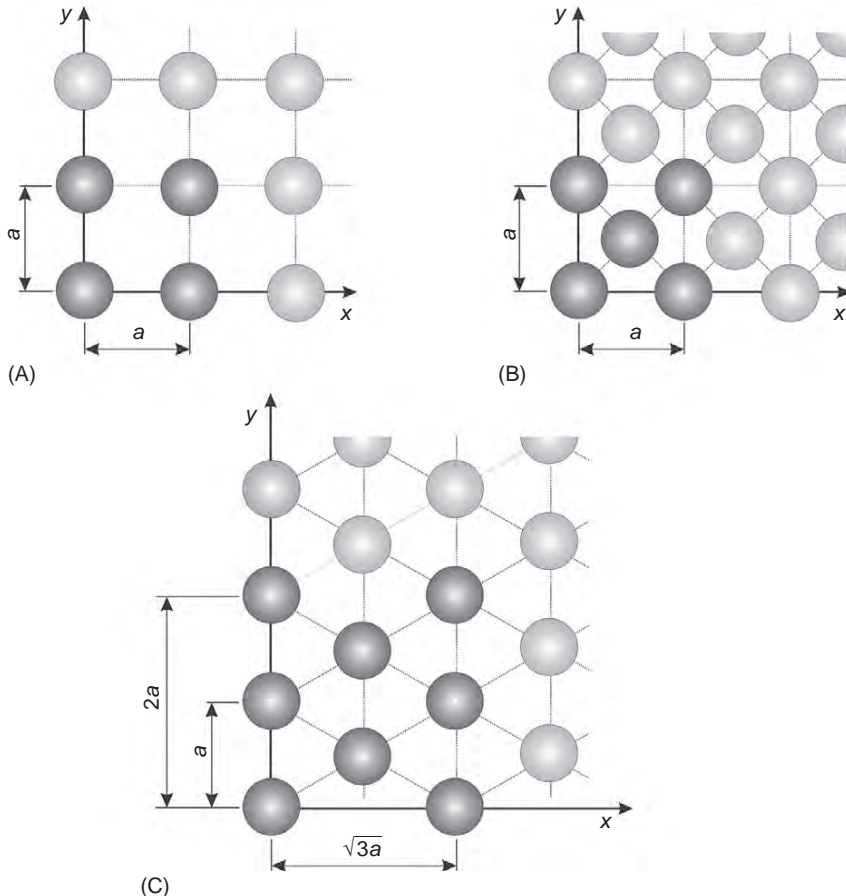


**Figure 2.1** Initial conditions for a two-dimensional system.

be taken from  $N = 1, 4, 9, 16, 25, 36, 49, 64, 81, 100$ , and so on. The number density of particles  $n$  is given by  $n = N/L^2$ , and the area fraction is given by  $\phi_s = \pi(d/2)^2 N/L^2$ , where  $d$  is the particle diameter. In practice, the number of particles  $N$  and the area fraction  $\phi_s$  are first chosen; then the values of  $Q$  and  $L$  are evaluated, from which the value of  $a$  can be determined. With these values, the initial configuration of particles can be assigned according to the simple lattice system shown in Figure 2.1A.

The lattice system shown in Figure 2.1B can yield a higher packing fraction and therefore may be applicable for an initial configuration of a gaseous or liquid state, but it has limited application to a solid state. Since there are two particles in the unit cell of this lattice, a system with total particle number  $N = 2Q^2$  of particles can be generated by replicating the unit cell ( $Q - 1$ ) times in each direction. In this case, the simulation region is also a square of side length  $L = Qa$ , and the possible value of  $N$  is taken from 2, 8, 18, 32, 50, 72, 98, 128, 162, 200, and so on. The number density of particles  $n$  is given by  $n = N/L^2$ , and the area fraction  $\phi_s$  is given by  $\phi_s = \pi(d/2)^2 N/L^2$ . Figure 2.1C shows the most compact lattice for a two-dimensional system. This lattice model may also be applicable to a solid system. If the dark particles are assumed to constitute the unit lattice, it follows that there are four particles in this unit lattice. Hence, by replicating the unit lattice ( $Q - 1$ ) times in each direction, the simulation region becomes a rectangle of side lengths  $L_x = 3^{1/2}aQ$  and  $L_y = 2aQ$ , with a total number of particles  $N = 4Q^2$ , where the possible value of  $N$  is taken from 4, 16, 36, 64, 100, 144, 196, 256, 324, 400, and so on. The particle number density  $n$  is given by  $n = N/L_x L_y$ , and the area fraction  $\phi_s$  is given by  $\phi_s = \pi(d/2)^2 N/L_x L_y$ . The actual assignment of the above-mentioned quantities for simulations is similar to that for Figure 2.1A.

Figure 2.2 shows several lattice models for a three-dimensional system. Figure 2.2A is the simple cubic lattice model, which is suitable as an initial configuration mainly for a gaseous or liquid system. Since there is only one particle in the unit cell, the number of particles in a system is given by  $N = Q^3$  by replicating the unit cell ( $Q - 1$ ) times in each direction. In this case the possible value of  $N$  is taken from  $N = 1, 8, 27, 64, 125, 216, 343, 512, 729, 1000$ , and so on.

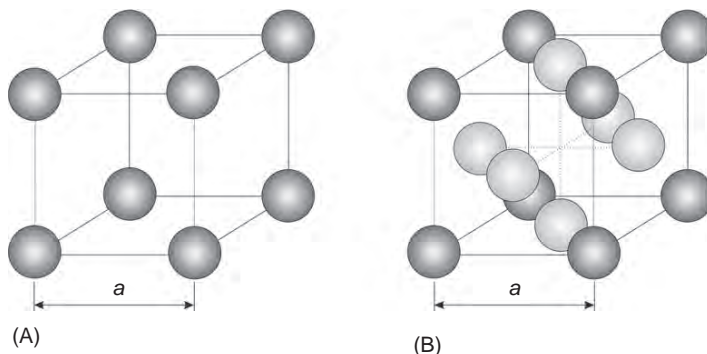


**Figure 2.2** Initial conditions for a three-dimensional system.

The simulation region is a cube of side length  $L = Qa$ . The number density  $n$  and the volumetric fraction  $\phi_V$  are given by  $n = N/L^3$  and  $\phi_V = 4\pi(d/2)^3N/3L^3$ , respectively. The face-centered cubic lattice model shown in Figure 2.2B is one of the close-packed lattices, and therefore may be applicable as an initial configuration of a solid state. Since there are four particles in the unit cell, the total number of particles in the simulation region is given by  $N = 4Q^3$  by replicating the unit cell ( $Q - 1$ ) times in each direction. In this case, the total number of particles is taken from  $N = 4, 32, 108, 256, 500, 864, 1372$ , and so on. The number density and the volumetric fraction are given by  $n = N/L^3$  and  $\phi_V = 4\pi(d/2)^3N/3L^3$ , respectively. As in a two-dimensional system, for the actual assignment of the above-mentioned quantities, the particle number  $N$  and the volumetric fraction  $\phi_V$  are first chosen, then  $Q$  and  $L$  are evaluated, and finally the lattice distance  $a$  is determined.

For a gaseous or liquid system, the simple lattice models shown in Figures 2.1A and 2.2A are applicable in a straightforward manner for developing a simulation program. In contrast, for the case of a solid system, the choice of an appropriate lattice used for the initial configuration of particles is usually determined by the known physical properties of the solid.

### 2.1.2 Nonspherical Particle Systems

The assignment of the initial configuration of particles for a spherical particle system, explained in the previous subsection, is quite clear because only the center of the particles needs to be considered. In this subsection we explain the method of setting the initial configuration for a system composed of nonspherical particles, using spherocylinders and disk-like particles as examples. For a nonspherical particle system, the orientation of the particles must be assigned in addition to their position, so that the technique for setting the initial configuration is a little more difficult than that for a spherical particle system. For this purpose, a versatile technique whereby a wide range of initial configurations can be assigned is desirable. If particle–particle interactions are large enough to induce the cluster formation of particles in a preferred direction, then an appropriately large initial configuration has to be adopted in order for the simulation to capture such characteristic aggregate structures.

We now consider the example of a system composed of spherocylinder particles with a magnetic moment at the particle center normal to the long particle axis. The spherocylinder is a cylinder with hemisphere caps at both the ends. An ensemble of these particles can be expected to aggregate to form raft-like clusters with the magnetic moments inclining in the applied magnetic field direction. Hence, a simulation region with sufficient length in the direction of the cluster formation has to be taken in order for the simulation particles to aggregate in a reasonable manner. We shall explain the technique for setting an initial configuration using Figure 2.3. The spherocylinder can be characterized by the ratio of the particle length  $l$  to the diameter  $d$  of the cylindrical part, known as the aspect ratio  $r_p = l/d$ . For the example in Figure 2.3 where  $r_p = 3$ , the particles are placed in contact with three and nine rows in the  $x$ - and  $y$ -directions, respectively, leading to a configuration of 27

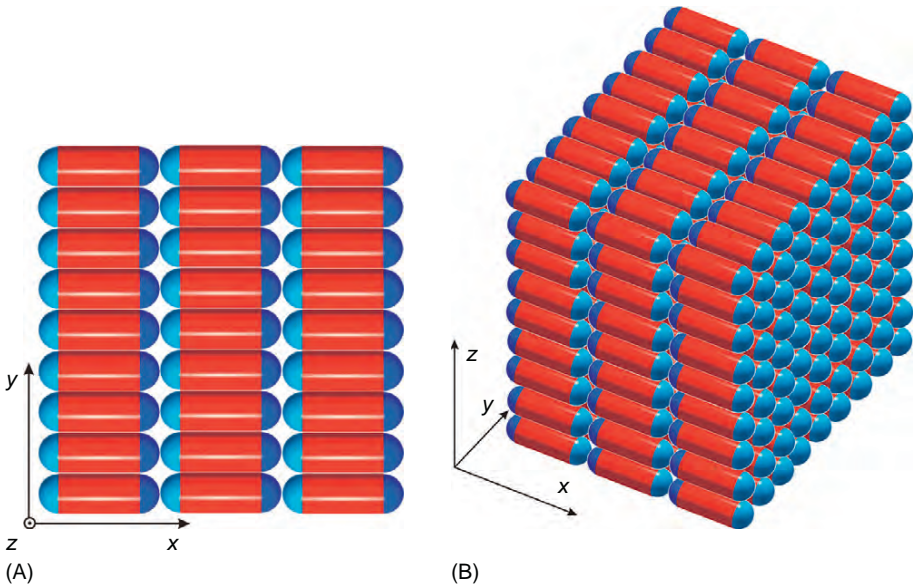


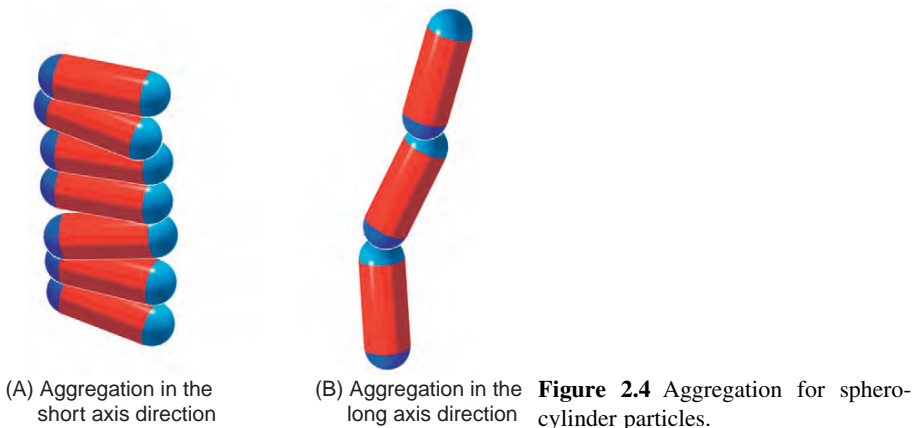
**Figure 2.3** Initial conditions for spherocylinder particles.

particles in a square region in the  $xy$ -plane. Extending this configuration to 18 layers in the  $z$ -direction yields an initial configuration of spherocylinder particles with a simulation region  $(L_x, L_y, L_z) = (3r_p d, 3r_p d, 6r_p d)$  with total number of particles  $N = 486$ ; if four rows are arranged in the  $x$ -direction, then a simulation region larger than the present case can be adopted with a simulation region  $(L_x, L_y, L_z) = (4r_p d, 4r_p d, 8r_p d)$ .

If the particle–particle distances are expanded equally in each direction to yield a desired volumetric fraction of particles  $\phi_V$ , then this expanded system may be used as an initial configuration for simulations. Such an expansion with a factor  $\alpha$  of particle–particle distances gives rise to the system volume  $V = 54r_p^3 d^3 \alpha^3$ . The volumetric fraction  $\phi_V$  is related to the system volume as  $\phi_V = NV_p/V$ , in which  $V_p$  is the volume of a spherocylinder particle, expressed as  $V_p = \pi d^3 (3r_p - 1)/12$ . From these expressions, the expansion ratio  $\alpha$  can be obtained as

$$\alpha = \frac{1}{r_p} \left( \frac{3\pi(3r_p - 1)}{4\phi_V} \right)^{1/3} \quad (2.1)$$

This initial configuration is applicable for a system in which particles are expected to aggregate in the direction of the particle short axis, as shown in Figure 2.4A. If particles are expected to aggregate in the direction of the particle long axis, as shown in Figure 2.4B, it is straightforward to follow a similar procedure with the spherocylinder particles aligned in the  $z$ -direction in Figure 2.3.



We now consider the method of setting an initial configuration of a disk-like particle system, in which particles are assumed to aggregate in a direction parallel to the disk plane surface, as shown in Figure 2.5B. Capturing such clusters in simulations requires a simulation region with suitable dimensions. As in the previous case of a spherocylinder particle system, a nearly close-packed configuration is first arranged. We here consider disk-like particles with particle aspect ratio  $r_p$  ( $= d_1/b_1 = 3$ ), in which the diameter of the circumference and the thickness are denoted by  $d_1$  and  $b_1$ , respectively, as shown in Figure 4.12. If three and nine particles are arranged in the  $x$ - and  $y$ -directions, respectively, the subtotal number of  $N = 27$  particles can be located in the  $xy$ -plane, as shown in Figure 2.5A. Extending this configuration with 12 layers in the  $z$ -direction leads to an initial configuration of 324 particles with particle–particle contact in the simulation region of  $(L_x, L_y, L_z) = (3r_p b_1, 3r_p b_1, 12r_p b_1)$ . By expanding particle–particle distances equally in each direction by the expansion factor  $\alpha$ , the volume of a system  $V$  becomes  $V = 108r_p^3b_1^3\alpha^3$ . Given the volume of a disk-like particle,  $V_p = (\pi/4)b_1^3(r_p - 1)^2 + (\pi^2/8)b_1^3(r_p - 1) + (\pi/6)b_1^3$ , the expansion factor  $\alpha$  can be derived as

$$\alpha = \frac{1}{2r_p} \left[ \frac{\pi}{\phi_V} \left\{ 6(r_p - 1)^2 + 3\pi(r_p - 1) + 4 \right\} \right]^{1/3} \quad (2.2)$$

In this derivation, the relationship of  $\phi_V = NV_p/V$  has been used.

The main procedure for setting the initial configuration is summarized as follows:

1. Consider an appropriate initial configuration, with sufficient consideration given to the physical phenomenon of interest.
2. Set a nearly close-packed situation as an initial configuration.
3. Calculate the total number of particles  $N$ .
4. Evaluate the expansion ratio  $\alpha$  from Eq. (2.1) or Eq. (2.2) to give rise to the desired volumetric fraction  $\phi_V$ .
5. Expand particle–particle distances equally by the factor  $\alpha$ .

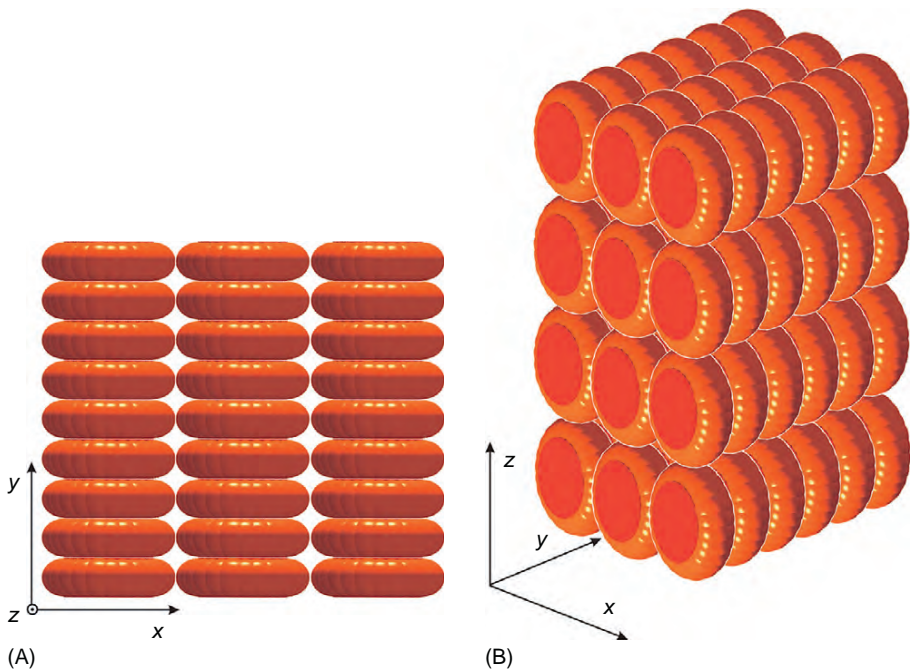


**Figure 2.5** Initial conditions for disk-like particles.

- Perturb the particle positions by small distances using random numbers in order to destroy the regularity of the initial configuration; otherwise, all particle–particle interactions may be zero and therefore the particles may not move with time.

## 2.2 Initial Velocities

### 2.2.1 Spherical Particle Systems

In the MD method, the motion of particles is described by pursuing their position and velocity over time, so these factors have to be specified as an initial condition. If the system of interest is in thermodynamic equilibrium with temperature  $T$ , the particle velocities are described by the following Maxwellian distribution [25]:

$$f(\mathbf{v}_i) = \left( \frac{m}{2\pi kT} \right)^{3/2} \exp \left\{ -\frac{m}{2kT} (v_{ix}^2 + v_{iy}^2 + v_{iz}^2) \right\} \quad (2.3)$$

in which  $k$  is Boltzmann's constant,  $m$  is the mass of particles, and  $\mathbf{v}_i = (v_{ix}, v_{iy}, v_{iz})$  is the velocity vector of particle  $i$ . Since the Maxwellian distribution  $f$  is the

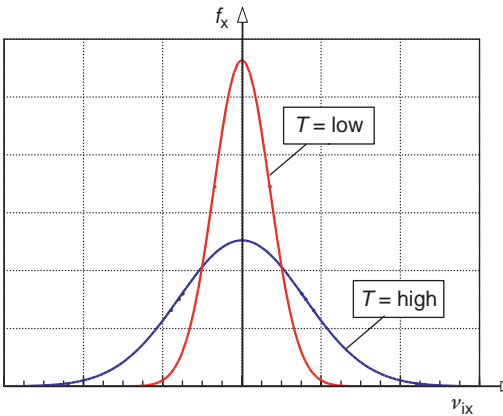


**Figure 2.6** Velocity distributions in equilibrium.

probability density distribution function, the probability of particle  $i$  being found in the infinitesimal velocity range between  $\mathbf{v}_i$  and  $(\mathbf{v}_i + d\mathbf{v}_i)$  becomes  $f(\mathbf{v}_i)d\mathbf{v}_i$ . Characteristics of this function can be understood more straightforwardly by treating the distribution function  $f_x$  as the  $x$ -velocity component. Figure 2.6 clearly shows that a higher system temperature leads to an increase in the probability of particles appearing with a larger velocity component  $v_{ix}$ . If we focus on the magnitude of the particle velocities instead of the velocity components, clearer discussion concerning such characteristics becomes possible. The probability density distribution function  $\chi(v_i)$  for the speed  $v_i = (\sqrt{v_{ix}^2 + v_{iy}^2 + v_{iz}^2})$  of particle  $i$  can be derived from Eq. (2.3) as

$$\chi(v_i) = 4\pi \left( \frac{m}{2\pi kT} \right)^{3/2} v_i^2 \exp\left(-\frac{m}{2kT} v_i^2\right) \quad (2.4)$$

This equation is derived, first, by a transformation from orthogonal to spherical coordinates, that is, from  $(v_{ix}, v_{iy}, v_{iz})$  to  $(v_i, \theta, \phi)$  with the relationship of  $(v_{ix}, v_{iy}, v_{iz}) = (v_i \sin \theta \cos \phi, v_i \sin \theta \sin \phi, v_i \cos \theta)$ , and second, from the integral with respect to  $\theta$  and  $\phi$  in the normalization equation of the Maxwellian distribution. The integrand in the normalization equation after this integral is the distribution function  $\chi(v_i)$ . Figure 2.7 shows the distribution  $\chi$  as a function of the particle speed  $v_i$  for several system temperatures. Figure 2.7 shows that the curve of  $\chi$  has a peak value position that moves further to the right with increasing value of the temperature. That is, the percentage of particles with larger velocities increases with the temperature. The particle speed  $v_{mp}$  yielding the peak value of the distribution can be derived from Eq. (2.4) as  $v_{mp} = (2kT/m)^{1/2}$ , which is called the “most probable velocity.” This means that particles with speed  $v_{mp}$  are likely to be the most numerous in the system. Note that the most probable speed is larger for a higher system temperature and a smaller mass.

For a given system temperature  $T$ , the initial velocities of particles for simulations can be assigned according to the probability density function in Eq. (2.3) or

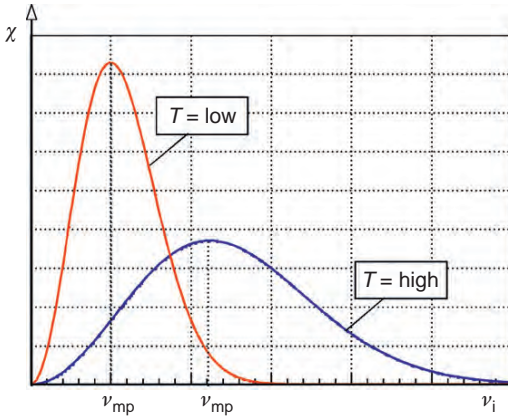


**Figure 2.7** Particle speed distributions in equilibrium.

Eq. (2.4). The detailed explanation is given in Appendix A2, so here we only show the final technique. With six different uniform random numbers,  $R_1, R_2, \dots, R_6$ , the initial velocity components ( $v_{ix}, v_{iy}, v_{iz}$ ) of particle  $i$  can be set as

$$\left. \begin{aligned} v_{ix} &= \left( -2 \frac{kT}{m} \ln R_1 \right)^{1/2} \cos(2\pi R_2) \\ v_{iy} &= \left( -2 \frac{kT}{m} \ln R_3 \right)^{1/2} \cos(2\pi R_4) \\ v_{iz} &= \left( -2 \frac{kT}{m} \ln R_5 \right)^{1/2} \cos(2\pi R_6) \end{aligned} \right\} \quad (2.5)$$

Note that each particle requires a new, that is, a different, set of random numbers.

The temperature which is evaluated from the initial particle velocities assigned by the above-mentioned method is approximately equal to the desired system temperature, but may not necessarily be satisfactory. Hence, an equilibration procedure is usually necessary before starting the main loop in an actual simulation program. This will be explained in the next subsection.

## 2.2.2 Nonspherical Particle Systems

For a nonspherical particle system, the initial angular velocities need to be assigned in addition to the translational velocities. Similar to the translational velocity  $\mathbf{v} = (v_x, v_y, v_z)$  discussed above, the angular velocity  $\boldsymbol{\omega} = (\omega_x, \omega_y, \omega_z)$  is also governed by the Maxwellian distribution  $f_\omega(\boldsymbol{\omega})$ . The expression for  $f_\omega(\boldsymbol{\omega})$  is

$$f_\omega(\boldsymbol{\omega}) = \left( \frac{I}{2\pi kT} \right)^{3/2} \exp \left\{ -\frac{I}{2kT} (\omega_x^2 + \omega_y^2 + \omega_z^2) \right\} \quad (2.6)$$

in which  $I$  is the inertia moment of a particle. The characteristics of the exponential function in Eq. (2.3) or Eq. (2.6) demonstrate that the probability of particles appearing with larger translational and angular velocities increases with the system temperature. Similar to  $v_{\text{mp}} = (2kT/m)^{1/2}$ ,  $\omega_{\text{mp}} = (2kT/I)^{1/2}$  is the most probable angular velocity to yield the maximum value of the Maxwellian distribution  $f_\omega$ . The method for setting the initial translational velocities using uniform random numbers, explained in the previous subsection, is applicable to the present angular velocity case. Here,  $m$  and  $(v_{ix}, v_{iy}, v_{iz})$  in Eq. (2.5) are replaced by  $I$  and  $(\omega_{ix}, \omega_{iy}, \omega_{iz})$ ; note that new uniform random numbers need to be used.

As already mentioned, an equilibration procedure may be necessary in order to obtain the desired system temperature  $T$ . In the example of a liquid, the temperature  $T_{\text{cal}}$ , which is calculated from averaging the assigned velocities of particles, may differ significantly from the desired system temperature  $T$ . This may be due to the energy exchange between the kinetic and the potential energies. Hence, an equilibration procedure is frequently necessary before starting the main loop in a simulation program. The temperatures calculated from the translational and angular velocities of particles are denoted by  $T_{\text{cal}}^{(t)}$  and  $T_{\text{cal}}^{(r)}$ , respectively, and written as

$$T_{\text{cal}}^{(t)} = \frac{1}{3N} \sum_{i=1}^N \frac{mv_i^2}{k}, \quad T_{\text{cal}}^{(r)} = \frac{1}{3N} \sum_{i=1}^N \frac{I\omega_i^2}{k} \quad (2.7)$$

in which  $N$  is the total number of particles, assumed to be  $N \gg 1$ .  $T_{\text{cal}}^{(t)}$  and  $T_{\text{cal}}^{(r)}$ , calculated from  $\mathbf{v}_i$  and  $\boldsymbol{\omega}_i$  ( $i = 1, 2, \dots, N$ ), are generally not equal to the desired temperature  $T$ . The equilibration procedure adjusts these temperatures to  $T$  during the simulation by using the method of scaling the translational and angular velocities of each particle. If  $T_{\text{cal}}^{(t)\text{ave}}$  and  $T_{\text{cal}}^{(r)\text{ave}}$  denote the averaged values of  $T_{\text{cal}}^{(t)}$  and  $T_{\text{cal}}^{(r)}$  taken, for example, over 50 time steps, then the scaling factors  $c_0^{(t)}$  and  $c_0^{(r)}$  are determined as

$$c_0^{(t)} = \sqrt{T/T_{\text{cal}}^{(t)\text{ave}}}, \quad c_0^{(r)} = \sqrt{T/T_{\text{cal}}^{(r)\text{ave}}} \quad (2.8)$$

With the scaling factors determined, the translational and angular velocities of all particles in a system are scaled as

$$\mathbf{v}'_i = c_0^{(t)} \mathbf{v}_i, \quad \boldsymbol{\omega}'_i = c_0^{(r)} \boldsymbol{\omega}_i \quad (i = 1, 2, \dots, N) \quad (2.9)$$

This treatment yields the desired system temperature  $T$ . In this example the scaling procedure would be conducted at every 50 time steps, but in practice an appropriate time interval must be adopted for each simulation case. The above-mentioned equilibration procedure is repeated to give rise to the desired system temperature with sufficient accuracy. (Note that if a system has a macroscopic velocity, i.e., if it is not in a quiescent state, the scaling procedure has to be slightly modified.)

## 2.3 Reduction Methods of Computation Time

### 2.3.1 Cutoff Distance

Computation time is an important factor for successfully obtaining reasonable results from molecular simulations. In some cases, due to an excessive restriction of the required computation time, only a small or two-dimensional system is able to be treated. The most time-consuming procedure is the calculation of interaction energies between particles in the MC method and that of forces and torques in the MD method. Even with the action–reaction law taken into account, the  $N(N - 1)/2$  calculations of energies or forces are necessary per unit time step (or unit MC step) for an  $N$ -particle system. Therefore, if it is possible to restrict the pairs of particles for the calculation, the computation time may significantly decrease. Fortunately, many particle–particle potentials are of short-range order, so that the potential energy between particles rapidly decreases with the particle–particle separation over a distance only several times the particle diameter. Therefore we may be able to treat only interactions within this range. Although magnetic or electrostatic forces are of long-range order, the above-mentioned concept is applicable to these interactions if the criterion separation between particles is taken to be of sufficient length.

#### 2.3.1.1 Spherical Particle Systems

An important concept in simulation methodology is that a significant limitation on the computation of interaction energies or forces between particles leads to an extraordinary reduction of the simulation time. To understand this concept, we consider the interaction energies between particles or potential curves. For example, the Lennard-Jones potential  $U_{\text{LJ}}$  is expressed as

$$U_{\text{LJ}} = 4\varepsilon \left\{ \left(\frac{\sigma}{r}\right)^{12} - \left(\frac{\sigma}{r}\right)^6 \right\} \quad (2.10)$$

This potential is usually used as a model potential for rare gases such as Ar molecule;  $\sigma$  is the quantity corresponding to the particle diameter, and  $r$  is the separation between particles (molecules). Figure 2.8 shows the curve of the Lennard-Jones potential, in which  $U_{\text{LJ}}$  and  $r$  are nondimensionalized by  $\varepsilon$  and  $\sigma$ . Figure 2.8 illustrates a steep potential barrier in the range of  $r \leq \sigma$ , which induces such a significant repulsive interaction that particles are prevented from significantly overlapping, and an attractive interaction in the range of  $r \geq \sigma$ , which rapidly decreases to zero. These characteristics of the potential curve indicate that the interaction energy after a distance of approximately  $r = 3\sigma$  can be assumed to be negligible. Hence, particle interaction energies or forces do not need to be calculated in the range of  $r > 3\sigma$  in actual simulations. The distance for cutting off the calculation of energies or forces is known as the cutoff distance or cutoff radius, denoted by  $r_{\text{cutoff}}$  in this book.

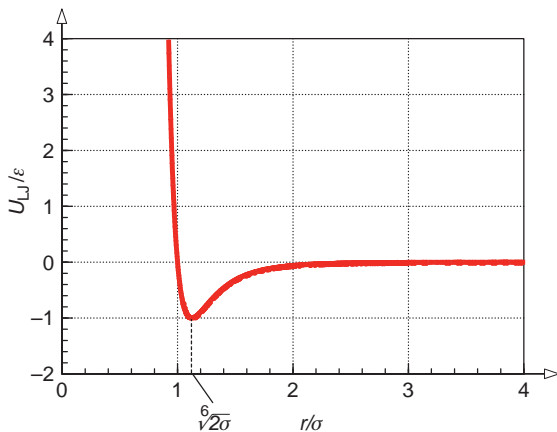


Figure 2.8 Lennard-Jones potential.

### 2.3.1.2 Nonspherical Particle Systems

The above cutoff procedure is directly applicable to a nonspherical particle system using the cutoff radius  $r_{\text{coff}}$  based on the particle center-to-center distance. That is, the calculation of energies or forces is unnecessary for  $r_{ij} \geq r_{\text{coff}}$  in simulations. For example, this applies to the case of rod-like particles that have a magnetic dipole moment at their particle center, as shown in Figure 2.9A. Unfortunately, the method is not suitable for the case of rod-like particles with plus and minus (NS) magnetic charges at the centers of hemisphere caps, as shown in Figure 2.9B. For this case, the most direct criterion is to calculate the distance between each pair of magnetic charges of the two interacting spherocylinder particles and compare this separation with a suitable cutoff radius  $r_{\text{coff}}$ . This will require the distances of the four pairs of magnetic charges to be calculated. However, with prior knowledge of the arrangement of the two spherocylinder particles, it is possible to determine certain cases where we may know, without calculating the distances for all the four pairs of charges, that there are only two pairs of the distances satisfying the relationship of  $r_{ij} \leq r_{\text{coff}}$ . Referring to Figure 2.10, if the center-to-center distance between particles  $i$  and  $j$  is denoted by  $r_{ij}$  and the distance between the magnetic charges in the particle is denoted by  $l$ , then the following three cases have to be considered for this assessment:

1. For  $r_{ij} \geq r_{\text{coff}} + l$   
No interactions.
2. For  $r_{\text{coff}} + l > r_{ij} > r_{\text{coff}}$   
A possibility of two pairs of interactions at the most.
3. For  $r_{ij} \leq r_{\text{coff}}$   
A possibility of all four pairs of interactions.

Figure 2.10A corresponds to case 1, in which the distance for any pair is beyond the cutoff radius. Figure 2.10B corresponds to case 2, in which there is a possibility of a certain magnetic charge interacting with both the magnetic charges in the other

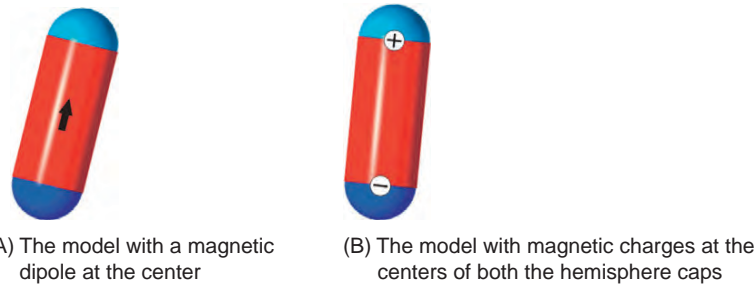


**Figure 2.9** Treatment of the cutoff distance for different rod-like particle models.

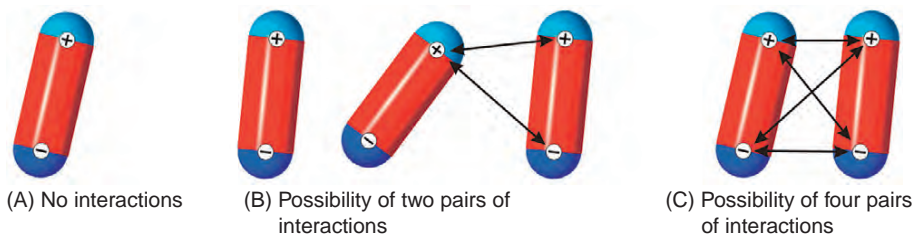


**Figure 2.10** Check for interactions in the criterion of the particle distance  $r_{ij}$ .

particle within the cutoff radius. Figure 2.10C corresponds to case 3, in which the two particles are proximate enough to give rise to a possibility of four pairs of magnetic charges being within the cutoff range. Hence, if case 1 holds, the calculation of energies or forces between particles is unnecessary, and for case 2, if two pairs of magnetic charges are found to be within the cutoff range, the further calculation of energies or forces is unnecessary.

Finally, it should be noted that the introduction of the cutoff radius by itself does not necessarily lead to a significant reduction in the computational time, since the  $N(N - 1)/2$  calculations have to be conducted in order to evaluate the distances between particles. Hence, the following cell index method, or the Verlet neighbor list method, is used with the cutoff method to accomplish a significant reduction in the computation time.

### 2.3.2 Cell Index Method

If in some way we had already determined the names of the particles within the cutoff range from each particle, the calculation of the particle-particle distances for all pairs of particles at each time step would be unnecessary. Several methods have been developed for grasping such particle names. We first explain the cell index method [27,28] in this subsection. In order for the reader to understand the method straightforwardly, we treat a two-dimensional system composed of the spherocylinder particles shown in Figure 2.9A. With reference

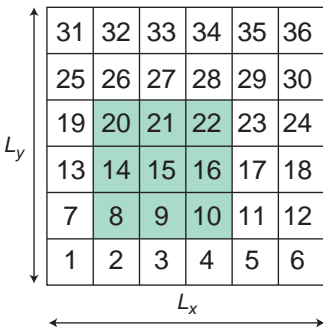


**Figure 2.11** Cell index method for grasping neighboring particles.

to Figure 2.11, the simulation region with dimensions of  $(L_x, L_y)$  is divided into  $(Q_x, Q_y)$  equal parts in each direction ( $Q_x = Q_y = 6$ ) in order to divide the whole region into small cells. Each cell has the dimensions of  $(L_x/Q_x, L_y/Q_y)$ , in which  $(Q_x, Q_y)$  are maximized to satisfy the relationships  $L_x/Q_x \geq r_{\text{coff}}$  and  $L_y/Q_y \geq r_{\text{coff}}$ . Since each side of a small cell is longer than the cutoff distance  $r_{\text{coff}}$ , the particles locating, for example, in the 15th cell in Figure 2.11, have a possibility to interact with those in their own cell 15 and those belonging to the neighboring cells, that is, in the 8th, 9th, 10th, 14th, 16th, 20th, 21st, and 22nd cells. Particles in other cells are beyond the cutoff area, so they are not used to calculate the distances between particles. Each cell needs to memorize the names of the particles which belong to it. As shown in Figure 2.11, the cell index method provides a significant reduction in the computation time for large values of  $(Q_x, Q_y)$ . For the case of the particles shown in Figure 2.9B, the method is simply applied if the values of  $(Q_x, Q_y)$  are adopted in such a way to satisfy the relationships of  $L_x/Q_x \geq r_{\text{coff}} + l$  and  $L_y/Q_y \geq r_{\text{coff}} + l$ .

### 2.3.3 Verlet Neighbor List Method

In the Verlet neighbor list method [29], a distance  $r_l$ , which is longer than the cut-off radius, is adopted, and each particle grasps the names of the particles within range of  $r_l$  from its center. Referring to Figure 2.12, it is clear that particles within range of  $r < r_{\text{coff}}$  are certainly within range of  $r < r_l$ . Hence, if the list of particles within range of  $r < r_l$  is renewed with such frequency that the particles outside the range of  $r = r_l$  cannot attain to the cutoff area, then it is sufficient to calculate the distances between the particle of interest and its neighboring particles being within range of  $r \leq r_l$ . If  $r_l$  is sufficiently short compared with the dimensions of a simulation region, and the information concerning the names of the neighboring particles is renewed, for example, at every 10 time steps, then a significant reduction in the computation time can be expected. The Verlet neighbor list method is applicable to the MD method as well as to the MC method. Note that the cutoff distance is usually taken as  $r_{\text{coff}} < L/2$  ( $L$  is the side length of a simulation region).

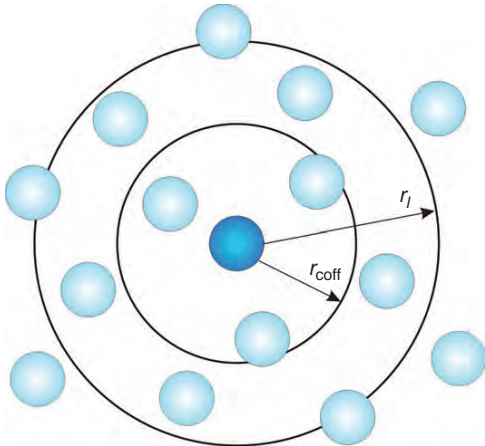


**Figure 2.12** Verlet neighbor list method.

## 2.4 Boundary Conditions

### 2.4.1 Periodic Boundary Condition

Fortunately, a system of one-mol-order size, being composed of about  $6 \times 10^{23}$  particles, never needs to be directly treated in molecular simulations for thermodynamic equilibrium (actually, it is impossible). The use of the periodic boundary condition, explained below, enables us to treat only a relatively small system of about 100–10,000 particles in order to obtain such reasonable results as to explain the corresponding experimental data accurately.

Figure 2.13 schematically illustrates the concept of the periodic boundary condition for a two-dimensional system composed of spherocylinder particles. The central square is a simulation region and the surrounding squares are virtual simulation boxes, which are made by replicating the main simulation box. As Figure 2.13 shows, the origin of the  $xy$ -coordinate system is taken at the center of the simulation region, and the dimensions of the simulation region in the  $x$ - and  $y$ -directions are denoted by  $L_x$  and  $L_y$ . The two specific procedures are necessary in treating the periodic boundary condition, that is, first the treatment of outgoing particles crossing the boundary surfaces of the simulation region and second the calculation of interaction energies or forces with virtual particles being in the replicated simulation boxes.

As shown in Figure 2.13, a particle crossing and exiting the left boundary surface has to enter from the right virtual box. This treatment can be expressed using the FORTRAN language as

```

IF(RXI.GE.LX/2.D0) THEN
    RXI=RXI-LX
ELSE IF(RXI.LT.-LX/2.D0) THEN
    RXI=RXI+LX
END IF

```

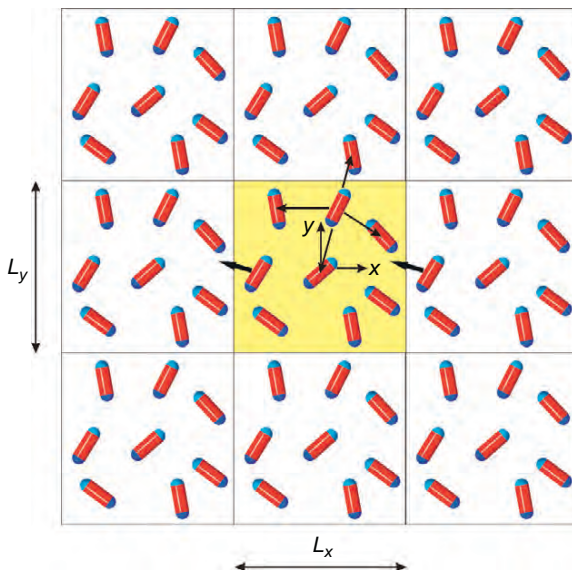


**Figure 2.13** Periodic boundary condition.

The rounding-up function DNINT can yield a simple one-line expression as

$$RXI = RXI - DNINT(RXI/LX)*LX$$

Note that the position of particle  $i$  is denoted by  $(RXI, RYI)$ . Similar procedures have to be conducted for the case of the  $y$ - and  $z$ -directions.

When the interaction energy or force of particle  $i$  with other particles, for example, particle  $j$ , is calculated, an appropriate particle  $j$  has to be chosen as an object from real and virtual particles  $j$ . This may be done in such a way that the distance between particle  $i$  and particle  $j$  is minimal. This treatment can be expressed using the FORTRAN language as

```
IF(RXIJ.GT.LX/2.D0) THEN
    RXIJ=RXIJ-LX
ELSE IF (RXIJ.LT.-LX/2.D0) THEN
    RXIJ=RXIJ+LX
END IF
```

The rounding-up function DNINT gives rise to a simple one-line expression as

$$RXIJ = RXIJ - DNINT(RXIJ/LX)*LX$$

in which  $RXIJ = RXI - RXJ$ , expressing the relative position of particles  $i$  to  $j$ . Similar procedures have to be conducted for the  $y$ - and  $z$ -directions. The above-mentioned procedures are applicable directly to a system composed of rod-like particles, such as that shown in Figure 2.9A, in which the interaction energies or forces are dependent only on the particle center-to-center distance. If we treat the pairs of magnetic charges instead of particle center-to-center interactions, the

above-mentioned procedures are also applicable, but in this case RXIJ and similar variables have to be taken as the distances between magnetic charges.

### 2.4.2 Lees–Edwards Boundary Condition

The periodic boundary condition is quite useful for molecular simulations of a system in thermodynamic equilibrium, but is this boundary condition still available for nonequilibrium situations? In treating the dynamic properties of a system in non-equilibrium, the most basic and important flow is a simple shear flow, as shown in Figure 2.14. The velocity profile, linearly varying from  $-U$  at the lower surface to  $U$  at the upper one, can be generated by sliding the lower and upper walls in the left and right directions with the velocity  $U$ , respectively. This flow field is called the “simple shear flow.” In generating such a simple shear flow in actual molecular simulations, the upper and lower replicated simulation boxes, shown in Figure 2.13, are made to slide in different directions with a certain constant speed. This sliding periodic boundary condition is called the “Lees–Edwards boundary condition” [30]. Figure 2.15 schematically depicts the concept of this boundary condition; the replicated boxes in the upper and lower layers slide in each direction by the distance  $\Delta X$ . If particles move out of the simulation box by crossing the boundary surface normal to the  $x$ -axis, as shown in Figure 2.15, they are made to come into the simulation box through the opposite boundary surface, which is exactly the same procedure as the periodic boundary condition. The important treatment in the Lees–Edwards boundary condition concerns the particles crossing the boundary surfaces normal to the  $y$ -axis. The same treatment of the periodic boundary condition is applied to the  $y$ -coordinate of such particles, but the  $x$ -coordinate should be shifted from  $x$  to  $(x - \Delta X)$  in the case of Figure 2.15. In addition, the  $x$ -component  $v_x$  of these particles needs to be modified to  $(v_x - U)$ , but the  $y$ -component  $v_y$  can be used without modification. The above-mentioned procedures concerning  $x$  and  $v_x$  can be expressed using the FORTRAN language as

```

IF (RYI.GE.LY/2.D0) THEN
    RXI=RXI-DX
    RXI=RXI-DNINT(RXI/LX)*LX
    VXI=VXI-U
ELSE (RYI.LT.-LY/2.D0) THEN
    RXI=RXI+DX
    RXI=RXI-DNINT(RXI/LX)*LX
    VXI=VXI+U
END IF

```

A slightly simplified expression can be written as

```

CORY=DNINT(RYI/LY)
RXI=RXI-CORY*DX
RXI=RXI-DNINT(RXI/LX)*LX
VXI=VXI-CORY*U

```

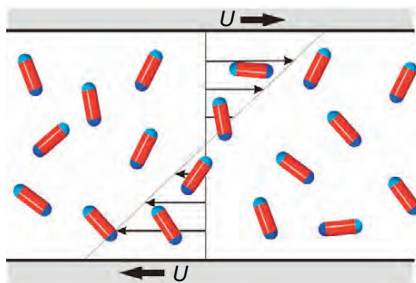


Figure 2.14 Simple shear flow.

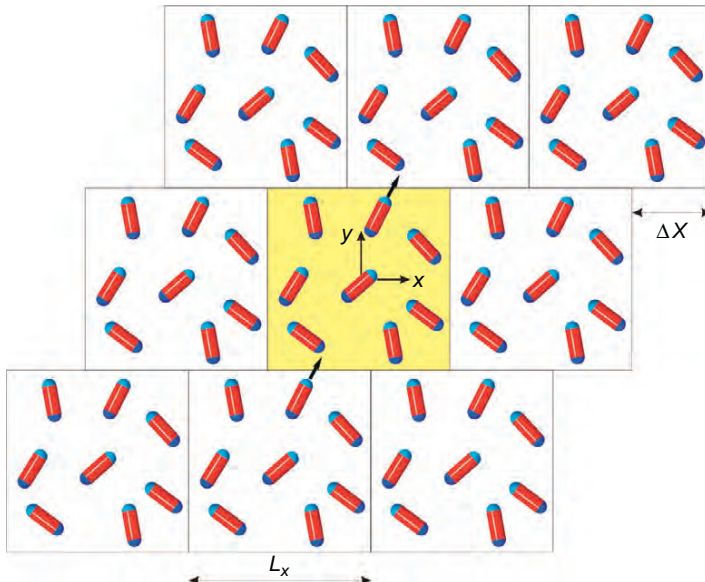


Figure 2.15 Lees-Edwards boundary condition.

The  $y$ - and  $z$ -coordinates are treated as in the periodic boundary condition, and the modification of  $v_y$  and  $v_z$  is unnecessary.

For the case of evaluating interaction energies or forces, the similar procedures have to be conducted for the particles interacting with virtual particles which are in the replicated simulation boxes in the upper or lower layers. This treatment can be expressed using the FORTRAN language as

```

IF (RYJI.GE.LY/2.D0) THEN
  RYJI=RYJI-LY
  RXJI=RXJI-DX
  RXJI=RXJI-DNINT(RXJI/LX)*LX
ELSE IF (RYJI.LT.-LY/2.D0) THEN

```

```
RYJI=RYJI+LY  
RXJI=RXJI+DX  
RXJI=RXJI-DNINT(RXJI/LX)*LX  
END IF
```

A slightly simplified expression can be written as

```
CORY=DNINT(RYJI/LY)  
RYJI=RYJI-CORY*LY  
RXJI=RXJI-CORY*DX  
RXJI=RXJI-DNINT(RXJI/LX)*LX
```

The relative position RZJI in the  $z$ -direction is treated according to the periodic boundary condition.

The above-mentioned procedures are valid for the particle model shown in Figure 2.9A and also apply to the model shown in Figure 2.9B by focusing on the interactions between magnetic charges instead of the particle centers.

This page intentionally left blank

# **3 Practice of Molecular Dynamics Simulations**

In the present and subsequent chapters, we consider examples of physical phenomena in order to explain a series of important procedures employed in conducting molecular simulations. In particular, we discuss the formalization of a problem and the method for nondimensionalizing quantities, and we make several analyses indispensable for developing a simulation program. These techniques are demonstrated in a sample simulation program with explanatory remarks included to clarify important features.

In this chapter, we consider two different physical phenomena as examples for the practice of molecular dynamics simulations. The first example discusses a diffusion problem with two kinds of molecules initially immersed in a small region in thermodynamic equilibrium. The simulation then follows the particle diffusion after the wall surrounding the region has been removed. For this case the Verlet algorithm is used for simulating the particle motion. The second example discusses the problem of the behavior of axisymmetric particles (spherocylinders in this case) in a simple shear flow. This case is an example of a more advanced type of molecular dynamics (MD) simulation where the translational and rotational motion of the particles is simulated simultaneously; therefore this exercise is considerably more advanced. The techniques demonstrated in this example are fundamental to many practical applications and may offer many valuable suggestions in developing a simulation program for systems such as DNA or polymer solutions.

## **3.1 Diffusion Phenomena in a System of Light and Heavy Molecules**

In this section we demonstrate a MD simulation employing only the translational motion of spherical molecules. A spherical molecule system is a basic form employed in molecular simulations, and the diffusion problem in this system is a useful example because almost all the important methodology for developing a simulation program is included in this exercise. A system composed of two kinds of molecules has been chosen because the extra complexity renders the example more useful and practical.

### 3.1.1 Physical Phenomena of Interest

The two kinds of molecules, that is, the  $N_A$  light molecules with mass  $m$  and  $N_B$  heavy molecules with mass  $M$ , are placed in a two-dimensional square cell with side length  $L$  in equilibrium with temperature  $T$ . Both kinds of molecules have the same diameter  $\sigma$ , and the interaction between molecules is assumed to be expressed by the Lennard-Jones potential. At the moment the wall surrounding the square retaining cell is removed, these molecules start to diffuse into the larger surrounding area. In this example, we will consider how this physical phenomenon depends on the system temperature and the mass ratio.

### 3.1.2 Specification of Problems in Equations

The starting point for the formalization of a problem is the development of the governing equation—in this case, the equation of motion of the molecules. The equation of motion of an arbitrary light molecule  $i$  and arbitrary heavy molecule  $j$  are written from Newton's equation of motion, respectively, as

$$m \frac{d^2 \mathbf{r}_i}{dt^2} = \mathbf{f}_i = \sum_{p=1}^N \mathbf{f}_{ip} \quad (3.1)$$

$$M \frac{d^2 \mathbf{r}_j}{dt^2} = \mathbf{f}_j = \sum_{p=1}^N \mathbf{f}_{jp} \quad (3.2)$$

in which  $N = N_A + N_B$ ,  $\mathbf{f}_{ip}$  is the force exerted by molecule  $p$  on molecule  $i$ , and  $\mathbf{f}_i$  is the total force acting on molecule  $i$  from all the other molecules irrespective of the type of molecule. This notation is similarly applicable to a heavy molecule  $j$ . The force acting between molecules can be derived from the Lennard-Jones potential. With the aid of the basic formulae of vector analysis, the force  $\mathbf{f}$  is derived from a potential  $U$  as

$$\mathbf{f} = -\nabla U = -\left( \mathbf{i} \frac{\partial U}{\partial x} + \mathbf{j} \frac{\partial U}{\partial y} + \mathbf{k} \frac{\partial U}{\partial z} \right) \quad (3.3)$$

The notation  $\nabla$  on the right-hand side is the nabla operator, which is defined by the last expression on the right-hand side, and  $(\mathbf{i}, \mathbf{j}, \mathbf{k})$  are the unit vectors in the  $(x, y, z)$  directions, respectively. Equation (3.3) implies that the force acts in the direction of the interaction energy decreasing at the maximum. By substituting Eq. (2.10) into Eq. (3.3), the force  $\mathbf{f}_{qp}$  exerted by molecule  $p$  on molecule  $q$  can be derived as

$$\mathbf{f}_{qp} = 24\epsilon \left\{ 2 \left( \frac{\sigma}{r_{qp}} \right)^{12} - \left( \frac{\sigma}{r_{qp}} \right)^6 \right\} \frac{\mathbf{r}_{qp}}{r_{qp}^2} \quad (3.4)$$

in which  $\mathbf{r}_{qp}$  is the relative position vector of molecule  $q$  to molecule  $p$ , expressed as  $\mathbf{r}_{qp} = \mathbf{r}_q - \mathbf{r}_p$ , and  $r_{qp} = |\mathbf{r}_{qp}|$ .

In practice, simulations usually treat a nondimensional system, in which the governing equations and all physical quantities are nondimensionalized by certain representative values. Therefore, in the following paragraphs, we show the method of nondimensionalizing the equations.

For a Lennard-Jones system, the following representative values are generally used for nondimensionalizing quantities:  $\sigma$  for distances,  $\varepsilon$  for energies,  $(\varepsilon/m)^{1/2}$  for velocities,  $\sigma(m/\varepsilon)^{1/2}$  for time,  $\varepsilon/\sigma$  for forces,  $\varepsilon/k$  for temperatures,  $1/\sigma^3$  for number densities, and  $m/\sigma^3$  for densities. Nondimensional quantities are expressed as the original quantities with superscript \*. Each quantity is expressed as a nondimensional quantity multiplied by the corresponding representative value. The substitution of these quantities into the original dimensional equation yields the desired nondimensional equation. These procedures give rise to the nondimensional form of Eqs. (3.1) and (3.2) expressed, respectively, as

$$\frac{d^2\mathbf{r}_i^*}{dt^{*2}} = \mathbf{f}_i^* = \sum_{p=1}^N \mathbf{f}_{ip}^* \quad (3.5)$$

$$K \frac{d^2\mathbf{r}_j^*}{dt^{*2}} = \mathbf{f}_j^* = \sum_{p=1}^N \mathbf{f}_{jp}^* \quad (3.6)$$

in which the force is nondimensionalized from Eq. (3.4) as

$$\mathbf{f}_{qp}^* = 24 \left\{ 2 \left( \frac{1}{r_{qp}^*} \right)^{12} - \left( \frac{1}{r_{qp}^*} \right)^6 \right\} \frac{\mathbf{r}_{qp}^*}{(r_{qp}^*)^2} \quad (3.7)$$

The parameter  $K$ , appearing in Eq. (3.6), is a nondimensional parameter expressing the mass ratio  $K = M/m$ , which arises due to the mass  $m$  being used as the representative mass. As in this example, it is usual for several additional nondimensional parameters to arise when equations and quantities are nondimensionalized. In order to compare the simulation with experimental results, appropriate values of these nondimensional parameters need to be adopted.

### 3.1.3 Verlet Algorithm

In this example we employ the Verlet algorithm in order to simulate the motion of the molecules. Referring to Eq. (1.6), the algebraic equations according to the Verlet algorithm can be expressed concerning a light molecule  $i$  and heavy molecule  $j$  as

$$\mathbf{r}_i^*(t^* + h^*) = 2\mathbf{r}_i^*(t^*) - \mathbf{r}_i^*(t^* - h^*) + h^{*2}\mathbf{f}_i^*(t^*) \quad (3.8)$$

$$\mathbf{r}_j^*(t^* + h^*) = 2\mathbf{r}_j^*(t^*) - \mathbf{r}_j^*(t^* - h^*) + \frac{h^{*2}}{K} \mathbf{f}_j^*(t^*) \quad (3.9)$$

As these equations indicate, in order to execute a simulation program, the Verlet algorithm needs the information of all the molecular positions at  $t^* = 0$  and the first time step  $t^* = h^*$ . If the initial positions and velocities of molecules and the system temperature  $T$  are assigned at  $t^* = 0$ , then the molecular positions at  $t^* = h^*$  may be evaluated from Eqs. (3.10) and (3.11).

For the given values of the molecular position  $\mathbf{r}_i^*(0)$  and velocity  $\mathbf{v}_i^*(0)$  at  $t^* = 0$ , the position  $\mathbf{r}_i^*(h^*)$  at  $t^* = h^*$  can be evaluated from Eq. (1.8) as

$$\mathbf{r}_i^*(h^*) = \mathbf{r}_i^*(0) + h^* \mathbf{v}_i^*(0) + \frac{h^{*2}}{2} \mathbf{f}_i^*(0) \quad (3.10)$$

Similarly, the equation for a heavy molecule  $j$  can be obtained as

$$\mathbf{r}_j^*(h^*) = \mathbf{r}_j^*(0) + h^* \mathbf{v}_j^*(0) + \frac{h^{*2}}{2K} \mathbf{f}_j^*(0) \quad (3.11)$$

Hence, if the initial position and velocity at  $t^* = 0$  are assigned, the position at the next time step can be evaluated from Eqs. (3.10) and (3.11), and the simulation can commence according to Eqs. (3.8) and (3.9).

### 3.1.4 Parameters for Simulations

In addition to the above assignment of the initial positions and velocities, it is necessary to assign the number of molecules  $N$ , the system temperature  $T^*$ , and the mass ratio  $K$ . Setting these parameters corresponds to the specification of the physical system of interest. Moreover, an appropriate time interval  $h^*$  and the total number of time steps needed for one simulation run must also be carefully specified in order to conduct a simulation successfully without serious problems, such as a system divergence. Additionally, other specifications may be necessary to assist the postprocessing analysis and visualization. For example, in making an animation, it may be necessary to write out various types of data at specific time steps.

The initial positions are usually assigned by a method employing uniform random numbers. The Maxwellian distribution function, which is the velocity distribution for thermodynamic equilibrium, can be written in nondimensional form for a two-dimensional system from Eq. (2.3) as

$$f^*(\mathbf{v}_j^*) = \left( \frac{K}{2\pi T^*} \right) \exp \left\{ -\frac{K}{2T^*} (v_{jx}^{*2} + v_{jy}^{*2}) \right\} \quad (3.12)$$

This equation is for a heavy molecule  $j$ , but it also holds for a light molecule  $i$  by replacing subscript  $j$  and  $K$  by  $i$  and unity, respectively. The method of assigning

the initial velocities according to this normal distribution function is explained in Appendix A2. Since the number of degrees of freedom for a two-dimensional system is different from that for a three-dimensional system, the relationship between the average velocity and the specified temperature has a slightly different expression from that in Eq. (2.7). If the square mean velocities of a light molecule  $i$  and heavy molecule  $j$  are denoted by  $v_i^{*2}$  and  $v_j^{*2}$ , respectively, these quantities are related to the system temperature by

$$T^* = \frac{\overline{v_i^{*2}}}{2} = K \frac{\overline{v_j^{*2}}}{2} \quad (3.13)$$

The number of light molecules  $N_A$  is taken to be equal to that of heavy molecules  $N_B$  where  $N_A = N_B = 20$  in this exercise. Note that in practice a personal computer can easily handle a much larger system, such as  $N_A = 1000$  or 10,000. Generally speaking, it is desirable to run a set of simulations where each parameter is given at least three different values in order to grasp how it may influence the simulation results. If there are many parameters governing a phenomenon, it is advisable that important parameters are taken in several different cases, with a typical value set assigned to the other parameters. In the present exercise, therefore, the temperature  $T^*$  and mass ratio  $K$  are taken as  $T^* = 1.5, 5$ , and  $10$ , and  $K = 2, 5$ , and  $10$ , respectively. The number density  $n^* (=n\sigma^2)$  is taken only for the single case of  $n^* = 0.1$ .

Finally, we discuss an appropriate value for the time interval, which has to be carefully determined because it has a significant influence on both the accuracy of the results and the stability of a simulation. If the mean speed of molecule  $i$  is assumed to be equal to the root mean square of velocity, the mean distance of travel for the translational motion during the time interval  $h$  is expected as  $h(\overline{v_i^2})^{1/2}$ . This distance is required to be much shorter than the characteristic distance of the Lennard-Jones potential. Referring to Figure 2.8, this can be expressed mathematically as

$$h(\overline{v_i^2})^{1/2} \ll 0.1 \times \sigma \quad (3.14)$$

Using Eq. (3.13) and expressing the average velocity as a function of  $T^*$ , it follows that Eq. (3.14) can be written in nondimensional form as

$$h^* \ll 0.1 / \sqrt{2T^*} \quad (3.15)$$

As is clearly shown in Eq. (3.15), a shorter time interval is required for a higher temperature; for example,  $h^*$  is taken as  $h^* = 0.005, 0.001$ , and  $0.0005$  for  $T^* = 1, 5$ , and  $10$ , respectively. Unless the time interval is sufficiently short, molecules will have a tendency to overlap in a manner that is physically unreasonable, which will induce divergence of the system. After determining an appropriate value of the time interval, one can determine the length of a simulation run, that is, the total number of time steps. For example, if  $T^*$  and  $h^*$  are adopted as  $T^* = 10$  and

$h^* = 0.0005$ , the mean travel distance of molecules per unit time step  $h^*(2T^*)^{1/2}$  is approximately equal to 0.002. Hence, if the total number of time steps is set to be 50,000, the paths of the molecules will be of sufficient length to examine the diffusion phenomenon.

### 3.1.5 Results of Simulations

We show some results of the snapshots of molecules in Figures 3.1 and 3.2, which were obtained by conducting the simulation program that is shown in the next subsection. The figures were obtained for a molecular mass ratio of  $K = 2$  and 10, respectively. Each figure shows two snapshots at  $t^* = 8$  for the two cases of the temperature  $T^* = 1.5$  and 5. These figures clearly show that both species of molecules move more actively and diffuse further in the higher-temperature case. If the snapshots for the same temperature are compared, the diffusion of heavy molecules is less active, and this situation is more significant for the larger mass ratio.

The sequence of snapshots in Figure 3.3 shows how molecules diffuse from the center toward the outer simulation boundaries with time for  $K = 10$  and  $T^* = 5$ . This sequence clearly shows that light molecules start to diffuse from the central area in the outward directions more significantly than heavy molecules.

These results indicate the main qualitative features of the diffusion phenomenon of light and heavy molecules. However, the above discussion is too simple from an academic point of view, therefore quantitative considerations and discussion based on the theoretical background are indispensable. How can we theoretically explain the qualitative features that both the light and heavy molecules diffuse more significantly for a higher temperature, and also that heavy molecules are less able to move for larger values of the mass ratio? This may be explained theoretically by considering that Eq. (3.13) implies the mean velocity is larger for a higher

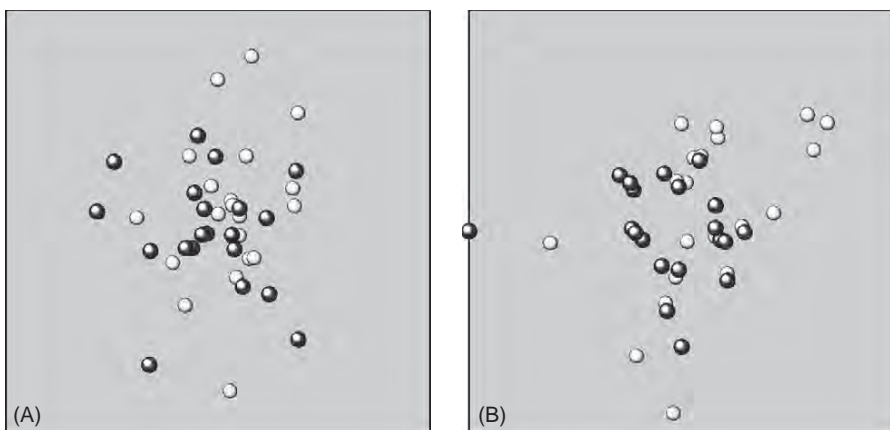


**Figure 3.1** Diffusion phenomena of molecules for the mass ratio  $K = 2$ : (A)  $T^* = 1.5$  and (B)  $T^* = 5$  (white and black molecules denote light and heavy molecules, respectively).

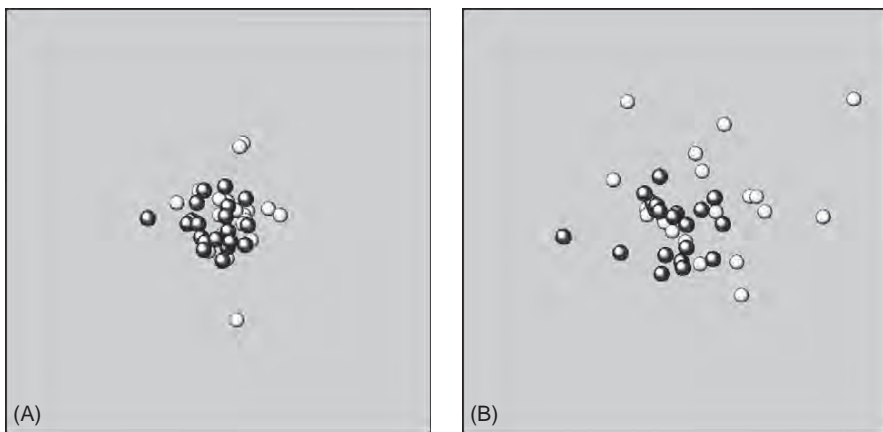


**Figure 3.2** Diffusion phenomena of molecules for the mass ratio  $K = 10$ : (A)  $T^* = 1.5$  and (B)  $T^* = 5$  (white and black molecules denote light and heavy molecules, respectively).

temperature and that the mean velocity of the heavier molecules is smaller for a larger mass ratio. This may be one of the key theoretical considerations in fully understanding the present simulation results. In academic simulations, such theoretical considerations are conducted in more complex form by combining different threads in order to form a uniformed conclusion about the results. These sophisticated considerations help one to avoid presenting erroneous simulation results, which sometimes happens, for a variety of reasons. Although we here show only the results in the form of snapshots, academic research would require comprehensive quantitative results that might include the change in the internal structures and analysis of the transport coefficients. Furthermore, it will usually be necessary to check the influence of the time interval and the size of a system on the results.

### 3.1.6 Simulation Program

We here show a sample simulation program to simulate the present diffusion phenomenon. The program is written in the FORTRAN language. Since the main program is usually written in order to clarify a flow of procedure in a straightforward way, the assignment of the initial positions and velocities is treated in a subroutine subprogram. The reader is advised to develop a simulation program with a clear logical flow, thereby simplifying the debugging of a program under development and making it, on completion, a straightforward and useful resource.

For these reasons, the important variables in a program need to be explained in comments at the beginning of the program and each subroutine. These comments provide the user an image of a specific physical meaning from the variable name. In scientific numerical simulations, double-precision variables are usually used for real-type variables, but higher is sometimes more desirable in certain cases, such as solving the problem of an inverse matrix. The following simple simulation program

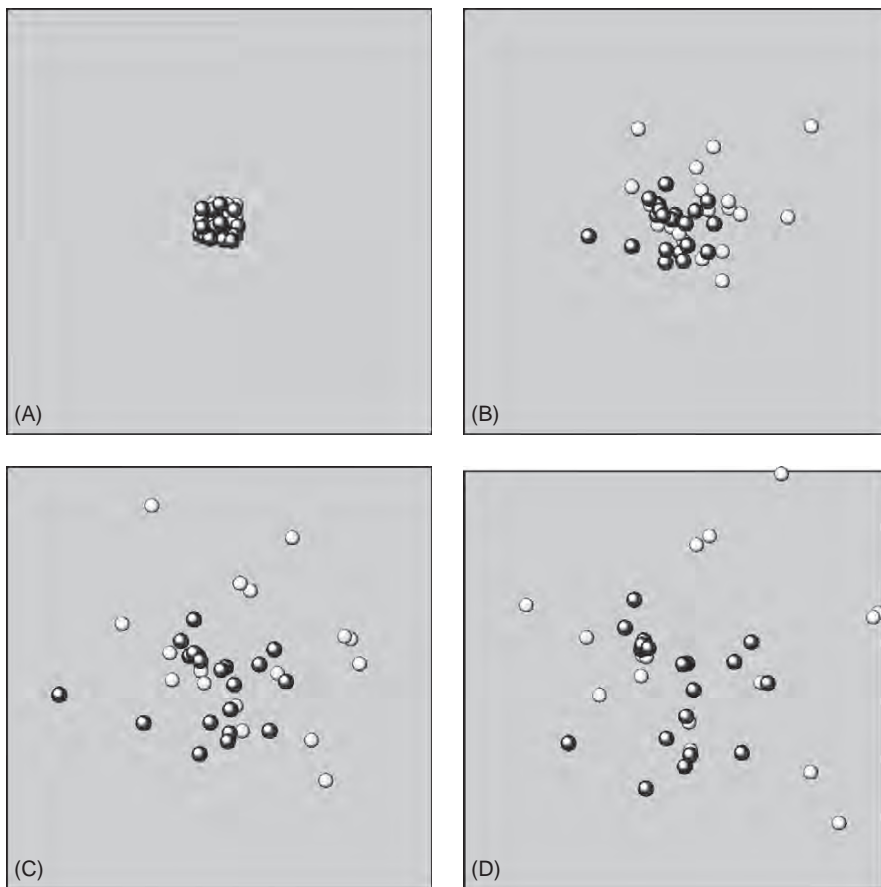


**Figure 3.3** Movement of molecules with time for the mass ratio  $K = 10$  and the temperature  $T^* = 5$ : (A)  $t^* = 0$ , (B)  $t^* = 6$ , (C)  $t^* = 12$ , and (D)  $t^* = 18$ .

has been developed according to these guidelines. The important variables are shown below to help the reader better understand the program.

$\text{RX}(I), \text{RY}(I)$	: $(x, y)$ coordinates of the position vector $\mathbf{r}_i^*$ of molecule $i$
$\text{RX0}(I), \text{RY0}(I)$	: Position vector $\mathbf{r}_i^*$ at the previous time step
$\text{FX}(I), \text{FY}(I)$	: Force $\mathbf{f}_i^*$ acting on molecule $i$
$N$	: Number of molecules in the system
$NA, NB$	: Numbers of light and heavy molecules, respectively
$K$	: Mass ratio $K = M/m$
$T$	: Desired temperature $T^*$
$H$	: Time interval $h^*$
$NDENS$	: Number density of molecules
$L$	: Side length of the square simulation region

RAN(J) : Uniform random numbers ranging 0~1 (J=1~NRANMX)  
 NRAN : Number of used random numbers

Several remarks are attached to the more important statements in the program for the benefit of the reader. Note that the line numbers are for the sake of convenience only and are not necessary during the execution of a simulation program.

```

0001 C*****  

0002 C*          diffuse.f  

0003 C*          *  

0004 C*          MOLECULAR DYNAMICS METHOD FOR MOLECULAR DIFFUSION PROBLEM  

0005 C*          --- TWO-DIMENSIONAL CASE ---  

0006 C*          *  

0007 C*          OPEN( 9,FILE= 'aaa1.data' ,STATUS='UNKNOWN' )  

0008 C*          OPEN(21,FILE='aaa001.data',STATUS='UNKNOWN') ; POSITION DATA  

0009 C*          OPEN(22,FILE='aaa011.data',STATUS='UNKNOWN') ; POSITION DATA  

0010 C*          OPEN(23,FILE='aaa021.data',STATUS='UNKNOWN') ; POSITION DATA  

0011 C*          OPEN(24,FILE='aaa031.data',STATUS='UNKNOWN') ; POSITION DATA  

0012 C*          OPEN(25,FILE='aaa041.data',STATUS='UNKNOWN') ; POSITION DATA  

0013 C*          *  

0014 C*          *  

0015 C*          VER.4 , BY A.SATOH , '04 3/13 *  

0016 C*****  

0017 C  

0018 C      RX(I) , RY(I) : POSITION OF I-TH MOLECULE  

0019 C      RX0(I),RY0(I) : POSITION OF I-TH MOLECULE AT PREVIOUS TIME  

0020 C      FX(I) , FY(I) : FORCE ACTING ON I-TH MOLECULE  

0021 C      T : TEMPERATURE  

0022 C      K : MASS RATIO = MB/MA  

0023 C      NDENS : NUMBER DENSITY OF MOLECULES  

0024 C      H : TIME DIFFERENCE  

0025 C      RC : CUTOFF RADIUS FOR FORCE  

0026 C      L : MAGNITUDE OF CAGE  

0027 C      NA : NUMBER OF MOLECULES OF SPECIES A  

0028 C      NB : NUMBER OF MOLECULES OF SPECIES B  

0029 C      N : TOTAL NUMBER OF MOLECULES  

0030 C      -L/2 < RX(I) < L/2 , -L/2 < RY(I) < L/2  

0031 C-----  

0032 C  

0033      IMPLICIT REAL*8 (A-H,O-Z), INTEGER (I-N)  

0034 C  

0035      COMMON /BLOCK1/ RX0 , RY0 , RX , RY  

0036      COMMON /BLOCK2/ FX , FY  

0037      COMMON /BLOCK3/ VELX, VELY  

0038      COMMON /BLOCK4/ H , RC , L , T , K , NDENS  

0039      COMMON /BLOCK5/ NRAN , RAN , IX  

0040 C  

0041      PARAMETER( NN=80, NRANMX=50000 )  

0042      PARAMETER( PI=3.141592653589793D0 )  

0043 C  

0044      REAL*8 RX0(NN), RY0(NN), RX(NN) , RY(NN)  

0045      REAL*8 FX(NN) , FY(NN) , VELX(NN), VELY(NN)  

0046      REAL*8 H , RC , L , T , K , NDENS  

0047 C  

0048      REAL RAN(NRANMX)  

0049      INTEGER NRAN , IX  

0050 C  

0051      REAL*8 RXI, RYI, TIME, HSQ, CC0, CC1  

0052      INTEGER N, NA, NB  

0053      INTEGER SWITCH, NTIME, NTIMEMX  

0054      INTEGER NP, NOPT, NGRAPH, NPRINT  

0055 C  

0056          OPEN( 9,FILE= 'aaa1.data' ,STATUS='UNKNOWN' )  

0057          OPEN(21,FILE='aaa001.data',STATUS='UNKNOWN')  

0058          OPEN(22,FILE='aaa011.data',STATUS='UNKNOWN')  

0059          OPEN(23,FILE='aaa021.data',STATUS='UNKNOWN')
```

- The given values and intermediate results are written out in @aa1.data and the molecular positions are done in aaa001 to aaa041.

```

0060          OPEN( 24,FILE='aaa031.data' ,STATUS='UNKNOWN' )
0061          OPEN( 25,FILE='aaa041.data' ,STATUS='UNKNOWN' )
0062                                              NP=9
0063 C
0064      T    = 5.0D0
0065      K    = 10.D0
0066      NA   = 20
0067      NB   = NA
0068      H    = 0.001D0
0069      RC   = 3.D0
0070      N    = NA + NB
0071      NDENS = 0.1D0
0072      L    = DSQRT( DBLE(N)/NDENS )
0073      HSQ  = H*H
0074 C
0075      NTIMEMX= 10000
0076      NPRINT = 1000
0077      NGRAPH = 2000
0078      NOPT   = 20
0079 C
0080      IX    = 0
0081      CALL RANCAL(NRANMX,IX,RAN)
0082      NRAN   = 1
0083 C
0084 C
0085 C----- INITIAL CONFIGURATION -----
0086 C
0087 C
0088 C
0089      CALL INIPOSIT( N , L )
0090 C
0091      CALL INIVEL( N , NA , NB , T , K , PI )
0092 C
0093      DO 10 I=1,N
0094      RX(I) = RX0(I)
0095      RY(I) = RY0(I)
0096 10 CONTINUE
0097 C
0098      SWITCH = 0
0099      CALL FORCE( N , L , RC , SWITCH )
0100 C
0101      CALL POSITR1( N , NA , H , K )
0102 C
0103 C----- PRINT OUT CONSTANTS -----
0104      WRITE(NP,5) T , K , NDENS , NA , NB , L , H , RC
0105 C
0106      CALL PRINTOUT( N , NA , TIME , NP )
0107 C
0108      TIME = 0.D0
0109 C
0110 C----- START OF MAIN LOOP -----
0111 C
0112 C
0113      SWITCH = 10
0114 C
0115      DO 100 NTIME=1 , NTIMEMX
0116 C
0117      CALL FORCE(N , L , RC,SWITCH)
0118      CC0 = 1.D0/K
0119      CC1 = 1.D0
0120 C
0121      DO 50 I=1,N
0122 C
0123      IF ( I .EQ. NA+1 ) CC1 = CC0
0124      RXI   = 2.D0*RX(I) - RX0(I) + FX(I)*HSQ*CC1
0125      RYI   = 2.D0*RY(I) - RY0(I) + FY(I)*HSQ*CC1
0126      RX0(I) = RX(I)
0127      RY0(I) = RY(I)
0128      RX(I) = RXI
0129      RY(I) = RYI
0130 C
0131      50 CONTINUE

```

• Temperature  $T^* = 5$ , mass ratio  $K = 10$ , numbers of light and heavy molecules  $N_A = N_B = 20$ , time interval  $\hbar^* = 0.001$ , cutoff distance  $\lambda_{\text{coff}}^* = 3$ , number density  $n^* = 0.1$ , and simulation region size  $L^* = (N/n^*)^{1/2}$ .

• The total number of time steps is 10,000, and the molecular positions are written out at every 2000 time steps for the postprocessing analysis.

• A sequence of uniform random numbers is prepared in advance and when necessary, random numbers are taken out from the variable RAN(\*).

• The periodic BC is used for SWITCH=0 but not for the other cases.

• The molecular positions are calculated at the next time step from Eqs. (3.10) and (3.11) in the subroutine POSITR1.

• The forces acting on each particle are calculated in the subroutine FORCE.

• The molecular positions are calculated from Eqs. (3.8) and (3.9). The previous molecular positions are saved in RX0(\*) and RY0(\*), and the present are saved in RX(\*) and RY(\*).

• The molecular positions are written out at every NPRINT time steps for subsequently checking the reliability of results.

```

0132 C          --- PRINT OUT DATA ---
0133      IF ( MOD(NTIME,NPRINT) .EQ. 0 ) THEN
0134          TIME = H*DBLE(NTIME)
0135          CALL PRINTOUT( N, NA, TIME, NP )
0136      END IF
0137 C          --- DATA OUTPUT FOR GRAPH ---
0138      IF ( MOD(NTIME,NGRAPH) .EQ. 0 ) THEN
0139          NOPT = NOPT + 1
0140          WRITE(NOPT,56) N, NA, NB, L, REAL(H)*REAL(NTIME)
0141 C
0142          DO 60 I =1,N
0143              IF( I .LE. NA ) THEN
0144                  R = 1.D0
0145              ELSE
0146                  R = 1.5D0
0147              END IF
0148              WRITE(NOPT,58) I, R, RX(I), RY(I)
0149      60 CONTINUE
0150      CLOSE(NOPT, STATUS='KEEP')
0151      END IF
0152 C
0153 C
0154      100 CONTINUE
0155 C
0156 C          -----
0157 C          ----- END OF MAIN LOOP -----
0158 C          -----
0159      CLOSE(NP, STATUS='KEEP')
0160 C
0161 C          ----- FORMAT -----
0162      5 FORMAT(/1H , '-----'
0163      &      /1H , ' MOLECULAR DYNAMICS SIMULATION '
0164      &      /1H , 'FOR TWO-DIMENSIONAL MOLECULAR DIFFUSION PROBLEM '
0165      &      /1H , '-----'
0166      &      /1H , 'TEMPERATURE= ',F6.2 ,2X, 'MASS RATIO= ',F6.2 ,2X,
0167      &      'NDENS= ',F6.3
0168      &      /1H , 'NUMBER OF MOLECULES OF SPECIES A= ',I4
0169      &      /1H , 'NUMBER OF MOLECULES OF SPECIES B= ',I4
0170      &      /1H , 'MAGNITUDE OF CAGE= ',F7.2 ,2X, 'TIME DIFF.= ',
0171      &      F8.5 ,2X, 'CUTOFF RADIUS= ',F6.2/)
0172      56 FORMAT( 3I6, 2B13.8 )
0173      58 FORMAT( I5, F8.3, 2E26.18 )
0174      STOP
0175      END
0176 C***** SUB PRINTOUT *****
0177 C***** SUBROUTINE PRINTOUT( N, NA, TIME, NP )
0178 C*****
0179 C
0180 C**** SUB PRINTOUT *****
0181      SUBROUTINE PRINTOUT( N, NA, TIME, NP )
0182 C
0183      IMPLICIT REAL*8 (A-H,O-Z), INTEGER (I-N)
0184 C
0185      COMMON /BLOCK1/ RX0, RY0, RX, RY
0186 C
0187      PARAMETER( NN=80 )
0188 C
0189      REAL*8 RX0(NN), RY0(NN), RX(NN), RY(NN)
0190      INTEGER N, NA, NP
0191 C
0192      WRITE(NP,2) TIME
0193      2 FORMAT(/1H , '----- TIME= ',E13.5/)
0194      WRITE(NP,*)
0195      WRITE(NP,*) 'MOLECULES OF SPECIES A'
0196      WRITE(NP,*) 
0197      DO 10 I=1,NA
0198          WRITE(NP,5) I, RX(I), RY(I)
0199      5 FORMAT(1H , 'I= ',I3 ,5X, 'RX= ',F8.2 ,5X, 'RY= ',F8.2)
0200      10 CONTINUE
0201      WRITE(NP,*)

```

• The molecular positions are written out at every NGRAPH time steps for the postprocessing analysis.

• The positions of light molecules are first written out and followed by those of the heavy molecules.

```

0202      WRITE(NP,*)'MOLECULES OF SPECIES B'
0203      WRITE(NP,*)
0204      DO 20 I=NA+1,N
0205         WRITE(NP,5) I,RX(I),RY(I)
0206 20 CONTINUE
0207      WRITE(NP,*)
0208
0209
0210 C**** SUB INIPOSIT *****
0211      SUBROUTINE INIPOSIT( N, L )
0212 C
0213      IMPLICIT REAL*8 (A-H,O-Z), INTEGER (I-N)
0214 C
0215      COMMON /BLOCK1/ RX0, RY0, RX, RY
0216      COMMON /BLOCK5/ NRAN , RAN , IX
0217 C
0218      PARAMETER( NN=80, NRANMX=50000 )
0219 C
0220      REAL*8 RX0(NN), RY0(NN), RX(NN), RY(NN), L
0221      REAL*8 RXIJ , RYIJ , RIJSQ , CRX0 , CRY0
0222      REAL   RAN(NRANMX)
0223      INTEGER N, NRAN
0224 C
0225      DO 10 I=1,N
0226 2      NRAN = NRAN + 1
0227      CRX0 = L*( DBLE(RAN(NRAN))-0.5D0)
0228      NRAN = NRAN + 1
0229      CRY0 = L*( DBLE(RAN(NRAN))-0.5D0)
0230      IF( I .NE. 1 ) THEN
0231         DO 5 J=1,I-1
0232            RXIJ = CRX0 - RX0(J)
0233            RYIJ = CRY0 - RY0(J)
0234            RXIJ = RXIJ - DNINT( RXIJ/L )*L
0235            RYIJ = RYIJ - DNINT( RYIJ/L )*L
0236            RIJSQ = RXIJ*RXIJ + RYIJ*RYIJ
0237            IF ( RIJSQ .LT. 1.D0 ) GOTO 2
0238 5      CONTINUE
0239      END IF
0240      RX0(I) = CRX0
0241      RY0(I) = CRY0
0242 C
0243 10 CONTINUE
0244
0245
0246 C**** SUB INIVEL *****
0247      SUBROUTINE INIVEL( N, NA, NB, T, K, PI )
0248 C
0249      IMPLICIT REAL*8 (A-H,O-Z), INTEGER (I-N)
0250 C
0251      COMMON /BLOCK3/ VELX , VELY
0252      COMMON /BLOCK5/ NRAN , RAN , IX
0253 C
0254      PARAMETER( NN=80, NRANMX=50000 )
0255 C
0256      INTEGER N, NA, NB, NRAN
0257      REAL*8 VELX(NN) , VELY(NN) , T , K , PI
0258      REAL   RAN(NRANMX)
0259      REAL*8 MOMXA, MOMYA, MOMXB, MOMYB
0260      REAL*8 CC0, CC1, CC10, CC11
0261 C
0262      CC0 = 1.D0/K
0263      CC1 = 1.D0
0264 C
0265      DO 10 I=1,N
0266      IF ( I .EQ. NA+1 ) CC1 = CC0
0267      NRAN = NRAN + 1
0268      CC10 = DSQRT( -2.D0*T*CC1*DLOG( DBLE(RAN(NRAN)) ) )
0269      NRAN = NRAN + 1
0270      CC11 = 2.D0*PI*DBLE(RAN(NRAN))
0271      VELX(I) = CC10*DCCOS(CC11)
0272      VELY(I) = CC10*DSIN(CC11)

```

• A subroutine for setting the initial molecular positions.

• Dissimilar to the regular configuration explained in Section 2.1, the initial molecular positions are assigned using random numbers. If  $r_{ij}^* < 1$ , such molecular positions are not employed because of an extraordinary overlap.

• A subroutine for setting the initial molecular velocities.

• The initial velocities are set according to Eq. (2.5) based on Eq. (3.12) using random numbers.

```

0273    10 CONTINUE
0274 C      MOMXA = 0.D0
0275      MOMYA = 0.D0
0276      MOMXB = 0.D0
0277      MOMYB = 0.D0
0278
0279 C      DO 20 I=1,N
0280        IF ( I .LE. NA ) THEN
0281          MOMXA = MOMXA + VELX(I)
0282          MOMYA = MOMYA + VELY(I)
0283        ELSE
0284          MOMXB = MOMXB + VELX(I)
0285          MOMYB = MOMYB + VELY(I)
0286        END IF
0287
0288    20 CONTINUE
0289 C      MOMXA = MOMXA/DBLE(NA)
0290      MOMYA = MOMYA/DBLE(NA)
0292      MOMXB = MOMXB/DBLE(NB)
0293      MOMYB = MOMYB/DBLE(NB)
0294 C
0295 C      --- CORRECT VELOCITIES TO SATISFY ---
0296 C      --- ZERO TOTAL MOMENTUM ---
0297 C
0298      CC10 = MOMXA
0299      CC11 = MOMYA
0300      DO 30 I=1,N
0301        IF ( I .EQ. NA+1 ) THEN
0302          CC10 = MOMXB
0303          CC11 = MOMYB
0304        END IF
0305        VELX(I) = VELX(I)-CC10
0306        VELY(I) = VELY(I)-CC11
0307
0308    30 CONTINUE
0309
0310 C**** SUB FORCE *****
0311      SUBROUTINE FORCE( N, L, RC, SWITCH )
0312 C      IMPLICIT REAL*8 (A-H,O-Z), INTEGER (I-N)
0314 C
0315      COMMON /BLOCK1/ RX0, RY0, RX, RY
0316      COMMON /BLOCK2/ FX , FY
0317 C
0318      PARAMETER( NN=80 )
0319 C
0320      INTEGER N, SWITCH
0321      REAL*8 RX0(NN), RY0(NN), RX(NN), RY(NN)
0322      REAL*8 FX(NN) , FY(NN)
0323      REAL*8 L, RC
0324      REAL*8 RXI, RYI, RXIJ, RYIJ, RIJSQ
0325      REAL*8 FXI, FYI, FXIJ, FYIJ, FIJ
0326      REAL*8 RCSQ, LINV
0327      REAL*8 SR2, SR6, SR12
0328 C
0329      RCSQ = RC*RC
0330      LINV = 1.D0/L
0331 C      DO 5 I=1,N
0332        FX(I) = 0.D0
0333        FY(I) = 0.D0
0334
0335    5 CONTINUE
0336 C      DO 20 I=1,N-1
0337        RXI = RX(I)
0338 C        RYI = RY(I)
0339        FXI = FX(I)
0340        FYI = FY(I)
0341
0342

```

• To make the system momentum zero, the total momentum is first calculated for each light and heavy molecule.

• The extra momentum per molecule is calculated from the total momentum.

• The total momentum is forced to be zero by subtracting the extra momentum per molecule from the velocity components of each molecule.

RETURN  
END

• A subroutine for calculating the forces acting on molecules.

• The force variables are initialized as zero before proceeding to the main loop.

--- FOR I-TH MOLECULE ---

• The action-reaction law enables us to calculate the forces of only pairs of particles satisfying  $j > i$ .

```

0343 C
0344      DO 10 J=I+1,N
0345 C
0346      RXIJ = RXI - RX(J)
0347      RYIJ = RYI - RY(J)
0348      IF ( SWITCH .EQ. 0 ) THEN
0349          RXIJ = RXIJ-DNINT( RXIJ*LINV )*L
0350          RYIJ = RYIJ-DNINT( RYIJ*LINV )*L
0351      END IF
0352      IF ( DABS(RXIJ) .GT. RC ) GOTO 10
0353      IF ( DABS(RYIJ) .GT. RC ) GOTO 10
0354      RIJSQ = RXIJ*RXIJ + RYIJ*RYIJ
0355      IF ( RIJSQ .GT. RCSQ )      GOTO 10
0356 C
0357      SR2   = 1.D0/RIJSQ
0358      SR6   = SR2**3
0359      SR12  = SR6**2
0360      FIJ   = ( 2.D0*SR12-SR6 )/RIJSQ
0361      FXIJ = FIJ*RXIJ
0362      FYIJ = FIJ*RYIJ
0363      FXI  = FXI + FXIJ
0364      FYI  = FYI + FYIJ
0365      FX(J) = FX(J) - FXIJ
0366      FY(J) = FY(J) - FYIJ
0367      10  CONTINUE
0368 C
0369      FX(I) = FXI
0370      FY(I) = FYI
0371 C
0372      20  CONTINUE
0373 C
0374      DO 30 I=1,N
0375      FX(I) = FX(I)*24.D0
0376      FY(I) = FY(I)*24.D0
0377      30  CONTINUE
0378
0379
0380 C**** SUB POSITR1 *****
0381      SUBROUTINE POSITR1( N, NA, H, K )
0382 C
0383      IMPLICIT REAL*8 (A-H,O-Z), INTEGER (I-N)
0384 C
0385      COMMON /BLOCK1/ RX0 , RY0, RX, RY
0386      COMMON /BLOCK2/ FX , FY
0387      COMMON /BLOCK3/ VELX, VELY
0388 C
0389      PARAMETER( NN=80 )
0390 C
0391      REAL*8 RX0(NN), RY0(NN), RX(NN) , RY(NN)
0392      REAL*8 FX(NN) , FY(NN) , VELX(NN), VELY(NN)
0393      REAL*8 H , K
0394      REAL*8 HSQ2, CC0, CC1
0395      INTEGER NA , N
0396 C
0397      HSQ2 = H*H/2.D0
0398      CC0 = 1.D0/K
0399      CC1 = 1.D0
0400 C
0401      DO 10 I=1,N
0402      IF( I .EQ. NA+1 ) CC1 = CC0
0403      RX(I) = RX0(I) + H*VELX(I) + HSQ2*FX(I)*CC1
0404      RY(I) = RY0(I) + H*VELY(I) + HSQ2*FY(I)*CC1
0405      10  CONTINUE
0406
0407
0408 C**** SUB RANCAL *****
0409      SUBROUTINE RANCAL( N, IX, X )
0410 C
0411      DIMENSION X(N)
0412      DATA INTEGMX/2147483647/
0413      DATA INTEGST,INTEG/584287,48828125/

```

--- FOR I-TH AND J-TH ---

- The periodic BC is used for SWITCH = 0.
- The particles separating over the cutoff distance  $r_{\text{cutoff}}^*$  are passed without calculation of forces.

• The forces between molecules are calculated from Eq. (3.7).

• The factor 24 in Eq. (3.7) will be multiplied later.

• The action-reaction law can provide the force FX(J) and FY(J) as (-FXIJ) and (-FYIJ).

RETURN  
END

• The starting value of the molecular positions is calculated from Eqs. (3.10) and (3.11).

RETURN  
END

• A subroutine for generating a uniform random number sequence.

```

0414 C
0415     AINTEGMX = REAL( INTEGMX )
0416 C
0417     IF ( IX.LT.0 ) PAUSE
0418     IF ( IX.EQ.0 ) IX = INEGST
0419     DO 30 I=1,N
0420         IX = IX*INTEG
0421         IF (IX) 10, 20, 20
0422 10     IX   = (IX+INTEGMX)+1
0423 20     X(I) = REAL(IX)/AINTEGMX
0424 30 CONTINUE
0425     RETURN
0426     END
0427 C*****THIS SUBROUTINE IS FOR GENERATING UNIFORM RANDOM NUMBERS ****
0428 C THIS SUBROUTINE IS FOR GENERATING UNIFORM RANDOM NUMBERS           *
0429 C (SINGLE PRECISION) FOR 64-BIT COMPUTER.                                *
0430 C   N      : NUMBER OF RANDOM NUMBERS TO GENERATE                      *
0431 C   IX     : INITIAL VALUE OF RANDOM NUMBERS (POSITIVE INTEGER)        *
0432 C   : LAST GENERATED VALUE IS KEPT                                     *
0433 C   X(N)  : GENERATED RANDOM NUMBERS (0<X(N)<1)                   *
0434 C*****SUB RANCAL ****
0435 CCC SUBROUTINE RANCAL( N, IX, X )
0436 CCC IMPLICIT REAL*8(A-H,O-Z),INTEGER*8 ( I-N )
0437 C
0438 CCC
0439 C
0440 CCC REAL      X(N)
0441 CCC INTEGER*8 INTEGMX, INTEG64, INEGST, INEG
0442 C
0443 CCC DATA INTEGMX/2147483647/
0444 CCC DATA INTEG64/2147483648/
0445 CCC DATA INEGST,INEG/584287,48828125/
0446 C
0447 CCC AINTEGMX = REAL( INTEGMX )
0448 CCC AINTEGMX = REAL( INEG64 )
0449 C
0450 CCC IF ( IX.LT.0 ) PAUSE
0451 CCC IF ( IX.EQ.0 ) IX = INEGST
0452 CCC DO 30 I=1,N
0453 CCC     IX = IX*INTEG
0454 CCC     IX = KMOD(IX,INTEG64)
0455 CCC     IF (IX) 10, 20, 20
0456 CCC10    IX   = (IX+INTEGMX)+1
0457 CCC20    X(I) = REAL(IX)/AINTEGMX
0458 CCC30 CONTINUE
0459 CCC RETURN
0460 CCC END

```

• This is for a 32-bit CPU based on the expression of two's complement.

• This is also a random number generating subroutine for a 64-bit CPU based on the expression of two's complement.

## 3.2 Behavior of Rod-like Particles in a Simple Shear Flow

In the present section, we consider the behavior of axisymmetric particles, known as spherocylinders, in a simple shear flow as the second demonstration of the MD method. MD simulations for rod-like particles are much more complex than those for a spherical particle system, since the translational and rotational motion of rod-like particles must be treated simultaneously. Hence, this exercise is of a considerably high level and may be applicable to a range of academic research fields. The present simulation method for a spherocylinder particle system is expected to offer many important suggestions in developing practical simulation programs, such as for the adsorption phenomenon between carbon-nanotubes and nonspherical molecules.

### 3.2.1 Physical Phenomena of Interest

The dispersion of interest in this exercise is composed of spherocylinder particles with mass  $m$  and inertia moment  $I$ , and it is subjected to a simple shear flow. The spherocylinder particle has a positive and negative magnetic charges (NS poles) at each center of the hemisphere cap situated at both ends of the cylindrical body. This magnetic particle is coated with a steric (surfactant) layer, which acts to prevent the particles from aggregating and thus sedimentation in the gravitational field. In this exercise we consider how such a dispersion behaves under the circumstance of an applied magnetic field in addition to the simple shear flow.

The main subjects for the formalization of this problem are explained in the following subsections. Essentially, they are the modeling of the particles, the formalization of the equation of motion, the derivation of forces and torques acting on particles, and the nondimensionalization of quantities.

### 3.2.2 Particle Model

As shown in Figure 3.4, a magnetic rod-like particle is modeled as a spherocylinder, with the magnetic charges  $\pm q$  at the center of each hemisphere cap, which has a length  $l_0$  and a cylindrical diameter  $d$  of the cylindrical part. The particle is covered with a uniform steric (surfactant) layer with thickness  $\delta$ , and the overlap of these steric layers induces a repulsive interaction between the particles. In the following we show magnetic forces and torques acting on the magnetic particles.

If a magnetic charge  $q$  and a magnetic dipole moment  $\mathbf{m}$  are acted upon by a uniform applied magnetic field  $\mathbf{H}$ , then the force  $\mathbf{F}$  acting on the charge and the torque  $\mathbf{T}$  acting on the dipole moment may be found from a standard textbook on magnetic material engineering as

$$\mathbf{F} = \mu_0 q \mathbf{H}, \quad \mathbf{T} = \mu_0 \mathbf{m} \times \mathbf{H} \quad (3.16)$$

The magnetic field  $\mathbf{H}^{(\text{ind})}$  at an arbitrary relative position  $\mathbf{r}$  ( $r = |\mathbf{r}|$ ) induced by the magnetic charge  $q$  is expressed as

$$\mathbf{H}^{(\text{ind})} = \frac{q}{4\pi r^2} \cdot \frac{\mathbf{r}}{r} \quad (3.17)$$

Note that in this book we employ such a unit system concerning magnetic properties that the magnetization corresponds to the magnetic field, that is,

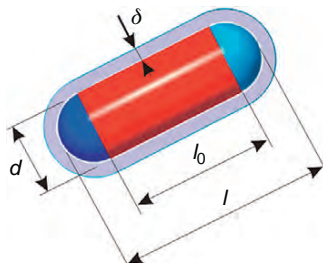


Figure 3.4 Particle model.

$\mathbf{B} = \mu_0(\mathbf{H} + \mathbf{M})$ ; the correspondence table between two representative unit systems is shown in Appendix A4. With these basic formulae, we derive the magnetic force and torque acting on the spherocylinder particle shown in Figure 3.4.

If the position vector of the center of particle  $i$  is denoted by  $\mathbf{r}_i$  and the particle direction by  $\mathbf{e}_i$ , then the position vectors  $\mathbf{r}_i^+$  and  $\mathbf{r}_i^-$  of the magnetic charges  $q$  and  $-q$  can be expressed as

$$\mathbf{r}_i^+ = \mathbf{r}_i + (l_0/2)\mathbf{e}_i, \quad \mathbf{r}_i^- = \mathbf{r}_i - (l_0/2)\mathbf{e}_i \quad (3.18)$$

The magnetic field  $\mathbf{H}_{ij}^+$  at the position  $\mathbf{r}_i^+$  induced by particle  $j$  can be written from Eq. (3.17) as

$$\begin{aligned} \mathbf{H}_{ij}^+ &= \frac{q}{4\pi} \cdot \frac{\mathbf{r}_i^+ - \mathbf{r}_j^+}{|\mathbf{r}_i^+ - \mathbf{r}_j^+|^3} - \frac{q}{4\pi} \cdot \frac{\mathbf{r}_i^+ - \mathbf{r}_j^-}{|\mathbf{r}_i^+ - \mathbf{r}_j^-|^3} \\ &= \frac{q}{4\pi} \left\{ \frac{\mathbf{r}_{ij} + \frac{l_0}{2}(\mathbf{e}_i - \mathbf{e}_j)}{|\mathbf{r}_{ij} + \frac{l_0}{2}(\mathbf{e}_i - \mathbf{e}_j)|^3} - \frac{\mathbf{r}_{ij} + \frac{l_0}{2}(\mathbf{e}_i + \mathbf{e}_j)}{|\mathbf{r}_{ij} + \frac{l_0}{2}(\mathbf{e}_i + \mathbf{e}_j)|^3} \right\} \end{aligned} \quad (3.19)$$

Similarly,  $\mathbf{H}_{ij}^-$  at  $\mathbf{r}_i^-$  induced by particle  $j$  is written as

$$\mathbf{H}_{ij}^- = \frac{q}{4\pi} \left\{ \frac{\mathbf{r}_{ij} - (l_0/2)(\mathbf{e}_i + \mathbf{e}_j)}{|\mathbf{r}_{ij} - (l_0/2)(\mathbf{e}_i + \mathbf{e}_j)|^3} - \frac{\mathbf{r}_{ij} - (l_0/2)(\mathbf{e}_i - \mathbf{e}_j)}{|\mathbf{r}_{ij} - (l_0/2)(\mathbf{e}_i - \mathbf{e}_j)|^3} \right\} \quad (3.20)$$

in which  $\mathbf{r}_{ij} = \mathbf{r}_i - \mathbf{r}_j$ . Hence, the magnetic forces acting on the positive and negative magnetic charges of particle  $i$ ,  $\mathbf{F}_{ij}^+$  and  $\mathbf{F}_{ij}^-$ , by the magnetic charges of particle  $j$ , are finally written as

$$\mathbf{F}_{ij}^+ = \mu_0 q \mathbf{H}_{ij}^+ = \frac{\mu_0 q^2}{4\pi} \left\{ \frac{\mathbf{r}_{ij} + (l_0/2)(\mathbf{e}_i - \mathbf{e}_j)}{|\mathbf{r}_{ij} + (l_0/2)(\mathbf{e}_i - \mathbf{e}_j)|^3} - \frac{\mathbf{r}_{ij} + (l_0/2)(\mathbf{e}_i + \mathbf{e}_j)}{|\mathbf{r}_{ij} + (l_0/2)(\mathbf{e}_i + \mathbf{e}_j)|^3} \right\} \quad (3.21)$$

$$\mathbf{F}_{ij}^- = -\mu_0 q \mathbf{H}_{ij}^- = -\frac{\mu_0 q^2}{4\pi} \left\{ \frac{\mathbf{r}_{ij} - (l_0/2)(\mathbf{e}_i + \mathbf{e}_j)}{|\mathbf{r}_{ij} - (l_0/2)(\mathbf{e}_i + \mathbf{e}_j)|^3} - \frac{\mathbf{r}_{ij} - (l_0/2)(\mathbf{e}_i - \mathbf{e}_j)}{|\mathbf{r}_{ij} - (l_0/2)(\mathbf{e}_i - \mathbf{e}_j)|^3} \right\} \quad (3.22)$$

Similarly, the magnetic torque about the particle axis of particle  $i$ ,  $\mathbf{T}_{ij}^+$ , due to the force acting on the positive charge by the magnetic charges of particle  $j$ , is obtained as

$$\mathbf{T}_{ij}^+ = \frac{l_0}{2} \mathbf{e}_i \times \mathbf{F}_{ij}^+ = \frac{\mu_0 q^2 l_0}{8\pi} \left\{ \frac{\mathbf{e}_i \times \mathbf{r}_{ij} + \frac{l_0}{2}(-\mathbf{e}_i \times \mathbf{e}_j)}{|\mathbf{r}_{ij} + \frac{l_0}{2}(\mathbf{e}_i - \mathbf{e}_j)|^3} - \frac{\mathbf{e}_i \times \mathbf{r}_{ij} + \frac{l_0}{2}(\mathbf{e}_i \times \mathbf{e}_j)}{|\mathbf{r}_{ij} + \frac{l_0}{2}(\mathbf{e}_i + \mathbf{e}_j)|^3} \right\} \quad (3.23)$$

Also, such a torque  $\mathbf{T}_{ij}^-$  due to the force acting on the negative charge is as follows:

$$\mathbf{T}_{ij}^- = -\frac{l_0}{2}\mathbf{e}_i \times \mathbf{F}_{ij}^- = \frac{\mu_0 q^2 l_0}{8\pi} \left\{ \frac{\mathbf{e}_i \times \mathbf{r}_{ij} - \frac{l_0}{2}(\mathbf{e}_i \times \mathbf{e}_j)}{\left| \mathbf{r}_{ij} - \frac{l_0}{2}(\mathbf{e}_i + \mathbf{e}_j) \right|^3} - \frac{\mathbf{e}_i \times \mathbf{r}_{ij} - \frac{l_0}{2}(-\mathbf{e}_i \times \mathbf{e}_j)}{\left| \mathbf{r}_{ij} - \frac{l_0}{2}(\mathbf{e}_i - \mathbf{e}_j) \right|^3} \right\} \quad (3.24)$$

From these equations, the total magnetic force and torque acting on particle  $i$  by particle  $j$  are written as

$$\mathbf{F}_{ij}^{(m)} = \mathbf{F}_{ij}^+ + \mathbf{F}_{ij}^-, \quad \mathbf{T}_{ij}^{(m)} = \mathbf{T}_{ij}^+ + \mathbf{T}_{ij}^- \quad (3.25)$$

It is noted that  $\mathbf{F}_{ji}^{(m)} = -\mathbf{F}_{ij}^{(m)}$  due to the action-reaction law.

A uniform applied magnetic field does not induce a force acting on a particle because there is no field gradient, but it does induce torque. Similar to the above derivation, the torque due to an applied magnetic field can be derived as

$$\mathbf{T}_i^{(H)} = \frac{l_0}{2}\mathbf{e}_i \times \mu_0 q \mathbf{H} - \frac{l_0}{2}\mathbf{e}_i \times (-\mu_0 q \mathbf{H}) = \mu_0(l_0 q \mathbf{e}_i) \times \mathbf{H} \quad (3.26)$$

Since the force and torque due to the overlap of the steric layers cannot be derived straightforwardly, we will discuss this interaction in detail later.

### 3.2.3 Equation of Motion and Molecular Dynamics Algorithm

The spherocylinder particle is axisymmetric and therefore we can employ the method shown in Section 1.1.2 for simulating the motion of particles. However, several modifications are necessary because we consider the behavior of the particles in a simple shear flow, not in a quiescent flow. If the particles are smaller than micron order, the inertia terms are negligible, which means that we can use the equations shown in Section 1.1.2. The equations of motion under the circumstance of a simple shear flow can be obtained by adding new terms due to the flow into Eqs. (1.42) and (1.43) as

$$\mathbf{v}_i^{\parallel} = \mathbf{U}^{\parallel}(\mathbf{r}_i) + \frac{1}{\eta X^A} \mathbf{F}_i^{\parallel}, \quad \mathbf{v}_i^{\perp} = \mathbf{U}^{\perp}(\mathbf{r}_i) + \frac{1}{\eta Y^A} \mathbf{F}_i^{\perp} \quad (3.27)$$

$$\boldsymbol{\omega}_i^{\parallel} = \boldsymbol{\Omega}^{\parallel} + \frac{1}{\eta X^C} \mathbf{T}_i^{\parallel}, \quad \boldsymbol{\omega}_i^{\perp} = \boldsymbol{\Omega}^{\perp} + \frac{1}{\eta Y^C} \mathbf{T}_i^{\perp} - \frac{Y^H}{Y^C} (\boldsymbol{\varepsilon} \cdot \mathbf{e}_i \mathbf{e}_i) : \mathbf{E} \quad (3.28)$$

in which an arbitrary vector is decomposed into the two vectors parallel and normal to the particle axis. These vectors are denoted by superscripts  $\parallel$  and  $\perp$ , respectively: for example,  $\mathbf{v}_i = \mathbf{v}_i^{\parallel} + \mathbf{v}_i^{\perp}$ . We here treat only the angular velocity  $\boldsymbol{\omega}_i^{\perp}$  and neglect  $\boldsymbol{\omega}_i^{\parallel}$  because the rotational motion about the particle axis does not affect the

particle orientation and the magnetic interactions. The velocity field  $\mathbf{U}(\mathbf{r})$  for a simple shear flow is defined as

$$\mathbf{U}(\mathbf{r}) = \dot{\gamma} \begin{bmatrix} 0 & 1 & 0 \\ 0 & 0 & 0 \\ 0 & 0 & 0 \end{bmatrix} \begin{bmatrix} x \\ y \\ z \end{bmatrix} \quad (3.29)$$

in which  $\mathbf{r}$  is the position vector from the origin of the coordinate system, expressed as  $\mathbf{r} = (x, y, z)$ . In this flow case, the rotational angular velocity  $\boldsymbol{\Omega}$  and the rate-of-strain tensor  $\mathbf{E}$  are derived from the definitions as

$$\boldsymbol{\Omega} = \frac{1}{2} \nabla \times \mathbf{U}(r) = -\frac{\dot{\gamma}}{2} \begin{bmatrix} 0 \\ 0 \\ 1 \end{bmatrix}, \quad \mathbf{E} = \frac{1}{2} (\nabla \mathbf{U} + (\nabla \mathbf{U})^t) = \frac{\dot{\gamma}}{2} \begin{bmatrix} 0 & 1 & 0 \\ 1 & 0 & 0 \\ 0 & 0 & 0 \end{bmatrix} \quad (3.30)$$

in which the superscript  $t$  denotes a transposed tensor, and  $\dot{\gamma}$  is the shear rate and a constant representing the strength of a shear flow. Also,  $\varepsilon$  appeared as the last term in the second equation of Eq. (3.28) is a third-rank tensor called “Eddington’s epsilon.” The  $ijk$ -component of this tensor,  $\varepsilon_{ijk}$ , is expressed as

$$\varepsilon_{ijk} = \begin{cases} 1 & \text{for } (i,j,k) = (x,y,z), (y,z,x), (z,x,y) \\ -1 & \text{for } (i,j,k) = (z,y,x), (y,x,z), (x,z,y) \\ 0 & \text{for the other cases} \end{cases} \quad (3.31)$$

With these characteristics of  $\varepsilon_{ijk}$  and  $\mathbf{E}$  in Eq. (3.30), the last term of the second equation in Eq. (3.28) can be simplified to

$$-\frac{Y^H}{Y^C} (\boldsymbol{\varepsilon} \cdot \mathbf{e}_i \mathbf{e}_i) : \mathbf{E} = -\frac{Y^H}{Y^C} \cdot \frac{\dot{\gamma}}{2} \begin{bmatrix} e_{iz} e_{ix} \\ -e_{iz} e_{iy} \\ e_{iy}^2 - e_{ix}^2 \end{bmatrix} \quad (3.32)$$

In obtaining Eq. (3.32), the following simple formulae have been used:

$$\mathbf{a}\mathbf{b} = \begin{bmatrix} a_x b_x & a_x b_y & a_x b_z \\ a_y b_x & a_y b_y & a_y b_z \\ a_z b_x & a_z b_y & a_z b_z \end{bmatrix} \quad (3.33)$$

$$\mathbf{A} : \mathbf{B} = A_{xx}B_{xx} + A_{xy}B_{yx} + A_{xz}B_{zx} + A_{yx}B_{xy} + A_{yy}B_{yy} + A_{yz}B_{zy} + A_{zx}B_{xz} + A_{zy}B_{yz} + A_{zz}B_{zz} \quad (3.34)$$

$$(\boldsymbol{\varepsilon} \cdot \mathbf{a}\mathbf{b}) : \mathbf{A} = \begin{bmatrix} a_z(b_x A_{xy} + b_y A_{yy} + b_z A_{zy}) - a_y(b_x A_{xz} + b_y A_{yz} + b_z A_{zz}) \\ a_x(b_x A_{xz} + b_y A_{yz} + b_z A_{zz}) - a_z(b_x A_{xx} + b_y A_{yx} + b_z A_{zx}) \\ a_y(b_x A_{xx} + b_y A_{yx} + b_z A_{zx}) - a_x(b_x A_{xy} + b_y A_{yy} + b_z A_{zy}) \end{bmatrix} \quad (3.35)$$

in which  $\mathbf{a}$  and  $\mathbf{b}$  are arbitrary one-rank tensors,  $\mathbf{A}$  and  $\mathbf{B}$  are arbitrary two-rank tensors, and  $\boldsymbol{\epsilon}$  is the three-rank tensor previously defined.

The quantities used to determine the translational and angular velocities from Eqs. (3.27) and (3.28) can be obtained from the force  $\mathbf{F}_i$  and torque  $\mathbf{T}_i$  acting on particle  $i$  and also from the particle direction  $\mathbf{e}_i$  as

$$\left. \begin{aligned} \mathbf{F}_i^{\parallel} &= (\mathbf{F}_i \cdot \mathbf{e}_i) \mathbf{e}_i, & \mathbf{F}_i^{\perp} &= \mathbf{F}_i - \mathbf{F}_i^{\parallel}, & \mathbf{T}_i^{\parallel} &= (\mathbf{T}_i \cdot \mathbf{e}_i) \mathbf{e}_i, \\ \mathbf{T}_i^{\perp} &= \mathbf{T}_i - \mathbf{T}_i^{\parallel}, & \boldsymbol{\Omega}_i^{\parallel} &= (\boldsymbol{\Omega}_i \cdot \mathbf{e}_i) \mathbf{e}_i, & \boldsymbol{\Omega}_i^{\perp} &= \boldsymbol{\Omega}_i - \boldsymbol{\Omega}_i^{\parallel} \end{aligned} \right\} \quad (3.36)$$

With the solutions of  $\mathbf{v}_i(t)$  and  $\boldsymbol{\omega}_i(t)$ , the particle position  $\mathbf{r}_i(t + \Delta t)$  and the particle direction  $\mathbf{e}_i(t + \Delta t)$  at the next time step can be evaluated from Eqs. (1.45) and (1.46). That is,

$$\mathbf{r}_i(t + \Delta t) = \mathbf{r}_i(t) + \Delta t \mathbf{v}_i(t) \quad (3.37)$$

$$\mathbf{e}_i(t + \Delta t) = \mathbf{e}_i(t) + \Delta t \boldsymbol{\omega}_i^{\perp}(t) \times \mathbf{e}_i(t) \quad (3.38)$$

Finally, we discuss the resistance functions  $X^A$ ,  $Y^A$ ,  $X^C$ ,  $Y^C$ , and  $Y^H$  [4,16–18]. There would be no difficulties for simulations if the solutions of these resistance functions were known for a spherocylinder particle. However, the solutions are known only for a cylindrical particle with sufficiently large aspect ratio, or for the spherical particle explained before. These solutions are for a solid particle, but in our case we are considering a solid particle coated with a soft steric layer, and the resistance functions have not yet been solved for this case.

Hence, in conducting MD simulations for the present particle dispersion, we have several options for overcoming the problem for the resistance functions. The first option is to tackle the difficult mathematical problem of solving these resistance functions. The second option is to apply the known solutions of a solid spheroidal particle as the first approximation. The third option is to introduce the modeling of the spherocylinder particle in order for the known solutions to be applied more accurately. Here we adopt the second option, that is, the solutions shown in Eqs. (1.35) and (1.36) for a solid spheroid are used for the resistance functions for the spherocylinder shown in Figure 3.4. In addition, the resistance function  $Y^H$  can be written as

$$Y^H = 8\pi a^3 \cdot \frac{4}{3} \cdot \frac{s^5}{-2s + (1 + s^2)L} \quad (3.39)$$

In the limiting case of  $s \ll 1$ , this can be approximated as

$$Y^H = 8\pi a^3 \left( \frac{1}{2}s^2 - \frac{1}{5}s^4 + \dots \right) \quad (3.40)$$

in which  $a$ ,  $b$ , and  $s$  are assumed to be expressed as  $a = l/2 + \delta$ ,  $b = d/2 + \delta$ , and  $s = \sqrt{(l/2 + \delta)^2 - (d/2 + \delta)^2}/(l/2 + \delta)$ , respectively.

### 3.2.4 Modeling of Steric Repulsive Interaction

If the two spherocylinder particles coated with a surfactant layer, shown in Figure 3.4, overlap, how should we write this repulsive interaction as a mathematical expression? To answer this question, we first need to analyze the behavior of the surfactant molecules in detail in such a situation. However, it may be possible to develop a physically acceptable model as a first approximation by combining the known solutions in a sophisticated manner. For a spherical particle system, an expression for the repulsive interaction has already been obtained. Hence, the extension of this potential to the present spherocylinder particle system enables us to overcome the problem of the unknown potential for a spherocylinder coated with a soft surfactant layer.

We consider a spherical particle modeled as a solid sphere of diameter  $d$  coated by a uniform surfactant layer of thickness  $\delta$ . An interaction energy arising from the overlap of these two particles has already been derived from the entropy calculation as [31,32]

$$u_{ij}^{(V)} = \frac{\pi d^2 n_s k T}{2} \left\{ 2 - \left( \frac{r_{ij}}{\delta} \right) \ln \left( \frac{d + 2\delta}{r_{ij}} \right) - \frac{r_{ij} - d}{\delta} \right\} \quad (3.41)$$

in which  $n_s$  is the number of surfactant molecules per unit area on the particle surface,  $k$  is Boltzmann's constant, and  $T$  is the system temperature. The force acting on particle  $i$ ,  $\mathbf{F}_{ij}^{(V)}$ , by particle  $j$  due to the overlap can be obtained from this equation as

$$\mathbf{F}_{ij}^{(V)} = -\frac{\partial}{\partial \mathbf{r}_i} u_{ij}^{(V)} = -\frac{\partial}{\partial \mathbf{r}_{ij}} u_{ij}^{(V)} = \frac{\pi d^2 n_s k T}{2\delta} \mathbf{t}_{ij} \ln \left( \frac{d + 2\delta}{r_{ij}} \right) \quad (\text{for } d \leq r_{ij} \leq d + 2\delta) \quad (3.42)$$

in which  $\mathbf{t}_{ij}$  ( $= \mathbf{r}_{ij}/r_{ij}$ ) is the unit vector. It is shown in Eq. (3.42) that this repulsive force acts along a line drawn between the two particles.

We now idealize the spherocylinder particle in order to apply Eq. (3.42). The most feasible model is a linear sphere-connected model shown in Figure 3.5. In this model, solid spheres are linearly connected in contact and covered by a uniform surfactant layer of thickness  $\delta$ . If the constituent spherical particles are located at each fixed position in the rod-like particle, this model does not necessarily yield

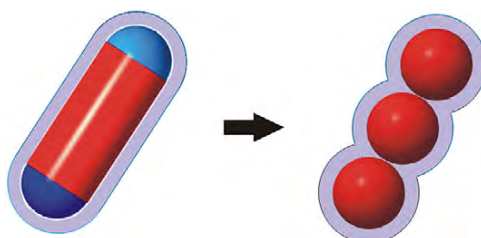


**Figure 3.5** Sphere-connected model for calculating repulsive interactions.

a maximum repulsive interaction energy at a position where the maximum energy is provided from the overlap of the original spherocylinder particles. In order to overcome this shortcoming, the above model must be slightly modified to yield a maximum repulsive energy at a position of minimum separation between the two spherocylinder particles. To do so, two spheres are first located at the positions in each spherocylinder, where a maximum repulsive energy is yielded, and then other spheres are linearly added on each side of these two spheres on the original particle to produce a modified sphere-connected model. This is the particle model we use for evaluating interaction energies due to particle overlap.

In the following paragraphs, we show a method for calculating the force and torque acting between particles  $i$  and  $j$  based on the above-mentioned sphere-connected model. An important task for evaluating such a force and torque is to find the positions along each particle axis at which the separation between the two spherocylinder particles is minimized for the given position and orientation of these two particles. Hence, we focus on a method for finding this minimum separation, including a way of assessing the particle overlap.

The notation  $\mathbf{r}_i$  is used for the center of spherocylinder particle  $i$  shown in Figure 3.4; similarly,  $\mathbf{r}_j$  is used for particle  $j$ . Figure 3.6 demonstrates that there is a view angle from which the two particles can be seen as existing in two parallel planes. In Figure 3.6, two points  $P_i$  and  $P_j$  are taken on each particle axis line such that the line drawn between these points is normal to the two parallel planes. Consideration of the two points  $P_i$  and  $P_j$  enables us to make a systematic and sophisticated assessment of the particle overlap. If the points  $P_i$  and  $P_j$  are denoted by  $(\mathbf{r}_i + k_i \mathbf{e}_i)$  and  $(\mathbf{r}_j + k_j \mathbf{e}_j)$ , respectively, the line  $\overline{P_i P_j}$  has to satisfy the following equation from the orthogonality condition:

$$\mathbf{e}_i \cdot \{(\mathbf{r}_i + k_i \mathbf{e}_i) - (\mathbf{r}_j + k_j \mathbf{e}_j)\} = 0, \quad \mathbf{e}_j \cdot \{(\mathbf{r}_i + k_i \mathbf{e}_i) - (\mathbf{r}_j + k_j \mathbf{e}_j)\} = 0 \quad (3.43)$$

The solutions of  $k_i$  and  $k_j$  satisfying this relationship leads to the determination of the specific positions of  $P_i$  and  $P_j$ . Equation (3.43) yields the final results as

$$\begin{bmatrix} k_i \\ k_j \end{bmatrix} = \frac{1}{1 - (\mathbf{e}_i \cdot \mathbf{e}_j)^2} \begin{bmatrix} -1 & \mathbf{e}_i \cdot \mathbf{e}_j \\ -\mathbf{e}_i \cdot \mathbf{e}_j & 1 \end{bmatrix} \begin{bmatrix} \mathbf{e}_i \cdot \mathbf{r}_{ij} \\ \mathbf{e}_j \cdot \mathbf{r}_{ij} \end{bmatrix} \quad (3.44)$$

This equation has been derived under the assumption of  $\mathbf{e}_i \cdot \mathbf{e}_j \neq \pm 1$ . This condition is necessary for the existence of the solution because  $\mathbf{e}_i \cdot \mathbf{e}_j = \pm 1$  implies a parallel

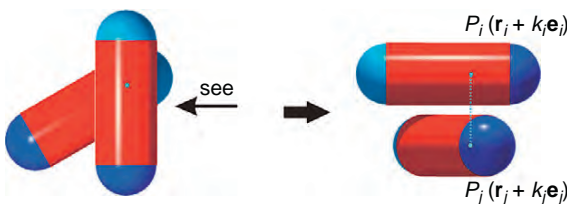


**Figure 3.6** Assessment of the particle overlap.

or line configuration of the particles. If the line  $\overline{P_i P_j}$  is longer than  $(d + 2\delta)$ , there is no particle overlap. Hence, we first consider the general case under the assumptions that  $\mathbf{e}_i \cdot \mathbf{e}_j \neq \pm 1$  and the line  $\overline{P_i P_j}$  is shorter than  $(d + 2\delta)$ .

There are three cases of overlap for the two spherocylinder particles: that is, hemisphere–hemisphere, hemisphere–cylinder, and cylinder–cylinder overlap. We first consider a cylinder–cylinder overlap between particles  $i$  and  $j$ . The condition for this overlap is derived as

$$|(\mathbf{r}_i + k_i \mathbf{e}_i) - (\mathbf{r}_j + k_j \mathbf{e}_j)| < d + 2\delta, \quad |k_i| < l_0/2, \quad |k_j| < l_0/2 \quad (3.45)$$

Next, we consider the criterion for the overlap between the cylindrical part of particle  $i$  and the hemisphere cap of particle  $j$ . In this case, the conditions of  $|k_i| < l_0/2$  and  $|k_j| \geq l_0/2$  are satisfied. A vertical line is drawn from the center of the hemisphere to the axis line of particle  $i$ , and the intersection point on this axis line of particle  $i$  is denoted by  $Q_{i(j)}$ , which is expressed as  $(\mathbf{r}_i + k_i^s \mathbf{e}_i)$  with an unknown constant  $k_i^s$ . The determination of  $k_i^s$  yields explicit specification of the position  $Q_{i(j)}$ . If the center of hemisphere of particle  $j$  is denoted by  $\mathbf{r}_j^s$  (similarly  $\mathbf{r}_i^s$  for particle  $i$ ), then  $k_i^s$  is solved from the orthogonality condition of  $(\mathbf{r}_i + k_i^s \mathbf{e}_i - \mathbf{r}_j^s)$  and  $\mathbf{e}_i$ :

$$k_i^s = \mathbf{e}_i \cdot (\mathbf{r}_j^s - \mathbf{r}_i) \quad (3.46)$$

The use of this solution of  $k_i^s$  gives rise to the criterion condition for the overlap between the cylindrical part of particle  $i$  and the hemisphere cap of particle  $j$  as

$$|k_i^s| \leq l_0/2, \quad |(\mathbf{r}_i + k_i^s \mathbf{e}_i) - \mathbf{r}_j^s| < d + 2\delta \quad (3.47)$$

Finally, the overlap between the hemisphere caps between particles  $i$  and  $j$  arises when the following condition is satisfied:

$$|k_i^s| > l_0/2, \quad |\mathbf{r}_i^s - \mathbf{r}_j^s| < d + 2\delta \quad (3.48)$$

The above-mentioned criterion conditions are summarized as follows:

1. For  $|(\mathbf{r}_i + k_i \mathbf{e}_i) - (\mathbf{r}_j + k_j \mathbf{e}_j)| \geq d + 2\delta$ , there is no overlap.
2. For  $|(\mathbf{r}_i + k_i \mathbf{e}_i) - (\mathbf{r}_j + k_j \mathbf{e}_j)| < d + 2\delta$ , there is a possibility of overlap.
  - 2.1. For  $|k_i| \leq l_0/2$  and  $|k_j| \leq l_0/2$ , an overlap occurs.
  - 2.2. For  $|k_i| \leq l_0/2$  and  $|k_j| > l_0/2$  and  $|k_i^s| < l_0/2$ , there is a possibility of overlap between the cylinder part of particle  $i$  and the hemisphere cap of particle  $j$ .
    - 2.2.1.  $|(\mathbf{r}_i + k_i^s \mathbf{e}_i) - \mathbf{r}_j^s| \geq d + 2\delta$ , there is no overlap.
    - 2.2.2.  $|(\mathbf{r}_i + k_i^s \mathbf{e}_i) - \mathbf{r}_j^s| < d + 2\delta$ , an overlap occurs.
  - 2.3. For  $|k_i| \leq l_0/2$  and  $|k_j| > l_0/2$  and  $|k_i^s| \geq l_0/2$ , there is a possibility of overlap between the hemisphere caps between particles  $i$  and  $j$ .
    - 2.3.1. For  $|\mathbf{r}_i^s - \mathbf{r}_j^s| \geq d + 2\delta$ , there is no overlap.
    - 2.3.2. For  $|\mathbf{r}_i^s - \mathbf{r}_j^s| < d + 2\delta$ , an overlap occurs.
  - 2.4. For  $|k_j| > |k_i| > l_0/2$  and  $|k_i^s| < l_0/2$ , there is a possibility of overlap between the cylinder part of particle  $i$  and the hemisphere cap of particle  $j$ .
    - 2.4.1. For  $|(\mathbf{r}_i + k_i^s \mathbf{e}_i) - \mathbf{r}_j^s| \geq d + 2\delta$ , there is no overlap.
    - 2.4.2. For  $|(\mathbf{r}_i + k_i^s \mathbf{e}_i) - \mathbf{r}_j^s| < d + 2\delta$ , an overlap occurs.

**2.5.** For  $|k_j| > |k_i| > l_0/2$  and  $|k_i^s| \geq l_0/2$ , there is a possibility of overlap between the hemisphere caps between particles  $i$  and  $j$ .

**2.5.1.** For  $|\mathbf{r}_i^s - \mathbf{r}_j^s| \geq d + 2\delta$ , there is no overlap.

**2.5.2.** For  $|\mathbf{r}_i^s - \mathbf{r}_j^s| < d + 2\delta$ , an overlap occurs.

These overlap criteria have been shown under the assumption of  $|k_j| > |k_i|$ . However, the above description is sufficient on the analysis level, because the exchange of subscripts  $i$  and  $j$  in a simulation program reduces to the same criterion procedure for particle overlap.

In addition to particle overlap in a general configuration, we need to consider several special cases, that is, particle overlap in a parallel or line configuration. The latter is straightforward to analyze and therefore we address the former case. According to the distance  $|k_{ij}^c|$  ( $= |\mathbf{r}_{ij} \cdot \mathbf{e}_i|$ ) between the centers of particles  $i$  and  $j$  along the particle axis, whether or not particles  $i$  and  $j$  overlap can be determined by the following procedures:

**1.** For  $|k_{ij}^c| \leq l_0$ , an overlap occurs.

**2.** For  $|k_{ij}^c| > l_0$ ,

**2.1.** For  $|\mathbf{r}_i^s - \mathbf{r}_j^s| \geq d + 2\delta$ , there is no overlap.

**2.2.** For  $|\mathbf{r}_i^s - \mathbf{r}_j^s| < d + 2\delta$ , an overlap occurs.

If the particle separation satisfies  $(|\mathbf{r}_{ij}|^2 - |k_{ij}^c|^2)^{1/2} \geq d + 2\delta$ , then overlap does not occur.

The above-assessing procedures concerning particle overlap enable us to recognize a specific configuration of the two particles in which the minimum distance can be obtained from the line of each particle axis. The notation  $\mathbf{r}_i^{(\min)}$  and  $\mathbf{r}_j^{(\min)}$  is used for expressing such positions on the axis lines. The present modified linear sphere-connected model for particle  $i$  can be constructed by placing other spheres on both sides of the sphere at  $\mathbf{r}_i^{(\min)}$  repeatedly. According to this model, a force acting on particle  $i$  by particle  $j$ , arising from the overlap of the steric layers, can be obtained by evaluating the interaction forces between the constituent spherical particles and then by summing these interactions. Similarly, a torque acting on particle  $i$  by particle  $j$  can be evaluated by performing the vector product of each force vector of the constituent spheres and the corresponding relative position vectors from the center of particle  $i$ .

### 3.2.5 Nondimensionalization of Basic Equations

In actual simulations, it is usual to treat a nondimensional system in which quantities are nondimensionalized by the corresponding representative values. The present simulation employs the following representative values for nondimensionalization:  $d$  for distances,  $1/\dot{\gamma}$  for time,  $\dot{\gamma}d$  for velocities,  $\dot{\gamma}$  for angular velocities,  $3\pi\eta\dot{\gamma}d^2$  for forces,  $\pi\eta\dot{\gamma}d^3$  for torques, and so on. With these representative values, the equations of motion in Eqs. (3.27) and (3.28) are nondimensionalized as

$$\mathbf{v}_i^{\parallel*} = \mathbf{U}^{\parallel*}(\mathbf{r}_i^*) + \frac{\mathbf{F}_i^{\parallel*}}{X^{A*}(l^* + 2\delta^*)}, \quad \mathbf{v}_i^{\perp*} = \mathbf{U}^{\perp*}(\mathbf{r}_i^*) + \frac{\mathbf{F}_i^{\perp*}}{Y^{A*}(l^* + 2\delta^*)} \quad (3.49)$$

$$\omega_i^{\perp*} = \Omega^{\perp*} + \frac{\mathbf{T}_i^{\perp*}}{Y^{C*}(l^* + 2\delta^*)^3} - \frac{Y^{H*}}{Y^{C*}}(\boldsymbol{\varepsilon} \cdot \mathbf{e}_i \mathbf{e}_i) : \mathbf{E}^* \quad (3.50)$$

in which

$$\left. \begin{aligned} X^{A*} &= \frac{X^A}{6\pi(l/2 + \delta)} = \frac{8}{3} \cdot \frac{s^3}{-2s + (1 + s^2)L} \\ Y^{A*} &= \frac{Y^A}{6\pi(l/2 + \delta)} = \frac{16}{3} \cdot \frac{s^3}{2s + (3s^2 - 1)L} \end{aligned} \right\} \quad (3.51)$$

$$Y^{C*} = \frac{Y^C}{8\pi(l/2 + \delta)^3} = \frac{4}{3} \cdot \frac{s^3(2 - s^2)}{-2s + (1 + s^2)L} \quad (3.52)$$

$$Y^{H*} = \frac{Y^H}{8\pi(l/2 + \delta)^3} = \frac{4}{3} \cdot \frac{s^5}{-2s + (1 + s^2)L} \quad (3.53)$$

$$\mathbf{E}^* = \frac{1}{2} \begin{bmatrix} 0 & 1 & 0 \\ 1 & 0 & 0 \\ 0 & 0 & 0 \end{bmatrix}, \quad \Omega^* = -\frac{1}{2} \begin{bmatrix} 0 \\ 0 \\ 1 \end{bmatrix}, \quad (\boldsymbol{\varepsilon} \cdot \mathbf{e}_i \mathbf{e}_i) : \mathbf{E}^* = \frac{1}{2} \begin{bmatrix} e_{iz}e_{ix} \\ -e_{iz}e_{iy} \\ e_{iy}^2 - e_{ix}^2 \end{bmatrix} \quad (3.54)$$

Also, Eqs. (3.37) and (3.38) can be written in nondimensionalized form as

$$\begin{aligned} \mathbf{r}_i^*(t^* + \Delta t^*) &= \mathbf{r}_i^*(t^*) + \Delta t^* \mathbf{v}_i^*(t^*), \\ \mathbf{e}_i(t^* + \Delta t^*) &= \mathbf{e}_i(t^*) + \Delta t^* \omega_i^{\perp*}(t^*) \times \mathbf{e}_i(t^*) \end{aligned} \quad (3.55)$$

The forces acting on the positive and negative magnetic charges of particle  $i$  in Eqs. (3.21) and (3.22) are nondimensionalized as

$$\mathbf{F}_{ij}^{+*} = \lambda_m \left\{ \frac{\mathbf{r}_{ij}^* + (l_0^*/2)(\mathbf{e}_i - \mathbf{e}_j)}{\left| \mathbf{r}_{ij}^* + (l_0^*/2)(\mathbf{e}_i - \mathbf{e}_j) \right|^3} - \frac{\mathbf{r}_{ij}^* + (l_0^*/2)(\mathbf{e}_i + \mathbf{e}_j)}{\left| \mathbf{r}_{ij}^* + (l_0^*/2)(\mathbf{e}_i + \mathbf{e}_j) \right|^3} \right\} \quad (3.56)$$

$$\mathbf{F}_{ij}^{-*} = -\lambda_m \left\{ \frac{\mathbf{r}_{ij}^* - (l_0^*/2)(\mathbf{e}_i + \mathbf{e}_j)}{\left| \mathbf{r}_{ij}^* - (l_0^*/2)(\mathbf{e}_i + \mathbf{e}_j) \right|^3} - \frac{\mathbf{r}_{ij}^* - (l_0^*/2)(\mathbf{e}_i - \mathbf{e}_j)}{\left| \mathbf{r}_{ij}^* - (l_0^*/2)(\mathbf{e}_i - \mathbf{e}_j) \right|^3} \right\} \quad (3.57)$$

in which  $ql_0$  is the magnitude of a magnetic moment, expressed as  $m = ql_0$ , and  $\lambda_m$  is the nondimensional parameter representing the strength of magnetic forces relative to the shear force of a simple shear flow, expressed as

$$\lambda_m = \frac{\mu_0 m^2}{12\pi^2 \eta \dot{\gamma} l_0^2 d^4} \quad (3.58)$$

The nondimensionalization procedure generally leads to the appearance of such nondimensional numbers; the most famous nondimensional number—the Reynolds number, in fluid mechanics—arises from a similar nondimensional procedure.

Similarly, the torque acting on particle  $i$  by particle  $j$  in Eqs. (3.23) and (3.24) is nondimensionalized as

$$\mathbf{T}_{ij}^{+*} = \frac{3l_0^*}{2} \lambda_m \left\{ \frac{\mathbf{e}_i \times \mathbf{r}_{ij}^* - (l_0^*/2)(\mathbf{e}_i \times \mathbf{e}_j)}{\left| \mathbf{r}_{ij}^* + (l_0^*/2)(\mathbf{e}_i - \mathbf{e}_j) \right|^3} - \frac{\mathbf{e}_i \times \mathbf{r}_{ij}^* + (l_0^*/2)(\mathbf{e}_i \times \mathbf{e}_j)}{\left| \mathbf{r}_{ij}^* + (l_0^*/2)(\mathbf{e}_i + \mathbf{e}_j) \right|^3} \right\} \quad (3.59)$$

$$\mathbf{T}_{ij}^{-*} = \frac{3l_0^*}{2} \lambda_m \left\{ \frac{\mathbf{e}_i \times \mathbf{r}_{ij}^* - (l_0^*/2)(\mathbf{e}_i \times \mathbf{e}_j)}{\left| \mathbf{r}_{ij}^* - (l_0^*/2)(\mathbf{e}_i + \mathbf{e}_j) \right|^3} - \frac{\mathbf{e}_i \times \mathbf{r}_{ij}^* + (l_0^*/2)(\mathbf{e}_i \times \mathbf{e}_j)}{\left| \mathbf{r}_{ij}^* - (l_0^*/2)(\mathbf{e}_i - \mathbf{e}_j) \right|^3} \right\} \quad (3.60)$$

The torque exerted by an applied magnetic field in Eq. (3.26) is written in non-dimensional form:

$$\mathbf{T}_i^{(H)*} = \lambda_H \mathbf{e}_i \times \mathbf{h} \quad (3.61)$$

in which  $\mathbf{h}$  is a unit vector denoting the magnetic field direction, expressed as  $\mathbf{h} = \mathbf{H}/H$ . As before,  $\lambda_H$  is a nondimensional parameter representing the strength of magnetic particle–field interactions relative to the torque due to the shear flow force, expressed as

$$\lambda_H = \frac{\mu_0 m H}{\pi \eta \dot{\gamma} d^3} \quad (3.62)$$

The repulsive force due to the overlap of the surfactant layers in Eq. (3.42) is nondimensionalized as

$$\mathbf{F}_{ij}^{(V)*} = \lambda_V \mathbf{t}_{ij} \ln \left( \frac{1 + 2\delta^*}{r_{ij}^*} \right) \quad (\text{for } 1 \leq r_{ij}^* \leq 1 + 2\delta^*) \quad (3.63)$$

in which  $\lambda_V$  is a nondimensional parameter representing the strength of such repulsive forces relative to the shear flow force.

We have finished nondimensionalizing almost all the quantities necessary for simulations. The nondimensional parameters characterizing the physical phenomenon are  $\lambda_m$  for magnetic particle–particle interactions,  $\lambda_H$  for magnetic particle–field interactions, and  $\lambda_V$  for steric repulsive interactions.

### 3.2.6 Treatment of the Criteria for Particle Overlap in Simulations

In the previous subsection on the modeling of steric repulsive interactions, we presented a mathematical discussion on the assessment for the overlap of the steric layers. In actual calculations in a simulation program, the systematic classification

of the overlapping regimes enables us to quickly grasp a logical flow of the calculation procedures; this subject may be on a technical side rather than a mathematical one. As shown in Table 3.1, particle overlapping can be classified into four cases: that is, a general overlap ( $\text{itree} = 1$ ), a linear overlap ( $\text{itree} = 0$ ), a normal overlap ( $\text{itree} = 2$ ), and a parallel overlap ( $\text{itree} = 3$ ). Note that the variable names “ $\text{itree}$ ” and “ $\text{ipath}$ ” are commonly used in a simulation program, so that the overlap treatment is conducted for the cases specified by “ $\text{itree}$ ” and “ $\text{ipath}$ ” in a simulation program. The important point in a simulation program is that if  $|k_j| < |k_i|$ , then the overlap regimes shown in Table 3.1 are easily applicable after the replacement of indices  $i$  and  $j$  by  $j$  and  $i$ . Hence, the assumption of the condition  $|k_j| \geq |k_i|$  for starting a mathematical analysis provides a relatively straightforward classification without losing our way in a mathematical labyrinth. The classification in the substage for each case depends on which hemisphere cap of particle  $j$  overlaps with particle  $i$ . That is, the directions of particles  $i$  and  $j$  are important for the successive treatment of repulsive interactions. For a linear overlapping case, the calculation of the repulsive force between only one pair of the spheres completes the overlapping treatment. On the other hand, for the other overlapping cases, two spheres are first placed at the nearest separation positions on each axis line, as previously explained, in order to calculate the force and torque for this pair of spheres. Then, other spheres are repeatedly added to the both ends of each sphere in linear formation to form the linear sphere-connected particles  $i$  and  $j$ . Finally, the interaction forces and torques are calculated for each pair of constituent spheres of particles  $i$  and  $j$ ; the summation of these forces and torques for each pair of spheres yields the total force and torque acting on particle  $i$  by particle  $j$ . For example, we briefly consider the case of  $\text{itree} = 1$  and  $\text{ipath} = 1$  in Table 3.1. The positions of the two spheres are first determined on each axis line, and then the next spheres are placed at each neighboring position in the  $(-\mathbf{n}_i)$  and  $(-\mathbf{n}_j)$  directions; the repulsive forces and torques are calculated for each pair of these constituent spheres.

### 3.2.7 Parameters for Simulations

We set the following initial conditions for simulations. A magnetic field is applied in the  $y$ -axis direction, and a simple shear flow is applied in the  $x$ -direction. The spherocylinder particles are expected to aggregate in the magnetic field direction ( $y$ -axis direction) because they are magnetized in the particle axis direction. Hence we employ a rectangular-parallelepiped simulation box, with its longer axis along the field direction with a square base. We first place six rows of particles in the  $x$ -axis direction with their particle axis pointing to the  $y$ -axis direction, then repeat this procedure in the  $z$ -direction to obtain the initial configuration of 36 particles in the  $xz$ -plane. Finally, we expand this configuration in the  $y$ -axis direction to obtain the total six layers of these particles. The initial configuration of 216 particles, therefore, can be assigned from this procedure. A rectangular-parallelepiped simulation box needs to be set, with an appropriate aspect ratio dependent upon the particle aspect ratio. The present simulation uses a simulation box where the length in the  $y$ -axis direction is twice the length in the  $x$ -axis direction; note that the

**Table 3.1** Regime of Overlap

1. itree = 1 <p> <b>ipath = 1</b>  <math>(\mathbf{n}_i \cdot \mathbf{n}_j \geq 0, k_j \geq 0)</math> </p> <p> <b>ipath = 2</b>  <math>(\mathbf{n}_i \cdot \mathbf{n}_j &lt; 0, k_j &lt; 0)</math> </p> <p> <b>ipath = 3</b>  <math>(\mathbf{n}_i \cdot \mathbf{n}_j &lt; 0, k_j \geq 0)</math> </p> <p> <b>ipath = 4</b>  <math>(\mathbf{n}_i \cdot \mathbf{n}_j \geq 0, k_j &lt; 0)</math> </p>			
2. itree = 0			
	<p> <b>ipath = 1</b>  <math>(\mathbf{n}_i \cdot \mathbf{n}_j \geq 0, \mathbf{t}_{ij} \cdot \mathbf{n}_j \geq 0)</math> </p>	<p> <b>ipath = 2</b>  <math>(\mathbf{n}_i \cdot \mathbf{n}_j \geq 0, \mathbf{t}_{ij} \cdot \mathbf{n}_j &lt; 0)</math> </p>	
	<p> <b>ipath = 3</b>  <math>(\mathbf{n}_i \cdot \mathbf{n}_j &lt; 0, \mathbf{t}_{ij} \cdot \mathbf{n}_j \geq 0)</math> </p>	<p> <b>ipath = 4</b>  <math>(\mathbf{n}_i \cdot \mathbf{n}_j &lt; 0, \mathbf{t}_{ij} \cdot \mathbf{n}_j &lt; 0)</math> </p>	
3. itree = 2			
	<p> <b>ipath = 1</b>  <math>(k_j \geq 0)</math> </p>	<p> <b>ipath = 2</b>  <math>(k_j &lt; 0)</math> </p>	
4. itree = 3			
	<p> <b>ipath = 1</b>  <math>(\mathbf{n}_i \cdot \mathbf{n}_j \geq 0)</math> </p>	<p> <b>ipath = 2</b>  <math>(\mathbf{n}_i \cdot \mathbf{n}_j &lt; 0, k_j^s \leq -l_0/2)</math> </p>	<p> <b>ipath = 3</b>  <math>(\mathbf{n}_i \cdot \mathbf{n}_j &lt; 0, k_j^s &gt; -l_0/2)</math> </p>

Note that  $\mathbf{n}_i$  is used as  $\mathbf{e}_i$ .

above-mentioned setting procedure is slightly different from that explained in Section 2.1.2. In the present simulation, the particle aspect ratio  $r_p$  is taken as  $r_p = 5$ , the volumetric fraction as  $\phi_V = 0.05$ , and the thickness of a surfactant layer as  $\delta^* = 0.15$ .

A shear flow and a magnetic field have a tendency to make the spherocylinder particles incline in the flow direction and in the applied direction, respectively. The orientational behavior of the magnetic spherocylinder particles, therefore, depends in a complicated manner on the strength of magnetic interactions as well as the flow shear rate. The main objective of the present simulation is to discuss the influences of magnetic particle–field, magnetic particle–particle, and steric repulsive interactions on the behavior of spherocylinder particles in a simple shear flow. Hence, simulations are carried out for various cases of the nondimensional parameters  $\lambda_m$  and  $\lambda_H$  such as  $\lambda_m = 0, 10, 20$ , and  $50$  and  $\lambda_H = 0, 10, 20, 50$ , and  $100$ . On the other hand,  $\lambda_V$  is taken to have the single value  $\lambda_V = 150$ ; a larger value of  $\lambda_V$  induces a large repulsive force at the particle overlapping.

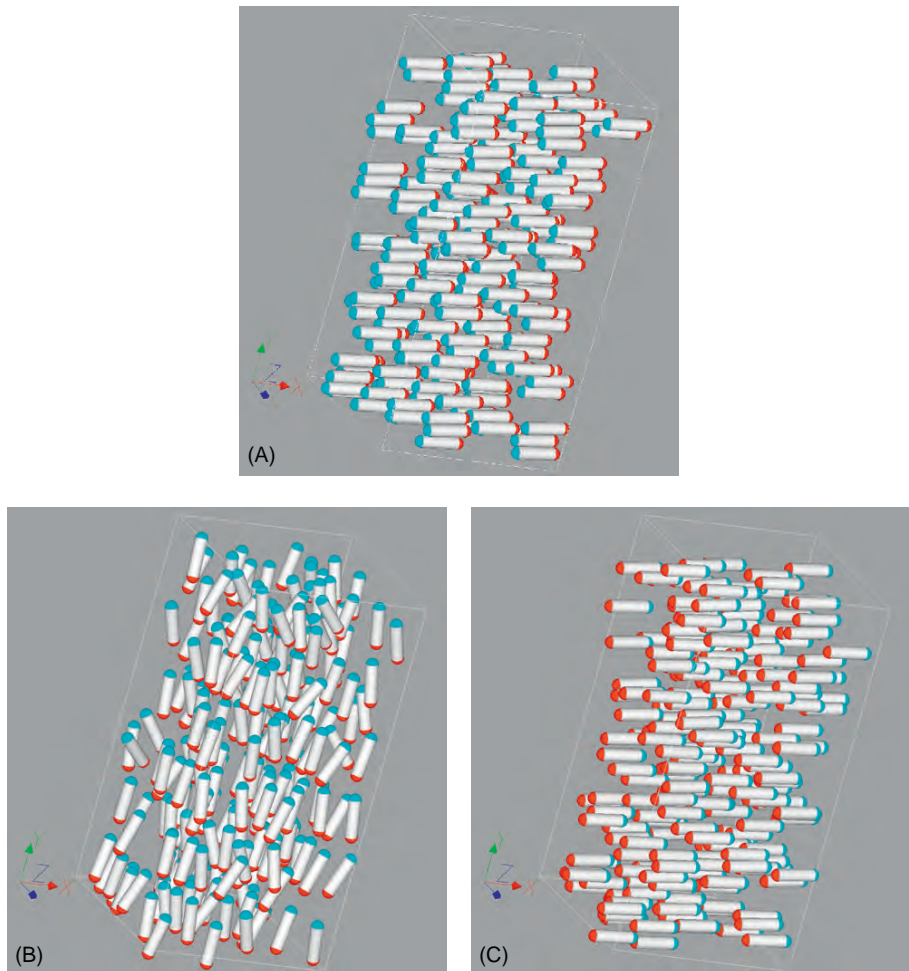
### 3.2.8 Results of Simulations

Figure 3.7 shows the change in aggregate structures with time for no applied magnetic field and no magnetic interactions between particles. The rod-like particles rotate in the  $xy$ -plane about the  $z$ -axis because there is no applied magnetic field. Describing in more detail, the particles incline in the flow direction ( $x$ -axis direction) during a long period as in Figures 3.7A and C. Once particles have been kicked below the  $x$ -axis, they quickly rotate toward the preferred direction, as shown in Figures 3.7A and C by way of a transient snapshot shown in Figure 3.7B. This is because much larger torques act on the rod-like particles when inclining in a direction normal to the flow.

Figure 3.8 shows a snapshot for no applied magnetic field under strong magnetic particle–particle interactions  $\lambda_m = 10$ . The figure on the left-hand side is a general snapshot viewed from a certain angle to grasp how nearly the particles incline in the flow direction. The figure on the right-hand side is an oblique view for grasping the formation of wall-like clusters along the flow direction, that is, it is viewed almost from the negative  $x$ -axis direction. In this case, even if no magnetic field is applied, rod-like particles seldom rotate from the situation in Figure 3.8 because magnetic particle–particle interactions become more dominant than viscous shear forces, and so the particles form complex three-dimensional aggregate structures. However, the individual particles have a tendency to incline in the shear flow direction.

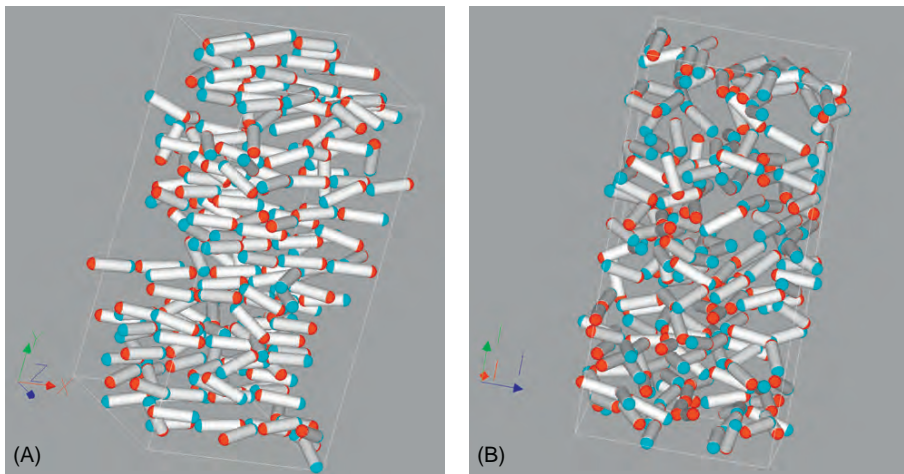
Figure 3.9 shows a snapshot for a strong applied magnetic field  $\lambda_H = 10$  and no magnetic interactions  $\lambda_m = 0$ . In this situation, the applied magnetic field makes rod-like particles incline in the magnetic field direction. The final particle orientation is determined by the balance of the torque due to the applied field and the torque due to a shear flow; in Figure 3.9 all rod-like particles tend to incline in the same direction (the direction of the flow) because there is no disturbance due to magnetic particle–particle interactions.

Figure 3.10 shows the result for magnetic interactions  $\lambda_m = 10$  and for an external magnetic field  $\lambda_H = 10$  as in Figure 3.9. A significant difference to the case of



**Figure 3.7** Time change in aggregate structures for  $\lambda_H = 0$  and  $\lambda_m = 0$ : (A)  $t = t_1$ , (B)  $t = t_2$ , and (C)  $t = t_3$ .

Figure 3.9 is that, to a certain degree, aggregates have wall-like structures along the flow direction. The particle aggregation is due to magnetic interactions between particles, and the viscous forces and torques induce more complex aggregates, such as these wall-like structures. Wall-like clusters are also observed for the case of magnetic spherical particles in an applied magnetic field subject to a simple shear flow. Magnetic particle–particle interactions emphasize the tendency of particles to incline in the flow direction, which is clearly seen by comparing with the case in Figure 3.9. Note that the particles in Figure 3.10 do not orient toward the same preferred direction.



**Figure 3.8** Aggregate structures for  $\lambda_H = 0$  and  $\lambda_m = 10$ : (A) an oblique view and (B) viewed nearly from the negative  $x$ -axis.

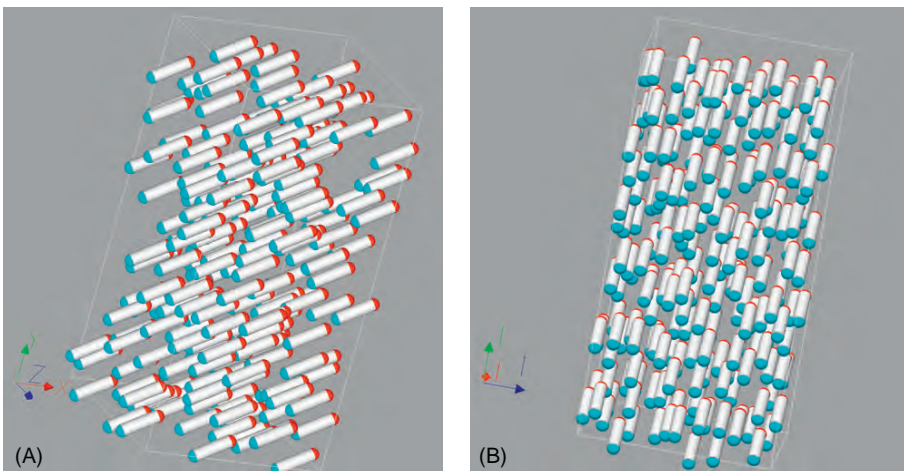


**Figure 3.9** Aggregate structures for  $\lambda_H = 10$  and  $\lambda_m = 0$ : (A) an oblique view and (B) viewed nearly from the negative  $x$ -axis.

Figure 3.11 is a snapshot for a significantly strong applied magnetic field  $\lambda_H = 50$ , but without magnetic particle–particle interactions. Since a magnetic field is significantly strong, each particle inclines to a higher degree in the magnetic field direction ( $y$ -axis direction) as compared with that in Figure 3.9. On the other hand, wall-like clusters are not formed in this case because there are no magnetic interactions.

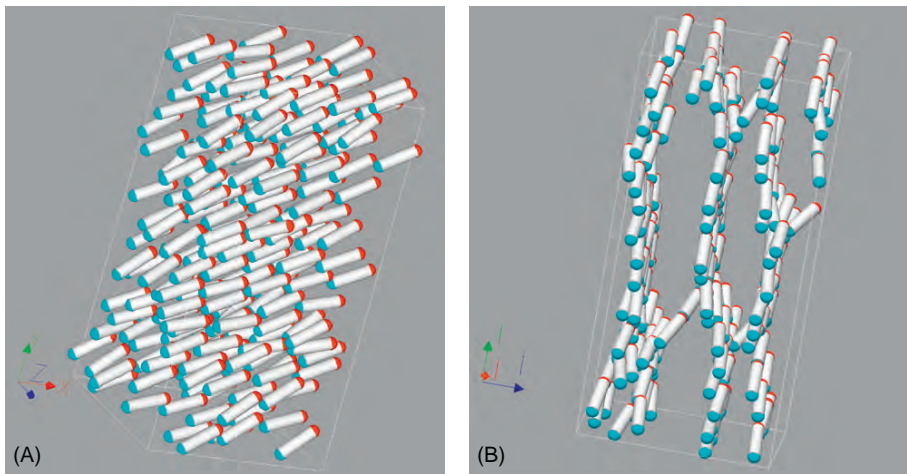


**Figure 3.10** Aggregate structures for  $\lambda_H = 10$  and  $\lambda_m = 10$ : (A) an oblique view and (B) viewed nearly from the negative  $x$ -axis.

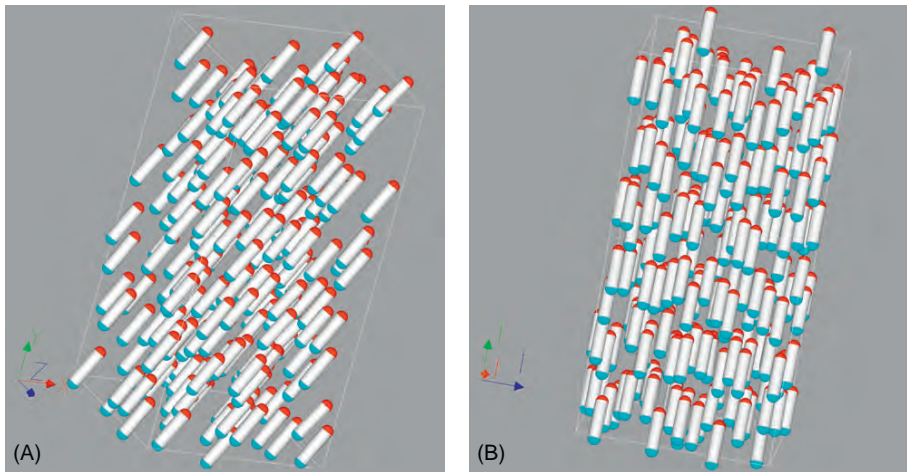


**Figure 3.11** Aggregate structures for  $\lambda_H = 50$  and  $\lambda_m = 0$ : (A) an oblique view and (B) viewed nearly from the negative  $x$ -axis.

Figure 3.12 also shows  $\lambda_H = 50$ , as in Figure 3.11, but magnetic interactions are  $\lambda_m = 10$  in this case. Comparison with Figure 3.10, clearly reveals that wall-like clusters are formed along the flow direction. The detailed observation of the internal structures of wall-like clusters indicates that the rod-like particles aggregate to

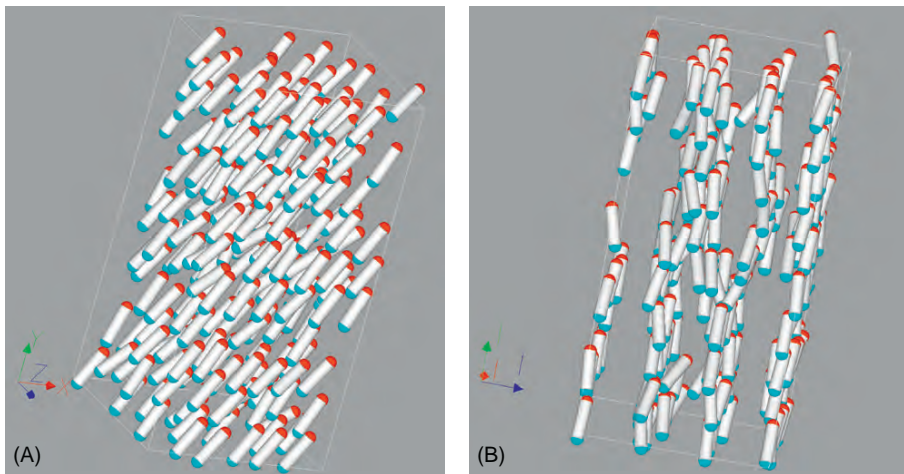


**Figure 3.12** Aggregate structures for  $\lambda_H = 50$  and  $\lambda_m = 10$ : (A) an oblique view and (B) viewed nearly from the negative  $x$ -axis.

form wall-like structures in such a way that one cluster is placed into two parallel clusters, with the plus magnetic charge of the center particle in contact with the minus magnetic charges of the two neighboring particles.

The above discussion has systematically used snapshots to present the properties of aggregates. However, this type of qualitative discussion is insufficient for an academic paper, and the addition of quantitative discussion is necessary. For this exercise, it would be suitable to discuss the radial, pair, and orientational distribution functions, whilst further investigation of the phenomena might necessitate Brownian dynamics in order to include random particle motion.

### 3.2.9 Simulation Program

The following sample simulation program has been written for the present simulation in FORTRAN. The important variables used in the simulation program are as follows:

$RX(I)$ , $RY(I)$ , $RZ(I)$	: $(x, y, z)$ components of the position vector $\mathbf{r}_i^*$ of particle $i$
$NX(I)$ , $NY(I)$ , $NZ(I)$	: $(x, y, z)$ components of the unit vector $\mathbf{n}_i (= \mathbf{e}_i)$ of particle $i$ denoting the particle and magnetic moment direction
$FX(I)$ , $FY(I)$ , $FZ(I)$	: $(x, y, z)$ components of the force $\mathbf{F}_i^*$ acting on particle $i$
$TX(I)$ , $TY(I)$ , $TZ(I)$	: $(x, y, z)$ components of the torque $\mathbf{T}_i^*$ acting on particle $i$
$XL$ , $YL$ , $ZL$	: Side lengths of the simulation box in the $(x, y, z)$ directions
$L$	: Length $l^*$ of the solid part of the spherocylinder particle
$D$	: Diameter $d^*$ of the solid cylinder part of the spherocylinder
$DEL$	: Thickness $\delta^*$ of the surfactant layer
$TD$	: Ratio $2\delta^*/(=2\delta/d)$ of the surfactant layer thickness to the particle radius

---

RP	:	Particle aspect ratio $r_p$ ( $=l/d$ )
RP1	:	Particle aspect ratio $r_p'$ ( $=l_0/d = r_p - 1$ )
N	:	Number of particles
VDENS	:	Volumetric fraction of particles $\phi_V$
NDENS	:	Number density of particles
HX, HY, HZ	:	(x,y,z) components of the unit vector denoting the magnetic field direction
RAM	:	Nondimensional parameter $\lambda_m$ representing the strength of magnetic particle-particle interactions
RAH	:	Nondimensional parameter $\lambda_H$ representing the strength of magnetic particle-field interactions
RAV	:	Nondimensional parameter $\lambda_V$ representing the strength of repulsive interactions due to the overlap of steric layers
H	:	Time interval
RCOFF	:	Cutoff distance for calculations of forces and torques
XA, YA, YC, YH	:	Resistance functions
GAMDOT	:	Shear rate $\dot{\gamma}^*$
MOMX (*), MOMEY (*),	:	Averaged values of the particle direction at each time step
MOMZ (*)		

As an aid for understanding the program, comments have been added to the important features. The line numbers shown at the beginning of each line are just for the reader's convenience and are unnecessary for executing the FORTRAN program.

We briefly explain quasi-random numbers, which are used in the subroutine "INITIAL" for setting an initial configuration. A quasi-random number is generated using an irrational. For example, if  $\sqrt{2}$  is used, the fractional parts of  $\sqrt{2}$ ,  $2\sqrt{2}$ ,  $3\sqrt{2}$ ,  $4\sqrt{2}, \dots$  provide a sequence of quasi-random numbers ranging from zero to unity.

```

0001 C*****
0002 C*                      mdcylndr1.f
0003 C*                      *
0004 C*          OPEN(9, FILE='@bbb1.dat', STATUS='UNKNOWN') *
0005 C*          OPEN(10,FILE='bbb11.dat', STATUS='UNKNOWN') *
0006 C*          OPEN(13,FILE='bbb41.mgf', STATUS='UNKNOWN') *
0007 C*          OPEN(21,FILE='bbb001.dat', STATUS='UNKNOWN') *
0008 C*          OPEN(22,FILE='bbb011.dat', STATUS='UNKNOWN') *
0009 C*          OPEN(23,FILE='bbb021.dat', STATUS='UNKNOWN') *
0010 C*          OPEN(24,FILE='bbb031.dat', STATUS='UNKNOWN') *
0011 C*          OPEN(25,FILE='bbb041.dat', STATUS='UNKNOWN') *
0012 C*          OPEN(26,FILE='bbb051.dat', STATUS='UNKNOWN') *
0013 C*          OPEN(27,FILE='bbb061.dat', STATUS='UNKNOWN') *
0014 C*          OPEN(28,FILE='bbb071.dat', STATUS='UNKNOWN') *
0015 C*          OPEN(29,FILE='bbb081.dat', STATUS='UNKNOWN') *
0016 C*          OPEN(30,FILE='bbb091.dat', STATUS='UNKNOWN') *
0017 C*          *
0018 C*          ----- MOLECULAR DYNAMICS SIMULATIONS -----
0019 C*          THREE-DIMENSIONAL MOLECULAR DYNAMICS SIMULATIONS OF *
0020 C*          A DISPERSION COMPOSED OF MAGNETIC SPHEROCYLINDERS *
0021 C*          IN A SIMPLE SHEAR FLOW. *
0022 C*          *
0023 C*          1. RODLIKE MODEL WITH ARBITRARY ASPECT RATIO. *
0024 C*          2. NO HYDRODYNAMIC INTERACTIONS AMONG PARTICLES. *
0025 C*          *
0026 C*          VER.1 BY A.SATOH , '08 5/23 *
0027 C*****

```

```

0028 C      N      : NUMBER OF PARTICLES
0029 C      D      : DIAMETER OF SOLID HEMISPHERE PARTICLE (=1)
0030 C      L      : LENGTH OF SOLID SPHEROCYLINDER
0031 C      RP     : ASPECT RATIO (=L/D)
0032 C      RP1    : ASPECT RATIO OF CYLINDER LENGTH TO D (=RP-1)
0033 C      NDENS   : NUMBER DENSITY
0034 C      VDENS   : VOLUMETRIC FRACTION
0035 C      RAM     : NONDIMENSIONAL PARAMETER OF PARTICLE-PARTICLE INTERACT
0036 C      RAH     : NONDIMENSIONAL PARAMETER OF PARTICLE-FIELD INTERACTION
0037 C      RAV     : NONDIMENSIONAL PARAMETER OF STERIC REPULSION
0038 C      RCOFF   : CUTOFF RADIUS FOR CALCULATION OF INTERACTION ENERGIES
0039 C      XL,YL,ZL : DIMENSIONS OF SIMULATION REGION
0040 C      BETA    : ASPECT RATIO OF SIMULATION BOX
0041 C      (HX,HY,HZ) : UNIT VECTOR DENOTING MAGNETIC FIELD DIRECTION
0042 C
0043 C      XA,YA : RESISTANCE FUNC. FOR TRANSLATIONAL MOTION
0044 C      YC     : RESISTANCE FUNC. FOR ROTATIONAL MOTION
0045 C      YH     : RESISTANCE FUNC. FOR SHEAR FLOW TERM
0046 C      RX(I),RY(I),RZ(I) : PARTICLE POSITION
0047 C      NX(N),NY(N),NZ(N) : DIRECTION OF PARTICLE MAJOR AXIS AND
0048 C                           MAGNETIC MOMENT
0049 C      FX(I),FY(I),FZ(I) : FORCES ACTING ON PARTICLE I
0050 C      TX(I),TY(I),TZ(I) : TORQUES ACTING ON PARTICLE I
0051 C      MOMX(**),MOMY(**) : MAG. MOMENT OF SYSTEM AT EACH TIME STEP
0052 C      MOMZ(**)
0053 C
0054 C      H      : INTERVAL OF TIME STEP FOR MOLE. DYNA. SIMULATIONS
0055 C      GAMDOT : SHEAR RATE (=1 FOR THIS CASE)
0056 C      NTIMEMX : MAXIMUM NUMBER OF TIME STEP
0057 C
0058 C      -XL/2 < RX < XL/2 , -YL/2 < RY < YL/2 , -ZL/2 < RZ < ZL/2
0059 C-----
0060 C
0061      IMPLICIT REAL*8 (A-H,O-Z), INTEGER (I-N)
0062 C
0063      COMMON /BLOCK1/ RX , RY , RZ
0064      COMMON /BLOCK2/ NX , NY , NZ
0065      COMMON /BLOCK3/ FX , FY , FZ
0066      COMMON /BLOCK4/ TX , TY , TZ
0067      COMMON /BLOCK5/ XL , YL , ZL
0068      COMMON /BLOCK6/ RP , RP1 , D , DEL , TD
0069      COMMON /BLOCK7/ XA , YA , YC , YH
0070      COMMON /BLOCK8/ N , NDENS , VDENS
0071      COMMON /BLOCK9/ H , RCOFF , GAMDOT , DX , CORY
0072      COMMON /BLOCK10/ RAM , RAH , RAV
0073      COMMON /BLOCK11/ HX , HY , HZ
0074      COMMON /BLOCK12/ MOMX , MOMEY , MOMZ
0075      COMMON /WORK20/ XRXI , YRYI , ZRZI , XRXJ , YRYJ , ZRZJ
0076      COMMON /WORK21/ FXIJS , FYIJS , FZIJS , FXJIS , FYJIS , FZJIS
0077      COMMON /WORK22/ TXIJS , TYIJS , TZIJS , TXJIS , TYJIS , TZJIS
0078      COMMON /WORK23/ RCOFF2 , RP102 , D1 , DISQ
0079      COMMON /WORK24/ CF0XA , CF0YA , CT0YC , CE0YHYC
0080 C
0081      PARAMETER( NN=1000 , NNS=500000 , PI=3.141592653589793D0 )
0082 C
0083      REAL*8 NDENS
0084      REAL*8 RX(NN) , RY(NN) , RZ(NN) , NX(NN) , NY(NN) , NZ(NN)
0085      REAL*8 FX(NN) , FY(NN) , FZ(NN) , TX(NN) , TY(NN) , TZ(NN)
0086      REAL     MOMX(NNS) , MOMEY(NNS) , MOMZ(NNS)
0087 C
0088      REAL*8 BETA
0089      REAL*8 RXI , RYI , RZI , NXI , NYI , NZI , FXI , FYI , FZI
0090      REAL*8 TXI , TYI , TZI , WXI , WYI , WZI , WXIN , WYIN , WZIN
0091      REAL*8 FXIP , FYIP , FZIP , FXIN , FYIN , FZIN
0092      REAL*8 TXIP , TYIP , TZIP , TXIN , TYIN , TZIN
0093      REAL*8 OMEIPX , OMEIPY , OMEIPZ , OMEINX , OMEINY , OMEINZ
0094      REAL*8 C1 , C2 , C3 , C00
0095      REAL*8 C1X , C1Y , C1Z , C2X , C2Y , C2Z
0096      REAL*8 C3X , C3Y , C3Z
0097      REAL*8 CCA1 , CCB1 , CCS1 , CCL1
0098      INTEGER NTIME , NTIMEMX , NGRAPH , DNSMPL , NP , NOPT

```

```

0099      INTEGER   NSMPL1 , NSMPL2
0100      INTEGER   NANIME , NANMCTR, NOPT1
0101 C
0102      OPEN(9,FILE='@bbb1.dat' , STATUS='UNKNOWN')
0103      OPEN(10,FILE='bbb11.dat' , STATUS='UNKNOWN')
0104      OPEN(13,FILE='bbb41.mgf' , STATUS='UNKNOWN')
0105      OPEN(21,FILE='bbb001.dat' , STATUS='UNKNOWN')
0106      OPEN(22,FILE='bbb011.dat' , STATUS='UNKNOWN')
0107      OPEN(23,FILE='bbb021.dat' , STATUS='UNKNOWN')
0108      OPEN(24,FILE='bbb031.dat' , STATUS='UNKNOWN')
0109      OPEN(25,FILE='bbb041.dat' , STATUS='UNKNOWN')
0110      OPEN(26,FILE='bbb051.dat' , STATUS='UNKNOWN')
0111      OPEN(27,FILE='bbb061.dat' , STATUS='UNKNOWN')
0112      OPEN(28,FILE='bbb071.dat' , STATUS='UNKNOWN')
0113      OPEN(29,FILE='bbb081.dat' , STATUS='UNKNOWN')
0114      OPEN(30,FILE='bbb091.dat' , STATUS='UNKNOWN')
0115
0116 C
0117 C
0118 C
0119 C
0120 C
0121 C
0122 C
0123 C
0124 C
0125 C
0126 C
0127 C
0128 C
0129 C
0130 N      = 216
0131 VDENS = 0.05D0
0132 RAM   = 20.D0
0133 RAH   = 10.0D0
0134 RAV   = 150.D0
0135 RP    = 5.D0
0136 RP1   = RP - 1.D0
0137 C
0138 H      = 0.0001D0
0139 GAMDOT = 1.D0
0140 TD    = 0.3D0
0141 RCOFF = 5.D0*RP
0142 DEL   = TD/2.D0
0143 HX   = 0.D0
0144 HY   = 1.D0
0145 HZ   = 0.D0
0146 C
0147 BETA  = 2.D0
0148 DX    = 0.D0
0149 D     = 1.0D0
0150 NDENS = ( 12.D0/( PI*(3.D0*RP-1.D0) ) )*VDENS
0151 C
0152 NTIMEMX = 200000
0153 NGRAPH = NTIMEMX/10
0154 NANIME = NTIMEMX/200
0155 DNSMPL = 2
0156 NOPT  = 20
0157 C
0158 CCA1  = RP/2.D0 + DEL
0159 CCB1  = 0.5D0 + DEL
0160 CCS1  = DSQRT( CCA1**2 - CCB1**2 ) / CCA1
0161 CCL1  = DLOG( (1.D0+CCS1)/(1.D0-CCS1) )
0162 XA    = (8.D0/3.D0)*CCS1**3
0163 &           / ( -2.D0*CCS1+(1.D0+CCS1**2)*CCL1 )
0164 YA    = (16.D0/3.D0)*CCS1**3
0165 &           / ( -2.D0*CCS1+(3.D0*CCS1**2-1.D0)*CCL1 )
0166 YC    = (4.D0/3.D0)* ( CCS1**3*(2.D0-CCS1**2) )
0167 &           / ( -2.D0*CCS1+(1.D0+CCS1**2)*CCL1 )
0168 YH    = (4.D0/3.D0)*CCS1**5
0169 &           / ( -2.D0*CCS1+(1.D0+CCS1**2)*CCL1 )

```

• The given values and the magnetic moment results are written out in @bbb1 and bbb11, the data for MicroAVS are done in bbb41, and the intermediate positions and directions are done in bbb001-bbb091 in the time sequential order.

NP=9

--- PARAMETER (1) ---

-----

N=5\*\*3(125), 6\*\*3(216), 7\*\*3(343), 8\*\*3(512)

-----

RAH	= 0.1	1.0	10.	100.
H	= 0.001	0.001	0.001	0.0001
+++++				
RAM	= 0.1	1.0	10.	100.
H	= 0.001	0.001	0.001	0.0001

-----

THE MINIMUM VALUE ON THE ABOVE LIST MUST BE  
USED FOR THE TIME INTERVAL H.

-----

• The particle number  $N=216$ , volumetric fraction  $\phi_V=0.05$ ,  $\lambda_m=20$ ,  $\lambda_r=10$ ,  $\lambda_v=150$ , and aspect ratio  $r_p=5$ .

--- PARAMETER (2) ---

-----

• The time interval  $h^*=0.0001$ ,  $t_0=0.3$ , cutoff radius  $r_{\text{cuff}}^*=5r_p$ , thickness of a surfactant layer  $\delta^*=0.15$ , and magnetic field direction  $\mathbf{h}=(0,1,0)$ .

-----

• BETA is used in determining the simulation region size. NDENS is the number density of particles.

-----

• The main loop is finished when NTIME arrives at 200,000.  
• The particle position and other data are written out at every NGRAPH time steps. 200 sets of data are written out for making an animation based on MicroAVS.

-----

--- PARAMETER (5) ---

-----

• The resistance functions  $X^A$ ,  $Y^A$ ,  $Y^C$ , and  $Y^H$  are calculated in advance.

```

0170 C
0171      RCOFF2 = RCOFF**2
0172      RP102 = RP1/2.D0
0173      D1 = 1.D0+TD
0174      D1SQ = D1**2
0175      CFOXA = 1.D0/( XA*(RP+2.D0*DEL ) )
0176      CFOYA = 1.D0/( YA*(RP+2.D0*DEL ) )
0177      CT0YC = 1.D0/( YC*(RP+2.D0*DEL )**3 )
0178      CE0YHYC = (YH/YC)*0.5D0
0179 C
0180 C -----
0181 C ----- INITIAL CONFIGURATION -----
0182 C -----
0183 C
0184 C
0185 CCC OPEN(19,FILE='qqq091.dat',STATUS='OLD')
0186 CCC READ(19,472) N , XL , YL , ZL , D , TD , RP , RP1 , DX
0187 CCC READ(19,474) (RX(I),I=1,N),(RY(I),I=1,N),(RZ(I),I=1,N),
0188 CCC & (NX(I),I=1,N),(NY(I),I=1,N),(NZ(I),I=1,N)
0189 CCC CLOSE(19,STATUS='KEEP')
0190 CCC GOTO 7
0191 C
0192 CALL INITIAL( BETA )
0193 C
0194 7 IF( RCOFF .GE. XL/2.D0 ) THEN
0195     RCOFF = XL/2.D0 - 0.0001D0
0196 END IF
0197 RCOFF2 = RCOFF**2
0198 C
0199      NTIME = 0
0200      CALL FORCECAL( NP, NTIME )
0201 C
0202 C
0203      WRITE(NP,12) N, VDENS, NDENS, RAM ,RAH ,RAV ,RP ,RP1 ,D ,DEL ,
0204      & TD , XA , YA , YC , YH , H , RCOFF , GAMDOT , BETA ,
0205      & XL , YL , ZL
0206      WRITE(NP,13) RP102, D1, CFOXA, CFOYA, CT0YC, CE0YHYC
0207      WRITE(NP,14) NTIMEMX, NGRAPH, DNSMPL
0208 C
0209 C
0210      NANMCTR = 0
0211      NSMPL = 0
0212 C
0213 C -----
0214 C ----- START OF MAIN LOOP -----
0215 C
0216 C
0217 DO 1000 NTIME = 1,NTIMEMX
0218 C
0219      DX = GAMDOT*YL*H*DBLE(NTIME)
0220      DX = DMOD( DX, XL )
0221 C
0222      DO 100 I = 1,N
0223 C
0224      NXI = NX(I)
0225      NYI = NY(I)
0226      NZI = NZ(I)
0227      FXI = FX(I)
0228      FYI = FY(I)
0229      FZI = FZ(I)
0230      TXI = TX(I)
0231      TYI = TY(I)
0232      TZI = TZ(I)
0233 C
0234 C
0235      C00 = FXI*NXI + FYI*NYI + FZI*NZI
0236      FXIP = C00*NXI
0237      FYIP = C00*NYI
0238      FZIP = C00*NZI
0239      FXIN = FXI - FXIP
0240      FYIN = FYI - FYIP

```

• CFOXA and CF0YA are the coefficients in the force term in Eq. (3.49), CT0YC is the coefficient in the torque term in Eq. (3.50), and CE0YHYC is a part of the coefficient of the shear rate in Eq. (3.50).

• These READ statements are for continuing the sequential simulation using the data saved previously.

• The particle initial positions and velocities are assigned.

• The forces and torques acting between particles are calculated.

• DX is  $\Delta X$  in Fig. 2.15.

• The force acting on particle  $i$  is decomposed into one in the particle direction and another in the direction normal to the particle axis according to Eq. (3.36).

```

0241      FZIN = FZI - FZIP
0242 C
0243      RXI = RX(I) + H*( CFOXA*FXIP+CF0YA*FXIN ) + RY(I)*GAMDOT*H
0244      RYI = RY(I) + H*( CFOXA*FYIP+CF0YA*FYIN )
0245      RZI = RZ(I) + H*( CFOXA*FZIP+CF0YA*FZIN )
0246      CORY = DNINT( RYI/YL )
0247      RXI = RXI - CORY*DX
0248      RX(I) = RXI - DNINT( RXI/XL )*XL
0249      RY(I) = RYI - CORY*YL
0250      RZ(I) = RZI - DNINT( RZI/ZL )*ZL
0251 C
0252 C
0253      C00 = TXI*NXI + TYI*NYI + TZI*NZI
0254      TXIP = C00*NXI
0255      TYIP = C00*NYI
0256      TZIP = C00*NZI
0257      TXIN = TXI - TXIP
0258      TYIN = TYI - TYIP
0259      TZIN = TZI - TZIP
0260 C
0261      C00 = -0.5D0*NZI
0262      OMEIPX = C00*NXI
0263      OMEIPY = C00*NYI
0264      OMEIPZ = C00*NZI
0265      OMEINX = - OMEIPX
0266      OMEINY = - OMEIPY
0267      OMEINZ = -0.5D0 - OMEIPZ
0268 C
0269      C1X = CT0YC*TXIN
0270      C1Y = CT0YC*TYIN
0271      C1Z = CT0YC*TZIN
0272      C2X = -CE0YHYC* ( NZI*NXI )
0273      C2Y = -CE0YHYC* (-NZI*NYI )
0274      C2Z = -CE0YHYC* ( NYI**2 - NXI**2 )
0275 C
0276      WXIN = OMEINX + C1X + C2X
0277      WYIN = OMEINY + C1Y + C2Y
0278      WZIN = OMEINZ + C1Z + C2Z
0279      C3X = WYIN*NZI - WZIN*NYI
0280      C3Y = WZIN*NXI - WXIN*NZI
0281      C3Z = WXIN*NYI - WYIN*NXI
0282 C
0283      NXI = NXI + H*C3X
0284      NYI = NYI + H*C3Y
0285      NZI = NZI + H*C3Z
0286      C00 = DSQRT( NXI**2 + NYI**2 + NZI**2 )
0287      NX(I) = NXI/C00
0288      NY(I) = NYI/C00
0289      NZ(I) = NZI/C00
0290 C
0291 100  CONTINUE
0292 C
0293      CALL FORCECAL( NP, NTIME )
0294 C
0295 C
0296 C
0297      IF( MOD(NTIME,DNSMPL) .EQ. 0 ) THEN
0298          NSMPL = NSMPL + 1
0299          C1 = 0.D0
0300          C2 = 0.D0
0301          C3 = 0.D0
0302          DO 450 J=1,N
0303              C1 = C1 + NX(J)
0304              C2 = C2 + NY(J)
0305              C3 = C3 + NZ(J)
0306        450  CONTINUE
0307          MOMX(NSMPL) = REAL(C1)/REAL(N)
0308          MOMY(NSMPL) = REAL(C2)/REAL(N)
0309          MOMZ(NSMPL) = REAL(C3)/REAL(N)
0310
0311      END IF
0312 C

```

--- (2) ROTATIONAL MOTION ---

• The torque acting on particle *i* is decomposed into one about the particle direction and another about a line normal to the particle direction through its center according to Eq. (3.36).

• The angular velocity is decomposed into two vectors in a similar way to the torque.

• The terms of the torque and the shear rate are calculated in the angular velocity in Eq. (3.50).

• The angular velocity in Eq.(3.50) is calculated.

• To evaluate the particle direction from Eq.(3.55), the vector product of the angular velocity and the particle direction is first calculated.

• The particle direction is evaluated from Eq. (3.55).

• The modification is made to yield the unit vector.

--- CAL FORCES ---

• Calculation of the forces and torques.

--- MOMENT OF SYSTEM ---

• To check the system convergence afterward, the average of the particle direction vector is calculated.

• The data of the particle positions and directions are written out at every NGRAPH time steps for the post processing analysis.

--- DATA OUTPUT (1) FOR GRAPHICS ---

```

0313      IF( MOD(NTIME,NGRAPH) .EQ. 0 ) THEN
0314          NOPT = NOPT + 1
0315          WRITE(NOPT,472) N , XL , YL , ZL , D , TD , RP , RP1 , DX
0316          WRITE(NOPT,474) (RX(I),I=1,N),(RY(I),I=1,N),(RZ(I),I=1,N),
0317          & (NX(I),I=1,N),(NY(I),I=1,N),(NZ(I),I=1,N)
0318          CLOSE(NOPT,STATUS='KEEP')
0319      END IF
0320 C
0321 C           --- DATA OUTPUT FOR ANIMATION (2) ---
0322      IF( MOD(NTIME,NANIME) .EQ. 0 ) THEN
0323          NANMCTR = NANMCTR + 1
0324          NOPT1 = 13
0325          CALL DATAOPUT( NOPT1, NANMCTR, NTIMEMX, NANIME, N )
0326      END IF
0327 C
0328 C
0329 1000 CONTINUE
0330 C
0331 C
0332 C           ----- END OF MOLECULAR DYNAMICS -----
0333 C
0334 C
0335 C           --- PRINT OUT (2) ---
0336      WRITE(NP,1011)
0337      NSMPL1 = 1
0338      NSMPL2 = NSMPL
0339      CALL PRNTDATA( NSMPL1 , NSMPL2 , NP )
0340      WRITE(NP,1013) NSMPL1 , NSMPL2
0341 C
0342      WRITE(10,1111) N , VDENS, NDENS, RAM, RAH, RAV
0343      WRITE(10,1113) RP, RP1, D, DEL, TD, XA, YA, YC, YH
0344      WRITE(10,1115) H, RCOFF, GAMDOT, BETA, XL, YL, ZL
0345      WRITE(10,1117) RP102, D1, CF0XA, CF0YA, CTOYC, CEOYHYC
0346      WRITE(10,1119) NTIMEMX, NGRAPH, DNSMPL
0347      WRITE(10,1121) ( MOMX(I),I=NSMPL1 , NSMPL2)
0348      & ,( MOMY(I),I=NSMPL1 , NSMPL2)
0349      & ,( MOMZ(I),I=NSMPL1 , NSMPL2)
0350 C
0351          CLOSE(9, STATUS='KEEP')
0352          CLOSE(10,STATUS='KEEP')
0353          CLOSE(13,STATUS='KEEP')
0354 C
0355 12 FORMAT(/1H ,-----'
0356  & /1H ,-' MOLECULAR DYNAMICS SIMULATIONS OF SPHERO-
0357  & /1H ,-' CYLINDER PARTICLES IN A SIMPLE SHEAR FLOW   -'
0358  & /1H ,-----'
0359  & //1H , 'I6 , 2X, 'VDENS=' ,F7.4 , 2X , 'NDENS=' ,F9.6
0360  & /1H , 'RAM=' ,F6.2 , 2X , 'RAH=' ,F6.2 , 2X , 'RAV=' ,F7.2
0361  & /1H , 'RP=' ,F5.2 , 2X , 'RP1=' ,F5.2 , 2X , 'D=' ,F5.2 , 2X ,
0362  & 'DEL=' ,F5.2 , 2X , 'TD=' ,F5.2
0363  & /1H , 'XA=' ,E12.4 ,2X , 'YA=' ,E12.4 ,2X , 'YC=' ,E12.4 ,2X ,
0364  & 'YH=' ,E12.4
0365  & /1H , 'H=' ,E12.4 ,3X , 'RCOFF=' ,F5.2 ,2X , 'GAMDOT=' ,F5.2 ,2X ,
0366  & 'BETA=' , F5.2
0367  & /1H , 'XL=' ,F6.2 ,2X , 'YL=' ,F6.2 ,2X , 'ZL=' ,F6.2 )
0368 13 FORMAT( 1H , 'RP102=' ,F5.2 ,2X , 'D1=' ,F5.2 ,2X ,
0369  & 'CF0XA=' ,E11.3 , 2X , 'CF0YA=' ,E11.3
0370  & /1H , 'CTOYC=' ,E11.3 , 2X , 'CEOYHYC=' ,E11.3 )
0371 14 FORMAT( 1H , 'NTIMEMX=' ,I8 , 2X , 'NGRAPH=' ,I8 ,2X , 'DNSMPL=' ,I8 /)
0372 472 FORMAT( I5 , 3F9.4 , 4F8.4 , E16.8 )
0373 474 FORMAT( (5F16.10) )
0374 1011 FORMAT(/1H ,'++++++++' )
0375  & /1H , MD SIMULATIONS
0376  & /1H , '++++++++' /)
0377 1013 FORMAT(//1H ,18X, 'START OF MD SAMPLING STEP=' ,I7 /
0378  & /1H ,18X, 'END OF MD SAMPLING STEP=' ,I7 /)
0379 1111 FORMAT( I5 , 2F7.4 , 3F12.5 )
0380 1113 FORMAT( 3F6.2 , 2F7.3 , 4E12.4 )
0381 1115 FORMAT( E11.3 , F8.3 , 2F7.4 , 3F9.3 )
0382 1117 FORMAT( 2F6.2 , 4E12.4 )
0383 1119 FORMAT( 3I8 )
0384 1121 FORMAT( (10F8.5) )

```

• The data of the particle positions and directions are written out at every NANIME time steps for making an animation based on MicroAVS.

• To check the system convergence afterward, the data of the particle directions are written out.

```

0385                                              STOP
0386                                              END
0387 C***** SUB PRNTDATA *****
0388 C***** SUBROUTINE PRNTDATA( MCSST, MCSMX, NP )
0389 C***** SUBROUTINE ***** SUBROUTINE ***** SUBROUTINE *****
0390 C
0391 C**** SUB PRNTDATA *****
0392     SUBROUTINE PRNTDATA( MCSST, MCSMX, NP )
0393 C
0394     IMPLICIT REAL*8 ( A-H,O-Z ), INTEGER ( I-N )
0395 C
0396     COMMON /BLOCK12/ MOMX , MOMEY , MOMZ
0397 C
0398     PARAMETER( NN=1000 , NNS=500000 , PI=3.141592653589793D0 )
0399 C
0400     INTEGER    MCSST      , MCSMX      , NP
0401     REAL       MOMX(NNS) , MOMEY(NNS) , MOMZ(NNS)
0402 C
0403     REAL       AMOMX(10) , AMOMY(10) , AMOMZ(10) , CO
0404     INTEGER    IC , IMC(0:10) , JS , JE
0405 C
0406 C                                              ----- KEIKA INSATU -----
0407     IC = ( MCSMX-MCSST+1 )/50
0408     DO 20 I= MCSST-1+IC , MCSMX , IC
0409       WRITE(NP,10) I, MOMX(I), MOMEY(I), MOMZ(I)
0410   20 CONTINUE
0411 C
0412     IC = ( MCSMX-MCSST+1 )/10
0413     DO 30 I=0,10
0414       IMC(I) = MCSST - 1 + IC*I
0415       IF( I .EQ. 10 ) IMC(I) = MCSMX
0416   30 CONTINUE
0417 C
0418 C
0419     DO 35 I=1,10
0420       AMOMX( I ) = 0.
0421       AMOMY( I ) = 0.
0422       AMOMZ( I ) = 0.
0423   35 CONTINUE
0424 C
0425     DO 50 I=1,10
0426       JS = IMC(I-1) + 1
0427       JE = IMC(I)
0428       DO 40 J=JS,JE
0429         AMOMX(I) = AMOMX( I ) + MOMX( J )
0430         AMOMY(I) = AMOMY( I ) + MOMEY( J )
0431         AMOMZ(I) = AMOMZ( I ) + MOMZ( J )
0432   40 CONTINUE
0433   50 CONTINUE
0434 C
0435     DO 70 I=1,10
0436       CO    = REAL( IMC(I)-IMC(I-1) )
0437       AMOMX(I) = AMOMX(I) /CO
0438       AMOMY(I) = AMOMY(I) /CO
0439       AMOMZ(I) = AMOMZ(I) /CO
0440   70 CONTINUE
0441 C                                              ----- STEP HEIKIN INSATU -----
0442     WRITE(NP,75)
0443     DO 90 I=1,10
0444       WRITE(NP,80) I, IMC(I-1)+1, IMC(I), AMOMX(I),AMOMY(I),AMOMZ(I)
0445   90 CONTINUE
0446 C
0447   10 FORMAT(1H , 'SMPL=' , I7, 1X , 'NX=' , F6.3, 1X , 'NY=' , F6.3,
0448   &                                1X , 'NZ=' , F6.3)
0449   75 FORMAT(//1H , '-----',
0450   &           /1H , '          TIME AVERAGE
0451   &           /)
0452   80 FORMAT(1H , 'I=' , I2, 2X , 'SMPLMN=' , I7, 2X , 'SMPLMX=' , I7
0453   &           /1H , 5X , 'NX=' , F6.3, 2X , 'NY=' , F6.3, 2X , 'NZ=' , F6.3 )
0454
0455
0456 C**** SUB INITIAL *****

```

• The total time steps are equally divided into 50 blocks, and the end value of each block is written out.

• The total time steps are equally divided into 10 blocks, and the subaverages are calculated for each block.

```

0457      SUBROUTINE INITIAL( BETA )
0458 C
0459      IMPLICIT REAL*8 (A-H,O-Z), INTEGER (I-N)
0460 C
0461      COMMON /BLOCK1/ RX , RY , RZ
0462      COMMON /BLOCK2/ NX , NY , NZ
0463      COMMON /BLOCK5/ XL , YL , ZL
0464      COMMON /BLOCK6/ RP , RP1 , D , DEL , TD
0465      COMMON /BLOCK8/ N , NDENS, VDENS
0466      COMMON /BLOCK9/ H , RCOFF, GAMDOT, DX , CORY
0467 C
0468      PARAMETER( NN=1000 , PI=3.141592653589793D0 )
0469 C
0470      REAL*8 NDENS
0471      REAL*8 RX(NN) , RY(NN) , RZ(NN) , NX(NN) , NY(NN) , NZ(NN)
0472 C
0473      INTEGER Q , PTCL
0474      REAL*8 A , XLUNT , YLUNT , ZLUNT, RAN1 , RAN2 , RAN3
0475      REAL*8 C1 , C2 , C3
0476 C
0477      A = 1.D0/( (BETA*NDENS)**(1./3. ) )
0478      Q = NINT( (REAL(N+1))**(.1./3. ) )
0479      XL = A*DBLE(Q)
0480      YL = A*DBLE(Q)*BETA
0481      ZL = A*DBLE(Q)
0482      XLUNT = A
0483      YLUNT = A*BETA
0484      ZLUNT = A
0485 C
0486      RAN1 = DSQRT( 2.0D0 )
0487      RAN2 = DSQRT( 7.0D0 )
0488      RAN3 = DSQRT( 11.0D0 )
0489      PTCL = 0
0490      DO 10 K=0,Q-1
0491      DO 10 J=0,Q-1
0492      DO 10 I=0,Q-1
0493      PTCL = PTCL + 1
0494      C1 = RAN1*DBLE(PTCL)
0495      C1 = C1 - DINT(C1)
0496      C1 = C1 - 0.5D0
0497      C2 = RAN2*DBLE(PTCL)
0498      C2 = C2 - DINT(C2)
0499      C2 = C2 - 0.5D0
0500      C3 = RAN3*DBLE(PTCL)
0501      C3 = C3 - DINT(C3)
0502      C3 = C3 - 0.5D0
0503      RX(PTCL) = DBLE(I)*XLUNT+XLUNT/3D0+C1*(XLUNT/8.D0)-XL/2.D0
0504      RY(PTCL) = DBLE(J)*YLUNT+YLUNT/3D0+C2*(YLUNT/8.D0)-YL/2.D0
0505      RZ(PTCL) = DBLE(K)*ZLUNT+ZLUNT/3D0+C3*(ZLUNT/8.D0)-ZL/2.D0
0506 10 CONTINUE
0507      N = PTCL
0508 C
0509      RAN1 = DSQRT( 2.0D0 )
0510      RAN2 = DSQRT( 3.0D0 )
0511      DO 20 I=1,N
0512      C1 = RAN1*DBLE(I)
0513      C1 = C1 - DINT(C1)
0514      C1 = C1 - 0.5D0
0515      C1 = PI/2.D0 + (5.D0/180.D0)*PI*C1
0516      C2 = RAN2*DBLE(I)
0517      C2 = C2 - DINT(C2)
0518      C2 = C2 - 0.5D0
0519      C2 = PI/2.D0 + (5.D0/180.D0)*PI*C2
0520      NX(I) = DSIN(C1)*DCOS(C2)
0521      NY(I) = DSIN(C1)*DSIN(C2)
0522      NZ(I) = DCOS(C1)
0523 20 CONTINUE
0524
0525
0526 C**** SUB DATAOPUT ****
0527      SUBROUTINE DATAOPUT( NOPT1, NANMCTR, NTIMEMX, NANIME, N )
0528 C

```

• A subroutine for setting the initial positions and velocities of particles.

• The volume occupied by one particle is  $\beta a^3$  and therefore  $a^* = 1/(\beta n)^{1/3}$  because of  $\beta a^3 n = 1$  ( $n$  is the number density).

• The side lengths of the unit cell are  $(a^*, \beta a^*, a^*)$  in each direction.

----- POSITION -----

- RAN1, RAN2, and RAN3 are quasi-random numbers.
- Q particles are located in each axis direction.
- Each particle is moved in parallel by (XLUNT/3, YLUNT/3, ZLUNT/3) to remove subtle situations at outer boundary surfaces. Also, to remove the regularity of the initial configuration, each particle is moved randomly by the maximum displacement  $(1/2)\times(XLUNT/8, YLUNT/8, ZLUNT/8)$  using quasi-random numbers.
- Each particle is moved in parallel by  $(1/2)\times(-XL, -YL, -ZL)$ , so that the simulation box center is the coordinate origin.

----- MOMENT -----

• The initial direction of each particle is randomly assigned with a certain angle range about the y-direction using quasi-random numbers.

RETURN  
END

```

0529      IMPLICIT REAL*8 (A-H,O-Z), INTEGER (I-N)
0530 C
0531      COMMON /BLOCK1/ RX    , RY    , RZ
0532      COMMON /BLOCK2/ NX    , NY    , NZ
0533      COMMON /BLOCK5/ XL    , YL    , ZL
0534      COMMON /BLOCK6/ RP    , RP1   , D     , DEL   , TD
0535      COMMON /BLOCK9/ H     , RCOFF, GAMDOT, DX    , CORY
0536 C
0537      PARAMETER( NN=1000 , PI=3.141592653589793D0 )
0538 C
0539      REAL*8   RX(NN) , RY(NN) , RZ(NN) , NX(NN) , NY(NN) , NZ(NN)
0540      REAL*8   RP102 , CRADIUS , CX1 , CY1 , CZ1 , CX2 , CY2 , CZ2
0541 C
0542      RP102 = RP1/2.D0
0543      CRADIUS = ( D + TD )/2.D0
0544      XL2   = XL/2.D0
0545      YL2   = YL/2.D0
0546      ZL2   = ZL/2.D0
0547 C
0548      IF( NANMCTR.EQ. 1 ) THEN
0549          WRITE(NOPT1,181) ( NTIMEMX/NANIME )
0550      END IF
0551 C
0552      IF( (NANMCTR.GE.1) .AND. (NANMCTR.LE.9) ) THEN
0553          WRITE(NOPT1,183) NANMCTR
0554      ELSE IF( (NANMCTR.GE.10) .AND. (NANMCTR.LE.99) ) THEN
0555          WRITE(NOPT1,184) NANMCTR
0556      ELSE IF( (NANMCTR.GE.100) .AND. (NANMCTR.LE.999) ) THEN
0557          WRITE(NOPT1,185) NANMCTR
0558      ELSE IF( (NANMCTR.GE.1000) .AND. (NANMCTR.LE.9999) ) THEN
0559          WRITE(NOPT1,186) NANMCTR
0560      END IF
0561 C
0562 C
0563      WRITE(NOPT1,211) N
0564      DO 250 I=1,N
0565          CX1 = RX(I) - NX(I)*RP102
0566          CY1 = RY(I) - NY(I)*RP102
0567          CZ1 = RZ(I) - NZ(I)*RP102
0568          CX2 = RX(I) + NX(I)*RP102
0569          CY2 = RY(I) + NY(I)*RP102
0570          CZ2 = RZ(I) + NZ(I)*RP102
0571          WRITE(NOPT1,248) CX1, CY1, CZ1, CX2, CY2, CZ2, (CRADIUS+1.D-5)
0572 250 CONTINUE
0573 C
0574 C
0575      WRITE(NOPT1,311) N
0576      DO 350 I=1,N
0577          CX1 = RX(I) - NX(I)*RP102
0578          CY1 = RY(I) - NY(I)*RP102
0579          CZ1 = RZ(I) - NZ(I)*RP102
0580          WRITE(NOPT1,348) CX1, CY1, CZ1, CRADIUS, 0.0, 0.8, 1.0
0581 350 CONTINUE
0582 C
0583 C
0584      WRITE(NOPT1,311) N
0585      DO 450 I=1,N
0586          CX1 = RX(I) + NX(I)*RP102
0587          CY1 = RY(I) + NY(I)*RP102
0588          CZ1 = RZ(I) + NZ(I)*RP102
0589          WRITE(NOPT1,348) CX1, CY1, CZ1, CRADIUS, 1.0, 0.0, 0.0
0590 450 CONTINUE
0591 C
0592 C
0593      WRITE(NOPT1,648) 17
0594      WRITE(NOPT1,649) -XL2, -YL2, -ZL2
0595      WRITE(NOPT1,649) XL2, -YL2, -ZL2
0596      WRITE(NOPT1,649) XL2, YL2, -ZL2
0597      WRITE(NOPT1,649) -XL2, YL2, -ZL2
0598      WRITE(NOPT1,649) -XL2, -YL2, -ZL2
0599      WRITE(NOPT1,649) -XL2, -YL2, ZL2
0600      WRITE(NOPT1,649) XL2, -YL2, ZL2

```

• A subroutine for writing out the data which can be used for making an animation based on the commercial software MicroAVS.

• MicroAVS can make a visualization or animation by reading the data from bbb41.mgf.

CYLINDER (1) ---

• Drawing of the cylindrical part of particles.

SPHERE MINUS (2) ---

• Drawing of the hemisphere of the negative charge.

SPHERE PLUS (3) ---

• Drawing of the hemisphere of the positive charge.

SIM.REGEON LINES (4) ---

• Drawing of the frame of the simulation box.

```

0601      WRITE(NOPT1,649)  XL2,   YL2,   ZL2
0602      WRITE(NOPT1,649) -XL2,   YL2,   ZL2
0603      WRITE(NOPT1,649) -XL2,  -YL2,   ZL2
0604      WRITE(NOPT1,649) -XL2,   YL2, -ZL2
0605      WRITE(NOPT1,649) -XL2,  -YL2, -ZL2
0606      WRITE(NOPT1,649)  XL2,  -YL2,   ZL2
0607      WRITE(NOPT1,649)  XL2,   YL2,   ZL2
0608      WRITE(NOPT1,649)  XL2,   YL2, -ZL2
0609      WRITE(NOPT1,649)  XL2,  -YL2, -ZL2
0610      WRITE(NOPT1,649)  XL2,  -YL2,   ZL2
0611 C
0612 C ----- FORMAT -----
0613 181 FORMAT('# Micro AVS Geom:2.00'
0614   &      '# Animation of DPD simulation results'
0615   &      /I4)
0616 183 FORMAT('step',I1)
0617 184 FORMAT('step',I2)
0618 185 FORMAT('step',I3)
0619 186 FORMAT('step',I4)
0620 211 FORMAT('column'/'cylinder'/'dvertex'/'32'/I7 )
0621 248 FORMAT( 6F10.3 , F6.2 )
0622 311 FORMAT( 'sphere'/'sphere_sample'/'color'/I7 )
0623 348 FORMAT( 3F10.3 , F6.2 , 3F5.2 )
0624 648 FORMAT( 'polyline'/'pline_sample'/'vertex'/I3 )
0625 649 FORMAT( 3F10.3 )
0626
0627
0628 C**** SUB FORCECAL *****
0629      SUBROUTINE FORCECAL( NP, NTIME )
0630 C
0631      IMPLICIT REAL*8 (A-H,O-Z), INTEGER (I-N)
0632 C
0633      COMMON /BLOCK1/ RX ,  RY ,  RZ
0634      COMMON /BLOCK2/ NX ,  NY ,  NZ
0635      COMMON /BLOCK3/ FX ,  FY ,  FZ
0636      COMMON /BLOCK4/ TX ,  TY ,  TZ
0637      COMMON /BLOCK5/ XL ,  YL ,  ZL
0638      COMMON /BLOCK6/ RP ,  RP1 , D ,  DEL , TD
0639      COMMON /BLOCK7/ XA ,  YA ,  YC ,  YH
0640      COMMON /BLOCK8/ N ,  NDENS, VDENS
0641      COMMON /BLOCK9/ H ,  RCOFF, GAMDOT, DX ,  CORY
0642      COMMON /BLOCK10/ RAM , RAH , RAV
0643      COMMON /BLOCK11/ HX ,  HY ,  HZ
0644      COMMON /WORK20/ XRI ,  YRYI ,  ZRZI ,  XRXJ ,  YRYJ ,  ZRZJ
0645      COMMON /WORK21/ FXIJS, FYIJS, FZIJS, FXJIS, FYJIS, FZJIS
0646      COMMON /WORK22/ TXIJS, TYIJS, TZIJS, TXJIS, TYJIS, TZJIS
0647      COMMON /WORK23/ RCOFP2 , RP102 , D1 ,  DISQ
0648      COMMON /WORK24/ CFOXA , CFOYA , CTOYC , CE0YHYC
0649 C
0650      PARAMETER( NN=1000 , PI=3.141592653589793D0 )
0651 C
0652      REAL*8 NDENS
0653      REAL*8 RX(NN) , RY(NN) , RZ(NN) , NX(NN) , NY(NN) , NZ(NN)
0654      REAL*8 FX(NN) , FY(NN) , FZ(NN) , TX(NN) , TY(NN) , TZ(NN)
0655 C
0656      REAL*8 RXI , RYI , RZI , RXIJ , RYIJ , RZIJ , RIJSQ , RIJ
0657      REAL*8 RXJ , RYJ , RZJ
0658      REAL*8 NXI , NYI , NZI , NXIJ , NYIJ , NZIJ
0659      REAL*8 NXJ , NYJ , NZJ , NXIJ2 , NYIJ2 , NZIJ2
0660      REAL*8 FXI , FYI , FZI , TXI , TYI , TZI
0661      REAL*8 FXIJP01 , FYIJP01, FZIJP01, FXIJP02, FYIJP02, FZIJP02
0662      REAL*8 FXIJM01 , FYIJM01, FZIJM01, FXIJM02, FYIJM02, FZIJM02
0663      REAL*8 FXIJP , FYIJP , FZIJP , FXJIP , FYJIP , FZJIP
0664      REAL*8 TXIJP , TYIJP , TZIJP , TXJIP , TYJIP , TZJIP
0665      REAL*8 FXIJM , FYIJM , FZIJM , FXJIM , FYJIM , FZJIM
0666      REAL*8 TXIJM , TYIJM , TZIJM , TXJIM , TYJIM , TZJIM
0667      REAL*8 TXIJ , TYIJ , TZIJ , TXIJO , TYIJO , TZIJO
0668      REAL*8 XI , YI , ZI , XJ , YJ , ZJ
0669      REAL*8 RRXI , RRYI , RRZI , RRXIJ , RRYIJ , RRZIJ , RRIJ
0670      REAL*8 RRXJ , RRYJ , RRZJ , RCHKSQ , RCHKSQ2
0671      REAL*8 RRXIC , RRYIC , RRZIC , RRXJC , RRYJC , RRZJC
0672      REAL*8 NNXI , NNYI , NNZI , NNXJ , NNYJ , NNZJ

```

• A subroutine for calculating the forces and torques acting between particles.

```

0673      REAL*8   R11 , R12 , R21 , R22
0674      REAL*8   KI , KJ , KKI , KKJ , KIS , KJS , KKIS , KKIS2
0675      REAL*8   CKI , CKJ , CKKI , CKKJ
0676      REAL*8   KKIC , KKJC , CKKIC , CKKIC2
0677      REAL*8   CNINJ , CRIJN1 , CRIJN2 , CRIJSQ , CWIDTH
0678      REAL*8   C01X, C01Y, C01Z
0679      REAL*8   C11X, C11Y, C11Z, C12X, C12Y, C12Z
0680      REAL*8   C21X, C21Y, C21Z, C22X, C22Y, C22Z
0681      REAL*8   C1R11, C1R12, C1R21, C1R22
0682      REAL*8   C2R11, C2R12, C2R21, C2R22
0683      REAL*8   C00 , C11 , C12 , C21 , C22
0684      INTEGER  ITREE , ISKIP , IPATH , ISUBTREE
0685      LOGICAL  KEEP
0686 C
0687      DO 10 I=1,N
0688         FX(I) = 0.D0
0689         FY(I) = 0.D0
0690         FZ(I) = 0.D0
0691         TX(I) = 0.D0
0692         TY(I) = 0.D0
0693         TZ(I) = 0.D0
0694 10 CONTINUE
0695 C
0696 C ----- MAIN LOOP START
0697 C
0698      DO 2000 I=1,N-1
0699 C
0700         RXI = RX(I)
0701         RYI = RY(I)
0702         RZI = RZ(I)
0703         NXI = NX(I)
0704         NYI = NY(I)
0705         NZI = NZ(I)
0706         FXI = FX(I)
0707         FYI = FY(I)
0708         FZI = FZ(I)
0709         TXI = TX(I)
0710         TYI = TY(I)
0711         TZI = TZ(I)
0712 C
0713      DO 1000 J=I+1,N
0714 C
0715         RXJ = RX(J)
0716         RYJ = RY(J)
0717         RZJ = RZ(J)
0718         NXJ = NX(J)
0719         NYJ = NY(J)
0720         NZJ = NZ(J)
0721 C
0722         RZIJ = RZI - RZJ
0723         IF( RZIJ .GT. ZL/2.D0 ) THEN
0724             RZIJ = RZIJ - ZL
0725             RZJ = RZJ + ZL
0726         ELSE IF( RZIJ .LT. -ZL/2.D0 ) THEN
0727             RZIJ = RZIJ + ZL
0728             RZJ = RZJ - ZL
0729         END IF
0730         IF( DABS(RZIJ) .GE. RCOFF )      GOTO 1000
0731 C
0732         RYIJ = RYI - RYJ
0733         CORY = - DNINT( RYIJ/YL )
0734         RYIJ = RYIJ + CORY*YL
0735         RYJ = RYJ - CORY*YL
0736         IF( DABS(RYIJ) .GE. RCOFF )      GOTO 1000
0737 C
0738         RXIJ = RXI - RXJ
0739         RXIJ = RXIJ + CORY*DX
0740         RXJ = RXJ - CORY*DX

```

• The treatment concerning particle *i* is conducted in the following.

• The treatment concerning particles *i* and *j* is conducted in the following.

• The treatment of the periodic BC.

• The treatment of the Lees–Edwards BC.

```

0741      IF( RXIJ .GT. XL/2.D0 ) THEN
0742          RXIJ = RXIJ - XL
0743          RXJ  = RXJ  + XL
0744      ELSE IF( RXIJ .LT. -XL/2.D0 ) THEN
0745          RXIJ = RXIJ + XL
0746          RXJ  = RXJ  - XL
0747      END IF
0748      IF( DABS(RXIJ) .GE. RCOFF )      GOTO 1000
0749 C
0750      RIJSQ= RXIJ**2 + RYIJ**2 + RZIJ**2
0751      IF( RIJSQ .GE. RCOFF2 )          GOTO 1000
0752      RIJ  = DSQRT(RIJSQ)
0753 C
0754 C----- START OF MAGNETIC FORCES ---
0755      NXIJ  = NXI - NXJ
0756      NYIJ  = NYI - NYJ
0757      NZIJ  = NZI - NZJ
0758      NXIJ2 = NXI + NXJ
0759      NYIJ2 = NYI + NYJ
0760      NZIJ2 = NZI + NZJ
0761 C
0762      FXIJP01 = RXIJ + RP102*NXIJ
0763      FYIJP01 = RYIJ + RP102*NYIJ
0764      FZIJP01 = RZIJ + RP102*NZIJ
0765      FXIJP02 = RXIJ + RP102*NXIJ2
0766      FYIJP02 = RYIJ + RP102*NYIJ2
0767      FZIJP02 = RZIJ + RP102*NZIJ2
0768      FXIJM01 = RXIJ - RP102*NXIJ2
0769      FYIJM01 = RYIJ - RP102*NYIJ2
0770      FZIJM01 = RZIJ - RP102*NZIJ2
0771      FXIJM02 = RXIJ - RP102*NXIJ
0772      FYIJM02 = RYIJ - RP102*NYIJ
0773      FZIJM02 = RZIJ - RP102*NZIJ
0774 C
0775      C2R11 = FXIJP01**2 + FYIJP01**2 + FZIJP01**2
0776      C2R12 = FXIJP02**2 + FYIJP02**2 + FZIJP02**2
0777      C2R21 = FXIJM01**2 + FYIJM01**2 + FZIJM01**2
0778      C2R22 = FXIJM02**2 + FYIJM02**2 + FZIJM02**2
0779      C1R11 = DSQRT( C2R11 )
0780      C1R12 = DSQRT( C2R12 )
0781      C1R21 = DSQRT( C2R21 )
0782      C1R22 = DSQRT( C2R22 )
0783      IF( C1R11 .GE. 1.D0 ) THEN
0784          R11 = C1R11*C2R11
0785      ELSE
0786          R11 = C1R11
0787      END IF
0788      IF( C1R12 .GE. 1.D0 ) THEN
0789          R12 = C1R12*C2R12
0790      ELSE
0791          R12 = C1R12
0792      END IF
0793      IF( C1R21 .GE. 1.D0 ) THEN
0794          R21 = C1R21*C2R21
0795      ELSE
0796          R21 = C1R21
0797      END IF
0798      IF( C1R22 .GE. 1.D0 ) THEN
0799          R22 = C1R22*C2R22
0800      ELSE
0801          R22 = C1R22
0802      END IF
0803 C
0804      C11X = FXIJP01/R11
0805      C11Y = FYIJP01/R11
0806      C11Z = FZIJP01/R11
0807      C12X = FXIJP02/R12
0808      C12Y = FYIJP02/R12
0809      C12Z = FZIJP02/R12
0810      FXIJP = C11X - C12X

```

• If the two particles are separated over the cutoff distance  $r_{\text{cutoff}}^*$ , the calculation of forces and torques is unnecessary.

• The magnetic force acting between particles  $i$  and  $j$  is calculated.

--- MAGNETIC FORCES ---

• To calculate the first and second terms of Eq. (3.56) and also Eq. (3.57) separately, we calculate quantities needed in order.

• The denominators of the first and second terms in Eq. (3.56) are calculated and saved in R11 and R12.

• Similarly, those in Eq. (3.57) are calculated and saved in R21 and R22.

• The first and second terms in Eq. (3.56) are calculated and saved in (C11X, C11Y, C11Z) and (C12X, C12Y, C12Z).

• Eq. (3.56) is calculated, but  $\lambda_m$  is multiplied in the final stage.

```

0811      FYIJP = C11Y - C12Y
0812      FZIJP = C11Z - C12Z
0813      C21X = FXIJM01/R21
0814      C21Y = FYIJM01/R21
0815      C21Z = FZIJM01/R21
0816      C22X = FXIJM02/R22
0817      C22Y = FYIJM02/R22
0818      C22Z = FZIJM02/R22
0819      FXIJM = - C21X + C22X
0820      FYIJM = - C21Y + C22Y
0821      FZIJM = - C21Z + C22Z
0822 C
0823      FXJIP = - C11X + C21X
0824      FYJIP = - C11Y + C21Y
0825      FZJIP = - C11Z + C21Z
0826      FXJIM = C12X - C22X
0827      FYJIM = C12Y - C22Y
0828      FZJIM = C12Z - C22Z
0829 C
0830      FXI = FXI + ( FXIJP + FXIJM ) * RAM
0831      FYI = FYI + ( FYIJP + FYIJM ) * RAM
0832      FZI = FZI + ( FZIJP + FZIJM ) * RAM
0833      FX(J) = FX(J) + ( FXJIP + FXJIM ) * RAM
0834      FY(J) = FY(J) + ( FYJIP + FYJIM ) * RAM
0835      FZ(J) = FZ(J) + ( FZJIP + FZJIM ) * RAM
0836 C
0837      TXIJP = ( NYI * FXIJP - NZI * FYIJP )
0838      TYIJP = ( NZI * FXIJP - NXI * FZIJP )
0839      TZIJP = ( NXI * FYIJP - NYI * FXIJP )
0840      TXIJM = - ( NYI * FZIJM - NZI * FYIJM )
0841      TYIJM = - ( NZI * FZIJM - NXI * FZIJM )
0842      TZIJM = - ( NXI * FYIJM - NYI * FXIJM )
0843      TXI = TXI + ( TXIJP + TXIJM ) * ( RP102 * 3.D0 ) * RAM
0844      TYI = TYI + ( TYIJP + TYIJM ) * ( RP102 * 3.D0 ) * RAM
0845      TZI = TZI + ( TZIJP + TZIJM ) * ( RP102 * 3.D0 ) * RAM
0846 C
0847      TXJIP = ( NYJ * FZJIP - NZJ * FYJIP )
0848      TYJIP = ( NZJ * FXJIP - NXJ * FZJIP )
0849      TZJIP = ( NXJ * FYJIP - NYJ * FXJIP )
0850      TXJIM = - ( NYJ * FZJIM - NZJ * FYJIM )
0851      TYJIM = - ( NZJ * FXJIM - NXJ * FZJIM )
0852      TZJIM = - ( NXJ * FYJIM - NYJ * FXJIM )
0853      TX(J) = TX(J) + ( TXJIP + TXJIM ) * ( RP102 * 3.D0 ) * RAM
0854      TY(J) = TY(J) + ( TYJIP + TYJIM ) * ( RP102 * 3.D0 ) * RAM
0855      TZ(J) = TZ(J) + ( TZJIP + TZJIM ) * ( RP102 * 3.D0 ) * RAM
0856 C
0857 C
0858 C
0859 C
0860 C
0861      CNINJ = NXI * NXJ + NYI * NYJ + NZI * NZJ
0862      TXIJ = RXIJ / RIJ
0863      TYIJ = RYIJ / RIJ
0864      TZIJ = RZIJ / RIJ
0865      C11 = TXIJ * NXJ + TYIJ * NYJ + TZIJ * NZJ
0866 C
0867      IF( DABS(CNINJ) .LT. 0.001D0 ) THEN
0868          ITREE = 2
0869      ELSE IF( DABS(CNINJ) .GT. 0.999D0 ) THEN
0870          IF( DABS(C11) .GT. 0.999D0 ) THEN
0871              ITREE = 0
0872          END IF
0873          ITREE = 3
0874      ELSE
0875          ITREE = 1
0876      END IF
0877 C
0878 C
0879 C
0880 C
0881 C
0882 C
  
```

• The first and second terms in Eq. (3.57) are calculated and saved in (C21X, C21Y, C21Z) and (C22X, C22Y, C22Z).  
 • Eq. (3.57) is calculated, but  $\lambda_m$  is multiplied in the final stage.

• The forces acting on the positive and negative charges of particle  $j$  can be obtained from the action-reaction law;  $\lambda_m$  is multiplied in the final stage.

• The force exerted by particle  $j$  is saved in the variable of particle  $i$ .  
 • Similarly, the force exerted by particle  $i$  is saved.

--- MAGNETIC TORQUES ---

• The torque acting on particle  $i$  is calculated from Eqs. (3.59) and (3.60).

• The torque acting on particle  $j$  is calculated from Eqs. (3.59) and (3.60).

----- END OF MAGNETIC FORCES -----

----- FORCES DUE TO STERIC INER. -----

• The repulsive force due to the overlap of surfactant layers is calculated below.  
 • The variable ITREE implies the particle overlapping regime, and the procedures are performed according to ITREE.

• The regime in Table 3.1 is determined to proceed to appropriate treatment, and after the calculation of the repulsive forces, the calculation procedure returns to the main loop.

ITREE=0: LINEAR  
 ITREE=1: GENERAL  
 ITREE=2: NORMALL  
 ITREE=3: PARALLEL

```

0883 C -----
0884 C
0885 C ----- (0) LINEAR -----
0886 IF( ITREE .EQ. 0 ) THEN
0887 C
0888   IF( CNINJ .GE. 0 ) THEN
0889     IF( C11 .GE. 0 ) THEN
0890 C
0891       XJ = RXJ + NXJ*RP102
0892       YJ = RYJ + NYJ*RP102
0893       ZJ = RZJ + NZJ*RP102
0894       XI = RXI - NXI*RP102
0895       YI = RYI - NYI*RP102
0896       ZI = RZI - NZI*RP102
0897     ELSE
0898 C
0899       XJ = RXJ - NXJ*RP102
0900       YJ = RYJ - NYJ*RP102
0901       ZJ = RZJ - NZJ*RP102
0902       XI = RXI + NXI*RP102
0903       YI = RYI + NYI*RP102
0904       ZI = RZI + NZI*RP102
0905     END IF
0906   ELSE
0907     IF( C11 .GE. 0 ) THEN
0908 C
0909       XJ = RXJ + NXJ*RP102
0910       YJ = RYJ + NYJ*RP102
0911       ZJ = RZJ + NZJ*RP102
0912       XI = RXI + NXI*RP102
0913       YI = RYI + NYI*RP102
0914       ZI = RZI + NZI*RP102
0915     ELSE
0916 C
0917       XJ = RXJ - NXJ*RP102
0918       YJ = RYJ - NYJ*RP102
0919       ZJ = RZJ - NZJ*RP102
0920       XI = RXI - NXI*RP102
0921       YI = RYI - NYI*RP102
0922       ZI = RZI - NZI*RP102
0923     END IF
0924   END IF
0925 C
0926   RRIJ = DSQRT( (XI-XJ)**2 + (YI-YJ)**2 + (ZI-ZJ)**2 )
0927   XRXI = XI - RXI
0928   YRYI = YI - RYI
0929   ZRZI = ZI - RZI
0930   XRXJ = XJ - RXJ
0931   YRYJ = YJ - RYJ
0932   ZRZJ = ZJ - RZJ
0933   ISKIP = 1
0934   CALL STEFORCE( RRIJ, RAV, ISKIP, TXIJ, TYIJ, TZIJ )
0935   FXI = FXI + FXIJS
0936   FYI = FYI + FYIJS
0937   FZI = FZI + FZIJS
0938   FX(J) = FX(J) + FXJIS
0939   FY(J) = FY(J) + FYJIS
0940   FZ(J) = FZ(J) + FZJIS
0941 C
0942   GOTO 1000
0943 C
0944 END IF
0945 C ----- END OF LINEAR --
0946
0947 IF( (ITREE .EQ. 1) .OR. (ITREE .EQ. 2) ) THEN
0948 C
0949   CRIJN1 = NXI*RXIJ + NYI*RYIJ + NZI*RZIJ
0950   CRIJN2 = NXJ*RXIJ + NYJ*RYIJ + NZJ*RZIJ
0951   C00 = 1.D0 / (1.D0 - CNINJ**2)
0952   KI = C00*( -CRIJN1 + CNINJ*CRIJN2 )
0953   KJ = C00*( CRIJN2 - CNINJ*CRIJN1 )
0954 C
0955   ----- CHECK OVERLAP -----

```

• The treatment for the linear arrangement in Table 3.1.

• The positions  $(X_i, Y_i, Z_i)$  and  $(X_j, Y_j, Z_j)$  of the magnetic charges of particles  $i$  and  $j$  are calculated.

• The calculation of torques is unnecessary, so ISKIP is set as ISKIP=1.

• The repulsive forces due to the overlap of the steric layers are calculated in the subroutine STEFORCE; the results concerning particles  $i$  and  $j$  are saved in  $(FXIJS, FYIJS, FZIJS)$  and  $(FXJIS, FYJIS, FZJIS)$ , respectively.

•  $k_i$  and  $k_j$  are calculated from Eq. (3.44).

```

0955      CRIJSQ = (RXIJ + KI*NXI - KJ*NXJ )**2
0956      &           + (RYIJ + KI*NYI - KJ*NYJ )**2
0957      &           + (RZIJ + KI*NZI - KJ*NZJ )**2
0958      IF( CRIJSQ .GE. DISQ ) GOTO 1000
0959 C
0960      IF( DABS(KJ) .GT. DABS(KI) ) THEN
0961          KEEP = .TRUE.
0962          II = I
0963          JJ = J
0964          RRXI = RXI
0965          RRYI = RYI
0966          RRZI = RZI
0967          RRXJ = RXJ
0968          RRYJ = RYJ
0969          RRZJ = RZJ
0970          RRXIJ = RXIJ
0971          RRYIJ = RYIJ
0972          RRZIJ = RZIJ
0973          NNXI = NXI
0974          NNYI = NYI
0975          NNZI = NZI
0976          NNXJ = NXJ
0977          NNYJ = NYJ
0978          NNZJ = NZJ
0979          KKI = KI
0980          KKJ = KJ
0981      ELSE
0982          KEEP = .FALSE.
0983          II = J
0984          JJ = I
0985          RRXI = RXJ
0986          RRYI = RYJ
0987          RRZI = RZJ
0988          RRXJ = RXI
0989          RRYJ = RYI
0990          RRZJ = RZI
0991          RRXIJ = -RXIJ
0992          RRYIJ = -RYIJ
0993          RRZIJ = -RZIJ
0994          NNXI = NXJ
0995          NNYI = NYJ
0996          NNZI = NZJ
0997          NNXJ = NXI
0998          NNYJ = NYI
0999          NNZJ = NZI
1000          KKI = KJ
1001          KKJ = KI
1002          TXIJ = -TXIJ
1003          TYIJ = -TYIJ
1004          TZIJ = -TZIJ
1005      END IF
1006 C
1007 C
1008 C
1009 C
1010      IF( DABS(KKJ) .GE. RP102 ) THEN
1011          ISUBTREE = 1
1012      ELSE
1013          ISUBTREE = 2
1014      END IF
1015 C
1016      END IF
1017 C
1018 C
1019 C
1020 C
1021 C
1022 C
1023      IF( ITREE .EQ. 1 ) GOTO 200
1024      IF( ITREE .EQ. 2 ) GOTO 400
1025      IF( ITREE .EQ. 3 ) GOTO 600
-----
```

- The subscripts are exchanged between  $i$  and  $j$  so as to satisfy  $|k_j| > |k_i|$ .
- As a result, the particle names  $i$  and  $j$  in Table 3.1 are expressed as II and JJ in the program.

-----

ISUBTREE=1: i(sphe,cyl)-j(sphe)  
 ISUBTREE=2: i(cyl) -j(cyl)

-----

• Which part of particle  $j$  has a possibility of the overlap with particle  $i$  is grasped; there is an overlapping possibility of the hemisphere part for ISUBTREE=1 and of the cylindrical part for SUBTREE=2.

-----

ITREE=0 : LINEAR  
 ITREE=1 : GENERAL  
 ITREE=2 : NORMALL  
 ITREE=3 : PARALLEL

-----

```

1026 C
1027 C ----- (1) GENERAL -----
1028 C ----- FOR II AND JJ -----
1029 200 CNINJ = NXI*NXJ + NYI*NYJ + NZI*NZJ
1030 IF( CNINJ .GT. 0.D0 ) THEN
1031   IF( KKJ .GE. 0.D0 ) THEN
1032     IPATH = 1
1033   ELSE
1034     IPATH = 4
1035   END IF
1036 ELSE
1037   IF( KKJ .GE. 0.D0 ) THEN
1038     IPATH = 3
1039   ELSE
1040     IPATH = 2
1041   END IF
1042 END IF
1043 C
1044 KKIS = CNINJ*RP102 - (RRXIJ*NNXI + RRYIJ*NNYI + RRZIJ*NNZI)
1045 KKIS2 = -CNINJ*RP102 - (RRXIJ*NNXI + RRYIJ*NNYI + RRZIJ*NNZI)
1046 C
1047 C1 = RP102 - KKJ
1048 C1 = DINT( C1 )
1049 C2 = RP102 - DABS( KKJ )
1050 C2 = DINT( C2 )
1051 C
1052 IF( IPATH .EQ. 1 ) THEN
1053 C
1054   C12 = -1.D0
1055   C22 = -1.D0
1056   IF( ISUBTREE .EQ. 1 ) THEN
1057     C11 = RP102
1058     C21 = KKIS
1059     IF( KKIS .GT. RP102 ) C21 = RP102
1060     IF( KKIS .LT. -RP102 ) C21 = -RP102
1061   ELSE
1062     C11 = KKJ + C1
1063     C21 = KKI + C1
1064   END IF
1065 C
1066 ELSE IF( IPATH .EQ. 2 ) THEN
1067   C12 = 1.D0
1068   C22 = -1.D0
1069   IF( ISUBTREE .EQ. 1 ) THEN
1070     C11 = -RP102
1071     C21 = KKIS2
1072     IF( KKIS2 .GT. RP102 ) C21 = RP102
1073     IF( KKIS2 .LT. -RP102 ) C21 = -RP102
1074   ELSE
1075     C11 = KKJ - C2
1076     C21 = KKI + C2
1077   END IF
1078 C
1079 ELSE IF( IPATH .EQ. 3 ) THEN
1080   C12 = -1.D0
1081   C22 = 1.D0
1082   IF( ISUBTREE .EQ. 1 ) THEN
1083     C11 = RP102
1084     C21 = KKIS
1085     IF( KKIS .LT. -RP102 ) C21 = -RP102
1086     IF( KKIS .GT. RP102 ) C21 = RP102
1087   ELSE
1088     C11 = KKJ + C1
1089     C21 = KKI - C1
1090   END IF
1091 C
1092 ELSE
1093   C12 = 1.D0
1094   C22 = 1.D0
1095   IF( ISUBTREE .EQ. 1 ) THEN
1096     C11 = -RP102
1097     C21 = KKIS2

```

• The treatment for itree=1 of the general arrangement in Table 3.1.  
 • The treatment is conducted for the four cases depending on the position relationship of the positive and negative charges of particles  $i$  and  $j$ ; IPATH is used for specifying the case chosen.

$k_i^s$  (KKIS) is calculated from Eq. (3.46). Similarly,  $k_j^s$  (KKIS2) concerning the negative magnetic charge of particle  $j$  is calculated.

• According to the repulsive force model shown in Section 3.2.4, the position of the first constituent sphere to be placed is determined. The variables used to do so are C11 and C21 for particles  $j$  and  $i$ , respectively.

--- PATH=2 ---

• The direction in which the next neighboring sphere is added to form the sphere-connected particle  $j$  is specified by C12; similarly, C22 is used for particle  $i$ . C12=1 means the particle axis direction. C12=-1 means the opposite direction to the particle axis.

--- PATH=3 ---

• The direction in which the next neighboring sphere is added to form the sphere-connected particle  $j$  is specified by C12; similarly, C22 is used for particle  $i$ . C12=1 means the particle axis direction. C12=-1 means the opposite direction to the particle axis.

--- PATH=4 ---

```

1098      IF( KKIS2 .LT. -RP102 ) C21 = -RP102
1099      IF( KKIS2 .GT. RP102 ) C21 = RP102
1100      ELSE
1101          C11 = KKJ - C2
1102          C21 = KKI - C2
1103      END IF
1104  END IF
1105 C
1106 C
1107      JJJE = IDNINT(RP1)
1108  DO 250 JJJ= 0, JJJE
1109 C
1110      CKKJ = C11 + C12*DBLE(JJJ)
1111      CKKI = C21 + C22*DBLE(JJJ)
1112      IF( ( DABS(CKKJ) .GT. RP102+1.D-10 ) .OR.
1113      & ( DABS(CKKI) .GT. RP102+1.D-10 ) ) GOTO 250
1114 C
1115      IF( ISUBTREE .EQ. 1 ) THEN
1116          IF( ( DABS(CKKI) .GT. RP102+1.D-10 ) .OR.
1117          & ( DABS(CKKJ) .GT. RP102+1.D-10 ) ) GOTO 1000
1118  END IF
1119 C
1120 245      XJ = RRXJ + NNXJ*CKKJ
1121      YJ = RRYJ + NNYJ*CKKJ
1122      ZJ = RRZJ + NNZJ*CKKJ
1123      XI = RRXI + NNXI*CKKI
1124      YI = RRYI + NNYI*CKKI
1125      ZI = RRZI + NNZI*CKKI
1126      RRIJ = DSQRT( (XI-XJ)**2 + (YI-YJ)**2 + (ZI-ZJ)**2 )
1127      IF( ISUBTREE .EQ. 1 ) THEN
1128          IF( RRIJ .GE. D1 ) GOTO 1000
1129      END IF
1130      XRXI = XI - RRXI
1131      YRYI = YI - RRYI
1132      ZRZI = ZI - RRZI
1133      XRXJ = XJ - RRXJ
1134      YRYJ = YJ - RRYJ
1135      ZRZJ = ZJ - RRZJ
1136      TXIJO= (XI-XJ)/RRIJ
1137      TYIJO= (YI-YJ)/RRIJ
1138      TZIJO= (ZI-ZJ)/RRIJ
1139      ISKIP = 0
1140      CALL STEFORCE( RRIJ,RAV,ISKIP,TXIJO,TYIJO,TZIJO )
1141      IF( .NOT. KEEP ) THEN
1142          C1 = FXIJS
1143          C2 = FYIJS
1144          C3 = FZIJS
1145          FXIJS = FXJIS
1146          FYIJS = FYJIS
1147          FZIJS = FZJIS
1148          FXJIS = C1
1149          FYJIS = C2
1150          FZJIS = C3
1151          C1 = TXIJS
1152          C2 = TYIJS
1153          C3 = TZIJS
1154          TXIJS = TXJIS
1155          TYIJS = TYJIS
1156          TZIJS = TZJIS
1157          TXJIS = C1
1158          TYJIS = C2
1159          TZJIS = C3
1160      END IF
1161      FXI = FXI + FXIJS
1162      FYI = FYI + FYIJS
1163      FZI = FZI + FZIJS
1164      FX(J) = FX(J) + FXJIS
1165      FY(J) = FY(J) + FYJIS
1166      FZ(J) = FZ(J) + FZJIS
1167      TXI = TXI + TXIJS
1168      TYI = TYI + TYIJS
1169      TZI = TZI + TZIJS

```

• The positions of the spheres of particle *i* and *j* are saved in (XI,YI,ZI) and (XJ,YJ, ZJ), respectively.

• To evaluate the torque, the relative position of the sphere from the rod-like particle center is calculated.

• The posttreatment for the case of the particle names exchanged.

```

1170      TX(J) = TX(J) + TXJIS
1171      TY(J) = TY(J) + TYJIS
1172      TZ(J) = TZ(J) + TZJIS
1173 C
1174 250  CONTINUE
1175 C
1176      GOTO 1000
1177 C      ----- (2) NORMAL ---
1178 C      --- FOR II AND JJ ---
1179 C
1180 400  IF( KKJ .GE. 0.D0 ) THEN
1181      IPATH = 1
1182 ELSE
1183      IPATH = 2
1184 END IF
1185 C
1186      CNINJ = NXI*NXJ + NYI*NYJ + NZI*NZJ
1187      KKIS = CNINJ*RP102 - (RRXIJ*NNXI + RRYIJ*NNYI + RRZIJ*NNZI)
1188      KKIS2 = -CNINJ*RP102 - (RRXIJ*NNXI + RRYIJ*NNYI + RRZIJ*NNZI)
1189 C
1190      C11 = KKJ
1191      C21 = KKI
1192      IF( IPATH .EQ. 1 ) THEN
1193 C          IF( ISUBTREE .EQ. 1 ) THEN
1194              C11 = RP102
1195              C21 = KKIS
1196              IF( KKIS .GT. RP102 ) C21 = RP102
1197              IF( KKIS .LT.-RP102 ) C21 =-RP102
1198          END IF
1199      ELSE
1200          IF( ISUBTREE .EQ. 1 ) THEN
1201              C11 =-RP102
1202              C21 = KKIS2
1203              IF( KKIS2 .GT. RP102 ) C21 = RP102
1204              IF( KKIS2 .LT.-RP102 ) C21 =-RP102
1205          END IF
1206      END IF
1207
1208 C
1209 C      CKKJ = C11
1210      CKKI = C21
1211      XJ = RRXJ + CKKJ*NNXJ
1212      YJ = RRYJ + CKKJ*NNYJ
1213      ZJ = RRZJ + CKKJ*NNZJ
1214      XI = RRXI + CKKI*NNXI
1215      YI = RRYI + CKKI*NNYI
1216      ZI = RRZI + CKKI*NNZI
1217      RRIJ = DSQRT( (XI-XJ)**2 + (YI-YJ)**2 + (ZI-ZJ)**2 )
1218      IF( RRIJ .GE. D1 ) GOTO 1000
1219
1220 C
1221      RXXI = XI - RRXI
1222      YRYI = YI - RRYI
1223      ZRZI = ZI - RRZI
1224      XRXJ = XJ - RRXJ
1225      YRYJ = YJ - RRYJ
1226      ZRZJ = ZJ - RRZJ
1227      TXIJ0= (XI-XJ)/RRIJ
1228      TYIJ0= (YI-YJ)/RRIJ
1229      TZIJ0= (ZI-ZJ)/RRIJ
1230      ISKIP = 0
1231      CALL STEFORCE( RRIJ, RAV, ISKIP, TXIJ0, TYIJ0, TZIJ0 )
1232      IF( .NOT. KEEP ) THEN
1233          C1 = FXIJS
1234          C2 = FYIJS
1235          C3 = FZIJS
1236          FXIJS = FXJIS
1237          FYIJS = FYJIS
1238          FZIJS = FZJIS
1239          FXJIS = C1
1240          FYJIS = C2

```

• The treatment for the normal arrangement in Table 3.1.

•  $k_i^s$  (KKIS) is calculated from Eq. (3.46). Similarly,  $k_i^{s'}$  (KKIS2) concerning the negative magnetic charge of particle  $j$  is calculated

• According to the repulsive force model shown in Section 3.2.4, the position of the first constituent sphere to be placed is determined. The variables used to do so are C11 and C21 for particles  $j$  and  $i$ , respectively.

• The positions of the spheres of particles  $i$  and  $j$  are saved in (Xi,Yi,Zi) and (Xj,Yj,Zj), respectively.

• To evaluate the torque, the relative position of the sphere from the rod-like particle center is calculated.

• The posttreatment for the case of the particle names exchanged.

```

1241      FZJIS = C3
1242      C1   = TXIJS
1243      C2   = TYIJS
1244      C3   = TZIJS
1245      TXIJS = TXJIS
1246      TYIJS = TYJIS
1247      TZIJS = TZJIS
1248      TXJIS = C1
1249      TYJIS = C2
1250      TZJIS = C3
1251  END IF
1252      FXI = FXI + FXIJS
1253      FYI = FYI + FYIJS
1254      FZI = FZI + FZIJS
1255      FX(J) = FX(J) + FXJIS
1256      FY(J) = FY(J) + FYJIS
1257      FZ(J) = FZ(J) + FZJIS
1258      TXI = TXI + TXIJS
1259      TYI = TYI + TYIJS
1260      TZI = TZI + TZIJS
1261      TX(J) = TX(J) + TXJIS
1262      TY(J) = TY(J) + TYJIS
1263      TZ(J) = TZ(J) + TZJIS
1264 C      GOTO 1000
1265 C      ----- (3) PARALLEL --
1266 C      --- FOR I AND J ---
1267 C
1268 C
1269 600  CNINJ = NXI*NXJ + NYI*NYJ + NZI*NZJ
1270  KIS = CNINJ*RP102 - (RXIJ*NXI + RYIJ*NYI + RZIJ*NZI)
1271  KJS = CNINJ*RP102 + (RXIJ*NXJ + RYIJ*NYJ + RZIJ*NZJ)
1272 C      --- CHECK OVERLAP ---
1273  CWIDTH = (RXIJ + KIS*NXI - RP102*NXJ )**2
1274 &      + (RYIJ + KIS*NYI - RP102*NYJ )**2
1275 &      + (RZIJ + KIS*NZI - RP102*NZJ )**2
1276  IF( CWIDTH .GE. D1SQ ) GOTO 1000
1277 C
1278  IF( CNINJ .GE. 0.D0 ) THEN
1279    IPATH = 1
1280  ELSE
1281    IF( KIS .LE. -RP102 ) THEN
1282      IPATH = 2
1283    ELSE
1284      IPATH = 3
1285    END IF
1286  END IF
1287 C
1288  KEEP = .TRUE.
1289  II  = I
1290  JJ  = J
1291  RRXI = RXI
1292  RRYI = RYI
1293  RRZI = RZI
1294  RRXJ = RXJ
1295  RRYJ = RYJ
1296  RRZJ = RZJ
1297  RRXIJ = RXIJ
1298  RRYIJ = RYIJ
1299  RRZIJ = RZIJ
1300  NNXI = NXI
1301  NNYI = NYI
1302  NNZI = NZI
1303  NNXJ = NXJ
1304  NNYJ = NYJ
1305  NNZJ = NZJ
1306  KKIS = KIS
1307  IF( (IPATH .EQ. 1) .AND. (KIS .GT. KJS) ) THEN
1308    KEEP = .FALSE.
1309    II  = J
1310    JJ  = I
1311    RRXI = RXJ
1312    RRYI = RYJ

```

• The treatment for the parallel arrangement in Table 3.1.

• The square distance between particles *i* and *j* is calculated and saved in CWIDTH. In this calculation, the length of the vertical line drawn from the positive magnetic charge of particle *j* to the axis line of particle *i* is evaluated.

```

1313          RRZI   = RZJ
1314          RRXJ   = RXI
1315          RRYJ   = RYI
1316          RRZJ   = RZI
1317          RRXIJ  = -RXIJ
1318          RRYIJ  = -RYIJ
1319          RRZIJ  = -RZIJ
1320          NNXI   = NXJ
1321          NNYI   = NYJ
1322          NNZI   = NZJ
1323          NNXJ   = NXI
1324          NNYJ   = NYI
1325          NNZJ   = NZI
1326          KKIS   = KJS
1327
1328 C      END IF
1329 C
1330          KKIC   = -( RRXIJ*NNXI+ RRYIJ*NNYI + RRZIJ*NNZI )
1331          KKJC   = ( RRXIJ*NNXJ+ RRYIJ*NNYJ + RRZIJ*NNZJ )
1332          CKKIC  = DABS( KKIC )
1333          CKKIC2 = CKKIC/2.0D
1334 C
1335          C11 = KKJC/2.0D
1336          C21 = KKIC/2.0D
1337          IF( IPATH .EQ. 1 ) THEN
1338 C
1339          C12 = 1.0D
1340          C22 = 1.0D
1341          IF( CKKIC2 .GT. RP102 ) THEN
1342          C11 = RP102
1343          C21 = -RP102
1344 C
1345          END IF
1346          ELSE IF( IPATH .EQ. 2 ) THEN
1347          C12 = -1.0D
1348          C22 = 1.0D
1349          IF( CKKIC2 .GT. RP102 ) THEN
1350          C11 = -RP102
1351          C21 = -RP102
1352          END IF
1353 C
1354          ELSE
1355          C12 = 1.0D
1356          C22 = -1.0D
1357          IF( CKKIC2 .GT. RP102 ) THEN
1358          C11 = RP102
1359          C21 = RP102
1360          END IF
1361 C
1362 C
1363          JJJE = IDNINT(RP102)
1364          DO 650 JJJ= 0, JJJE
1365 C
1366          CKKJ = C11 + C12*DBLE(JJJ)
1367          CKKI = C21 + C22*DBLE(JJJ)
1368          IF( JJJ .EQ. 0 ) GOTO 645
1369          IF( ( DABS(CKKI) .GT. RP102+1.D-10 ) .OR.
1370          &           ( DABS(CKKJ) .GT. RP102+1.D-10 ) ) GOTO 1000
1371 C
1372 645      XJ   = RRXJ + NNXJ*CKKJ
1373          YJ   = RRYJ + NNYJ*CKKJ
1374          ZJ   = RRZJ + NNZJ*CKKJ
1375          XI   = RRXI + NNXI*CKKI
1376          YI   = RRYI + NNYI*CKKI
1377          ZI   = RRZI + NNZI*CKKI
1378          RRIJ = DSQRT( (XI-XJ)**2 + (YI-YJ)**2 + (ZI-ZJ)**2 )
1379          IF( RRIJ .GE. 1.0 ) GOTO 1000
1380          XRXI = XI - RRXI
1381          YRYI = YI - RRYI
1382          ZRZI = ZI - RRZI
1383          XRXJ = XJ - RRXJ

```

• The point at which the vertical line drawn from the center of particle  $j$  intersects the axis line of particle  $i$  is assumed to be denoted by  $\mathbf{r}_i + k_i^c \mathbf{e}_p$ ,  $k_i^c$ , and a similar quantity  $k_j^c$  is evaluated.

--- FOR II AND JJ ---

• According to the repulsive force model in Section 3.2.4, the position of the first sphere to be placed is determined. The variables used to do so are C11 and C21 for particles  $j$  and  $i$ , respectively.

--- PATH=1 ---

• The direction in which the next neighboring sphere is added to form the sphere-connected particle  $j$  is specified by C12.

--- PATH=2 ---

• Similarly, C22 is used for particle  $i$ . C12=1 means the particle axis direction; C12=-1 means the opposite direction to the particle axis.

--- PATH=3 ---

• The positions of the spheres of particles  $i$  and  $j$  are saved in (XI,YI,ZI) and (XJ,YJ,ZJ), respectively.

```

1384      YRYJ = YJ - RRYJ
1385      ZRZJ = ZJ - RRZJ
1386      TXIJ0= (XI-XJ)/RRIJ
1387      TYIJ0= (YI-YJ)/RRIJ
1388      TZIJ0= (ZI-ZJ)/RRIJ
1389      ISKIP = 0
1390      CALL STEFORCE( RRIJ,RAV,ISKIP,TXIJ0,TYIJ0,TZIJ0 )
1391      IF( .NOT. KEEP ) THEN
1392          C1 = FXIJS
1393          C2 = FYIJS
1394          C3 = FZIJS
1395          FXIJS = FXJIS
1396          FYIJS = FYJIS
1397          FZIJS = FZJIS
1398          FXJIS = C1
1399          FYJIS = C2
1400          FZJIS = C3
1401          C1 = TXIJS
1402          C2 = TYIJS
1403          C3 = TZIJS
1404          TXIJS = TXJIS
1405          TYIJS = TYJIS
1406          TZIJS = TZJIS
1407          TXJIS = C1
1408          TYJIS = C2
1409          TZJIS = C3
1410      END IF
1411      FXI = FXI + FXIJS
1412      FYI = FYI + FYIJS
1413      FZI = FZI + FZIJS
1414      FX(J) = FX(J) + FXJIS
1415      FY(J) = FY(J) + FYJIS
1416      FZ(J) = FZ(J) + FZJIS
1417      TXI = TXI + TXIJS
1418      TYI = TYI + TYIJS
1419      TZI = TZI + TZIJS
1420      TX(J) = TX(J) + TXJIS
1421      TY(J) = TY(J) + TYJIS
1422      TZ(J) = TZ(J) + TZJIS
1423 C      --- COUNT JUST ONCE FOR CENTRAL PLACE ---
1424      IF( JJJ .EQ. 0 ) GOTO 650
1425 C
1426      XJ = RRXJ - NNXJ*CKKJ
1427      YJ = RRYJ - NNYJ*CKKJ
1428      ZJ = RRZJ - NNZJ*CKKJ
1429      XI = RRXI - NNXI*CKKI
1430      YI = RRYI - NNYI*CKKI
1431      ZI = RRZI - NNZI*CKKI
1432      RRIJ = DSQRT( (XI-XJ)**2 + (YI-YJ)**2 + (ZI-ZJ)**2 )
1433      XRXI = XI - RRXI
1434      YRYI = YI - RRYI
1435      ZRZI = ZI - RRZI
1436      XRXJ = XJ - RRXJ
1437      YRYJ = YJ - RRYJ
1438      ZRZJ = ZJ - RRZJ
1439      TXIJ0= (XI-XJ)/RRIJ
1440      TYIJ0= (YI-YJ)/RRIJ
1441      TZIJ0= (ZI-ZJ)/RRIJ
1442      ISKIP = 0
1443      CALL STEFORCE( RRIJ,RAV,ISKIP,TXIJ0,TYIJ0,TZIJ0 )
1444      IF( .NOT. KEEP ) THEN
1445          C1 = FXIJS
1446          C2 = FYIJS
1447          C3 = FZIJS
1448          FXIJS = FXJIS
1449          FYIJS = FYJIS
1450          FZIJS = FZJIS
1451          FXJIS = C1
1452          FYJIS = C2
1453          FZJIS = C3

```

• To evaluate the torque, the relative position of the sphere from the rod-like particle center is calculated.

• The posttreatment for the case of the particle names exchanged.

• Because of the parallel arrangement, a similar calculation of the repulsive forces is carried out for the particles placed on the particle axis in the opposite direction.

```

1454      C1      = TXIJS
1455      C2      = TYIJS
1456      C3      = TZIJS
1457      TXIJS = TXJIS
1458      TYIJS = TYJIS
1459      TZIJS = TZJIS
1460      TXJIS = C1
1461      TYJIS = C2
1462      TZJIS = C3
1463      END IF
1464      FXI    = FXI    + FXIJS
1465      FYI    = FYI    + FYIJS
1466      FZI    = FZI    + FZIJS
1467      FX(J) = FX(J) + FXJIS
1468      FY(J) = FY(J) + FYJIS
1469      FZ(J) = FZ(J) + FZJIS
1470      TXI    = TXI    + TXIJS
1471      TYI    = TYI    + TYIJS
1472      TZI    = TZI    + TZIJS
1473      TX(J) = TX(J) + TXJIS
1474      TY(J) = TY(J) + TYJIS
1475      TZ(J) = TZ(J) + TZJIS
1476 C
1477 650  CONTINUE
1478 C
1479      GOTO 1000
1480 C
1481 C      ----- END OF ENERGY DUE TO STERIC INER. ---
1482 C
1483 1000 CONTINUE
1484 C
1485      FX(I) = FXI
1486      FY(I) = FYI
1487      FZ(I) = FZI
1488      TX(I) = TXI
1489      TY(I) = TYI
1490      TZ(I) = TZI
1491 C
1492 2000 CONTINUE
1493 C
1494 C      --- TORQUES DUE TO MAG. FIELD ---
1495 DO 2010 I=1,N
1496      TX(I) = TX(I) + ( NY(I)*HZ - NZ(I)*HY )*RAH
1497      TY(I) = TY(I) + ( NZ(I)*HX - NX(I)*HZ )*RAH
1498      TZ(I) = TZ(I) + ( NX(I)*HY - NY(I)*HX )*RAH
1499 2010 CONTINUE
1500
1501
1502 C**** SUB STEFORCE ****
1503      SUBROUTINE STEFORCE( RRIJ, RAV, ISKIP, TXIJ, TYIJ, TZIJ )
1504 C
1505      IMPLICIT REAL*8 ( A-H,O-Z ), INTEGER ( I-N )
1506 C
1507      COMMON /WORK20/ XRXI , YRYI , ZRZI , XRXJ , YRYJ , ZRZJ
1508      COMMON /WORK21/ FXIJS, FYIJS, FZIJS, FXJIS, FYJIS, FZJIS
1509      COMMON /WORK22/ TXIJS, TYIJS, TZIJS, TXJIS, TYJIS, TZJIS
1510      COMMON /WORK23/ RCOFF2 , RP102 , D1      , DISQ
1511 C
1512      REAL*8 FXIJ , FYIJ , FZIJ , CO
1513 C
1514      FXIJ  = 0.D0
1515      FYIJ  = 0.D0
1516      FZIJ  = 0.D0
1517 C
1518      IF( RRIJ .LT. D1 ) THEN
1519          IF( RRIJ .LE. 1.D0 ) RRIJ = 1.0001D0
1520          C0  = DLOG( D1 / RRIJ )
1521          FXIJ = TXIJ*C0
1522          FYIJ = TYIJ*C0
1523          FZIJ = TZIJ*C0
1524      END IF

```

• The torque due to the external magnetic field is calculated and added to the corresponding variable.

• A subroutine for calculating the repulsive forces resulting from the overlap of the surfactant layers according to Eq. (3.63).

```
1525 C
1526   FXIJS = FXIJ*RAV
1527   FYIJS = FYIJ*RAV
1528   FZIJS = FZIJ*RAV
1529   FXJIS = - FXIJS
1530   FYJIS = - FYIJS
1531   FZJIS = - FZIJS
1532   IF( ISKIP .EQ. 1 )  RETURN
1533 C
1534   TXIJS = YRYI*FZIJS - ZRZI*FYIJS
1535   TYIJS = ZRZI*FXIJS - XRXI*FZIJS
1536   TZIJS = XRXI*FYIJS - YRYI*FXIJS
1537   TXJIS = YRYJ*FZJIS - ZRZJ*FYJIS
1538   TYJIS = ZRZJ*FXJIS - XRXJ*FZJIS
1539   TZJIS = XRXJ*FYJIS - YRYJ*FXJIS
1540
1541
```

- The torques acting on particles *i* and *j* due to the repulsive forces are calculated and saved in (TXIJS,TYIJS,TZIJS) and (TXJIS, TYJIS,TZJIS), respectively.

--- TORQUES ---

RETURN  
END

# 4 Practice of Monte Carlo Simulations

In the present chapter we demonstrate the two examples of an Monte Carlo (MC) simulation by considering the aggregation phenomena of magnetic particles in an applied magnetic field. The first exercise treats a two-dimensional suspension composed of magnetic spherocylinder particles with the purpose of discussing the dependence of the particle behavior on the magnetic particle–particle and the particle–field interactions. The second exercise treats a three-dimensional suspension composed of magnetic disk-like particles for discussing similar particle behavior in thermodynamic equilibrium. Understanding the MC method for simulations of these nonspherical systems is an important first step in treating a more complex system, such as DNA, polymeric liquids, or carbon-nanotubes. The sample simulation programs that follow each exercise have been taken from real-life academic-oriented research projects and are therefore realistic examples for guidance in writing an academic or commercial simulation program. In both examples demonstrated here, the canonical MC algorithm is used under the physical conditions of a given number of particles, temperature, and volume of the system.

## 4.1 Orientational Phenomena of Rod-like Particles in an Applied Magnetic Field

In the present section we consider a suspension composed of magnetic rod-like particles as a two-dimensional system that is in thermodynamic equilibrium under the conditions of a constant number of particles, temperature, and volume. A sample simulation program written in the FORTRAN language completes the exercise.

### 4.1.1 Physical Phenomena of Interest

The system, assumed to be in thermodynamic equilibrium, is composed of  $N$  ferromagnetic particles with diameter  $d$  and length  $l_0 (=l + d)$  that are dispersed in a base liquid. Each magnetic rod-like particle is modeled as a spherocylinder, as already explained in Section 3.2, with magnetic plus and minus charges at the centers of each hemisphere cap; it is therefore magnetized in the particle axis direction. Each particle is coated with a surfactant layer for stabilization purposes. In this type of dispersion, the aggregation phenomenon of magnetic particles is strongly dependent on the magnetic field strength, magnetic interactions, and the number

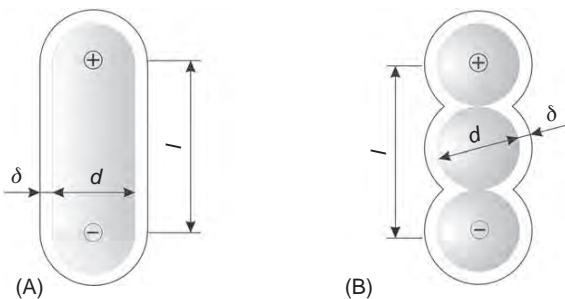


**Figure 4.1** Rod-like particle model with a steric layer: (A) the spherocylinder model and (B) the sphere-connected model.

density. In this example we discuss the influence of these effects on particle aggregation by means of a canonical MC simulation.

#### 4.1.2 Specification of Problems in Equations

The main consideration in formulating the present problem is the interaction energy between the particles. Similar to Section 3.2, it is necessary to take into account magnetic interactions and steric repulsive interactions acting between particles for the spherocylinder particle model shown in Figure 4.1A. The treatment of the steric interactions due to particle overlap is difficult even in the present two-dimensional case. Therefore, in evaluating the steric interactions, we employ the simple linear sphere-connected model shown in Figure 4.1B. In this model, each constituent sphere is covered by a uniform steric layer. Hence, a repulsive interaction energy due to the overlap of the two steric layers can be obtained by summing all interaction energies for each pair of spheres belonging to the two different rod-like particles. This is a characteristic feature of the sphere-connected model, which is different from the model employed in Section 3.2 in that the constituent spheres are in fixed positions in the present case.

It is difficult to treat the particle overlap in a manner that results in an efficient simulation program, even for the two-dimensional case, and therefore considerable effort is required to address this problem for a three-dimensional system. In many cases, rather than directly addressing the three-dimensional system, it is more effective to first develop a two-dimensional simulation program and then extend it to the three-dimensional case. The three-dimensional simulation program shown in Section 3.2 has been developed using this approach from the present two-dimensional program, which will be shown in Section 4.1.6.

We use the notation  $\mathbf{r}_i$  for the position vector of the center of particle  $i$  ( $i = 1, 2, \dots, N$ ),  $\mathbf{e}_i$  for the particle axis direction vector, and  $\pm q$  for the plus and minus magnetic charges at both hemispheres. The interaction energy with an applied magnetic field  $\mathbf{H}$  is expressed similar to the spherical particles as

$$u_i = -\mu_0 \mathbf{m}_i \cdot \mathbf{H} \quad (4.1)$$

in which  $\mathbf{m}_i$  is the magnetic moment, expressed as  $\mathbf{m}_i = q \mathbf{e}_i$  ( $= m \mathbf{e}_i$ ). Eq. (4.1) implies that a rod-like particle tends to incline in the magnetic field direction, leading to a minimum interaction energy.

We first show an expression for the interaction energy  $u$  between magnetic charges  $q$  and  $q'$ . If the magnetic charges are separated by distance  $r$ , the interaction energy is expressed as

$$u = \frac{\mu_0 q q'}{4\pi r} \quad (4.2)$$

This equation is quite well known [31]. Eq. (4.2) is applied to the present magnetic rod-like particle shown in Figure 4.1. The interaction energy for the rod-like particles shown in Figure 4.1B can be obtained by summing the interaction energies for the four pairs of magnetic charges. If the position vectors of the plus and minus charges of an arbitrary particle  $i$  are denoted by  $\mathbf{r}_i^+$  and  $\mathbf{r}_i^-$ , respectively, they are written as

$$\mathbf{r}_i^+ = \mathbf{r}_i + (l/2)\mathbf{e}_i, \quad \mathbf{r}_i^- = \mathbf{r}_i - (l/2)\mathbf{e}_i \quad (4.3)$$

With this notation, the magnetic interaction energy  $u_{ij}$  between rod-like particles  $i$  and  $j$  is expressed as

$$u_{ij} = \frac{\mu_0 q^2}{4\pi} \left\{ \frac{1}{|\mathbf{r}_i^+ - \mathbf{r}_j^+|} - \frac{1}{|\mathbf{r}_i^+ - \mathbf{r}_j^-|} - \frac{1}{|\mathbf{r}_i^- - \mathbf{r}_j^+|} + \frac{1}{|\mathbf{r}_i^- - \mathbf{r}_j^-|} \right\} \quad (4.4)$$

The first term on the right-hand side is an interaction energy between the plus charges of particles  $i$  and  $j$ . The second term is an energy between the plus charge of particle  $i$  and the minus charge of particle  $j$ . The third term is an energy between the minus charge of particle  $i$  and the plus charge of particle  $j$ . The fourth term is an energy between the minus charges of particles  $i$  and  $j$ . Substitution of Eq. (4.3) into Eq. (4.4) leads to

$$u_{ij} = \frac{\mu_0 q^2}{4\pi} \left\{ \frac{1}{|\mathbf{r}_{ij} + l(\mathbf{e}_i + \mathbf{e}_j)/2|} - \frac{1}{|\mathbf{r}_{ij} + l(\mathbf{e}_i + \mathbf{e}_j)/2|} - \frac{1}{|\mathbf{r}_{ij} - l(\mathbf{e}_i + \mathbf{e}_j)/2|} + \frac{1}{|\mathbf{r}_{ij} - l(\mathbf{e}_i + \mathbf{e}_j)/2|} \right\} \quad (4.5)$$

in which  $\mathbf{r}_{ij} = \mathbf{r}_i - \mathbf{r}_j$  and  $\mathbf{e}_{ij} = \mathbf{e}_i - \mathbf{e}_j$ .

We now consider an interaction energy  $u_{ij}^{(V)}$  arising from the overlap of the steric layers. For a spherical particle with diameter  $d$  covered by a uniform surfactant layer with thickness  $\delta$ , an overlap of these two particles yields a repulsive interaction energy  $u_{ij}^{(V)}$ , as already shown in Eq. (3.41):

$$u_{ij}^{(V)} = kT\lambda_V \left\{ 2 - \frac{2r_{ij}/d}{t_\delta} \ln \left( \frac{d + 2\delta}{r_{ij}} \right) - 2 \frac{r_{ij}/d - 1}{t_\delta} \right\} \quad (4.6)$$

in which  $r_{ij}$  is the separation between particles  $i$  and  $j$  (center-to-center distance),  $t_\delta$  is the ratio of the steric layer thickness to the particle radius expressed as  $t_\delta = 2\delta/d$ ,  $\lambda_V$  is a nondimensional parameter representing the strength of steric repulsive interactions expressed as  $\lambda_V = \pi d^2 n_s/2$ , and  $n_s$  is the number of surfactant molecules per

unit area on the particle surface. If the particle separation satisfies  $r_{ij} < d + 2\delta$ , the two steric layers of particles  $i$  and  $j$  overlap. In the following, we apply this interaction energy to the two spherocylinder particles shown in Figure 4.1B.

The sphere-connected model enables us to employ the evaluation approach, which has been used for calculating magnetic interactions. That is, the net steric interaction energy between the two rod-like particles can be obtained by summing a steric interaction energy for each pair of constituent spherical particles belonging to the two different rod-like particles. However, this approach becomes inefficient, or requires enormous computation time, as the rod-like particle becomes longer (i.e., for an increase in the number of spherical particles). Since the steric layer is thin compared with the particle diameter, the pair-wise calculation of the repulsive interactions implies that, for some calculations, the result is negligible. We therefore need to develop an alternative technique for calculating the steric interactions. This kind of difficulty frequently appears in developing a simulation program, so the process of overcoming this problem provides a good opportunity for the development of a higher-level simulation program. Therefore, in the following we discuss this problem in more detail.

The spatial relationship of two rod-like particles  $i$  and  $j$  is a function of the particle position vectors  $\mathbf{r}_i$  and  $\mathbf{r}_j$  and the particle direction (unit) vectors  $\mathbf{e}_i$  and  $\mathbf{e}_j$ . In practice, a two-dimensional system is considerably more straightforward than a three-dimensional system in treating the overlap assessment. Referring to Figure 4.2, we now discuss the overlap between particles  $i$  and  $j$ . Assessing how the two rod-like particles overlap first requires finding the intersection point of each particle axis. If the two axis lines intersect at the positions  $(\mathbf{r}_i + k_i \mathbf{e}_i)$  and  $(\mathbf{r}_j + k_j \mathbf{e}_j)$  of particles  $i$  and  $j$ , respectively, then the unknown constants  $k_i$  and  $k_j$  have to satisfy the following equation:

$$\mathbf{r}_i + k_i \mathbf{e}_i = \mathbf{r}_j + k_j \mathbf{e}_j \quad (4.7)$$

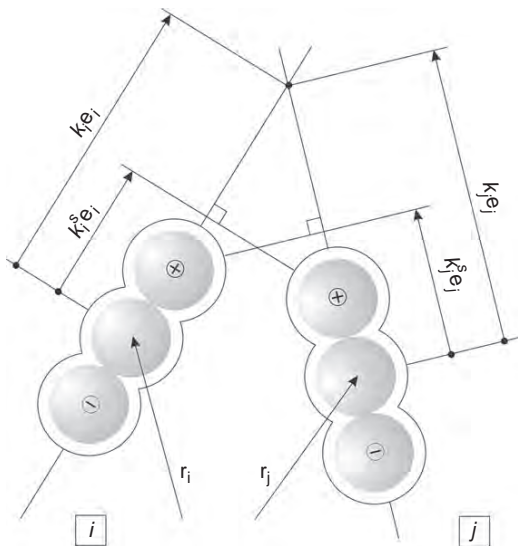


**Figure 4.2** Analysis of the overlap condition of steric layers.

Vector product of  $\mathbf{e}_j$  (or  $\mathbf{e}_i$ ) on both sides of this equation yields  $|k_i|$  (or  $|k_j|$ ):

$$|k_i| = \frac{|\mathbf{r}_{ij} \times \mathbf{e}_j|}{|\mathbf{e}_i \times \mathbf{e}_j|}, \quad |k_j| = \frac{|\mathbf{r}_{ij} \times \mathbf{e}_i|}{|\mathbf{e}_i \times \mathbf{e}_j|} \quad (4.8)$$

These equations are valid for a nonparallel configuration. For parallel cases, the treatment of the particle overlap is quite straightforward and will be explained later.

Next we need to find the point  $(\mathbf{r}_i + k_i^s \mathbf{e}_i)$  on the axis line of particle  $i$ , which is the intersection point of the line drawn from the position  $\mathbf{r}_j^+$  of the plus magnetic charge of particle  $j$  that perpendicularly intersects the axis line of particle  $i$ . The orthogonality condition of this vertical line and the particle direction vector  $\mathbf{e}_i$  provides the solution of the unknown constant  $k_i^s$  as

$$k_i^s = \frac{l}{2} \mathbf{e}_i \cdot \mathbf{e}_j - \mathbf{r}_{ij} \cdot \mathbf{e}_i \quad (4.9)$$

The solution of  $k_j^s$  can be obtained by exchanging the subscripts  $i$  and  $j$  in this equation. Similarly, if a line drawn from the position  $\mathbf{r}_j^-$  perpendicularly intersects the axis line of particle  $i$  at the position  $(\mathbf{r}_i + k_i^{s'} \mathbf{e}_i)$ , the above-mentioned mathematical procedure gives rise to the solution of  $k_i^{s'}$  as

$$k_i^{s'} = -\frac{l}{2} \mathbf{e}_i \cdot \mathbf{e}_j - \mathbf{r}_{ij} \cdot \mathbf{e}_i \quad (4.10)$$

The use of these intersection points enables us to calculate effectively the repulsive interaction energy between particles  $i$  and  $j$  arising from the overlap of the steric layers. First, the solutions of  $k_i$  and  $k_j$  are obtained from Eqs. (4.7) and (4.8). From the large-or-small relationship and the positive-or-negative sign of  $k_i$  and  $k_j$ , we see which sphere of particle  $i$  has a possibility of interacting with which sphere of particle  $j$ . For example, since  $k_j > k_i > 0$  in Figure 4.2, there is a possibility of the plus magnetic charged sphere of particle  $j$  interacting with any constituent spheres of particle  $i$ . Which sphere of particle  $i$  interacts with the plus charged sphere of particle  $j$  can be determined by the solution  $k_i^s$  in Eq. (4.9). Because  $k_i^s > l/2$  in Figure 4.2, it has a possibility to interact with the plus magnetic charged sphere of particle  $i$ . At this stage, we have identified the first pair of constituent spheres of the particles  $i$  and  $j$  required for calculating the interaction energy due to the overlap of the steric layers.

After this calculation, we shift our attention to the next neighboring constituent spheres of each particle and calculate their interaction energy. Repeating this procedure finally yields the total interaction energy due to the particle overlap of particles  $i$  and  $j$ . An important advantage of this procedure is that the nonoverlap of the constituent spheres can be used to terminate the calculation. In other words, this method becomes much more efficient with an increasing particle length when compared to the simple calculation method, in which all possible pairs of constituent

spheres are treated. Note that there may be situations where one constituent sphere of particle  $j$  may interact with two constituent spheres of particle  $i$ . For example, in Figure 4.2, this situation may arise if the two axis lines intersect under the condition of  $-l/2 < k_i^s < l/2$ ; in this case, the sphere of particle  $j$  is located at a position between the two constituent spheres of particle  $i$ .

The parallel configuration and the linear configuration do not require values of  $k_i$  and  $k_j$  for the calculation of the steric interaction energy. The linear configuration satisfies the relationships of  $|\mathbf{e}_i \cdot \mathbf{e}_j| = |\mathbf{e}_i \cdot \mathbf{t}_{ij}| = 1$ , in which  $\mathbf{t}_{ij}$  is the unit vector between particles  $i$  and  $j$ , expressed as  $\mathbf{t}_{ij} = \mathbf{r}_{ij}/r_{ij}$ . Only the two spheres at the end of each particle have a possibility to overlap for the linear configuration, so that just one calculation is sufficient for this case; these spheres can be straightforwardly specified by the signs of  $\mathbf{e}_i \cdot \mathbf{e}_j$  and  $\mathbf{e}_i \cdot \mathbf{t}_{ij}$ . For the parallel configuration, a value of  $k_i^s$  in Eq. (4.9) provides information as to how the two particles are shifted in separation along the particle axis direction. The value of  $k_i^s$  or  $k_j^s$  indicates which sphere of particle  $j$  interacts with which sphere of particle  $i$  in the nearest configuration.

In the above discussion, we have explained the fundamental and mathematical aspects of evaluating the steric interaction between the particles. The technical aspect of this treatment, required for developing a simulation program, will be discussed in detail later in the next subsection on the MC algorithm.

Finally, we show the nondimensional expressions of the important physical quantities. If distances and energies are nondimensionalized by the particle diameter  $d$  and the thermal energy  $kT$ , respectively, Eqs. (4.1), (4.4), (4.5), and (4.6) are nondimensionalized as

$$u_i^* = u_i/kT = -\xi \mathbf{e}_i \cdot \mathbf{h} \quad (4.11)$$

$$u_{ij}^* = u_{ij}/kT = \lambda_0 \left\{ \frac{1}{|\mathbf{r}_i^{+*} - \mathbf{r}_j^{+*}|} - \frac{1}{|\mathbf{r}_i^{+*} - \mathbf{r}_j^{-*}|} - \frac{1}{|\mathbf{r}_i^{-*} - \mathbf{r}_j^{+*}|} + \frac{1}{|\mathbf{r}_i^{-*} - \mathbf{r}_j^{-*}|} \right\} \quad (4.12)$$

$$\begin{aligned} u_{ij}^* &= u_{ij}/kT \\ &= \lambda_0 \left\{ \frac{1}{|\mathbf{r}_{ij}^* + r_p \mathbf{e}_{ij}/2|} - \frac{1}{|\mathbf{r}_{ij}^* + r_p(\mathbf{e}_i + \mathbf{e}_j)/2|} - \frac{1}{|\mathbf{r}_{ij}^* - r_p(\mathbf{e}_i + \mathbf{e}_j)/2|} + \frac{1}{|\mathbf{r}_{ij}^* - r_p \mathbf{e}_{ij}/2|} \right\} \end{aligned} \quad (4.13)$$

$$u_{ij}^{(V)*} = u_{ij}^{(V)}/kT = \lambda_V \left\{ 2 - \frac{2r_{ij}^*}{t_\delta} \ln \left( \frac{1+t_\delta}{r_{ij}^*} \right) - 2 \frac{r_{ij}^* - 1}{t_\delta} \right\} \quad (4.14)$$

in which  $r_p$  is the particle aspect ratio, defined as  $r_p = l/d$ . In addition, the nondimensional parameters  $\xi$  and  $\lambda_0$  are expressed as

$$\xi = \mu_0 m H / kT, \quad \lambda_0 = \mu_0 (qd)^2 / 4\pi d^3 kT \quad (4.15)$$

in which  $\mathbf{h} = \mathbf{H}/H (H = |\mathbf{H}|)$  and the quantities with superscript \* are dimensionless quantities. As previously explained in Eqs. (3.62) and (3.58), the meanings of  $\xi$  and  $\lambda_0$  are the strengths of magnetic particle–field and magnetic particle–particle interactions, respectively. A slightly different nondimensional parameter  $\lambda = r_p^2 \lambda_0$  is introduced for discussion.

#### 4.1.3 Canonical Monte Carlo Algorithm

The system is in thermodynamic equilibrium, composed of  $N$  rod-like particles with specified volume  $V$  (i.e., area in this two-dimensional case) and temperature  $T$ , and it is appropriate to use the canonical MC algorithm for the simulation. The total system potential energy is evaluated by summing the magnetic particle–field and the particle–particle interaction energy together with the steric repulsive interaction energy due to the overlap of the steric layers. That is,

$$U^* = \sum_{i=1}^N u_i^* + \sum_{i=1}^N \sum_{j=1(j>i)}^N \left( u_{ij}^* + u_{ij}^{(V)*} \right) \quad (4.16)$$

We now consider a transition from the present microscopic state  $k$ , which has a system potential energy  $U_k$ . A new microscopic state  $l$  is generated by selecting one particle and moving it to a new position by using random numbers, which yields a new system potential energy  $U_l$ . The transition probability from microscopic state  $k$  to  $l$ ,  $p_{kl}$ , is given by Eq. (1.49), but in this case the probability density ratio is

$$\frac{\rho_l}{\rho_k} = \exp \left\{ -\frac{1}{kT} (U_l - U_k) \right\} = \exp \left\{ -(U_l^* - U_k^*) \right\} \quad (4.17)$$

After this treatment of the translational displacement of the particle, a similar procedure is conducted for the rotational displacement. A series of trials for the translational and rotational displacement, when applied to all the system particles, is called an “MC step,” which corresponds to a time step in the molecular dynamics method.

From the viewpoint of developing a simulation program, we now show the scheme for calculating the interaction energy due to the overlap of the steric layers. Figure 4.3 shows the categories of overlap for the two particles. There are four typical overlap regimes: linear (itree = 0), general (itree = 1), perpendicular (itree = 2), and parallel (itree = 3). Any overlap of the steric layers can be classified into one of these four regimes. Note that the variables itree and ipath (appearing later) have no physical meaning but are used for the sake of convenience; these variables are used in the sample simulation program with consistent meaning. We explain the four overlap cases in more detail in the following paragraphs.

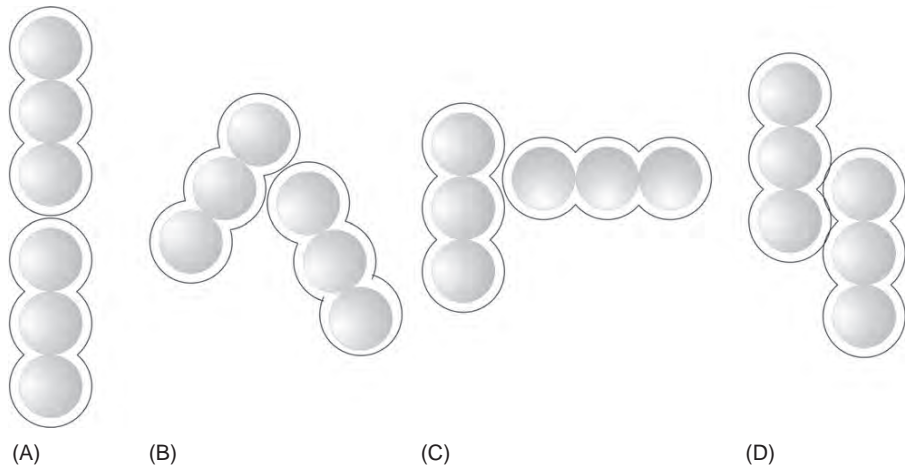


**Figure 4.3** Typical overlap regime of the steric layers: (A) linear ( $itree = 0$ ), (B) general ( $itree = 1$ ), (C) perpendicular ( $itree = 2$ ), and (D) parallel ( $itree = 3$ ).

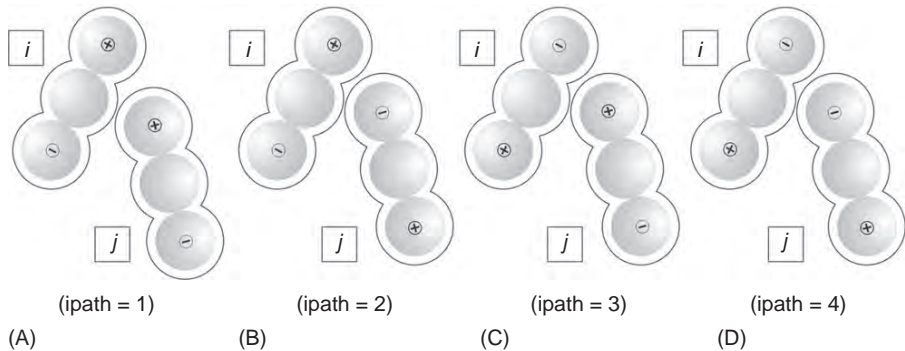


**Figure 4.4** Overlap in the general situation ( $itree = 1$ ).

#### 4.1.3.1 General Overlap Case ( $itree = 1$ )

In this case, there are four types of overlap dependent upon the location of the plus and minus magnetic charges, which are schematically shown in Figure 4.4. In order to treat the particle overlap consistently in a simulation program, the names of the two particles may be exchanged in such a way so as to satisfy the relationship  $|k_i| < |k_j|$ . This condition is assumed to be satisfied in the following discussion. Figures 4.4A and C show the possibility of the plus magnetic charge of particle  $j$  overlapping with particle  $i$ . Figures 4.4B and D are for the overlap of the minus magnetic charge of particle  $j$  with particle  $i$ .

The four types of particle overlaps in Figure 4.4 can be identified in the following way. By reason of  $|k_i| < |k_j|$ , the particle on the left-hand side in Figure 4.4 is

particle  $i$ , and the particle on the right-hand side is particle  $j$ . For the case of  $\mathbf{e}_i \cdot \mathbf{e}_j \geq 0$ , the overlap regime is ipath = 1 or ipath = 4, and for the case of  $\mathbf{e}_i \cdot \mathbf{e}_j < 0$ , it is ipath = 2 or ipath = 3. Furthermore, the sign of  $k_j$  enables us to identify whether ipath = 1 or ipath = 4 arises for the overlap, which is also applicable to the identification of ipath = 2 or ipath = 3. For example, for the case of  $\mathbf{e}_i \cdot \mathbf{e}_j \geq 0$  and  $k_j \geq 0$ , there is a possibility of particle overlap in the situation ipath = 1.

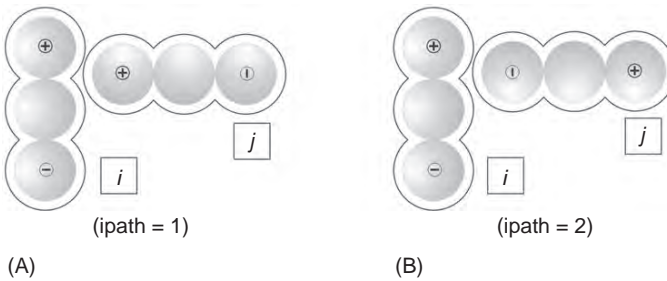
We now discuss which constituent sphere of particle  $i$  interacts with the magnetic charged sphere of particle  $j$ . Since the principle is the same for all cases, we focus on the case of ipath = 1. The value of  $k_i^s$  can allow us to identify which sphere of particle  $i$  has the possibility to interact with the plus magnetic charged sphere of particle  $j$ . For simplification, we name the constituent spheres in the rod-like particle in such a way that the plus magnetic charged sphere is called “subparticle 1,” the next neighboring sphere is called “subparticle 2,” and so on. For  $k_i^s \geq l/2$ , subparticle 1 of particle  $j$  may overlap with subparticle 1 of particle  $i$ ; similarly,  $l/2 > k_i^s \geq (l/2 - d)$  overlaps with subparticle 1 or subparticle 2; and  $(l/2 - d) > k_i^s \geq (l/2 - 2d)$  overlaps with subparticle 2 or subparticle 3. Even if the rod-like particle is composed of numerous subparticles, the above-mentioned procedure can provide us with a method to find which subparticle of particle  $i$  overlaps with particle  $j$ .

We now consider the case in which subparticle 1 of particle  $j$  overlaps with subparticle 2 or 3 of particle  $i$ . The total repulsive interaction energy between particles  $i$  and  $j$  can be obtained by calculating the interaction energy in Eq. (4.14) for this pair of subparticles and by repeating this calculation procedure for the neighboring subparticles for subparticle 2 of particle  $j$  and subparticle 3 or 4 (note that subparticle 4 does not exist for the present three-sphere-connected model) of particle  $i$ , and so on. The calculation procedure can be terminated when a pair of the subparticles is found to be separated by more than the distance  $(d + 2\delta)$ . In the case of Figure 4.4A, only the first two calculations are needed to obtain the total steric repulsive interaction energy between particles  $i$  and  $j$ . This discussion clearly suggests that the present method becomes much more effective for a longer rod-like particle. In the sample simulation program shown later, the above-mentioned procedures are employed for calculating the steric interaction energy together with the variables itree and ipath with the same meaning as above.

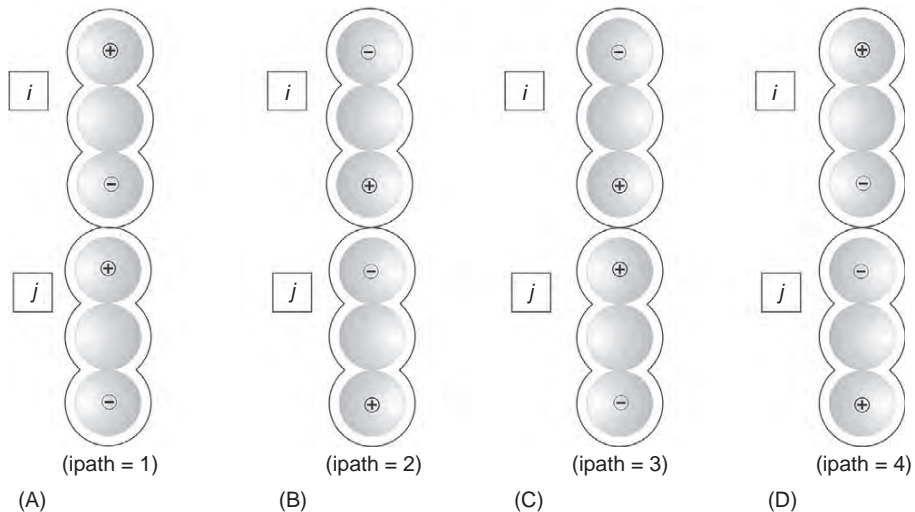
#### 4.1.3.2 Normal Overlap Case (itree = 2)

Figure 4.5 shows the two categories of particle overlap in a normal orientation. As in the general overlap case, the subscripts  $i$  and  $j$  may be exchanged in order to satisfy  $|k_i| < |k_j|$ . Figure 4.5A shows an overlap between subparticle 1 of particle  $j$  and particle  $i$ , and Figure 4.5B is for the case of the other end subparticle of particle  $j$  overlapping with particle  $i$ . These two categories can be identified by the value of  $k_j$ ; that is, there is a possibility of particle overlap in the situation ipath = 1 or ipath = 2 for  $k_j > 0$  or  $k_j < 0$ , respectively.

We treat the case ipath = 1 shown in Figure 4.5 to consider which subparticle of particle  $i$  possibly overlaps with the subparticle of particle  $j$ . As in the general



**Figure 4.5** Overlap in the normal situation (*itree* = 2).



**Figure 4.6** Overlap in the linear situation (*itree* = 0).

overlap situation, subparticle 1 possibly overlaps with subparticle 1 of particle *j* for  $k_i^s \geq l/2$ , subparticle 1 or 2 overlaps with particle *j* for  $l/2 > k_i^s \geq (l/2 - d)$ , and subparticle 2 or 3 does so for  $(l/2 - d) > k_i^s \geq (l/2 - 2d)$ . For the case where the rod-like particle is composed of numerous subparticles, the above-mentioned procedure is repeated to find a pair or two pairs of interacting subparticles.

#### 4.1.3.3 Linear Overlap Case (*itree* = 0)

In the linear overlap case, there are four types of overlap possibility, as shown in Figure 4.6. The four categories can be identified by assessing the signs of  $\mathbf{e}_i \cdot \mathbf{e}_j$  and  $\mathbf{e}_j \cdot \mathbf{t}_{ij}$ . That is, the relationship  $\mathbf{e}_i \cdot \mathbf{e}_j > 0$  provides an overlap for ipath = 1 or ipath = 2, and  $\mathbf{e}_i \cdot \mathbf{e}_j < 0$  provides an overlap for ipath = 3 or ipath = 4. For the case of  $\mathbf{e}_i \cdot \mathbf{e}_j > 0$ , the sign of  $\mathbf{e}_j \cdot \mathbf{t}_{ij}$  can identify whether the overlap is for ipath = 1 or ipath = 2. Subsequently, there is a possibility of particle overlap in the situation

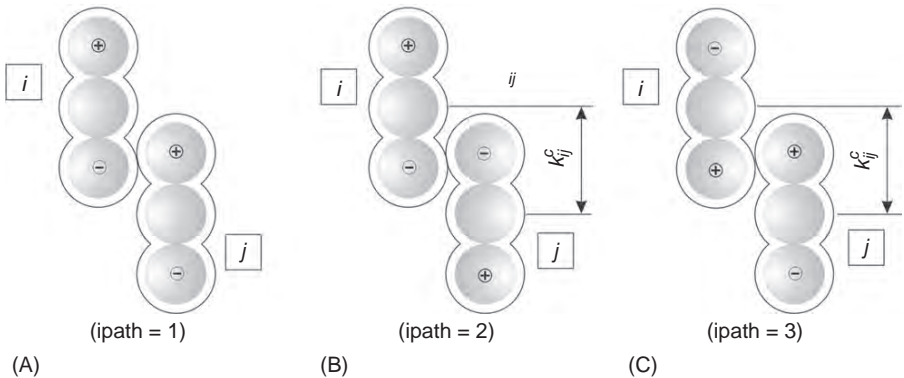


**Figure 4.7** Overlap in the parallel situation ( $itree = 3$ ).

where  $ipath = 1$  for  $\mathbf{e}_i \cdot \mathbf{e}_j > 0$  and  $\mathbf{e}_j \cdot \mathbf{t}_{ij} > 0$ ,  $ipath = 2$  for  $\mathbf{e}_i \cdot \mathbf{e}_j > 0$  and  $\mathbf{e}_j \cdot \mathbf{t}_{ij} < 0$ ,  $ipath = 3$  for  $\mathbf{e}_i \cdot \mathbf{e}_j < 0$  and  $\mathbf{e}_j \cdot \mathbf{t}_{ij} > 0$ , and  $ipath = 4$  for  $\mathbf{e}_i \cdot \mathbf{e}_j < 0$  and  $\mathbf{e}_j \cdot \mathbf{t}_{ij} < 0$ . Once the type of particle overlap is identified, the pair of the overlapping subparticles is readily identified in order to calculate the interaction energy.

#### 4.1.3.4 Parallel Overlap Case ( $itree = 3$ )

For the parallel overlap case, there are three types of particle overlap, as shown in Figure 4.7. For the case of  $ipath = 1$  in Figure 4.7A, the relationship  $k_i^s \leq k_j^s$  needs to be satisfied by exchanging the particle names. The overlap regime is identified by assessing the sign of  $\mathbf{e}_i \cdot \mathbf{e}_j$  with a value of  $k_i^s$ . That is, the overlap regime is  $ipath = 1$  for  $\mathbf{e}_i \cdot \mathbf{e}_j > 0$ ,  $ipath = 2$  for  $\mathbf{e}_i \cdot \mathbf{e}_j < 0$  and  $k_i^s \leq -l/2$ , and  $ipath = 3$  for  $\mathbf{e}_i \cdot \mathbf{e}_j < 0$  and  $k_i^s > -l/2$ .

We focus on the cases  $ipath = 2$  and  $3$  for discussion, since the treatment for  $ipath = 1$  is almost the same as in the general overlap case. For  $ipath = 2$  and  $3$ , the determination of the separation between the particle centers makes the subsequent treatment more straightforward. The separation between the particle centers along the particle axis,  $k_{ij}^c$ , is expressed as  $k_{ij}^c = |k_i^s| - l/2$  for  $ipath = 2$ , and as  $k_{ij}^c = k_i^s + l/2$  for  $ipath = 3$ . Because of the similarity in the treatment for  $ipath = 2$  and  $3$ , we explain only the case of  $ipath = 2$ . The value of  $k_{ij}^c$  allows us to find which subparticle of particle  $i$  overlaps with the minus magnetic charged sphere of particle  $j$ . There is a possibility of the overlap with subparticle 1 or 2 of particle  $i$  for  $d \geq k_{ij}^c > 0$  and of the overlap with subparticle 2 or 3 for  $2d \geq k_{ij}^c > d$ . This calculation procedure is repeated until the end-sphere of particle  $i$  obtains the total steric interaction energy.

#### 4.1.4 Parameters for Simulations

We employed the following parameters for conducting the simulations. It is presumed that the rod-like particles aggregate to form chain-like clusters along the

applied field direction (i.e.,  $y$ -axis direction). We therefore choose to employ a rectangular simulation region dependent upon the particle aspect ratio; we therefore adopt a rectangular region having a side length in the  $y$ -direction twice that of in the  $x$ -direction. The results shown in the next subsection were obtained under the assumption that a rod-like particle may be represented by three spherical subparticles. The area fraction  $\phi_V = 0.2$ , the nondimensional parameter  $\lambda_V$ , representing the strength of steric repulsive interactions, is set as  $\lambda_V = 150$ . The thickness of the steric layer is assumed as  $t_\delta = 0.3$ . The maximum distance  $\delta r_{\max}^*$  and angle  $\delta\theta_{\max}$  per one trial in the MC algorithm are taken as  $\delta r_{\max}^* = 0.1$  and  $\delta\theta_{\max} = 5^\circ$ . The MC simulations were carried out for various cases of the magnetic particle–field and the particle–particle interactions,  $\xi$  and  $\lambda$ , respectively.

#### 4.1.5 Results of Simulations

Figures 4.8–4.11 show the results relating to the aggregate structures, which were obtained by conducting the sample simulation program shown in the next subsection. Figure 4.8 was obtained for  $\lambda_0 = 0.75$ , Figure 4.9 for  $\lambda_0 = 1.75$ , Figure 4.10 for  $\lambda_0 = 4$ , and Figure 4.11 for  $\lambda_0 = 7.5$ . Each figure has two snapshots: one for the case of no external field, and the other for the case of a strong applied magnetic field.

For the case of  $\lambda_0 = 0.75$ , shown in Figure 4.8, the magnetic interaction between particles is of the same order of the thermal energy and therefore no aggregates are observed in Figures 4.8A and B. Figure 4.8A is for the case of no external field and therefore the rod-like particles have no specifically favored directional characteristic. On the other hand, the rod-like particles tend to incline in the magnetic field direction in Figure 4.8B because  $\xi = 20$  represents a significantly strong magnetic field.

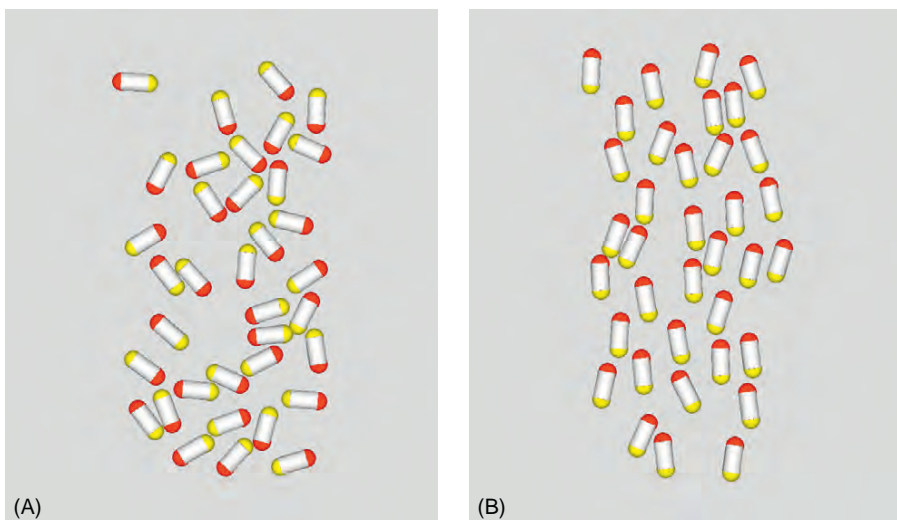


**Figure 4.8** Snapshots of aggregate structures for  $\lambda = 3$  ( $\lambda_0 = 0.75$ ): (A)  $\xi = 0$  and (B)  $\xi = 20$ .

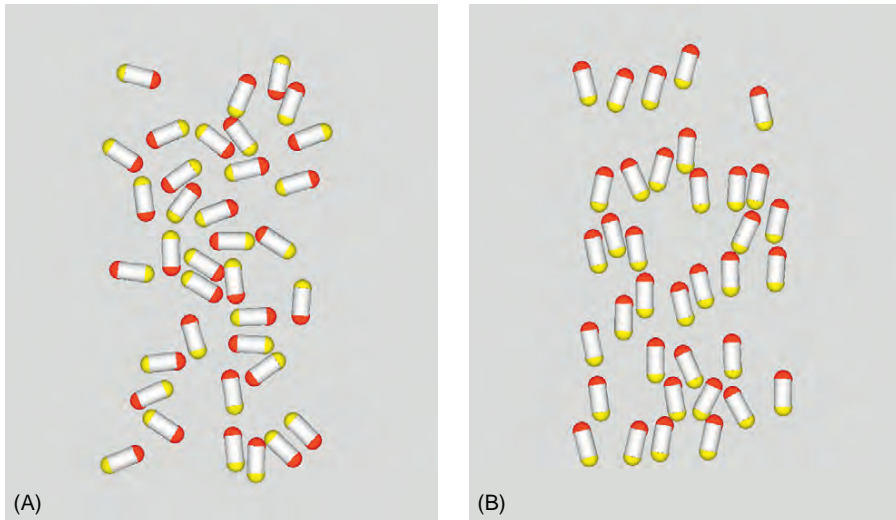


**Figure 4.9** Snapshots of aggregate structures for  $\lambda = 7$  ( $\lambda_0 = 1.75$ ): (A)  $\xi = 0$  and (B)  $\xi = 20$ .

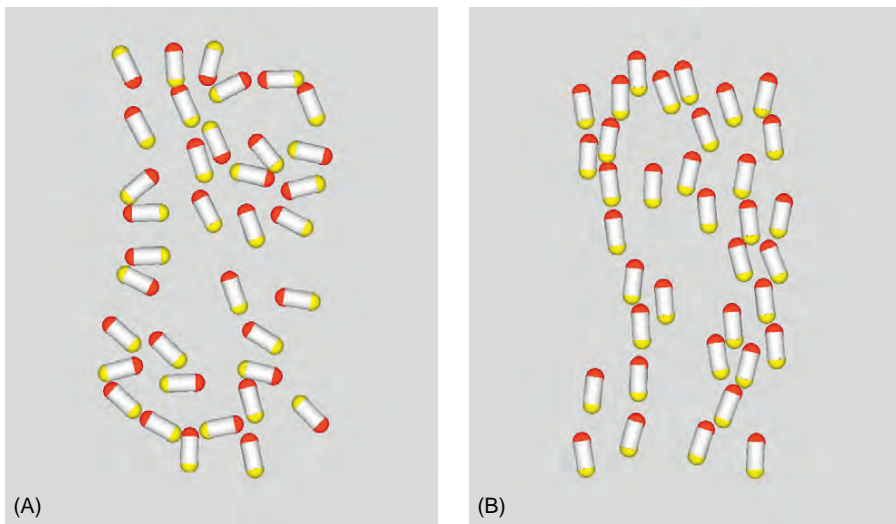


**Figure 4.10** Snapshots of aggregate structures for  $\lambda = 16$  ( $\lambda_0 = 4$ ): (A)  $\xi = 0$  and (B)  $\xi = 20$ .

Figure 4.9 shows snapshots for the slightly stronger interaction  $\lambda_0 = 1.75$ . These snapshots are similar to Figure 4.8, because  $\lambda_0 = 1.75$  is not significantly larger than the thermal energy.

For the stronger case of  $\lambda_0 = 4$ , shown in Figure 4.10, the magnetic interaction between particles is now more dominant than the thermal energy, and thus significant aggregate structures are observed. In the case of no applied magnetic field,

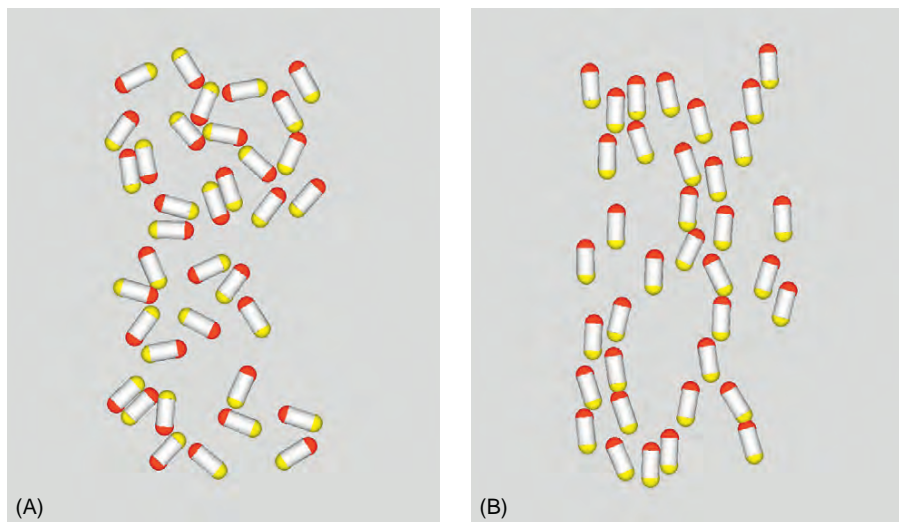


**Figure 4.11** Snapshots of aggregate structures for  $\lambda = 30$  ( $\lambda_0 = 7.5$ ): (A)  $\xi = 0$  and (B)  $\xi = 20$ .

shown in Figure 4.10A, loop-like clusters can be observed. Since the arrangement of the contact of the plus and minus magnetic charged spheres gives rise to a lower magnetic interaction energy, this type of connection is repeated and may result in the formation of necklace-like clusters. In the case of no external magnetic field there is no mechanism for forming chain-like clusters. In Figure 4.10B, the external magnetic field is significantly strong in comparison to the thermal energy, and therefore rod-like particles tend to aggregate to form chain-like clusters in the field direction.

These characteristics exhibited by aggregate structures can be recognized more clearly in the case of the much stronger interaction  $\lambda_0 = 7.5$  shown in Figure 4.11. In addition to the necklace-like clusters, star-like clusters are partially observed in Figure 4.11A. The snapshot in Figure 4.11B suggests the possibility that large-scale network-like or thick chain-like clusters may be formed in the field direction for stronger magnetic interaction cases.

#### 4.1.6 Simulation Program

We now show a sample simulation program written in the FORTRAN language employing the simulation techniques described above in the present demonstration of the MC method.

The important variables used in the program are described below.

$RX(I)$ , $RY(I)$	:	$(x,y)$ components of the position vector $\mathbf{r}_i^*$ of particle $i$
$NX(I)$ , $NY(I)$	:	$(x,y)$ components of the unit vector $\mathbf{e}_i$ of particle $i$ denoting the particle direction

$XL$ , $YL$	:	Side lengths of the simulation box in the $(x,y)$ directions
$N$	:	Number of particles
$D$	:	Particle diameter ( $D = 1$ in this case)
$VDENS$	:	Area fraction of particles $\phi_V$
$RA$	:	Nondimensional parameter $\lambda$ representing the strength of magnetic particle-particle interactions
$KU$	:	Nondimensional parameter $\xi$ representing the strength of magnetic particle-field interactions
$RV$	:	Nondimensional parameter $\lambda_V$ representing the strength of repulsive interactions due to the overlap of the steric layers
$RCOFF$	:	Cutoff distance for calculations of interaction energies
$DELR$	:	$\delta r_{\max}^*$
$DELT$	:	$\delta \theta_{\max}$
$RAN(J)$	:	Uniform random numbers ranging $0 \sim 1$ ( $J = 1 \sim NRANMX$ )
$NRAN$	:	Number of used random numbers
$E(i)$	:	Energy of particle $i$ interacting with other particles
$MOMX(*)$ , $MOMY(*)$	:	Mean value of the particle direction at each MC step
$MEANENE(*)$	:	Mean value of the system energy at each MC step

As an aid for the reader, comments have been placed beside important programming features. The line numbers are added for convenience and are unnecessary for the execution of the simulation program.

Finally, note that the cluster-moving method [4] may not be required for the case of a rod-like particle suspension, although it is indispensable for a spherical particle system in order to obtain physically reasonable aggregate structures in a strongly interacting system.

```

0001 C*****
0002 C*          mccyclin3.f
0003 C*
0004 C*          ----- MONTE CARLO SIMULATIONS -----
0005 C*          TWO-DIMENSIONAL MONTE CARLO SIMULATION OF
0006 C*          FERROMAGNETIC COLLOIDAL DISPERSIONS COMPOSED OF
0007 C*          RODLIKE PARTICLES
0008 C*
0009 C*          OPEN(9,FILE='@daa1.data', STATUS='UNKNOWN'); parameters
0010 C*          OPEN(10,FILE='daa11.data', STATUS='UNKNOWN'); para. & data
0011 C*          OPEN(21,FILE='daa001.data',STATUS='UNKNOWN'); particle pos.
0012 C*          OPEN(22,FILE='daa011.data',STATUS='UNKNOWN'); particle pos.
0013 C*          OPEN(23,FILE='daa021.data',STATUS='UNKNOWN'); particle pos.
0014 C*          OPEN(24,FILE='daa031.data',STATUS='UNKNOWN'); particle pos.
0015 C*          OPEN(25,FILE='daa041.data',STATUS='UNKNOWN'); particle pos.
0016 C*          OPEN(26,FILE='daa051.data',STATUS='UNKNOWN'); particle pos.
0017 C*          OPEN(27,FILE='daa061.data',STATUS='UNKNOWN'); particle pos.
0018 C*          OPEN(28,FILE='daa071.data',STATUS='UNKNOWN'); particle pos.
0019 C*          OPEN(29,FILE='daa081.data',STATUS='UNKNOWN'); particle pos.
0020 C*          OPEN(30,FILE='daa091.data',STATUS='UNKNOWN'); particle pos.
0021 C*
0022 C*          1. WITHOUT CLUSTER MOVEMENT.
0023 C*          2. RODLIKE MODEL COMPOSED OF ARBITRARY NUMBER
0024 C*              OF PARTICLES.
0025 C*
0026 C*
0027 C*          VER.1 BY A.SATOH , '03 11/20
0028 C*****

```

```

0029 C      N      : NUMBER OF PARTICLES
0030 C      D      : DIAMETER OF PARTICLE ( =1 FOR THIS CASE )
0031 C      VDENS : VOLUMETRIC FRACTION OF PARTICLES
0032 C      RA     : NONDIMENSIONAL PARAMETER OF PARTICLE-PARTICLE INTERACT
0033 C      KU     : NONDIMENSIONAL PARAMETER OF PARTICLE-FIELD INTERACTION
0034 C      RV     : NONDIMENSIONAL PARAMETER OF STERIC REPULSION
0035 C      RCOFF : CUTOFF RADIUS FOR CALCULATION OF INTERACTION ENERGIES
0036 C      XL,YL : DIMENSIONS OF SIMULATION REGION
0037 C
0038 C      RX(N),RY(N) : PARTICLE POSITION
0039 C      NX(N),NY(N) : DIRECTION OF MAGNETIC MOMENT
0040 C      E(I)       : INTERACTION ENERGY OF PARTICLE I WITH THE OTHERS
0041 C      MOMX(**),MOMY(**) : MAGNETIC MOMENT OF SYSTEM AT EACH MC STEP
0042 C      MEANENE(**)   : MEAN ENERGY OF SYSTEM AT EACH MC STEP
0043 C
0044 C      DELR    : MAXIMUM MOVEMENT DISTANCE
0045 C      DELT    : MAXIMUM MOVEMENT IN ORIENTATION
0046 C
0047 C      -XL/2 < RX(*) < XL/2 , -YL/2 < RY(*) < YL/2
0048 C-----
0049 C
0050 IMPLICIT REAL*8 (A-H,O-Z), INTEGER (I-N)
0051 C
0052 COMMON /BLOCK1/ RX      , RY
0053 COMMON /BLOCK2/ NX      , NY
0054 COMMON /BLOCK3/ XL      , YL
0055 COMMON /BLOCK4/ RA      , KU      , RV      , TD      , RP
0056 COMMON /BLOCK5/ VDENS   , N       , NPTC   , RCOFF  , D      , NPTCHF
0057 COMMON /BLOCK6/ E       , ENEW   , EOLD
0058 COMMON /BLOCK7/ NRAN   , RAN    , IX
0059 COMMON /BLOCK8/ DELR   , DELT
0060 COMMON /BLOCK9/ MOMX   , MOMY   , MEANENE
0061 C
0062 PARAMETER( NN=1000 , NNS=200000 )
0063 PARAMETER( NRANMX=500000 , PI=3.141592653589793D0 )
0064 C
0065 REAL*8   RX(NN) , RY(NN) , NX(NN) , NY(NN) , E(NN)
0066 REAL*8   VDENS   , KU
0067 REAL     MOMX(NNS) , MOMY(NNS) , MEANENE(NNS)
0068 INTEGER  N , NPTC , NDNSMX , NPTCHF
0069 C
0070 REAL     RAN(NRANMX)
0071 INTEGER NRAN , IX , NRANCHK
0072 C
0073 REAL*8   RXCAN   , RYCAN   , NXCAN   , NYCAN
0074 REAL*8   RXI     , RYI     , NXI     , NYI
0075 REAL*8   RXIJ    , RYIJ    , RIJ     , RIJSQ   , RCOFF2
0076 REAL*8   ECAN   , C1      , C2      , C3      , CX      , CY
0077 INTEGER MCSMPL , MCSMPLMX , MCSMPL1 , MCSMPL2
0078 INTEGER NGRAPH , NOPT
0079 LOGICAL OVRLAP
0080 C
0081 OPEN(9,FILE='@daa1.data', STATUS='UNKNOWN')
0082 OPEN(10,FILE='daa11.data', STATUS='UNKNOWN')
0083 OPEN(21,FILE='daa001.data', STATUS='UNKNOWN')
0084 OPEN(22,FILE='daa011.data', STATUS='UNKNOWN')
0085 OPEN(23,FILE='daa021.data', STATUS='UNKNOWN')
0086 OPEN(24,FILE='daa031.data', STATUS='UNKNOWN')
0087 OPEN(25,FILE='daa041.data', STATUS='UNKNOWN')
0088 OPEN(26,FILE='daa051.data', STATUS='UNKNOWN')
0089 OPEN(27,FILE='daa061.data', STATUS='UNKNOWN')
0090 OPEN(28,FILE='daa071.data', STATUS='UNKNOWN')
0091 OPEN(29,FILE='daa081.data', STATUS='UNKNOWN')
0092 OPEN(30,FILE='daa091.data', STATUS='UNKNOWN')
0093 C

```

```

0094
0095 C
0096 C
0097      N      = 36
0098      VDENS   = 0.2D0
0099      RA      = 5.0D0
0100      KU      = 8.0D0
0101      RV      = 150.D0
0102      D       = 1.0D0
0103      TD      = 0.3D0
0104      RP      = 2.0D0
0105      NPTC    = 3
0106      RCOFF   = 5.D0*RP
0107      NPTCHF  = (NPTC-1)/2
0108 C
0109      DELR    = 0.1D0
0110      DELT    = (5.D0/180.D0 )*PI
0111 C
0112      MCSMPLMX = 10000
0113      NGRAPH  = MCSMPLMX/10
0114      NOPT    = 20
0115      RCOFF2  = RCOFF**2
0116 C
0117      IX = 0
0118      CALL RANCAL( NRANMX, IX, RAN )
0119      NRAN    = 1
0120      NRANCHK = NRANMX - 10*N
0121 C
0122 C
0123 C      ----- INITIAL CONFIGURATION -----
0124 C
0125 C
0126 C
0127 CCC      OPEN(19,FILE='daa091.dat',STATUS='OLD')
0128 CCC      READ(19,462) N, XL, YL, D, DT, NPTC
0129 CCC      READ(19,464) (RX(I),I=1,N) , (RY(I),I=1,N) ,
0130 CCC      &           (NX(I),I=1,N) , (NY(I),I=1,N)
0131 CCC      CLOSE(19,STATUS='KEEP')
0132 CCC      GOTO 7
0133 C
0134      CALL INITIAL( VDENS , N , NPTC )
0135 C
0136 C
0137      7 WRITE(NP,12) N, VDENS, RA, KU, RV, D, TD, XL, YL, RCOFF,
0138      &           RP, NPTC, DELR, DELT
0139      WRITE(NP,14) MCSMPLMX, NGRAPH
0140 C
0141 C
0142 C
0143 C
0144 C      ----- START OF MONTE CARLO PART -----
0145 C
0146 C
0147 C
0148      DO 500 MCSMPL = 1 , MCSMPLMX
0149 C
0150      DO 400 I=1,N
0151 C
0152 C      ----- POSITION -----
0153      RXI = RX(I)
0154      RYI = RY(I)
0155      NXI = NX(I)
0156      NYI = NY(I)
0157      CALL ENECAL( I , RXI, RYI, NXI, NYI, RCOFF2 , ECAN, OVRLAP )
0158      EOLD = ECAN
0159 C
0160 C      ----- OLD ENERGY -----
0161      NRAN = NRAN + 1
0162      RXCAN = RX(I) + DELR*( 1.D0 - 2.D0*DBLE(RAN(NRAN)) )
0163      RXCAN = RXCAN - DNINT(RXCAN/XL)*XL
0164      NRAN = NRAN + 1
0165      RYCAN = RY(I) + DELR*( 1.D0 - 2.D0*DBLE(RAN(NRAN)) )

```

NP=9

- The given values and subaveraged values are written out in @daa1.data and daa11.data; @daa1 is for confirming the values assigned for simulations and the results calculated, and daa11.data is for the postprocessing analysis.
- The particle positions and directions are written out in daa001 – daa091 for the postprocessing analysis.

--- PARAMETER (3) ---

- The total number of MC steps is 10,000, and the particle positions are written out at every NGRAPH steps for the postprocessing analysis.

----- INITIAL CONFIGURATION -----

--- SET INITIAL CONFIG. ---

- A sequence of uniform random numbers are prepared in advance and, when necessary, random numbers are taken out from the variable RAN(\*)

----- PRINT OUT -----

- The READ statements are for continuing the sequential simulation using the data saved previously.

----- INITIALIZATION -----

----- START OF MONTE CARLO PART -----

----- POSITION -----

----- OLD ENERGY -----

- The interaction energies are calculated between particle  $i$  and its interacting particles.
- After particle  $i$  is slightly moved according to Eq. (1.52), the interaction energy is calculated for this new microscopic state.

```

0166      RYCAN = RYCAN - DNINT(RYCAN/YL)*YL
0167 C
0168      CALL ENECAL(I, RXCAN, RYCAN, NXI, NYI, RCOFF2, ECAN, OVRAP)
0169      IF( OVRAP ) THEN
0170          ENEW = EOLD
0171          GOTO 150
0172      END IF
0173 C
0174 C
0175      C3 = ECAN - EOLD
0176      IF( C3 .GE. 0.0D0 )THEN
0177          NRAN = NRAN + 1
0178          IF( DBLE(RAN(NRAN)) .GE. DEXP(-C3) )THEN
0179              ENEW = EOLD
0180              GOTO 150
0181          END IF
0182      END IF
0183 C
0184 C
0185 C
0186      RX(I) = RXCAN
0187      RY(I) = RYCAN
0188      ENEW = ECAN
0189      E(I) = ECAN
0190 C
0191 C
0192      150    RXI = RX(I)
0193      RYI = RY(I)
0194      NXI = NX(I)
0195      NYI = NY(I)
0196 C
0197      EOLD = ENEW
0198 C
0199 C
0200      NRAN = NRAN + 1
0201      C1 = DELT*DBLE(RAN(NRAN))
0202      NRAN = NRAN + 1
0203      C1 = DSIGN( C1 , DBLE(RAN(NRAN))-0.5 )
0204      CX = DSIN(C1)
0205      CY = DCOS(C1)
0206      NXCAN = NXI*CY + NYI*CX
0207      NYCAN = NYI*CY - NXI*CX
0208 C
0209 C
0210      CALL ENECAL(I, RXI, RYI, NXCAN, NYCAN, RCOFF2, ECAN, OVRAP)
0211      IF( OVRAP ) GOTO 400
0212 C
0213 C
0214 C
0215      C3 = ECAN - EOLD
0216      IF( C3 .GE. 0.0D0 )THEN
0217          NRAN = NRAN + 1
0218          IF( DBLE(RAN(NRAN)) .GE. DEXP(-C3) )THEN
0219              GOTO 400
0220          END IF
0221      END IF
0222 C
0223 C
0224 C
0225      NX(I) = NXCAN
0226      NY(I) = NYCAN
0227      E(I) = ECAN
0228 C
0229 ccc      if( i.eq.1) then
0230 ccc          write(6,*) 'smpl,rx,ry',mcsmpl, rx(1), ry(1)
0231 ccc          end if
0232 C
0233      400  CONTINUE
0234 C
0235 C
0236 C
0237      C1 = 0.0D0
0238      C2 = 0.0D0

```

• The adoption of the new state is determined according to the transition probability in Eq. (1.49).

• The procedure after the acceptance of the new state.

----- (3) CANDIDATE -----

• After the direction of particle  $i$  is slightly changed according to a similar equation to Eq. (1.52), the interaction energy is calculated for this new microscopic state.

----- (4) ENERGY HANDAN -----

• The adoption of the new state is determined according to the transition probability in Eq. (1.49).

• The procedure after the acceptance of the new state.

----- MOMENT AND ENERGY OF SYSTEM -----

• The system energy can be obtained by summing the energy of each particle.

```

0239      C3 = 0.0D
0240      DO 450 J=1,N
0241          C1 = C1 + NY(J)
0242          C2 = C2 + NX(J)
0243          C3 = C3 + E(J)
0244 450    CONTINUE
0245      MOMY(MCSMPL)     = REAL(C1)/REAL(N)
0246      MOMX(MCSMPL)     = REAL(C2)/REAL(N)
0247      MEANENE(MCSMPL)  = REAL(C3-KU*C1)/REAL(2*N)
0248 C
0249 C                                         --- DATA OUTPUT FOR GRAPHICS (1) ---
0250 C
0251 IF( MOD(MCSMPL,NGRAPH) .EQ. 0 ) THEN
0252     NOPT = NOPT + 1
0253     WRITE(NOPT,462) N, XL, YL, D, DT, NPTC
0254     WRITE(NOPT,464) (RX(I),I=1,N), (RY(I),I=1,N),
0255     & (NX(I),I=1,N), (NY(I),I=1,N)
0256     CLOSE(NOPT,STATUS='KEEP')
0257 END IF
0258 C
0259 C                                         --- CHECK OF THE SUM OF RANDOM NUMBERS ---
0260 C
0261 IF( NRAN .GE. NRANCHK )THEN
0262     CALL RANCAL( NRANMX, IX, RAN )
0263     NRAN = 1
0264 END IF
0265 C
0266 C
0267 500 CONTINUE
0268 C
0269 C
0270 C----- END OF MONTE CARLO PART -----
0271 C
0272 C
0273      WRITE(NP,592)
0274      MCSMPL1 = 1
0275      MCSMPL2 = MCSMPLMX
0276      CALL PRNTDATA( MCSMPL1, MCSMPL2, NP )
0277      WRITE(NP,612) MCSMPL1, MCSMPL2
0278 C
0279 C                                         --- DATA OUTPUT FOR GRAPHICS (2) ---
0280      WRITE(10,1012) N, VDENS, RA, KU, RV, D, TD, XL, YL
0281      WRITE(10,1013) RCOFF, RP, NPTC, DELR, DELT
0282      WRITE(10,1014) MCSMPLMX, NGRAPH
0283      & WRITE(10,1016) ( MEANENE(I),I=MCSMPL1, MCSMPL2)
0284      & , ( MOMX(I), I=MCSMPL1, MCSMPL2)
0285      & , ( MOME(Y(I), I=MCSMPL1, MCSMPL2)
0286 C
0287      CLOSE(9, STATUS='KEEP')
0288      CLOSE(10, STATUS='KEEP')
0289 C
0290 12 FORMAT(/1H,'-----',
0291      & /1H,'- MONTE CARLO METHOD -',
0292      & /1H,'-----',
0293      & //1H,'N=',I4, 2X, 'VDENS=',F5.2, 2X,
0294      & 'RA=',F5.2, 2X, 'KU=',F6.2, 2X, 'RV=',F6.2, 2X,
0295      & 'D=',F5.2, 2X, 'TD=',F5.2
0296      & /1H,'XL=',F6.2, 2X, 'YL=',F6.2, 2X, 'RCOFF=',F6.2, 2X,
0297      & 'RP=',F7.4, 2X, 'NPTC=',I3
0298      & /1H,'DELR=',F7.4, 2X, 'DELT=',F7.4)
0299 14 FORMAT( 1H,'MCSMPMX=',I8, 2X, 'NGRAPH=',I8/)
0300 462 FORMAT( 15, 4F9.4, I5 )
0301 464 FORMAT( (8F10.5) )
0302 592 FORMAT(/1H,'+++++++',I8, '+-----')
0303      & /1H,' WITHOUT CLUSTER MOVEMENT '
0304      & /1H,'+++++++',I8, '+-----')
0305 612 FORMAT(///1H,18X, 'START OF MC SAMPLING STEP=',I7
0306      & /1H,18X, 'END OF MC SAMPLING STEP=',I7/)
0307 1007 FORMAT(/1H,'***** NUMBER DENSITY OF CLUSTERS *****',
0308      & /1H,'Q (MEAN LENGTH OF CLUSTERS)=',F10.5, 5X,
0309      & 'NDNSMX=',I8
0310      & /1H, 'NDNSCLS(1), NDNSCLS(2), NDNSCLS(3), .....',
0311      & /(1H, 6E13.6) )
0312 1012 FORMAT( 17, 8F9.4 )
0313 1013 FORMAT( 2F9.5, 14, 2F8.5 )

```

• Since each interaction energy is counted twice, the magnetic particle-field interaction is also added twice. The system energy can finally be obtained by dividing the result by two.

• The number of the random numbers used is checked. If over NRANCHK, a uniform random number sequence is renewed.

```

0314 1014 FORMAT( 2I8 )
0315 1016 FORMAT( 5E16.9 )                                     STOP
0316                                         END
0317
0318 C*****SUBROUTINE PRNTDATA *****
0319 C*****SUBROUTINE PRNTDATA( MCSST, MCSMX, NP )           *
0320 C*****SUBROUTINE PRNTDATA( MCSST, MCSMX, NP )           *
0321 C
0322 C**** SUB PRNTDATA *****
0323      SUBROUTINE PRNTDATA( MCSST, MCSMX, NP )
0324 C
0325      IMPLICIT REAL*8 ( A-H,O-Z ), INTEGER ( I-N )
0326 C
0327      COMMON /BLOCK9/  MOMX , MOMEY , MEANENE
0328 C
0329      PARAMETER( NN=1000 , NNS=200000 )
0330      PARAMETER( NRANMX=500000 , PI=3.141592653589793D0 )
0331 C
0332      INTEGER    MCSST      , MCSMX      , NP
0333      REAL       MOMX(NNS)   , MOMEY(NNS)  , MEANENE(NNS)
0334 C
0335      REAL       AMOMX(10)   , AMOMY(10)
0336      INTEGER    IC         , IMC(0:10)   , JS , JE
0337 C
0338 C
0339      IC = ( MCSMX-MCSST+1 )/50
0340      DO 20 I= MCSST-1+IC , MCSMX , IC
0341          WRITE(NP,10) I ,MOMX(I) ,MOMEY(I) ,MEANENE(I)
0342      20 CONTINUE
0343 C
0344      IC = ( MCSMX-MCSST+1 )/10
0345      DO 30 I=0,10
0346          IMC(I) = MCSST - 1 + IC*I
0347          IF( I .EQ. 10 ) IMC(I) = MCSMX
0348      30 CONTINUE
0349 C
0350 C
0351      DO 35 I=1,10
0352          AMOMY(I) = 0.
0353          AMOMX(I) = 0.
0354          AMEANENE(I) = 0.
0355      35 CONTINUE
0356 C
0357      DO 50 I=1,10
0358          JS = IMC(I-1) + 1
0359          JE = IMC(I)
0360          DO 40 J=JS,JE
0361              AMOMY(I) = AMOMY(I) + MOMEY(J)
0362              AMOMX(I) = AMOMX(I) + MOMX(J)
0363              AMEANENE(I) = AMEANENE(I) + MEANENE(J)
0364      40 CONTINUE
0365      50 CONTINUE
0366 C
0367      DO 70 I=1,10
0368          CO      = REAL( IMC(I)-IMC(I-1) )
0369          AMOMY(I) = AMOMY(I) /CO
0370          AMOMX(I) = AMOMX(I) /CO
0371          AMEANENE(I) = AMEANENE(I)/CO
0372      70 CONTINUE
0373 C
0374      WRITE(NP,75)
0375      DO 90 I=1,10
0376          WRITE(NP,80) I,IMC(I-1)+1,IMC(I),AMOMX(I),AMOMY(I),AMEANENE(I)
0377      90 CONTINUE
0378 C
0379      10 FORMAT(1H , 'MCSMLN=' , I5 , 3X , 'MOMENT(X)' , F7.4, 3X ,
0380      &           'MOMENT(Y)' , F7.4, 3X , 'MEAN ENERGY=' , E12.5)
0381      75 FORMAT(//1H , '-----' ,
0382      &           /1H , '          MONTE CARLO HEIKIN
0383      &           /)
0384      80 FORMAT(1H , 'I=' , I2 , 2X , 'SMPLMN=' , I5 , 2X , 'SMPLMX=' , I5
0385      &           /1H , 15X , 'MOMENT(X)' , F7.4, 3X ,
0386      &           'MOMENT(Y)' , F7.4, 3X , 'MEAN ENERGY=' , E12.5/)
0387                                         RETURN
0388                                         END

```

• The total MC steps are equally divided into 50 blocks, and the end value of each block is written out.

• The particle direction and the averaged energy are written out.

• The total MC steps are equally divided into 10 blocks, and the subaverages are calculated for each block.

```

0389 C**** SUB INITIAL *****
0390      SUBROUTINE INITIAL( VDENS , N , NPTC )
0391 C
0392      IMPLICIT REAL*8 ( A-H,O-Z ), INTEGER ( I-N )
0393 C
0394      COMMON /BLOCK1/ RX    , RY
0395      COMMON /BLOCK2/ NX    , NY
0396      COMMON /BLOCK3/ XL    , YL
0397 C
0398      PARAMETER( NN=1000 )
0399      PARAMETER( NRANMX=500000 , PI=3.141592653589793D0 )
0400 C
0401      REAL*8   RX(NN) , RY(NN) , NX(NN) , NY(NN)
0402      REAL*8   VDENS
0403 C
0404      INTEGER   Q , PTCL
0405      REAL*8   A , XLUNT , YLUNT , RAN , RAN1 , RAN2 , C1 , C2
0406 C
0407      A = DSQRT( DBLE(NPTC)*PI/(8.D0*VDENS) )
0408      Q = NINT( SQRT(REAL(N+1)) )
0409      XL = A*DBLE(Q)
0410      YL = A*DBLE(2*Q)
0411      XLUNT = A
0412      YLUNT = A*DBLE(2)
0413 C
0414      RAN1 = DSQRT( 2.D0 )
0415      RAN2 = DSQRT( 7.D0 )
0416      PTCL=0
0417      DO 10 J=0,Q-1
0418         DO 10 I=0,Q-1
0419            PTCL = PTCL + 1
0420            C1 = RAN1*DBLE(PTCL)
0421            C1 = C1 - DINT(C1)
0422            C1 = C1 - 0.5D0
0423            C2 = RAN2*DBLE(PTCL)
0424            C2 = C2 - DINT(C2)
0425            C2 = C2 - 0.5D0
0426            RX(PTCL) = DBLE(I)*XLUNT+XLUNT/2.D0+C1*(XLUNT/6.D0)-XL/2.D0
0427            RY(PTCL) = DBLE(J)*YLUNT+YLUNT/2.D0+C2*(YLUNT/6.D0)-YL/2.D0
0428 10 CONTINUE
0429      N = PTCL
0430 C
0431      RAN = DSQRT( 2.D0 )
0432      DO 20 I=1,N
0433        C1 = RAN*DBLE(I)
0434        C1 = C1 - DINT(C1)
0435        C1 = C1 - 0.5D0
0436        C1 = (5.D0/180.D0)*PI*C1
0437        NX(I) = DSIN( C1 )
0438        NY(I) = DCOS( C1 )
0439 20 CONTINUE
0440
0441
0442 C**** SUB ENECAL *****
0443      SUBROUTINE ENECAL(I, RXI, RYI, NXI, NYI, RCOFF2 ,ECAN, OVRLAP)
0444 C
0445      IMPLICIT REAL*8 ( A-H,O-Z ), INTEGER ( I-N )
0446 C
0447      COMMON /BLOCK1/ RX    , RY
0448      COMMON /BLOCK2/ NX    , NY
0449      COMMON /BLOCK3/ XL    , YL
0450      COMMON /BLOCK4/ RA    , KU    , RV    , TD    , RP
0451      COMMON /BLOCK5/ VDENS , N     , NPTC , RCOFF , D     , NPTCHF
0452      COMMON /BLOCK6/ E     , ENEW , EOLD
0453 C
0454      PARAMETER( NN=1000 , PI=3.141592653589793D0 )
0455 C
0456      REAL*8   RX(NN) , RY(NN) , NX(NN) , NY(NN) , E(NN)
0457      REAL*8   VDENS , KU
0458      LOGICAL  OVRLAP
0459 C
0460      REAL*8   RXI , RXJ , RYI , RXIJ , RYIJ , RIJ , RIJSQ
0461      REAL*8   NXI , NYI , NXJ , NYJ , NXIJ , NYIJ , NXIJ2 , NYIJ2
0462      REAL*8   RRXI , RRYI , RRXJ , RRYJ , RRXIJ , RRYIJ
0463      REAL*8   NNXI , NNYI , NNXJ , NNYJ

```

• A subroutine for setting the initial position and velocity of each particle.

• The area occupied by one particle is ( $a^* \times 2a^*$ ) and therefore the relationship between the area fraction  $\phi_V$  and  $a^*$  is expressed as  $\phi_V = (NPTC)^* \pi / 8a^*{}^2$ .

----- POSITION -----

• The particles are initially set in the simple lattice unit formation in Figure 2.1A; the side lengths of the unit cell are ( $a^*, 2a^*$ ) in each direction.  
 • Each particle is moved in parallel by (XLUNT/2, YLUNT/2) to remove subtle situations at outer boundary surfaces. Also, to remove the regularity of the initial configuration, each particle is moved randomly by the maximum displacement  $0.5 \times (XLUNT/6, YLUNT/6)$  using quasi-random numbers.

----- MOMENT -----

• To save pseudo-random numbers, quasi-random numbers based on irrational numbers are used for randomly setting the particle direction within a small angle range.

RETURN  
END

• A subroutine for calculating the interaction energies between particles.

```

0464      REAL*8   TXIJ , TYIJ , R00 , R01 , R10 , R11
0465      REAL*8   C11 , C12 , C21 , C22 , C31 , C32 , C41 , C42
0466      REAL*8   C00 , C01 , C02
0467      REAL*8   CNINJ , CNINJ2 , CRIJN12 , CRIJN2 , CKI , CKJ
0468      REAL*8   KI , KJ , KKI , KKJ , KIS , KJS , KKIS , KKIS2 , KKIJC
0469      REAL*8   DSQ, RCHKSQ , RCHKSQ2
0470      REAL*8   XI , YI , XJ , YJ , ENESTER
0471      INTEGER  ITREE , IPATH , II , JJ , JJS , JJE , IIDEF, IINUMBR
0472 C
0473      OVLAP = .FALSE.
0474      ECAN = - KU*NYI
0475      DSQ = ( 1.D0 + TD )**2
0476 C
0477      DO 1000 J=1,N
0478 C
0479      IF( J .EQ. I )           GOTO 1000
0480 C
0481      RXJ = RX(J)
0482      RYJ = RY(J)
0483      RXIJ = RXI - RXJ
0484      RXIJ = RXIJ - DNINT(RXIJ/XL)*XL
0485      IF( DABS(RXIJ) .GE. RCOFF ) GOTO 1000
0486      RYIJ = RYI - RYJ
0487      RYIJ = RYIJ - DNINT(RYIJ/YL)*YL
0488      IF( DABS(RYIJ) .GE. RCOFF ) GOTO 1000
0489      RIJSQ= RXIJ**2 + RYIJ**2
0490      IF( RIJSQ .GE. RCOFF2 )    GOTO 1000
0491      RIJ = DSQRT(RIJSQ)
0492 C
0493      IF( DABS(RXIJ) .GT. XL/2.D0 ) THEN
0494          IF( RXIJ .GT. 0.D0 ) RXJ = RXJ + XL
0495          IF( RXIJ .LE. 0.D0 ) RXJ = RXJ - XL
0496      END IF
0497      IF( DABS(RYIJ) .GT. YL/2.D0 ) THEN
0498          IF( RYIJ .GT. 0.D0 ) RYJ = RYJ + YL
0499          IF( RYIJ .LE. 0.D0 ) RYJ = RYJ - YL
0500      END IF
0501      NXJ = NX(J)
0502      NYJ = NY(J)
0503      NXIJ = NXI - NXJ
0504      NYIJ = NYI - NYJ
0505      NXIJ2 = NXI + NXJ
0506      NYIJ2 = NYI + NYJ
0507 C
0508      C11 = RXIJ*NXIJ + RYIJ*NYIJ
0509      C21 = RXIJ*NXIJ2 + RYIJ*NYIJ2
0510      C12 = 1.D0 - ( NXI*NXJ + NYI*NYJ )
0511      C22 = 1.D0 + ( NXI*NXJ + NYI*NYJ )
0512      C00 = RA/(RP**2)
0513      C01 = RP/RIJSQ
0514      C02 = RP**2/(2.D0*RIJSQ)
0515 C
0516      R00 = RIJ*(1.D0 + C01*C11 + C02*C12)**0.5
0517      R11 = RIJ*(1.D0 - C01*C11 + C02*C12)**0.5
0518      R01 = RIJ*(1.D0 + C01*C21 + C02*C22)**0.5
0519      R10 = RIJ*(1.D0 - C01*C21 + C02*C22)**0.5
0520      IF( (R00 .LT. 1.D0) .OR. (R11 .LT. 1.D0)
0521      & .OR. (R01 .LT. 1.D0) .OR. (R10 .LT. 1.D0) ) THEN
0522          OVLAP = .TRUE.
0523          RETURN
0524      END IF
0525 C
0526      ECAN = ECAN + C00*( 1.D0/R00 + 1.D0/R11 - 1.D0/R01 - 1.D0/R10 )
0527 C
0528 C
0529 C
0530 C
0531      CNINJ = NXI*NXJ + NYI*NYJ
0532      IF( DABS(CNINJ) .LT. 0.2D0 ) THEN
0533          ITREE = 2
0534      ELSE IF( DABS(CNINJ) .GT. 0.9999D0 ) THEN
0535          ITREE = 3

```

• The treatment concerning particle *i*.

• The treatment of the periodic BC.  
• If the two particles are separated over the cutoff distance  $r_{\text{coff}}$ , the calculation is unnecessary.

• The position of the partner particle *j* is modified according to the periodic BC.

• The magnetic interaction energy is calculated from Eq. (4.13).  
• The distance between the magnetic charges is first calculated.

• The interaction energy is summed for the four pairs of magnetic charges.

• The interaction energy due to the overlap of the steric layers is calculated in the following.

```

0536      ELSE
0537          ITREE = 1
0538      END IF
0539 C      TXIJ = RXIJ/RIJ
0540      TYIJ = RYIJ/RIJ
0542      C11 = TXIJ*NXJ + TYIJ*NYJ
0543      IF( (DABS(CNINJ).GT.0.9999D0).AND.(DABS(C11).GT.0.9999D0) ) THEN
0544          ITREE=0
0545      END IF
0546 C
0547 C
0548 C
0549 C
0550 C
0551 C
0552 C
0553 C
0554 C      -----
0555 C      IF( ITREE .EQ. 0 ) THEN
0556          IF( CNINJ .GE. 0 ) THEN
0557              IF( C11 .GE. 0 ) THEN
0558 C
0559          XJ = RXJ + NXJ*DBLE(NPTCHF)
0560          YJ = RYJ + NYJ*DBLE(NPTCHF)
0561          XI = RXI - NXI*DBLE(NPTCHF)
0562          YI = RYI - NYI*DBLE(NPTCHF)
0563          ECAN = ECAN + ENESTER( XI, YI, XJ, YJ, TD, RV, OVRLAP )
0564          IF ( OVRLAP ) RETURN
0565      ELSE
0566          ----- (0) LINEAR ---
0567          XJ = RXJ - NXJ*DBLE(NPTCHF)
0568          YJ = RYJ - NYJ*DBLE(NPTCHF)
0569          XI = RXI + NXI*DBLE(NPTCHF)
0570          YI = RYI + NYI*DBLE(NPTCHF)
0571          ECAN = ECAN + ENESTER( XI, YI, XJ, YJ, TD, RV, OVRLAP )
0572          IF ( OVRLAP ) RETURN
0573      END IF
0574      ELSE
0575          IF( C11 .GE. 0 ) THEN
0576 C
0577          XJ = RXJ + NXJ*DBLE(NPTCHF)
0578          YJ = RYJ + NYJ*DBLE(NPTCHF)
0579          XI = RXI + NXI*DBLE(NPTCHF)
0580          YI = RYI + NYI*DBLE(NPTCHF)
0581          ECAN = ECAN + ENESTER( XI, YI, XJ, YJ, TD, RV, OVRLAP )
0582          IF ( OVRLAP ) RETURN
0583      ELSE
0584          ----- IPATH=1
0585          XJ = RXJ - NXJ*DBLE(NPTCHF)
0586          YJ = RYJ - NYJ*DBLE(NPTCHF)
0587          XI = RXI - NXI*DBLE(NPTCHF)
0588          YI = RYI - NYI*DBLE(NPTCHF)
0589          ECAN = ECAN + ENESTER( XI, YI, XJ, YJ, TD, RV, OVRLAP )
0590          IF ( OVRLAP ) RETURN
0591      END IF
0592      END IF
0593 C      ----- IPATH=2
0594      GOTO 1000
0595 C
0596      END IF
0597 C      ----- IPATH=3
0598
0599      IF( (ITREE .EQ. 1) .OR. (ITREE .EQ. 2) ) THEN
0600 C
0601          CNINJ2 = NXJ*NYI - NYJ*NXI
0602          CRIJN12 = RXIJ*NYI - RYIJ*NXI
0603          CRIJNJ2 = RXIJ*NYJ - RYIJ*NXJ
0604          CKJ = DABS( CRIJN12/CNINJ2 )
0605          CKI = DABS( CRIJNJ2/CNINJ2 )
0606 C
0607          C11 = RXIJ + CKI*NXI - CKJ*NXJ
0608          C12 = RYIJ + CKI*NYI - CKJ*NYJ
0609          C21 = RXIJ - CKI*NXI - CKJ*NXJ
0610          C22 = RYIJ - CKI*NYI - CKJ*NYJ

```

• The regime shown in Figure 4.3 is determined to proceed to the appropriate treatment, and after the calculation of the interaction energy, the calculation procedure returns to the main program.

• The treatment for a linear arrangement in Figure 4.6.

• The position ( $X_i, Y_i$ ) and ( $X_j, Y_j$ ) of the spheres of particles  $i$  and  $j$  are calculated.

• The absolute values ( $C_{KI}, C_{KJ}$ ) of ( $k_i, k_j$ ) are calculated from Eq. (4.8).

```

0611 C31 = RXIJ + CKI*NXI + CKJ*NXJ
0612 C32 = RYIJ + CKI*NYI + CKJ*NYJ
0613 C41 = RXIJ - CKI*NXI + CKJ*NXJ
0614 C42 = RYIJ - CKI*NYI + CKJ*NYJ
0615 C00 = 1.0D-8
0616 IF( (DABS(C11).LT. C00) .AND. (DABS(C12).LT. C00) )THEN
0617   KI = CKI
0618   KJ = CKJ
0619   GOTO 110
0620 END IF
0621 IF( (DABS(C21).LT. C00) .AND. (DABS(C22).LT. C00) )THEN
0622   KI = -CKI
0623   KJ = CKJ
0624   GOTO 110
0625 END IF
0626 IF( (DABS(C31).LT. C00) .AND. (DABS(C32).LT. C00) )THEN
0627   KI = CKI
0628   KJ = -CKJ
0629   GOTO 110
0630 END IF
0631 IF( (DABS(C41).LT. C00) .AND. (DABS(C42).LT. C00) )THEN
0632   KI = -CKI
0633   KJ = -CKJ
0634   GOTO 110
0635 END IF
0636 C
0637 110 IF( CKJ .GT. CKI ) THEN
0638   II = I
0639   JJ = J
0640   RRXI = RXI
0641   RRYI = RYI
0642   RRXJ = RXJ
0643   RRYJ = RYJ
0644   RRXIJ = RXIJ
0645   RRYIJ = RYIJ
0646   NNXI = NXI
0647   NNYI = NYI
0648   NNXJ = NXJ
0649   NNYJ = NYJ
0650   KKI = KI
0651   KKJ = KJ
0652 ELSE
0653   II = J
0654   JJ = I
0655   RRXI = RXJ
0656   RRYI = RYJ
0657   RRXJ = RXI
0658   RRYJ = RYI
0659   RRXIJ = -RXIJ
0660   RRYIJ = -RYIJ
0661   NNXI = NXJ
0662   NNYI = NYJ
0663   NNXJ = NXI
0664   NNYJ = NYI
0665   KKI = KJ
0666   KKJ = KI
0667 END IF
0668 C
0669 END IF
0670 C
0671 C
0672 C
0673 C
0674 C
0675 C
0676 IF( ITREE .EQ. 1 ) GOTO 200
0677 IF( ITREE .EQ. 2 ) GOTO 400
0678 IF( ITREE .EQ. 3 ) GOTO 600
0679 C
0680 C
0681 200 CNINJ = NXI*NXJ + NYI*NYJ
0682 IF( CNINJ .GT. 0.D0 ) THEN
0683   IF( KKJ .GE. 0.D0 ) THEN
0684     IPATH = 1
0685   ELSE
----- (1) GENERA
----- ITREE=0: LINEAR
----- ITREE=1: GENERAL
----- ITREE=2: NORMAL
----- ITREE=3: PARALLEL
----- (1) GENERA
----- The treatment for a general
----- Figure 4.4.

```

- The final results of  $k_i$  and  $k_j$  are obtained by checking the sign of  $k_i$  and  $k_j$ .

- The subscripts are exchanged between  $i$  and  $j$  so as to satisfy  $|k_i| > |k_j|$ .
  - As a result, the particle names  $i$  and  $j$  in Figure 4.2 are expressed as II and JJ in the program.

ITREE=0: LINEAR  
ITREE=1: GENERAL  
ITREE=2: NORMALL  
ITREE=3: PARALLE

### (1) GENERAL

- The treatment for a general arrangement in Figure 4.4.

```

0686      IPATH = 4
0687      END IF
0688      ELSE
0689      IF( KKJ .GE. 0.D0 ) THEN
0690          IPATH = 3
0691      ELSE
0692          IPATH = 2
0693      END IF
0694  END IF
0695 C
0696      KKIS = CNINJ*DBLE(NPTCHF) - ( RRXIJ*NNXI + RRYIJ*NNYI )
0697      KKIS2 = -CNINJ*DBLE(NPTCHF) - ( RRXIJ*NNXI + RRYIJ*NNYI )
0698      RCHKSQ = ( RRXIJ + KKIS *NNXI - NNXJ*DBLE(NPTCHF) )**2
0699      & +( RRYIJ + KKIS *NNYI - NNYJ*DBLE(NPTCHF) )**2
0700      & RCHKSQ2=( RRXIJ + KKIS2*NNXI + NNXJ*DBLE(NPTCHF) )**2
0701      & +( RRYIJ + KKIS2*NNYI + NNYJ*DBLE(NPTCHF) )**2
0702 C
0703      IF( IPATH .EQ. 1 ) THEN
0704 C
0705      IF( RCHKSQ .GE. DSQ ) GOTO 1000
0706 C
0707      IF( KKIS .GE. 0.D0 ) THEN
0708          IKKIS = IDINT(KKIS) + 1
0709      ELSE
0710          IKKIS = IDINT(KKIS)
0711      END IF
0712      IF( IKKIS .GT. NPTCHF ) IKKIS = NPTCHF
0713      JJS = NPTCHF
0714      IIDEF = NPTCHF - IKKIS
0715      JJE = -NPTCHF + IIDEF
0716 C
0717      DO 250 JJ= JJS, JJE, -1
0718      XJ = RRXJ + DBLE(JJ)*NNXJ
0719      YJ = RRYJ + DBLE(JJ)*NNYJ
0720      DO 250 II= JJ-IIDEF, JJ-IIDEF-1, -1
0721      IF( II .LT. -NPTCHF ) GOTO 250
0722      XI = RRXI + DBLE(II)*NNXI
0723      YI = RRYI + DBLE(II)*NNYI
0724      ECAN = ECAN + ENESTER( XI, YI, XJ, YJ, TD, RV, OVRLAP )
0725      IF( OVRLAP ) RETURN
0726 250  CONTINUE
0727 C
0728      ELSE IF( IPATH .EQ. 2 ) THEN
0729 C
0730      IF( RCHKSQ2 .GE. DSQ ) GOTO 1000
0731 C
0732      IF( KKIS2 .GE. 0.D0 ) THEN
0733          IKKIS2 = IDINT(KKIS2) + 1
0734      ELSE
0735          IKKIS2 = IDINT(KKIS2)
0736      END IF
0737      IF( IKKIS2 .GT. NPTCHF ) IKKIS2 = NPTCHF
0738      JJS = NPTCHF
0739      IIDEF = NPTCHF - IKKIS2
0740      JJE = -NPTCHF + IIDEF
0741 C
0742      DO 252 JJ= JJS, JJE, -1
0743      JJJ= -JJ
0744      XJ = RRXJ + DBLE(JJJ)*NNXJ
0745      YJ = RRYJ + DBLE(JJJ)*NNYJ
0746      DO 252 II= JJ-IIDEF, JJ-IIDEF-1, -1
0747      IF( II .LT. -NPTCHF ) GOTO 252
0748      XI = RRXI + DBLE(II)*NNXI
0749      YI = RRYI + DBLE(II)*NNYI
0750      ECAN = ECAN + ENESTER( XI, YI, XJ, YJ, TD, RV, OVRLAP )
0751      IF( OVRLAP ) RETURN
0752 252  CONTINUE
0753 C
0754      ELSE IF( IPATH .EQ. 3 ) THEN
0755 C
0756      IF( RCHKSQ .GE. DSQ ) GOTO 1000
0757 C
0758      IF( -KKIS .GE. 0.D0 ) THEN
0759          IKKIS = IDINT(-KKIS) + 1
0760      ELSE
0761          IKKIS = IDINT(-KKIS)

```

- After the assessment of the particle overlap regime,  $k_i^s$  (KKIS) and  $k_j^s$  (KKIS2) are calculated from Eqs. (4.9) and (4.10).

- The constituent spheres in the rod-like particle are named in such a way that the central sphere is 0, the neighboring spheres are 1,2,..., in the particle direction, and -1,-2,..., in the opposite direction.

- The interaction energy between the sphere IKKIS of particle  $i$  and the sphere JJS of particle  $j$  is checked.
- The two spheres of particle  $i$  are checked as an object interacting with the sphere of particle  $j$ .

- The center of the sphere of particle  $i$  is denoted by (XI,YI) and, similarly, (XJ,YJ) for the sphere of particle  $j$ .

--- PATH=2 ---

--- PATH=3 ---

```

0762      END IF
0763      IF( IKKIS .GT. NPTCHF )  IKKIS = NPTCHF
0764      JJS = NPTCHF
0765      IIDEF = NPTCHF - IKKIS
0766      JJE = -NPTCHF + IIDEF
0767 C
0768      DO 254 JJ= JJS, JJE, -1
0769      XJ = RRXJ + DBLE(JJ)*NNXJ
0770      YJ = RRYJ + DBLE(JJ)*NNYJ
0771      DO 254 II= JJ-IIDEF, JJ-IIDEF-1, -1
0772      IF( II .LT. -NPTCHF )  GOTO 254
0773      III = -II
0774      XI = RRXI + DBLE(III)*NNXI
0775      YI = RRYI + DBLE(III)*NNYI
0776      ECAN = ECAN + ENESTER( XI, YI, XJ, YJ, TD, RV, OVRLAP )
0777      IF ( OVRLAP ) RETURN
0778      254  CONTINUE
0779 C
0780      ELSE IF( IPATH .EQ. 4 ) THEN
0781 C
0782      IF( RCHKSQ2 .GE. DSQ ) GOTO 1000
0783 C
0784      IF( -KKIS2 .GE. 0.D0 ) THEN
0785          IKKIS2 = IDINT(-KKIS2) + 1
0786      ELSE
0787          IKKIS2 = IDINT(-KKIS2)
0788      END IF
0789      IF( IKKIS2 .GT. NPTCHF )  IKKIS2 = NPTCHF
0790      JJS = NPTCHF
0791      IIDEF = NPTCHF - IKKIS2
0792      JJE = -NPTCHF + IIDEF
0793 C
0794      DO 256 JJ= JJS, JJE, -1
0795      JJJ = -JJ
0796      XJ = RRXJ + DBLE(JJJ)*NNXJ
0797      YJ = RRYJ + DBLE(JJJ)*NNYJ
0798      DO 256 II= JJ-IIDEF, JJ-IIDEF-1, -1
0799      IF( II .LT. -NPTCHF )  GOTO 256
0800      III = -II
0801      XI = RRXI + DBLE(III)*NNXI
0802      YI = RRYI + DBLE(III)*NNYI
0803      ECAN = ECAN + ENESTER( XI, YI, XJ, YJ, TD, RV, OVRLAP )
0804      IF ( OVRLAP ) RETURN
0805      256  CONTINUE
0806 C
0807      END IF
0808 C
0809      GOTO 1000
0810 C
0811 C
0812 400  IF( KKJ .GE. 0.D0 ) THEN
0813      IPATH = 1
0814  ELSE
0815      IPATH = 2
0816  END IF
0817 C
0818      CNINJ = NXI*NXJ + NYI*NYJ
0819      KKIS = CNINJ*DBLE(NPTCHF) - ( RRXIJ*NNXI + RRYIJ*NNYI )
0820      KKIS2 = - CNINJ*DBLE(NPTCHF) - ( RRXIJ*NNXI + RRYIJ*NNYI )
0821      & RCHKSQ = ( RRXIJ + KKIS *NNXI - NNXJ*DBLE(NPTCHF) )**2
0822      & +( RRYIJ + KKIS *NNYI - NNYJ*DBLE(NPTCHF) )**2
0823      RCHKSQ2=( RRXIJ + KKIS2*NNXI + NNXJ*DBLE(NPTCHF) )**2
0824      & +( RRYIJ + KKIS2*NNYI + NNYJ*DBLE(NPTCHF) )**2
0825 C
0826      IF( IPATH .EQ. 1 ) THEN
0827          IF( RCHKSQ .GE. DSQ ) GOTO 1000
0828      ELSE
0829          IF( RCHKSQ2 .GE. DSQ ) GOTO 1000
0830      END IF
0831 C
0832      IF( IPATH .EQ. 2 )  KKIS = KKIS2
0833 C
0834      IF( KKIS .GE. 0.D0 ) THEN
0835          IKKIS = IDINT(KKIS) + 1
0836      ELSE

```

• The treatment for a normal arrangement in Figure 4.5.

----- (2) NORMAL -----

• After the assessment of the particle overlap regime,  $k_i^s$  (KKIS) and  $k_i^{s'}$  (KKIS2) are calculated from Eqs. (4.9) and (4.10).

• The constituent spheres in the rod-like particle are named in such a way that the central sphere is 0, the neighboring spheres are 1, 2,..., in the particle direction, and -1, -2,..., in the opposite direction.

```

0837      IKKIS = IDINT(KKIS)
0838      END IF
0839      IF( IKKIS .GT. NPTCHF )  IKKIS = NPTCHF + 1
0840      IIDEF = NPTCHF - IKKIS
0841 C
0842      JJJ = NPTCHF
0843      IF( IPATH .EQ. 1 ) THEN
0844          JJ = JJJ
0845      ELSE
0846          JJ = -JJJ
0847      END IF
0848 C
0849
0850      XJ = RRXJ + DBLE(JJ)*NNXJ
0851      YJ = RRYJ + DBLE(JJ)*NNYJ
0852      DO 450 II= JJJ-IIDEF, JJJ-IIDEF-1, -1
0853          IF( II .GT. NPTCHF )  GOTO 450
0854          IF( II .LT. -NPTCHF ) GOTO 450
0855          XI = RRXI + DBLE(II)*NNXI
0856          YI = RRYI + DBLE(II)*NNYI
0857          ECAN = ECAN + ENESTER( XI, YI, XJ, YJ, TD, RV, OVRLAP )
0858          IF ( OVRLAP ) RETURN
0859      450 CONTINUE
0860 C
0861      GOTO 1000
0862 C
0863 C
0864      600 CNINJ = NXI*NXJ + NYI*NYJ
0865      KIS = CNINJ*DBLE(NPTCHF) - ( RXIJ*NXI + RYIJ*NYI )
0866      KJS = CNINJ*DBLE(NPTCHF) + ( RXIJ*NXJ + RYIJ*NYJ )
0867      IF( CNINJ .GE. 0.D0 ) THEN
0868          IPATH = 1
0869      ELSE
0870          IF( KIS .LE. -DBLE(NPTCHF) ) THEN
0871              IPATH = 2
0872          ELSE
0873              IPATH = 3
0874          END IF
0875      END IF
0876 C
0877      II    = I
0878      JJ    = J
0879      RRXI = RXI
0880      RRYI = RYI
0881      RRXJ = RXJ
0882      RRYJ = RYJ
0883      RRXIJ = RXIJ
0884      RRYIJ = RYIJ
0885      NNXI = NXI
0886      NNYI = NYI
0887      NNXJ = NXJ
0888      NNYJ = NYJ
0889      KKIS = KJS
0890      IF( (IPATH .EQ. 1) .AND. (KIS .GT. KJS) ) THEN
0891          II    = J
0892          JJ    = I
0893          RRXI = RXJ
0894          RRYI = RYJ
0895          RRXJ = RXI
0896          RRYJ = RYI
0897          RRXIJ = -RXIJ
0898          RRYIJ = -RYIJ
0899          NNXI = NXJ
0900          NNYI = NYJ
0901          NNXJ = NXI
0902          NNYJ = NYI
0903          KKIS = KJS
0904      END IF
0905 C
0906      & RCHKSQ = ( RRXIJ + KKIS *NNXI - NNXJ*DBLE(NPTCHF) )**2
0907          + ( RRYIJ + KKIS *NNYI - NNYJ*DBLE(NPTCHF) )**2
0908      IF( RCHKSQ .GE. DSQ ) GOTO 1000

```

• The interaction energy between the sphere IKKIS of particle *i* and the sphere JJ of particle *j* is treated.  
• The two spheres of particle *i* are checked as an object interacting with the sphere of particle *j*.

• The center of the sphere of particle *i* is denoted by (XI,YI) and, similarly, (XJ,YJ) for the sphere of particle *j*

• The treatment for a parallel arrangement in Figure 4.7.  
----- (3) PARALLEL -----

• After the assessment of the particle overlap regime,  $k_i^s$ (KIS) and  $k_j^s$ (KJS) are calculated from Eq. (4.9).

• The subscripts are exchanged between *i* and *j* so as to satisfy  $k_j^s > k_i^s$ .  
• As a result, the particle names *i* and *j* in Figure 4.7 are expressed as II and JJ in the program.

• The constituent spheres in the rod-like particle are named in such a way that the central sphere is 0, the neighboring spheres are 1,2,..., in the particle direction, and -1,-2,..., in the opposite direction.

```

0909 C
0910      IF( IPATH .EQ. 1 ) THEN
0911 C
0912          IF( KKIS .GE. 0.0D0 ) THEN
0913              IKKIS = IDINT(KKIS) + 1
0914          ELSE
0915              IKKIS = IDINT(KKIS)
0916          END IF
0917          IIDEF = NPTCHF - IKKIS
0918 C
0919          XJ = RRXJ + DBLE(NPTCHF)*NNXJ
0920          YJ = RRYJ + DBLE(NPTCHF)*NNYJ
0921          IINUMBR = NPTC + 1 - IIDEF
0922          DO 650 II= NPTCHF-IIDEF, NPTCHF-IIDEF-1, -1
0923              IF( II .LT. -NPTCHF ) GOTO 650
0924              XI = RRXI + DBLE(II)*NNXI
0925              YI = RRYI + DBLE(II)*NNYI
0926              IINUMBR = IINUMBR - 1
0927              ECAN = ECAN + DBLE(IINUMBR)*
0928          &          ENESTER( XI, YI, XJ, YJ, TD, RV, OVRLAP )
0929          IF ( OVRLAP ) RETURN
0930      650      CONTINUE
0931      END IF
0932 C
0933          KKIJC = DABS( KKIS ) - DBLE(NPTCHF)
0934 C
0935          IF( IPATH .EQ. 2 ) THEN
0936 C
0937              IKKIJC = IDINT( KKIJC )
0938              IIDEF = IKKIJC
0939              XJ = RRXJ - DBLE(NPTCHF)*NNXJ
0940              YJ = RRYJ - DBLE(NPTCHF)*NNYJ
0941              IINUMBR = NPTC + 1 - IIDEF
0942              DO 652 II= NPTCHF-IIDEF, NPTCHF-IIDEF-1, -1
0943                  IF( II .LT. -NPTCHF ) GOTO 652
0944                  XI = RRXI + DBLE(II)*NNXI
0945                  YI = RRYI + DBLE(II)*NNYI
0946                  IINUMBR = IINUMBR - 1
0947                  ECAN = ECAN + DBLE(IINUMBR)*
0948          &          ENESTER( XI, YI, XJ, YJ, TD, RV, OVRLAP )
0949          IF ( OVRLAP ) RETURN
0950      652      CONTINUE
0951      END IF
0952 C
0953          KKIJC = KKIS + DBLE(NPTCHF)
0954 C
0955          IF( IPATH .EQ. 3 ) THEN
0956 C
0957              IKKIJC = IDINT( KKIJC )
0958              IIDEF = IKKIJC
0959              XJ = RRXJ + DBLE(NPTCHF)*NNXJ
0960              YJ = RRYJ + DBLE(NPTCHF)*NNYJ
0961              IINUMBR = NPTC + 1 - IIDEF
0962              DO 654 II= NPTCHF-IIDEF, NPTCHF-IIDEF-1, -1
0963                  IF( II .LT. -NPTCHF ) GOTO 654
0964                  III = -II
0965                  XI = RRXI + DBLE(III)*NNXI
0966                  YI = RRYI + DBLE(III)*NNYI
0967                  IINUMBR = IINUMBR - 1
0968                  ECAN = ECAN + DBLE(IINUMBR)*
0969          &          ENESTER( XI, YI, XJ, YJ, TD, RV, OVRLAP )
0970          IF ( OVRLAP ) RETURN
0971      654      CONTINUE
0972      END IF
0973 C
0974      GOTO 1000
0975 C
0976 C      ----- END OF ENERGY DUE TO STERIC INER. ---
0977 C
0978 1000 CONTINUE
0979
0980
0981 C#### FUN ENESTER ####
0982      DOUBLE PRECISION FUNCTION ENESTER(XI, YI, XJ, YJ, TD, RV, OVRLAP)
0983 C
0984      IMPLICIT REAL*8 (A-H,O-Z), INTEGER (I-N)

```

• The interaction energy between the sphere of the positive magnetic charge of particle  $j$  and the sphere IKKIS (and (IKKIS-1)) of particle  $i$  is calculated. There are IINUMBR pairs of particles.

• The center of the sphere of particle  $i$  is denoted by (XI,YI) and, similarly, (XJ,YJ) for particle  $j$ .

• The separation between the central spheres of particles  $i$  and  $j$  along the particle axis,  $k_j^i(KKIJC)$ , is calculated.

--- PATH=2 ---

• The sphere of particle  $i$  is determined as an object according to Section 4.1.3.4. There are IINUMBR pairs of particles yielding such an arrangement.

--- PATH=3 ---

RETURN  
END

```

0985 C
0986     LOGICAL    OVRLAP
0987 C
0988     RIJ = DSQRT( ( XI-XJ )**2 + ( YI-YJ )**2 )
0989     X  = 2.D0*(RIJ-1.D0)
0990     IF( X .LT. 0.D0 ) THEN
0991         OVRLAP = .TRUE.
0992         ENESTER = 1.D9
0993         RETURN
0994     END IF
0995 ccc   write(6,*)'xi,yi,xj,yj', xi,yi,xj,yj
0996 C
0997     IF( RIJ .LE. ( TD+1.D0 ) ) THEN
0998         C1 = ( X+2.D0)/TD
0999         C2 = DLOG( ( TD+1.D0)/(X/2.D0+1.D0) )
1000         C3 = X/TD
1001         ENESTER = RV*( 2.D0 - C1*C2 - C3 )
1002         RETURN
1003     ELSE
1004         ENESTER = 0.D0
1005         RETURN
1006     END IF
1007
1008                                         RETURN
1009 C**** SUB RANCAL *****
1010     SUBROUTINE RANCAL( N, IX, X )
1011 C
1012     DIMENSION X(N)
1013     DATA INTEGMX/2147483647/
1014     DATA INTEGST,INTEG/584287,48828125/
1015 C
1016     AINTEGMX = REAL( INTEGMX )
1017 C
1018     IF ( IX.LT.0 ) PAUSE
1019     IF ( IX.EQ.0 ) IX = INTEGST
1020     DO 30 I=1,N
1021         IX = IX*INTEG
1022         IF ( IX ) 10, 20, 20
1023 10      IX = (IX+AINTEGMX)+1
1024 20      X(I) = REAL(IX)/AINTEGMX
1025 30      CONTINUE
1026      RETURN
1027
1028 C*****
1029 C THIS SUBROUTINE IS FOR GENERATING UNIFORM RANDOM NUMBERS *
1030 C ( SINGLE PRECISION ) FOR 64-BIT COMPUTER. *
1031 C     N : NUMBER OF RANDOM NUMBERS TO GENERATE *
1032 C     IX : INITIAL VALUE OF RANDOM NUMBERS ( POSITIVE INTEGER ) *
1033 C           : LAST GENERATED VALUE IS KEPT *
1034 C     X(N) : GENERATED RANDOM NUMBERS ( 0<X(N)<1 ) *
1035 C*****
1036 C**** SUB RANCAL999 *****
1037 ccc   SUBROUTINE RANCAL999( N, IX, X )
1038 C
1039 ccc   IMPLICIT REAL*8 (A-H,O-Z), INTEGER*8 (I-N)
1040 C
1041 ccc   REAL      X(N)
1042 ccc   INTEGER*8 INTEGMX, INTEG64, INTEGST, INTEG
1043 C
1044 CCC   DATA INTEGMX/2147483647/
1045 CCC   DATA INTEG64/2147483648/
1046 CCC   DATA INTEGST,INTEG/584287,48828125/
1047 C
1048 CCC   AINTEGMX = REAL( INTEGMX )
1049 CCC   AINTEGMX = REAL( INTEG64 )
1050 C
1051 ccc   IF ( IX.LT.0 ) PAUSE
1052 ccc   IF ( IX.EQ.0 ) IX = INTEGST
1053 ccc   DO 30 I=1,N
1054 ccc       IX = IX*INTEG
1055 ccc       IX = KMOD(IX,INTEG64)
1056 CCC       IF ( IX ) 10, 20, 20
1057 CCC10      IX = (IX+AINTEGMX)+1
1058 CCC20      X(I) = REAL(IX)/AINTEGMX
1059 CCC30      CONTINUE
1060 CCC      RETURN
1061 CCC      END

```

• A function subprogram for calculating the interaction energy due to the overlap of the surfactant layers according to Eq. (4.14).

• A subroutine for generating a uniform random number sequence.

• This is for a 32-bit CPU based on the expression of two's complement.

## 4.2 Aggregation Phenomena in a Dispersion of Plate-like Particles

In this section, we consider aggregation phenomena in a suspension composed of disk-like particles. As seen in the rod-like particle system, there are several obstacles to developing a simulation program employing a nonspherical particle system. That is, we need to first make a mathematical analysis of particle overlap and then express the overlap criterion in the language of a simulation program. Hence, in this section we show the mathematical analysis from the viewpoint of developing a simulation program. The exercise of interest is a circular disk-like particle with a magnetic dipole moment at the particle center. We discuss the influences of magnetic particle–particle interactions and the magnetic field strength on aggregation phenomena. The subject of the present exercise is partly under our research group’s study, and therefore the sample simulation program has an academic emphasis. The system of interest is in thermodynamic equilibrium and has a given number of particles, temperature, and volume; therefore, the canonical MC algorithm is employed.

### 4.2.1 Physical Phenomena of Interest

It is assumed that the system composed of disk-like particles with a magnetic moment at the particle center is in thermodynamic equilibrium. In the present exercise, we discuss aggregation phenomena in this type of dispersion under the influence of an applied magnetic field by means of an MC simulation.

The main points in formalizing this demonstration are to develop the particle model, to express the potential energy between particles, and to analyze the criterion for particle overlap. We explain these important subjects in detail below.

### 4.2.2 Particle Model

As shown in Figure 4.12, we here employ a disk-like particle with a magnetic moment  $\mathbf{m}$  (along the disk surface) normal to the particle axis at the particle center with the section shape of a spherocylinder. The central part of this disk-like particle is a short cylinder with diameter  $d$  and thickness  $b_1$ . The side of the cylinder is surrounded by the semi-shape of a torus shape, resulting in a particle circumcircle with dimension  $d_1$  ( $=d + b_1$ ), as shown in Figure 4.12. The configurational state of a single axisymmetric particle  $i$  is specified by the position of the particle center  $\mathbf{r}_i$ , the particle direction (normal to the disk surface)  $\mathbf{e}_i$ , and the magnetic moment direction  $\mathbf{n}_i$  where  $\mathbf{e}_i$  and  $\mathbf{n}_i$  are the unit vectors. In the MC method, knowledge of only the position and direction of each particle is sufficient to advance an MC step, while both the translational and angular velocities need to be treated in the MD method. The magnetic moment is assumed to be fixed in the particle body, so that only the rotation of the particle can provide a change in the magnetic moment direction.

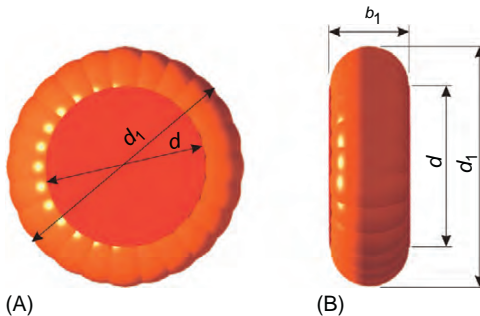


**Figure 4.12** Particle model: (A) plane view and (B) side view.

The interaction energy  $u_i$  between the magnetic moment  $\mathbf{m}_i$  and an applied magnetic field  $\mathbf{H}$  is expressed as

$$u_i = -\mu_0 \mathbf{m}_i \cdot \mathbf{H} \quad (4.18)$$

in which  $\mu_0$  is the permeability of free space. This expression clearly implies that the inclination of the magnetic moment along the field direction yields a minimum interaction energy; that is, the particle has a tendency to orient in such a way that the magnetic moment will incline in the field direction.

The magnetic interaction energy  $u_{ij}$  between particles  $i$  and  $j$  is expressed as [31]

$$u_{ij} = \frac{\mu_0}{4\pi r_{ij}^3} \left\{ \mathbf{m}_i \cdot \mathbf{m}_j - \frac{3}{r_{ij}^2} (\mathbf{m}_i \cdot \mathbf{r}_{ij})(\mathbf{m}_j \cdot \mathbf{r}_{ij}) \right\} \quad (4.19)$$

in which  $\mathbf{r}_i$  is the position vector of particle  $i$  ( $i = 1, 2, \dots, N$ ),  $\mathbf{r}_{ij} = \mathbf{r}_i - \mathbf{r}_j$ , and  $r_{ij} = |\mathbf{r}_{ij}|$ . Eq. (4.19) implies that a minimum interaction energy can be obtained when both magnetic moments incline in the same direction along a line drawn between the particle centers. However, note that a thermodynamic equilibrium state will be determined by the balance of the decrease in the system energy and the increase in the system entropy; that is, the entropy should be treated in addition to the energy in order to discuss the thermodynamic equilibrium state. This approach may provide an important facility to molecular simulation methods as a tool for analyzing physical phenomena at the microscopic level. In addition to magnetic forces, the interactions due to electric double layers and steric layers are important considerations, but in this example we have chosen to neglect these interactions for simplification and clarification of the method.

In our approach, by treating a nondimensional form of the system, we are able to discuss the physical phenomenon of interest in a much more reasonable manner, since several important factors governing the physical phenomenon appear as explicit terms in the nondimensional equations. In the nondimensionalization procedure the representative values used are particle thickness  $b_1$  for distances and

thermal energy  $kT$  for energies. With these representative values, Eqs. (4.18) and (4.19) are written as

$$u_i^* = u_i/kT = -\xi \mathbf{n}_i \cdot \mathbf{h} \quad (4.20)$$

$$u_{ij}^* = u_{ij}/kT = \lambda \frac{1}{r_{ij}^{*3}} \{ \mathbf{n}_i \cdot \mathbf{n}_j - 3(\mathbf{n}_i \cdot \mathbf{t}_{ij})(\mathbf{n}_j \cdot \mathbf{t}_{ij}) \} \quad (4.21)$$

in which  $\mathbf{n}_i = \mathbf{m}_i/m$ ,  $m = |\mathbf{m}_i|$ ,  $\mathbf{h} = \mathbf{H}/H$ ,  $H = |\mathbf{H}|$ ,  $\mathbf{t}_{ij} = \mathbf{r}_{ij}/r_{ij}$ , and the superscript \* implies nondimensionalized quantities;  $\mathbf{n}_i$  and  $\mathbf{h}$  are the unit vectors denoting the magnetic moment direction and the magnetic field direction, respectively. The procedure gives rise to the nondimensional parameters  $\xi$  and  $\lambda$  that are defined as

$$\xi = \mu_0 m H / kT, \quad \lambda = \mu_0 m^2 / 4\pi b_1^3 kT \quad (4.22)$$

This is a typical example of the nondimensionalizing procedure giving rise to the appearance of nondimensional parameters or nondimensional numbers. In the present exercise, the physical phenomenon is governed by the magnetic particle–field interactions, the particle–particle interactions, and the random forces and torques acting on each particle. It is therefore reasonable that the ratios of these factors appear in the basic equations as nondimensional parameters  $\xi$  and  $\lambda$  in Eq. (4.22). These parameters imply the strengths of the magnetic particle–field and the particle–particle interactions relative to the thermal energy, respectively.

### 4.2.3 Criterion of the Particle Overlap

Assessing the overlap of the two disk-like particles shown in Figure 4.12 is significantly different from that of a pair of spherical particles. Both the torus parts may overlap, or the torus part and the disk part may overlap. Taking into account all the possible overlap regimes during a simulation requires probing into the essence of the overlap and then making a systematic analysis based on the insight gained from a careful investigation of the problem. This is usually undertaken in advance as part of the preparation required in writing a computer simulation program. In the previous case of the spherocylinder, systematic analysis on the particle overlap criterion was achieved by viewing a pair from such a direction that the planes including the corresponding particles are seen to be parallel. For our disk-like particle, a systematic analysis may be possible by focusing on the line of intersection generated by the two corresponding planes. Hence, we first consider the case of nonparallel planes, in which the intersection line can certainly be defined. The use of the maximum section circle of diameter  $d_1$  of the disk-like particle enables us to indicate the typical overlap patterns schematically in Figure 4.13. Figure 4.13A is for the case of the intersection line penetrating each particle (circle), Figures 4.13B and C are for the intersection line penetrating only one particle, and Figure 4.13D is for the intersection line located outside both particles. Since the present disk-like particles have a definite thickness, the above-mentioned regimes of the particle

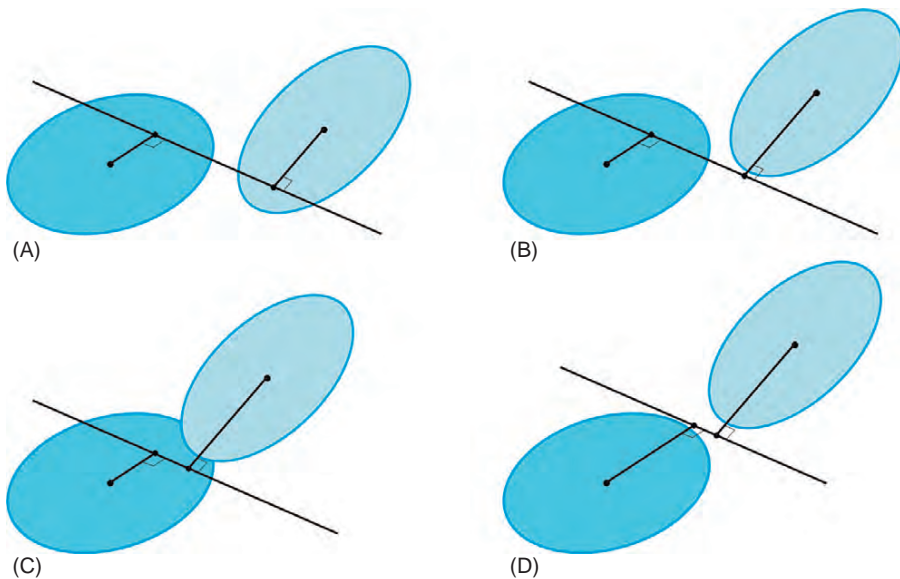


**Figure 4.13** Overlap of circular disk-like particles with infinitesimal thin thickness.

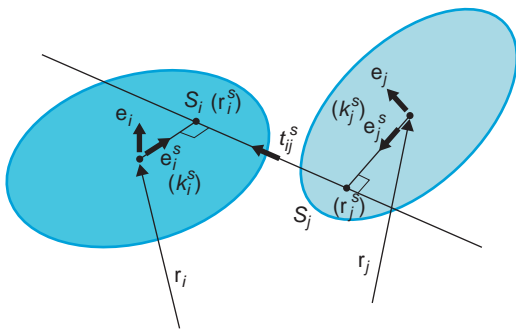


**Figure 4.14** Analysis of circles with radius  $r_0$  ( $=d/2$ ).

overlap need to be slightly modified. That is, in each regime, the particle overlap is assessed by calculating the minimum separation between the two particles. We discuss this method of assessing an overlap in detail below.

Advancing our analysis, we now consider the configuration of particles  $i$  and  $j$  shown in Figure 4.14, with the notion  $\mathbf{r}_i$  for the particle center position, the unit vector  $\mathbf{e}_i$  for denoting the particle direction (normal to the disk surface), the point  $S_i$  for the intersection point of the vertical line drawn from  $\mathbf{r}_i$  to the intersection line, the position vector  $\mathbf{r}_i^s$  for point  $S_i$ , and the unit vector  $\mathbf{e}_i^s$  for denoting the direction of  $(\mathbf{r}_i^s - \mathbf{r}_i)$ , with similar notation for particle  $j$ . In addition, the notation  $\mathbf{t}_{ij}^s$  is used as the unit vector denoting the direction of the line drawn from points  $S_j$  to  $S_i$ . In the following paragraphs, these quantities are first evaluated for a pair of particles and then they are used to discuss the criterion for particle overlap.

The unit vector  $\mathbf{t}_{ij}^s$  along the intersection line is normal to both the vectors  $\mathbf{e}_i$  and  $\mathbf{e}_j$ , so that  $\mathbf{t}_{ij}^s$  can be expressed from the formula of vector product as

$$\mathbf{t}_{ij}^s = \mathbf{e}_j \times \mathbf{e}_i / |\mathbf{e}_j \times \mathbf{e}_i| \quad (4.23)$$

in which  $\mathbf{t}_{ij}^s$  is necessarily taken from  $S_j$  toward  $S_i$ . Since  $\mathbf{e}_i^s$  is normal to both  $\mathbf{e}_i$  and  $\mathbf{t}_{ij}^s$  and, similarly,  $\mathbf{e}_j^s$  is normal to  $\mathbf{e}_j$  and  $\mathbf{t}_{ij}^s$ , the use of the vector  $\mathbf{t}_{ij}^s$  provides the solutions of  $\mathbf{e}_i^s$  and  $\mathbf{e}_j^s$  as

$$\mathbf{e}_i^s = -\mathbf{e}_i \times \mathbf{t}_{ij}^s, \quad \mathbf{e}_j^s = \mathbf{e}_j \times \mathbf{t}_{ij}^s \quad (4.24)$$

In the particle configuration shown in Figure 4.14, it is clear that the unit vectors  $\mathbf{e}_i^s$  and  $\mathbf{e}_j^s$  in Eq. (4.24) point toward the intersection line from the center of each particle. In certain situations, however, these vectors may point in the opposite direction. The treatment of ensuring that  $\mathbf{e}_i^s$  and  $\mathbf{e}_j^s$  point toward the intersection line will be discussed in detail in Section 4.2.5. If the distance between the center of particle  $i$  and point  $S_i$  is denoted by  $k_i^s$  (similarly,  $k_j^s$  for particle  $j$ ), and the separation between points  $S_i$  and  $S_j$  is denoted by  $k_{ij}^s$ , the expression of point  $S_i$  in the two different forms yields the following equation:

$$\mathbf{r}_i + k_i^s \mathbf{e}_i^s = \mathbf{r}_j + k_j^s \mathbf{e}_j^s + k_{ij}^s \mathbf{t}_{ij}^s \quad (4.25)$$

The left- and right-hand sides in this equation are related to the same position vector  $\mathbf{r}_i^s$ , which is traced from the center of particles  $i$  and  $j$ , respectively. With the orthogonality condition of the unit vectors, Eq. (4.25) provides the following expressions:

$$k_i^s = -\frac{\mathbf{e}_j \cdot \mathbf{r}_{ij}}{\mathbf{e}_j \cdot \mathbf{e}_i^s}, \quad k_j^s = \frac{\mathbf{e}_i \cdot \mathbf{r}_{ij}}{\mathbf{e}_i \cdot \mathbf{e}_j^s}, \quad k_{ij}^s = \mathbf{r}_{ij} \cdot \mathbf{t}_{ij}^s \quad (4.26)$$

Another preliminary discussion is necessary before proceeding to the analysis of the particle overlap. Figure 4.15 shows the possibility of the torus part of particle  $j$  overlapping with the disk surface part of particle  $i$ , where the angle between the two planes including each particle is denoted by  $\theta_0$ . A line is drawn from the nearest point  $Q_j$  at the torus center circle of particle  $j$  so that it is perpendicular to the plane of particle  $i$ , and this line will intersect the plane at a point denoted by  $Q_{i(j)}$ , as shown in Figure 4.15. The length of the vertical line  $k_{i(j)}^Q$  can be straightforwardly obtained from a simple geometric relationship as

$$k_{i(j)}^Q = (k_j^s - d/2) |\mathbf{e}_j^s \cdot \mathbf{e}_i| \quad (4.27)$$

The position vector  $\mathbf{r}_{i(j)}^Q$  of point  $Q_{i(j)}$  can therefore be written as

$$\mathbf{r}_{i(j)}^Q = \mathbf{r}_j + (d/2) \mathbf{e}_j^s - k_{i(j)}^Q \mathbf{e}_i \quad (4.28)$$

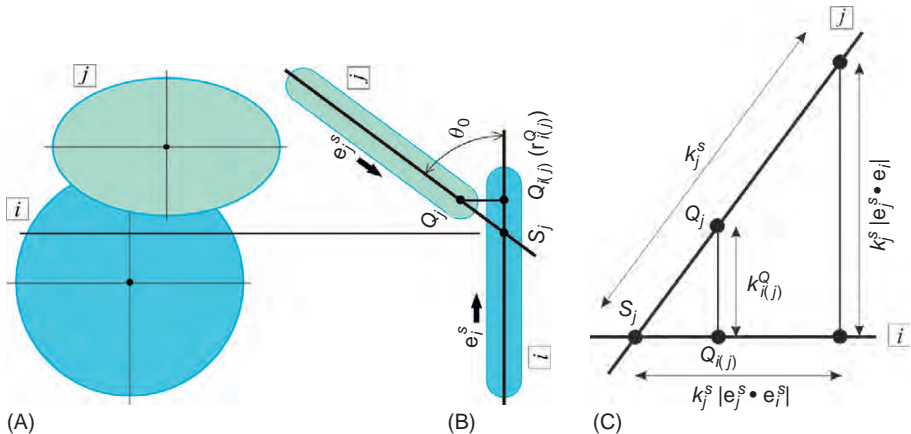


**Figure 4.15** Analysis of the overlap of the flat part of particle  $i$  and the circumference of particle  $j$ : (A) plane view, (B) side view, and (C) vector expression.

Note that Eqs. (4.27) and (4.28) are valid for  $k_j^S \geq d/2$ , as shown in Figure 4.15. In the case of  $k_j^S < d/2$ , the following expressions are used instead of Eqs. (4.27) and (4.28):

$$k_{i(j)}^Q = (d/2 - k_j^S) |\mathbf{e}_j^S \cdot \mathbf{e}_i| \quad (4.29)$$

$$\mathbf{r}_{i(j)}^Q = \mathbf{r}_j + (d/2) \mathbf{e}_j^S + k_{i(j)}^Q \mathbf{e}_i \quad (4.30)$$

We have now completed the preparatory analysis and are able to begin discussion of the particle overlap conditions. For simplicity, the condition  $k_i^S \leq k_j^S$  is assumed to be satisfied in the following. It is reasonable to discuss the particle overlap condition for the three different cases with regard to the directions of  $\mathbf{e}_i$  and  $\mathbf{e}_j$ :

1. Case of  $\mathbf{e}_i \neq \pm \mathbf{e}_j$  (general overlap).
2. Case of  $\mathbf{e}_i = \pm \mathbf{e}_j$  and  $\mathbf{e}_i \cdot \mathbf{r}_{ij} = 0$  (two particles being in the same plane).
3. Case of  $\mathbf{e}_i = \pm \mathbf{e}_j$  and  $\mathbf{e}_i \cdot \mathbf{r}_{ij} \neq 0$  (two particles being in the two parallel planes).

The procedure for assessing the particle overlap with regard to particles  $i$  and  $j$  is as follows:

1. For  $\mathbf{e}_i = \pm \mathbf{e}_j$  and  $\mathbf{e}_i \cdot \mathbf{r}_{ij} = 0$  (both particles being in one plane).
  - 1.1. For  $|\mathbf{r}_i - \mathbf{r}_j| \geq d_1$ , no overlap.
  - 1.2. For  $|\mathbf{r}_i - \mathbf{r}_j| < d_1$ , an overlap.
2. For  $\mathbf{e}_i = \pm \mathbf{e}_j$  and  $\mathbf{e}_i \cdot \mathbf{r}_{ij} \neq 0$  (particles  $i$  and  $j$  being in two parallel planes).
  - 2.1. For  $|\mathbf{e}_i \cdot \mathbf{r}_{ij}| \geq b_1$ , no overlap.
  - 2.2. For  $|\mathbf{e}_i \cdot \mathbf{r}_{ij}| < b_1$ , a possibility of overlap.

The line drawn between  $\mathbf{r}_i$  and  $\mathbf{r}_j$  is projected onto each plane. The projected lines will intersect the corresponding torus center circles at points  $P_i$  and  $P_j$ , respectively. Then the unit vector  $\mathbf{e}_i^p$  denoting the direction from the particle center to point  $P_i$  (similarly  $\mathbf{e}_j^p$ ) can be expressed as

$$\mathbf{e}_j^p = \frac{(\mathbf{e}_i \times \mathbf{r}_{ij}) \times \mathbf{e}_i}{|(\mathbf{e}_i \times \mathbf{r}_{ij}) \times \mathbf{e}_i|} = \frac{\mathbf{r}_{ij} - (\mathbf{e}_i \cdot \mathbf{r}_{ij})\mathbf{e}_i}{|\mathbf{r}_{ij} - (\mathbf{e}_i \cdot \mathbf{r}_{ij})\mathbf{e}_i|}, \quad \mathbf{e}_i^p = -\mathbf{e}_j^p \quad (4.31)$$

$$\mathbf{r}_{ij}^p = \mathbf{r}_{ij} - (\mathbf{e}_i \cdot \mathbf{r}_{ij})\mathbf{e}_i \quad (4.32)$$

With these vectors,

**2.2.1.** For  $|\mathbf{r}_{ij}^p| < d$ , an overlap.

**2.2.2.** For  $|\mathbf{r}_{ij}^p| \geq d_1$ , no overlap.

**2.2.3.** For  $|\mathbf{r}_{ij}^p| \geq d$  and  $|(\mathbf{r}_i + (d/2)\mathbf{e}_i^p) - (\mathbf{r}_j + (d/2)\mathbf{e}_j^p)| < b_1$ , an overlap.

**2.2.4.** For  $|\mathbf{r}_{ij}^p| \geq d$  and  $|(\mathbf{r}_i + (d/2)\mathbf{e}_i^p) - (\mathbf{r}_j + (d/2)\mathbf{e}_j^p)| \geq b_1$ , no overlap.

**3.** For  $\mathbf{e}_i \neq \pm \mathbf{e}_j$  (general overlap situations)

**3.1.** For  $k_j^s > d/2$ ,

**3.1.1.** For  $k_{i(j)}^Q \geq b_1$ , no overlap irrespective of values of  $|\mathbf{r}_{i(j)}^Q - \mathbf{r}_i|$ .

**3.1.2.** For  $k_{i(j)}^Q < b_1$ , a possibility of overlap.

a. For  $|\mathbf{r}_{i(j)}^Q - \mathbf{r}_i| < d/2$ , an overlap.

b. For  $|\mathbf{r}_{i(j)}^Q - \mathbf{r}_i| \geq d/2$ , a possibility of overlap.

b.1. For  $r_{ij}^{(min)} \geq b_1$ , no overlap.

b.2. For  $r_{ij}^{(min)} < b_1$ , an overlap.

**3.2.** For  $k_i^s < d/2$  and  $k_j^s \leq d/2$ , depending on the value of  $r_{ij}^{(min)}$  (defined later)

**3.2.1.** For  $|\mathbf{r}_{i(j)}^Q - \mathbf{r}_i| < d/2$ , an overlap.

**3.2.2.** For  $|\mathbf{r}_{i(j)}^Q - \mathbf{r}_i| \geq d/2$ , a possibility of overlap.

a. For  $r_{ij}^{(min)} \geq b_1$ , no overlap.

b. For  $r_{ij}^{(min)} < b_1$ , an overlap.

The above-mentioned analysis has effectively generated an algorithm for assessing the particle overlap. Notice that the algorithm has been organized from the viewpoint of developing a simulation program, so it can be readily translated into a programming language.

Figure 4.16 shows a method of evaluating the minimum distance  $r_{ij}^{(min)}$ , which has already been used in the analysis but not yet given an exact definition. The particle coordinate system XYZ is fixed at the center of the torus circle of particle  $i$ ,

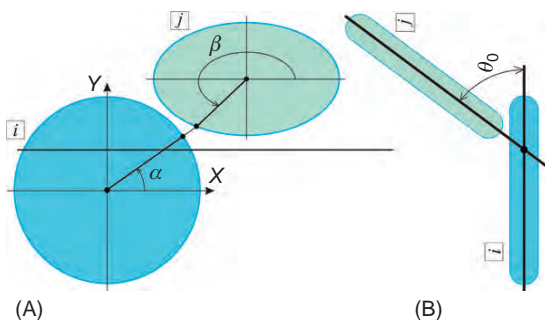


**Figure 4.16** Evaluation of the minimum distance of particles  $i$  and  $j$  using the particle-fixed coordinate system XYZ: (A) plane view and (B) side view.

and the center of particle  $j$  is assumed to be expressed as  $(x_0, y_0, z_0)$  in this coordinate system, where the  $X$ -axis is taken parallel to the intersection line. The angle between the two planes that include particles  $i$  and  $j$  is denoted by the angle  $\theta_0$ , as shown in Figure 4.16B. An arbitrary position vector  $\mathbf{x}_1 = (x_1, y_1, z_1)$  on the torus center circle line of particle  $i$  is taken in the counterclockwise direction by the angle  $\alpha$ . Similarly, an arbitrary position vector  $\mathbf{x}_2 = (x_2, y_2, z_2)$  on the torus center circle line of particle  $j$  is taken in a similar way by the angle  $\beta$ , as shown in Figure 4.16A. Then  $\mathbf{x}_1$  and  $\mathbf{x}_2$  are expressed as

$$\mathbf{x}_1 = (r_0 \cos \alpha, r_0 \sin \alpha, 0) \quad (4.33)$$

$$\mathbf{x}_2 = (r_0 \cos \beta + x_0, r_0 \sin \beta \cos \theta_0 + y_0, r_0 \sin \beta \sin \theta_0 + z_0) \quad (4.34)$$

in which  $r_0 = d/2$ . The square separation between  $\mathbf{x}_1$  and  $\mathbf{x}_2$  is a function of the angles  $\alpha$  and  $\beta$ , expressed as

$$\begin{aligned} g(\alpha, \beta) &= (x_2 - x_1)^2 + (y_2 - y_1)^2 + (z_2 - z_1)^2 \\ &= (r_0 \cos \beta + x_0 - r_0 \cos \alpha)^2 + (r_0 \sin \beta \cos \theta_0 + y_0 - r_0 \sin \alpha)^2 \\ &\quad + (r_0 \sin \beta \sin \theta_0 + z_0)^2 \end{aligned} \quad (4.35)$$

Certain values of  $\alpha$  and  $\beta$  give rise to a minimum value of  $g(\alpha, \beta)$ . It is clear that the positions  $\mathbf{x}_1$  and  $\mathbf{x}_2$  on the different torus center circles specified by the angles  $\alpha$  and  $\beta$  that minimize the function  $g$  yield their minimum separation distance. The values of  $\alpha$  and  $\beta$  to satisfy a minimum  $g(\alpha, \beta)$  can be obtained by solving the equations of  $\partial g / \partial \alpha = \partial g / \partial \beta = 0$ . The equation  $\partial g / \partial \alpha = 0$  yields the following relationship:

$$\tan \alpha = \frac{y_2}{x_2} \quad (4.36)$$

Furthermore, the expression  $\partial g / \partial \beta = 0$  gives rise to the following relationship:

$$\tan \beta = \frac{y_0 - y_1}{x_0 - x_1} \cos \theta_0 + \frac{z_0}{x_0 - x_1} \sin \theta_0 \quad (4.37)$$

The solutions of  $\alpha$  and  $\beta$  can be obtained by solving Eqs. (4.36) and (4.37). However, because of the difficulty of an analytical approach, we here employ Newton's iteration method [33] for numerically solving these equations. From the particle configuration in Figure 4.16, we reasonably expect that Newton's iteration method will effectively provide a converged solution after several iterations, because  $g(\alpha, \beta)$  has a relatively simple form. We show the algorithm of Newton's iteration method in the following steps:

1. Suppose a starting value  $\beta_n$ , around an expected solution, for  $\beta$ .
2. Calculate  $(x_2, y_2, z_2)$ .

3. Calculate  $(x_1, y_1, z_1) = \left(r_0 x_2 / \sqrt{x_2^2 + y_2^2}, r_0 y_2 / \sqrt{x_2^2 + y_2^2}, 0\right)$  from Eqs. (4.36) and (4.33).
4. Evaluate  $f(\beta_n)$  from Eq. (4.37).

$$f(\beta_n) = \tan \beta_n - \frac{y_0 - y_1}{x_0 - x_1} \cos \theta_0 - \frac{z_0}{x_0 - x_1} \sin \theta_0 \quad (4.38)$$

5. Evaluate the derivative of  $f(\beta)$  with respect to  $\beta$ .

$$f'(\beta_n) = \frac{1}{\cos^2 \beta_n} - \frac{\cos \theta_0}{(x_0 - x_1)^2} \left\{ -\frac{\partial y_1}{\partial \beta} (x_0 - x_1) + \frac{\partial x_1}{\partial \beta} (y_0 - y_1) \right\} - z_0 \sin \theta_0 \frac{\partial x_1 / \partial \beta}{(x_0 - x_1)^2} \quad (4.39)$$

in which

$$\left. \begin{aligned} \frac{\partial x_1}{\partial \beta} &= r_0 \cdot \frac{\frac{\partial x_2}{\partial \beta} \sqrt{x_2^2 + y_2^2} - \left( x_2 \frac{\partial x_2}{\partial \beta} + y_2 \frac{\partial y_2}{\partial \beta} \right) x_2 / \sqrt{x_2^2 + y_2^2}}{x_2^2 + y_2^2} \\ \frac{\partial y_1}{\partial \beta} &= r_0 \cdot \frac{\frac{\partial y_2}{\partial \beta} \sqrt{x_2^2 + y_2^2} - \left( x_2 \frac{\partial x_2}{\partial \beta} + y_2 \frac{\partial y_2}{\partial \beta} \right) y_2 / \sqrt{x_2^2 + y_2^2}}{x_2^2 + y_2^2} \end{aligned} \right\} \quad (4.40)$$

The right-hand sides are evaluated by setting  $\beta = \beta_n$ .

6. Evaluate the next approximation  $\beta_{n+1}$  from Newton's method:

$$\beta_{n+1} = \beta_n - \frac{f(\beta_n)(x_0 - x_1)^2}{f'(\beta_n)(x_0 - x_1)^2} \quad (4.41)$$

7. Go to step 8 in the case of sufficiently convergence such as  $|\beta_{n+1} - \beta_n| < \varepsilon$  ( $\varepsilon$  is infinitesimal small), otherwise repeat from step 2 by regarding  $\beta_{n+1}$  as  $\beta_n$ .
8. Calculate  $\alpha_{n+1}$  from Eq. (4.36) with the converged value of  $\beta_{n+1}$ , and evaluate  $g(\alpha_{n+1}, \beta_{n+1})$  from Eq. (4.35), yielding the desired minimum distance  $r_{ij}^{(\min)} = \sqrt{g(\alpha_{n+1}, \beta_{n+1})}$ .

We here employ a value satisfying  $x_2 = x_0/2$  as a starting value of  $\beta$ . With this value,  $\beta$  can be obtained from Eq. (4.34) as  $\beta = \cos^{-1}(-x_0/2r_0)$ : although there are two solutions of the equation of  $\cos \beta = -x_0/2r_0$ , such a solution as satisfying  $z_2 < z_0$  is adopted for  $\beta$ . This solution  $\beta$  provides the values of  $y_2$  and  $z_2$  from Eq. (4.34).

#### 4.2.4 Canonical Monte Carlo Algorithm

As already indicated, we consider a system composed of  $N$  magnetic particles in an applied magnetic field in thermodynamic equilibrium. The canonical MC method is therefore adopted for a given system temperature  $T$ , volume  $V$ , and number of particles  $N$ . The system potential energy  $U^*$  can be expressed as the summation of the magnetic particle–particle interaction energy  $u_{ij}^*$  and the magnetic particle–field interaction energy  $u_i^*$  as

$$U^* = \sum_{i=1}^N u_i^* + \sum_{i=1}^N \sum_{j=1(j>i)}^N u_{ij}^* \quad (4.42)$$

in which  $u_i^*$  and  $u_{ij}^*$  have already been shown in Eqs. (4.20) and (4.21).

The canonical MC algorithm has been explained in Chapter 1 for a nonspherical particle system. According to Eq. (1.52), an arbitrary particle is translated into an adjacent position using random numbers. If the energy  $U^*$  decreases, the movement is accepted, but if it increases, it is employed according to the probability shown in Eq. (1.49). The rotational movement is first attempted and then accepted or rejected in a similar procedure. Although the simultaneous attempt of the translational and rotational movements is possible, the above-mentioned separate attempts will become more effective in the case of a strongly interacting system.

#### 4.2.5 Treatment of the Criterion of the Particle Overlap in Simulations

The criterion of the particle overlap has already been discussed in detail from a mathematical point of view. In this subsection, we address important points to be noted with regard to the actual treatment of particle overlap in the simulation.

**1. Exchange of the particle names  $i$  and  $j$ :**

The particle subscripts  $i$  and  $j$  are exchanged in such a way to satisfy  $k_i^s \leq k_j^s$ . That is, in the case of  $k_i^s > k_j^s$ , the subscripts  $i$  and  $j$  are replaced with  $j$  and  $i$ , respectively; therefore the criterion for particle overlap in Section 4.2.3 is directly applicable.

**2. Reversal of the directions of the unit vectors  $\mathbf{e}_i$  and  $\mathbf{e}_j$ :**

As shown in Figures (4.14) and (4.15), the unit vectors  $\mathbf{e}_i$  and  $\mathbf{e}_j$  are temporarily reversed in such a way that the angle  $\theta_0$  will satisfy  $0 \leq \theta_0 \leq \pi/2$ . In the case of  $\mathbf{r}_{ji} \cdot \mathbf{e}_i \geq 0$ ,  $\mathbf{e}_i$  is unchanged, otherwise  $\mathbf{e}_i$  is temporarily reversed in direction as  $\mathbf{e}_i \rightarrow -\mathbf{e}_i$ . For this new  $\mathbf{e}_i$ ,  $\mathbf{e}_j$  is unchanged for  $\mathbf{e}_i \cdot \mathbf{e}_j \geq 0$ ; otherwise  $\mathbf{e}_j$  is temporarily reversed for the successive procedure. These treatments confirm that  $\theta_0$  becomes an acute angle, as shown in Figure 4.14. Note that the exchange of the subscripts  $i$  and  $j$  may be necessary in the following procedures.

**3. Reversal of the direction of the unit vector  $\mathbf{t}_{ij}^s$ :**

The unit vector  $\mathbf{t}_{ij}^s$  is taken in the direction from point  $S_j$  to  $S_i$ . For  $\mathbf{t}_{ij}^s$  evaluated from Eq. (4.23), if  $\mathbf{t}_{ij}^s \cdot \mathbf{r}_{ij} \geq 0$ ,  $\mathbf{t}_{ij}^s$  is unchanged, otherwise  $\mathbf{t}_{ij}^s$  is temporarily reversed as  $\mathbf{t}_{ij}^s \rightarrow -\mathbf{t}_{ij}^s$ . This treatment ensures that  $\mathbf{t}_{ij}^s$  is from point  $S_j$  toward point  $S_i$  even if particle  $j$  is on the left-hand side.

**4. Reversal of the unit vectors  $\mathbf{e}_i$  and  $\mathbf{e}_j$ :**

With the unit vectors  $\mathbf{e}_i^s$  and  $\mathbf{e}_j^s$  evaluated from Eq. (4.24), the solutions  $k_i^s$  and  $k_j^s$  can be obtained from Eq. (4.26). However, note that the definition of these unit vectors

pointing toward the intersection line from each particle center is not necessarily satisfied but depends on the interaction position. In other words, since the sign of  $k_i^s$  or  $k_j^s$  is not necessarily positive,  $\mathbf{e}_i^s$  or  $\mathbf{e}_j^s$  may be reversed in this situation. In the case of  $k_i^s \geq 0$ ,  $\mathbf{e}_i^s$  is unchanged, and in the case of  $k_i^s < 0$ ,  $\mathbf{e}_i^s$  is reversed as  $\mathbf{e}_i^s \rightarrow -\mathbf{e}_i^s$ , making  $k_i^s$  positive. Similar treatment is made for  $k_j^s$  and  $\mathbf{e}_j^s$ .

These procedures ensure that the previous algorithm for assessing the particle overlap and Newton's iteration method for finding the minimum separation are directly applicable without any changes.

#### 4.2.6 Particle-Fixed Coordinate System and the Absolute Coordinate System

We here explain the particle-fixed coordinate system and the absolute coordinate system, which are necessary for a rotation of the particle and a rotation of the magnetic moment. As previously defined, we use the notation  $\mathbf{e}$  for the particle direction and  $\mathbf{n}$  for the magnetic moment direction, as shown in Figure 4.17. We call the coordinate system fixed at the particle the “particle-fixed coordinate system,” simply expressed as the  $XYZ$ -coordinate system, centered at the particle center with the  $Z$ -axis along the particle axis direction. On the other hand, the coordinate system fixed, for example, on the computational cell is called the “absolute coordinate system,” simply expressed as the  $xyz$ -coordinate system. Note that each particle has its own particle-fixed coordinate system centered at its particle center.

We briefly consider the rotation of the  $xyz$ -coordinate system about the  $z$ -axis by an angle  $\phi$ , and then the rotation of the rotated  $xyz$ -coordinate system about the  $y$ -axis by an angle  $\theta$  to generate the  $XYZ$ -coordinate system. For these rotations, the rotational matrix  $\mathbf{R}$  can be written as

$$\begin{aligned}\mathbf{R} &= \begin{pmatrix} \cos \theta & 0 & -\sin \theta \\ 0 & 1 & 0 \\ \sin \theta & 0 & \cos \theta \end{pmatrix} \begin{pmatrix} \cos \phi & \sin \phi & 0 \\ -\sin \phi & \cos \phi & 0 \\ 0 & 0 & 1 \end{pmatrix} \\ &= \begin{pmatrix} \cos \theta \cos \phi & \cos \theta \sin \phi & -\sin \theta \\ -\sin \phi & \cos \phi & 0 \\ \sin \theta \cos \phi & \sin \theta \sin \phi & \cos \theta \end{pmatrix}\end{aligned}\quad (4.43)$$

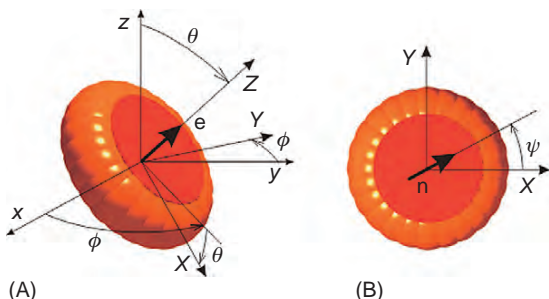


**Figure 4.17** Particle-fixed coordinate system and absolute coordinate system.

This rotational matrix will allow us to express the relationship between an arbitrary position  $\mathbf{a}^b = (a_x^b, a_y^b, a_z^b)$  in the *XYZ*-coordinate system and  $\mathbf{a} = (a_x, a_y, a_z)$  in the *xyz*-coordinate system as

$$\mathbf{a}^b = \mathbf{R} \cdot \mathbf{a} \quad (4.44)$$

The inverse matrix  $\mathbf{R}^{-1}$  of  $\mathbf{R}$  is equal to the transpose matrix  $\mathbf{R}'$  of  $\mathbf{R}$ , so that  $\mathbf{a}$  can be obtained from  $\mathbf{a}^b$  as

$$\mathbf{a} = \mathbf{R}^{-1} \cdot \mathbf{a}^b \quad (4.45)$$

Thus, the particle direction  $\mathbf{e}$  and the magnetic moment direction  $\mathbf{n}$  of an arbitrary particle can be expressed as

$$\mathbf{e} = \mathbf{R}^{-1} \cdot \mathbf{e}^b, \quad \mathbf{n} = \mathbf{R}^{-1} \cdot \mathbf{n}^b \quad (4.46)$$

Since the *XYZ*-coordinate system is adopted so that the *Z*-axis is pointing in the particle direction, the unit vector  $\mathbf{e}^b$  satisfies  $\mathbf{e}^b = (0, 0, 1)$ . This gives rise to the particle direction  $\mathbf{e}$  in the *xyz*-coordinate system expressed as  $\mathbf{e} = (e_x, e_y, e_z) = (\sin \theta \cos \phi, \sin \theta \sin \phi, \cos \theta)$ . If necessary, known values of  $(e_x, e_y, e_z)$  yield the sine and cosine functions of  $\theta$  and  $\phi$  as  $\cos \theta = e_z$ ,  $\sin \theta = \sqrt{1 - e_z^2}$ ,  $\cos \phi = e_x / \sin \theta$ , and  $\sin \phi = e_y / \sin \theta$ , in which it is noted that  $\theta$  is defined in the range of  $0 \leq \theta \leq \pi/2$ . Several special features arising from this definition of range will be explained later.

We briefly explain the method for expressing the magnetic moment direction  $\mathbf{n}$ . As shown in Figure 4.17B, the direction of the magnetic moment can be specified by an angle  $\psi$  in the counterclockwise direction from the *X*-axis in the *XYZ*-coordinate system. That is, the magnetic moment direction  $\mathbf{n}^b$  is expressed as  $\mathbf{n}^b = (\cos \psi, \sin \psi, 0)$ , so that the vector  $\mathbf{n}$  in the *xyz*-coordinate system can be obtained from Eq. (4.46) as  $\mathbf{n} = \mathbf{R}^{-1} \cdot \mathbf{n}^b$ .

#### 4.2.7 Attempt of Small Angular Changes in the Particle Axis and the Magnetic Moment

In MC simulations, an attempt is made to move each particle in translation and rotation with small displacements using uniform random numbers. Since the attempt of the translational movement is similar to that for a spherical particle system, we here show the method of rotating the particle direction and the magnetic moment direction.

We first consider the rotation of the particle direction. As shown previously, the particle direction  $(\theta, \phi)$  of an arbitrary particle is assumed to be made as  $(\theta + \Delta\theta, \phi + \Delta\phi)$ , with the small change  $(\Delta\theta, \Delta\phi)$ . Special treatment will be necessary if  $(\theta + \Delta\theta)$  or  $(\phi + \Delta\phi)$  is then larger than  $\pi/2$  for  $\theta$  or  $2\pi$  for  $\phi$  and also if smaller than zero for  $\theta$  or  $\phi$ , because the angles  $\theta$  and  $\phi$  are defined within the ranges of  $0 \leq \theta \leq \pi/2$  and  $0 \leq \phi < 2\pi$ .

**1. For the case of  $\theta + \Delta\theta < 0$ :**

We make a modification such that  $\theta' = -(\theta + \Delta\theta)$ ,  $\phi' = \phi + \Delta\phi + \pi$ , and  $\psi' = \psi + \pi$ , and use these values  $(\theta', \phi', \psi')$  for the rotational movement. Note that  $(\phi' - 2\pi)$  needs to be adopted as  $\phi'$  if  $\phi' \geq 2\pi$  since  $\phi'$  is defined in the range of  $0 \leq \phi' < 2\pi$ . Similar treatment is required for  $\psi'$ .

**2. For the case of  $\theta + \Delta\theta \geq \pi/2$ :**

We make a modification such that  $\theta' = \pi - (\theta + \Delta\theta)$ ,  $\phi' = \phi + \Delta\phi + \pi$ , and  $\psi' = 2\pi - \psi$ . If  $\phi'$  or  $\psi'$  is outside the range of  $0 \leq \phi', \psi' < 2\pi$ , the above-mentioned treatment is applicable.

**3. For the case of  $0 \leq \theta + \Delta\theta < \pi/2$ :**

In this case, a special modification is unnecessary and  $(\theta', \phi', \psi')$  are merely expressed as  $\theta' = \theta + \Delta\theta$ ,  $\phi' = \phi + \Delta\phi$ , and  $\psi' = \psi$ , except that  $\phi'$  is modified as in the previous case if  $\phi'$  is outside the defined range.

For the above-modified  $\theta'$ ,  $\phi'$ , and  $\psi'$ , the rotational displacement is attempted and determined by the MC assessing procedure.

We next consider the rotation of the magnetic moment. The angle  $\psi$  specifying the direction is slightly displaced as  $(\psi + \Delta\psi)$ . Since  $\psi$  is defined in the range of  $0 \leq \psi < 2\pi$ ,  $\psi'$  is modified such that  $\psi' = \psi + \Delta\psi - 2\pi$  for  $\psi + \Delta\psi \geq 2\pi$ ,  $\psi' = \psi + \Delta\psi + 2\pi$  for  $\psi + \Delta\psi < 0$  and  $\psi' = \psi + \Delta\psi$  for the other cases. With this modified  $\psi'$ , the magnetic moment direction  $\mathbf{n}'^b$  is specified as  $\mathbf{n}'^b = (\cos \psi', \sin \psi', 0)$  in the XYZ-coordinate system, and therefore the vector  $\mathbf{n}'$  in the xyz-coordinate system can be obtained as  $\mathbf{n}' = \mathbf{R}^{-1} \cdot \mathbf{n}'^b$  from Eq. (4.46). The magnetic interaction energies are calculated for the new magnetic moment direction, and the MC procedure determines whether this new state is accepted or rejected.

## 4.2.8 Parameters for Simulations

### 4.2.8.1 Initial Conditions

The assignment of an initial configuration of the circular disk-like particles explained in Section 2.1.2 is applied to the present system with different number of particles. As shown in Figure 2.5, four disk-like particles are located linearly along the  $x$ -axis, with the particles aligning in the  $y$ -direction. This stack of 4 particles is repeatedly placed in the  $y$ -direction, giving rise to 48 disk-like particles in the  $xy$ -plane at this stage. These particles are expanded in the  $z$ -direction to total 6 layers, giving a final sum of 288 particles placed in the simulation region. In this contact configuration, the size of the simulation region ( $L_x, L_y, L_z$ ) is  $(4r_p b_1, 12b_1, 6r_p b_1)$ . The expansion of the distance between each pair of particles by  $\alpha$  times each side length yields the desired volumetric fraction of particles  $\phi_V$ . The relationship between  $\alpha$  and  $\phi_V$  can be expressed as

$$\alpha = \left[ \frac{\pi}{24r_p^2 \phi_V} \{ 6(r_p - 1)^2 + 3\pi(r_p - 1) + 4 \} \right]^{\frac{1}{3}} \quad (4.47)$$

This configuration is perfectly regular, and therefore each particle is given a small translational displacement in order for the initial configuration to be able to transform to an equilibrium state straightforwardly. Then the direction of each particle is assigned as  $\mathbf{e}_i = (0, 1, 0)$  ( $i = 1, 2, \dots, N$ ).

Finally the direction of the magnetic moment is set to be arbitrary using random numbers. Thus, setting the  $\psi$  in the XY-plane gives rise to  $\mathbf{n}^b = (n_x^b, n_y^b, 0) = (\cos \psi, \sin \psi, 0)$  and Eq. (4.46) finally yields the direction  $\mathbf{n}$  in the xyz-coordinate system.

#### 4.2.8.2 Assignment of Parameters

The simulations were conducted for the particle number  $N = 288$  and the volumetric fraction ranging  $\phi_V = 0.05 \sim 0.3$ . An external magnetic field is applied in the z-direction as  $\mathbf{h} = (0, 0, 1)$ . We here employ the cutoff distance  $r_{\text{cuff}}^* = 5d_1^*$  for calculating magnetic interaction energies; an academic study may require a longer cutoff distance because magnetic energies are of long-range order. The nondimensional parameters  $\xi$  and  $\lambda$  representing the strengths of magnetic particle–field and particle–particle interactions are taken as  $\xi = 0, 1, 10$ , and  $30$  and  $\lambda = 0, 1, 10, 30$ , and  $60$ . Note that the situation where  $\xi \gg 1$  or  $\lambda \gg 1$  means that the magnetic field or the magnetic particle–particle interaction is more dominant than the Brownian motion, respectively. The total number of MC steps  $N_{\text{mcsmplemx}}$  is usually taken as  $N_{\text{mcsmplemx}} = 100,000 \sim 1,000,000$ , but the present exercise is only for the purpose of demonstration and therefore we employ a smaller value  $N_{\text{mcsmplemx}} = 100,000$ .

#### 4.2.9 Results of Simulations

Figures 4.18–4.21 show the snapshots of the aggregate structures, which were obtained using the sample simulation program presented in the next subsection. Figure 4.18 is for no magnetic interactions between particles, that is,  $\lambda = 0$ , and

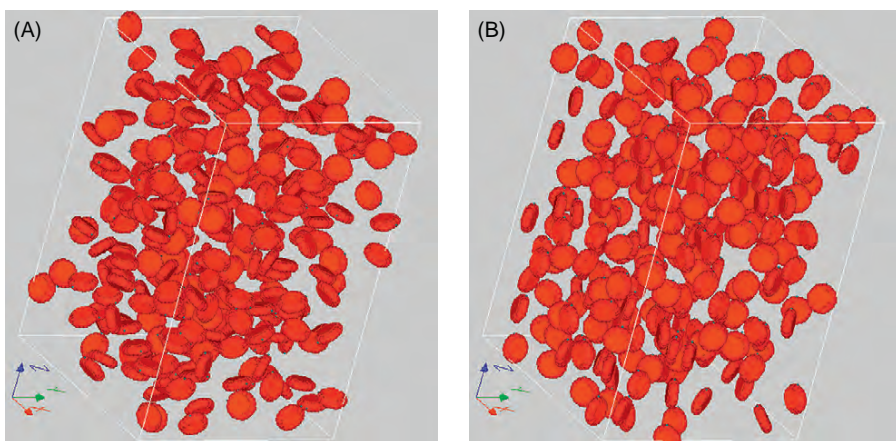


**Figure 4.18** Aggregate structures for  $\lambda = 0$ : (A)  $\xi = 0$  and (B)  $\xi = 30$ .

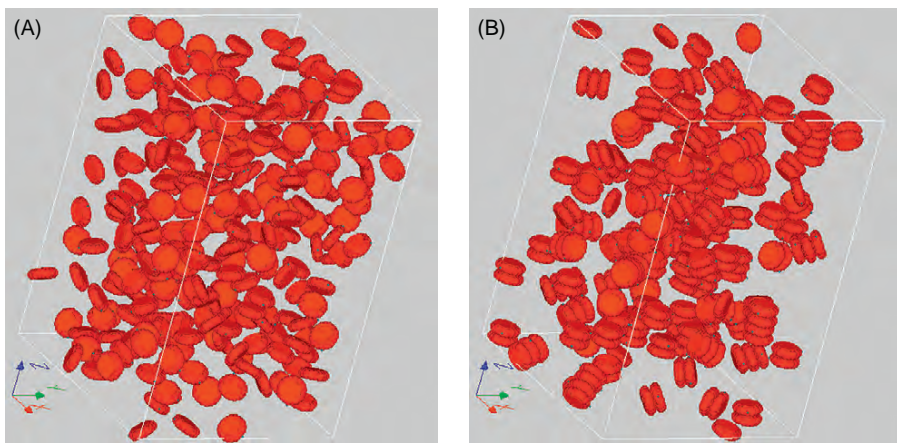


**Figure 4.19** Aggregate structures for  $\xi = 0$ : (A)  $\lambda = 10$  and (B)  $\lambda = 30$ .

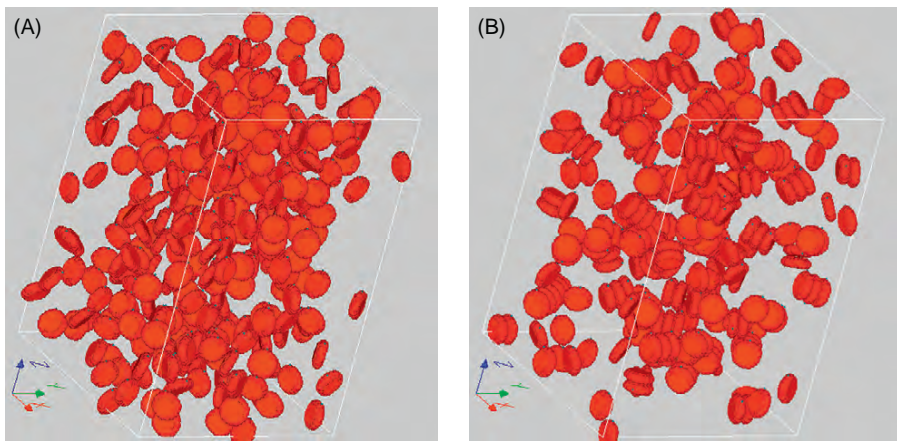


**Figure 4.20** Aggregate structures for  $\xi = 10$ : (A)  $\lambda = 10$  and (B)  $\lambda = 30$ .

Figures 4.19–4.21 are for the magnetic field strength  $\xi = 0$  (i.e., no field), 10, and 30, respectively.

For the case of  $\lambda = 0$  in Figure 4.18, no aggregates are formed because magnetic particle–particle interactions are absent. In addition, since an external magnetic field is also absent in Figure 4.18A, the particles do not show a specifically favored direction in their orientational characteristics. On the other hand, the application of a strong magnetic field, as shown in Figure 4.17B, makes the magnetic moment of each particle incline almost in the field direction (i.e.,  $z$ -direction), resulting in the particle direction significantly fixed in the  $xy$ -plane.

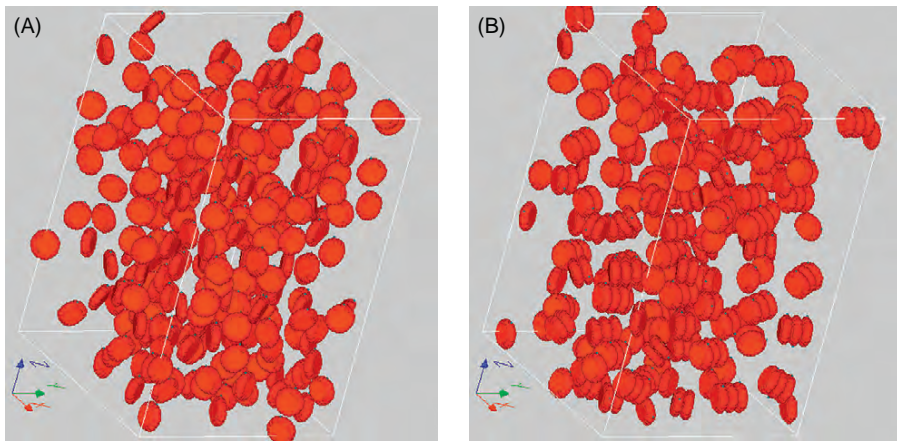


**Figure 4.21** Aggregate structures for  $\xi = 30$ : (A)  $\lambda = 30$  and (B)  $\lambda = 60$ .

Figure 4.19 is for no applied magnetic field  $\xi = 0$ , so that the particles have no tendency to incline in a specifically favored direction. In the case of  $\lambda = 10$  shown in Figure 4.19A, short aggregates are found but are not significant. On the other hand, for the case of  $\lambda = 30$  shown in Figure 4.19B, the disk-like particles aggregate to form column-like clusters in the particle direction (i.e., in the direction normal to the disk surface); each cluster inclines in its favored direction. This is because the magnetic particle–particle interaction is much more dominant than the Brownian motion. A careful observation of the column-like clusters indicates that the disk-like particles in the column-like cluster have their magnetic moments alternating in direction with the neighboring particles. This is because this type of internal structure gives rise to a minimum interaction energy for the magnetic particle–particle interaction. In the case of an external magnetic field of  $\xi = 10$ , shown in Figure 4.20B, the characteristic of the internal structure is the same as in Figure 4.19B because the magnetic interaction of  $\lambda = 30$  is much more dominant than the applied magnetic field strength  $\xi = 10$ ; that is, the magnetic particle–particle interaction tends to determine the internal structures of column-like clusters.

In contrast, for the strong applied magnetic field  $\xi = 30$  shown in Figure 4.21A, column-like clusters obtained in Figure 4.20B are not formed, but the magnetic moment of each particle tends to incline toward the field direction and the particles move singly without forming clusters. The field strength  $\xi = 30$  implies that an applied magnetic field significantly governs the aggregation process, so that the snapshot in Figure 4.21A is not essentially different from that in Figure 4.18B. A stronger interaction  $\lambda = 60$  shown in Figure 4.21B recovers the formation of the column-like clusters that were seen in Figure 4.20B; in this case, the magnetic interactions significantly govern the aggregation process as compared with the external magnetic field. These discussions demonstrate that the internal structures

of the aggregates are dependent on which factor is more dominant among the Brownian motion, the magnetic particle–particle interaction, and the magnetic field strength.

#### 4.2.10 *Simulation Program*

We now present the sample simulation program, written in FORTRAN, for simulating the present physical phenomenon. The important variables used in the program are explained as follows:

$\text{RX}(I)$ , $\text{RY}(I)$ , $\text{RZ}(I)$	: $(x,y,z)$ components of the position vector $\mathbf{r}_i^*$ of particle $i$
$\text{EX}(I)$ , $\text{EY}(I)$ , $\text{EZ}(I)$	: $(x,y,z)$ components of the unit vector $\mathbf{e}_i$ of particle $i$ denoting the particle direction
$\text{NX}(I)$ , $\text{NY}(I)$ , $\text{NZ}(I)$	: $(x,y,z)$ components of the unit vector $\mathbf{n}_i$ of particle $i$ denoting the magnetic moment direction
$\text{XL}$ , $\text{YL}$ , $\text{ZL}$	: Side lengths of the simulation box in the $(x,y,z)$ directions
$N$	: Number of particles
$D1$	: Diameter of the circular disk-like particle $d_1^*$
$D$	: Diameter of the cylinder part of the circular disk-like particle $d^*$
$RP$	: Particle aspect ratio $d_1^*(=d_1/b_1)$
$VP$	: Volume of the disk-like particle
$VDENS$	: Volumetric fraction $\phi_V$
$\text{HX}$ , $\text{HY}$ , $\text{HZ}$	: $(x,y,z)$ components of the unit vector $\mathbf{h}$ denoting the field direction
$RA$	: Nondimensional parameter $\lambda$ representing the strength of magnetic particle–particle interactions
$KU$	: Nondimensional parameter $\xi$ representing the strength of magnetic particle–field interactions
$\text{RCOFF}$	: Cutoff distance for calculations of interaction energies
$\text{DELR}$	: Maximum displacement in the translational movement
$\text{DELT}$	: Maximum angle in the rotational movement
$\text{RAN}(J)$	: Uniform random numbers ranging $0 \sim 1$ $(J = 1 \sim \text{NRANMX})$
$\text{NRAN}$	: Number of used random numbers
$E(I)$	: Energy of particle $i$ interacting with other particles
$\text{MOMX}(*), \dots, \text{MOMZ}(*)$	: Mean value of the particle direction at each MC step
$\text{MEANENE}(*)$	: Mean value of the system energy at each MC step

Brief comments have been added to the important features of the program in order to clarify the meaning for the reader. Note that the line numbers are merely for convenience and are unnecessary for the execution of the program.

The use of quasi-random numbers for saving the pseudo-random numbers  $\text{RAN}(*)$  has already been explained in Section 3.2.9.

```

0001 C*****C*****C*****C*****C*****C*****C*****C*****C*****C*****C*****
0002 C*                                     *
0003 C*      mcdisk3.f                      *
0004 C*                                     *
0005 C*          OPEN(9, FILE='aaa1.dat', STATUS='UNKNOWN')   *
0006 C*          OPEN(10,FILE='aaa11.dat', STATUS='UNKNOWN')   *
0007 C*          OPEN(13,FILE='aaa41.mgf', STATUS='UNKNOWN')   *
0008 C*          OPEN(21,FILE='aaa001.dat',STATUS='UNKNOWN')   *
0009 C*          OPEN(22,FILE='aaa011.dat',STATUS='UNKNOWN')   *
0010 C*          OPEN(23,FILE='aaa021.dat',STATUS='UNKNOWN')   *
0011 C*          OPEN(24,FILE='aaa031.dat',STATUS='UNKNOWN')   *
0012 C*          OPEN(25,FILE='aaa041.dat',STATUS='UNKNOWN')   *
0013 C*          OPEN(26,FILE='aaa051.dat',STATUS='UNKNOWN')   *
0014 C*          OPEN(27,FILE='aaa061.dat',STATUS='UNKNOWN')   *
0015 C*          OPEN(28,FILE='aaa071.dat',STATUS='UNKNOWN')   *
0016 C*          OPEN(29,FILE='aaa081.dat',STATUS='UNKNOWN')   *
0017 C*          OPEN(30,FILE='aaa091.dat',STATUS='UNKNOWN')   *
0018 C*                                     *
0019 C*      ----- MONTE CARLO SIMULATIONS ----- *
0020 C*      THREE-DIMENSIONAL MONTE CARLO SIMULATION OF   *
0021 C*      MAGNETIC COLLOIDAL DISPERSIONS COMPOSED OF   *
0022 C*      MAGNETIC DISK-LIKE PARTICLES                 *
0023 C*                                     *
0024 C*      1. A PARTICLE IS MODELED AS A CIRCULAR DISK-LIKE PARTICLE.   *
0025 C*      2. THE CLUSTER-MOVING METHOD IS NOT USED.           *
0026 C*      3. A STERIC LAYER IS NOT TAKEN INTO ACCOUNT.       *
0027 C*                                     *
0028 C*      VER.1 BY A.SATOH , '08 5/2 * *
0029 C*****C*****C*****C*****C*****C*****C*****C*****C*****C*****C*****
0030 C      N : NUMBER OF PARTICLES (N=INIPX*INIPY*INIPZ)
0031 C      D1 : DIAMETER OF OUTER CIRCLE OF A DISK-LIKE PARTICLE
0032 C      D : DIAMETER OF THE PART OF CYLINDER
0033 C      B1 : THICKNESS OF PARTICLE (=1 FOR THIS CASE)
0034 C      RP : ASPECT RATIO (=D1/B1) (=D1 FOR THIS CASE)
0035 C      VP : VOLUME OF THE PARTICLE
0036 C      NDENS : NUMBER DENSITY
0037 C      VDENS : VOLUMETRIC FRACTION
0038 C      IPTCLMDL : =1 FOR DIPOLE IN THE CENTER, =2 FOR TWO POINT CHARGES
0039 C      RA : NONDIMENSIONAL PARAMETER OF PARTICLE-PARTICLE INTERACT
0040 C      RA0 : =RA/RP**3 FOR IPTCLMDL=1, =RA/RP FOR IPTCLMDL=2
0041 C      KU : NONDIMENSIONAL PARAMETER OF PARTICLE-FIELD INTERACTION
0042 C      HX,HY,HZ : MAGNETIC FIELD DIRECTION (UNIT VECTOR)
0043 C      RCOFF : CUTOFF RADIUS FOR CALCULATION OF INTERACTION ENERGIES
0044 C      XL,YL,ZL : DIMENSIONS OF SIMULATION REGION
0045 C      (XL,YL,ZL)=(INIPX*RP, INIPY, INIPZ*RP) *ALPHA
0046 C      (1) RP=3
0047 C          INITTREE=1 : (INIPX,INIPY,INIPZ)=( 3, 9,12), N= 324
0048 C          INITTREE=2 : (INIPX,INIPY,INIPZ)=( 4,12, 6), N= 288
0049 C      (2) RP=4
0050 C          INITTREE=3 : (INIPX,INIPY,INIPZ)=( ?, ?, ?), N= ?
0051 C          INITTREE=4 : (INIPX,INIPY,INIPZ)=( ?, ?, ?), N= ?
0052 C      (3) RP=5
0053 C          INITTREE=5 : (INIPX,INIPY,INIPZ)=( ?, ?, ?), N= ?
0054 C          INITTREE=6 : (INIPX,INIPY,INIPZ)=( ?, ?, ?), N= ?
0055 C      RX(N),RY(N),RZ(N) : PARTICLE POSITION
0056 C      EX(N),EY(N),EZ(N) : DIRECTION OF RODLIKE PARTICLE
0057 C      NX(N),NY(N),NZ(N) : DIRECTION OF MAGNETIC MOMENT
0058 C      E(I) : INTERACTION ENERGY OF PARTICLE I WITH THE OTHERS
0059 C      MOMX(**),MOMY(**) : MAG. MOMENT OF SYSTEM AT EACH TIME STEP
0060 C      MOMZ(**)
0061 C      MEANENE(**) : MEAN ENERGY OF SYSTEM AT EACH MC STEP
0062 C      ETHETA(N),EPHI(N) : ANGLES DENOTING THE PARTICLE DIRECTION
0063 C      NPSI(N) : ANGLE DENOTING THE MAG.MOM. DIRECTION
0064 C      RMAT(3,3,N) : ROTATIONAL MATRIX
0065 C      NXB(N), NYB(N) : DIREC. OF MAG. MOM. IN THE BODY-FIXED AXIS
0066 C                           SYSTEM
0067 C
0068 C      DELR : MAXIMUM MOVEMENT DISTANCE
0069 C      DELT : MAXIMUM MOVEMENT IN ORIENTATION
0070 C
0071 C          0 < RX < XL , 0 < RY < YL , 0 < RZ < ZL
0072 C-----*
0073 C      IMPLICIT REAL*8 (A-H,O-Z), INTEGER (I-N)
0074 C
0075 C      COMMON /BLOCK1/ RX , RY , RZ

```

```

0076      COMMON /BLOCK2/ NX      , NY      , NZ
0077      COMMON /BLOCK3/ N       , NDENS   , VDENS
0078      COMMON /BLOCK4/ D       , D1      , RP      , VP      , IPTCLMDL
0079      COMMON /BLOCK5/ XL     , YL     , ZL     , INIPX  , INIPY  , INIPZ  , INITREE
0080      COMMON /BLOCK6/ RA     , RA0    , KU     , HX     , HY     , HZ
0081      COMMON /BLOCK7/ E      , ENEW   , EOLD
0082      COMMON /BLOCK8/ RCOFF  , DELR   , DELT
0083      COMMON /BLOCK10/ MOMX  , MOMEY  , MOMZ  , MEANENE
0084      COMMON /BLOCK11/ EX     , EY     , EZ
0085      COMMON /BLOCK12/ NXB   , NYB
0086      COMMON /BLOCK13/ ETHETA , EPHI   , NPSI   , RMAT
0087      COMMON /BLOCK30/ NRAN  , RAN   , IX
0088 C
0089      PARAMETER( NN=1360 , NNS=200000 )
0090      PARAMETER( NRANMX=1000000 , PI=3.141592653589793D0 )
0091 C
0092      REAL*8   KU      , NDENS   , VDENS
0093      REAL*8   RX(NN)  , RY(NN)  , RZ(NN)
0094      REAL*8   NX(NN)  , NY(NN)  , NZ(NN)  , E(NN)
0095      REAL*8   EX(NN)  , EY(NN)  , EZ(NN)
0096      REAL*8   NXB(NN) , NYB(NN)
0097      REAL*8   ETHETA(NN), EPHI(NN), NPSI(NN), RMAT(3,3,NN)
0098      REAL    MOMX(NNS), MOMEY(NNS), MOMZ(NNS), MEANENE(NNS)
0099 C
0100      REAL    RAN(NRANMX)
0101      INTEGER NRAN , IX , NRANCHK
0102 C
0103      REAL*8   RXCAN , RYCAN , RZCAN
0104      REAL*8   NXCAN , NYCAN , NZCAN
0105      REAL*8   EXCAN , EYCAN , EZCAN
0106      REAL*8   RXI , RYI , RZI , NXI , NYI , NZI
0107      REAL*8   EXI , EYI , EZI
0108      REAL*8   RXIJ , RYIJ , RZIJ , RIJ , RIJSQ , RCOFF2
0109      REAL*8   NXBI , NYBI , NXBC , NYBC , NXC , NYC , NZC
0110      REAL*8   ETHETAI , EPHII , NPSII , ETHETAC , EPHIC , NPSIC
0111      REAL*8   RMATC(3,3)
0112      REAL*8   ECAN , C1 , C2 , C3 , C4
0113      REAL*8   CX , CY , CZ
0114      INTEGER MCSMPL , MCSMPLMX , MCSMPL1 , MCSMPL2 , NSMPL
0115      INTEGER INGRAPH , NOPT , DN , DNSMPL
0116      INTEGER ITHETA , IPHAI , IT , IP
0117      INTEGER NANIME , NANMCTR , NOPT1
0118      LOGICAL OVRLAP
0119 C
0120      OPEN(9,FILE='@babal.dat' , STATUS='UNKNOWN')
0121      OPEN(10,FILE='babal1.dat' , STATUS='UNKNOWN')
0122      OPEN(13,FILE='baba41.mgf' , STATUS='UNKNOWN')
0123      OPEN(21,FILE='baba001.dat' , STATUS='UNKNOWN')
0124      OPEN(22,FILE='baba011.dat' , STATUS='UNKNOWN')
0125      OPEN(23,FILE='baba021.dat' , STATUS='UNKNOWN')
0126      OPEN(24,FILE='baba031.dat' , STATUS='UNKNOWN')
0127      OPEN(25,FILE='baba041.dat' , STATUS='UNKNOWN')
0128      OPEN(26,FILE='baba051.dat' , STATUS='UNKNOWN')
0129      OPEN(27,FILE='baba061.dat' , STATUS='UNKNOWN')
0130      OPEN(28,FILE='baba071.dat' , STATUS='UNKNOWN')
0131      OPEN(29,FILE='baba081.dat' , STATUS='UNKNOWN')
0132      OPEN(30,FILE='baba091.dat' , STATUS='UNKNOWN')
0133                                         NP=9
0134 C
0135 C
0136 C
0137 C
0138 C
0139      IPTCLMDL= 1
0140      VDENS = 0.1D0
0141      KU = 10.0D0
0142      RA = 10.0D0
0143      INITREE = 2
0144      N = 288
0145 CCC  INITREE = 1
0146 CCC  N = 324
0147 C
0148      HX = 0.D0
0149      HY = 0.D0
0150      HZ = 1.D0
0151      RP = 3.D0

```

• The given values are written out in @babal, sampled magnetic moment directions are done in baba11, and data for MicroAVS are done in baba41. The particle positions and directions are written out in baba001 – baba091.

--- PARAMETER (1) ---

BE CAREFUL IN SETTING N, INIPX, ..., INITREE !!!

• The number of particles  $N=288$ , volumetric fraction  $\phi_V=0.1$ ,  $\lambda=10$ , and  $\xi=10$ . The size of the simulation region is varied using INITREE.  
• The aspect ratio  $r_p=3$  and the field direction  $\mathbf{h}=(0,0,1)$ .

--- PARAMETER (2) ---

• The cutoff distance  $r_{\text{cuff}}^*=5r_p$ , the volume of the particle VP, and the number density NDENS.

```

0152      D1      = RP
0153      D      = D1 - 1.D0
0154      RCOFF   = 5.D0*D1
0155      VP      = (PI/24.D0)*(6.D0*(RP-1.D0)**2+3.D0*PI*(RP-1.D0)+4.D0)
0156      NDENS   = VDENS/VP
0157      IF( IPTCLMDL .EQ. 1 ) RA0 = RA/RP**3
0158      IF( IPTCLMDL .EQ. 2 ) RA0 = RA/RP
0159 C
0160      DELR    = 0.2D0
0161      DELT    = (5.D0/180.D0 )*PI
0162 C
0163 CCC  MCSMPLMX= 100000
0164      MCSMPLMX= 10000
0165      NGRAPH  = MCSMPLMX/10
0166      NANIME  = MCSMPLMX/200
0167      DN      = 10
0168      DNSMPL  = 10
0169      NOPT    = 20
0170      RCOFF2  = RCOFF**2
0171 C
0172      IX = 0
0173      CALL RANCAL( NRANMX, IX, RAN
0174      NRAN   = 1
0175      NRANCHK = NRANMX - 12*N
0176 C
0177 C
0178 C      ----- INITIAL CONFIGURATION -----
0179 C
0180 C
0181 C
0182 CCC  OPEN(19,FILE='aaba091.dat',STATUS='OLD')
0183 CCC  READ(19,472) N , XL , YL , ZL , D , D1 , RP
0184 CCC  READ(19,473) (RX(I) ,I=1,N), (RY(I) ,I=1,N), (RZ(I) ,I=1,N)
0185 CCC  READ(19,474) (NX(I) ,I=1,N), (NY(I) ,I=1,N), (NZ(I) ,I=1,N),
0186 CCC  & (EX(I) ,I=1,N), (EY(I) ,I=1,N), (EZ(I) ,I=1,N),
0187 CCC  & (NXB(I) ,I=1,N), (NYB(I) ,I=1,N)
0188 CCC  READ(19,473) (ETHETA(I) ,I=1,N), (EPHI(I) ,I=1,N), (NPSI(I) ,I=1,N)
0189 CCC  READ(19,474) ( ( (RMAT(IJ,JJ,I),IJ=1,3 ), JJ=1,3 ), I=1,N )
0190 CCC  CLOSE(19,STATUS='KEEP')
0191 CCC  GOTO 7
0192 C
0193      CALL INITIAL
0194 C
0195      7 IF( XL .LE. YL ) THEN
0196          IF( RCOFF .GE. XL/2.D0 ) THEN
0197              RCOFF = XL/2.D0 - 0.00001D0
0198          END IF
0199      ELSE
0200          IF( RCOFF .GE. YL/2.D0 ) THEN
0201              RCOFF = YL/2.D0 - 0.00001D0
0202          END IF
0203      END IF
0204      RCOFF2 = RCOFF**2
0205      CRAD   = ( XL*YL*ZL/DBLE(N*N) ) / ( 4.D0*PI*DR )
0206 C
0207 C
0208 C      ----- PRINT OUT (1) ---
0209      WRITE(NP,12) IPTCLMDL, N, VDENS, NDENS, RA, RA0, KU, RP,
0210      & D, D1, XL, YL, ZL, RCOFF, DELR, DELT
0211      WRITE(NP,14) MCSMPLMX, NGRAPH, DN, DNSMPL
0212      WRITE(NP,15) HX, HY, HZ
0213 C
0214 C
0215      NANMCTR = 0
0216      NSMPL   = 0
0217 C
0218 C      ----- START OF MONTE CARLO PROGRAM -----
0219 C
0220 C
0221      DO 1000 MCSMPL = 1 , MCSMPLMX
0222 C
0223          DO 400 I=1,N
0224 C
0225 C          RXI = RX(I)
0226

```

• The maximum displacements in the MC method are  $\delta r_{\max}^* = 0.2$  and  $\delta \theta_{\max} = (5/180)\pi$ .  
--- PARAMETER (4) ---

• The total number of MC steps is MCSMPLMX=10000 and sampling is carried out at every DNSMPL steps.  
• The particle positions are written out at every NGRAPH steps. 200 sets of data are written out for making an animation.

--- PARAMETER (5) ---

• A sequence of uniform random numbers is prepared in advance. When necessary, random numbers are taken out from the variable RAN(\*)

--- SET INITIAL CONFIG. ---

• These READ statements are for continuing the sequential simulation using the data saved previously.

• The initial positions and directions of particles are assigned.

• RCOFF has to be taken shorter than  $XL/2$  and  $YL/2$ .

----- POSITION ++++++  
--- OLD ENERGY ---

• The treatment concerning particle *i*.

```

0227 RYI = RY(I)
0228 RZI = RZ(I)
0229 NXI = NX(I)
0230 NYI = NY(I)
0231 NZI = NZ(I)
0232 EXI = EX(I)
0233 EYI = EY(I)
0234 EZI = EZ(I)
0235 ITREE = 0
0236 CALL ENECAL( I, RXI, RYI, RZI, EXI, EYI, EZI, NXI, NYI, NZI,
0237 & RCOFF2, EOLD, OVRLAP, ITREE, J )
0238 C
0239 C
0240 NRAN = NRAN + 1
0241 RXCAN = RX(I) + DELR*( 1.D0 - 2.D0*DBLE(RAN(NRAN)) )
0242 IF( RXCAN .GE. XL ) THEN
0243   RXCAN = RXCAN - XL
0244 ELSE IF( RXCAN .LT. 0.D0 ) THEN
0245   RXCAN = RXCAN + XL
0246 END IF
0247 NRAN = NRAN + 1
0248 RYCAN = RY(I) + DELR*( 1.D0 - 2.D0*DBLE(RAN(NRAN)) )
0249 IF( RYCAN .GE. YL ) THEN
0250   RYCAN = RYCAN - YL
0251 ELSE IF( RYCAN .LT. 0.D0 ) THEN
0252   RYCAN = RYCAN + YL
0253 END IF
0254 NRAN = NRAN + 1
0255 RZCAN = RZ(I) + DELR*( 1.D0 - 2.D0*DBLE(RAN(NRAN)) )
0256 IF( RZCAN .GE. ZL ) THEN
0257   RZCAN = RZCAN - ZL
0258 ELSE IF( RZCAN .LT. 0.D0 ) THEN
0259   RZCAN = RZCAN + ZL
0260 END IF
0261 C
0262 ITREE = 0
0263 CALL ENECAL( I, RXCAN, RYCAN, RZCAN, EXI, EYI, EZI,
0264 & NXI, NYI, NZI, RCOFF2, ECAN, OVRLAP, ITREE, J )
0265 C
0266 IF( OVRLAP ) THEN
0267   GOTO 150
0268 END IF
0269 C
0270 C3 = ECAN - EOLD
0271 IF( C3 .GE. 0.D0 )THEN
0272   NRAN = NRAN + 1
0273   IF( DBLE(RAN(NRAN)) .GE. DEXP(-C3) )THEN
0274     GOTO 150
0275   END IF
0276 END IF
0277 C
0278 C
0279 C
0280 RX(I) = RXCAN
0281 RY(I) = RYCAN
0282 RZ(I) = RZCAN
0283 EOLD = ECAN
0284 E(I) = ECAN
0285 C
0286 C
0287 150 RXI = RX(I)
0288 RYI = RY(I)
0289 RZI = RZ(I)
0290 EXI = EX(I)
0291 EYI = EY(I)
0292 EZI = EZ(I)
0293 NXI = NX(I)
0294 NYI = NY(I)
0295 NZI = NZ(I)
0296 NXBI= NXB(I)
0297 NYBI= NYB(I)
0298 ETHETA1 = ETHETA(I)
0299 EPHII = EPHI(I)
0300 NPSII = NPSI(I)
0301 C

```

• The interaction energies between particle *i* and its interacting particles.

----- (1) CANDIDATE

• Particle *i* is slightly moved according to Eq. (1.52).

• The treatment of the periodic BC.

• The interaction energies are calculated for this new state after the movement of particle *i*.

--- NEW ENERGY ---

----- (2) ENERGY HANDAN

• The adoption of the new state is determined according to the transition probability in Eq. (1.49).

+++++  
CANDIDATES ARE ACCEPTED  
+++++

• The procedure after the acceptance of the new state.

+++++ ROTATION +++++

• The procedure for the rotation.

• The particle direction is described by the zenithal and azimuthal angles ETHETA1 and EPHII. The magnetic moment direction is described by the angle NPSII taken counter clockwise from the X-axis about the Z-axis.

```

0302      NPSIC = NPSII
0303      NXBC = NXBI
0304      NYBC = NYBI
0305 C      NRAN = NRAN + 1
0306      C1 = DELT*DBLE(RAN(NRAN))
0308      NRAN = NRAN + 1
0309      C1 = DSIGN( C1 , DBLE(RAN(NRAN))-0.5 )
0310      ETHETAC = ETHETAC + C1
0311      NRAN = NRAN + 1
0312      C1 = DELT*DBLE(RAN(NRAN))
0313      NRAN = NRAN + 1
0314      C1 = DSIGN( C1 , DBLE(RAN(NRAN))-0.5 )
0315      EPHIC = EPHIC + C1
0316 C      IF( ETHETAC .LT. 0.D0 ) THEN
0317          ETHETAC = DABS( ETHETAC )
0318          EPHIC = EPHIC + PI
0319          IF( EPHIC .GE. 2.D0*PI ) EPHIC = EPHIC - 2.D0*PI
0320          NPSIC = NPSII + PI
0321          IF( NPSIC .GE. 2.D0*PI ) NPSIC = NPSIC - 2.D0*PI
0322          NXBC = -NXBI
0323          NYBC = -NYBI
0325 ELSE IF ( ETHETAC .GT. PI/2.D0 ) THEN
0326     ETHETAC = PI - ETHETAC
0327     EPHIC = EPHIC + PI
0328     IF( EPHIC .GE. 2.D0*PI ) EPHIC = EPHIC - 2.D0*PI
0329     NPSIC = 2.D0*PI - NPSIC
0330 ELSE
0331     IF( EPHIC .GE. 2.D0*PI ) EPHIC = EPHIC - 2.D0*PI
0332     IF( EPHIC .LT. 0.D0 ) EPHIC = EPHIC + 2.D0*PI
0333 END IF
0334 C      --- RMATC(3,3) ---
0335     C11 = DCOS( ETHETAC )
0336     C12 = DSIN( ETHETAC )
0337     C21 = DCOS( EPHIC )
0338     C22 = DSIN( EPHIC )
0339     RMATC(1,1) = C11*C21
0340     RMATC(2,1) = C11*C22
0341     RMATC(3,1) = -C12
0342     RMATC(1,2) = -C22
0343     RMATC(2,2) = C21
0344     RMATC(3,2) = 0.D0
0345     RMATC(1,3) = C12*C21
0346     RMATC(2,3) = C12*C22
0347     RMATC(3,3) = C11
0348 C      EXC = RMATC(1,3)
0349      EYC = RMATC(2,3)
0350      EZC = RMATC(3,3)
0351      NXC = NXBC*RMATC(1,1) + NYBC*RMATC(1,2)
0352      NYC = NXBC*RMATC(2,1) + NYBC*RMATC(2,2)
0353      NZC = NXBC*RMATC(3,1) + NYBC*RMATC(3,2)
0354 C      --- NEW ENERGY ---
0355 ITREE = 0
0356 CALL ENECAL( I , RXI, RYI, RZI, EXC, EYC, EZC,
0357           NXC, NYC, NZC, RCOFF2, ECAN, OVRALP, ITREE, J )
0358 &      IF( OVRALP ) THEN
0359 C      GOTO 250
0360      END IF
0361      IF( OVRALP ) THEN
0362          GOTO 250
0363 C      END IF
0364 C      --- (4) ENERGY HANDAN ---
0365     C3 = ECAN - EOLD
0366     IF( C3 .GE. 0.D0 )THEN
0367         NRAN = NRAN + 1
0368         IF( DBLE(RAN(NRAN)) .GE. DEXP(-C3) )THEN
0369             GOTO 250
0370             END IF
0371             END IF
0372 C      ++++++ CANDIDATES ARE ACCEPTED ++++++
0373 C      ++++++ CANDIDATES ARE ACCEPTED ++++++
0374 C      EX(I) = EXC
0375      EY(I) = EYC

```

• The zenithal and azimuthal angles are slightly changed using random numbers to change the particle direction; the new angles are saved in ETHETAC and EPHIC.

• The treatment shown in Section 4.2.7.

• The rotational matrix  $R^{-1}$  (RMATC) is evaluated for the particle direction.

• The particle direction  $e$  and the magnetic moment direction  $n$  are calculated from Eq. (4.46).

• The interaction energies are calculated for the new direction of particle  $i$ .

• The adoption of the new state is determined according to the transition probability in Eq. (1.49).

• The procedure after the acceptance of the new state.

```

0377      EZ(I) = EZC
0378      NX(I) = NXC
0379      NY(I) = NYC
0380      NZ(I) = NZC
0381      NXB(I) = NXBC
0382      NYB(I) = NYBC
0383      ETHETA(I) = ETHETAC
0384      EPHI(I) = EPHIC
0385      NPSI(I) = NPSIC
0386      DO 110 II=1,3
0387      DO 110 JJ=1,3
0388      RMAT(II,JJ,I) = RMATC(II,JJ)
0389 110  CONTINUE
0390      EOLD = ECAN
0391      E(I) = ECAN
0392 C
0393 C      ++++++MOMENT+++++
0394 250  RXI = RX(I)
0395  RYI = RY(I)
0396  RZI = RZ(I)
0397  NXI = NX(I)
0398  NYI = NY(I)
0399  NZI = NZ(I)
0400  EXI = EX(I)
0401  EYI = EY(I)
0402  EZI = EZ(I)
0403  NXBI = NXB(I)
0404  NYBI = NYB(I)
0405  ETHETAI = ETHETA(I)
0406  EPHII = EPHI(I)
0407  NPSII = NPSI(I)
0408 C
0409  NRAN = NRAN + 1
0410  C1 = DELT*DBLE(RAN(NRAN))
0411  NRAN = NRAN + 1
0412  C1 = DSIGN( C1 , DBLE(RAN(NRAN))-0.5 )
0413  NPSIC = NPSII + C1
0414 C
0415  IF( NPSIC .GE. 2.0D+0 ) THEN
0416    NPSIC = NPSIC - 2.0D+0
0417  ELSE IF ( NPSIC .LT. 0.D0 ) THEN
0418    NPSIC = NPSIC + 2.0D+0
0419  END IF
0420 C
0421  NXBC = DCOS( NPSIC )
0422  NYBC = DSIN( NPSIC )
0423  NXC = RMAT(1,1,I)*NXBC + RMAT(1,2,I)*NYBC
0424  NYC = RMAT(2,1,I)*NXBC + RMAT(2,2,I)*NYBC
0425  NZC = RMAT(3,1,I)*NXBC + RMAT(3,2,I)*NYBC
0426 C
0427 C      ITREE = 1
0428  CALL ENECAL( I , RXI, RYI, RZI, EXI, EYI, EZI,
0429                NXC, NYC, NZC, RCOFF2, ECAN, OVRLAP, ITREE, J )
0430 &
0431 C
0432 CCC  IF( OVRLAP ) THEN
0433 CCC    GOTO 400
0434 CCC  END IF
0435 C
0436 C
0437  C3 = ECAN - EOLD
0438  IF( C3 .GE. 0.D0 )THEN
0439    NRAN = NRAN + 1
0440    IF( DBLE(RAN(NRAN)) .GE. DEXP(-C3) )THEN
0441      GOTO 400
0442    END IF
0443  END IF
0444 C
0445 C
0446 C      NX(I) = NXC
0447  NY(I) = NYC
0448  NZ(I) = NZC
0449  NXB(I) = NXBC
0450  NYB(I) = NYBC
0451

```

• The particle direction, magnetic moment direction, and zenithal and azimuthal angles are renewed.  
• The rotational matrix is renewed.  
• The interaction energy of particle *i* is saved in *E*(*i*).

• The attempt for changing the magnetic moment direction.

• The particle direction is described by the zenithal and azimuthal angles *ETHETAI* and *EPHII*. The magnetic moment direction is described by the angle *NPSII*.

----- (5) CANDIDATE

• The magnetic moment direction is slightly changed using random numbers; this new angle is saved in *NPSIC*.

• The new magnetic moment direction is evaluated from Eq. (4.46). The rotational matrix is unchanged, still valid.

•  $\mathbf{n}^b = (\text{NXBC}, \text{NYBC}, 0)$  and  
 $\mathbf{n} = \mathbf{R}^{-1} \bullet \mathbf{n}^b$ .

--- NEW ENERGY ---

• The interaction energies are calculated for this new state of particle *i*.

----- (6) ENERGY HANDAN -----

• The adoption of the new state is determined according to the transition probability in Eq. (1.49).

++++++  
CANDIDATES ARE ACCEPTED  
++++++

• The procedure after the acceptance of the new state.

```

0452           NPSI(I) = NPSIC
0453           E(I)     = ECAN
0454 C
0455 C
0456 400    CONTINUE
0457 C
0458 C
0459 C
0460 C           ----- MOMENT AND ENERGY OF SYSTEM -----
0461 IF( MOD(MCSMPL,DNSMPL) .EQ. 0 ) THEN
0462   NSMPL = NSMPL + 1
0463   C1 = 0.D0
0464   C2 = 0.D0
0465   C3 = 0.D0
0466   C4 = 0.D0
0467   DO 420 J=1,N
0468     C1 = C1 + NX(J)
0469     C2 = C2 + NY(J)
0470     C3 = C3 + NZ(J)
0471     C4 = C4 + E(J)
0472   420    CONTINUE
0473   MOMX(NSMPL) = REAL(C1)/REAL(N)
0474   MOMY(NSMPL) = REAL(C2)/REAL(N)
0475   MOMZ(NSMPL) = REAL(C3)/REAL(N)
0476   MEANENE(NSMPL) = REAL( C4-KU*(C1*XH+C2*HY+C3*HZ) )/REAL(2*N)
0477 END IF
0478 C
0479 IF( MOD(MCSMPL,NGRAPH) .EQ. 0 ) THEN
0480   NOPT = NOPT + 1
0481   WRITE(NOPT,472) N , XL , YL , ZL , D , D1 , RP
0482   WRITE(NOPT,473) (RX(I),I=1,N),(RY(I),I=1,N),(RZ(I),I=1,N),
0483   WRITE(NOPT,474) (NX(I),I=1,N),(NY(I),I=1,N),(NZ(I),I=1,N),
0484   & (EX(I),I=1,N),(EY(I),I=1,N),(EZ(I),I=1,N),
0485   & (NKB(I),I=1,N),(NYB(I),I=1,N)
0486   WRITE(NOPT,473) (ETHETA(I),I=1,N), (EPHI(I),I=1,N),
0487   & (NPSI(I),I=1,N)
0488   & WRITE(NOPT,474) ( ( (RMAT(II,JJ,I),II=1,3), JJ=1,3 ),
0489   &                                I=1,N )
0490   & CLOSE(NOPT,STATUS='KEEP')
0491 END IF
0492 C
0493 C
0494 IF( MOD(MCSMPL,NANIME) .EQ. 0 ) THEN
0495   NANMCTR = NANMCTR + 1
0496   NOPT1 = 13
0497   CALL ANIMEDAT( NOPT1, NANMCTR, MCSMPLMX, NANIME, N )
0498 END IF
0499 C
0500 C           --- CHECK OF THE SUM OF RANDOM NUMBERS ---
0501 C
0502 IF( NRAN .GE. NRANCHK )THEN
0503   CALL RANCAL( NRANMX, IX, RAN )
0504   NRAN = 1
0505 END IF
0506 C
0507 IF( MOD(MCSMPL,DN) .EQ. 0 ) THEN
0508   DO 490 I=1,N
0509     C1 = DSQRT( NX(I)**2 + NY(I)**2 + NZ(I)**2 )
0510     NX(I) = NX(I)/C1
0511     NY(I) = NY(I)/C1
0512     NZ(I) = NZ(I)/C1
0513     C1 = DSQRT( EX(I)**2 + EY(I)**2 + EZ(I)**2 )
0514     EX(I) = EX(I)/C1
0515     EY(I) = EY(I)/C1
0516     EZ(I) = EZ(I)/C1
0517     C1 = DSQRT( NXB(I)**2 + NYB(I)**2 )
0518     NXB(I) = NXB(I)/C1
0519     NYB(I) = NYB(I)/C1
0520   490    CONTINUE
0521 END IF
0522 C
0523 C
0524 1000 CONTINUE
0525 C

```

• To check the system convergence afterward, the average of the particle direction vector is calculated.

• The data of the particle positions and directions are written out at every NGRAPH MC steps for the postprocessing analysis.

• The data of the particle positions and directions are written out at every NANIME MC steps for making an animation.

• The number of the used random numbers is checked. If over NRANCHK, a uniform random number sequence is renewed.

--- NORMALIZATION ---

• Each unit vector is modified at every DN steps so as to yield unit length.

```

0526 C ----- END OF MONTE CARLO PROGRAM -----
0527 C -----
0528 C -----
0529 C -----
0530 C ----- --- PRINT OUT (2) ---
0531      WRITE(NP,1002)
0532      MCSMPL1 = 1
0533 CCC MCSMPL2 = MCSMPLMX
0534 MCSMPL2 = NSMPL
0535 CALL PRNTDATA( MCSMPL1 , MCSMPL2 , NP )
0536 WRITE(NP,1004) MCSMPL1 , MCSMPL2
0537 C
0538 C ----- DATA OUTPUT FOR GRAPHICS (3) ---
0539 WRITE(10,1012) IPTCLMDL, N, VDENS, NDENS, RA, RA0, KU
0540 WRITE(10,1014) RP, D, D1, XL, YL, ZL, RCOFF
0541 WRITE(10,1016) DELR, DELT
0542 WRITE(10,1017) HX, HY, HZ
0543 WRITE(10,1018) MCSMPLMX, NGRAPH, DN, DNSMPL
0544 WRITE(10,1022) MCSMPL1, MCSMPL2
0545 WRITE(10,1024) ( MEANENE(I), I=MCSMPL1, MCSMPL2)
0546 & ,( MOMX(I), I=MCSMPL1, MCSMPL2)
0547 & ,( MOMY(I), I=MCSMPL1, MCSMPL2)
0548 C
0549                               CLOSE(9, STATUS='KEEP')
0550                               CLOSE(10, STATUS='KEEP')
0551                               CLOSE(13, STATUS='KEEP')
0552 C ----- FORMAT -----
0553 12 FORMAT(1H ,-----'
0554 & /1H ,'-          MONTE CARLO METHOD          -'
0555 & /1H ,-----'
0556 & //1H , 'IPTCLMDL=' ,I4
0557 & /1H , 'N=' ,I4, 2X, 'VDENS=' ,F4.2, 2X , 'NDENS=' ,F7.4
0558 & /1H , 'RA=' ,F6.2, 2X, 'RA0=' ,F9.2, 2X , 'KU=' ,F6.2, 2X ,
0559 & 'RP=' , F7.4
0560 & /1H , 'D=' ,F5.2, 2X , 'D1=' ,F5.2, 2X,
0561 & 'XL=' ,F6.2, 2X, 'YL=' ,F6.2, 2X, 'ZL=' ,F6.2, 2X,
0562 & 'RCOFF=' ,F6.2
0563 & /1H , 'DELR=' ,F7.4, 2X , 'DELT=' ,F7.4)
0564 14 FORMAT( 1H , 'MCSMPLMX=' ,I8, 2X, 'NGRAPH=' ,I8, 2X, 'DN=' ,I4, 2X,
0565 & 'DNSMPL=' ,I4/)
0566 15 FORMAT( 1H , '(HX,HY,HZ)=' , 3F5.1 )
0567 472 FORMAT( I5 , 3F9.4 , 3F8.4 )
0568 473 FORMAT( (5F16.10) )
0569 474 FORMAT( (11F7.3) )
0570 1002 FORMAT(1H , '+++++++' )
0571 & /1H , ' WITHOUT CLUSTER MOVEMENT '
0572 & /1H , '+++++++' )
0573 1004 FORMAT(//1H ,18X, 'START OF MC SAMPLING STEP=' ,I9
0574 & /1H ,18X, 'END OF MC SAMPLING STEP=' ,I9)
0575 1012 FORMAT( I2 , I5 , 2F9.4 , 4F9.3 )
0576 1014 FORMAT( 3F7.2 , 3F9.3 , F9.3 )
0577 1016 FORMAT( 2F9.5 )
0578 1017 FORMAT( 3F7.2 )
0579 1018 FORMAT( 6I9 )
0580 1020 FORMAT( 2F7.3 , I4 , F7.3 , E12.4 )
0581 1022 FORMAT( 2I9 )
0582 1024 FORMAT( (7E11.4) )
0583 1367 FORMAT( 3I9, 2F9.4 )
0584 1368 FORMAT( I6 , F8.4 , 3F10.5 )
0585 1392 FORMAT( 2I9 )
0586 1394 FORMAT( (7E11.4) )
0587 1501 FORMAT( I8 )
0588 1502 FORMAT( (10F8.3) )
0589 1511 FORMAT( I8 )
0590 1513 FORMAT( (10I8) )
0591 1515 FORMAT( (10F8.3) )
0592 1521 FORMAT( I8 )
0593 1523 FORMAT( 2I8 )
0594 1525 FORMAT( (10F8.3) )
0595 1541 FORMAT( I8 )
0596 1543 FORMAT( (10I8) )
0597 1545 FORMAT( (10F8.3) )

```

STOP  
END

```

0600 C***** SUBROUTINE PRNTDATA *****
0601 C***** SUBROUTINE PRNTDATA( MCSST, MCSMX, NP )
0602 C***** IMPLICIT REAL*8 ( A-H,O-Z ), INTEGER ( I-N )
0603 C
0604 C**** SUB PRNTDATA *****
0605 SUBROUTINE PRNTDATA( MCSST, MCSMX, NP )
0606 C
0607 IMPLICIT REAL*8 ( A-H,O-Z ), INTEGER ( I-N )
0608 C
0609 COMMON /BLOCK10/ MOMX , MOMEY , MOMZ , MEANENE
0610 C
0611 PARAMETER( NN=1360 , NNS=200000 )
0612 PARAMETER( NRANMX=1000000 , PI=3.141592653589793D0 )
0613 C
0614 INTEGER MCSST , MCSMX , NP
0615 REAL MOMX(NNS) , MOMEY(NNS) , MOMZ(NNS) , MEANENE(NNS)
0616 C
0617 REAL AMOMX(10) , AMOMY(10) , AMOMZ(10) , AMEANENE(10) , CO
0618 INTEGER IC , IMC(0:10) , JS , JE
0619 C
0620 C ----- KEIKA INSATU -----
0621 IC = ( MCSMX-MCSST+1 )/50
0622 DO 20 I= MCSST-1+IC , MCSMX , IC
0623 WRITE(NP,10) I, MOMX(I), MOMEY(I), MOMZ(I), MEANENE(I)
0624 20 CONTINUE
0625 C ----- MONTE CARLO STEP HEIKIN -----
0626 IC = ( MCSMX-MCSST+1 )/10
0627 DO 30 I=0,10
0628 IMC(I) = MCSST - 1 + IC*I
0629 IF( I .EQ. 10 ) IMC(I) = MCSMX
0630 30 CONTINUE
0631 C
0632 C
0633 DO 35 I=1,10
0634 AMOMX(I) = 0.
0635 AMOMY(I) = 0.
0636 AMOMZ(I) = 0.
0637 AMEANENE(I) = 0.
0638 35 CONTINUE
0639 C
0640 DO 50 I=1,10
0641 JS = IMC(I-1) + 1
0642 JE = IMC(I)
0643 DO 40 J=JS,JE
0644 AMOMX(I) = AMOMX(I) + MOMX(J)
0645 AMOMY(I) = AMOMY(I) + MOMEY(J)
0646 AMOMZ(I) = AMOMZ(I) + MOMZ(J)
0647 AMEANENE(I) = AMEANENE(I) + MEANENE(J)
0648 40 CONTINUE
0649 50 CONTINUE
0650 C
0651 DO 70 I=1,10
0652 C0 = REAL( IMC(I)-IMC(I-1) )
0653 AMOMX(I) = AMOMX(I) /C0
0654 AMOMY(I) = AMOMY(I) /C0
0655 AMOMZ(I) = AMOMZ(I) /C0
0656 AMEANENE(I) = AMEANENE(I)/C0
0657 70 CONTINUE
0658 C ----- STEP HEIKIN INSATU -----
0659 WRITE(NP,75)
0660 DO 90 I=1,10
0661 WRITE(NP,80) I,IMC(I-1)+1,IMC(I),AMOMX(I),AMOMY(I),AMOMZ(I),
0662 & AMEANENE(I)
0663 90 CONTINUE
0664 C
0665 10 FORMAT(1H , 'MCSMPL=',I8, 2X , 'MOMENT(X)=',F7.4, 2X ,
0666 & 'MOMENT(Y)=',F7.4, 2X , 'MOMENT(Z)=',F7.4
0667 & /1H , 53X , 'MEAN ENERGY=',E12.5)
0668 75 FORMAT(/1H , '-----'
0669 & /1H , ' MONTE CARLO HEIKIN '
0670 & /)
0671 80 FORMAT(1H , 'I=',I2, 2X , 'SMPLMN=',I8, 2X , 'SMPLMX=',I8
0672 & /1H ,15X , 'MOMENT(X)=',F7.4, 2X ,
0673 & 'MOMENT(Y)=',F7.4, 2X , 'MOMENT(Z)=',F7.4
0674 & /1H ,53X , 'MEAN ENERGY=',E12.5/)

```

• The total MC steps are equally divided into 50 blocks, and the end value of each block is written out.

• The total MC steps are equally divided into 10 blocks, and the subaverages are calculated for each block.

```

0675          RETURN
0676          END
0677 C**** SUB ANIMEDAT *****
0678      SUBROUTINE ANIMEDAT( NOPT1, NANMCTR, MCSMPLMX, NANIME, N )
0679 C
0680      IMPLICIT REAL*8 ( A-H,O-Z ), INTEGER ( I-N )
0681 C
0682      COMMON /BLOCK1/   RX    , RY    , RZ
0683      COMMON /BLOCK2/   NX    , NY    , NZ
0684      COMMON /BLOCK4/   D     , D1    , RP    , VP    , IPTCLMDL
0685      COMMON /BLOCK5/   XL    , YL    , ZL    , INIPX , INIPY , INIPZ , INITREE
0686      COMMON /BLOCK11/  EX    , EY    , EZ
0687 C
0688      PARAMETER( NN=1360 , PI=3.141592653589793D0 )
0689 C
0690      REAL*8    RX(NN) , RY(NN) , RZ(NN)
0691      REAL*8    NX(NN) , NY(NN) , NZ(NN)
0692      REAL*8    EX(NN) , EY(NN) , EZ(NN)
0693      REAL*8    D02   , D102  , CX1  , CY1  , CZ1  , CX2  , CY2  , CZ2
0694      REAL*8    CNX(50) , CNY(50) , CNZ(50)
0695 C
0696      D02     = D/2.D0
0697      D102    = D1/2.D0
0698 C
0699      IF( NANMCTR .EQ. 1 ) THEN
0700         WRITE(NOPT1,181) (MCSMPLMX/NANIME)
0701      END IF
0702 C
0703      IF( (NANMCTR.GE.1) .AND. (NANMCTR.LE.9) ) THEN
0704         WRITE(NOPT1,183) NANMCTR
0705      ELSE IF( (NANMCTR.GE.10) .AND. (NANMCTR.LE.99) ) THEN
0706         WRITE(NOPT1,184) NANMCTR
0707      ELSE IF( (NANMCTR.GE.100) .AND. (NANMCTR.LE.999) ) THEN
0708         WRITE(NOPT1,185) NANMCTR
0709      ELSE IF( (NANMCTR.GE.1000) .AND. (NANMCTR.LE.9999) ) THEN
0710         WRITE(NOPT1,186) NANMCTR
0711      END IF
0712 C
0713 C ----- CYLINDER (1) ---
0714      WRITE(NOPT1,211) N
0715      DO 250 I=1,N
0716         CX1 = RX(I) - EX(I)*0.5D0
0717         CY1 = RY(I) - EY(I)*0.5D0
0718         CZ1 = RZ(I) - EZ(I)*0.5D0
0719         CX2 = RX(I) + EX(I)*0.5D0
0720         CY2 = RY(I) + EY(I)*0.5D0
0721         CZ2 = RZ(I) + EZ(I)*0.5D0
0722         WRITE(NOPT1,248) CX1,CY1,CZ1, CX2,CY2,CZ2, D02, 1.0, 0.0, 0.0
0723      250 CONTINUE
0724 C
0725 C ----- SPHERE (1) ---
0726 C
0727      WRITE(NOPT1,311) N*16
0728      DO 350 I=1,N
0729         CNX(1) = NX(I)
0730         CNY(1) = NY(I)
0731         CNZ(1) = NZ(I)
0732 C
0733         C1X = EY(I)*NZ(I) - EZ(I)*NY(I)
0734         C1Y = EZ(I)*NX(I) - EX(I)*NZ(I)
0735         C1Z = EX(I)*NY(I) - EY(I)*NX(I)
0736         C1 = DSQRT( C1X**2 + C1Y**2 + C1Z**2 )
0737         CNX(2) = C1X/C1
0738         CNY(2) = C1Y/C1
0739         CNZ(2) = C1Z/C1
0740         CNX(3) = - CNX(2)
0741         CNY(3) = - CNY(2)
0742         CNZ(3) = - CNZ(2)
0743 C
0744         CNX(4) = ( CNX(1) + CNX(2) )/1.4142D0
0745         CNY(4) = ( CNY(1) + CNY(2) )/1.4142D0
0746         CNZ(4) = ( CNZ(1) + CNZ(2) )/1.4142D0
0747         CNX(5) = ( CNX(1) + CNX(3) )/1.4142D0
0748         CNY(5) = ( CNY(1) + CNY(3) )/1.4142D0
0749         CNZ(5) = ( CNZ(1) + CNZ(3) )/1.4142D0

```

• A subroutine for writing out the data, which can be directly used for making an animation based on MicroAVS.

• MicroAVS can make a visualization or animation by reading the data file baba41.mgf.

• Drawing of the cylindrical part.

• Drawing of the disk-like particle in Figure 4.12 by having the short cylinder surrounded by numerous spheres.

```

0750 C
0751      CNY(6) = ( CNX(1) + CNX(4) )/1.8478D0
0752      CNY(6) = ( CNY(1) + CNY(4) )/1.8478D0
0753      CNZ(6) = ( CNZ(1) + CNZ(4) )/1.8478D0
0754      CNX(7) = ( CNX(2) + CNX(4) )/1.8478D0
0755      CNY(7) = ( CNY(2) + CNY(4) )/1.8478D0
0756      CNZ(7) = ( CNZ(2) + CNZ(4) )/1.8478D0
0757      CNX(8) = ( CNX(1) + CNX(5) )/1.8478D0
0758      CNY(8) = ( CNY(1) + CNY(5) )/1.8478D0
0759      CNZ(8) = ( CNZ(1) + CNZ(5) )/1.8478D0
0760      CNX(9) = ( CNX(3) + CNX(5) )/1.8478D0
0761      CNY(9) = ( CNY(3) + CNY(5) )/1.8478D0
0762      CNZ(9) = ( CNZ(3) + CNZ(5) )/1.8478D0
0763 C
0764      CNX(10) = - CNX(1)
0765      CNY(10) = - CNY(1)
0766      CNZ(10) = - CNZ(1)
0767      CNX(11) = - CNX(4)
0768      CNY(11) = - CNY(4)
0769      CNZ(11) = - CNZ(4)
0770      CNX(12) = - CNX(5)
0771      CNY(12) = - CNY(5)
0772      CNZ(12) = - CNZ(5)
0773      CNX(13) = - CNX(6)
0774      CNY(13) = - CNY(6)
0775      CNZ(13) = - CNZ(6)
0776      CNX(14) = - CNX(7)
0777      CNY(14) = - CNY(7)
0778      CNZ(14) = - CNZ(7)
0779      CNX(15) = - CNX(8)
0780      CNY(15) = - CNY(8)
0781      CNZ(15) = - CNZ(8)
0782      CNX(16) = - CNX(9)
0783      CNY(16) = - CNY(9)
0784      CNZ(16) = - CNZ(9)
0785 C
0786      DO 340 J=1,16
0787      CX1 = RX(I) + CNX(J)*D02
0788      CY1 = RY(I) + CNY(J)*D02
0789      CZ1 = RZ(I) + CNZ(J)*D02
0790      WRITE(NOPT1,348) CX1, CY1, CZ1, 0.499 , 1.0, 0.2, 0.2
0791      340 CONTINUE
0792 C
0793      350 CONTINUE
0794 C
0795 C ----- SPHERE (2) ---
0796 C ----- FOR MAG MOMENT ---
0797      WRITE(NOPT1,311) N
0798      DO 450 I=1,N
0799      CX1 = RX(I) + NX(I)*D102
0800      CY1 = RY(I) + NY(I)*D102
0801      CZ1 = RZ(I) + NZ(I)*D102
0802      WRITE(NOPT1,348) CX1, CY1, CZ1, 0.12 , 0.0, 0.8, 1.0
0803      450 CONTINUE
0804 C
0805 C ----- SIM.REGEON LINES (3) ---
0806      WRITE(NOPT1,648) 17
0807      WRITE(NOPT1,649) 0. , 0. , 0.
0808      WRITE(NOPT1,649) XL , 0. , 0.
0809      WRITE(NOPT1,649) XL , YL , 0.
0810      WRITE(NOPT1,649) 0. , YL , 0.
0811      WRITE(NOPT1,649) 0. , 0. , 0.
0812      WRITE(NOPT1,649) 0. , 0. , ZL
0813      WRITE(NOPT1,649) XL , 0. , ZL
0814      WRITE(NOPT1,649) XL , YL , ZL
0815      WRITE(NOPT1,649) 0. , YL , ZL
0816      WRITE(NOPT1,649) 0. , 0. , ZL
0817      WRITE(NOPT1,649) 0. , 0. , 0.
0818      WRITE(NOPT1,649) 0. , YL , 0.
0819      WRITE(NOPT1,649) 0. , YL , ZL
0820      WRITE(NOPT1,649) XL , YL , ZL
0821      WRITE(NOPT1,649) XL , YL , 0.
0822      WRITE(NOPT1,649) XL , 0. , 0.
0823      WRITE(NOPT1,649) XL , 0. , ZL
0824 C

```

• The magnetic moment direction is described by adding a small sphere to the surface of the torus part.

• Drawing the frame of the simulation box.

```

0825 C ----- FORMAT -----
0826 181 FORMAT('# Micro AVS Geom:2.00'
0827   &      '# Animation of MC simulation results'
0828   &      /I4)
0829 183 FORMAT('step',I1)
0830 184 FORMAT('step',I2)
0831 185 FORMAT('step',I3)
0832 186 FORMAT('step',I4)
0833 211 FORMAT('column'/'cylinder'/'dvertex_and_color'/'32'/I7 )
0834 248 FORMAT( 6F10.3 , F6.2 , 3F4.1)
0835 311 FORMAT( 'sphere'/'sphere_sample'/'color'/I7 )
0836 348 FORMAT( 3F10.3 , F6.2 , 3F5.2 )
0837 648 FORMAT( 'polyline'/'pline_sample'/'vertex'/I3 )
0838 649 FORMAT( 3F10.3 )
0839
0840
0841 C**** SUB INITIAL ****
0842      SUBROUTINE INITIAL
0843 C
0844      IMPLICIT REAL*8 (A-H,O-Z), INTEGER (I-N)
0845 C
0846      COMMON /BLOCK1/ RX , RY , RZ
0847      COMMON /BLOCK2/ NX , NY , NZ
0848      COMMON /BLOCK3/ N , NDENS, VDENS
0849      COMMON /BLOCK4/ D , D1 , RP , VP , IPTCLMDL
0850      COMMON /BLOCK5/ XL , YL , ZL , INIPX , INIPY , INIPZ , INITREE
0851      COMMON /BLOCK11/ EX , EY , EZ
0852      COMMON /BLOCK12/ NXB , NYB
0853      COMMON /BLOCK13/ ETHETA , EPHI , NPSI , RMAT
0854 C
0855      PARAMETER( NN=1360 , PI=3.141592653589793D0 )
0856 C
0857      REAL*8 NDENS
0858      REAL*8 RX(NN) , RY(NN) , RZ(NN) , NX(NN) , NY(NN) , NZ(NN)
0859      REAL*8 EX(NN) , EY(NN) , EZ(NN)
0860      REAL*8 NXB(NN) , NYB(NN)
0861      REAL*8 ETHETA(NN) , EPHI(NN) , NPSI(NN) , RMAT(3,3,NN)
0862 C
0863      INTEGER PTCL , ICNTR
0864      REAL*8 XLUNT , YLUNT , ZLUNT , RAN1 , RAN2 , RAN3
0865      REAL*8 VDENSMX , CRATIO , C0 , C1 , C2 , C3
0866 C
0867      IF( INITREE .EQ. 1 ) THEN
0868          INIPX = 3
0869          INIPY = 9
0870          INIPZ = 12
0871          N = 324
0872      ELSE IF( INITREE .EQ. 2 ) THEN
0873          INIPX = 4
0874          INIPY = 12
0875          INIPZ = 6
0876          N = 288
0877      ELSE
0878          WRITE(6,*)
0879          STOP
0880      END IF
0881 C
0882 C
0883      VMN = DBLE( INIPX*INIPY*INIPZ )*RP**2
0884      CRATIO = ( ( DBLE(N)*VP )/( VMN*VDENS ) )**(.1/3.)
0885      XLUNT = RP
0886      YLUNT = 1.D0
0887      ZLUNT = RP
0888      XLUNT = XLUNT*CRATIO
0889      YLUNT = YLUNT*CRATIO
0890      ZLUNT = ZLUNT*CRATIO
0891      XL = XLUNT*DBLE( INIPX )
0892      YL = YLUNT*DBLE( INIPY )
0893      ZL = ZLUNT*DBLE( INIPZ )
0894 C

```

• A subroutine for setting the initial position and direction of each particle.

• (INIPX, INIPY, INIPZ) particles are placed in the x-, y-, and z-directions, respectively.

• The volumetric fraction  $\phi_V$  satisfies  $\phi_V = V_p \times N(\alpha^3 \times V_{mn})$ , so that  $\alpha$  can be obtained as  $\alpha = (V_p \times N(\phi_V \times V_{mn}))^{1/3}$ , in which  $VMN = V_{mn}$  and  $CRATIO = \alpha$ .

• As shown in Figure 2.5, VMN is the minimum volume for a contact arrangement of the particles.

----- POSITION -----

```

0895      RAN1 = DSQRT( 2.D0 )
0896      RAN2 = DSQRT( 7.D0 )
0897      RAN3 = DSQRT( 11.D0 )
0898      C0 = 1.D-4
0899      PTCL = 0
0900      DO 10 K=0, INIPZ-1
0901      DO 10 J=0, INIPY-1
0902      DO 10 I=0, INIPX-1
0903      PTCL = PTCL + 1
0904      C1 = RAN1*DBLE(PTCL)
0905      C1 = C1 - DINT(C1)
0906      C1 = C1 - 0.5D0
0907      C2 = RAN2*DBLE(PTCL)
0908      C2 = C2 - DINT(C2)
0909      C2 = C2 - 0.5D0
0910      C3 = RAN3*DBLE(PTCL)
0911      C3 = C3 - DINT(C3)
0912      C3 = C3 - 0.5D0
0913      RX(PTCL) = DBLE(I)*XLUNT + C1*C0 + C0
0914      RY(PTCL) = DBLE(J)*YLUNT + C2*C0 + C0
0915      RZ(PTCL) = DBLE(K)*ZLUNT + C3*C0 + C0
0916 10 CONTINUE
0917      N = PTCL
0918 C      RAN1 = DSQRT( 2.D0 )
0919      RAN2 = DSQRT( 3.D0 )
0920      DO 80 I=1,N
0921      C1 = PI/2.D0
0922      C2 = PI/2.D0
0923      EX(I) = DSIN(C1)*DCOS(C2)
0924      EY(I) = DSIN(C1)*DSIN(C2)
0925      EZ(I) = DCOS(C1)
0926
0927      ETHETA(I) = C1
0928      EPHI(I) = C2
0929      RMAT(1,1,I) = DCOS(C1)*DCOS(C2)
0930      RMAT(2,1,I) = DCOS(C1)*DSIN(C2)
0931      RMAT(3,1,I) = -DSIN(C1)
0932      RMAT(1,2,I) = -DSIN(C2)
0933      RMAT(2,2,I) = DCOS(C2)
0934      RMAT(3,2,I) = 0.D0
0935      RMAT(1,3,I) = DSIN(C1)*DCOS(C2)
0936      RMAT(2,3,I) = DSIN(C1)*DSIN(C2)
0937      RMAT(3,3,I) = DCOS(C1)
0938
0939 80 CONTINUE
0940 C      RAN1 = DSQRT( 2.D0 )
0941      DO 90 I=1,N
0942      C1 = RAN1*DBLE(I)
0943      C1 = C1 - DINT(C1)
0944      NPSI(I) = 2.D0*PI*C1
0945      NXB(I) = DCOS(NPSI(I))
0946      NYB(I) = DSIN(NPSI(I))
0947      NX(I) = RMAT(1,1,I)*NXB(I) + RMAT(1,2,I)*NYB(I)
0948      NY(I) = RMAT(2,1,I)*NXB(I) + RMAT(2,2,I)*NYB(I)
0949      NZ(I) = RMAT(3,1,I)*NXB(I) + RMAT(3,2,I)*NYB(I)
0950
0951 90 CONTINUE
0952
0953
0954 C**** SUB ENECAL *****
0955      SUBROUTINE ENECAL( I, RXI, RYI, RZI, EXI, EYI, EZI, NXI, NYI,
0956      &                      NZI, RCOFF2, ECAN, OVRALP, ISTREET, JPTCL0 )
0957 C
0958      IMPLICIT REAL*8 (A-H,O-Z), INTEGER (I-N)
0959 C
0960      COMMON /BLOCK1/ RX    , RY    , RZ
0961      COMMON /BLOCK2/ NX    , NY    , NZ
0962      COMMON /BLOCK3/ N     , NDENS, VDENS
0963      COMMON /BLOCK4/ D     , D1    , RP    , VP    , IPTCLMDL
0964      COMMON /BLOCK5/ XL    , YL    , ZL    , INIPX , INIPY , INIPZ , INITREE
0965      COMMON /BLOCK6/ RA    , RAO   , KU    , HX    , HY    , HZ
0966      COMMON /BLOCK7/ E     , ENEW  , EOLD
0967      COMMON /BLOCK8/ RCOFF, DELR  , DELT
0968      COMMON /BLOCK11/ EX   , EY    , EZ
0969      COMMON /BLOCK12/ NXB  , NYB

```

• (XLUNT, YLUNT, ZLUNT) are the distances between the neighboring particles in each axis direction.

• RAN1, RAN2, and RAN3 are quasi-random numbers.  
• (INIPX, INIPY, INIPZ) particles are placed in each direction.  
• Each particle is moved in parallel by the distance C0 to remove subtle situations at outer boundary surfaces. Also, to remove the regularity of the initial configuration, each particle is moved randomly by (C1\*C0, C2\*C0, C3\*C0) in each direction.

----- DIRECTION -----

• All the particles are set so as to point in the y-direction.

• The rotational matrix  $R^{-1}$  (=RMAT) can be evaluated as a transpose matrix in Eq. (4.43) using the particle direction data.

----- MOMENT -----

• The magnetic moment direction is randomly assigned using quasi-random numbers.

• A subroutine for calculating the interaction energies between particles.

RETURN  
END

```

0970 C      COMMON /BLOCK13/ ETHETA , EPHI , NPSI , RMAT
0971 C      PARAMETER( NN=1360 , PI=3.141592653589793D0 )
0972 C
0973 C      REAL*8   NDENS , KU
0974 C      REAL*8   RX(NN) , RY(NN) , RZ(NN)
0975 C      REAL*8   NX(NN) , NY(NN) , NZ(NN) , E(NN)
0976 C      REAL*8   EX(NN) , EY(NN) , EZ(NN)
0977 C      REAL*8   NXB(NN) , NYB(NN)
0978 C      REAL*8   ETHETA(NN), EPHI(NN) , NPSI(NN) , RMAT(3,3,NN)
0979 C      LOGICAL  OVLAP
0980 C
0981 C      REAL*8   RXI , RYI , RZI , RXJ , RYJ , RZJ
0982 C      REAL*8   RXIP , RYIP , RZIP , RXJP , RYJP , RZJP
0983 C      REAL*8   RXIJ , RYIJ , RZIJ , RXJI , RYJI , RZJI
0984 C      REAL*8   RXIJQ , RYIJQ , RZIJQ
0985 C      REAL*8   NXI , NYI , NZI , NXJ , NYJ , NZJ
0986 C      REAL*8   NXIJ , NYIJ , NZIJ
0987 C      REAL*8   NXIJ2 , NYIJ2 , NZIJ2
0988 C      REAL*8   TXIJ , TYIJ , TZIJ , TXIJS , TYIJS , TZIJS
0989 C      REAL*8   EXI , EYI , EZI , EXJ , EYJ , EZJ
0990 C      REAL*8   EXIP , EYIP , EZIP , EXJP , EYJP , EZJP
0991 C      REAL*8   EXIS , EYIS , EZIS , EXJS , EYJS , EZJS
0992 C      REAL*8   KIS , KJS , KIJS , KIQ
0993 C      REAL*8   RRXI , RRYI , RRZI , RRXJ , RRYJ , RRZJ
0994 C      REAL*8   RRXIJ , RRYIJ , RRZIJ , RRXJI , RRYJI , RRZJI
0995 C      REAL*8   TTXIJ , TTYIJ , TTZIJ , TTXIJS , TTYIJS , TTZIJS
0996 C      REAL*8   EEXI , EEXY , EEXZ , EEXJ , EEXY , EEXZ
0997 C      REAL*8   EEXIS , EEXYIS , EEZIS , EEXJS , EEXYS , EEZJS
0998 C      REAL*8   KKIS , KKJS , KKIJS
1000 C      REAL*8   RIJ , RIJSQ , RIJ3 , R00 , R01 , R10 , R11
1001 C      REAL*8   RIJMN , RIJMNFUN
1002 C      REAL*8   ECAN , RCOFF2 , RCHKSQ , RCHKSQ2
1003 C      REAL*8   DSQ , D1 , DISQ , D02 , CHCK0 , CHCK1
1004 C      REAL*8   C0 , C1 , C2 , C00 , C01 , C02 , C03
1005 C      REAL*8   C11 , C21 , C12 , C22
1006 C      REAL*8   C1X , C1Y , C1Z , C1SQ
1007 C      REAL*8   CEIEJ , CEIRIJ , CEJEIX , CEJEIY , CEJEIZ
1008 C      INTEGER ITREE , IPATH , JPTCL
1009 C
1010 C      OVLAP = .FALSE.
1011 C      ECAN = - KU*( NXI*HX + NYI*HY + NZI*HZ )
1012 C      D1SQ = D1**2
1013 C      DSQ = D**2
1014 C      D02 = D/2.D0
1015 C
1016 C      ----- MAIN LOOP START
1017 C
1018 DO 1000 JPTCL=1,N
1019 C
1020 J = JPTCL
1021 IF( J .EQ. I ) GOTO 1000
1022 C
1023 RXJ = RX(J)
1024 RYJ = RY(J)
1025 RZJ = RZ(J)
1026 C
1027 RXIJ = RXI - RXJ
1028 IF( RXIJ .GT. XL/2.D0 ) THEN
1029   RXIJ = RXIJ - XL
1030   RXJ = RXJ + XL
1031 ELSE IF( RXIJ .LT. -XL/2.D0 ) THEN
1032   RXIJ = RXIJ + XL
1033   RXJ = RXJ - XL
1034 END IF
1035 IF( DABS(RXIJ) .GE. RCOFF ) GOTO 1000
1036 C
1037 RYIJ = RYI - RYJ
1038 IF( RYIJ .GT. YL/2.D0 ) THEN
1039   RYIJ = RYIJ - YL
1040   RYJ = RYJ + YL
1041 ELSE IF( RYIJ .LT. -YL/2.D0 ) THEN
1042   RYIJ = RYIJ + YL
1043   RYJ = RYJ - YL
1044 END IF

```

• The treatment concerning particle *i*.

• The treatment concerning particles *i* and *j*.

• The treatment of the periodic BC.

```

1045      IF( DABS(RYIJ) .GE. RCOFF ) GOTO 1000
1046 C
1047      RZIJ = RZI - RZJ
1048      IF( RZIJ .GT. ZL/2.D0 ) THEN
1049          RZIJ = RZIJ - ZL
1050          RZJ = RZJ + ZL
1051      ELSE IF( RZIJ .LT. -ZL/2.D0 ) THEN
1052          RZIJ = RZIJ + ZL
1053          RZJ = RZJ - ZL
1054      END IF
1055      IF( DABS(RZIJ) .GE. RCOFF ) GOTO 1000
1056 C
1057      RIJSQ= RXIJ**2 + RYIJ**2 + RZIJ**2
1058      IF( RIJSQ .GE. RCOFF2 ) GOTO 1000
1059      IF( RIJSQ .LT. 1.D0 ) THEN
1060          OVR LAP = .TRUE.
1061          RETURN
1062      END IF
1063 C
1064      RIJ = DSQRT(RIJSQ)
1065 C
1066 C----- START OF MAGNETIC ENERGY ---
1067      IF( IPTCLMDL .EQ. 1 ) THEN
1068 C
1069          NXJ = NX(J)
1070          NYJ = NY(J)
1071          NZJ = NZ(J)
1072          EXJ = EX(J)
1073          EYJ = EY(J)
1074          EZJ = EZ(J)
1075          RXJI = -RXIJ
1076          RYJI = -RYIJ
1077          RZJI = -RZIJ
1078 C
1079          C00 = NXJ*NXJ + NYJ*NYJ + NZJ*NZJ
1080          C01 = NXJ*RXIJ + NYJ*RYIJ + NZJ*RZIJ
1081          C02 = NXJ*RXIJ + NYJ*RYIJ + NZJ*RZIJ
1082          RIJ3 = RIJ*RIJSQ
1083 C
1084          C1 = (RA/RIJ3)*( C00 - 3.D0*C01*C02/RIJSQ )
1085 C
1086          ECAN = ECAN + C1
1087 C
1088      ELSE IF( IPTCLMDL .EQ. 2 ) THEN
1089 C
1090          NXJ = NX(J)
1091          NYJ = NY(J)
1092          NZJ = NZ(J)
1093          NXIJ = NXI - NXJ
1094          NYIJ = NYI - NYJ
1095          NZIJ = NZI - NZJ
1096          NXIJ2 = NXI + NXJ
1097          NYIJ2 = NYI + NYJ
1098          NZIJ2 = NZI + NZJ
1099          EXJ = EX(J)
1100          EYJ = EY(J)
1101          EZJ = EZ(J)
1102          RXJI = -RXIJ
1103          RYJI = -RYIJ
1104          RZJI = -RZIJ
1105 C
1106          C11 = RXIJ*NXIJ + RYIJ*NYIJ + RZIJ*NZIJ
1107          C21 = RXIJ*NXIJ2 + RYIJ*NYIJ2 + RZIJ*NZIJ2
1108          C12 = 1.D0 - ( NXI*NXJ + NYI*NYJ + NZI*NZJ )
1109          C22 = 1.D0 + ( NXI*NXJ + NYI*NYJ + NZI*NZJ )
1110          C01 = D/RIJSQ
1111          C02 = D**2/(2.D0*RIJSQ)
1112 C
1113          R00 = RIJ*( 1.D0 + C01*C11 + C02*C12 )**0.5
1114          R11 = RIJ*( 1.D0 - C01*C11 + C02*C12 )**0.5
1115          R01 = RIJ*( 1.D0 + C01*C21 + C02*C22 )**0.5
1116          R10 = RIJ*( 1.D0 - C01*C21 + C02*C22 )**0.5
1117          IF( (R00 .LT. 1.D0) .OR. (R11 .LT. 1.D0) .OR.
1118          & (R01 .LT. 1.D0) .OR. (R10 .LT. 1.D0) ) THEN
1119          OVR LAP = .TRUE.

```

• If the two particles are separated over the cutoff distance  $r_{\text{coff}}^*$ , the calculation is unnecessary.

• The magnetic interaction energies are calculated.

• The treatment for the particle model with a magnetic dipole at the particle center.

• The treatment for the particle model with a plus and a minus magnetic charge at the torus part; this model is not used in the present exercise.

```

1120           RETURN
1121         END IF
1122 C
1123       &      ECAN = ECAN
1124             + RA*( 1.D0/R00 + 1.D0/R11 - 1.D0/R01 - 1.D0/R10 )
1125 C
1126     END IF
1127 C   ----- END OF MAGNETIC ENERGY -----
1128 C
1129   IF( ISTREET .EQ. 1 ) GOTO 1000
1130 C
1131   IF( RIJ .GE. D1 ) THEN
1132     OVRLAP = .FALSE.
1133     GOTO 1000
1134   END IF
1135 C
1136 C
1137 C   ----- CHECK THE OVERLAP OF PARTICLES I AND J -----
1138 C
1139 C
1140   CEIEJ = EXI*EXJ + EYI*EYJ + EZI*EZJ
1141   TXIJ = RXIJ/RIJ
1142   TYIJ = RYIJ/RIJ
1143   TZIJ = RZIJ/RIJ
1144   C11 = TXIJ*EXI + TYIJ*EYI + TZIJ*EZI
1145 C
1146   IF( DABS(CEIEJ) .GT. 0.999D0 ) THEN
1147     IF( DABS(C11) .LT. 0.001D0 )THEN
1148       ITREE = 2
1149     ELSE
1150       ITREE = 3
1151     END IF
1152   ELSE
1153     ITREE = 1
1154   END IF
1155 C
1156 C
1157 C
1158 C
1159 C
1160 C
1161 C
1162 C   ----- (1) ITREE=2 -----
1163 C
1164   IF( ITREE .EQ. 2 ) THEN
1165     IF( RIJ .GE. D1 ) THEN
1166       OVRLAP = .FALSE.
1167       GOTO 1000
1168     ELSE
1169       OVRLAP = .TRUE.
1170     RETURN
1171   END IF
1172 END IF
1173 C
1174 C
1175 C   ----- (2) ITREE=3 -----
1176   IF( ITREE .EQ. 3 ) THEN
1177     CEIRIJ = EXI*RXIJ + EYI*RYIJ + EZI*RZIJ
1178     IF( DABS(CEIRIJ) .GE. 1.D0 ) THEN
1179       OVRLAP = .FALSE.
1180       GOTO 1000
1181     END IF
1182
1183 C
1184     RXIP = RXIJ - CEIRIJ*EXI
1185     RYIP = RYIJ - CEIRIJ*EYI
1186     RZIP = RZIJ - CEIRIJ*EZI
1187     C0 = DSQRT( RXIP**2 + RYIP**2 + RZIP**2 )
1188     IF( C0 .LE. D ) THEN
1189       OVRLAP = .TRUE.
1190     RETURN
1191     ELSE IF( C0 .GE. D1 ) THEN
1192       OVRLAP = .FALSE.
1193       GOTO 1000
1194     END IF

```

• The assessment of the overlap between particles *i* and *j*.

• The regime of particle overlap is assessed. There are three regimes: a general arrangement ( $ITREE=1$ ), a one-plane arrangement ( $ITREE=2$ ), and a parallel arrangement ( $ITREE=3$ ).

-----  
ITREE=1: GENERAL  
ITREE=2: ONE PLANE  
ITREE=3: TWO PARALLEL PLANES-----

• The treatment for a one-plane arrangement ( $ITREE=2$ ).  
• The occurrence of a particle overlap can be assessed by only the particle-particle distance.

• The treatment for a parallel arrangement ( $ITREE=3$ ).  
• No overlap if the condition (2.1) in Section 4.2.3 is satisfied.  
•  $r_{ij}^P$  in Eq. (4.32) is evaluated.

• An overlap in the case of 2.2.1 in Section 4.2.3.  
• No overlap in the case of 2.2.2 in Section 4.2.3.

```

1195      EXJP = RXIP/C0
1196      EYJP = RYIP/C0
1197      EZJP = RZIP/C0
1198      EXIP = -EXJP
1199      EYIP = -EYJP
1200      EZIP = -EZJP
1201      C1X = RXI + D02*EXIP - ( RXJ + D02*EXJP )
1202      C1Y = RYI + D02*EYIP - ( RYJ + D02*EYJP )
1203      C1Z = RZI + D02*EZIP - ( RZJ + D02*EZJP )
1204      C1SQ = C1X**2 + C1Y**2 + C1Z**2
1205      IF( C1SQ .LT. 1.0D ) THEN
1206          OVRALP = .TRUE.
1207          RETURN
1208      ELSE
1209          OVRALP = .FALSE.
1210          GOTO 1000
1211      END IF
1212 C
1213      END IF
1214 C
1215 C ----- TIJS ---
1216      CEJEIX = EYJ*EZI - EZJ*EYI
1217      CEJEIY = EZJ*EXI - EXJ*EZI
1218      CEJEIZ = EXJ*EYI - EYJ*EXI
1219      C1 = DSQRT( CEJEIX**2 + CEJEIY**2 + CEJEIZ**2 )
1220      TXIJS = CEJEIX / C1
1221      TYIJS = CEJEIY / C1
1222      TZIJS = CEJEIZ / C1
1223 C
1224 C ----- EIS , EJS ---
1225      EXIS = -( EYI*TZIJS - EZI*TYIJS )
1226      EYIS = -( EZI*TXIJS - EXI*TZIJS )
1227      EZIS = -( EXI*TYIJS - EYI*TXIJS )
1228      EXJS = ( EYJ*TZIJS - EZJ*TYIJS )
1229      EYJS = ( EZJ*TXIJS - EXJ*TZIJS )
1230      EZJS = ( EXJ*TYIJS - EYJ*TXIJS )
1231 C
1232 C ----- KIS , KJS ---
1233      KIS = -(EXJ*RXIJ + EYJ*RYIJ + EZJ*RZIJ) /
1234      & (EXJ*EXIS + EYJ*EYIS + EZJ*EZIS)
1235      KJS = (EXI*RXIJ + EYI*RYIJ + EZI*RZIJ) /
1236      & (EXI*EXJS + EYI*EYJS + EZI*EZJS)
1237      KIJS = RXIJ*TXIJS + RYIJ*TYIJS + RZIJ*TZIJS
1238 C
1239 C ----- REPLACEMENT OF PARTICLES I AND J ---
1240      IF( DABS(KJS) .GE. DABS(KIS) ) THEN
1241          II = I
1242          JJ = J
1243          RRXI = RXI
1244          RRYI = RYI
1245          RRZI = RZI
1246          RRXJ = RXJ
1247          RRYJ = RYJ
1248          RRZJ = RZJ
1249          RRXIJ = RXIJ
1250          RRYIJ = RYIJ
1251          RRZIJ = RZIJ
1252          RRXJI = RXJI
1253          RRYJI = RYJI
1254          RRZJI = RZJI
1255          TTXIJ = TXIJ
1256          TTYIJ = TYIJ
1257          TTZIJ = TZIJ
1258          TTXIJS= TXIJS
1259          TTYIJS= TYIJS
1260          TTZIJS= TZIJS
1261          EEXI = EXI
1262          EEEYI = EYI
1263          EEEZI = EZI
1264          EEXXJ = EXJ
1265          EEEYJ = EYJ
1266          EEEZJ = EZJ
1267          EEXIS = EXIS
1268          EEEYIS = EYIS
1269          EEEZIS = EZIS

```

• An overlap in the case of 2.2.3 in Section 4.2.3.

• No overlap in the case of 2.2.4 in Section 4.2.3.

•  $t_{ij}^s$  ( $= (TXIJS, TYIJS, TZIJS)$ ) in Eq. (4.23) is evaluated.

•  $e_i^s$  and  $e_j^s$  in Eq. (4.24) are evaluated.

•  $k_i^s$ ,  $k_j^s$ , and  $k_{ij}^s$  in Eq. (4.26) are evaluated.

• Treatment (1) shown in Section 4.2.5. The subscripts are exchanged between  $i$  and  $j$  so as to satisfy  $|k_i^s| > |k_j^s|$ .

• As a result, the particle names  $i$  and  $j$  are expressed as II and JJ in the program.

```

1270      EEXJS = EXJS
1271      EYJJS = EYJS
1272      EZJJS = EZJS
1273      KIS = KKIS
1274      KJS = KKJS
1275      KIJS = KKIJS
1276      ELSE
1277          II = J
1278          JJ = I
1279          RXJI = RXJ
1280          RYJI = RYJ
1281          RZJI = RZJ
1282          RXIJ = RXI
1283          RYIJ = RYI
1284          RRZJ = RZI
1285          RRXIJ = -RXIJ
1286          RRYIJ = -RYIJ
1287          RRZIJ = -RZIJ
1288          RRXJI = -RXJI
1289          RRYJI = -RYJI
1290          RRZJI = -RZJI
1291          TTXIJ = -TXIJ
1292          TTYIJ = -TYIJ
1293          TTZIJ = -TZIJ
1294          TTXIJS = -TXIJS
1295          TTYIJS = -TYIJS
1296          TTZIJS = -TZIJS
1297          EEXI = EXJ
1298          EYI = EYJ
1299          EZI = EZJ
1300          EEXJ = EXI
1301          EYJ = EYI
1302          EZJ = EZI
1303          EEXIS = EXJS
1304          EYVIS = EYJS
1305          EZVIS = EZJS
1306          EEXJS = EXIS
1307          EYJS = EYIS
1308          EZJS = EZIS
1309          KIS = KKIS
1310          KJS = KKJS
1311          KIJS = KKIJS
1312      END IF
1313 C ----- REPLACEMENT OF DIRECTIONS OF EI AND EJ ---
1314 CHCK0 = RRXJI*EEXI + RRYJI*EYI + RRZJI*EEZI
1315 IF( CHCK0 .LT. 0.D0 ) THEN
1316     EEXI = -EEXI
1317     EYI = -EYI
1318     EZI = -EEZI
1319 END IF
1320
1321 C ----- REPLACEMENT OF DIRECTIONS OF EI AND EJ ---
1322 CEIEJ = EEXI*EEXJ + EYI*EYJ + EZI*EEZJ
1323 IF( CEIEJ .LT. 0.D0 ) THEN
1324     EEXJ = -EEXJ
1325     EYJ = -EYJ
1326     EZJ = -EEZJ
1327     CEIEJ = -CEIEJ
1328 END IF
1329 C ----- REPLACEMENT OF DIRECTION OF TIJS ---
1330 CHCK0 = TTXIJS*RRXIJ + TTYIJS*RRIJ + TTZIJS*RRZIJ
1331 IF( CHCK0 .LT. 0.D0 ) THEN
1332     TTXIJS = -TTXIJS
1333     TTYIJS = -TTYIJS
1334     TTZIJS = -TTZIJS
1335 END IF
1336
1337 C ----- REPLACEMENT OF DIRECTIONS OF EIS,EJS,KIS,KJS,KIJS ---
1338 IF( KKIS .LT. 0.D0 ) THEN
1339     KKIS = -KKIS
1340     EEXIS = -EEXIS
1341     EYVIS = -EYVIS
1342     EZVIS = -EEZIS
1343 END IF
1344

```

• Treatment (2) shown in Section 4.2.5.

• Treatment (3) shown in Section 4.2.5.

• Treatment (4) shown in Section 4.2.5.

```

1345      IF( KKJS .LT. 0.D0 ) THEN
1346          KKJS = -KKJS
1347          EEXJS = -EEXJS
1348          EEYJS = -EEYJS
1349          EEZJS = -EEZJS
1350      END IF
1351      IF( KKIJS .LT. 0.D0 ) THEN
1352          KKIJS = -KKIJS
1353      END IF
1354 C
1355 C
1356 C
1357 C
1358      IF( ITREE .EQ. 1 ) THEN
1359      &          • The treatment for a general arrangement (ITREE=1).
1360 C
1361          KIJQ = DABS( EEXJS*EEXI + EEYJS*EEYI + EEZJS*EEZI )
1362          IF( KKJS .GE. D02 ) THEN
1363              KIJQ = ( KKJS - D02 ) *KIJQ
1364              RXIJQ = RRXJ + D02*EEXJS - KIJQ*EEXI
1365              RYIJQ = RRYJ + D02*EEYJS - KIJQ*EEYI
1366              RZIJQ = RRZJ + D02*EEZJS - KIJQ*EEZI
1367              IPATH = 1
1368          ELSE
1369              KIJQ = ( D02 - KKJS ) *KIJQ
1370              RXIJQ = RRXJ + D02*EEXJS + KIJQ*EEXI
1371              RYIJQ = RRYJ + D02*EEYJS + KIJQ*EEYI
1372              RZIJQ = RRZJ + D02*EEZJS + KIJQ*EEZI
1373              IPATH = 2
1374          END IF
1375          CHCK1 = DSQRT( (RXIJQ-RRXJ)**2 + (RYIJQ-RRYI)**2
1376          &                                + (RZIJQ-RRZI)**2 )
1377          IF( CHCK1 .LE. D02 ) THEN
1378          &          --- (3)-1 INNER CIRCLE ---
1379              IF( IPATH .EQ. 2 ) THEN
1380                  OVRLAP = .TRUE.
1381                  RETURN
1382              ELSE IF( IPATH .EQ. 1 ) THEN
1383                  IF( KIJQ .LT. 1.D0 ) THEN
1384                      OVRLAP = .TRUE.
1385                      RETURN
1386                  ELSE
1387                      OVRLAP = .FALSE.
1388                      GOTO 1000
1389                  END IF
1390              END IF
1391          ELSE
1392          &          --- (3)-2 OUTER CIRCLE ---
1393              IF( IPATH .EQ. 1 ) THEN
1394          &          --- (3)-2-1 IPATH=1 ---
1395                  IF( KIJQ .GE. 1.D0 ) THEN
1396                      OVRLAP = .FALSE.
1397                      GOTO 1000
1398                  ELSE
1399                      RIJMNFUN( EEXI, EEYI, EEZI, EEXJ, ERYJ, EEZJ,
1400                               EEXIS, EYYS, EEZIS, EEXJS, EYJS, EEZJS,
1401                               KKIS, KKJS, KKIJS, RRXIJ, RRYIJ, RRZIJ, D )
1402                  IF( RIJMNFUN .GE. 1.D0 ) THEN
1403                      OVRLAP = .FALSE.
1404                      GOTO 1000
1405                  ELSE
1406                      OVRLAP = .TRUE.
1407                      RETURN
1408                  END IF
1409              END IF
1410          ELSE IF( IPATH .EQ. 2 ) THEN
1411          &          --- (3)-2-2 IPATH=2 ---
1412              RIJMNFUN( EEXI, EEYI, EEZI, EEXJ, EYJ, EEZJ,
1413                               EEXIS, EYYS, EEZIS, EEXJS, EYJS, EEZJS,
1414                               KKIS, KKJS, KKIJS, RRXIJ, RRYIJ, RRZIJ, D )
1415              IF( RIJMNFUN .GE. 1.D0 ) THEN
1416                  OVRLAP = .FALSE.
1417                  GOTO 1000
1418          ELSE

```

•  $K_{ij}^Q$  in Eq. (4.27) and  $r_{ij}^Q$  in Eq. (4.28) are evaluated.  
IPATH=1 means  $k_j^s \geq d/2$ .

•  $K_{ij}^Q$  in Eq. (4.29) and  $r_{ij}^Q$  in Eq. (4.30) are evaluated.  
IPATH=2 means  $k_j^s < d/2$ .

• An overlap in the case of 3.2.1 in Section 4.2.3.

• An overlap in the case of 3.1.2.a in Section 4.2.3.

• No overlap in the case of 3.1.1 in Section 4.2.3.

• No overlap in the case of 3.1.1 in Section 4.2.3.

• No overlap in the case of 3.1.2.b.1 in Section 4.2.3.

• An overlap in the case of 3.1.2.b.2 in Section 4.2.3.

• No overlap in the case of 3.2.2.a in Section 4.2.3.

```

1419          OVLAP = .TRUE.
1420          RETURN
1421      END IF
1422 C
1423      END IF
1424 C
1425      END IF
1426 C
1427 C
1428      END IF
1429 C
1430 C
1431 1000 CONTINUE
1432
1433
1434 C#### FUN RIJMNFUN #####
1435      DOUBLE PRECISION FUNCTION RIJMNFUN( EXI, EYI, EZI, EXJ,EYJ,EZJ,
1436      &                                         EXIS, EYIS, EZIS, EXJS, EYJS, EZJS,
1437      &                                         KIS, KJS, KIJS, RXIJ, RYIJ, RZIJ, D )
1438 C
1439      IMPLICIT REAL*8 (A-H,O-Z), INTEGER (I-N)
1440 C
1441      PARAMETER( PI=3.141592653589793D0 )
1442 C
1443      REAL*8     KIS, KJS, KIJS
1444 C
1445      REAL*8     X0 , Y0 , Z0 , X1 , Y1 , Z1 , X2 , Y2 , Z2
1446      REAL*8     D02 , CS , SN , BETAN1 , BETAN2 , BETAN , DBETAN
1447      REAL*8     FBETAN , FPBETAN , GAB , GABMN
1448      REAL*8     DX1DB , DY1DB , DX2DB , DY2DB
1449      REAL*8     CX0X1 , CX0X1SQ , CY0CY1
1450      REAL*8     SNBETA , CSBETA , CR2 , CRSQ , CHCK0 , DDEG
1451      REAL*8     DELX , DELY , DELZ , C0 , C1 , C2
1452      INTEGER     ICTR
1453 C
1454      DDEG = 10.D0 * (PI/180.D0)
1455      D02 = D/2.D0
1456      CS = EXI*EXJ + EYI*EYJ + EZI*EZJ
1457      SN = DSQRT( 1.D0 - CS**2 )
1458      X0 = KIJS
1459      CHCK0 = EXIS*EXJ + EYIS*EYJ + EZIS*EZJ
1460      IF( CHCK0 .LE. 0.D0 ) THEN
1461          DELX = EXIS
1462          DELY = EYIS
1463          DELZ = EZIS
1464      ELSE
1465          DELX = -EXIS
1466          DELY = -EYIS
1467          DELZ = -EZIS
1468      END IF
1469      Y0 = -( RXIJ*DELX + RYIJ*DELY + RZIJ*DELZ )
1470      Z0 = KJS*DABS( EXJS*EXI + EYJS*EYI + EZJS*EZI )
1471 C
1472 C
1473 C
1474      IF( DABS(X0) .LE. 0.05D0 ) THEN
1475          X2 = X0
1476          Y2 = Y0 - D02*CS
1477          Z2 = Z0 - D02*SN
1478          X1 = 0.D0
1479          Z1 = 0.D0
1480          IF( Y2 .GE. 0.D0 ) THEN
1481              Y1 = D02
1482          ELSE
1483              Y1 = -D02
1484          END IF
1485          GAB = (X2-X1)**2 + (Y2-Y1)**2 + (Z2-Z1)**2
1486          RIJMNFUN = DSQRT( GAB )
1487          RETURN
1488      END IF
1489 C
1490      X2     = X0 / 2.D0
1491      C1     = 1.0D0
1492      C2     = -X0/D
1493      IF( DABS(C2) .GE. 1.D0 ) C2 = DSIGN( C1, C2 )

```

• An overlap in the case of 3.2.2.b in Section 4.2.3.

• A function subprogram for evaluating  $r_{ij}^{(min)}$  by means of Newton's method.

•  $CS=\cos(\theta_0)$  and  $SN=\sin(\theta_0)$ .  
 •  $x_0=(x_0, y_0, z_0)$  is evaluated.

--- FOR THE CASE OF  $\cos(\beta)=0$  ---  
 - VALID ONLY FOR OUTER CIRCLE -

• The case of  $x_0=(0, y_0, z_0)$  and  $|r_{ij}^Q-r_i| \geq d/2$  enables us to conduct simple treatment.

• A starting value of  $x_2$  is given. It is first assumed that  $X2=X0/2$ , yielding a starting value of  $\beta=BETAN$ .

```

1494      BETAN1 = DACOS( C2 )
1495      BETAN2 = 2.D0*PI - BETAN1
1496      C1      = DSIN(BETAN1)
1497      C2      = DSIN(BETAN2)
1498      IF( C1 .GE. C2 ) THEN
1499          BETAN = BETAN2
1500      ELSE
1501          BETAN = BETAN1
1502      END IF
1503 C      -----
1504 C      ----- START OF NEWTON PROCEDURE -----
1505 C
1506      GABMN = 1.D5
1507      ICTR = 0
1508      10 ICTR = ICTR + 1
1509      SNBETA = DSIN( BETAN )
1510      CSBETA = DCOS( BETAN )
1511      X2 = D02*CSBETA + X0
1512      Y2 = D02*SNBETA*CS + Y0
1513      Z2 = D02*SNBETA*SN + Z0
1514 C
1515      CR2 = X2**2 + Y2**2
1516      CRSQ = DSQRT( CR2 )
1517      X1 = (X2/CRSQ)*D02
1518      Y1 = (Y2/CRSQ)*D02
1519      Z1 = 0.D0
1520      C1 = (X2-X1)**2 + (Y2-Y1)**2 + (Z2-Z1)**2
1521      IF( C1 .LT. GABMN ) GABMN = C1
1522 C
1523      CX0X1 = X0 - X1
1524      CX0X1SQ = CX0X1**2
1525      CY0Y1 = Y0 - Y1
1526      FBETAN = CX0X1*( CX0X1*SNBETA/CSBETA - CS*CY0Y1 - SN*Z0 )
1527 C
1528      DX2DB = -D02*SNBETA
1529      DY2DB = D02*CSBETA*CS
1530      C0 = X2*DX2DB + Y2*DY2DB
1531      C1 = CRSQ/CR2
1532      C2 = C0/(CRSQ*CR2)
1533      DX1DB = ( C1*DX2DB - C2*X2 )*D02
1534      DY1DB = ( C1*DY2DB - C2*Y2 )*D02
1535      CY0Y1 = Y0 - Y1
1536      FPBETAN = CX0X1SQ/CSBETA**2 - CS* ( -DY1DB*CX0X1 + DX1DB*CY0Y1 )
1537      & - Z0*SN*DX1DB
1538 C
1539      BETAN1 = BETAN - FBETAN/FPBETAN
1540 C
1541      DBETAN = DABS(BETAN1-BETAN)
1542      IF( DBETAN .GT. 0.01D0 ) THEN
1543          IF( DBETAN .GT. DDEG ) THEN
1544              BETAN = DSIGN( DDEG, (BETAN1-BETAN) ) + BETAN
1545          ELSE
1546              BETAN = BETAN1
1547          ENDIF
1548          IF( ICTR .GT. 10 ) GOTO 900
1549          GOTO 10
1550      END IF
1551 C
1552      900 GAB = (X2-X1)**2 + (Y2-Y1)**2 + (Z2-Z1)**2
1553      IF( GAB .GT. GABMN ) GAB = GABMN
1554      RIJMNFUN = DSQRT( GAB )
1555 C
1556      RETURN
1557 C*****
1558 C THIS SUBROUTINE IS FOR GENERATING UNIFORM RANDOM NUMBERS      *
1559 C (SINGLE PRECISION) FOR 32-BIT COMPUTER.                      *
1560 C      N : NUMBER OF RANDOM NUMBERS TO GENERATE                 *
1561 C      IX : INITIAL VALUE OF RANDOM NUMBERS (POSITIVE INTEGER)   *
1562 C      : LAST GENERATED VALUE IS KEPT                            *
1563 C      X(N) : GENERATED RANDOM NUMBERS (0<X(N)<1)            *
1564 C*****
1565 C**** SUB RANCAL ****
1566      SUBROUTINE RANCAL( N, IX, X )
1567 C
1568      IMPLICIT REAL*8 (A-H,O-Z), INTEGER (I-N)
1569 C

```

• The minimum value of  $g(\alpha, \beta)$  is saved in GABMN.

• The start of the iteration procedure of Newton's method.

•  $\mathbf{x}_2 = (X_2, Y_2, Z_2)$  is calculated using BETAN which is an expected value of the solution  $\beta$ .

•  $\mathbf{x}_1 = (X_1, Y_1, Z_1)$  is calculated from procedure 3 of Newton's method in Section 4.2.3.

•  $(x_0 - x_1)^2 f'(\beta_n) = FBETAN$  is evaluated.

•  $\partial x_2 / \partial \beta = DX2DB$  and  $\partial y_2 / \partial \beta = DY2DB$ .  
•  $\partial x_1 / \partial \beta = DX1DB$  and  $\partial y_1 / \partial \beta = DY1DB$ .

•  $(x_0 - x_1)^2 f'(\beta_n) = FPBETAN$  is evaluated.

•  $\beta_{x+1} = BETAN1$  is evaluated from Eq. (4.41).

• A subroutine for generating a uniform random number sequence.

```
1570      REAL      X(N)
1571      INTEGER    INTEGMX, INEGST, INEG
1572 C
1573      DATA INTEGMX/2147483647/
1574      DATA INEGST,INEG/584287,48828125/
1575 C
1576      AINTEGMX = REAL( INTEGMX )
1577 C
1578      IF ( IX.LT.0 ) STOP
1579      IF ( IX.EQ.0 ) IX = INEGST
1580      DO 30 I=1,N
1581          IX = IX*INEG
1582          IF (IX .LT. 0 ) IX = (IX+INTEGMX)+1
1583          X(I) = REAL(IX)/AINTEGMX
1584 30 CONTINUE
1585      RETURN
1586      END
```

- This is for a 32-bit CPU based on the expression of two's complement.

# 5 Practice of Brownian Dynamics Simulations

In the previous chapters, we have shown how the MD method and MC method are applied in a practical simulation. In the present and successive chapters, we follow the same approach and demonstrate the microsimulation methods required for the application of the Brownian Dynamics (BD) method, the DPD method, and the lattice Boltzmann method. These further methods are very useful as simulation tools for a colloidal dispersion or a suspension composed of dispersed particles. These simulation methods have many applications in the pharmaceutical field, as well as in science and engineering.

The exercise in the present chapter is for a BD simulation to discuss how Lennard-Jones particles sediment in the gravitational field for cases when the Brownian motion is expected to be significant. This example of a physical phenomenon becomes attractive as a research subject when the particle aggregation is strongly related to the sedimentation. The sample simulation program is written in the C programming language.

## 5.1 Sedimentation Phenomena of Lennard-Jones Particles

We consider a thermodynamic equilibrium state of  $N$  Brownian particles with mass  $m$  dispersed in a base liquid contained in a rectangular parallelepiped box. For simplification, the Brownian particles are assumed to be the Lennard-Jones particle, where the particle–particle interactions can be expressed as a Lennard-Jones potential. The objective of the present practice is to discuss how the Brownian particles in thermodynamic equilibrium sediment after the gravitational field is switched on. The system temperature, gravitational force, and particle–particle interactions are expected to significantly influence the sedimentation phenomenon.

## 5.2 Specification of Problems in Equations

Since the particles sediment under the effect of the Brownian motion in a gravitational field, we are required to use the BD method, explained in Section 1.3, in order to simulate this phenomenon. In contrast to a magnetic particle system in which the particle rotation is restricted by an external magnetic field, the Lennard-Jones particles are only influenced by the isotropic force due to the Lennard-Jones potential. We

therefore only need to treat the translational motion of the Brownian particles. The particles hydrodynamically interact through their ambient fluid, but it is difficult to take into account these multibody hydrodynamic interactions, even for the relatively simple spherical particle system. It is still more so for a nonspherical particle system, such as a rod-like or disk-like particle suspension. The difficulty of treating multibody hydrodynamic interactions forces us to take into account only the friction term as a first approximation, even in the case of a nondilute suspension. In the present exercise, we therefore take into account the nonhydrodynamic interaction but neglect the multi-body hydrodynamic interaction among the particles.

If the position vector of an arbitrary particle  $i$  is denoted by  $\mathbf{r}_i$ , the velocity by  $\mathbf{v}_i$ , the nonhydrodynamic force by  $\mathbf{f}_i$ , and the random force by  $\mathbf{f}_i^B$ , then the equation of motion of particle  $i$  is expressed as [1,4]

$$m \frac{d^2 \mathbf{r}_i}{dt^2} = \mathbf{f}_i - \xi \mathbf{v}_i + \mathbf{f}_i^B \quad (5.1)$$

in which  $\xi$  is the friction coefficient, expressed as  $\xi = 3\pi\eta d$  ( $\eta$  is the liquid viscosity) under the assumption that the Lennard-Jones particles are spherical with diameter  $d$ . The random force  $\mathbf{f}_i^B = (f_{ix}^B, f_{iy}^B, f_{iz}^B)$  must satisfy the following stochastic properties:

$$\langle f_{ix}^B(t) \rangle = \langle f_{iy}^B(t) \rangle = \langle f_{iz}^B(t) \rangle = 0 \quad (5.2)$$

$$\left\langle \left\{ f_{ix}^B(t) \right\}^2 \right\rangle = \left\langle \left\{ f_{iy}^B(t) \right\}^2 \right\rangle = \left\langle \left\{ f_{iz}^B(t) \right\}^2 \right\rangle = 2\xi kT \delta(t - t') \quad (5.3)$$

The force  $\mathbf{f}_{ij}$  acting on particle  $i$  by particle  $j$  due to the Lennard-Jones potential is expressed as

$$\mathbf{f}_{ij} = 24\varepsilon \left\{ 2 \left( \frac{d}{r_{ij}} \right)^{12} - \left( \frac{d}{r_{ij}} \right)^6 \right\} \frac{\mathbf{r}_{ij}}{r_{ij}^2} \quad (5.4)$$

in which  $\mathbf{r}_{ij}$  is the position vector of particle  $i$  relative to particle  $j$ , expressed as  $\mathbf{r}_{ij} = \mathbf{r}_i - \mathbf{r}_j$ , and  $r_{ij}$  is the magnitude of  $\mathbf{r}_{ij}$ , that is,  $r_{ij} = |\mathbf{r}_{ij}|$ . The total force acting on particle  $i$ ,  $\mathbf{f}_i$ , can be obtained by summing  $\mathbf{f}_{ij}$  from the contributions of all the ambient particles.

The method of nondimensionalizing quantities is described in the next section.

### 5.3 Brownian Dynamics Algorithm

As explained in Section 1.3, the Ermak–McCammon method [24] enables us to transform the equation of motion in Eq. (5.1) into Eq. (1.59). We here show the non-dimensional expressions in the following. It may be inappropriate to use the

representative values usually employed for the Lennard-Jones system, because we consider a dispersion of fine particles—which are regarded as a Lennard-Jones particle performing Brownian motion—and not a pure molecular system. We therefore use the following representative values: the particle diameter  $d$  for distances;  $mg/(3\pi\eta d)$  for the velocities, which is obtained by equating the friction force to the gravitational force; and the gravitational force  $mg$  for forces. With these representative values, the equation of an arbitrary particle  $i$  is written in nondimensional form as

$$\mathbf{r}_i^*(t^* + h^*) = \mathbf{r}_i^*(t^*) + h^* \mathbf{f}_i^*(t^*) + \Delta \mathbf{r}_i^{B*} \quad (5.5)$$

in which the components  $(\Delta x_i^{B*}, \Delta y_i^{B*}, \Delta z_i^{B*})$  of the random displacement  $\Delta \mathbf{r}_i^{B*}$  must satisfy the following stochastic characteristics:

$$\langle \Delta x_i^{B*} \rangle = \langle \Delta y_i^{B*} \rangle = \langle \Delta z_i^{B*} \rangle = 0 \quad (5.6)$$

$$\langle (\Delta x_i^{B*})^2 \rangle = \langle (\Delta y_i^{B*})^2 \rangle = \langle (\Delta z_i^{B*})^2 \rangle = 2R_B h^* \quad (5.7)$$

in which  $R_B$  is a nondimensional parameter representing the strength of the random force relative to the gravitational force, expressed as  $R_B = kT/(mgd)$ . The gravitational force  $\mathbf{f}_i^{(g)}$  acting on particle  $i$  and the force  $\mathbf{f}_{ij}^{(LJ)}$  due to the Lennard-Jones interaction are expressed in nondimensional form as

$$\mathbf{f}_i^{(g)*} = \hat{\mathbf{g}} \quad (5.8)$$

$$\mathbf{f}_{ij}^{(LJ)*} = 24R_{LJ} \left\{ 2 \left( \frac{1}{r_{ij}^*} \right)^{12} - \left( \frac{1}{r_{ij}^*} \right)^6 \right\} \frac{\mathbf{r}_{ij}^*}{(r_{ij}^*)^2} \quad (5.9)$$

in which  $R_{LJ}$  is a nondimensional parameter presenting the strength of the force due to the Lennard-Jones potential relative to the gravitational force, expressed as  $R_{LJ} = \varepsilon/(mgd)$ , and  $\hat{\mathbf{g}}$  is the unit vector, denoting the gravitational direction. The consideration of these forces provides the nondimensional force  $\mathbf{f}_i^*$  acting on particle  $i$  as

$$\mathbf{f}_i^* = \mathbf{f}_i^{(g)*} + \sum_{j(\neq i)} \mathbf{f}_{ij}^{(LJ)*} = \hat{\mathbf{g}} + 24R_{LJ} \sum_{j(\neq i)} \left\{ 2 \left( \frac{1}{r_{ij}^*} \right)^{12} - \left( \frac{1}{r_{ij}^*} \right)^6 \right\} \frac{\mathbf{r}_{ij}^*}{(r_{ij}^*)^2} \quad (5.10)$$

Since the particles sediment in the gravitational field direction, assumed to be the negative direction of the  $y$ -axis, the periodic boundary condition is not applicable at the sedimentation surface, but it is applicable to the boundary surfaces normal to the  $x$ - and  $z$ -directions. On the sedimentation surface, the elastic reflection condition is here employed for the boundary in order to ensure that a particle cannot cross the boundary surface. In the concrete treatment of a reflecting particle, the velocity component parallel to the boundary surface is unchanged, but the velocity component normal to the boundary surface is reversed in direction.

The main procedure of the BD simulation is summarized as follows. First, we set the number of particles  $N$ , the size of simulation region  $(L_x^*, L_y^*, L_z^*)$ , and the volumetric fraction  $\phi_v$ . Then, the assignment of the initial position of the particles enables us to begin the main loop in a simulation program. The particles are simulated according to the basic equations shown in Eq. (5.5) together with generating the random displacements of the particles based on the stochastic properties in Eqs. (5.6) and (5.7); these random displacements are sampled from the normal distribution specified by Eqs. (5.6) and (5.7). In order that we may discuss quantitatively the particle sedimentation phenomenon, the time variation in the local densities is evaluated for each thin-sliced volume along the  $y$ -direction. The pair correlation function is usually employed for an accurate quantitative discussion of the internal particle structure of a system, but we here focus only on the method of snapshots and employ the local number density.

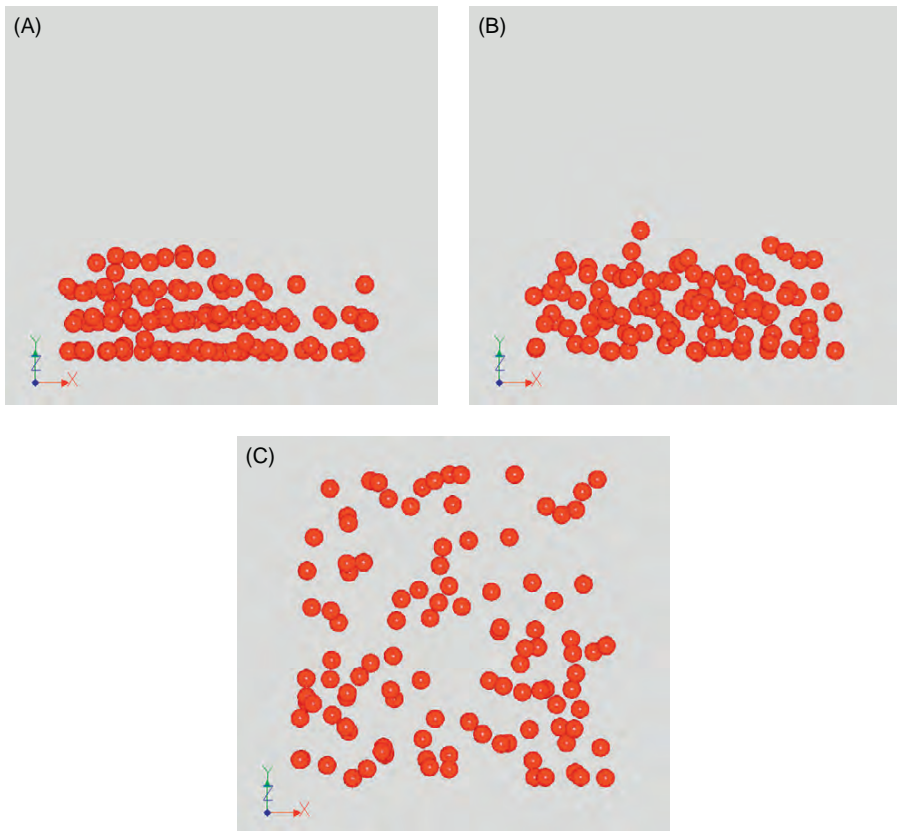
## 5.4 Parameters for Simulations

In conducting the following BD simulations, the number of particles is taken as  $N = 108$ , and the volumetric fraction is taken as  $\phi_v = 0.1$  to give a number density  $n^* = 6\phi_v/\pi$ . The face-centered cubic lattice system shown in Figure 2.2B is employed as an initial configuration of particles, yielding the lattice constant  $a^* = (4/n^*)^{1/3}$  and  $Q = (N/4)^{1/3}$ ; the replication of the unit cell ( $Q - 1$ ) times in each direction generates the particle configuration for the whole simulation region. The dimensions of the region are therefore  $(L_x^*, L_y^*, L_z^*) = (Qa^*, Qa^*, Qa^*)$ . An appropriate time interval  $h^*$  has to be chosen with sufficient consideration. Setting an unreasonably large time interval is likely to induce a serious particle overlap problem, which will result in the instability of the system. Choice of the appropriate time interval is strongly dependent on the nondimensional parameters  $R_{\text{LJ}}$  and  $R_B$ . The larger these quantities, the smaller the time interval (i.e.,  $h^* \ll 1$ ). In the present demonstration,  $h^* = 0.00005$  was adopted for the case of  $R_{\text{LJ}} = R_B = 1$ . The simulations were carried out for various cases of  $R_{\text{LJ}}$  and  $R_B$ , where we have used  $R_{\text{LJ}} = 1$  and 5 and also  $R_B = 0.1, 1$ , and 5.

## 5.5 Results of Simulations

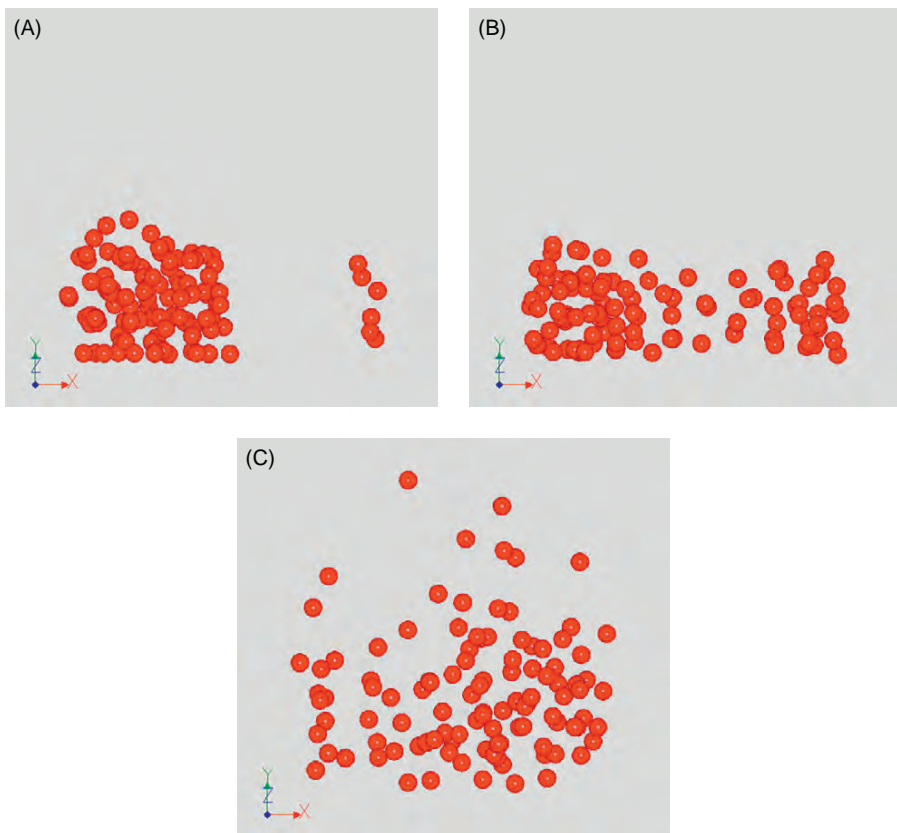
Figures 5.1–5.3 show the snapshots of the Lennard-Jones particles in the sedimentation process under the influence of the gravitational field, which were obtained by conducting the sample simulation program explained in the next section. The snapshots in Figures 5.1 and 5.2 were obtained for different cases of  $R_B$  after the particle distribution attains to a steady state (in the macroscopical meaning). Those in Figure 5.3 are from the visualization of the sedimentation process with advancing time.

Figure 5.1A clearly shows that the particles have sedimented on the base surface area under the gravitational field. This is because the value of the nondimensional parameter  $R_B = 0.1$  implies a significant influence of the gravitational force over the random Brownian force. On the other hand, in the case of  $R_{\text{LJ}} = 5$  in



**Figure 5.1** Snapshots in a steady state for  $R_{\text{LJ}} = 1$ : (A)  $R_B = 0.1$ , (B)  $R_B = 1$ , and (C)  $R_B = 5$ .

Figure 5.2A, the Lennard-Jones interactions significantly affect the sedimentation process, exhibiting characteristic aggregates formed differently from those in Figure 5.1A. For the case of the influence of the random force being equal to that of the gravitational force in Figure 5.2B, the particles have almost completely sedimented on the base area, but the internal structure seems to be considerably different from that found in Figure 5.1A. This is an example where the use of quantitative results from the pair correlation function would be required for a deeper discussion. In the case of  $R_B = 5$  shown in Figures 5.1 and 5.2, the particles actively exhibit the Brownian motion without sedimenting on the base surface area; however, the particles tend to aggregate to form clusters with increasing values of  $R_{\text{LJ}}$  even in the case of  $R_B = 5$ . From these snapshots, we may conclude that the gravitational force mainly governs the sedimentation process, and the Lennard-Jones interactions between particles mainly determine the internal structures of the aggregates formed during the sedimentation process. As already pointed out, a higher-level academic study



**Figure 5.2** Snapshots in a steady state for  $R_{\text{LJ}} = 5$ : (A)  $R_B = 0.1$ , (B)  $R_B = 1$ , and (C)  $R_B = 5$ .

would require quantitative results, such as the pair correlation function, in addition to the qualitative results visualized here.

Figure 5.3 shows how the particles sediment with time, that is, the particle sedimentation process for the case of  $R_{\text{LJ}} = 1$  and  $R_B = 0.1$ : Figures 5.3A–C are for nondimensional time  $t^* = 1, 4$ , and  $8$ , respectively. In this case of  $R_B = 0.1$ , the gravitational force is much more dominant than the random force (i.e., the Brownian motion), so that the particles sediment, attain at the bottom surface, and form layer structures from the base with time.

Figure 5.4 shows the results of the local number density of particles  $n^*$  at the position  $y^*$  of each sliced layer taken from the base surface in the opposite direction to the gravitational field. Note that the nondimensional time is used, and the data or subaveraged values were calculated at every certain number of time steps. This figure demonstrates quantitative characteristics of the sedimentation process with time, which clearly suggests the layered structures of sedimented particles indicated previously.

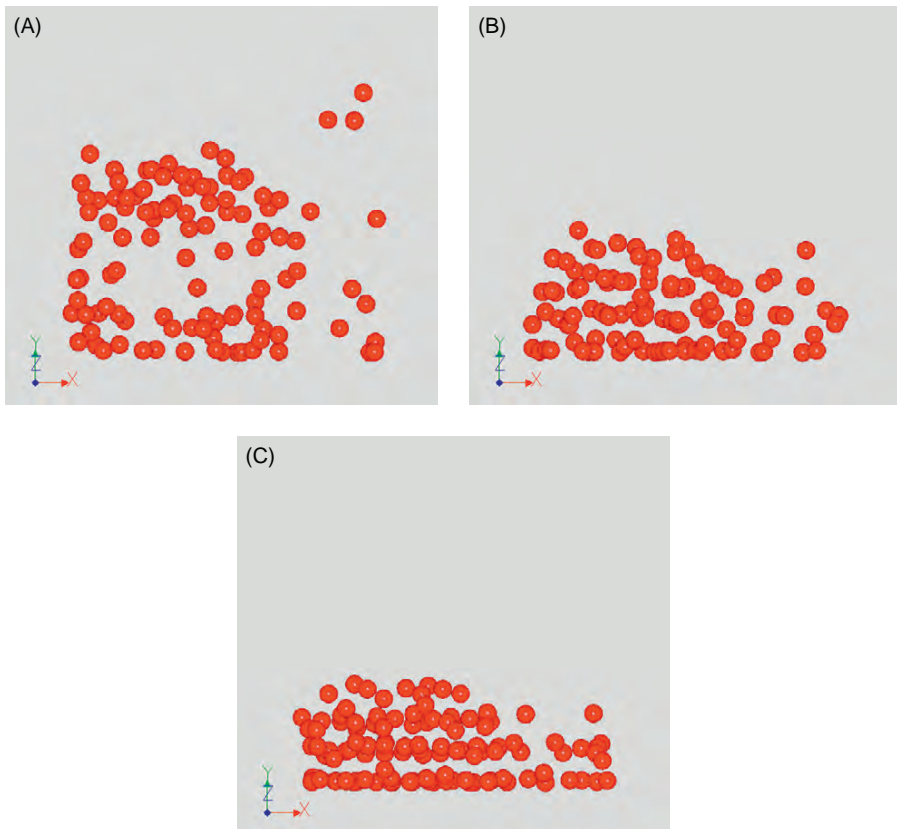


**Figure 5.3** Time change of aggregate structures for  $R_{\text{LJ}} = 1$  and  $R_B = 0.1$ : (A)  $t^* = 1$ , (B)  $t^* = 4$ , and (C)  $t^* = 8$ .

## 5.6 Simulation Program

We show a sample simulation program for the example of the present sedimentation phenomenon in the following. The program is written in the C language.

To aid the reader's understanding, the important variables used in the program are shown as follows:

$\text{RX}[i], \text{RY}[i], \text{RZ}[i]$	: $(x,y,z)$ components of the position vector $\mathbf{r}_i^*$ of particle $i$
$\text{FX}[i], \text{FY}[i], \text{FZ}[i]$	: $(x,y,z)$ components of the force $\mathbf{f}_i^*$ acting on particle $i$
$\text{RXB}[i], \text{RYB}[i],$	: $(x,y,z)$ components of the random displacements $\Delta\mathbf{r}_i^{\text{B}*}$ of
$\text{RZB}[i]$	particle $i$
$\text{XL}, \text{YL}, \text{ZL}$	: Side lengths of the simulation box in the $(x,y,z)$ directions
$h$	: Time interval $h^*$
$\text{ndens0}$	: Initial number density of particles
$\text{phaiv0}$	: Initial volumetric fraction of particles

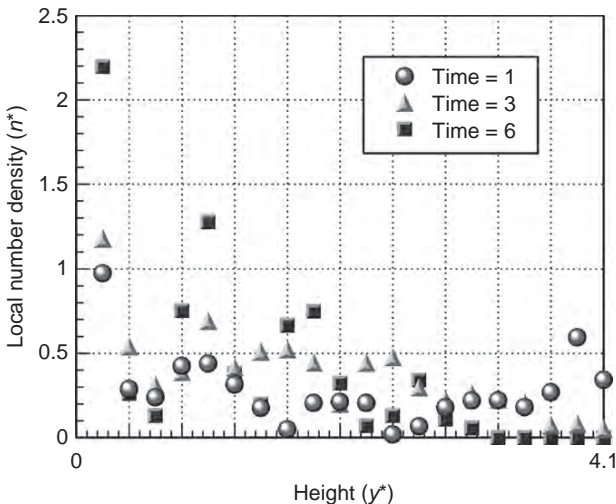


**Figure 5.4** Time change in the local number density distribution for  $R_{\text{LJ}} = 1$  and  $R_B = 0.1$ .

RLJ, RB	:	Nondimensional parameters $R_{\text{LJ}}$ and $R_B$
n	:	Number of particles
RAN[j]	:	Uniform random numbers ranging $0 \sim 1$ ( $j=1 \sim \text{NRANMX}$ )
NRAN	:	Number of used random numbers

Note that the line numbers are added for convenience and are grammatically unnecessary.

In the following program, several explanatory comments have been added to the important features to assist the reader's understanding.

```

0001 /*-----*/
0002 /*-----*/ bdsedim1.c */ */
0003 /*-----*/ */
0004 /*-----*/ */
0005 /*-----*/ - Brownian dynamics simulation of the sedimentation of - */
0006 /*-----*/ - spherical particles in gravity field. - */
0007 /*-----*/ */
0008 /*-----*/ */
0009 /*-----*/ np1     = fopen("@eaal.data", "w"); parameters */
0010 /*-----*/ np2     = fopen("eaa11.data", "w"); parameters */
0011 /*-----*/ np[1]   = fopen("eaa001.data", "w"); particle position */
0012 /*-----*/ np[2]   = fopen("eaa011.data", "w"); particle position */
0013 /*-----*/ np[3]   = fopen("eaa021.data", "w"); particle position */
0014 /*-----*/ np[4]   = fopen("eaa031.data", "w"); particle position */
0015 /*-----*/ np[5]   = fopen("eaa041.data", "w"); particle position */
0016 /*-----*/ np[6]   = fopen("eaa051.data", "w"); particle position */
0017 /*-----*/ np[7]   = fopen("eaa061.data", "w"); particle position */
0018 /*-----*/ np[8]   = fopen("eaa071.data", "w"); particle position */
0019 /*-----*/ np[9]   = fopen("eaa081.data", "w"); particle position */
0020 /*-----*/ np[10]  = fopen("eaa091.data", "w"); particle position */
0021 /*-----*/ */
0022 /*-----*/ 1. Lennard-Jones particle system. */
0023 /*-----*/ */
0024 /*-----*/ */
0025 /*-----*/ Ver.2 by A.Satoh , '04 3/10 */
0026 /*-----*/ */

```

```

0027 /*          */
0028 /*      RX[i],RY[i],RZ[i] : particle position           */
0029 /*      RXB[i],RYB[i],RZB[i] : random displace. due to Brownian motion */
0030 /*      FX[i],FY[i],FZ[i]   : forces acting on particle i      */
0031 /*      XL, YL, ZL : size of simulation box along each axis    */
0032 /*      h           : time interval                         */
0033 /*      ndens0       : number density                      */
0034 /*      phai0        : volumetric fraction                 */
0035 /*      RB, RG, RLJ : nondimensional parameters            */
0036 /*      ychk[*]     : is used to calculate number density distribution */
0037 /*      dnsmpl,dtsmpl : data is sub-averaged using dnsmpl-data */
0038 /*      : through dtsmpl-time                                */
0039 /*      ndens[*][+] : number density distribution             */
0040 /*      ntimemx     : maximum number of time step           */
0041 /*      */
0042 /*      0<RX[i]<XL , 0<RY[i]<YL , 0<RZ[i]<ZL           */
0043 /*-----*/
0044 #include <stdio.h>
0045 #include <math.h>
0046 #define PI      3.141592653589793
0047 #define NN      501
0048 #define NS      2001
0049 #define NRANMX 2001
0050 double RX[NN] , RY[NN] , RZ[NN] ;
0051 double RXB[NN] , RYB[NN] , RZB[NN] ;
0052 double FX[NN] , FY[NN] , FZ[NN] ;
0053 double XL, YL, ZL ;
0054 double RB, RG, RLJ ;
0055 float  RAN[NRANMX] ;
0056 int    NRAN, IX ;
0057
0058 /*----- main function ---*/
0059 main()
0060 {
0061     int   n , nychk , dnsmpl ;
0062     double h , ndens0 , phai0 ;
0063     double ndens[NN][NS] , ychk[NN] ;
0064     double cndns[NN] ;
0065     double dtsmpl ;
0066     FILE *fopen() , *np[11] , *np1 , *np2 ;
0067
0068     double rcoff , rcoff2 , rxi , ryi , rzi ;
0069     int    ntime , ntimemx , ntimemx1 , nsmpl , inp , ngraph ;
0070     int    i , j , nranchk ;
0071
0072     np1   = fopen("@eaa1.data" , "w");
0073     np2   = fopen("eaa11.data" , "w");
0074     np[1] = fopen("eaa001.data" , "w");
0075     np[2] = fopen("eaa011.data" , "w");
0076     np[3] = fopen("eaa021.data" , "w");
0077     np[4] = fopen("eaa031.data" , "w");
0078     np[5] = fopen("eaa041.data" , "w");
0079     np[6] = fopen("eaa051.data" , "w");
0080     np[7] = fopen("eaa061.data" , "w");
0081     np[8] = fopen("eaa071.data" , "w");
0082     np[9] = fopen("eaa081.data" , "w");
0083     np[10] = fopen("eaa091.data" , "w");
0084
0085     /*--- parameter (1) ---*/
0086     /******n=32, 108, 256, 500, 864, 1372, 2048 must be chosen. */
0087     /******n=108, 256, 500, 864, 1372, 2048 must be chosen. */
0088
0089     n   = 108 ;
0090     rcoff = 2.5 ;
0091     h   = 0.00005 ;
0092     rcoff2 = rcoff*rcoff ;
0093
0094     RB   = 1.0 ;
0095     RLJ  = 1.0 ;  RG     = 1.0 ;
0096     phai0 = 0.1 ;
0097     ndens0 = phai0*6./PI ;
0098     nychk = 40 ;
0099
0100    ntimemx = 200000 ;
0101    dnsmpl = 200 ;
0102    dtsmpl = (double)dnsmpl*h ;
0103    ntimemx1= ntimemx/10 ;
0104    ngraph = ntimemx/10 ;
0105    inp   = 0 ;
0106    IX    = 0 ;

```

• The given values and results are written out in @eaa1.data and eaa11.data.  
• @eaa1 is for confirming the values set for starting a simulation, and eaa11 is for the postprocessing analysis.

• The particle position data are written out in eaa001-eaa091 for the postprocessing analysis.

• The particle number  $N=108$ , cutoff distance  $r_{\text{coff}}^*=2.5$ , and time interval  $h^*=0.00005$ .

•  $R_B=1$ ,  $R_L=1$ , volumetric fraction  $\phi_V=0.1$ , and number density  $n^*=6\phi/\pi$ . The simulation box is sliced into  $nychk$  equal pieces in the  $y$ -direction.

• The total number of time steps is 200,000 and data are sampled at every 200 time steps. The equilibration procedure is conducted until  $ntimemx1$  steps. The particle positions are written out at every  $ngraph$  steps for the postprocessing analysis.

```

0108 rancal() ;
0109 NRAN = 1 ;
0110 nranchk = NRANMX - 6*n ;
0111 /*
0112 *----- initial configuration -----*/
0113 /*----- set initial positions ---*/
0114 /*----- calculate energy ---*/
0115 initpos( n, ndens0 ) ; YL = XL ; ZL = XL ;
0116 /*----- set grid for num.dens.dist. ---*/
0117 gridcal( nychk, ychk ) ;
0118 /*----- cal random displacement ---*/
0119 forcecal( n, rcoff, rcoff2 ) ;
0120 randisp( n, h ) ;
0121 /*----- print out constants ---*/
0122 fprintf(np1,"-----\n");
0123 fprintf(np1," Brownian dynamics method\n");
0124 fprintf(np1," +++ Lennard-Jones particles system +++\n");
0125 fprintf(np1,"n=%4d ndens=%8.3f phaiv0=%6.3f rcoff=%6.3f h=%10.8f\n",
0126 n, ndens0, phaiv0, rcoff, h );
0127 fprintf(np1,"XL=%6.3f YL=%6.3f\n", XL, YL, ZL) ;
0128 fprintf(np1,"RB=%12.4e RG=%12.4e RLJ=%12.4e\n", RB, RG, RLJ) ;
0129 fprintf(np1,"ntimemx=%8d nychk=%4d dnsmples=%8d dtmpl=%12.4e\n",
0130 ntimemx, nychk, dnsmples, dtmpl);
0131 fprintf(np1,"-----\n");
0132 /*----- initialization ---*/
0133 for( i=1 ; i <= nychk ; i++ ) {
0134     cndns[i] = 0. ;
0135 }
0136 nsmpl = 0 ;
0137 /*----- equilibration -----*/
0138 /*----- The variables are initialized for saving the local number densities afterward. */
0139 /*----- The equilibration procedure is conducted below. */
0140 /*----- The particle positions at the next time step are calculated from Eq. (5.5). */
0141 /*----- The periodic BC is used for the x- and z-directions. */
0142 /*----- The elastic collision model at the boundary surface is used for the y-direction. */
0143 /*----- The forces acting on particles are calculated in the function forcecal. The random displacements are generated in the function randisp. */
0144 /*----- check of random numbers used ---*/
0145 if ( NRAN >= nranchk ) {
0146     rancall() ; NRAN = 1 ;
0147 }
0148 /*----- start of main loop -----*/
0149 /*----- The particle positions at the next time step are evaluated according to Eq. (5.5). */
0150 /*----- The periodic BC is used for the x- and z-directions. */
0151 /*----- The elastic collision model at the boundary surface is used for the y-direction. */
0152 rx1 = RX[i] + h*FX[i] + RXB[i] ;
0153 ry1 = RY[i] + h*FY[i] + RYB[i] ;
0154 rzi = RZ[i] + h*FZ[i] + RZB[i] ;
0155 rx1 += -rint( rx1/XL - 0.5 )*XL ;
0156 rzi += -rint( rzi/ZL - 0.5 )*ZL ;
0157 if( ry1 < 0. ) ry1 = -ry1 ;
0158 if( ry1 > YL ) ry1 = YL - ( ry1 - YL ) ;
0159 RX[i] = rx1 ;
0160 RY[i] = ry1 ;
0161 RZ[i] = rzi ;
0162 }
0163 forcecal( n, rcoff, rcoff2 ) ;
0164 randisp( n, h ) ;
0165 /*----- The number of the used random numbers is checked. If over nranchk, a uniform random number sequence is renewed. */
0166 /*----- The particle positions at the next time step are evaluated according to Eq. (5.5). */
0167 /*----- The periodic BC is used for the x- and z-directions. */
0168 /*----- The elastic collision model at the boundary surface is used for the y-direction. */
0169 /*----- The particle positions at the next time step are evaluated according to Eq. (5.5). */
0170 /*----- The periodic BC is used for the x- and z-directions. */
0171 /*----- The elastic collision model at the boundary surface is used for the y-direction. */
0172 /*----- The particle positions at the next time step are evaluated according to Eq. (5.5). */
0173 /*----- The periodic BC is used for the x- and z-directions. */
0174 /*----- The elastic collision model at the boundary surface is used for the y-direction. */
0175 /*----- The particle positions at the next time step are evaluated according to Eq. (5.5). */
0176 /*----- The periodic BC is used for the x- and z-directions. */
0177 /*----- The elastic collision model at the boundary surface is used for the y-direction. */
0178 for( i=1 ; i <= n ; i++ ) {
0179     FY[i] = FY[i] - RG ;
0180     rx1 = RX[i] + h*FX[i] + RXB[i] ;
0181     ry1 = RY[i] + h*FY[i] + RYB[i] ;
0182     rzi = RZ[i] + h*FZ[i] + RZB[i] ;
0183     rx1 += -rint( rx1/XL - 0.5 )*XL ;
0184     rzi += -rint( rzi/ZL - 0.5 )*ZL ;
0185     if( ry1 < 0. ) ry1 = -ry1 ;
0186     if( ry1 > YL ) ry1 = YL - ( ry1 - YL ) ;
0187 }
```

```

0189      RX[i] = rxi ;      • The forces acting on particles are calculated in the function forcecal.
0190      RY[i] = ryi ;      The random displacements are generated in the function randisp.
0191      RZ[i] = rzi ;
0192  }
0193 }                                     /*--- cal force ---*/
0194 forcecal( n , rcoff , rcoff2 ) ;    /*--- cal random displacement ---*/
0195 randisp( n , h ) ;
0196
0197 /*-----*/
0198
0199 /*-----*/
0200
0201 ndnscal( n , nychk , ychk , cndns ) ;  • The value divided by the sampling number
0202                                         yields its average value, and then the average
0203                                         value divided by the volume of one sliced piece
0204                                         gives rise to the number density ndens[*]
0205 if( (ntime % dnsmpl) == 0 ) {
0206   nsmpl += 1 ;
0207   for ( j=1 ; j<=nychk ; j++ ) {
0208     cndns[j] /= (double)dnsmpl ;
0209     ndens[j][nsmpl] = cndns[j] / (XL*ZL*ychk[1]) ;
0210     cndns[j] = 0. ;
0211   }
0212   /*--- data output for graphics (1) ---*/
0213   if( (ntime % ngraph) == 0 ) {
0214     inp += 1 ;
0215     fprintf(np[inp],"%d%10.3f%10.3f%10.3f\n", n, XL, YL, ZL ) ;
0216     for ( i=1 ; i<=n ; i++ ) {
0217       fprintf(np[inp],"%18.10e%18.10e%18.10e\n",
0218
0219     }
0220     fclose(np[inp]) ;  • The particle position data are written out at every ngraph time
0221   }                     steps for the postprocessing analysis.
0222   /*--- check of random numbers used ---*/
0223   if ( NRAN >= nranchk ) {  • The number of the used random numbers is checked. If over
0224     rancal() ; NRAN = 1 ;
0225   }
0226 }
0227
0228 /*-----*/
0229 /*----- end of main loop -----*/
0230 /*-----*/
0231
0232 fprintf(np1,"nsmpl=%8d dnsmpl=%8d dtsmpl=%12.4e\n",
0233                               nsmpl, dnsmpl, dtsmpl) ;
0234 for ( i= nsmpl/10 ; i<= nsmpl ; i += nsmpl/10 ) {
0235   fprintf(np1,"i=%8d time=%12.4e\n",
0236           i, dtsmpl*(double)i - dtsmpl/2. ) ;
0237   fprintf(np1,"ndens(1), ndens(2), ndens(3),...,ndens(nychk)\n" );
0238   for ( j=1 ; j<=nychk ; j += 10 ) {
0239     fprintf(np1,
0240             "%8.4f%8.4f%8.4f%8.4f%8.4f%8.4f%8.4f%8.4f%8.4f\n",
0241             ndens[j][i] , ndens[j+1][i], ndens[j+2][i], ndens[j+3][i],
0242             ndens[j+4][i], ndens[j+5][i], ndens[j+6][i], ndens[j+7][i],
0243             ndens[j+8][i], ndens[j+9][i] ) ;
0244   }
0245 }
0246 /*--- data output (2)---*/
0247 fprintf(np2,"%4d%8.5f%8.5f%8.4f%14.6e%14.6e%14.6e\n",
0248         n, ndens0, phai0, rcoff, h, XL, YL, ZL ) ;
0249 fprintf(np2,"%14.6e%14.6e%14.6e\n", RB, RG, RLJ ) ;
0250 fprintf(np2,"%8d%8d\n", ntimemx, nychk ) ;
0251 /*--- data output (3)---*/
0252 fprintf(np2,"%8d%8d%14.6e\n", nsmpl, dnsmpl, dtsmpl) ;
0253 for ( i= 1 ; i<=nsmpl ; i++ ) {
0254   fprintf(np2,"%8d%14.6e\n", i, dtsmpl*(double)i-dtsmpl/2) ;
0255   for ( j=1 ; j<=nychk ; j += 5 ) {
0256     fprintf(np2,"%12.4e%12.4e%12.4e%12.4e\n",
0257             ndens[j][i], ndens[j+1][i], ndens[j+2][i], ndens[j+3][i],
0258             ndens[j+4][i] ) ;
0259   }
0260 }
0261   fclose (np1) ;
0262   fclose (np2) ;
0263 }
0264 /*-----*/
0265 /*----- functions -----*/
0266 /*-----*/
0267 /*-----*/
0268 /*+++ fun iniposit +++*/

```

```

0269     iniposit( n , ndens )
0270
0271     double  ndens ;
0272     int      n ;
0273
0274     {   double  rxi, ryi, rzi, rx0, ry0, rz0 , c0 ;
0275       int      q , k , ix , iy , iz , iface ;
0276
0277       c0 = pow( (4./ndens) , (1./3.) ) ;
0278       q  = rint( pow( (double)(n/4) , (1./3.) ) ) ;
0279       XL = c0*(double)q ;
0280
0281       /*--- start ----*/
0282
0283       /*--- set initial positions ---*/
0284       k = 0 ;
0285       for( iface=1 ; iface<=4 ; iface++ ) {
0286
0287         if( iface == 1 ) {
0288           rx0 = 0.0001 ; ry0 = 0.0001 ; rz0 = 0.0001 ;
0289         } else if( iface == 2 ) {
0290           rx0 = c0/2. ; ry0 = c0/2. ; rz0 = 0.0001 ;
0291         } else if( iface == 3 ) {
0292           rx0 = c0/2. ; ry0 = 0.0001 ; rz0 = c0/2. ;
0293         } else {
0294           rx0 = 0.0001 ; ry0 = c0/2. ; rz0 = c0/2. ;
0295
0296         for( iz=0 ; iz <= q-1 ; iz++ ) {
0297           rzi = (double)iz*c0 + rz0 ;
0298           if( rzi >= XL ) break ;
0299           for( iy=0 ; iy <= q-1 ; iy++ ) {
0300             ryi = (double)iy*c0 + ry0 ;
0301             if( ryi >= XL ) break ;
0302             for( ix=0 ; ix <= q-1 ; ix++ ) {
0303               rxi = (double)ix*c0 + rx0 ;
0304               if( rxi >= XL ) break ;
0305
0306               k += 1 ;
0307               RX[k] = rxi ; RY[k] = ryi ; RZ[k] = rzi ;
0308
0309             }
0310           }
0311         }
0312     /*+++ fun gridcal +++*/
0313     gridcal( nychk, ychk )
0314
0315     int      nychk ;
0316     double  ychk[NN] ;
0317
0318     {   double  cl ;
0319       int      i ;
0320
0321       cl = YL/(double)nychk ;
0322       for( i=1 ; i<= nychk ; i++ ) {
0323         ychk[i] = cl * (double)i ;
0324       }
0325     /*+++ ndnsscal +++*/
0326     ndnsscal( n, nychk, ychk, cndns )
0327
0328     int      n , nychk ;
0329     double  ychk[NN], cndns[NN] ;
0330
0331     {   int    i, j ;
0332
0333       for( i=1 ; i<=n      ; i++ ) {
0334         for( j=1 ; j<=nychk ; j++ ) {
0335           if( ychk[j] >= RY[i] ) {
0336             cndns[j] += 1. ;
0337             goto L2 ;
0338           }
0339         }
0340         cndns[nychk] += 1. ;
0341       L2:   continue ;
0342     }
0343
0344     /*+++ forcecal +++*/
0345     forcecal( n, rcoff, rcoff2 )
0346
0347     double  rcoff, rcoff2 ;
0348     int      n ;
0349   }

```

• A function for setting the initial particle positions.

•  $n^* = 4/a^3$ ,  $a^* = (4/n^*)^{1/3}$ , and  $Q = (N/4)^{1/3}$ .  $a^*$  and  $Q$  are saved in the variables  $c0$  and  $q$ , respectively.

• The particles are placed in the face-centered cubic lattice formation shown in Figure 2.2(B).  
 • The four ways of setting provides this initial formation of particles.  
 • Each particle is moved in parallel by a small distance 0.0001 to remove subtle situations at outer boundary surfaces.

• In order to evaluate the local number densities, the simulation box is divided into equal volumes sliced in the  $y$ -direction.  
 • The  $y$ -axis side length of each volume is  $YL/nychk$ , in which  $nychk$  is the number of the sliced volumes.

• The number of the particles belonging to each volume is calculated in order to evaluate the local number density.  
 • The later procedure of dividing  $cndns[*]$  by the volume, leading to the number density of particles.

• A function for calculating the forces acting on particles.

```

0350     double rxi , ryi , rzi , rxij , ryij , rzijsq ;
0351     double fxi , fyi , fzi , fxij , fyij , fzij , fij ;
0352     double sr2 , sr6 , sr12 ;
0353     int i , j ;
0354
0355     for ( i=1 ; i<=n ; i++ ) {
0356         FX[i] = 0. ; FY[i] = 0. ; FZ[i] = 0. ;
0357     }
0358
0359     for ( i=1 ; i<=n-1 ; i++ ) {
0360
0361         rxi = RX[i] ; ryi = RY[i] ; rzi = RZ[i] ;
0362         fxi = FX[i] ; fyi = FY[i] ; fzi = FZ[i] ;
0363
0364         for ( j=i+1 ; j<=n ; j++ ) {
0365
0366             rxij = rxi - RX[j] ;
0367             rxij += - rint(rxij/XL)*XL ;
0368             if( fabs(rxij) >= rcoff ) goto L10 ;
0369             ryij = ryi - RY[j] ;
0370             ryij += - rint(ryij/YL)*YL ;
0371             if( fabs(ryij) >= rcoff ) goto L10 ;
0372             rzijsq= rxijsq ;
0373             rzijsq = rxij*rxij + ryij*ryij + rzijsq ;
0374             if( rzijsq >= rcoff2 ) goto L10 ;
0375
0376             rzijsq= rxij*rxij + ryij*ryij + rzijsq ;
0377             if( rzijsq >= rcoff2 ) goto L10 ;
0378
0379             sr2 = 1./rzijsq ; sr6 = sr2*sr2*sr2 ; sr12 = sr6*sr6 ;
0380             fij = ( 2.*sr12 - sr6 )/rzijsq ;
0381             fxij = fij*rxij ;
0382             fyij = fij*ryij ;
0383             fzij = fij*rzijsq ;
0384             fxi += fxij ;
0385             fyi += fyij ;
0386             fzi += fzij ;
0387
0388             FX[j] += - fxij ;
0389             FY[j] += - fyi ;
0390             FZ[j] += - fzi ;
0391
0392 L10:    continue ;
0393 }
0394
0395     FX[i] = fxi ;
0396     FY[i] = fyi ;
0397     FZ[i] = fzi ;
0398
0399 }
0400
0401     for( i=1 ; i<= n ; i++ ) {
0402         FX[i] *= RLJ*24. ;
0403         FY[i] *= RLJ*24. ;
0404         FZ[i] *= RLJ*24. ;
0405     }
0406 }
0407 /*+++ randisp +++*/
0408 randisp( n , h )
0409
0410     int n ;
0411     double h ;
0412 {
0413     double ran1, ran2 ;
0414     int i , j ;
0415
0416     for ( i=1 ; i<= n ; i++ ) {
0417         NRAN += 1 ;
0418         ran1 = (double)( RAN[NRAN] ) ;
0419         NRAN += 1 ;
0420         ran2 = (double)( RAN[NRAN] ) ;
0421         RXB[i] = pow( -2.* (2.*h*RB)*log(ran1) , 0.5 ) * cos(2.*PI*ran2) ;
0422         /*--- random disp x ---*/
0423
0424         NRAN += 1 ;
0425         ran1 = (double)( RAN[NRAN] ) ;

```

• The variables for saving forces are initialized.

• The consideration of the action-reaction law enables us to calculate only the pairs of particles satisfying  $i < j$ .

• The treatment of the periodic BC.  
• If the two particles are separated over the cutoff distance  $r_{\text{coff}}$ , the calculation is unnecessary.

• The forces acting on particles are calculated according to Eq. (5.9); the constant 24 is multiplied in the later procedure.  
• The action-reaction law can provide the force acting on particle  $j$  as  $(-f_{xij}, -f_{yij}, -f_{zij})$ .

• The random displacements can be generated from Eq. (A2.3) with the variance of the right-hand side term in Eq. (5.7).

```

0426      NRAN += 1 ;
0427      ran2 = (double)( RAN[NRAN] ) ;
0428      RYB[i] = pow( -2.*(2.*h*RB)*log(ran1) , 0.5 ) * cos(2.*PI*ran2);
0429      /*--- random disp z ---*/
0430      NRAN += 1 ;
0431      ran1 = (double)( RAN[NRAN] ) ;
0432      NRAN += 1 ;
0433      ran2 = (double)( RAN[NRAN] ) ;
0434      RZB[i] = pow( -2.*(2.*h*RB)*log(ran1) , 0.5 ) * cos(2.*PI*ran2);
0435  }
0436 }
0437 /*--- rancal ---*/
0438 rancal()
0439 {
0440   float aintegmx ;
0441   int integmx, integst, integ ;
0442   int i ;
0443
0444   integmx = 2147483647 ;
0445   integst = 584287 ;
0446   integ = 48828125 ;
0447
0448   aintegmx = (float)integmx ;
0449
0450   if ( IX == 0 ) IX = integst ;
0451   for (i=1 ; i<NRANMX ; i++ ) {
0452     IX *= integ ;
0453     if (IX < 0 ) IX = (IX+integmx)+1 ;
0454     RAN[i] = (float)IX/aintegmx ;
0455   }
0456 }
```

• A function for generating a uniform random number sequence.

• This is for a 32-bit CPU based on the expression of two's complement.

# 6 Practice of Dissipative Particle Dynamics Simulations

In this chapter we consider an alternative microsimulation method called the dissipative particle dynamics (DPD) method,” which is also available for simulating a particle suspension system. In the DPD method [4–8], the fluid is assumed to be composed of virtual fluid particles called “dissipative particles,” and therefore the solution of a flow field can be obtained from the motion of the dissipative particles in a way similar to the MD method. A significant advantage of this method is that when it is applied to the simulation of a particle suspension, the multibody hydrodynamic interaction is taken into account without introducing a special technique. This characteristic of the DPD method provides it with a great potential as a simulation tool for particle suspensions; the present method is thus available for various fields of scientific research, including the pharmaceutical sciences and specialized engineering fields. The sample simulation program is written in the FORTRAN programming language.

## 6.1 Aggregation Phenomena of Magnetic Particles

For our example, a system composed of  $N$  magnetic particles with mass  $m$  dispersed in a base liquid is assumed to be in thermodynamic equilibrium. The main objective of the present exercise is to discuss the feasibility of the DPD method for successfully capturing the aggregate formations of the magnetic particles, which are dependent on the strength of magnetic particle–particle interactions. It is important to note that in the present demonstration we assume the applied magnetic field to be very strong, so that we only need to consider the translational motion of magnetic particles. The rotational motion may be neglected.

## 6.2 Specification of Problems in Equations

### 6.2.1 Kinetic Equation of Dissipative Particles

A ferromagnetic colloidal suspension is composed of ferromagnetic particles and the molecules of a base liquid. If a base liquid is regarded as being composed of dissipative particles, the motion of magnetic particles is governed by the interaction with both the other magnetic particles and the ambient dissipative particles. In the following, we show the kinetic equation for the dissipative particles.

Three kinds of forces act on dissipative particle  $i$ : a repulsive conservative force  $\mathbf{F}_{ij}^C$ , exerted by the other particles; a dissipative force  $\mathbf{F}_{ij}^D$ , providing a viscous drag to the system; and a random or stochastic force  $\mathbf{F}_{ij}^R$ , inducing the thermal motion of particles. The force acting on the dissipative particles by magnetic particles is not taken into account in this subsection, since that force will be addressed later. The equation of motion of particle  $i$  is therefore written as

$$m_d \frac{d\mathbf{v}_i}{dt} = \sum_{j(j \neq i)} \mathbf{F}_{ij}^C + \sum_{j(j \neq i)} \mathbf{F}_{ij}^D + \sum_{j(j \neq i)} \mathbf{F}_{ij}^R \quad (6.1)$$

in which

$$\mathbf{F}_{ij}^D = -\gamma w_D(r_{ij})(\mathbf{e}_{ij} \cdot \mathbf{v}_{ij})\mathbf{e}_{ij}, \quad \mathbf{F}_{ij}^R = \sigma w_R(r_{ij})\mathbf{e}_{ij}\zeta_{ij}, \quad \mathbf{F}_{ij}^C = \alpha w_R(r_{ij})\mathbf{e}_{ij} \quad (6.2)$$

In these equations,  $m_d$  is the mass of particle  $i$ , and  $\mathbf{v}_i$  is the velocity. Regarding the use of subscripts, as an example,  $\mathbf{F}_{ij}^C$  is the force acting on particle  $i$  by particle  $j$ . Moreover,  $\alpha$ ,  $\gamma$ , and  $\sigma$  are constants representing the strengths of the repulsive, the dissipative, and the random forces, respectively. The weight functions  $w_D(r_{ij})$  and  $w_R(r_{ij})$  are introduced such that the interparticle force decreases with increasing particle–particle separation. The expression for  $w_R(r_{ij})$  is written as

$$w_R(r_{ij}) = \begin{cases} 1 - \frac{r_{ij}}{d_c} & \text{for } r_{ij} \leq d_c \\ 0 & \text{for } r_{ij} > d_c \end{cases} \quad (6.3)$$

The weight functions  $w_D(r_{ij})$  and  $w_R(r_{ij})$ , as well as  $\gamma$  and  $\sigma$ , must satisfy the following relationships, respectively:

$$w_D(r_{ij}) = w_R^2(r_{ij}), \quad \sigma^2 = 2\gamma kT \quad (6.4)$$

In the above equations,  $d_c$  is the apparent diameter of dissipative particles,  $\mathbf{r}_{ij}$  is the relative position ( $r_{ij} = |\mathbf{r}_{ij}|$ ), given by  $\mathbf{r}_{ij} = \mathbf{r}_i - \mathbf{r}_j$ ;  $\mathbf{e}_{ij}$  is the unit vector denoting the direction of particle  $i$  relative to particle  $j$ , expressed as  $\mathbf{e}_{ij} = \mathbf{r}_{ij}/r_{ij}$ ;  $\mathbf{v}_{ij}$  is the relative velocity, expressed as  $\mathbf{v}_{ij} = \mathbf{v}_i - \mathbf{v}_j$ ;  $k$  is Boltzmann's constant; and  $T$  is the liquid temperature. Also,  $\zeta_{ij}$  is a random variable inducing the random motion of the particles.

If Eq. (6.1) is integrated with respect to time over a small time interval  $\Delta t$  from  $t$  to  $t + \Delta t$ , then the finite difference equations governing the particle motion in simulations can be obtained as

$$\Delta\mathbf{r}_i = \mathbf{v}_i \Delta t \quad (6.5)$$

$$\begin{aligned} \Delta\mathbf{v}_i &= \frac{\alpha}{m_d} \sum_{j(j \neq i)} w_R(r_{ij})\mathbf{e}_{ij}\Delta t - \frac{\gamma}{m_d} \sum_{j(j \neq i)} w_R^2(r_{ij})(\mathbf{e}_{ij} \cdot \mathbf{v}_{ij})\mathbf{e}_{ij}\Delta t \\ &\quad + \frac{(2\gamma kT)^{1/2}}{m_d} \sum_{j(j \neq i)} w_R(r_{ij})\mathbf{e}_{ij}\theta_{ij}\sqrt{\Delta t} \end{aligned} \quad (6.6)$$

in which  $\theta_{ij}$  is the stochastic variable that must satisfy the following stochastic properties:

$$\langle \theta_{ij} \rangle = 0, \quad \langle \theta_{ij} \theta_{i'j'} \rangle = (\delta_{ii'} \delta_{jj'} + \delta_{ij'} \delta_{ji'}) \quad (6.7)$$

in which  $\delta_{ij}$  is the Kronecker delta. During the simulation, the stochastic variable  $\theta_{ij}$  is sampled from a uniform or normal distribution with zero average value and unit variance.

### 6.2.2 Model of Particles

A magnetic particle is idealized as a spherical particle with a central point dipole and is coated with a uniform steric layer (or surfactant layer). Using the notation  $d_s$  for the diameter of the particle,  $\delta$  for the thickness of the steric layer, and  $d (=d_s + 2\delta)$  for the diameter, including the steric layer, then the magnetic interaction energy between particles  $i$  and  $j$ ,  $u_{ij}^{(m)}$ , and the particle–field interaction energy,  $u_i^{(H)}$ , and the interaction energy arising due to the overlap of the steric layers,  $u_{ij}^{(V)}$ , are expressed, respectively, as [31]

$$u_{ij}^{(m)} = \frac{\mu_0}{4\pi r_{ij}^3} \{ \mathbf{m}_i \cdot \mathbf{m}_j - 3(\mathbf{m}_i \cdot \mathbf{t}_{ij})(\mathbf{m}_j \cdot \mathbf{t}_{ij}) \} \quad (6.8)$$

$$u_i^{(H)} = -\mu_0 \mathbf{m}_i \cdot \mathbf{H} \quad (6.9)$$

$$u_{ij}^{(V)} = kT\lambda_V \left\{ 2 - \frac{2r_{ij}/d_s}{t_\delta} \ln \left( \frac{d}{r_{ij}} \right) - 2 \frac{r_{ij}/d_s - 1}{t_\delta} \right\} \quad (6.10)$$

in which  $\mu_0$  is the permeability of free space,  $\mathbf{m}_i$  is the magnetic moment ( $m_0 = |\mathbf{m}_i|$ ),  $\mathbf{t}_{ij}$  is the unit vector given by  $\mathbf{r}_{ij}/r_{ij}$ ,  $\mathbf{r}_{ij} = \mathbf{r}_i - \mathbf{r}_j$ ,  $r_{ij} = |\mathbf{r}_{ij}|$ ,  $\mathbf{H}$  is the applied magnetic field ( $H = |\mathbf{H}|$ ), and  $t_\delta$  is the ratio of the thickness of the steric layer  $\delta$  to the radius of the solid part of the particle, equal to  $2\delta/d_s$ . The nondimensional parameter  $\lambda_V$ , appearing in Eq. (6.10), represents the strength of the steric particle–particle interaction relative to the thermal energy, expressed as  $\lambda_V = \pi d_s^2 n_s / 2$ , in which  $n_s$  is the number of surfactant molecules per unit area on the particle surface.

From Eqs. (6.8) and (6.10), the forces acting on particle  $i$  are derived as

$$\mathbf{F}_{ij}^{(m)} = -\frac{3\mu_0}{4\pi r_{ij}^4} [ -(\mathbf{m}_i \cdot \mathbf{m}_j) \mathbf{t}_{ij} + 5(\mathbf{m}_i \cdot \mathbf{t}_{ij})(\mathbf{m}_j \cdot \mathbf{t}_{ij}) \mathbf{t}_{ij} - \{ (\mathbf{m}_j \cdot \mathbf{t}_{ij}) \mathbf{m}_i + (\mathbf{m}_i \cdot \mathbf{t}_{ij}) \mathbf{m}_j \} ] \quad (6.11)$$

$$\mathbf{F}_{ij}^{(V)} = \frac{kT\lambda_V}{\delta} \cdot \frac{\mathbf{r}_{ij}}{r_{ij}} \ln \left( \frac{d}{r_{ij}} \right) \quad (d_s \leq d_{ij} \leq d) \quad (6.12)$$

In addition to these forces, the forces due to dissipative particles have to be taken into account, but are not treated here, since they will be addressed in the following subsection.

The motion of magnetic particles is specified by Newton's equations and are discretized in time to obtain the finite difference equations governing the particle motion in simulations:

$$\Delta \mathbf{r}_i = \mathbf{v}_i \Delta t \quad (6.13)$$

$$\Delta \mathbf{v}_i = \sum_{j(\neq i)} \mathbf{F}_{ij} \Delta t / m_m \quad (6.14)$$

in which  $m_m$  is the mass of magnetic particles and  $\mathbf{F}_{ij} = \mathbf{F}_{ij}^{(m)} + \mathbf{F}_{ij}^{(V)}$ .

### 6.2.3 Model Potential for Interactions Between Dissipative and Magnetic Particles

Each colloidal particle is modeled as a group of dissipative particles. In the ordinary application of the method, the interaction of a magnetic particle with the ambient dissipative particles is treated as the interaction between the ambient dissipative particles and the constituent dissipative particles of the magnetic particle. However, in a real dispersion, the interaction between colloidal particles and the solvent molecules should depend on the characteristics of the dispersion of interest. Such interactions are strongly dependent on the ratio of the mass and the diameter of the colloidal particles to that of solvent molecules together with the properties of the interaction potential.

Therefore, instead of regarding a colloidal particle as a group of dissipative particles, it may be possible to use a model potential to describe the interaction between the magnetic and the ambient dissipative particles.

The simplest potential model may be the hard sphere potential, in which magnetic particles are regarded as a hard sphere and dissipative particles are elastically reflected on the contact with a magnetic particle. Another simple potential model may be the Lennard-Jones potential. Although the present exercise adopts the latter model potential and attempts to discuss its validity, the simple form of the Lennard-Jones potential based on each particle center may cause a nonphysical overlap. Hence, as shown in Figure 6.1, we consider an inscribed sphere with the same diameter as the dissipative particles, which is located on the line connecting each center of dissipative and magnetic particle. The Lennard-Jones potential is then employed using the inscribed particle and dissipative particles such that the interaction energy  $u_{ip}$  for dissipative particle  $p$  and magnetic particle  $i$  is expressed as

$$u_{ip} = 4\epsilon \left\{ \left( \frac{d_c}{r_{ip}} \right)^m - \left( \frac{d_c}{r_{ip}'} \right)^n \right\} \quad (6.15)$$

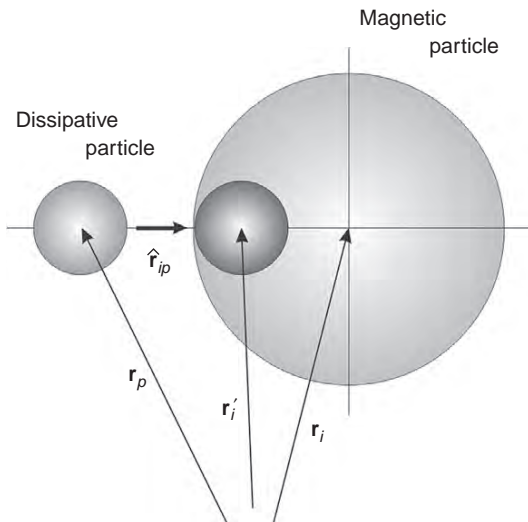


**Figure 6.1** Model of the interaction between magnetic and dissipative particles.

in which  $\varepsilon$  is a constant representing the strength of such an interaction,  $\mathbf{r}_{ip}' = \mathbf{r}_i' - \mathbf{r}_p$ ,  $r_{ip}' = |\mathbf{r}_{ip}'|$ ,  $\mathbf{r}_i$  is the position vector of the center of magnetic particle  $i$ ,  $\mathbf{r}_p$  is similarly the position vector of dissipative particle  $p$ , and  $\mathbf{r}_i'$  is the position vector of the inscribed sphere. The expression for  $\mathbf{r}_i'$  is written as

$$\mathbf{r}_i' = \mathbf{r}_i - (d - d_c/2)\hat{\mathbf{r}}_{ip} \quad (6.16)$$

in which  $\hat{\mathbf{r}}_{ip} = \mathbf{r}_{ip}/r_{ip}$ ,  $\mathbf{r}_{ip} = \mathbf{r}_i - \mathbf{r}_p$ , and  $r_{ip} = |\mathbf{r}_{ip}|$ . If we set  $m = 12$  and  $n = 6$  in Eq. (6.15), the model potential leads to the well-known Lennard-Jones 12–6 potential, and this potential is employed in the present simulation.

From the expression of the interaction energy in Eq. (6.15), the force acting on dissipative particle  $p$  by magnetic particle  $i$ ,  $\mathbf{F}_{ip}^{(\text{int})}$  is derived as

$$\mathbf{F}_{ip}^{(\text{int})} = 4n\varepsilon \left\{ \frac{m}{n} \left( \frac{d_c}{r_{ip}'} \right)^m - \left( \frac{d_c}{r_{ip}'} \right)^n \right\} \frac{\hat{\mathbf{r}}_{ip}}{r_{ip}'} \quad (6.17)$$

#### 6.2.4 Nondimensionalization of the Equation of Motion and Related Quantities

For the nondimensionalization of each quantity, the following representative values are used:  $d$  for distances,  $m_m$  for masses,  $kT$  for energies,  $(kT/m_m)^{1/2}$  for velocities,  $d(m_m/kT)^{1/2}$  for time,  $kT/d$  for forces, and so forth. With these representative values, Eqs. (6.5) and (6.6) are nondimensionalized as

$$\Delta \mathbf{r}_i^* = \mathbf{v}_i^* \Delta t^* \quad (6.18)$$

$$\begin{aligned}\Delta \mathbf{v}_i^* = & \frac{1}{m_d^* d_c^*} \alpha^* \sum_{j \neq i} w_R(r_{ij}^*) \mathbf{e}_{ij} \Delta t^* - \frac{1}{(m_d^*)^{1/2} d_c^*} \gamma^* \sum_{j \neq i} w_R^2(r_{ij}^*) (\mathbf{e}_{ij} \cdot \mathbf{v}_{ij}^*) \mathbf{e}_{ij} \Delta t^* \\ & - \frac{1}{(m_d^*)^{3/4} d_c^{*1/2}} (2\gamma^*)^{1/2} \sum_{j \neq i} w_R(r_{ij}^*) \mathbf{e}_{ij} \theta_{ij} \sqrt{\Delta t^*} - \frac{1}{m_d^*} \sum_k \mathbf{F}_{ki}^{(\text{int})*} \Delta t^*\end{aligned}\quad (6.19)$$

in which

$$w_R(r_{ij}^*) = \begin{cases} 1 - r_{ij}^*/d_c^* & \text{for } r_{ij}^*/d_c^* \leq 1 \\ 0 & \text{for } r_{ij}^*/d_c^* > 1 \end{cases} \quad (6.20)$$

$$\alpha^* = \alpha \frac{d_c}{kT}, \quad \gamma^* = \gamma \frac{d_c}{(m_d kT)^{1/2}} \quad (6.21)$$

In the above equations, the superscript \* indicates the nondimensionalized quantities. Note that Eq. (6.19) includes the forces due to the interaction with magnetic particles, described in Section 6.2.3.

Similarly, the nondimensional form of Eqs. (6.13), (6.14), (6.11), and (6.12) are expressed as

$$\Delta \mathbf{r}_i^* = \mathbf{v}_i^* \Delta t^* \quad (6.22)$$

$$\Delta \mathbf{v}_i^* = \sum_{j \neq i} \mathbf{F}_{ij}^* \Delta t^* + \sum_p \mathbf{F}_{ip}^{(\text{int})*} \Delta t^* \quad (6.23)$$

$$\mathbf{F}_{ij}^{(\text{m})*} = -3\lambda \frac{1}{r_{ij}^{4*}} [-(\mathbf{n}_i \cdot \mathbf{n}_j) \mathbf{t}_{ij} + 5(\mathbf{n}_i \cdot \mathbf{t}_{ij})(\mathbf{n}_j \cdot \mathbf{t}_{ij}) \mathbf{t}_{ij} - \{(\mathbf{n}_j \cdot \mathbf{t}_{ij}) \mathbf{n}_i + (\mathbf{n}_i \cdot \mathbf{t}_{ij}) \mathbf{n}_j\}] \quad (6.24)$$

$$\mathbf{F}_{ij}^{(\text{V})*} = \lambda_V \frac{1}{t_\delta^*} \cdot \mathbf{t}_{ij} \ln\left(\frac{1}{r_{ij}^{*s}}\right) \quad (d_s^* \leq r_{ij}^* \leq 1) \quad (6.25)$$

in which  $\mathbf{F}_{ij}^* = \mathbf{F}_{ij}^{(\text{m})*} + \mathbf{F}_{ij}^{(\text{V})*}$ ,  $\mathbf{n}_i$  is the unit vector denoting the direction of the magnetic moment  $\mathbf{m}_i$ , expressed as  $\mathbf{n}_i = \mathbf{m}_i/m_0$  ( $m_0 = |\mathbf{m}_i|$ ). The nondimensional parameter  $\lambda$  in Eq. (6.24) is the strength of magnetic particle interactions relative to the thermal energy, expressed as  $\lambda = \mu_0 m_0^2 / 4\pi d^3 kT$ . A slightly different parameter  $\lambda_s = (d/d_s)^3 \lambda$  ( $= \mu_0 m_0^2 / 4\pi d_s^3 kT$ ), which is defined based on the diameter of the solid part, will be useful in order to compare the present results with the previous MC and BD simulations.

The expression of the force between a dissipative and a magnetic particle is written in nondimensional form as

$$\mathbf{F}_{ip}^* = \lambda_\varepsilon \left\{ \frac{m}{n} \left( \frac{d_c^*}{r_{ip}^{*\prime}} \right)^m - \left( \frac{d_c^*}{r_{ip}^{*\prime}} \right)^n \right\} \frac{\hat{\mathbf{r}}_{ip}}{r_{ip}^{*\prime}/d_c^*} \quad (6.26)$$

in which  $\lambda_\varepsilon$  is a nondimensional parameter representing the strength of the interaction, expressed as  $\lambda_\varepsilon = 4n\varepsilon/(kT d_c^*)$ .

In the present simulation we consider a two-dimensional system in thermodynamic equilibrium, and therefore the relationship between the system temperature and the mean kinetic energy of one dissipative particle is expressed from the equipartition law of energies as

$$\frac{1}{2} m_d v_d^2 = 2 \frac{kT}{2} \quad (6.27)$$

From this equation, the mean square velocity of dissipative particles  $\overline{v_d^{*2}}$  is written as

$$\overline{v_d^{*2}} = 2/m_d^* \quad (6.28)$$

Similarly, the mean square velocity of magnetic particles  $\overline{v_m^{*2}}$  is expressed as

$$\overline{v_m^{*2}} = 2 \quad (6.29)$$

The number density of dissipative particles is nondimensionalized as

$$n_d^* = n_d d^2 = n_d d_c^2 (d/d_c)^2 = \hat{n}_d^*/d_c^2 \quad (6.30)$$

In addition to  $n_d^*$ , the nondimensional density  $\hat{n}_d^*$  based on the diameter of dissipative particles may be useful for quantifying the packing characteristics of the dissipative particles. The nondimensional number density of magnetic particles is expressed as  $n_m^* = n_m d^2$ .

### 6.3 Parameters for Simulations

In this chapter, we are considering a two-dimensional dispersion composed of ferromagnetic particles in order to investigate the validity of using the method for this type of problem. The equations of motion of a dissipative particle include many indefinite factors, so we have chosen to focus on a simplified case in which the external magnetic field is strong enough that we may neglect the rotational motion of magnetic particles. In this situation, each magnetic moment will point along the magnetic field direction. Also, we will only focus on the one specific model potential of  $(m,n) = (12,6)$ . Representative parameters used for the present simulations are  $\gamma^* = 10$ ,  $\alpha^* = \gamma^*/10$ ,  $m_d^* = 0.01$ ,  $d_c^* = 0.4$ ,  $\lambda_\varepsilon = 10$ ,  $\hat{n}_d^* = 1$ , and  $\Delta t^* = 0.0001$ .

Eq. (6.19) shows that the displacement distance of a dissipative particle per unit time step becomes greater with decreasing values of  $m_d^*$  and  $d_c^*$ , and for this reason the time interval  $\Delta t^*$  will be adjusted in proportion to the product of  $m_d^*$  and  $d_c^*$ . In this way, a smaller value of the time interval is employed as the value of  $m_d^* d_c^*$  decreases. The total number of simulation steps,  $N_{\text{timemx}}$ , is expected to be sufficient when the condition of  $\Delta t^* N_{\text{timemx}} = 100$  is satisfied.

## 6.4 Results of Simulations

We treat a multiparticle system with the number density of  $n_m^* \simeq 0.4$ , composed of 81 magnetic particles, to investigate the influence of the mass of dissipative particles on the aggregate structures. Figure 6.2 illustrates the results for aggregate structures in thermodynamic equilibrium for two cases of magnetic particle–particle interactions,  $\lambda_s = 10$  and 3. Unless specifically noted, all simulation results were obtained for the case of  $d_c^* = 0.4$  using the other representative values of the parameters given in Section 6.3. Figures 6.2A and B are for a value of the mass of dissipative particles,  $m_d^* = 0.05$ . Figures 6.2C and D are for  $m_d^* = 0.01$ . Figures 6.2E and F are for  $m_d^* = 0.005$ . Figures 6.2A, C, and E were obtained for  $\lambda_s = 10$ . Figures 6.2B, D, and F are for  $\lambda_s = 3$ . In the figures, small and large circles indicate the dissipative and magnetic particles, respectively.

Since the magnetic particle–particle interaction is much more dominant than the thermal energy for  $\lambda_s = 10$ , magnetic particles tend to aggregate to form chain-like clusters along the magnetic field direction, which was clearly shown in the

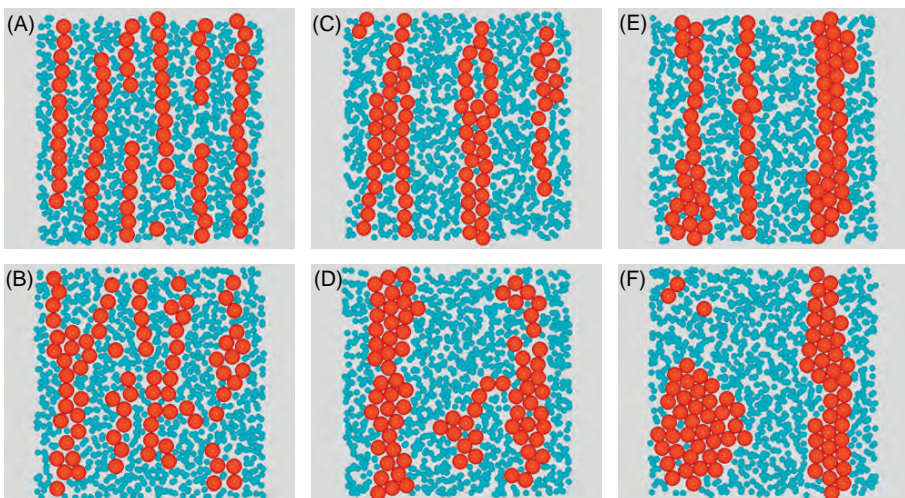


**Figure 6.2** Influence of the particle mass  $m_d^*$  on the aggregate structures for  $d_c^* = 0.4$ : (A) for  $m_d^* = 0.05$  and  $\lambda_s = 10$ , (B) for  $m_d^* = 0.05$  and  $\lambda_s = 3$ , (C) for  $m_d^* = 0.01$  and  $\lambda_s = 10$ , (D) for  $m_d^* = 0.01$  and  $\lambda_s = 3$ , (E) for  $m_d^* = 0.005$  and  $\lambda_s = 10$ , and (F) for  $m_d^* = 0.005$  and  $\lambda_s = 3$ .

previous MC simulations. As shown in Figures 6.2A, C, and E, the present DPD simulation results also reproduce this type of cluster formation well. However, the aggregate structures seem to be strongly dependent on the mass of the dissipative particles. That is, although only thin chain-like clusters are formed for the case of a relatively large mass, such as  $m_d^* = 0.05$ , magnetic particles form thicker chain-like clusters with decreasing values of the particle mass.

Now, we consider why much thicker chain-like clusters tend to form with decreasing mass of the dissipative particles. If the mass of dissipative particles is small, the magnetic particles should move easily by separating the ambient dissipative particles so they can force a path and approach each other. The thin chain-like clusters shown in Figure 6.2A, therefore, have a sufficient probability to aggregate to form the thicker chain-like clusters shown in Figure 6.2E. On the other hand, Eq. (6.28) shows that dissipative particles with smaller mass move with larger average velocity for a given system temperature. Hence, although a chain-like cluster can thicken to a certain degree, after that further growth is limited by the Brownian motion of the magnetic particles due to the influence of the active motion of dissipative particles. Since the magnetic particle–particle interaction is of a slightly larger order than the thermal energy for the case of  $\lambda_s = 3$ , significant aggregates should not be formed. However, the present DPD simulations exhibit significant cluster formation with decreasing mass of dissipative particles; such unexpected aggregate formation is significant for  $m_d^* = 0.005$ , and we also find that relatively long chain-like clusters are formed even for the case of  $m_d^* = 0.05$ . In order to explain these results, the first consideration must be that we do not use an equation of motion which can simulate the rotational motion of the magnetic particles, although the transnational motion is taken into account in the present exercise. Another consideration must be the model potential we have employed for the interaction between the magnetic and the dissipative particles.

For reference, the aggregate structures for  $d_c^* = 0.2$  are shown in Figure 6.3 under the same conditions as in Figure 6.2 except for the particle diameter. We here focus on the differences between the aggregate structures in Figures 6.2 and 6.3 without addressing the features of each aggregate structure in detail. The aggregates in Figure 6.3 have a more compact or denser internal structure, and it appears that large clusters are formed to a certain degree but do not grow any further. It seems as if the Brownian motion of the magnetic particles due to the interaction with the dissipative particles is not significant. The snapshot in Figure 6.3F also shows aggregates with a dense internal structure, and the effect of the particle Brownian motion does not appear significantly in the formation of these internal structures.

Finally, we consider what the appropriate mass of a dissipative particle should be for obtaining physically reasonable results. As pointed out previously, dissipative particles are virtual and regarded as groups or clusters of the real solvent molecules, so that it seems to be reasonable for the mass density of dissipative particles to be taken as roughly equal to the mass density of the base liquid of the dispersion system, which one must consider for evaluating physical quantities experimentally. In the present demonstration, for example, we consider a ferromagnetic colloidal

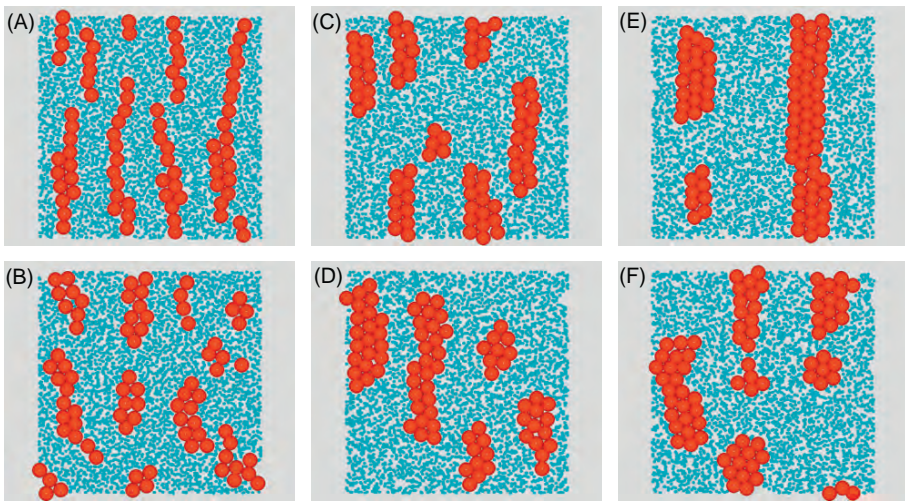


**Figure 6.3** Influence of the particle mass  $m_d^*$  on aggregate structures for  $d_c^* = 0.2$ : (A) for  $m_d^* = 0.05$  and  $\lambda_s = 10$ , (B) for  $m_d^* = 0.05$  and  $\lambda_s = 3$ , (C) for  $m_d^* = 0.01$  and  $\lambda_s = 10$ , (D) for  $m_d^* = 0.01$  and  $\lambda_s = 3$ , (E) for  $m_d^* = 0.005$  and  $\lambda_s = 10$ , and (F) for  $m_d^* = 0.005$  and  $\lambda_s = 3$ .

dispersion in which metallic ferromagnetic fine particles are assumed to be dispersed into a base liquid, such as kerosene or water. In this case, if the ratio of the mass density of magnetic particles to dissipative ones is regarded as 5–8, then the ratio of mass is 0.013–0.008 for  $d_c^* = 0.4$ , and 0.0016–0.001 for  $d_c^* = 0.2$ . Hence, it is for the case of  $d_c^* = 0.4$  and  $m_d^* = 0.01$  that physically reasonable aggregate structures can be regarded as being reproduced. This consideration is verified by comparing it with the results obtained by MC and BD simulations.

In addition to the previous discussion, it may be necessary to verify that the aggregate formation is truly induced by the magnetic interaction between magnetic particles in a physically reasonable manner and not by certain false mechanisms arising from the improper interaction between dissipative and magnetic particles. Figure 6.4A and B show the results that were obtained for the strength of magnetic interaction  $\lambda_s = 0$  by using the aggregate structures in Figures 6.2C and 6.3C as an initial configuration. Since the snapshot in Figure 6.4B from an initial configuration in Figure 6.3C for  $d_c^* = 0.2$  and  $m_d^* = 0.01$  exhibits the formation of large aggregates, we may conclude that this case does not give rise to physically reasonable results. In contrast, for the case of an initial configuration in Figure 6.2C for  $d_c^* = 0.4$  and  $m_d^* = 0.01$ , Figure 6.4A shows that the thick chain-like clusters, formed in the field direction, are dissociated sufficiently. However, a large aggregate (i.e., not chain-like) still remains, although the internal structure of this aggregate is considerably looser. The dissociation of the chain-like clusters indicates that the Brownian motion has been sufficiently effective. On the other hand, this type of loose aggregate structure of magnetic particles may be the result of employing a kinetic equation without including the rotational motion, as adopted here, or from

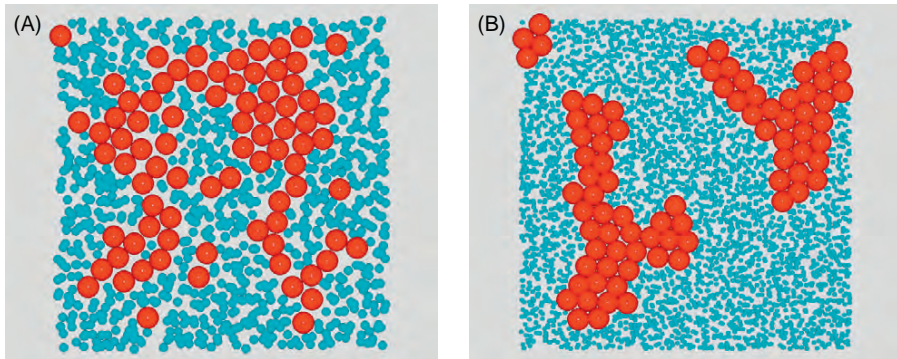


**Figure 6.4** Snapshots for  $\lambda_s = 0$  for the two initial configurations: Figures 6.2C and 6.3C were used as an initial configuration for (A) and (B), respectively.

employing the model potential for the interaction between dissipative and magnetic particles.

## 6.5 Simulation Program

A sample simulation program is shown below for conducting the simulation of the present exercise: the program is written in FORTRAN.

The important variables used in the program are explained as follow:

<code>RX(I), RY(I)</code>	: ( $x,y$ ) coordinates of the position vector $\mathbf{r}_i^*$ of magnetic particle $i$
<code>NX(I), NY(I)</code>	: ( $x,y$ ) coordinates of the magnetic moment direction $\mathbf{n}_i^*$
<code>VX(I), VY(I)</code>	: ( $x,y$ ) coordinates of the velocity $\mathbf{v}_i^*$ of magnetic particle $i$
<code>FX(I), FY(I)</code>	: ( $x,y$ ) coordinates of the magnetic force $\mathbf{F}_i^*$ acting on magnetic particle $i$
<code>FXMD(I), FYMD(I)</code>	: ( $x,y$ ) coordinates of the force acting on magnetic particle $i$ by dissipative particles
<code>N, NDENS, VDENS</code>	: Number of particles $N$ , number density $n^*$ , volumetric fraction $\phi_V^*$ concerning magnetic particles
<code>D, DS, DEL</code>	: Diameter, the diameter of solid part, the thickness of the steric layer of magnetic particles
<code>(XL, YL)</code>	: Side lengths of the simulation box in the ( $x,y$ ) directions
<code>RAS, RA, RV, RE</code>	: Nondimensional parameters $\lambda_s$ , $\lambda$ , $\lambda_V$ , and $\lambda_\varepsilon$
<code>OVRLAP(I)</code>	: <code>OVERLAP(I) = .TRUE.</code> in the case of an extraordinary overlap of magnetic particles
<code>RXD(I), RYD(I)</code>	: Position vector $\mathbf{r}_i^*$ of dissipative particle $i$
<code>VXD(I), VYD(I)</code>	: Velocity vector $\mathbf{v}_i^*$ of dissipative particle $i$
<code>FDXD(I), FDYD(I)</code>	: Dissipative force $\mathbf{F}_i^{D*}$ acting on dissipative particle $i$
<code>FCXD(I), FCYD(I)</code>	: Conservative force $\mathbf{F}_i^{C*}$ acting on dissipative particle $i$
<code>FRXD(I), FRYD(I)</code>	: Random force $\mathbf{F}_i^{R*}$ acting on dissipative particle $i$

---

FXDM(I), FYDM(I)	:	Force acting on dissipative particle $i$ by magnetic particles
ND, MD, DC, VDENSD	:	Number of particles, mass $m_d^*$ , diameter $d_c^*$ , volumetric fraction concerning dissipative particles
NDENSD, NDENSDH	:	Number densities of dissipative particles $n_d^*$ , $\hat{n}_d^*$
TMX(I), TABLE(*, I)	:	Names of cells to which dissipative particles interacting with the magnetic particle of interest belong
VTMX(I), VTABLE(#)	:	Names of magnetic particles interacting with the magnetic particle of interest
VPLACE(I)	:	Information starts to appear from the position VPLACE(I) in the variable VTABLE(I) concerning magnetic particles interacting with magnetic particle $i$
TMXD(GRP), TABLED(*, GRP))	:	Cell index method for dissipative particles
GRPX(I), GRPY(I)	:	Name of cell to which dissipative particle $i$ belongs is saved
ALP, GAM	:	Parameters $\alpha^*$ and $\gamma^*$ representing the strengths of repulsive and dissipative forces acting between dissipative particles, respectively

As an aid to understanding the program, explanatory comments have been added to important features. The line numbers are only for the reader's convenience, and unnecessary for executing a FORTRAN program.

```

0001 C*****
0002 C*          dpdmag3.f
0003 C*          *
0004 C*          OPEN(9, FILE='@daa1.data', STATUS='UNKNOWN'); parameters
0005 C*          OPEN(10,FILE='daa11.data', STATUS='UNKNOWN'); para. & data
0006 C*          OPEN(11,FILE='daa21.mgf', STATUS='UNKNOWN'); anime data
0007 C*          OPEN(21,FILE='daa001.data',STATUS='UNKNOWN'); particle pos.
0008 C*          OPEN(22,FILE='daa011.data',STATUS='UNKNOWN'); particle pos.
0009 C*          OPEN(23,FILE='daa021.data',STATUS='UNKNOWN'); particle pos.
0010 C*          OPEN(24,FILE='daa031.data',STATUS='UNKNOWN'); particle pos.
0011 C*          OPEN(25,FILE='daa041.data',STATUS='UNKNOWN'); particle pos.
0012 C*          OPEN(26,FILE='daa051.data',STATUS='UNKNOWN'); particle pos.
0013 C*          OPEN(27,FILE='daa061.data',STATUS='UNKNOWN'); particle pos.
0014 C*          OPEN(28,FILE='daa071.data',STATUS='UNKNOWN'); particle pos.
0015 C*          OPEN(29,FILE='daa081.data',STATUS='UNKNOWN'); particle pos.
0016 C*          OPEN(30,FILE='daa091.data',STATUS='UNKNOWN'); particle pos.
0017 C*          *
0018 C*          ----- DPD SIMULATION OF MAGNETIC PARTICLES -----
0019 C*          TWO-DIMENSIONAL DPD SIMULATION OF MAGNETIC SPHERICAL
0020 C*          PARTICLES IN DISSIPATIVE PARTICLES
0021 C*          *
0022 C*          1. FOR A STRONG MAGNETIC FIELD CASE (Y-DIRECTION).
0023 C*          2. FERROMAGNETIC SPHERICAL PARTICLES WITH STERIC LAYER.
0024 C*          3. LENNARD-JONES MODEL FOR INTERACTIONS BETWEEN
0025 C*          MAGNETIC AND DISSIPATIVE PARTICLES.
0026 C*          4. NNN SHOULD BE SUFFICIENTLY LARGE (NNN=10000)
0027 C*          5. OVRALP(*) IS INTRODUCED.
0028 C*          *
0029 C*          VER.1 BY A.SATOH, '09 4/5 *
0030 C*****
0031 C
0032 C      N   : NUMBER OF MAGNETIC PARTICLES (M. PTCL.)
0033 C      D   : DIAMETER OF PARTICLE INCLUDING SURFACTANT LAYER
0034 C           (=1 FOR THIS CASE )
0035 C      DS  : DIAMETER OF SOLID PARTICLE WITHOUT STERIC LAYER
0036 C      DEL : THICKNESS OF STERIC LAYER
0037 C      TD  : DIMENSIONLESS THICKNESS OF STERIC LAYER BASED ON RADIUS
0038 C      NDENS: NUMBER DENSITY OF M. PTCL.

```

---

```

0039 C VDENS : VOLUMETRIC FRACTION OF PARTICLES
0040 C RA   : NONDIMENSIONAL PARAMETER OF PARTICLE-PARTICLE INTERACT
0041 C RAS  : NONDIMENSIONAL PARAMETER OF PARTICLE-PARTICLE INTERACT
0042 C      BASED ON THE DIAMETER OF THE SOLID PART
0043 C KU   : NONDIMENSIONAL PARAMETER OF PARTICLE-FIELD INTERACTION
0044 C RV   : NONDIMENSIONAL PARAMETER OF STERIC REPULSION (=120)
0045 C RVS  : NONDIMENSIONAL PARAMETER OF STERIC REPULSION
0046 C      BASED ON THE DIAMETER OF THE SOLID PART (=150)
0047 C RE   : NONDIMENSIONAL PARAMETER OF M.PTCL.-D.PTCL INTERACTION
0048 C RCOFF : CUTOFF RADIUS FOR CALCULATION OF MAG. FORCES
0049 C RCOFFMD :CUTOFF RADIUS FOR FORCES BETWEEN M.PTCL. AND D.PTCL.
0050 C RCOFFDDM :CUTOFF RADIUS FOR FORCES BETWEEN P.PTCL. AND VIRTUAL
0051 C      PTCL. INSIDE M.PTCL.
0052 C XL,YL : DIMENSIONS OF SIMULATION REGION
0053 C H   : TIME INTERVAL FOR DPD SIMULATIONS
0054 C (HX,HY,HZ) : APPLIED MAGNETIC FIELD (UNIT VECTOR)
0055 C VELTHRY : AVERAGE OF (VX**2+VY**2) (DESIRED) FOR M-PTCL
0056 C VELTHRYD : AVERAGE OF (VX**2+VY**2) (DESIRED) FOR D-PTCL
0057 C NVELSC  : VELOCITIES OF M-PTCL ARE SCALED EVERY NVELSC
0058 C      TIME STEP TO SATISFY THE DESIRED VELOCITY
0059 C NVELSCD : VELOCITIES OF D-PTCL ARE SCALED EVERY NVELSCD
0060 C      TIME STEP TO SATISFY THE DESIRED VELOCITY
0061 C
0062 C RX(N),RY(N) : PARTICLE POSITION
0063 C NX(N),NY(N) : DIRECTION OF MAGNETIC MOMENT
0064 C VX(N),VY(N) : PARTICLE VELOCITY
0065 C FX(N),FY(N) : PARTICLE FORCE DUE TO MAGNETIC FORCES
0066 C FXMD(N),FYMD(N) : PARTICLE FORCE BY D. PTCL. ON M. PTCL.
0067 C TMX(I) : TOTAL NUMBER OF INDEX CELLS OF D. PTCL. WHICH MAY
0068 C      INTERACT WITH M. PTCL. I
0069 C TABLE(*,I) : NAME OF INDEX CELLS WHICH MAY INTERACT WITH M. PTCL.
0070 C VTMX(I) : TOTAL NUMBER OF NEIGHBORING M.PTCL. WHICH MAY
0071 C      INTERACT WITH M.PTCL. WITHIN THE CUTOFF RANGE
0072 C VTABLE(NNN) : NAME OF M.PTCL. IS SAVED IN ORDER (VERLET METHOD)
0073 C VPLACE(I) : THE FIRST PTCL., WHICH INTERACTS WITH PTCL. I,
0074 C      APPEARS AT VPLACE(I) IN THE TABLE OF VTABLE(**)
0075 C VRADIUS : CUTOFF RADIUS FOR VERLET METHOD
0076 C NVTABLE : VERLET TABLE IS RENEWED EVERY NVTABLE TIME STEP
0077 C
0078 C OVRLAP(*) : OVRLAP(I)=.TRUE. FOR OVERLAPING
0079 C
0080 C ND   : NUMBER OF DISSIPATIVE PARTICLES (D.PTCL.)
0081 C MD   : MASS OF D.PTCL.
0082 C DC   : DIAMETER OF D.PTCL.
0083 C RCOFFD : CUTOFF DISTANCE FOR INTERACTIONS BETWEEN D. PTCL.
0084 C ALP  : COEFFICIENT REPRESENTING REPULSIVE FORCE OF D.PTCL.
0085 C GAM  : COEFFICIENT REPRESENTING DISSIPATIVE FORCE OF D.PTCL.
0086 C
0087 C RXD(ND),RYD(ND) : POSITIONS OF D.PTCL.
0088 C VXD(ND),VYD(ND) : VELOCITIES OF D.PTCL.
0089 C FCXD(ND),FCYD(ND) : CONSERVATIVE FORCES ACTING ON A PARTICLE
0090 C FDXD(ND),FDYD(ND) : DISSIPATIVE FORCES ACTING ON A PARTICLE
0091 C FRXD(ND),FRYD(ND) : RANDOM FORCES ACTING ON A PARTICLE
0092 C FXMD(ND),FYMD(ND) : PARTICLE FORCE BY M. PTCL. ON D. PTCL.
0093 C NDENSDH : NUMBER DENSITY WITH HAT
0094 C NDENSD : NUMBER DENSITY OF D.PTCL.
0095 C VDENSD : VOLUMETRIC FRACTION OF D.PTCL.
0096 C
0097 C GRPX(ND),GRPY(ND) : GROUP TO WHICH D.PTCL. I BELONGS
0098 C PXD   : NUMBER OF CUT-OFF CELLS IN EACH DIRECTION
0099 C TMXD(GRP) : TOTAL NUMBER OF PTCL. BELONGING TO GROUP(GRP)
0100 C TABLED(*,GRP) : NAME OF PTCL. BELONGING TO GROUP(GRP)
0101 C GRPLXD(PXD) : IS USED FOR DETERMINE THE CELL TO WHICH A
0102 C      PARTICLE IS BELONG
0103 C
0104 C RAN(NRANMX) : RANDOM NUMBERS BETWEEN 0 AND 1
0105 C
0106 C      -XL/2 <RX(I) <XL/2 , -YL/2 <RY(I)< YL/2
0107 C-----
0108 C IMPLICIT REAL*8 (A-H,O-Z), INTEGER (I-N)
0109 C
0110 C COMMON /BLOCK1/ RX , RY

```

```

0111      COMMON /BLOCK2/  VX ,  VY
0112      COMMON /BLOCK3/  NX ,  NY
0113      COMMON /BLOCK5/  FX ,  FY
0114      COMMON /BLOCK7/  N ,  NDENS ,  VDENS ,  D ,  DS ,  DEL ,  TD
0115      COMMON /BLOCK8/  RA ,  RV ,  RE
0116      COMMON /BLOCK9/  TMX ,  TABLE
0117      COMMON /BLOCK10/ VTMX ,  VTABLE ,  VPLACE ,  NVTABLE ,  VRADIUS
0118      COMMON /BLOCK11/ FXMD ,  FYMD ,  RCOFFMD ,  RCOFFDMD
0119      COMMON /BLOCK13/ OVRLAP
0120      COMMON /BLOCK15/ H ,  XL ,  YL ,  RCOFF
0121      COMMON /BLOCK16/ VELTHRY ,  VELTHRYD ,  NVELSC ,  NVELSCD
0122 C
0123      COMMON /BLOCK21/ RXD ,  RYD
0124      COMMON /BLOCK22/ VXD ,  VYD
0125      COMMON /BLOCK23/ FCXD ,  FCYD
0126      COMMON /BLOCK24/ FDXD ,  FDYD
0127      COMMON /BLOCK25/ FRXD ,  FRYD
0128      COMMON /BLOCK26/ ND ,  NDENSDH ,  NDENSD ,  VDENSD ,  MD
0129      COMMON /BLOCK27/ DC ,  ALP ,  GAM ,  RCOFFD
0130      COMMON /BLOCK28/ GRPX ,  GRPY
0131      COMMON /BLOCK29/ TMXD ,  TABLED
0132      COMMON /BLOCK30/ PXD ,  GRPLXD ,  PXYD
0133      COMMON /BLOCK31/ FXDM ,  FYDM
0134 C
0135      COMMON /BLOCK35/ NRAN ,  RAN ,  IX
0136 C
0137      INTEGER      TT, PPXD, PPXYD, TTD
0138      PARAMETER( NN=100 ,  NNN=10000 ,  TT=500 )
0139      PARAMETER( NRANMX=100000000 )
0140      PARAMETER( PI=3.141592653589793D0 )
0141      PARAMETER( NND=50000 ,  PPXD=500 ,  PPXYD=250000 ,  TTD=20 )
0142 C
0143      REAL*8      RX(NN) ,  RY(NN) ,  VX(NN) ,  VY(NN)
0144      REAL*8      FX(NN) ,  FY(NN) ,  NX(NN) ,  NY(NN)
0145      REAL*8      NDENS
0146      REAL*8      FXMD(NN) ,  FYMD(NN)
0147      INTEGER      TMX(NN) ,  TABLE(TT,NN)
0148      INTEGER      VTMX(NN) ,  VTABLE(NNN) ,  VPLACE(NN)
0149      LOGICAL      OVRLAP(NN)
0150 C
0151      REAL*8      RXD(NND) ,  RYD(NND) ,  VXD(NND) ,  VYD(NND)
0152      REAL*8      FCXD(NND) ,  FCYD(NND) ,  FDXD(NND) ,  FDYD(NND)
0153      REAL*8      FRXD(NND) ,  FRYD(NND) ,  FXDM(NND) ,  FYDM(NND)
0154      REAL*8      NDENSDH ,  NDENSD ,  MD
0155      REAL*8      GRPLXD(PPXD)
0156      INTEGER      GRPX(NND) ,  GRPY(NND)
0157      INTEGER      TMXD(PPXYD) ,  TABLED(TTD,PPXYD) ,  PXD ,  PXYD
0158 C
0159      REAL*8      VELTHRY ,  VELTHRYD
0160      INTEGER      NVELSC ,  NVELSCD
0161 C
0162      REAL      RAN(NRANMX)
0163      INTEGER      NRAN ,  IX ,  NRANCHK
0164 C
0165      REAL*8      RXI ,  RYI ,  RXID ,  RYID ,  RCOFF2 ,  HSQ2 ,  H2
0166      REAL*8      VXI ,  VYI ,  VXA ,  VYA ,  VELAV ,  VELAVD
0167      REAL*8      VELMX ,  VELDMX
0168      REAL*8      EVELX ,  EVELY ,  EVELSQ ,  EVELXD ,  EVELYD ,  EVELSQD
0169      INTEGER      NTIME ,  NTIMEMX ,  NGRAPH ,  NANIME ,  NANMCTR
0170      INTEGER      NVELAV ,  NVELAVD ,  NP ,  NOPT
0171      INTEGER      TMX00 ,  TMXDOO ,  VTABLE00
0172 C
0173      OPEN(9, FILE='acka1.data' ,  STATUS='UNKNOWN')
0174      OPEN(10,FILE='acka11.data' ,  STATUS='UNKNOWN')
0175      OPEN(11,FILE='acka21.mgf' ,  STATUS='UNKNOWN')
0176      OPEN(21,FILE='acka001.data' ,  STATUS='UNKNOWN')
0177      OPEN(22,FILE='acka011.data' ,  STATUS='UNKNOWN')
0178      OPEN(23,FILE='acka021.data' ,  STATUS='UNKNOWN')
0179      OPEN(24,FILE='acka031.data' ,  STATUS='UNKNOWN')
0180      OPEN(25,FILE='acka041.data' ,  STATUS='UNKNOWN')
0181      OPEN(26,FILE='acka051.data' ,  STATUS='UNKNOWN')
0182      OPEN(27,FILE='acka061.data' ,  STATUS='UNKNOWN')

```

• The given values are written out in @acka1 and acka11.

```

0183          OPEN( 28,FILE='acka071.data' ,STATUS='UNKNOWN' )
0184          OPEN( 29,FILE='acka081.data' ,STATUS='UNKNOWN' )
0185          OPEN( 30,FILE='acka091.data' ,STATUS='UNKNOWN' )
0186
0187 C           NP=9
0188 C           ++++++ N=25, 36, 49, 64, 81, 100, 121, ...
0189 C           H=0.001 FOR RAS=10
0190 C           ++++++
0191 C
0192     N      = 81
0193     VDENS = 0.3D0
0194     NDENS = VDENS*(4.D0/PI)
0195     RAS   = 10.D0
0196     RV    = 120.D0
0197     RE    = 10.D0
0198     D     = 1.D0
0199     TD    = 0.3D0
0200     DEL   = TD/2.D0
0201     DS    = 1.D0 - TD
0202     RCOFF = 8.D0
0203     VRADIUS = RCOFF*1.3D0
0204     RCOFF2 = RCOFF**2
0205     VELMX = 2.D0*5.5D0**2
0206     RA    = RAS*DS**3
0207 C
0208     NDENSDH = 1.0D0
0209     DC     = 0.4D0
0210     NDENSD = NDENSDH/DC**2
0211     VDENSD = NDENSDH*PI/4.D0
0212     GAM   = 10.D0
0213     ALP   = GAM/10.D0
0214     MD    = 0.05D0
0215     RCOFFD = DC
0216     RCOFFDDM= 3.D0*DC
0217     RCOFFMD = 0.5D0 + RCOFFDDM - DC/2.D0
0218     VELDMX = (2.D0/MD)*5.5D0**2
0219 C
0220     H      = 0.001D0
0221     NTIMEMX = 100000
0222     NGRAPH = NTIMEMX/10
0223     NANIME = NTIMEMX/200
0224     NVTABLE = INT( 0.0001D0/H )
0225     IF( NVTABLE .LE. 0 ) NVTABLE = 1
0226 C
0227     NVELSC = INT( 0.1D0 /H + 0.001D0)
0228     NVELSCD= INT( 0.01D0/H + 0.001D0)
0229     VELTHRY = 2.D0**0.5
0230     VELTHRYD= (2.D0/MD)**0.5
0231     IF( NVELSC .LE. 0 ) NVELSC = 1
0232     IF( NVELSCD .LE. 0 ) NVELSCD = 1
0233 C
0234     IX    = 0
0235     CALL RANCAL( NRANMX, IX, RAN )
0236     NRAN  = 1
0237 C
0238 C
0239 C           ----- INITIAL CONFIGURATION -----
0240 C
0241 C
0242 CCC     --- SET INITIAL POSIT. AND VEL. ---
0243 CCC     OPEN(19,FILE='acka091.data' ,STATUS='OLD')
0244 CCC     READ(19,592) N , XL, YL
0245 CCC     READ(19,594) (RX(I),I=1,N) , (RY(I),I=1,N) ,
0246 CCC     &           (VX(I),I=1,N) , (VY(I),I=1,N) ,
0247 CCC     &           (NX(I),I=1,N) , (NY(I),I=1,N)
0248 CCC     READ(19,596) ND
0249 CCC     READ(19,598) (RxD(I),I=1,ND) , (RYD(I),I=1,ND) ,
0250 CCC     &           (VxD(I),I=1,ND) , (VYD(I),I=1,ND)
0251 CCC     CLOSE(19,STATUS='KEEP')
0252 C
0253     GOTO 7
0254
0255     CALL INIPOSIT( N , VDENS , NDENS, PI , VRADIUS )

```

• The positions and velocities of particles are written out in acka001 to acka091, and the data for MicroAVS are written out in acka21.

Concerning magnetic particles:  
 • The number of particles  $N=81$ , volumetric fraction  $\phi^*=0.3$ ,  $\lambda_s=10$ ,  $\lambda_v=120$  and  $\lambda_e=10$ . The particle diameter  $d^*=1$ , the surfactant layer thickness  $\delta^*=0.15$  and  $t_0=0.3$ .  
 • The cutoff distance  $r_{\text{cutoff}}^*=8$ ,  $r_j^*$  is used for the Verlet neighbor list method (see Figure 2.12).

Concerning dissipative particles:  
 • The number density  $\hat{n}_d=1$ , diameter  $d_c^*=0.4$  and mass  $m_d^*=0.05$ .  $\gamma^*=10$ ,  $\alpha^*=\gamma^*/10$ , and cutoff distance  $d_c^*$ .  
 • The cutoff distance between magnetic and dissipative particles is denoted by RCOFFMD.  
 • The maximum velocity is assumed to be VELDMX.

• Time interval  $h^*=0.001$ .

• The number of the total time steps is 100,000. The particle positions are written out at every NGRAPH time steps, and 200 sets of data are written out for making an animation.

• The data table in the Verlet neighbor list method is renewed at every NVTABLE time steps. The velocity scaling of magnetic and dissipative particles is carried out at every NVELSC and NVELSCD, respectively. The theoretical averaged velocities of magnetic and dissipative particles are denoted by VELTHRY and VELTHRYD, respectively.

• Pseudo-random numbers are saved in the variable RAN(").

• The initial positions of magnetic and dissipative particles are assigned in the subroutines INIPOSIT and INIPOSID. Similarly, the initial velocities are set in INIVEL and INIVELD.

```

0254      CALL INIPOSID( DC , RCOFFD , N )
0255      CALL INIVEL( N , PI , VELMX )
0256      CALL INIVELD( ND , MD , PI , VELDMX )
0257 C          --- (A1)
0258      7 CALL GRIDGENE( XL , RCOFFD )
0259 C          --- (A2)
0260      CALL GROUP( ND )
0261 C
0262      CALL TABLECAL( ND , PXD )
0263 C          --- (B1)
0264 C          -           FOR M. PTCL. -
0265      CALL VTABLEDP( N , RCOFFD , RCOFFMD , XL , YL , DC )
0266 C          --- (B2) SET UP VERLET TABLE OF M.PTCL ---
0267 C          -           FOR M. PTCL. -
0268      CALL VTABLEMA( N , XL , YL )
0269 C
0270      CALL FORCEMAG( RCOFF2 , NTIME )
0271      CALL FORCEDPD( PI )
0272      CALL FORCEINT( N , ND , RE , DC )
0273 C
0274 C          --- PRINT OUT CONSTANTS ---
0275      WRITE(NP,10) N, VDENS, NDENS, RAS, RA, RV, RE, D, TD, DEL, DS,
0276      &           RCOFF, VRADIUS, RCOFFMD, RCOFFDDM, XL, YL, H
0277      WRITE(NP,12) ND, NDENSDH, DC, NDENSD, VDENSD, MD, ALP, GAM,
0278      &           RCOFFD
0279      WRITE(NP,14) H, NTIMEMX, NGRAPH, NVTABLE
0280 C
0281 C
0282      NVELAV = 0
0283      VELAV = 0.D0
0284      NVELAVD = 0
0285      VELAVD = 0.D0
0286      NOPT = 20
0287      NRANCHK = NRANMX - ND*ND
0288      NANMCTR = 0
0289 C
0290      EVELX = 0.D0
0291      EVELY = 0.D0
0292      EVELSQ = 0.D0
0293      EVELXD = 0.D0
0294      EVELYD = 0.D0
0295      EVELSQD = 0.D0
0296 C
0297 C          -----
0298 C          ----- START OF MAIN LOOP ----- C
0299 C
0300 C
0301 DO 1000 NTIME = 1,NTIMEMX
0302 C
0303 C
0304      DO 100 I = 1,ND
0305 C
0306      RXID = RXD(I) + VXD(I)*H
0307      RYID = RYD(I) + VYD(I)*H
0308      RXID = RXID - DNINT( RXID/XL )*XL
0309      RYID = RYID - DNINT( RYID/YL )*YL
0310      RXD(I) = RXID
0311      RYD(I) = RYID
0312 C          -----
0313      VXID = VXD(I) + FCXD(I) + FDXD(I) + FRXD(I) + FXDM(I)*H/MD
0314      VYID = VYD(I) + FCYD(I) + FDYD(I) + FRYD(I) + FYDM(I)*H/MD
0315      VXD(I) = VXID
0316      VYD(I) = VYID
0317      C1 = VXID**2 + VYID**2
0318      IF( C1 .GT. VELDMX ) THEN
0319          C1 = DSQRT( VELDMX/C1 )
0320          VXD(I) = VXID*C1
0321          VYD(I) = VYID*C1
0322      END IF
0323 C
0324      IF( NTIME .GT. NTIMEMX/2 ) VELAVD=VELAVD+VXD(I)**2+VYD(I)**2

```

• Cells are set for using the cell index method.

• The name of the cell to which each dissipative particle belongs is grasped. Also, the name of dissipative particles belonging to each cell is grasped.

• The names of the cells interacting with each magnetic particle are grasped.

• The names of magnetic particles interacting with each magnetic particle are grasped in VTABLEMA.

• The forces acting on magnetic and dissipative particles are calculated in the subroutines FORCEMAG and FORCEDPD, respectively. The forces acting between magnetic and dissipative particles are calculated in FORCEINT.

----- (1) D. PTCL. CASE -----

• The positions of dissipative particles at the next time step are evaluated according to Eq. (6.18).

• The treatment of the periodic BC.

• The velocities of dissipative particles at the next time step are evaluated according to Eq. (6.19).

• The velocity of each particle is modified so as to be smaller than the maximum value.

```

0325 C
0326 100  CONTINUE
0327 C
0328     IF( NTIME .GT. NTIMEMX/2 )      NVELAVD = NVELAVD + 1
0329 C                                     ----- (2) M. PTCL. CASE ---
0330     HSQ2 = H*H/2.D0
0331     H2   = H/2.D0
0332     DO 200 I = 1,N
0333     ccc          RXI    = RX(I) + VX(I)*H + ( FX(I)+FXMD(I) )*HSQ2
0334     ccc          RYI    = RY(I) + VY(I)*H + ( FY(I)+FYMD(I) )*HSQ2
0335     RXI    = RX(I) + VX(I)*H
0336     RYI    = RY(I) + VY(I)*H
0337     C1    = VX(I)**2 + VY(I)**2
0338     IF( C1 .GT. VELMX ) THEN
0339         C1 = DSQRT( VELMX/C1 )
0340         VXI = VX(I)*C1
0341         VYI = VY(I)*C1
0342         RXI = RX(I) + VXI*H
0343         RYI = RY(I) + VYI*H
0344     END IF
0345     RXI = RXI - DNINT( RXI/XL )*XL
0346     RYI = RYI - DNINT( RYI/YL )*YL
0347     RX(I) = RXI
0348     RY(I) = RYI
0349 C
0350     IF( OVRLAP(I) ) THEN
0351         VXI = VX(I) + FX(I) * H
0352         VYI = VY(I) + FY(I) * H
0353     ELSE
0354         VXI = VX(I) + ( FX(I)+FXMD(I) )*H
0355         VYI = VY(I) + ( FY(I)+FYMD(I) )*H
0356     END IF
0357     VX(I) = VXI
0358     VY(I) = VYI
0359     C1 = VXI**2 + VYI**2
0360     IF( C1 .GT. VELMX ) THEN
0361         C1 = DSQRT( VELMX/C1 )
0362         VX(I) = VXI*C1
0363         VY(I) = VYI*C1
0364     END IF
0365 200  CONTINUE
0366 C
0367     CALL GROUP( ND )
0368     CALL TABLECAL( ND , PXD )
0369     CALL VTABLEDP( N , RCOFFD , RCOFFMD , XL , YL , DC )
0370     IF( MOD(NTIME,NVTABLE) .EQ. 0 ) THEN
0371         CALL VTABLEMA( N , XL , YL )
0372     END IF
0373 C
0374     CALL FORCEMAG( RCOFF2 , NTIME )
0375     CALL FORCEDPD( PI )
0376     CALL FORCEINT( N , ND , RE , DC )
0377 C
0378     DO 220 I = 1,N
0379         IF( NTIME .GT. NTIMEMX/2 )  VELAV = VELAV+VX(I)**2+VY(I)**2
0380 220  CONTINUE
0381 C
0382     IF( NTIME .GT. NTIMEMX/2 )      NVELAV = NVELAV + 1
0383 C
0384 C----- FOR VELOCITY SCALING ---
0385     DO 255 I = 1, N
0386         EVELX = EVELX + VX(I)
0387         EVELY = EVELY + VY(I)
0388         EVELSQ = EVELSQ + VX(I)**2 + VY(I)**2
0389 255  CONTINUE
0390     DO 260 I = 1, ND
0391         EVELXD = EVELXD + VXD(I)
0392         EVELYD = EVELYD + VYD(I)
0393         EVELSQD = EVELSQD + VXD(I)**2 + VYD(I)**2
0394 260  CONTINUE
0395 C

```

--- PART (1) OF VEL ---

- The positions of magnetic particles at the next time step are evaluated according to Eq. (6.22).

--- SAMPLING ---

- The treatment of the periodic BC.

--- MAG VELOCITY SCALING ---

- The treatment in the case of the solid parts of the two magnetic particles overlapping.

- The velocities of magnetic particles at the next time step are evaluated according to Eq. (6.23).

- The velocity of each particle is modified so as to be smaller than the maximum value.

- The information in the cell index table and in the Verlet neighbor list table is renewed.

- The forces acting between magnetic particles, between dissipative particles, and between magnetic and dissipative particles are calculated.

- The velocities are sampled for scaling the particle velocities afterward.

```

0396      IF( MOD(NTIME,NVELSC) .EQ. 0 ) THEN
0397          EVELX = EVELX /DBLE(N*NVELSC)
0398          EVELY = EVELY /DBLE(N*NVELSC)
0399          EVELSQ = EVELSQ/DBLE(N*NVELSC)
0400          CALL SCALEVEL( N, VX, VY, VELTHRY, EVELX, EVELY, EVELSQ )
0401          EVELX = 0.D0
0402          EVELY = 0.D0
0403          EVELSQ = 0.D0
0404      END IF
0405 C          --- DPD VELOCITY SCALING ---
0406      IF( MOD(NTIME,NVELSCD) .EQ. 0 ) THEN
0407          EVELXD = EVELXD /DBLE(ND*NVELSCD)
0408          EVELYD = EVELYD /DBLE(ND*NVELSCD)
0409          EVELSQD = EVELSQD/DBLE(ND*NVELSCD)
0410          CALL SCALEVEL( ND,VXD,VYD,VELTHRD,EVELXD,EVELYD,EVELSQD )
0411          EVELXD = 0.D0
0412          EVELYD = 0.D0
0413          EVELSQD = 0.D0
0414      END IF
0415 C
0416 C
0417 C
0418 C          --- DATA OUTPUT FOR GRAPHICS (1) ---
0419      IF( MOD(NTIME,NGRAPH) .EQ. 0 ) THEN
0420          NOPT = NOPT + 1
0421          WRITE(NOPT,592) N , XL, YL
0422          &          WRITE(NOPT,594) (RX(I),I=1,N) , (RY(I),I=1,N) ,
0423          &          (VX(I),I=1,N) , (VY(I),I=1,N) ,
0424          &          (NX(I),I=1,N) , (NY(I),I=1,N)
0425          &          WRITE(NOPT,596) ND
0426          &          WRITE(NOPT,598) (RXD(I),I=1,ND) , (RYD(I),I=1,ND) ,
0427          &          (VXD(I),I=1,ND) , (VYD(I),I=1,ND)
0428          CLOSE(NOPT,STATUS='KEEP')
0429      END IF
0430 C          --- DATA OUTPUT (2) FOR ANIMATION ---
0431      IF( MOD(NTIME,NANIME) .EQ. 0 ) THEN
0432          NANMCTR = NANMCTR + 1
0433 C          IF( NANMCTR .EQ. 1 ) THEN
0434              WRITE(11,381) (NTIMEMX/NANIME)
0435          END IF
0436 C          IF( (NANMCTR.GE.1) .AND. (NANMCTR.LE.9) ) THEN
0437              WRITE(11,383) NANMCTR
0438          ELSE IF( (NANMCTR.GE.10) .AND. (NANMCTR.LE.99) ) THEN
0439              WRITE(11,384) NANMCTR
0440          ELSE IF( (NANMCTR.GE.100) .AND. (NANMCTR.LE.999) ) THEN
0441              WRITE(11,385) NANMCTR
0442          ELSE IF( (NANMCTR.GE.1000) .AND. (NANMCTR.LE.9999) ) THEN
0443              WRITE(11,386) NANMCTR
0444          END IF
0445 C          WRITE(11,388) ( N+ND )
0446 C          DO 400 I=1,N
0447              WRITE(11,398) RX(I) ,RY(I) ,0.0, D/2.D0, 1.0, 0.0, 0.0
0448          CONTINUE
0449 C          DO 410 I=1,ND
0450              WRITE(11,398) RXD(I),RYD(I),0.0, DC/2.D0, 0.0, 0.8, 1.0
0451          CONTINUE
0452      END IF
0453 C          --- CHECK RANDOM NUMBERS USED ---
0454      IF( NRAN .GT. NRANCHK ) THEN
0455          CALL RANCAL( NRANMX, IX, RAN )
0456          NRAN = 1
0457      END IF
0458 C
0459      IF( NRAN .GT. NRANCHK ) THEN
0460          CALL RANCAL( NRANMX, IX, RAN )
0461          NRAN = 1
0462      END IF
0463 C
0464 C
0465      1000 CONTINUE
0466 C
0467 C

```

• The velocities of magnetic particles are scaled so as to yield the desired system temperature.

• The velocities of dissipative particles are scaled so as to yield the desired system temperature.

• The data are written out for making an animation based on the commercial software MicroAVS.

• The number of the used random numbers is checked. If over NRANCHK, a uniform random number sequence is renewed.

```

0468 C      ----- END OF MAIN LOOP -----
0469 C
0470 C
0471     VELAV   = VELAV /DBLE(NVELAV*N)
0472     VELAVD = VELAVD/DBLE(NVELAVD*ND)
0473 C
0474     TMX00 = 0
0475     TMXD00 = 0
0476     DO 1006 I=1,N
0477       IF( TMX(I) .GT. TMX00 ) TMX00 = TMX(I)
0478 1006 CONTINUE
0479     DO 1007 I=1,PXYD
0480       IF( TMXD(I) .GT. TMXD00 ) TMXD00 = TMXD(I)
0481 1007 CONTINUE
0482     VTABLE00 = VPLACE(N) + VTMX(N) - 1
0483 C
0484 C      ---- PRINT OUT (1) ----
0485     WRITE(NP,1011) TMX00 , TMXD00 , VTABLE00 ,
0486     &           REAL(TMX00)/REAL(TT) , REAL(TMXD00)/REAL(TTD) ,
0487     &           REAL(VTABLE00)/REAL(NNN) , REAL(PXYD)/REAL(PXXYD)
0488     WRITE(NP,1013) PXD , PXYD
0489     WRITE(NP,1014) DSQRT(VELAV) , DSQRT(VELAVD) ,
0490     &           DSQRT(VELAV/2.D0) , DSQRT(VELAVD*MD/2.D0)
0491 C
0492 C      ---- DATA OUTPUT FOR GRAPHICS (1) ----
0493     WRITE(10,1210) N, VDENS, NDENS, RAS, RA, RV, RE, D, TD, DEL, DS
0494     WRITE(10,1211) RCOFF, VRADIUS, RCOFFMD, RCOFFDDM, XL, YL, H
0495     WRITE(10,1213) ND, NDENSDH, DC, NDENSD, VDENSD, MD, ALP, GAM,
0496     &           RCOFFD
0497     WRITE(10,1214) H, NTIMEMX, NGRAPH, NVTABLE
0498 C
0499           CLOSE( 9,STATUS='KEEP' )
0500           CLOSE(10,STATUS='KEEP' )
0501           CLOSE(11,STATUS='KEEP' )
0502 C
0503 C      ---- FORMAT -----
0504 10 FORMAT(/1H , '
0505     &           /1H , ' DPD SIMULATION OF MAGNETIC PARTICLES '
0506     &           /1H , ' IN DISSIPATIVE PARTICLES IN EQUILIBRIUM '
0507     &           /1H , ' +++ TWO-DIMENSIONAL EQUILIBRIUM CASE +++ '
0508     &           /1H , '
0509     &           //1H , 'N=' ,I3 , 2X, 'VDENS=' , F6.3 , 2X, 'NDENS=' ,F6.3 , 2X,
0510     &           'RAS=' , F7.3 , 2X, 'RA=' , F7.3 , 2X, 'RV=' , F8.2
0511     &           /1H , 'RE=' , F7.3 , 2X, 'D=' , F3.1 , 2X, 'TD=' , F4.2 , 2X,
0512     &           'DEL=' , F5.3 , 2X, 'DS=' , F5.2
0513     &           /1H , 'RCOFF=' ,F6.2 , 2X, 'VRADIUS=' ,F6.2 , 2X, 'RCOFFMD=' ,
0514     &           F5.2 , 2X, 'RCOFFDDM=' , F5.2
0515     &           /1H , 'XL=' , F6.2 , 2X, 'YL=' , F6.2 , 2X, 'H=' , E9.2)
0516 12 FORMAT(/1H , 'ND=' ,I4 , 2X, 'NDENSDH=' , F6.3 , 2X, 'DC=' , F6.2 , 2X,
0517     &           'NDENSD=' , F6.2 , 2X, 'VDENSD=' , F6.2 , 2X, 'MD=' ,F5.3
0518     &           /1H , 'ALP=' , F6.2 , 2X, 'GAM=' , F6.2 , 2X, 'RCOFFD=' , F6.2)
0519 14 FORMAT(/1H , 'H=' , E9.2 , 2X, 'NTIMEMX=' , I8 , 2X, 'NGRAPH=' ,I7 ,
0520     &           2X, 'NVTABLE=' , I4/)
0521 381 FORMAT('# Micro AVS Geom:2.00'
0522     &           '# Animation of DPD simulation results'/I4)
0523 383 FORMAT('step',I1)
0524 384 FORMAT('step',I2)
0525 385 FORMAT('step',I3)
0526 386 FORMAT('step',I4)
0527 388 FORMAT( 'sphere'/'sphere_sample'/'color'/I7 )
0528 398 FORMAT( 3F10.4 , F6.2 , 3F5.2 )
0529 592 FORMAT( I8 , 2F12.6 )
0530 594 FORMAT( (5E16.8) )
0531 596 FORMAT( I8 )
0532 598 FORMAT( (5E16.8) )
0533 1011 FORMAT(/1H , 'TMX00=' ,I5 , 2X, 'TMXD00=' ,I5 , 2X, 'VTABLE00=' ,I5
0534     &           /1H , 'REAL(TMX00)/REAL(TT)=' ,F5.3 , 2X,
0535     &           'REAL(TMXD00)/REAL(TTD)=' ,F5.3
0536     &           /1H , 'REAL(VTABLE00)/REAL(NNN)=' ,F5.3 , 2X,
0537     &           'REAL(PXYD)/REAL(PXXYD)=' ,F5.3)
0538 1013 FORMAT(1H , 'PXD=' , I5 , 2X, 'PXYD=' , I6/ )
0539 1014 FORMAT(1H , 'VELAV=' , F9.4 , 2X, 'VELAVD=' , F9.4

```

```

0540      &           /1H , 'VELAV/THEORY=' , F9.4, 2X, 'VELAVD/THEORY=' , F9.4)
0541 1210 FORMAT( I4 , 2F6.3 , 3F8.3 , 5F7.3 )
0542 1211 FORMAT( 6F8.3 , E11.3 )
0543 1213 FORMAT( I4 , F6.3 , 7F8.3 )
0544 1214 FORMAT( E11.3 , 3I8 )
0545                                         STOP
0546                                         END
0547 ****
0548 C***** SUBROUTINE ***** SUBROUTINE ****
0549 C***** ****
0550 C
0551 C**** SUB INIPOSIT ****
0552     SUBROUTINE INIPOSIT( N , VDENS , NDENS , PI , VRADIUS )
0553 C
0554     IMPLICIT REAL*8 ( A-H,O-Z ), INTEGER ( I-N )
0555 C
0556     COMMON /BLOCK1/ RX , RY
0557     COMMON /BLOCK3/ NX , NY
0558     COMMON /BLOCK15/ H , XL , YL , RCOFF
0559 C
0560     PARAMETER( NN=100 )
0561 C
0562     REAL*8    RX(NN) , RY(NN) , NX(NN) , NY(NN) , NDENS
0563     REAL*8    A , RAN , C1
0564     INTEGER    Q , PTCL
0565 C
0566     A = DSQRT( PI/(4.0D0*VDENS) )
0567     Q = NINT( SQRT(REAL(N+1)) )
0568     XL = A*DBLE(Q)
0569     YL = XL
0570 C
0571     RAN1 = DSQRT(2.0D0)
0572     RAN2 = DSQRT(3.0D0)
0573     PTCL = 0
0574     DO 10 J=0,Q-1
0575     DO 10 I=0,Q-1
0576       PTCL = PTCL + 1
0577       C1 = RAN1*DBLE(PTCL)
0578       C1 = C1 - DINT(C1)
0579       C1 = C1 - 0.5D0
0580       C2 = RAN2*DBLE(PTCL)
0581       C2 = C2 - DINT(C2)
0582       C2 = C2 - 0.5D0
0583       RX(PTCL) = DBLE(I)*A - XL/2.0D0 + 0.1D0 + C1*0.091D0
0584       RY(PTCL) = DBLE(J)*A - YL/2.0D0 + 0.1D0 + C2*0.091D0
0585   10 CONTINUE
0586     N = PTCL
0587 C
0588     DO 20 I=1,N
0589       NX(I) = 0.0D0
0590       NY(I) = 1.0D0
0591   20 CONTINUE
0592 C
0593     IF( VRADIUS .GT. XL/2.0D0 ) THEN
0594       VRADIUS = XL/2.0D0
0595       RCOFF   = XL/2.0D0
0596     END IF
0597
0598
0599 C**** SUB INIPOSID *****
0600     SUBROUTINE INIPOSID( DC , RCOFFD , N )
0601 C
0602     IMPLICIT REAL*8 ( A-H,O-Z ), INTEGER ( I-N )
0603 C
0604     COMMON /BLOCK1/ RX , RY
0605     COMMON /BLOCK15/ H , XL , YL , RCOFF
0606     COMMON /BLOCK21/ RXD , RYD
0607     COMMON /BLOCK26/ ND , NDENSDH , NDENSD , VDENSD , MD
0608 C
0609     PARAMETER( NN=100 , NND=50000 )
0610 C
0611     REAL*8    RX(NN) , RY(NN) , RXD(NND) , RYD(NND)

```

• A subroutine for setting the initial positions of magnetic particles.

•  $\phi_V=(\pi/4)a^2$ ,  $a^*=(\pi/(4\phi_V))^{1/2}$  and  $Q=N^{1/2}$ . The values of  $a^*$  and  $Q$  are saved in  $A$  and  $Q$ , respectively.

----- POSITION -----

• RAN1 and RAN2 are quasi-random numbers.  
• Each particle is moved in parallel by the distance  $(0.1, 0.1)$  to remove subtle situations at the outer boundary surfaces. Also, to remove the regularity of the initial configuration, each particle is moved randomly by the maximum displacement  $(1/2)\times(0.091, 0.091)$  using quasi-random numbers.

• Additionally each particle is moved in parallel by  $(1/2)\times(-XL, -YL)$  so that the center of the simulation box is the origin of the coordinate system.

• The direction of each magnetic moment is set in the  $y$ -direction.

RETURN  
END

• A subroutine for setting the initial positions of dissipative particles.

```

0612      REAL*8    NDENSDH, NDENSD , MD , B , RSQCHK , RXID , RYID
0613      REAL*8    RXI , RYI , RXIJ , RYIJ , RIJSQ, RCOFFMN, RCOFFMN2
0614      INTEGER   P , PTCL
0615 C
0616      B = DSQRT( 1.D0/NDENSD )
0617      P = INT( XL/B )
0618      RSQCHK = ( 0.5D0 + DC/2.D0)**2
0619      RCOFFMN = 0.5D0 + ( DC/2.D0 )*0.3D0
0620      RCOFFMN2 = RCOFFMN**2
0621 C
0622      PTCL=0
0623      DO 120 IY=0,P-1
0624          RXID = DBLE(IY)*B - YL/2.D0 + 0.0001D0
0625          IF( RXID .GE. YL/2.D0 ) GOTO 120
0626      DO 100 IX=0,P-1
0627          RXID = DBLE(IX)*B - XL/2.D0 + 0.0001D0
0628          IF( RXID .GE. XL/2.D0 ) GOTO 100
0629 C
0630      DO 50 I=1,N
0631          RXI = RX(I)
0632          RYI = RY(I)
0633          RXIJ = RXID - RXI
0634          RXIJ = RXIJ - DNINT(RXIJ/XL)*XL
0635          IF( DABS(RXIJ) .GT. RCOFFMN ) GOTO 50
0636          RYIJ = RYID - RYI
0637          RYIJ = RYIJ - DNINT(RYIJ/YL)*YL
0638          IF( DABS(RYIJ) .GT. RCOFFMN ) GOTO 50
0639          RIJSQ= RXIJ**2 + RYIJ**2
0640          IF( RIJSQ .LT. RCOFFMN2 ) GOTO 100
0641      50  CONTINUE
0642 C
0643      PTCL = PTCL + 1
0644      RXD(PTCL) = RXID
0645      RYD(PTCL) = RYID
0646      100 CONTINUE
0647      120 CONTINUE
0648      ND = PTCL
0649
0650
0651 C**** SUB INIVEL *****
0652      SUBROUTINE INIVEL( N , PI , VELMX )
0653 C
0654      IMPLICIT REAL*8 ( A-H,O-Z) , INTEGER ( I-N )
0655 C
0656      COMMON /BLOCK2/ VX , VY
0657      COMMON /BLOCK35/ NRAN , RAN , IX
0658 C
0659      PARAMETER( NN=100 , NRANMX=100000000 )
0660 C
0661      REAL*8 VX(NN) , VY(NN) , MOMX , MOMY , CC1 , CC2
0662      REAL     RAN(NRANMX)
0663 C
0664      DO 10 I=1,N
0665          NRAN = NRAN + 1
0666          CC1 = DSQRT( -2.D0*(1.D0)*DLOG( DBLE(RAN(NRAN)) ) )
0667          NRAN = NRAN + 1
0668          CC2 = 2.D0*PI*DBLE(RAN(NRAN))
0669          VX(I) = CC1*DCOS(CC2)
0670 C
0671          NRAN = NRAN + 1
0672          CC1 = DSQRT( -2.D0*(1.D0)*DLOG( DBLE(RAN(NRAN)) ) )
0673          NRAN = NRAN + 1
0674          CC2 = 2.D0*PI*DBLE(RAN(NRAN))
0675          VY(I) = CC1*DSIN(CC2)
0676 C
0677          C1 = VX(I)**2 + VY(I)**2
0678          IF( C1 .GT. VELMX ) THEN
0679              C1 = DSQRT( VELMX/C1 )
0680              VX(I) = VX(I)*C1
0681              VY(I) = VY(I)*C1
0682          END IF
0683      10 CONTINUE

```

•  $n_d^* = 1/b^2$  and  $b^* = (1/n_d^*)^{1/2}$ . Particles are placed in each axis direction.

• Each particle is moved in parallel by  $(1/2)(-XL, -YL)$ , so that the center of the simulation box is the origin of the coordinate system.

• The dissipative particles are not placed if the separation between magnetic and dissipative particles is shorter than RCOFFMN.

• A subroutine for setting the initial velocities of magnetic particles.

• The initial velocities are assigned according to Eq. (A2.3).

• The initial velocities are modified so as to be smaller than the maximum velocity.

```

0684 C
0685     MOMX = 0.D0
0686     MOMY = 0.D0
0687     DO 20 I=1,N
0688         MOMX = MOMX + VX(I)
0689         MOMY = MOMY + VY(I)
0690     20 CONTINUE
0691     MOMX = MOMX/DBLE(N)
0692     MOMY = MOMY/DBLE(N)
0693 C                                     --- SET TOTAL MOMENTUM ZERO ---
0694 C                                     •The velocities are modified so as to yield
0695     DO 30 I=1,N                         zero total system momentum.
0696         VX(I) = VX(I) - MOMX
0697         VY(I) = VY(I) - MOMY
0698     30 CONTINUE
0699
0700
0701 C**** SUB INIVELD *****
0702     SUBROUTINE INIVELD( ND , MD , PI , VELDMX )
0703 C
0704     IMPLICIT REAL*8 (A-H,O-Z), INTEGER (I-N)
0705 C
0706     COMMON /BLOCK22/ VXD , VYD
0707     COMMON /BLOCK35/ NRAN , RAN , IX
0708 C
0709     PARAMETER( NND=50000 , NRANMX=100000000 )
0710 C
0711     REAL*8 VXD(NND) , VYD(NND) , MD , MOMX , MOMY , CC1 , CC2
0712     REAL      RAN(NRANMX)
0713 C
0714     DO 10 I=1,ND
0715         NRAN = NRAN + 1
0716         CC1 = DSQRT( -2.D0*(1.D0/MD)*DLOG( DBLE(RAN(NRAN)) ) )
0717         NRAN = NRAN + 1
0718         CC2 = 2.D0*PI*DBLE(RAN(NRAN))
0719         VXD(I) = CC1*DCOS(CC2)
0720 C
0721         NRAN = NRAN + 1
0722         CC1 = DSQRT( -2.D0*(1.D0/MD)*DLOG( DBLE(RAN(NRAN)) ) )
0723         NRAN = NRAN + 1
0724         CC2 = 2.D0*PI*DBLE(RAN(NRAN))
0725         VYD(I) = CC1*DSIN(CC2)
0726 C
0727         C1      = VXD(I)**2 + VYD(I)**2
0728         IF( C1 .GT. VELDMX ) THEN
0729             C1 = DSQRT( VELDMX/C1 )
0730             VXD(I) = VXD(I)*C1
0731             VYD(I) = VYD(I)*C1
0732         END IF
0733     10 CONTINUE
0734 C                                     --- SET TOTAL MOMENTUM ZERO ---
0735     MOMX = 0.D0
0736     MOMY = 0.D0
0737     DO 20 I=1,ND
0738         MOMX = MOMX + VXD(I)
0739         MOMY = MOMY + VYD(I)
0740     20 CONTINUE
0741     MOMX = MOMX/DBLE(ND)
0742     MOMY = MOMY/DBLE(ND)
0743 C                                     --- CORRECT VELOCITIES TO SATISFY ---
0744 C                                     --- ZERO TOTAL MOMENTUM ---
0745     DO 30 I=1,ND
0746         VXD(I) = VXD(I) - MOMX
0747         VYD(I) = VYD(I) - MOMY
0748     30 CONTINUE
0749
0750
0751 C**** SUB SCALEVEL *****
0752     SUBROUTINE SCALEVEL( N, VX, VY, VELTHRY, VELX, VELY, VELSQ )

```

RETURN  
END

• A subroutine for setting the initial velocities of dissipative particles.

• The initial velocities are assigned according to Eq. (A2.3).

• The initial velocities are modified so as to be smaller than the maximum velocity.

• The velocities are modified so as to yield zero total system momentum.

```

0753 C      IMPLICIT REAL*8 (A-H,O-Z), INTEGER (I-N)
0754      VX(N), VY(N)
0755 C      REAL*8   VX(N), VY(N)
0756      --- ZERO TOTAL MOMENTUM FOR EACH AXIS ---
0757 C      DO 10 I = 1,N
0758      VX(I) = VX(I) - VELX
0759      VY(I) = VY(I) - VELY
0760      10 CONTINUE
0761      --- CORRECT VELOCITIES TO SATISFY ---
0762 C      - SPECIFIED TEMPERATURE -
0763 C      C1 = VELTHRY/DSQRT( VELSQ - VELX**2 - VELY**2 )
0764      DO 50 I = 1,N
0765      VXI = VX(I)
0766      VVI = VY(I)
0767      VX(I) = VXI*C1
0768      VY(I) = VVI*C1
0769      50 CONTINUE
0770      RETURN
0771
0772
0773 C**** SUB GRIDGENE *****
0774      SUBROUTINE GRIDGENE( XL , RCOFFD )
0775 C      IMPLICIT REAL*8 (A-H,O-Z), INTEGER (I-N)
0776      COMMON /BLOCK30/ PXD , GRPLXD , PXYD
0777 C
0778      INTEGER     PPXD
0779 C      PARAMETER( PPXD=500 )
0780 C
0781      REAL*8   GRPLXD(PPXD) , C0
0782 C      INTEGER     PXD , PXYD
0783 C
0784      PXD = INT( XL/RCOFFD )
0785 C      PXYD = PXD**2
0786      C0 = XL/DBLE(PXD)
0787      DO 10 I=1,PXD
0788      GRPLXD(I) = C0*DBLE(I) - XL/2.D0
0789      10 CONTINUE
0790      RETURN
0791
0792
0793 C**** SUB GROUP *****
0794      SUBROUTINE GROUP( ND )
0795      IMPLICIT REAL*8 (A-H,O-Z), INTEGER (I-N)
0796 C
0797      COMMON /BLOCK21/ RXD , RYD
0798      COMMON /BLOCK28/ GRPX , GRPY
0799      COMMON /BLOCK30/ PXD , GRPLXD , PXYD
0800 C
0801      INTEGER     PPXD, PXYD, TTD
0802 C      PARAMETER( NND=50000 , PPXD=500 , PXYD=250000 , TTD=20 )
0803 C
0804      REAL*8   RXD(NND) , RYD(NND)
0805 C      REAL*8   GRPLXD(PPXD)
0806      INTEGER     GRPX(NND), GRPY(NND) , PXD , PXYD
0807 C
0808      DO 100 I=1,ND
0809 C
0810      DO 10 J=1,PXD
0811 C      IF( GRPLXD(J) .GT. RXD(I) ) THEN
0812 C          GRPX(I) = J
0813 C          GOTO 15
0814 C      END IF
0815 C
0816      10 CONTINUE
0817      GRPX(I) = PXD
0818 C
0819 C      15 DO 20 J=1,PXD
0820 C          IF( GRPLXD(J) .GT. RYD(I) ) THEN
0821 C              GRPY(I) = J
0822 C              GOTO 100
0823 C          END IF
0824 C

```

• A subroutine for scaling the velocities  
 (common for both magnetic and dissipative particles).

• The velocities are modified so as to yield zero total momentum.

• The velocities are modified so as to yield the desired system temperature.

• A subroutine for generating cells for the cell index method in the case of dissipative particles.

• The cells are made by dividing the simulation box into PXD equal cells in each axis-direction. The position of the x-coordinate (equal to y-coordinate) is saved in GRPLXD.

• A subroutine for grasping the name of the cell to which each dissipative particle belongs.

--- X AXIS ---

• If particle  $i$  belongs to the cell which is assumed to be the (GRPX( $i$ )-th, GRPY( $i$ )-th) cell in x- and y-directions, the name of the cell is GP=GRPX( $i$ )+(GRPY( $i$ )-1)\*PXD.

--- Y AXIS ---

```

0825    20  CONTINUE
0826          GRPY(I) = PXD
0827 C
0828    100 CONTINUE
0829
0830
0831 C**** SUB TABLECAL *****
0832      SUBROUTINE TABLECAL( ND , PXD )
0833 C
0834      IMPLICIT REAL*8 (A-H,O-Z), INTEGER (I-N)
0835 C
0836      COMMON /BLOCK28/ GRPX , GRPY
0837      COMMON /BLOCK29/ TMXD , TABLED
0838 C
0839      INTEGER PPXD, PPXYD, TTD
0840      PARAMETER( NND=50000 , PPXD=500 , PPXYD=250000 , TTD=20 )
0841 C
0842      INTEGER GRPX(NND), GRPY(NND)
0843      INTEGER TMXD(PPXYD), TABLED(TTD,PPXYD) , PXD , GX , GY , GP
0844 C
0845      DO 10 GY=1,PXD
0846      DO 10 GX=1,PXD
0847          GP = GX + (GY-1)*PXD
0848          TMXD(GP) = 0
0849          TABLED(1,GP) = 0
0850    10 CONTINUE
0851 C
0852      DO 20 I=1,ND
0853          GX = GRPX(I)
0854          GY = GRPY(I)
0855          GP = GX + (GY-1)*PXD
0856          TMXD(GP) = TMXD(GP) + 1
0857          TABLED( TMXD(GP),GP ) = I
0858    20 CONTINUE
0859
0860
0861 C**** SUB VTABLEDP *****
0862      SUBROUTINE VTABLEDP( N , RCOFFD , RCOFFMD , XL , YL , DC )
0863 C
0864      IMPLICIT REAL*8 (A-H,O-Z), INTEGER (I-N)
0865 C
0866      COMMON /BLOCK1/ RX , RY
0867      COMMON /BLOCK9/ TMX , TABLE
0868      COMMON /BLOCK30/ PXD , GRPLXD , PXYD
0869 C
0870      INTEGER TT, PPXD
0871      PARAMETER( NN=100 , NNN=10000 , TT=500 , PPXD=500 )
0872 C
0873      INTEGER TMX(NN) , TABLE(TT,NN) , PXD , PXYD
0874      REAL*8 RX(NN) , RY(NN) , GRPLXD(PPXD)
0875      REAL*8 RX1, RY1, RX1, RY1, RX2, RY2, XI, YI, CL, MODX, MODY
0876      REAL*8 RSQCHK , RSQCHK2 , RRISQ , RCHK
0877      INTEGER GPX1 , GPX2 , GPY1 , GPY2 , GP
0878 C
0879      CL = GRPLXD(2) - GRPLXD(1)
0880      RCHK = RCOFFMD + (CL/2.D0)*1.415D0
0881      RSQCHK = RCHK**2
0882      RSQCHK2 = ( 0.5D0-DC/2.D0-(CL/2.D0)*1.415D0 )**2
0883      DO 10 I=1,N
0884          TMX(I) = 0
0885          TABLE(1,I) = 0
0886    10 CONTINUE
0887 C
0888      DO 200 I=1,N
0889          RX1 = RX(I)
0890          RY1 = RY(I)
0891          RX1 = RX1 - RCHK
0892          RY1 = RY1 - RCHK
0893          RX2 = RX1 + RCHK
0894          RY2 = RY1 + RCHK

```

• A subroutine for grasping the names of dissipative particles belonging to each cell.

• If particle  $i$  belongs to the cell which is assumed to be the  $(GX\text{-}th, GY\text{-}th)$  cell in the  $x$ - and  $y$ -directions, the name of the cell is  $GP=GX+(GY-1)*PXD$ .  
• The name of particle  $i$  is therefore saved in the variable in  $\text{TABLED}(*,GP)$  concerning cell  $GP$ .

• A subroutine for grasping the cells in which dissipative particles possibly interact with magnetic particles.

```

0895      GPX1 = INT( (RX1+XL/2.D0)/CL ) - 1
0896      GPX2 = INT( (RX2+XL/2.D0)/CL ) + 2
0897      GPY1 = INT( (RY1+YL/2.D0)/CL ) - 1
0898      GPY2 = INT( (RY2+YL/2.D0)/CL ) + 2
0899 C
0900      DO 150 IY0 = GPY1, GPY2
0901          IY = IY0
0902          MODY = 0.D0
0903          IF( IY0 .LE. 0 ) THEN
0904              IY = IY0 + PXD
0905              MODY = -YL
0906          END IF
0907          IF( IY0 .GT. PXD ) THEN
0908              IY = IY0 - PXD
0909              MODY = YL
0910          END IF
0911          YI = GRPLXD(IY) - CL/2.D0 + MODY
0912 C
0913      DO 140 IX0 = GPX1, GPX2
0914          IX = IX0
0915          MODX = 0.D0
0916          IF( IX0 .LE. 0 ) THEN
0917              IX = IX0 + PXD
0918              MODX = -XL
0919          END IF
0920          IF( IX0 .GT. PXD ) THEN
0921              IX = IX0 - PXD
0922              MODX = XL
0923          END IF
0924          XI = GRPLXD(IX) - CL/2.D0 + MODX
0925 C
0926          GP = IX + PXD*(IY-1)
0927          RRISQ= (XI-RXI)**2 + (YI-RYI)**2
0928          IF( RRISQ .GE. RSQCHK ) GOTO 140
0929          IF( RRISQ .LE. RSQCHK2 ) GOTO 140
0930 C
0931          TMX(I) = TMX(I) + 1
0932          TABLE( TMX(I),I ) = GP
0933      140 CONTINUE
0934      150 CONTINUE
0935      200 CONTINUE
0936
0937
0938 C**** SUB VTABLEMA *****
0939      SUBROUTINE VTABLEMA( N , XL , YL )
0940 C
0941      IMPLICIT REAL*8 (A-H,O-Z), INTEGER (I-N)
0942 C
0943      COMMON /BLOCK1/ RX , RY
0944      COMMON /BLOCK10/ VT MX , VTABLE , VPLACE , NVTABLE , VRADIUS
0945 C
0946      PARAMETER( NN=100 , NNN=10000 )
0947 C
0948      REAL*8 RX(NN) , RY(NN)
0949      INTEGER VT MX(NN) , VTABLE(NNN) , VPLACE(NN) , N2
0950      REAL*8 RXI , RYI , RXIJ , RYIJ , RIJ2 , VRADIUS2
0951 C
0952      VRADIUS2 = VRADIUS**2
0953      N2 = N**2
0954      IF( N2 .GT. NNN ) N2 = NNN
0955      DO 10 I=1,N
0956          VT MX(I) = 0
0957          VPLACE(I) = 0
0958      10 CONTINUE
0959      DO 15 I=1,N2
0960          VTABLE(I) = 0
0961      15 CONTINUE
0962 C
0963 C
0964      DO 200 I=1,N
0965 C
0966          RXI = RX(I)

```

- The dissipative particles only in the neighboring cells possibly interact with magnetic particle *i*.

- The treatment of the periodic BC.

- If the distance between magnetic particle *i* and a cell is shorter than RSQCHK, the cell is regarded as a possible interacting cell.

RETURN  
END

- A subroutine for grasping the names of magnetic particles interacting with magnetic particle themselves according to the Verlet neighbor list method.

- The number of the magnetic particles interacting with particle *i* is saved in VT MX(*i*), and the names of the interacting particles are saved in VTABLE(\*). The name of the particle interacting with particle *i* first appears in the VPLACE(*i*)-th position of the variable VTABLE(\*)).

```

0967      RYI    = RY(I)
0968      IF( I .EQ. 1 ) THEN
0969          VPLACE(I) = 1
0970      ELSE
0971          VPLACE(I) = VPLACE(I-1) + VTMX(I-1)
0972      END IF
0973 C
0974      DO 150 J=1,N
0975 C
0976      IF( J.EQ.I )           GOTO 150
0977      RXIJ = RXI - RX(J)
0978      RXIJ = RXIJ - DNINT(RXIJ/XL)*XL
0979      IF( DABS(RXIJ) .GE. VRADIUS )   GOTO 150
0980      RYI = RYI - RY(J)
0981      RYIJ = RYIJ - DNINT(RYIJ/YL)*YL
0982      IF( DABS(RYIJ) .GE. VRADIUS )   GOTO 150
0983 C
0984      RIJ2 = RXIJ*RXIJ + RYI*RYIJ
0985      IF( RIJ2 .GE. VRADIUS2 )     GOTO 150
0986 C
0987      VTMX(I) = VTMX(I) + 1
0988      VTABLE( VPLACE(I) + VTMX(I) - 1 ) = J
0989 C
0990      150 CONTINUE
0991      200 CONTINUE
0992
0993
0994 C**** SUB FORCEMAG *****
0995      SUBROUTINE FORCEMAG( RCOFF2 , NTIME )
0996 C
0997      IMPLICIT REAL*8 ( A-H,O-Z ), INTEGER ( I-N )
0998 C
0999      COMMON /BLOCK1/  RX , RY
1000      COMMON /BLOCK2/  VX , VY
1001      COMMON /BLOCK3/  NX , NY
1002      COMMON /BLOCK5/  FX , FY
1003      COMMON /BLOCK7/  N , NDENS , VDENS , D , DS , DEL , TD
1004      COMMON /BLOCK8/  RA , RV , RE
1005      COMMON /BLOCK10/ VTMX , VTABLE , VPLACE , NVTABLE , VRADIUS
1006      COMMON /BLOCK13/ OVR LAP
1007      COMMON /BLOCK15/ H , XL , YL , RCOFF
1008 C
1009      INTEGER       TT
1010      PARAMETER( NN=100 , NNN=10000 , TT=500 )
1011 C
1012      REAL*8   RX(NN) , RY(NN) , VX(NN) , VY(NN)
1013      REAL*8   FX(NN) , FY(NN) , NX(NN) , NY(NN)
1014      REAL*8   NDENS
1015      LOGICAL  OVR LAP(NN)
1016      INTEGER   VTMX(NN) , VTABLE(NNN) , VPLACE(NN)
1017 C
1018      REAL*8   RXI , RYI , RXIJ , RYIJ
1019      REAL*8   NXI , NYI , NXJ , NYJ
1020      REAL*8   FXI , FYI , FXIJ , FYIJ
1021      REAL*8   TXIJ , TYIJ , RIJ , RIJ2 , RIJ4 , RIJORG N
1022      REAL*8   RA3 , RMN , RMN2
1023      REAL*8   C0 , C1 , C2 , C3
1024      INTEGER   IVPLACE
1025 C
1026      RA3 = 3.D0*RA
1027      RMN = DS
1028      RMN2 = RMN**2
1029      DO 10 I=1,N
1030          FX(I) = 0.D0
1031          FY(I) = 0.D0
1032          OVR LAP(I) = .FALSE.
1033      10 CONTINUE
1034 C
1035 C
1036      DO 100 I=1,N
1037 C

```

• The treatment for the periodic BC.

• If the distance between magnetic particles is within VRADIUS, the names of the magnetic particles are saved in VTABLE(\*)..

• A subroutine for calculating the magnetic forces acting on magnetic particles.

• Whether or not an overlap of the solid parts of the two magnetic particles appears is described by the logical variable OVR LAP(\*)..

```

1038      RXI = RX(I)
1039      RYI = RY(I)
1040      NXI = NX(I)
1041      NYI = NY(I)
1042      FXI = FX(I)
1043      FYI = FY(I)
1044 C      IF( VTMX(I) .EQ. 0 )          GOTO 100
1045 C      IVPLACE = VPLACE(I)
1046 C      DO 50 JJ=1, VTMX(I)
1047 C
1048 C      J = VTABLE( IVPLACE + JJ - 1 )
1049 C      IF( J.EQ.I )                  GOTO 50
1050 C      RXIJ = RXI - RX(J)
1051 C      RXIJ = RXIJ - DNINT(RXIJ/XL)*XL
1052 C      IF( DABS(RXIJ) .GE. RCOFF )   GOTO 50
1053 C      RYIJ = RYI - RY(J)
1054 C      RYIJ = RYIJ - DNINT(RYIJ/YL)*YL
1055 C      IF( DABS(RYIJ) .GE. RCOFF )   GOTO 50
1056 C
1057 C      RIJ2 = RXIJ*RXIJ + RYIJ*RYIJ
1058 C      IF( RIJ2 .GE. RCOFF2 )       GOTO 50
1059 C      RIJ = DSQRT(RIJ2)
1060 C      RIJORGN = RIJ
1061 C
1062 C      IF( RIJ2 .LT. RMN2 ) THEN
1063 C          RXIJ = RMN*RXIJ/RIJ
1064 C          RYIJ = RMN*RYIJ/RIJ
1065 C          RIJ = RMN
1066 C          RIJ2 = RMN2
1067 C
1068 C          OVRALP(I) = .TRUE.
1069 C          OVRALP(J) = .TRUE.
1070 C
1071 C          END IF
1072 C          RIJ4 = RIJ2**2
1073 C          TXIJ = RXIJ/RIJ
1074 C          TYIJ = RYIJ/RIJ
1075 C          NXJ = NX(J)
1076 C          NYJ = NY(J)
1077 C
1078 C          C1 = NXI*NXJ + NYI*NYJ
1079 C          C2 = NXI*TXIJ + NYI*TYIJ
1080 C          C3 = NXJ*TXIJ + NYJ*TYIJ
1081 C
1082 C          FXIJ = - ( RA3/RIJ4 ) * ( ( - C1 + 5.D0*C2*C3 )*TXIJ
1083 C                           - ( C3*NXI + C2*NXJ ) )
1084 C          FYIJ = - ( RA3/RIJ4 ) * ( ( - C1 + 5.D0*C2*C3 )*TYIJ
1085 C                           - ( C3*NYI + C2*NYJ ) )
1086 C
1087 C          IF( RIJORGN .LT. 1.D0 ) THEN
1088 C              C0 = DLOG( 1.D0 / RIJORGN )
1089 C              FXIJ = FXIJ + RV*TXIJ*C0/DEL
1090 C              FYIJ = FYIJ + RV*TYIJ*C0/DEL
1091 C
1092 C          END IF
1093 C          FXI = FXI + FXIJ
1094 C          FYI = FYI + FYIJ
1095 C
1096      50  CONTINUE
1097 C
1098      FX(I) = FXI
1099      FY(I) = FYI
1100 C
1101      100 CONTINUE
1102
1103
1104 C**** SUB FORCEDPD *****
1105      SUBROUTINE FORCEDPD( PI )
1106 C
1107      IMPLICIT REAL*8 (A-H,O-Z), INTEGER (I-N)
1108 C

```

- The name of the particles interacting with particle  $i$  first appears in the VPLACE( $i$ )-th position of the variable VTABLE(\*). The number of the magnetic particles interacting with particle  $i$  is VTMX( $i$ ).

- The treatment for the periodic BC.

- If the solid particles overlap, OVRALP( $i$ )=OVRALP( $j$ )=.TRUE. are set.

- The magnetic forces acting on particles are calculated according to Eq. (6.24).

--- MAGNETIC FORCE ---  

$$\begin{aligned} FXIJ = & - ( RA3/RIJ4 ) * ( ( - C1 + 5.D0*C2*C3 ) * TXIJ \\ & \quad - ( C3*NXI + C2*NXJ ) ) \\ FYIJ = & - ( RA3/RIJ4 ) * ( ( - C1 + 5.D0*C2*C3 ) * TYIJ \\ & \quad - ( C3*NYI + C2*NYJ ) ) \end{aligned}$$
  
--- STERIC REPULSION ---

- The repulsive force arising from the overlap of the surfactant layers is calculated according to Eq. (6.25).

RETURN  
END

- A subroutine for calculating the forces acting between dissipative particles.

```

1109      COMMON /BLOCK15/ H , XL , YL , RCOFF
1110      COMMON /BLOCK21/ RXD , RYD
1111      COMMON /BLOCK22/ VXD , VYD
1112      COMMON /BLOCK23/ FCXD , FCYD
1113      COMMON /BLOCK24/ FDXD , FDYD
1114      COMMON /BLOCK25/ FRXD , FRYD
1115      COMMON /BLOCK26/ ND , NDENSDH , NDENSD , VDENSD , MD
1116      COMMON /BLOCK27/ DC , ALP , GAM , RCOFFD
1117      COMMON /BLOCK28/ GRPX , GRPY
1118      COMMON /BLOCK29/ TMXD , TABLED
1119      COMMON /BLOCK30/ PXD , GRPLXD , PXYD
1120      COMMON /BLOCK35/ NRAN , RAN , IX
1121 C
1122      INTEGER     PPXD, PPXYD, TTD
1123      PARAMETER( NND=50000 , PPXD=500 , PPXYD=250000 , TTD=20 )
1124      PARAMETER( NRANMX=100000000 )
1125 C
1126      REAL*8    RXD(NND) , RYD(NND) , VXD(NND) , VYD(NND)
1127      REAL*8    FCXD(NND) , FCYD(NND) , FDXD(NND) , FDYD(NND)
1128      REAL*8    FRXD(NND) , FRYD(NND)
1129      REAL*8    NDENSDH , NDENSD , MD
1130      REAL*8    GRPLXD(PPXD)
1131      INTEGER   GRPX(NND), GRPY(NND)
1132      INTEGER   TMXD(PPXYD), TABLED(TTD,PPXYD) , PXD , PXYD
1133 C
1134      REAL     RAN(NRANMX)
1135      INTEGER   NRAN , IX , NRANCHK
1136 C
1137      REAL*8    RXI , RYI , RXIJ , RYIJ , RIJSQ , RIJ
1138      REAL*8    VXI , VYI , VVXIJ , VVYIJ
1139      REAL*8    FCXI , FCYI , FCXIJ , FCYIJ
1140      REAL*8    FDXI , FDYI , FDXIJ , FDYIJ
1141      REAL*8    FRXI , FRYI , FRXIJ , FRYIJ
1142      REAL*8    FXIJ , FYIJ
1143      REAL*8    EXIJ , EYIJ
1144      REAL*8    WR , WR2 , TTAIJ , RAN1 , RAN2 , RCOFFD2
1145      REAL*8    MODX , MODY , C1
1146      INTEGER   GX , GY , GRP
1147 C
1148      RCOFFD2 = RCOFFD**2
1149      DO 10 I=1,ND
1150          FCXD(I) = 0.D0
1151          FCYD(I) = 0.D0
1152          FDXD(I) = 0.D0
1153          FDYD(I) = 0.D0
1154          FRXD(I) = 0.D0
1155          FRYD(I) = 0.D0
1156 10 CONTINUE
1157 C
1158      DO 500 I=1,ND
1159 C
1160          RXI = RXD(I)
1161          RYI = RYD(I)
1162          VXI = VXD(I)
1163          VYI = VYD(I)
1164          FCXI = FCXD(I)
1165          FCYI = FCYD(I)
1166          FDXI = FDXD(I)
1167          FDYI = FDYD(I)
1168          FRXI = FRXD(I)
1169          FRYI = FRYD(I)
1170 C
1171      DO 300 JJ=-1,1
1172          GY = GRPY(I) + JJ
1173          IF( GY .EQ. 0 ) THEN
1174              GY = PXD
1175              MODY = -YL
1176              GOTO 150
1177          END IF
1178          IF( GY .EQ. PXD+1 ) THEN
1179              GY = 1
1180              MODY = YL

```

- The conservative force, i.e., the first term on the right-hand side of Eq. (6.19), is saved in FCXD(\*) and FCYD(\*). Similarly, the dissipative term, i.e., the second term, is saved in FDXD(\*) and FDYD(\*). The random term, i.e., the third term, is saved in FRXD(\*) and FRYD(\*).

+++ NEIGHBORING GROUP +++

- The name of the cell in which the particles possibly interact with particle *i* of interest is GRP=GX+(GY-1)\*PXD.
- (MODX, MODY) are used in treating the periodic BC.

```

1181           GOTO 150
1182       END IF
1183       MODY = 0.D0
1184 C
1185   150  DO 300 II=-1,1
1186       GX = GRPX(I) + II
1187       IF( GX .EQ. 0 ) THEN
1188           GX = PXD
1189           MODX = -XL
1190           GOTO 160
1191       END IF
1192       IF( GX .EQ. PXD+1 ) THEN
1193           GX = 1
1194           MODX = XL
1195           GOTO 160
1196       END IF
1197       MODX = 0.D0
1198 C
1199   160  GRP = GX + (GY-1)*PXD
1200       IF( TMXD(GRP) .EQ. 0 )          GOTO 300
1201 C
1202       DO 200 JJJ=1,TMXD(GRP)          +++ ENERGY +++
1203 C
1204       J = TABLED(JJJ,GRP)
1205       IF( J .LE. I )                  GOTO 200
1206 C
1207       RXIJ = RXI - (RXD(J) + MODX)
1208       IF( DABS(RXIJ) .GE. RCOFFD )    GOTO 200
1209       RYIJ = RYI - (RYD(J) + MODY)
1210       IF( DABS(RYIJ) .GE. RCOFFD )    GOTO 200
1211       RIJSQ = RXIJ**2 + RYIJ**2
1212       IF( RIJSQ .GE. RCOFFD2 )       GOTO 200
1213       RIJ = DSQRT(RIJSQ)
1214       VXIJ = VXI - VXD(J)
1215       VYIJ = VYI - VYD(J)
1216 C
1217       EXIJ = RXIJ/RIJ
1218       EYIJ = RYIJ/RIJ
1219       IF(RIJ .LE. DC ) THEN
1220           WR = 1.D0 - RIJ/DC
1221           WR2 = WR*WR
1222       ELSE
1223           WR = 0.D0
1224           WR2 = 0.D0
1225       END IF
1226 C
1227       FCXIJ = WR*EXIJ
1228       FCYIJ = WR*EYIJ
1229       FCXI = FCXI + FCXIJ
1230       FCYI = FCYI + FCYIJ
1231       FCXD(J)= FCXD(J) - FCXIJ
1232       FCYD(J)= FCYD(J) - FCYIJ
1233 C
1234       C1 = EXIJ*VXIJ + EYIJ*VYIJ
1235       FDXIJ = - WR2*C1*EXIJ
1236       FDYIJ = - WR2*C1*EYIJ
1237       FDXI = FDXI + FDXIJ
1238       FDYI = FDYI + FDYIJ
1239       FDXD(J)= FDXD(J) - FDXIJ
1240       FDYD(J)= FDYD(J) - FDYIJ
1241 C
1242       NRAN = NRAN + 1
1243       RAN1 = DBLE(RAN(NRAN))
1244       IF( RAN1 .LE. 0.D0 ) RAN1 = 0.99999D0
1245       NRAN = NRAN + 1
1246       RAN2 = DBLE(RAN(NRAN))
1247       TTAIJ = DSQRT(-2.D0*DLOG(RAN1))*DCOS(2.D0*PI*RAN2)
1248 CCC
1249       IF( DABS(TTAIJ) .GT. 6.D0 ) TTAIJ = DSIGN( 6.D0, TTAIJ )
1249 C

```

- The treatment of the periodic BC.
- If the two particles are separated over the cutoff distance RCOFFD, the calculation is unnecessary.

- The action-reaction law can provide the force acting on particle *j* as  $(-FCXIJ)$  and  $(-FCYIJ)$ .

--- FC ---

- The calculation of the first conservative force in Eq. (6.19).

--- FD ---

- The calculation of the second dissipative force in Eq. (6.19).

--- FR ---

- The calculation of the third random force in Eq. (6.19).

```

1250          FRXIJ = WR*EXIJ*TTAIJ
1251          FRYIJ = WR*EYIJ*TTAIJ
1252          FRXI = FRXI + FRXIJ
1253          FRYI = FRYI + FRYIJ
1254          FRXD(J) = FRXD(J) - FRXI
1255          FRYD(J) = FRYD(J) - FRYIJ
1256 C
1257      200    CONTINUE
1258 C
1259      300    CONTINUE
1260 C
1261          FCXD(I) = FCXI
1262          FCYD(I) = FCYI
1263          FDXD(I) = FDXI
1264          FDYD(I) = FDYI
1265          FRXD(I) = FRXI
1266          FRYD(I) = FRYI
1267 C
1268      500    CONTINUE
1269 C
1270      DO 520 I=1,ND
1271          FCXD(I) = FCXD(I)*H*ALP/(MD*DC)
1272          FCYD(I) = FCYD(I)*H*ALP/(MD*DC)
1273          FDXD(I) = FDXD(I)*H*GAM/(DC*MD**0.5)
1274          FDYD(I) = FDYD(I)*H*GAM/(DC*MD**0.5)
1275          FRXD(I) = FRXD(I)*(H*2.D0*GAM)**0.5/(MD**0.75*DC*0.5)
1276          FRYD(I) = FRYD(I)*(H*2.D0*GAM)**0.5/(MD**0.75*DC*0.5)
1277      520    CONTINUE
1278
1279
1280 C**** SUB FORCEINT *****
1281      SUBROUTINE FORCEINT( N , ND , RE , DC )
1282 C
1283      IMPLICIT REAL*8 ( A-H,O-Z) , INTEGER ( I-N)
1284 C
1285      COMMON /BLOCK1/ RX , RY
1286      COMMON /BLOCK9/ TMX , TABLE
1287      COMMON /BLOCK11/ FXMD , FYMD , RCOFFMD , RCOFFDDM
1288      COMMON /BLOCK15/ H , XL , YL , RCOFF
1289      COMMON /BLOCK21/ RXD , RYD
1290      COMMON /BLOCK29/ TMXD , TABLED
1291      COMMON /BLOCK31/ FXDM , FYDM
1292 C
1293      INTEGER TT, PPXD, PPXYD, TTD
1294      PARAMETER( NN=100 , NNN=10000 , TT=500 )
1295      PARAMETER( NND=50000 , PPXD=500 , PPXYD=250000 , TTD=20 )
1296 C
1297      REAL*8 RX(NN) , RY(NN) , FXMD(NN) , FYMD(NN)
1298      REAL*8 RXD(NND) , RYD(NND) , FXDM(NND) , FYDM(NND)
1299      INTEGER TMX(NN) , TABLE(TT,NN)
1300      INTEGER TMXD(PPXYD) , TABLED(TTD,PPXYD)
1301 C
1302      REAL*8 RCOFFMD2 , RCOFFDDM , RCOFFMN , RCOFFMN2
1303      REAL*8 RXI , RYI , RXIJ , RYIJ , RZIJ , RIJ , RIJ2
1304      REAL*8 RXID , RYID , RRIJ , TXIJ , TYIJ
1305      REAL*8 FIJ , FXIJ , FYIJ , SR2 , SR4
1306      INTEGER GP
1307 C
1308      RCOFFMD2 = RCOFFMD**2
1309      RCOFFDDM = 2.D0*(DC/RCOFFDDM)**12 - (DC/RCOFFDDM)**6
1310      RCOFFMN = 0.5D0 + ( DC/2.D0 )*0.3D0
1311      RCOFFMN2 = RCOFFMN**2
1312      DO 10 I=1,N
1313          FXMD(I) = 0.D0
1314          FYMD(I) = 0.D0
1315      10 CONTINUE
1316      DO 12 I=1,ND
1317          FXDM(I) = 0.D0
1318          FYDM(I) = 0.D0
1319      12 CONTINUE
1320 C

```

• TTAIJ means  $\theta_{ij}$

RETURN  
END

• A subroutine for calculating the forces between magnetic and dissipative particles.

• The force acting on magnetic particle  $i$  by dissipative particles is saved in FXMD( $i$ ) and FYMD( $i$ ). The force acting on dissipative particle  $i$  by magnetic particles is saved in FXDM( $i$ ) and FYDM( $i$ ).

```

1321 C
1322      DO 200 I=1,N
1323      RXI = RX(I)
1324      RYI = RY(I)
1325      IF( TMX(I) .EQ. 0 )          GOTO 200
1326 C
1327      DO 150 J=1, TMX(I)
1328      GP = TABLE(J,I)
1329      IF( TMXD(GP) .EQ. 0 )        GOTO 150
1330 C
1331      DO 120 K=1, TMXD(GP)
1332      II = TABLED(K,GP)
1333      RXID = RXD(II)
1334      RYID = RYD(II)
1335 C
1336      RXIJ = RXI - RXID
1337      RXIJ = RXIJ - DNINT(RXIJ/XL)*XL
1338      IF( DABS(RXIJ) .GE. RCOFFMD )      GOTO 120
1339      RYIJ = RYI - RYID
1340      RYIJ = RYIJ - DNINT(RYIJ/YL)*YL
1341      IF( DABS(RYIJ) .GE. RCOFFMD )      GOTO 120
1342      RIJ2 = RXIJ**2 + RYIJ**2
1343      IF( RIJ2 .GT. RCOFFMD2 )          GOTO 120
1344      IF( RIJ2 .LT. RCOFFMN2 )          RIJ2 = RCOFFMN2
1345 C
1346      RIJ = DSQRT( RIJ2 )
1347      TXIJ = RXIJ/RIJ
1348      TYIJ = RYIJ/RIJ
1349      RRIJ = RIJ - 0.5D0 + DC/2.D0
1350      SR1 = (DC/RRIJ)
1351      SR2 = (DC/RRIJ)**2
1352      SR4 = SR2*SR2
1353      SR6 = SR2*SR4
1354      SR12 = SR6*SR6
1355      FIJ = (RE*DC/RRIJ)*( 2.D0*SR12 - SR6 - FCOFFDDM )
1356      FXIJ = FIJ*TXIJ
1357      FYIJ = FIJ*TYIJ
1358 C
1359      FXMD(I) = FXMD(I) + FXIJ
1360      FYMD(I) = FYMD(I) + FYIJ
1361      FXDM(II) = FXDM(II) - FXIJ
1362      FYDM(II) = FYDM(II) - FYIJ
1363 C
1364      120    CONTINUE
1365      150    CONTINUE
1366      200    CONTINUE
1367
1368
1369 C*****
1370 C  THIS SUBROUTINE IS FOR GENERATING UNIFORM RANDOM NUMBERS *
1371 C  (SINGLE PRECISION) FOR 32-BIT COMPUTER. *
1372 C  N      : NUMBER OF RANDOM NUMBERS TO GENERATE   *
1373 C  IX     : INITIAL VALUE OF RANDOM NUMBERS (POSITIVE INTEGER) *
1374 C      : LAST GENERATED VALUE IS KEPT                 *
1375 C  X(N)   : GENERATED RANDOM NUMBERS (0<X(N)<1)   *
1376 C*****
1377 C*** SUB RANCAL ***
1378      SUBROUTINE RANCAL( N, IX, X )
1379 C
1380      IMPLICIT REAL*8 (A-H,O-Z), INTEGER (I-N)
1381 C
1382      REAL      X(N)
1383      INTEGER    INTEGMX, INEGST, INEG
1384 C
1385      DATA INTEGMX/2147483647/
1386      DATA INEGST,INEG/584287,48828125/
1387 C
1388      AINTEGMX = REAL( INTEGMX )
1389 C
1390      IF ( IX.LT.0 ) STOP

```

• The name of the cell in which the dissipative particles possibly interact with magnetic particle *i* is GP. The names of such dissipative particles are read from the variable TABLED (\*,GP).

• If the magnetic particle and the dissipative particle are separated over RCOFFMD, the force is regarded to be zero. If the two particles significantly overlap, the separation is regarded as RCOFFMN in order to prevent the system from diverging.

• The forces are calculated according to Eq. (6.26).

• A subroutine for generating a uniform random number sequence.

• This is for a 32-bit CPU based on the expression of two's complement.

```
1391      IF ( IX.EQ.0 ) IX = INTEGST
1392      DO 30 I=1,N
1393          IX = IX*INTEG
1394          IF (IX .LT. 0 ) IX   = (IX+INTEGMX)+1
1395          X(I) = REAL(IX)/AINTEGMX
1396 30 CONTINUE
1397      RETURN
1398      END
```

# 7 Practice of Lattice Boltzmann Simulations

In this chapter, we consider the lattice Boltzmann method, which is generally used as a simulation technique for a pure liquid system but has a different approach to the molecular simulation and microsimulation methods. The lattice Boltzmann method is also a potential simulation technique for taking into account multibody hydrodynamic interactions among particles in a particle suspension or polymers in a polymeric liquid. Therefore, the lattice Boltzmann method may be a promising simulation tool in various fields in science and engineering.

In treating fluid properties, such as the flow field, the lattice Boltzmann method employs an abstract approach that makes use of the particle distribution function, whereas the usual fluid simulation method deals with quantities that are intuitively understandable, such as velocities and pressures. The reader may therefore find that the basic principle behind the lattice Boltzmann method is slightly more difficult to understand. However, once mastered, the concept of the particle distribution function and the theoretical background of this simulation method will enable a research scientist to apply the lattice Boltzmann method to various types of flow problems in a relatively straightforward manner.

The present exercise addresses a uniform flow around a circular cylinder, which will be a foundation for applying the lattice Boltzmann method to flow problems in a particle dispersion or a polymeric liquid. The validity of the solution obtained by this method can be evaluated by comparing it with that obtained by a fully developed simulation method, such as the finite difference method. The sample simulation program has been developed from the viewpoint of applying it to a particle suspension; it may thus be very valuable in a practical context.

## 7.1 Uniform Flow Around a Two-Dimensional Circular Cylinder

We here consider solving the problem of uniform flow past a circular cylinder by means of the lattice Boltzmann method. In a certain limited range of the Reynolds number, a pair of vortices appears behind the cylinder. The formation of these vortices is very sensitive to the type of boundary model used for the interaction between the cylinder and the neighboring virtual fluid particles.

## 7.2 Specification of Problems in Equations

The important task in the formalization of the present problem is the treatment of the boundary condition between the cylinder and the virtual fluid particles in the neighboring lattice sites in addition to the outer boundary conditions.

We consider a uniform flow past a two-dimensional circular cylinder in the  $x$ -direction, as shown in Figure 7.1. The present flow problem is treated as a two-dimensional flow, so we use the D2Q9 lattice model, as explained in Section 1.5. The simulation region is divided into the lattice system shown in Figure 7.2. The two-dimensional circular cylinder with diameter  $D$  is fixed at the origin of the coordinate system. Numbering the velocity direction  $\alpha$  in the unit cell is as shown in Figure 1.5B, and  $\alpha$  is taken as  $\alpha = 0, 1, 2, \dots, 8$ . If  $\mathbf{r}$  is the position vector of an arbitrary lattice point and  $f_\alpha(\mathbf{r}, t)$  is the particle distribution function at time  $t$ , the function after the time interval  $\Delta t$ ,  $f_\alpha(\mathbf{r} + \mathbf{c}_\alpha \Delta t, t + \Delta t)$ , can be evaluated from Eq. (1.91) as

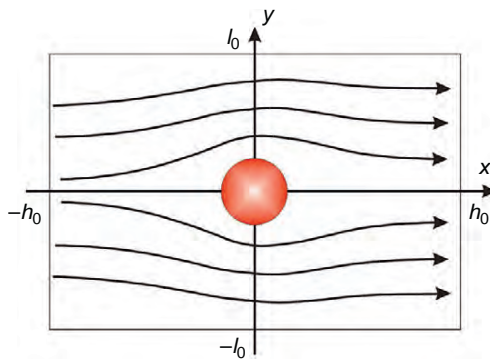


**Figure 7.1** Uniform flow past a circular cylinder.

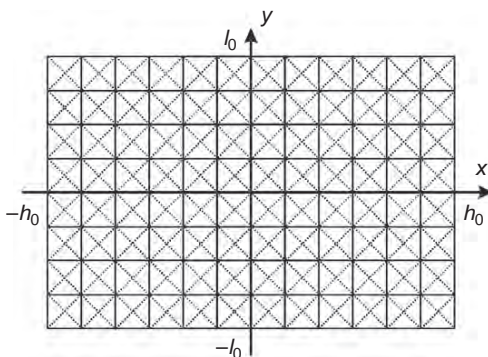


**Figure 7.2** Simulation region made up of square lattices.

$$\left. \begin{aligned} f_\alpha(\mathbf{r} + \mathbf{c}_\alpha \Delta t, t + \Delta t) &= \tilde{f}_\alpha(\mathbf{r}, t) \\ \tilde{f}_\alpha(\mathbf{r}, t) &= f_\alpha(\mathbf{r}, t) + \frac{1}{\tau} \{ f_\alpha^{(0)}(\mathbf{r}, t) - f_\alpha(\mathbf{r}, t) \} \end{aligned} \right\} \quad (7.1)$$

in which  $\tau$  is the relaxation time,  $f_\alpha^{(0)}$  is the thermodynamic equilibrium distribution function, and  $\mathbf{c}_\alpha$  is the lattice velocity in the  $\alpha$ -direction. With the notation  $\mathbf{u}$  for the macroscopic velocity and  $\rho$  for the density, the equilibrium distribution function is written as

$$f_\alpha^{(0)} = \rho w_\alpha \left\{ 1 + 3 \frac{\mathbf{c}_\alpha \cdot \mathbf{u}}{c^2} - \frac{3u^2}{2c^2} + \frac{9}{2} \cdot \frac{(\mathbf{c}_\alpha \cdot \mathbf{u})^2}{c^4} \right\} \quad (7.2)$$

in which  $w_\alpha$  is a weighting constant. For the case of the D2Q9 model, these terms are written as

$$w_\alpha = \begin{cases} 4/9 & \text{for } \alpha = 0 \\ 1/9 & \text{for } \alpha = 1, 2, 3, 4 \\ 1/36 & \text{for } \alpha = 5, 6, 7, 8 \end{cases} \quad |\mathbf{c}_\alpha| = \begin{cases} 0 & \text{for } \alpha = 0 \\ c & \text{for } \alpha = 1, 2, 3, 4 \\ \sqrt{2}c & \text{for } \alpha = 5, 6, 7, 8 \end{cases} \quad (7.3)$$

In these expressions,  $c$  is the velocity of the movement for the shortest lattice distance, expressed as  $c = \Delta x / \Delta t$ , in which  $\Delta x$  is the shortest distance between two neighboring sites. The lattice velocities given in Eq. (7.3) guarantee that the fluid particles can move from site to site during the time interval  $\Delta t$ . If the particle distributions  $f_\alpha$  ( $\alpha = 0, 1, 2, \dots, 8$ ) are known for all the directions, the macroscopic density and momentum can be evaluated from Eqs. (1.88) and (1.89). That is,

$$\rho(\mathbf{r}, t) = \sum_{\alpha=0}^8 f_\alpha(\mathbf{r}, t), \quad \rho(\mathbf{r}, t) \mathbf{u}(\mathbf{r}, t) = \sum_{\alpha=0}^8 f_\alpha(\mathbf{r}, t) \mathbf{c}_\alpha \quad (7.4)$$

In the present case, a uniform flow is generated by employing a thermodynamic equilibrium distribution with a given uniform velocity at the upstream boundary surface at  $x = -h_0$ . In order to ensure that we obtain reasonable solutions for the present flow problem, we must give careful attention to the interaction between the cylinder and the neighboring lattice sites, and to the outer boundary condition. In the next section we consider the treatment of the boundary conditions.

### 7.3 Boundary Conditions

We are now ready to formalize the boundary conditions that complement the basic equations explained previously. The boundary surfaces to be treated are the upstream and downstream boundaries, both outer side boundaries, and the cylinder surface boundary. Among these boundary surfaces, the boundary between the cylinder

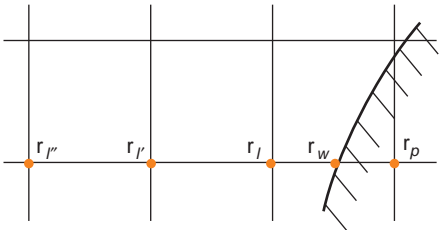


**Figure 7.3** Boundary condition on the material surface.

and its neighboring lattice points is the most important and complex. In the following paragraphs, the boundary conditions relating to the cylinder surface are treated first.

We first explain the Yu–Mei–Luo–Shyy (YMLS) model [34] using Figure 7.3. The particle distribution function in the  $\alpha$ -direction is considered ( $\alpha = 2$  in Figure 7.3). In Figure 7.3,  $\mathbf{r}_w$  is the point at the cylinder surface,  $\mathbf{r}_p$  is the neighboring point inside the cylinder,  $\mathbf{r}_l$  is the neighboring site in the liquid area, and  $\mathbf{r}_{l'}$  is the next neighboring point. Since the next point of  $\mathbf{r}_l$  in the direction of  $\alpha = 1$  is inside the cylinder,  $f_2(\mathbf{r}_l, t + \Delta t)$  cannot be obtained from Eq. (7.1). That is,  $f_2(\mathbf{r}_l, t + \Delta t)$  is dependent on the particle distribution function at the cylinder surface  $\mathbf{r}_w$ , and not on that at  $\mathbf{r}_p$ . If the particle distribution function at  $\mathbf{r}_w$ ,  $f_2(\mathbf{r}_w, t + \Delta t)$  is known,  $f_2(\mathbf{r}_l, t + \Delta t)$  at  $\mathbf{r}_l$  can be evaluated from the linear interpolation method using those at  $\mathbf{r}_{l'}$  and  $\mathbf{r}_w$  as

$$f_2(\mathbf{r}_l, t + \Delta t) = \frac{\Delta_w}{1 + \Delta_w} f_2(\mathbf{r}_{l'}, t + \Delta t) + \frac{1}{1 + \Delta_w} f_2(\mathbf{r}_w, t + \Delta t) \quad (7.5)$$

in which  $\Delta_w = |\mathbf{r}_l - \mathbf{r}_w| / |\mathbf{r}_l - \mathbf{r}_p|$ . Figure 7.3 shows the treatment for the direction of  $\bar{\alpha} = 2$  (in the opposite direction to  $\alpha = 1$ ), and Eq. (7.5) is simply applied to the direction  $\bar{\alpha} = 2$ , in which the connecting line in the opposite direction ( $\alpha = 1$ ) crosses the cylinder surface. In order to evaluate  $f_2(\mathbf{r}_l, t + \Delta t)$  from Eq. (7.5),  $f_2(\mathbf{r}_w, t + \Delta t)$  at the surface is necessary, and this method uses the following equation:

$$f_2(\mathbf{r}_w, t + \Delta t) = (1 - \Delta_w) \tilde{f}_1(\mathbf{r}_{l'}, t) + \Delta_w \tilde{f}_1(\mathbf{r}_l, t) \quad (7.6)$$

This expression means that the particle distribution function on the right-hand side, which is obtained from the linear interpolation method, becomes that in the opposite direction at the next time step. The linear YMLS method [34] uses the linear interpolation procedure with Eqs. (7.5) and (7.6) to obtain  $f_2(\mathbf{r}_l, t + \Delta t)$ . In this method, only two lattice points are used for the interpolation procedure, so it is suitable for many particle dispersions in which a near-contact situation of particles frequently arises.

In addition to the present YMLS boundary model, for the purpose of study, we will employ three other methods explained in Chapter 8: the historical bounce-back rule [35,36] in Eq. (8.106); the quadratic YMLS method, based on the quadratic curve with the additional point  $\mathbf{r}_{l''}$  (Eq. (8.121)); and the Bouzidi–Firdauss–Lallemand (BFL)

model [37] in Eqs. (8.113) and (8.116), or in Eqs. (8.117) and (8.118), which uses the slightly different interpolation scheme. The two different procedures are adopted for  $\Delta_w \leq 1/2$  and  $\Delta_w > 1/2$  in order not to lose the accuracy of the interpolation.

Next, we specify the treatment at the upstream and downstream surfaces. At the upstream surface, the equilibrium distribution with a given uniform velocity  $U$  is specified. On the other hand, the extrapolation condition, which is widely used in numerical analysis methods, may be employed at the downstream boundary surface. As will be shown in Chapter 8, the extrapolation method regards the last three values at  $\mathbf{r}_{N-2}$ ,  $\mathbf{r}_{N-1}$ , and  $\mathbf{r}_N$  as having a linear relationship, expressed as

$$f_{\bar{\alpha}}(\mathbf{r}_N, t + \Delta t) = 2f_{\bar{\alpha}}(\mathbf{r}_{N-1}, t + \Delta t) - f_{\bar{\alpha}}(\mathbf{r}_{N-2}, t + \Delta t) \quad (7.7)$$

in which  $\bar{\alpha}$  is the direction leaving the outer boundary toward the inside of the simulation region.

Similarly, the zero-gradient condition may be applicable, and in this condition the differential away from the boundary is regarded as zero:

$$f_{\bar{\alpha}}(\mathbf{r}_N, t + \Delta t) = f_{\bar{\alpha}}(\mathbf{r}_{N-1}, t + \Delta t) \quad (7.8)$$

This condition is inferior to the previous extrapolation in accuracy but superior on the point of divergence. In addition, the uniform flow condition is employed, in which a uniform flow is assumed outside the simulation region.

Finally, the outer side boundary surfaces of the simulation region are specified. If the simulation region is sufficiently large compared with the cylinder diameter, the periodic boundary condition, which is generally used in molecular simulations, is applicable. With this condition, the particle distribution function at the upper surface in Figure 7.1,  $f_{\alpha}(x,y,t)|_{\text{upper}}$  ( $\alpha = 0, 1, \dots, 8$ ), is regarded as equal to  $f_{\alpha}(x,y,t)|_{\text{lower}}$  at the lower surface. Also, the equilibrium distribution in Eq. (7.2) and the bounce-back rule may be applied at both side boundaries. However, these boundary models may cause significant distortion of the flow field, unless a sufficiently large simulation region is employed. The most effective method for removing the influences of the outer boundary surfaces is expected to be the extrapolation condition. Hence, we next discuss the relative accuracy of the uniform flow condition (i.e., the equilibrium distribution condition), the extrapolation condition, and the zero-gradient condition.

## 7.4 Various Treatments in the Simulation Program

### 7.4.1 Definition and Evaluation of the Drag Coefficient

The cylinder located in the fluid acts as a resistance to the smooth fluid flow. The drag coefficient  $C_D$  for a uniform flow past a two-dimensional circular cylinder can be evaluated using the force  $F$  per unit length in the flow direction exerted by the ambient fluid, defined as

$$C_D = \frac{F}{\rho U^2 D / 2} \quad (7.9)$$

in which  $\rho$  is the density of the fluid,  $U$  is the uniform flow velocity, and  $D$  is the cylinder diameter.

We now show the method of evaluating  $F$ . It is assumed that the point  $\mathbf{r}_l^{\text{cyl}}$  is the nearest neighbor site in the liquid to the cylinder surface, and the neighbor lattice point from the site in the  $\alpha$ -direction is inside the cylinder. The momentum toward the cylinder surface from  $\mathbf{r}_l^{\text{cyl}}$  at time  $t$  is  $\mathbf{c}_{\alpha_l^{\text{cyl}}} \tilde{f}_{\alpha_l^{\text{cyl}}}(\mathbf{r}_l^{\text{cyl}}, t) \Delta x \Delta y$ , and that after the collision with the cylinder surface at  $(t + \Delta t)$  is  $-\mathbf{c}_{\alpha_l^{\text{cyl}}} f_{\alpha_l^{\text{cyl}}}(\mathbf{r}_l^{\text{cyl}}, t + \Delta t) \Delta x \Delta y$ . The change in the momentum during the time interval  $\Delta t$  is equal to the impulse  $\mathbf{F}_{\alpha_l^{\text{cyl}}} \Delta t$ . Hence,  $\mathbf{F}_{\alpha_l^{\text{cyl}}} \Delta t$  can be obtained as

$$\mathbf{F}_{\alpha_l^{\text{cyl}}} = \left\{ \mathbf{c}_{\alpha_l^{\text{cyl}}} \tilde{f}_{\alpha_l^{\text{cyl}}}(\mathbf{r}_l^{\text{cyl}}, t) \Delta x \Delta y + \mathbf{c}_{\alpha_l^{\text{cyl}}} f_{\alpha_l^{\text{cyl}}}(\mathbf{r}_l^{\text{cyl}}, t + \Delta t) \Delta x \Delta y \right\} / \Delta t \quad (7.10)$$

The force acting on the cylinder by the fluid  $\mathbf{F}$  can be evaluated by summing the contributions from the neighbor lattice sites interacting with the cylinder as

$$\mathbf{F} = \sum_l \sum_{\alpha_l^{\text{cyl}}} \mathbf{F}_{\alpha_l^{\text{cyl}}} \quad (7.11)$$

In the present flow, the absolute value of  $F = |\mathbf{F}|$  is used to calculate the drag coefficient in Eq. (7.9).

The flow field and the drag coefficient have already been obtained theoretically and numerically as a function of the Reynolds number  $Re$  for a uniform flow past a cylinder, so the accuracy of the present results can be evaluated by comparison with such theoretical and numerical solutions. The Reynolds number  $Re$  is defined as  $Re = DU/\nu$ , in which the kinematic viscosity  $\nu$  is expressed in Eq. (8.94) for the D2Q9 model. That is,

$$\nu = \frac{\Delta t c^2}{3} (\tau - 1/2) \quad (7.12)$$

#### 7.4.2 Choice of the Procedures by Coloring Lattice Sites

All the lattice points can be classified into one of several groups. That is, the group is composed of (1) lattice points at the upstream and downstream boundary surfaces, (2) lattice points at the outer side boundary surfaces, (3) lattice points interacting with the cylinder, (4) lattice points inside the cylinder, and (5) all other usual lattice points. In the simulation program, this discrimination is expressed using the function “color.” The following values are given to  $\text{color}(i)$  in the sample program:

- $\text{color}(i) = 0$  : all the lattice points in the simulation region not included below
- $\text{color}(i) = 1$  : lattice points at the upstream boundary (both end points are included)

- $color(i) = 2$  : lattice points at the downstream boundary (both end points are included)
- $color(i) = 3$  : lattice points at the outer upper boundary surfaces (neither end point is included)
- $color(i) = 4$  : lattice points at the outer lower boundary surfaces (neither end point is included)
- $color(i) = 5$  : lattice points interacting with the cylinder
- $color(i) = 6$  : lattice points inside the cylinder, interacting with the neighboring outside points
- $color(i) = 7$  : lattice points inside the cylinder, not interacting with the neighboring outside points

In the present study, since the cylinder is fixed and does not move, the above checking procedure is only required once before starting the main loop in the program. The introduction of the *color* variable is useful to make the logical flow clear in the program, which is important in developing a simulation program. Moreover, this approach is directly applicable when the dispersed particles move with time, so that the checking procedure must be regularly undertaken until the end of the simulation.

### 7.4.3 Treatment of Interactions on the Cylinder Surface

In order to use the above-mentioned boundary conditions at the cylinder surface, the quantity  $\Delta_w = |\mathbf{r}_l - \mathbf{r}_w|/|\mathbf{r}_l - \mathbf{r}_p|$  must be evaluated. Since the point  $\mathbf{r}_w$  is at the cylinder surface, the following equation has to be satisfied:

$$|(1 - \Delta_w)(\mathbf{r}_l - \mathbf{r}_p) + \mathbf{r}_p - \mathbf{r}_{cyl}| = R_{cyl} \quad (7.13)$$

in which  $R_{cyl}$  is the cylinder radius ( $R_{cyl} = D/2$ ), and  $\mathbf{r}_{cyl}$  is the cylinder position vector ( $\mathbf{r}_{cyl} = 0$  in the present exercise). Equation (7.13) reduces to an easily solved quadratic equation:

$$\Delta_w = \frac{(\hat{\mathbf{r}}_l^2 - \hat{\mathbf{r}}_p \cdot \hat{\mathbf{r}}_l) - \sqrt{(\hat{\mathbf{r}}_l^2 - \hat{\mathbf{r}}_p \cdot \hat{\mathbf{r}}_l)^2 - (\hat{\mathbf{r}}_l - \hat{\mathbf{r}}_p)^2(\hat{\mathbf{r}}_l^2 - R_{cyl}^2)}}{(\hat{\mathbf{r}}_l - \hat{\mathbf{r}}_p)^2} \quad (7.14)$$

in which the notation of  $\hat{\mathbf{r}}_l = \mathbf{r}_l - \mathbf{r}_{cyl}$  and  $\hat{\mathbf{r}}_p = \mathbf{r}_p - \mathbf{r}_{cyl}$  is used for simplification. In simulations, the value of  $\Delta_w$  for all pairs of the two interacting points on either side of the cylinder surface is calculated and saved.

### 7.4.4 Evaluation of the Velocity and Density

In order to employ the equilibrium distribution function, the macroscopic velocity  $\mathbf{u}$  and density  $\rho$  at an arbitrary lattice point must be evaluated. The definition of the lattice velocities and the coordinate system are shown in Figure 1.4 and Figure 7.1, respectively. First, the density  $\rho(\mathbf{r}, t)$  at an arbitrary point  $\mathbf{r}$  is evaluated from

Eq. (7.4), and then the velocity  $\mathbf{u} = (u_x, u_y)$  is calculated from the following equations:

$$\begin{aligned}\rho(\mathbf{r}, t)u_x(\mathbf{r}, t) &= c(f_1(\mathbf{r}, t) - f_2(\mathbf{r}, t)) + \sqrt{2}c\left(\frac{\sqrt{2}}{2}f_5(\mathbf{r}, t) - \frac{\sqrt{2}}{2}f_6(\mathbf{r}, t)\right) \\ &\quad + \sqrt{2}c\left(\frac{\sqrt{2}}{2}f_7(\mathbf{r}, t) - \frac{\sqrt{2}}{2}f_8(\mathbf{r}, t)\right) \\ &= c(f_1(\mathbf{r}, t) - f_2(\mathbf{r}, t) + f_5(\mathbf{r}, t) - f_6(\mathbf{r}, t) + f_7(\mathbf{r}, t) - f_8(\mathbf{r}, t))\end{aligned}\quad (7.15)$$

$$\rho(\mathbf{r}, t)u_y(\mathbf{r}, t) = c(f_3(\mathbf{r}, t) - f_4(\mathbf{r}, t) + f_5(\mathbf{r}, t) - f_6(\mathbf{r}, t) - f_7(\mathbf{r}, t) + f_8(\mathbf{r}, t)) \quad (7.16)$$

## 7.5 Nondimensionalization of the Basic Equations

In simulations, it is usual practice for each quantity to be nondimensionalized and for the nondimensionalized equations to be treated. Since this has been explained in Section 8.6, we briefly show the nondimensionalized results. Here time is nondimensionalized by  $\Delta t$ , velocities by  $c$  ( $= \Delta x / \Delta t$ ), and the particle distribution function by  $\rho_0$ , so that the basic equation (7.1) is expressed in nondimensional form as

$$\left. \begin{aligned}f_{\alpha}^*(\mathbf{r}^* + \mathbf{c}_{\alpha}^*, t^* + 1) &= \tilde{f}_{\alpha}^*(\mathbf{r}^*, t^*) \\ \tilde{f}_{\alpha}^*(\mathbf{r}^*, t^*) &= f_{\alpha}^{(0)*}(\mathbf{r}^*, t^*) + \frac{1}{\tau} \{f_{\alpha}^{(0)*}(\mathbf{r}^*, t^*) - f_{\alpha}^*(\mathbf{r}^*, t^*)\}\end{aligned}\right\} \quad (7.17)$$

in which

$$f_{\alpha}^{(0)*} = w_{\alpha}^* \rho \left\{ 1 + 3\mathbf{c}_{\alpha}^* \cdot \mathbf{u}^* + \frac{9}{2} (\mathbf{c}_{\alpha}^* \cdot \mathbf{u}^*)^2 - \frac{3}{2} u^{*2} \right\} \quad (7.18)$$

$$|\mathbf{c}_{\alpha}^*| = \begin{cases} 0 & \text{for } \alpha = 0 \\ 1 & \text{for } \alpha = 1, 2, 3, 4 \\ \sqrt{2} & \text{for } \alpha = 5, 6, 7, 8 \end{cases} \quad (7.19)$$

In these equations,  $w_{\alpha}$  has already been shown in Eq. (7.3), and  $\tau$  is originally a nondimensional quantity. Note that the relationship  $c^* = 1$  has been taken into account in the above derivations. The nondimensional expressions of Eq. (7.4) are:

$$\rho^*(\mathbf{r}^*, t^*) = \sum_{\alpha=0}^8 f_{\alpha}^*(\mathbf{r}^*, t^*), \quad \rho^*(\mathbf{r}^*, t^*)\mathbf{u}^*(\mathbf{r}^*, t^*) = \sum_{\alpha=0}^8 f_{\alpha}^*(\mathbf{r}^*, t^*)\mathbf{c}_{\alpha}^* \quad (7.20)$$

Since the velocities of fluid particles are nondimensionalized by the lattice speed  $c$ , the nondimensional speed of sound  $c_s^*$  is expressed as  $c_s^* = 1/\sqrt{3}$  in Eq. (8.46). Hence, it should be noted that one needs to treat flow problems for a macroscopic velocity  $u^*$  of  $u^* \ll 1$ , unless the density significantly varies in the simulation region. The nondimensional kinematic viscosity, which is necessary for evaluating the Reynolds number, is expressed as  $\nu^* = (2\tau - 1)/6$ .

## 7.6 Conditions for Simulations

### 7.6.1 Initial Distribution

As an initial distribution, the equilibrium distribution with a uniform velocity  $U$  and density  $\rho_0$  is used here for the inner simulation region, as well as for the entrance boundary surface. It is possible to use an equilibrium distribution with zero velocity, but this may induce a divergence of the system with time. It is important to discuss the validity of the various initial conditions adopted in order to clarify the characteristics of the simulation program.

### 7.6.2 Parameters for Simulations

The solution of the flow field and the drag coefficient for the case of a uniform flow past a two-dimensional circular cylinder has already been solved theoretically for  $Re \leq 1$  and numerically for  $Re \geq 1$ . Since a pair of stable vortices appears behind the cylinder in the range of  $7 \leq Re \leq 40$ , it is quite reasonable to focus on a pair of vortices for  $7 \leq Re \leq 40$ ; these vortices are very sensitive to the type of surface model employed. Hence, the present simulations have been conducted within the range of  $1 \leq Re \leq 20$ . The Reynolds number can be expressed as  $Re = U^* D^*/((2\tau - 1)/6)$ , so that in order to take a large Reynolds number, the relaxation time  $\tau$  is chosen as  $\tau \simeq 1/2$ . The uniform velocity  $U^*$  cannot be large due to the restriction of the use of a slow uniform velocity compared with the speed of sound. From these considerations, the uniform flow velocity is taken as  $U^* = 0.005 - 0.01$  and the relaxation time as  $\tau = 0.515 - 0.8$ . The cylinder diameter  $D^*$  is  $D^* = 3 - 20$ , and the size of the simulation region is taken as  $2h_0^* = 4D^* - 14D^*$  and  $2l_0^* = 3D^* - 11D^*$ . The influence of the boundary model will appear to be more significant for a smaller simulation region.

## 7.7 Results of Simulations

It is known that the flow field for outer flow problems is significantly distorted unless a sufficiently large simulation region is used. The results for a relatively small simulation region ( $2h_0^*, 2l_0^*$ ) = ( $7D^*, 6D^*$ ) are shown in Figure 7.4 for  $Re = 20$ . Figures 7.4A and B depict the uniform flow condition and the zero-gradient

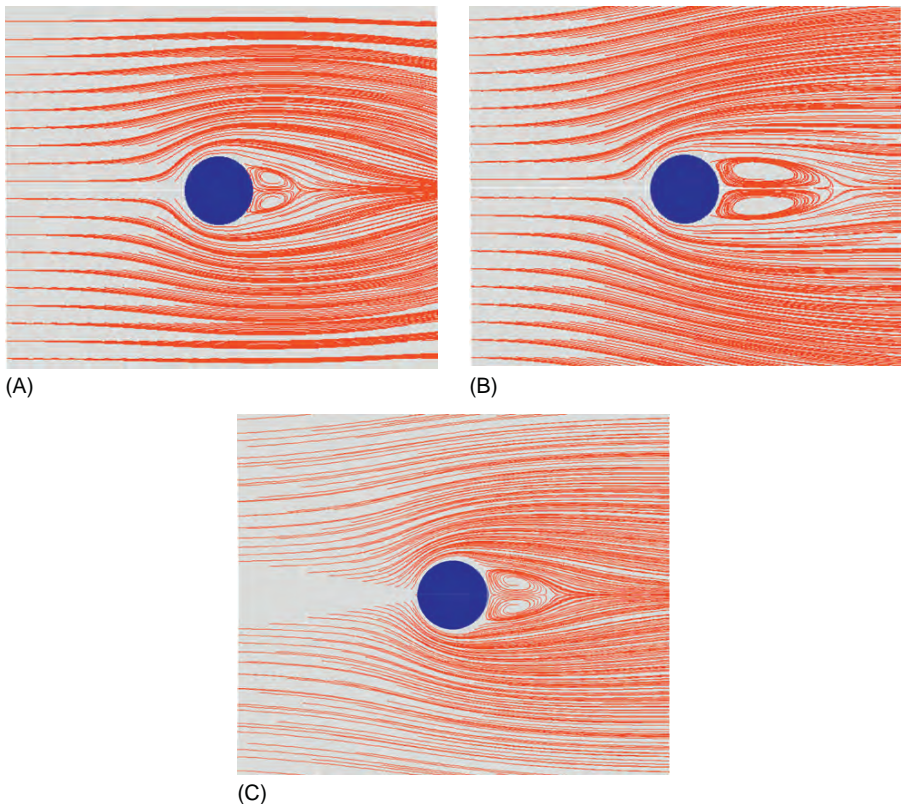


**Figure 7.4** Dependence of the flow field on the outer boundary conditions for  $Re = 20$ ; the bounce-back rule is used for the cylinder surface: (A) uniform flow condition, (B) zero-gradient condition, and (C) numerical solution of Navier–Stokes equation.

condition, respectively, and Figure 7.4C shows the Navier–Stokes solution. The historical bounce-back rule has been used for the treatment of the interactions with the cylinder. In the case of  $Re = 20$ , the length of the pair of vortices is approximately the same as the cylinder diameter, and the formation of these vortices is quite sensitive to the outer boundary condition that has been adopted. The result in Figure 7.4C is the numerical solution obtained by the ordinary finite difference method, and it can be regarded as an exact solution. As shown in Figure 7.4A, for the uniform flow condition (the equilibrium distribution case), the pair of vortices behind the cylinder is significantly distorted and shortened, and the fluid flows along and does not tend to cross the outer side boundary surfaces. This is quite understandable in this case, because a uniform flow is assumed just outside the boundary surfaces; therefore, the flow crossing the boundaries does not tend to arise. The pair of distorted vortices is due to a similar reason—the flow crossing the downstream boundary surface is

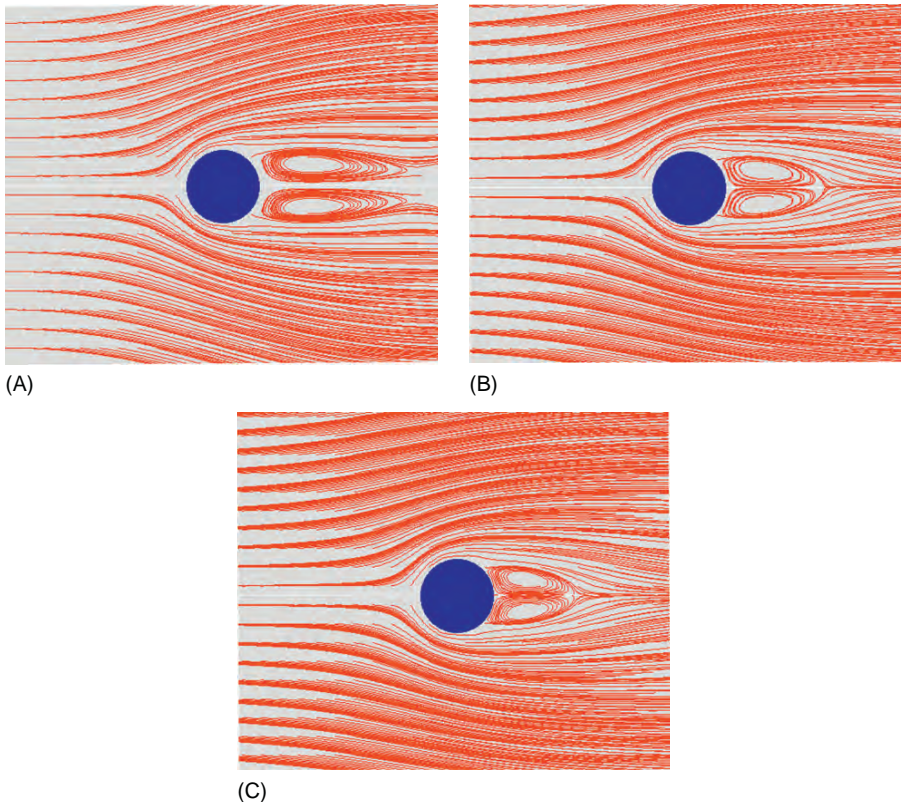


**Figure 7.5** Dependence of the flow field on the size of the simulation region ( $Re = 20$ , the bounce-back method): (A)  $(2h_0^*, 2l_0^*) = (6D^*, 5D^*)$ ; (B)  $(2h_0^*, 2l_0^*) = (9D^*, 7D^*)$ ; and (C)  $(2h_0^*, 2l_0^*) = (14D^*, 11D^*)$ .

significantly distorted. These results clearly show that a uniform flow condition has the tendency to distort the flow field significantly unless a sufficiently large simulation region is used, although this condition is found to exhibit less divergence in the calculation procedures during a simulation run. In contrast, the result for the zero-gradient condition shown in Figure 7.4B is in agreement with the Navier–Stokes solution, but the pair of vortices is significantly distorted. As discussed in the following, this is again due to the use of a small simulation region. For the extrapolation boundary condition, it was found that stable solutions could not be obtained because the flow field diverged during the advance of the time steps.

Figure 7.5 shows the influence of the size of the simulation region on the formation of a pair of vortices for the three cases of  $(2h_0^*, 2l_0^*) = (6D^*, 5D^*)$ ,  $(9D^*, 7D^*)$ , and  $(14D^*, 11D^*)$ , which correspond to Figure 7.5A–C, respectively. The bounce-back rule has been used for the collision with the cylinder, and the zero-gradient

condition has been used for the boundaries of the simulation box. The Reynolds number  $Re$  is 20, as in the previous case. For the case of our smallest simulation region, shown in Figure 7.5A, the pair of vortices unreasonably lengthens in the downstream area due to the significantly small region used. The results obtained by the lattice Boltzmann method tend to approach the Navier–Stokes solution shown in Figure 7.4C with the size of the simulation region, and the flow field is in agreement with the exact solution. This clearly demonstrates the importance of grasping the influence of this effect by investigating several cases with different size simulation regions.

Figure 7.6 shows the influence of the boundary model employed at the cylinder surface on the formation of the pair of vortices. Figure 7.6A–D illustrate the bounce-back rule, the linear YMLS method, the liner BFL method, and the Navier–Stokes solution. These results were obtained for  $Re = 20$ , the simulation region  $(2h_0^*, 2l_0^*) = (14D^*, 11D^*)$ , and the zero-gradient condition for the outer boundary surfaces. The quadratic YMLS and BFL methods give rise to a divergence of the flow field. As clearly seen in Figure 7.6, no significant difference can be observed among these flow fields, and these three boundary models show agreement concerning the formation of the pair of vortices behind the cylinder. Qualitative and quantitative agreement with the exact solution was also confirmed

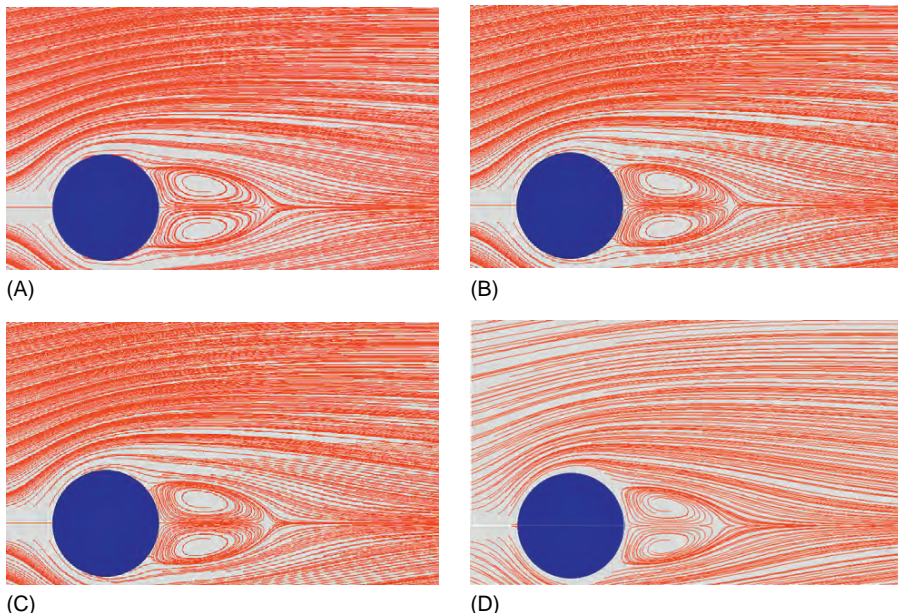


**Figure 7.6** Dependence of the flow field on the surface models on the cylinder surface ( $Re = 20$ , the zero-gradient condition): (A) bounce-back rule, (B) linear YMLS method, (C) linear BFL method, and (D) numerical solution of Navier–Stokes equation.

concerning the drag coefficient and the velocity distributions, although not shown here. In particular, agreement for the linear YMLS method is good, which may indicate there is some advantage to be found in the application of this boundary method for particle dispersions. As previously discussed, this is because the method that uses the fewer lattice points in the interpolation scheme is the most desirable.

## 7.8 Simulation Program

The following list is an example simulation program written in FORTRAN for the case discussed in this chapter, and it explains the significance of the important variables used in the program:

$\text{RX}(\text{I}, \text{J}), \text{RY}(\text{I}, \text{J})$	:	$(x,y)$ components of the position $\mathbf{r}_{i,j}^*$ of lattice site $(i,j)$ $(\text{I} = 0, 1, \dots, \text{PX}; \text{J} = 0, 1, \dots, \text{PY})$
$\text{VX}(\text{I}, \text{J}), \text{VY}(\text{I}, \text{J})$	:	Macroscopic velocity $\mathbf{u}_{i,j}^*$ at lattice site $(i,j)$
$\text{RHO}(\text{I}, \text{J})$	:	Macroscopic density at lattice site $(i,j)$
$\text{F}(\text{I}, \text{J}, \text{K})$	:	Particle distribution function ( $\text{K} = 0, 1, \dots, 8$ ) at lattice site $(i,j)$
$\text{FTILD}(\text{I}, \text{J}, \text{K})$	:	Particle distribution function after the collision at lattice $(i,j)$
$\text{W}(\text{K})$	:	Weighting constant $w_\alpha$
$\text{CVEL}(2, \text{K})$	:	Lattice velocity $\mathbf{c}_\alpha$ ( $\text{CVEL}(1, \text{K})$ is $x$ -component, and $\text{CVEL}(2, \text{K})$ is $y$ -component)
$\text{XL}, \text{YL}$	:	Dimensions of the simulation region in the $(x,y)$ directions
$\text{DNS0}$	:	Density of an inflow fluid
$\text{DCYL}$	:	Diameter of the cylinder
$\text{UVELX}$	:	Uniform flow velocity $U^*$
$\text{RE}$	:	Reynolds number $Re$
$\text{TAU}$	:	Relaxation time $\tau$
$\text{RXYCYL}, \text{RZYCYL}$	:	Center of the cylinder (equal to the origin in this practice)
$\text{ICYL}, \text{JCYL}$	:	Lattice site (in the $(x,y)$ direction) representing the cylinder center
$\text{COLOR}(\text{ITH})$	:	<i>Color</i> function representing the type of lattice site $(i,j)$ $(\text{ITH} = (1 + \text{PX}) * \text{J} + \text{I} + 1)$
$\text{TBLNAM}(\text{II})$	:	Save the name of lattice sites interacting with the cylinder
$\text{POSINTBL}(\text{ITH})$	:	Save the order in which each lattice site appears in $\text{TBLNAM}$
$\text{TBLPOS}(\text{II})$	:	Save the order in which quantities relate to lattice site $\text{TBLNAM}(\text{II})$ appear in the variable $\text{TBLDW}$
$\text{TBLNUM}(\text{II})$	:	Save the number of velocities interacting with the cylinder concerning lattice site $\text{TBLNAM}(\text{II})$
$\text{TBLDW}(\text{III})$	:	Save the value of $\Delta_w$
$\text{TBLAL}(\text{III})$	:	Save the name of the lattice directions $\alpha$ interacting with the cylinder

In order to assist the reader in understanding the program, explanatory statements have been added to the important features.

```

0001 C***** ****
0002 C*          LBcyl5.f
0003 C*
0004 C*      OPEN(9, FILE='@bbba1.dat', STATUS='UNKNOWN'); para, results
0005 C*      OPEN(11,FILE='bbba11.dat', STATUS='UNKNOWN'); parameters
0006 C*      OPEN(12,FILE='bbba21.dat', STATUS='UNKNOWN'); VEL data
0007 C*      OPEN(21,FILE='bbba001.dat', STATUS='UNKNOWN'); VEL field
0008 C*      OPEN(22,FILE='bbba011.dat', STATUS='UNKNOWN'); VEL field
0009 C*      OPEN(23,FILE='bbba021.dat', STATUS='UNKNOWN'); VEL field
0010 C*      OPEN(24,FILE='bbba031.dat', STATUS='UNKNOWN'); VEL field
0011 C*      OPEN(25,FILE='bbba041.dat', STATUS='UNKNOWN'); VEL field
0012 C*      OPEN(26,FILE='bbba051.dat', STATUS='UNKNOWN'); VEL field
0013 C*      OPEN(27,FILE='bbba061.dat', STATUS='UNKNOWN'); VEL field
0014 C*      OPEN(28,FILE='bbba071.dat', STATUS='UNKNOWN'); VEL field
0015 C*      OPEN(29,FILE='bbba081.dat', STATUS='UNKNOWN'); VEL field
0016 C*      OPEN(30,FILE='bbba091.dat', STATUS='UNKNOWN'); VEL field
0017 C*      OPEN(41,FILE='avsvell.fld', STATUS='UNKNOWN'); MicroAVS fld
0018 C*      OPEN(42,FILE='avsvell.dat', STATUS='UNKNOWN'); MicroAVS data
0019 C*
0020 C*      ----- LATTICE BOLTZMANN SIMULATION OF A FLOW PAST -----
0021 C*      A CIRCULAR CYLINDER IN A TWO-DIMENSIONAL SYSTEM
0022 C*
0023 C*      VER.1:
0024 C*          1. D2Q9 MODEL IS USED
0025 C*          2. EQUILIBRIUM BC WITH GIVEN UNIFORM VEL. IS USED FOR
0026 C*              UPSTREAM BC
0027 C*          3. THREE FOLLOWING BC'S ARE USED FOR BOTH SIDES BC OF CYL
0028 C*              (1) EXTRAPOLATION BC (ITREESID=1)
0029 C*              (2) DEF=0 (ITREESID=2)
0030 C*              (3A) UIFORM FLOW (Const)(ITREESID=3)
0031 C*              (3B) UIFORM FLOW (DEF=0)(ITREESID=4)
0032 C*              (3C) UIFORM FLOW (Extra)(ITREESID=5)
0033 C*          4. THREE FOLLOWING BC'S ARE USED FOR DOWNSTREAM BC
0034 C*              (1) EXTRAPOLATION BC (ITREEDWN=1)
0035 C*              (2) DEF=0 (ITREEDWN=2)
0036 C*              (3A) UIFORM FLOW (Const)(ITREEDWN=3)
0037 C*              (3B) UIFORM FLOW (DEF=0)(ITREEDWN=4)
0038 C*              (3C) UIFORM FLOW (Extra)(ITREEDWN=5)
0039 C*          5. THREE FOLLOWING BC'S ARE USED FOR COLLISION BETWEEN
0040 C*              SITES AND CYLINDER
0041 C*              (1) BOUNCE-BACK (ITREECYL=1)
0042 C*              (2A) YMLS METHOD(Quadratic) (ITREECYL=2)
0043 C*              (2B) YMLS METHOD(Liner) (ITREECYL=3)
0044 C*              (3A) BFL METHOD(Quadratic) (ITREECYL=4)
0045 C*              (3B) BFL METHOD(Linear) (ITREECYL=5)
0046 C*
0047 C*          VER.1 BY A.SATOH, '08 7/4
0048 C***** ****
0049 C      ---- THE FOLLOWING NOTATIONS ARE USED FOR LATTICE BOLTZMANN ---
0050 C      F(I,J,K) : DENSITY DISTRIBUTION FUNCTION
0051 C          I=0,1,2,...,PX : J=0,1,2,...PY : K=0,1,...,8
0052 C      FTILD(I,J,K) : DENSITY DISTRIBUTION FUNCTION BEFORE TRAVEL
0053 C      CVEL(2,K) : C_ALPHA
0054 C          C_0=(0,0)
0055 C          C_1=(1,0), C_2=(-1, 0), C_3=(0, 1), C_4=( 0,-1)
0056 C          C_5=(1,1), C_6=(-1,-1), C_7=(1,-1), C_8=(-1, 1)
0057 C      W(K) : WEIGHT CONSTANTS
0058 C          W(0)=4/9, W(ALPHA)=1/9 (ALPHA=1,2,3,4),
0059 C          W(ALPHA)=1/36 (ALPHA=5,6,7,8)
0060 C      ALPHAMX : =8 FOR D2Q9
0061 C      IINC(2,K) : INCREMENT IN EACH DIRECTION FOR TRANSFER
0062 C          FOR ALPHA DIRECTION
0063 C          (E.X., IINC(1,1)=1, IINC(2,1)=0)
0064 C      ANTIALPH(K) : NAME OF THE OPPOSITE DIRECTION SITE FOR ALPHA
0065 C          (E.X., ANTIALPH(1)=2)
0066 C      RHO(I,J) : DENSITY AT (I,J)
0067 C      RX(I,J),RY(I,J) : LATTICE POSITION
0068 C      VX(I,J),VY(I,J) : VELOCITY COMPONENTS IN X- AND Y-DIRECTIONS
0069 C      DNS0 : MEAN DENSITY (CONSTANT FOR NON-COMPRESSIVE FLOW)
0070 C      PX,PY : NUMBER OF CELLS IN EACH DIRECTION (EVEN VALUES)
0071 C      PXY : = (PX+1)*(PY+1)
0072 C      XL,YL : LENGTHS OF SIMULATION REGION IN EACH DIRECTION
0073 C      TAU : NON-DIMENSIONAL RELAXATION TIME
0074 C      DX : UNIT LENGTH (=1)
0075 C      DT : TIME INTERVAL(=1)
0076 C      CLAT : LATTICE VELOCITY (=1)
0077 C      (UVELX,UVELY) : UNIFORM VELOCITY COMPONENTS
0078 C
0079 C      ----- THE FOLLOWING NOTATIONS ARE USED FOR THE CYLINDER -----

```

```

0080 C      DCYL      : DIAMETER OF CYLINDER
0081 C      RXCYL, RYCYL : POSITION OF CYLINDER(=(0,0) FOR THE PRESENT CASE)
0082 C      ICYL , JCYL : SITE POSITION OF CYLINDER
0083 C      COLOR(PXY) : COLOR FOR DISTINGUISHING PROCEDURES FOR EACH SITE
0084 C      POSINTBL(PXY) : POSITION OF THE SITE IN TBLNAM(*) FOR EACH SITE
0085 C      TBLNAM(NTBL) : NAMES OF INTERACTING SITES WITH CYLINDER
0086 C      TBLNUM(NTBL) : NUMBERS OF INTERACTING ALPHA-VELS FOR EACH SITE
0087 C      TBLPOS(NTBL) : POSITION OF THE SITE APPEARING IN TBLDW(*) AND
0088 C          TBLA(*)*
0089 C      TBLDW(NTBLDW) : VALUES OF DW ARE SAVED IN TBLDW(*) FOR EACH SITE
0090 C      TBLAL(NTBLDW) : VALUES OF ALPHA-VEL ARE SAVED FOR EACH SITE
0091 C      TBLNAMIN(NTBLNAMI) : THE NAMES OF SITES INSIDE CYLINDER
0092 C
0093 C      ----- CONCERNING DRAG COEFFICIENT -----
0094 C      CD        : DRAG COEFFICIENT
0095 C      CDFORCE(NSMPLCD) : FORCE IS SAVED FOR EACH TIME STEP
0096 C      CDFORCE0 : COEFFICIENT (U**2)D/2 IS USED FOR CAL. CD
0097 C      NSMPLCD : TOTAL SAMPLING NUMBER
0098 C      RE        : REYNOLDS NUMBER
0099 C          U=0.005 D=20 TAU=0.80 Re= 1
0100 C          U=0.005 D=20 TAU=0.60 Re= 3
0101 C          U=0.005 D=20 TAU=0.55 Re= 6
0102 C          U=0.005 D=20 TAU=0.53 Re= 10
0103 C          U=0.005 D=20 TAU=0.52 Re= 15
0104 C          U=0.005 D=20 TAU=0.515 Re= 20
0105 C          U=0.005 D=20 TAU=0.51 Re= 30
0106 C
0107 C      +++ -XL1<RX(I)<XL2 , -YL1<RY(I)<YL2 , -ZL1<RZ(I)<ZL2 +++
0108 C-
0109 IMPLICIT REAL*8 (A-H,O-Z), INTEGER (I-N)
0110 C
0111 COMMON /BLOCK1/ F   , FTILD
0112 COMMON /BLOCK2/ CVEL , W   , IINC , ANTIALPH, ALPHAMX
0113 COMMON /BLOCK3/ RHO  , RX  , RY  , VX  , VY
0114 COMMON /BLOCK4/ DNSO  TAU , DX  , DT , CLAT
0115 COMMON /BLOCK5/ XL   , YL  , XL1 , YL1 , XL2 , YL2 , PX , PY , PXY
0116 COMMON /BLOCK6/ UVELX , UVELY
0117 C
0118 COMMON /BLOCK14/ RXCYL , RYCYL , ICYL , JCYL , DCYL
0119 COMMON /BLOCK15/ COLOR   , POSINTBL
0120 COMMON /BLOCK16/ TBLNAM , TBLNUM , TBLPOS , NTBL
0121 COMMON /BLOCK17/ TBLDW   , TBLAL  , NTBLDW
0122 COMMON /BLOCK18/ TBLNAMIN , NTBLNAMI
0123 C
0124 COMMON /BLOCK21/ CD , CDFORCE0 , CDFORCE , RE , NSMPLCD
0125 C
0126 C
0127 INTEGER PP , QQ , KK
0128 PARAMETER( PP=300 , QQ=400 , KK=8 , PI=3.141592653589793D0 )
0129 C
0130 REAL*8   F(0:PP,0:QQ,0:KK) , FTILD(0:PP,0:QQ,0:KK)
0131 REAL*8   CVEL(2,0:KK)       , W(0:KK)
0132 REAL*8   RHO(0:PP,0:QQ)
0133 REAL*8   RX( 0:PP,0:QQ)     , RY(0:PP,0:QQ)
0134 REAL*8   VX( 0:PP,0:QQ)     , VY(0:PP,0:QQ)
0135 INTEGER  ALPHAMX , IINC(2,0:KK) , ANTIALPH(0:KK)
0136 INTEGER  PX , PY , PXY
0137 C
0138 INTEGER  PPXY
0139 PARAMETER( PPXY=150000 , NNTBL=2200 , NNTBL2=4400 , NNTBL3=4400 )
0140 C
0141 REAL*8   TBLDW(NNTBL2)
0142 INTEGER  COLOR( PXY ) , POSINTBL(PPXY)
0143 INTEGER  TBLNAM(NNTBL) , TBLNUM(NNTBL) , TBLPOS(NNTBL) , NTBL
0144 INTEGER  TBLAL(NNTBL2) , NTBLDW
0145 INTEGER  TBLNAMIN(NNTBL3) , NTBLNAMI
0146 C
0147 INTEGER  NNCD
0148 PARAMETER( NNCD=1000000 )
0149 C
0150 REAL*8   CDFORCE(NNCD)
0151 C
0152 REAL*8   VXSUM(0:PP,0:QQ) , VYSUM(0:PP,0:QQ) , RHOSUM(0:PP,0:QQ)
0153 REAL*8   H , DCYL2SQ , CD99 , C1
0154 INTEGER  NTIMEMX , NGRAPH , NANIME , NOPT , NSMPLCD , NDM
0155 INTEGER  NTHROW , NSMPLVEL , NANMCTR , NSMPL1
0156 INTEGER  ITREECYL , ITREESID , ITREEDWN

```

• The given values are written out in @bbbd1 and bbbd11, and the velocities are written out in bbbd21.

```

0157 C
0158      OPEN(9,FILE='@bbbd1.dat' , STATUS='UNKNOWN')
0159      OPEN(11,FILE='bbbd11.dat' , STATUS='UNKNOWN')
0160      OPEN(12,FILE='bbbd21.dat' , STATUS='UNKNOWN')
0161      OPEN(21,FILE='bbbd001.dat' , STATUS='UNKNOWN')
0162      OPEN(22,FILE='bbbd011.dat' , STATUS='UNKNOWN')
0163      OPEN(23,FILE='bbbd021.dat' , STATUS='UNKNOWN')
0164      OPEN(24,FILE='bbbd031.dat' , STATUS='UNKNOWN')
0165      OPEN(25,FILE='bbbd041.dat' , STATUS='UNKNOWN')
0166      OPEN(26,FILE='bbbd051.dat' , STATUS='UNKNOWN')
0167      OPEN(27,FILE='bbbd061.dat' , STATUS='UNKNOWN')
0168      OPEN(28,FILE='bbbd071.dat' , STATUS='UNKNOWN')
0169      OPEN(29,FILE='bbbd081.dat' , STATUS='UNKNOWN')
0170      OPEN(30,FILE='bbbd091.dat' , STATUS='UNKNOWN')
0171      OPEN(41,FILE='avsvell.fld', STATUS='UNKNOWN')
0172      OPEN(42,FILE='avsvell.dat', STATUS='UNKNOWN')

0173          NP=9
0174 C          --- PARAMETER (1) ---
0175 C          ++ PX=140, PY=120 ; PX=280, PY=220 ++
0176 C          ++ PX=180, PY=140 ; PX=320, PY=260 ++
0177 C          ++ PX=220, PY=180 ; PX=340, PY=280 ++
0178 AU      = 0.515D0
0179 UVELX = 0.005D0 •  $\tau=0.515$  and  $U^*=0.005$ . The numbers of the lattice points in the x- and
0180 UVELY = 0.0D0 y-directions are (PX, PY), respectively.  $\alpha=0,\dots,8$ . The size of the
0181 PX     = 140 simulation box is (XL,YL) in each direction.
0182 PY     = 120
0183 C          --- PARAMETER (2) ---
0184 ALPHAMX = 8
0185 XL     = DBLE(PX)
0186 YL     = DBLE(PY)
0187 XL1    = XL/2.D0
0188 YL1    = YL/2.D0
0189 XL2    = XL - XL1
0190 YL2    = YL - YL1
0191 DNS0   = 1. DO
0192 DX     = 1.D0
0193 DT     = 1.D0
0194 CLAT   = 1.D0
0195 PXY    = (PX+1)*(PY+1)
0196 C          --- PARAMETER (2) ---
0197 DCYL   = 20.D0 - 0.0001D0
0198 DCYL2SQ = DCYL**2 / 4.D0
0199 RXCYL  = 0.D0
0200 RYCYL  = 0.D0
0201 C          --- PARAMETER (4) ---
0202 C          ++ (1) BOUNCE-BACK (ITREECYL=1) ++
0203 C          ++ (2A) YMLES METHOD(Quadratic) (ITREECYL=2) ++
0204 C          ++ (2B) YMLES METHOD(Liner) (ITREECYL=3) ++
0205 C          ++ (3A) BFL METHOD(Quadratic) (ITREECYL=4) ++
0206 C          ++ (3B) BFL METHOD(Linear) (ITREECYL=5) ++
0207 C          ++ (1) EXTRAPOLATION BC (ITREESID=1) ++
0208 C          ++ (2) DEF=0 (ITREESID=2) ++
0209 C          ++ (3A) UNIFORM FLOW(Const) (ITREESID=3) ++
0210 C          ++ (3B) UNIFORM FLOW(DEF=0) (ITREESID=4) ++
0211 C          ++ (3C) UNIFORM FLOW(Extra) (ITREESID=5) ++
0212 C          ++ (1) EXTRAPOLATION BC (ITREEDWN=1) ++
0213 C          ++ (2) DEF=0 (ITREEDWN=2) ++
0214 C          ++ (3A) UNIFORM FLOW(Const) (ITREEDWN=3) ++
0215 C          ++ (3B) UNIFORM FLOW(DEF=0) (ITREEDWN=4) ++
0216 C          ++ (3C) UNIFORM FLOW(Extra) (ITREEDWN=5) ++
0217 ITREECYL= 1
0218 ITREESID= 2
0219 ITREEDWN= 2
0220 C
0221 NTIMEMX = 200000
0222 NGRAPH  = NTIMEMX/10
0223 NANIME  = NTIMEMX/10
0224 NOPT    = 20
0225 C          --- PARAMETER (5) ---
0226 C          - NSMPLCD FOR CD -
0227 C
0228 NSMPLCD = NTIMEMX
0229 NSMPL1  = 5
0230 NTHROW  = NTIMEMX/10
0231 C          --- PARAMETER (6) ---
0232 CDFORCE0= (DNS0*(UVELX)**2)*DCYL /2.D0
0233 RE      = UVELX*DCYL/( (2.D0*TAU - 1.D0 )/6.D0 )
0234 C
0235 C----- INITIAL SETTING -----
0236 C-----
```

• The velocities and densities are written out in bbbd001 to bbbd091, and the data are written out in avsvell for MicroAVS.

•  $\tau=0.515$  and  $U^*=0.005$ . The numbers of the lattice points in the x- and y-directions are (PX, PY), respectively.  $\alpha=0,\dots,8$ . The size of the simulation box is (XL,YL) in each direction.

• The name of the first lattice point is 0, so that the total number of the lattice points is  $PXY=(PX+1)\times(PY+1)$ .

• The cylinder diameter centered at the origin is DCYL=20, and its center is therefore (RXCYL,RYCYL)=(0,0).

• The boundary condition is adopted according to the values of ITREECYL, ITREESID, and ITREEDWN.

• The total number of time steps is NTIMEMX= 200000. The velocity field data are written out at every NGRAPH time steps.

• 10 sets of data are written out for making an animation based on MicroAVS.

• The velocities and positions of the lattice points are assigned.

```

0237 C ----- --- SET C_VEL(2,8),W(8),IINC(2,8),ANTIALPH(8) ---
0238 C CALL INICVEL --- SET LATTICE POSITION RX(*,*),RY(*,*) ---
0239 C
0240 C CALL INILAT --- SET INITIAL POSIT. AND VEL. ---
0241 C
0242 C
0243 C
0244 CCC OPEN(19,FILE='bbbd091.dat',STATUS='OLD')
0245 CCC READ(19,201) PX, PY, ALPHAMX
0246 CCC READ(19,202) ( ( F(I,J,K),K=0,ALPHAMX ),J=0,PY ), I=0,PX )
0247 CCC READ(19,204) ( ( RX( I,J ),J=0,PY ),I=0,PX )
0248 CCC READ(19,204) ( ( RY( I,J ),J=0,PY ),I=0,PX )
0249 CCC READ(19,206) ( ( VX( I,J ),J=0,PY ),I=0,PX )
0250 CCC READ(19,206) ( ( VY( I,J ),J=0,PY ),I=0,PX )
0251 CCC READ(19,208) ( ( RHO(I,J),J=0,PY ),I=0,PX )
0252 CCC CLOSE(19,STATUS='KEEP')
0253 CCC GOTO 7
0254 C
0255 C CALL INIDIST( DNS0 , ALPHAMX ) --- SET
0256 C
0257 C
0258 7 CALL INICOLOR( PX , PY , DCYL2SQ ) --- MAKE
0259 C --- WITH CYLINDER
0260 C - WITH CYLINDER
0261 CALL MAKETBLE( DCYL2SQ , NTBL , NTBLDW ) --- SET ZERO
0262 C
0263 C
0264 DO 9 J=0, PY
0265 DO 8 I=0, PX
0266 ITH = (PX+1)*J + (I+1)
0267 IF( (COLOR(ITH).EQ.6) .OR. (COLOR(ITH).EQ.7) ) THEN
0268   VX( I,J ) = 0.D0
0269   VY( I,J ) = 0.D0
0270   RHO(I,J) = DNS0
0271 END IF
0272 8 CONTINUE
0273 9 CONTINUE
0274 C ----- PRINT OUT CONSTANTS ---
0275 WRITE(NP,10) DNS0, TAU, DX, DT, CLAT, ALPHAMX
0276 WRITE(NP,11) PX, PY, PXY, XL, YL, XL1, YL1, XL2, YL2,
0277 & UVELX, UVELY
0278 WRITE(NP,13) DCYL, ITREECYL, ITREESID, ITREEDWN
0279 WRITE(NP,14) NTIMEMX, NGRAPH, NANIME, NSMPLCD, NTHROW, NSMPL1
0280 WRITE(NP,15) CDFORCE0, RE
0281 C ----- INITIALIZATION ---
0282 C
0283 C ----- INITIALIZE(1) ---
0284 NSMPLCD = 0
0285 DO 20 I=1, NTIMEMX
0286   CDFORCE(I) = 0.D0
0287 20 CONTINUE
0288 C ----- INITIALIZE(2) ---
0289 DO 30 J=0, PY
0290 DO 25 I=0, PX
0291   VXSUM( I,J ) = 0.D0
0292   VYSUM( I,J ) = 0.D0
0293   RHOSUM(I,J) = 0.D0
0294 25 CONTINUE
0295 30 CONTINUE
0296 NSMPLVEL = 0
0297 C
0298 NANMCTR = 0
0299 C
0300 C ----- START OF MAIN LOOP -----
0301 C
0302 C
0303 C
0304 DO 1000 NTIME = 1,NTIMEMX
0305 C
0306 C ----- CAL. VEL AT EACH LAT. POS. ---
0307 C - VX(*,*),VY(*,*),RHO(*,*) -
0308 CALL VELCAL( COLOR , ITREESID , ITREEDWN, NTIME )
0309 C --- COLLISION PROCEDURE FTILD(*,*,8) ---
0310 CALL COLLPROC( COLOR , ALPHAMX )
0311 C --- PROPAGATION PROCEDURE,FORCE EVALUATION ---
0312 C - F(*,*,8) WITHOUT BC -
0313 NSMPLCD = NSMPLCD + 1
0314 CALL MOVEPROC( PX , PY , ANTIALPH , RHO , DNS0 , ITREECYL )
0315 C --- BOUNDARY CONDITION PROC. ---

• The initial values of the distribution function are assigned, and the values of the variable color in Section 7.4.2 are evaluated. This procedure is conducted only once because of the cylinder being fixed.

• The lattice points interacting with the cylinder are checked.

• The velocities at the lattice points inside the cylinder are set to be zero.

• The following procedure is conducted in the main loop: (1) the velocities at each lattice point are evaluated in VELCAL, (2) the collision treatment is carried out in COLLPROC, (3) the transfer of the distribution function is conducted in MOVEPROC, and (4) the BC treatment is conducted in BCPROC.
```

```

0316 C                                     -          FX(*,*,8) FOR BC      -
0317      CALL BCPROC( PX , PY , DNS0 , ALPHAMX , ITREESID ,
0318      &                                         ITREEDWN )
0319 C
0320 C                                     --- DATA OUTPUT (1) FOR GRAPHICS ---
0321 C
0322      IF( MOD(NTIME,NGRAPH) .EQ. 0 ) THEN
0323 C
0324      CALL VELCAL( COLOR , ITREESID , ITREEDWN , NTIME )
0325 C
0326      NOPT = NOPT + 1
0327      WRITE(NOPT,201) PX, PY, ALPHAMX
0328      WRITE(NOPT,202) ( ( F(I,J,K),K=0,ALPHAMX ),J=0,PY ),
0329      &                                         I=0,PX )
0330      WRITE(NOPT,204) ( ( RX( I,J ),J=0,PY ),I=0,PX )
0331      WRITE(NOPT,204) ( ( RY( I,J ),J=0,PY ),I=0,PX )
0332      WRITE(NOPT,206) ( ( VX( I,J ),J=0,PY ),I=0,PX )
0333      WRITE(NOPT,206) ( ( VY( I,J ),J=0,PY ),I=0,PX )
0334      WRITE(NOPT,208) ( ( RHO(I,J),J=0,PY ),I=0,PX )
0335 C
0336      CLOSE(NOPT,STATUS='KEEP')
0337 END IF
0338 C                                     --- DATA OUTPUT (2) FOR ANIMATION ---
0339 C
0340      IF( MOD(NTIME,NANIME) .EQ. 0 ) THEN
0341 C
0342      CALL VELCAL( COLOR , ITREESID , ITREEDWN , NTIME )
0343 C
0344      NANMCTR = NANMCTR + 1
0345      CALL GRAPHVEL( NANMCTR )
0346 C
0347 END IF
0348 C
0349 C                                     --- DATA BETWEEN NTIME=0 AND ---
0350 C                                     --- =NTHROW ARE THROWN AWAY. ---
0351 IF( NTIME .LT. NTHROW ) GOTO 1000
0352 C
0353 C
0354 IF( NTIME .EQ. NTHROW ) THEN
0355 C
0356      NSMPLCD = 0
0357      DO 302 I=1, NTIMEMX
0358      CDFORCE(I) = 0.D0
0359      302      CONTINUE
0360 C
0361      DO 310 J=0, PY
0362      DO 305 I=0, PX
0363      VXSUM( I,J ) = 0.D0
0364      VYSUM( I,J ) = 0.D0
0365      RHOSUM(I,J) = 0.D0
0366      305      CONTINUE
0367      310      CONTINUE
0368      NSMPLVEL = 0
0369 C
0370      GOTO 1000
0371 END IF
0372 C                                     --- CAL. SUM OF VELOCITIES ---
0373 C
0374 IF( MOD(NTIME,NSMPL1) .EQ. 0 )THEN
0375      NSMPLVEL = NSMPLVEL + 1
0376      CALL VELCAL( COLOR , ITREESID , ITREEDWN , NTIME )
0377 C
0378      DO 500 J=0, PY
0379      DO 490 I=0, PX
0380      VXSUM( I,J ) = VXSUM( I,J ) + VX( I,J )
0381      VYSUM( I,J ) = VYSUM( I,J ) + VY( I,J )
0382      RHOSUM(I,J) = RHOSUM(I,J) + RHO(I,J)
0383      490      CONTINUE
0384      500      CONTINUE
0385 END IF
0386 C
0387 C
0388 1000 CONTINUE
0389 C
0390 C
0391 C                                     --- END OF MAIN LOOP ---
0392 C
0393 C
0394 C                                     --- CAL. CD ---
0395      C1 = 0.D0
0396      DO 1100 I=1, NSMPLCD

```

• The velocity data, etc., are written out at every NGRAPH time steps for the post processing analysis.

• The velocity data, etc., are written out at every NANIME time steps for making an animation.

• In order to evaluate average values, the velocity data, etc., are sampled at every NSMPL1 time steps.

```

0397      C1 = C1 + CDFORCE(I)
0398 1100 CONTINUE
0399      CD = ( C1/DBLE(NSMPLCD) ) / CDFORCE0
0400      CD99 = CDFORCE( NSMPLCD ) / CDFORCE0
0401 C
0402 C           --- CAL AVE. AND PRINT OUT CONSTANTS (1) ---
0403     CALL AVECAL( NP, NSMPLVEL, VXSUM, VYSUM, RHOSUM,
0404     &                                         PX, PY, ALPHAMX )
0405 C
0406 C           --- DATA OUTPUT (3) ---
0407     WRITE(11,1101) DNS0, TAU, DX, DT, CLAT, ALPHAMX
0408     WRITE(11,1103) PX, PY, PXY, XL, YL, XL1, XL2, YL1, YL2
0409     WRITE(11,1105) UVELUX, UVELY
0410     WRITE(11,1107) DCYL, ITREECYL, ITREESID, ITREEDWN
0411     WRITE(11,1109) NTIMEMX, NGRAPH, NANIME, NSMPLCD, NTHROW, NSMPL1
0412     WRITE(11,1111) CD, RE
0413 C           --- DATA OUTPUT (4) ---
0414     WRITE(12,1121) PX, PY
0415     WRITE(12,1123) ( ( VXSUM( I,J),J=0,PY ), I=0,PX )
0416     WRITE(12,1123) ( ( VYSUM( I,J),J=0,PY ), I=0,PX )
0417     WRITE(12,1125) ( ( RHOSUM(I,J),J=0,PY ), I=0,PX )
0418 C
0419 C           --- PRINT OUT (2) ---
0420     WRITE(NP,1131) CD99 , CD , RE
0421 C           --- DATA OUTPUT (5) ---
0422     WRITE(12,1133) CD , RE , NSMPLCD
0423     WRITE(12,1135) ( CDFORCE(I), I=1, NSMPLCD )
0424 C
0425             CLOSE( 9,STATUS='KEEP' )
0426             CLOSE(11,STATUS='KEEP' )
0427             CLOSE(12,STATUS='KEEP' )
0428             CLOSE(41,STATUS='KEEP' )
0429             CLOSE(42,STATUS='KEEP' )
0430 C
0431 C           ----- FORMAT -----
0432 C
0433 10 FORMAT(/1H ,-----
0434   &      /1H ,1X,'LATTICE BOLTZMANN SIMULATION OF',
0435   &      ' A FLOW AROUND A CYLINDER'
0436   &      /1H ,10X,'+++ TWO-DIMENSIONAL FLOW +++'
0437   &      /1H ,-----
0438   &      //1H , 'DNS0=', F6.3, 2X, 'TAU=',F6.4,
0439   &      2X, 'DX=', F6.2, 2X, 'DT=', F6.2, 2X, 'CLAT=' ,
0440   &      F6.3
0441   &      /1H , 'ALPHAMX=', I3)
0442 11 FORMAT(1H , 'PX=', I3, 1X, 'PY=', I3, 1X, 'PXY=', I6, 1X,
0443   &      'XL=', F6.2, 1X, 'YL=', F6.2, 1X, 'XL1=', F6.2, 1X,
0444   &      'YL1=', F6.2
0445   &      /1H , 'XL2=', F6.2, 1X, 'YL2=', F6.2, 2X,
0446   &      'UVELX=', F6.2, 2X, 'UVELY=', F6.2)
0447 13 FORMAT(1H , 'DCYL=', F7.3, 2X, 'ITREECYL=',I3, 2X, 'ITREESID=',I3,
0448   &      2X, 'ITREEDWN=',I3)
0449 14 FORMAT(1H , 'NTIMEMX=', I8, 2X, 'NGRAPH=', I8, 2X, 'NANIME=', I8
0450   &      /1H , 'NSMPLCD=', I8, 2X, 'NTHROW=',I8, 2X, 'NSMPL1=',I8)
0451 15 FORMAT(1H , 'CDFORCE0=', F9.4, 2X, 'RE=', F9.3)
0452 201 FORMAT( 3I9 )
0453 202 FORMAT( (6E13.6) )
0454 204 FORMAT( (6E13.6) )
0455 206 FORMAT( (6E13.6) )
0456 208 FORMAT( (6E13.6) )
0457 1103 FORMAT( 5F9.4, I8 )
0458 1103 FORMAT( 3I8, 6F9.3 )
0459 1105 FORMAT( 2F11.5 )
0460 1107 FORMAT( F6.2 , 3I3 )
0461 1109 FORMAT( 6I10 )
0462 1111 FORMAT( 2F12.6 )
0463 1121 FORMAT( 2I10 )
0464 1123 FORMAT( ( 8E10.3 ) )
0465 1125 FORMAT( ( 8E10.3 ) )
0466 1131 FORMAT(/1H , 'CD99=', F10.5, 3X, 'CD=', F10.5, 3X, 'RE=', F10.5)
0467 1133 FORMAT( 2F10.4 , I9 )
0468 1135 FORMAT( ( 7E11.4 ) )
0469
0470                                     STOP
0471 C*****
0472 C*****          SUBROUTINE *****
0473 C*****          *****
0474 C
0475 C****  SUB AVECAL *****
0476     SUBROUTINE AVECAL( NP, NSMPLVEL, VXSUM, VYSUM, RHOSUM,

```

```

0477   &                                     PX, PY, ALPHAMX )
0478 C   IMPLICIT REAL*8 (A-H,O-Z), INTEGER (I-N)
0479   INTEGER PP, QQ, KK
0480 C   PARAMETER( PP=300, QQ=400, KK=8, PI=3.141592653589793D0 )
0481   INTEGER PX, PY, ALPHAMX
0482   REAL*8 VXSUM(0:PP,0:QQ), VYSUM(0:PP,0:QQ), RHOSUM(0:PP,0:QQ)
0483 C
0484   --- CAL VELOCITY FIELD ---
0485   DO 1010 J=0, PY
0486   DO 1008 I=0, PX
0487 C
0488   VXSUM( I,J ) = VXSUM( I,J ) / DBLE(NSMPLVEL)
0489   VYSUM( I,J ) = VYSUM( I,J ) / DBLE(NSMPLVEL)
0490   RHOSUM(I,J) = RHOSUM(I,J) / DBLE(NSMPLVEL)
0491   1008 CONTINUE
0492   1010 CONTINUE
0493 C
0494   --- PRINT OUT (2) VELOCITY FIELD ---
0495 C
0496 C
0497   WRITE(NP,1021)
0498   DO 1030 I=0, PX
0499   DO 1029 J=0, PY, 17
0500   &           WRITE(NP,1026) VXSUM(I,J),VXSUM(I,J+ 1),VXSUM(I,J+ 2),
0501   &           VXSUM(I,J+ 3),VXSUM(I,J+ 4),VXSUM(I,J+ 5),
0502   &           VXSUM(I,J+ 6),VXSUM(I,J+ 7),VXSUM(I,J+ 8),
0503   &           VXSUM(I,J+ 9),VXSUM(I,J+10),VXSUM(I,J+11),
0504   &           VXSUM(I,J+12),VXSUM(I,J+13),VXSUM(I,J+14),
0505   &           VXSUM(I,J+15),VXSUM(I,J+16)
0506   1029 CONTINUE
0507   1030 CONTINUE
0508 C
0509   WRITE(NP,1041)
0510   DO 1050 I=0, PX
0511   DO 1049 J=0, PY, 17
0512   &           WRITE(NP,1026) VYSUM(I,J),VYSUM(I,J+ 1),VYSUM(I,J+ 2),
0513   &           VYSUM(I,J+ 3),VYSUM(I,J+ 4),VYSUM(I,J+ 5),
0514   &           VYSUM(I,J+ 6),VYSUM(I,J+ 7),VYSUM(I,J+ 8),
0515   &           VYSUM(I,J+ 9),VYSUM(I,J+10),VYSUM(I,J+11),
0516   &           VYSUM(I,J+12),VYSUM(I,J+13),VYSUM(I,J+14),
0517   &           VYSUM(I,J+15),VYSUM(I,J+16)
0518   1049 CONTINUE
0519   1050 CONTINUE
0520 C
0521   WRITE(NP,1061)
0522   DO 1070 I=0, PX
0523   DO 1069 J=0, PY, 17
0524   &           WRITE(NP,1062) RHOSUM(I,J),RHOSUM(I,J+ 1),RHOSUM(I,J+ 2),
0525   &           RHOSUM(I,J+ 3),RHOSUM(I,J+ 4),RHOSUM(I,J+ 5),
0526   &           RHOSUM(I,J+ 6),RHOSUM(I,J+ 7),RHOSUM(I,J+ 8),
0527   &           RHOSUM(I,J+ 9),RHOSUM(I,J+10),RHOSUM(I,J+11),
0528   &           RHOSUM(I,J+12),RHOSUM(I,J+13),RHOSUM(I,J+14),
0529   &           RHOSUM(I,J+15),RHOSUM(I,J+16)
0530   1069 CONTINUE
0531   1070 CONTINUE
0532 C
0533   1021 FORMAT(/1H,' VX1, VX2, VX3, VX4, VX5, VX6,...')
0534   1026 FORMAT( (7E11.4) )
0535   1041 FORMAT(/1H,' VY1, VY2, VY3, VY4, VY5, VY6,...')
0536   1061 FORMAT(/1H,' RHO1, RHO2, RHO3, RHO4, RHO5, RHO6,...')
0537   1062 FORMAT( (6E13.6) )
0538
0539
0540 C**** SUB INICVEL *****
0541   SUBROUTINE INICVEL
0542 C
0543   IMPLICIT REAL*8 (A-H,O-Z), INTEGER (I-N)
0544 C
0545   COMMON /BLOCK2/  CVEL, W, IINC, ANTIALPH, ALPHAMX
0546 C
0547   INTEGER PP, QQ, KK
0548   PARAMETER( PP=300, QQ=400, KK=8, PI=3.141592653589793D0 )
0549 C
0550   REAL*8 CVEL(2,0:KK), W(0:KK)
0551   INTEGER ALPHAMX, IINC(2,0:KK), ANTIALPH(0:KK)
0552 C
0553   CVEL(1,0) = 0.D0
0554   CVEL(2,0) = 0.D0
0555   CVEL(1,1) = 1.D0
0556   CVEL(2,1) = 0.D0
0557   CVEL(1,2) = -1.D0

```

• The velocity field is calculated by an averaging procedure.

• A subroutine for setting the lattice velocities, etc.

• The lattice velocity  $c_a$  is set.

```

0558      CVEL(2,2) = 0.D0
0559      CVEL(1,3) = 0.D0
0560      CVEL(2,3) = 1.D0
0561      CVEL(1,4) = 0.D0
0562      CVEL(2,4) = -1.D0
0563      CVEL(1,5) = 1.D0
0564      CVEL(2,5) = 1.D0
0565      CVEL(1,6) = -1.D0
0566      CVEL(2,6) = -1.D0
0567      CVEL(1,7) = 1.D0
0568      CVEL(2,7) = -1.D0
0569      CVEL(1,8) = -1.D0
0570      CVEL(2,8) = 1.D0
0571 C
0572      W(0) = 4.D0/9.D0
0573      W(1) = 1.D0/9.D0
0574      W(2) = W(1)
0575      W(3) = W(1)
0576      W(4) = W(1)
0577      W(5) = 1.D0/36.D0
0578      W(6) = W(5)
0579      W(7) = W(5)
0580      W(8) = W(5)
0581 C
0582      IINC(1,1) = 1
0583      IINC(2,1) = 0
0584      IINC(1,2) = -IINC(1,1)
0585      IINC(2,2) = -IINC(2,1)
0586      IINC(1,3) = 0
0587      IINC(2,3) = 1
0588      IINC(1,4) = -IINC(1,3)
0589      IINC(2,4) = -IINC(2,3)
0590      IINC(1,5) = 1
0591      IINC(2,5) = 1
0592      IINC(1,6) = -IINC(1,5)
0593      IINC(2,6) = -IINC(2,5)
0594      IINC(1,7) = 1
0595      IINC(2,7) = -1
0596      IINC(1,8) = -IINC(1,7)
0597      IINC(2,8) = -IINC(2,7)
0598 C
0599      ANTIALPH(1) = 2
0600      ANTIALPH(2) = 1
0601      ANTIALPH(3) = 4
0602      ANTIALPH(4) = 3
0603      ANTIALPH(5) = 6
0604      ANTIALPH(6) = 5
0605      ANTIALPH(7) = 8
0606      ANTIALPH(8) = 7
0607
0608
0609 C**** SUB INILAT *****
0610      SUBROUTINE INILAT
0611 C
0612      IMPLICIT REAL*8 (A-H,O-Z), INTEGER (I-N)
0613 C
0614      COMMON /BLOCK3/ RHO , RX , RY , VX , VY
0615      COMMON /BLOCK5/ XL , YL , XLL , YLL , XL2 , YL2 , PX , PY , PXY
0616 C
0617      INTEGER      PP , QQ , KK
0618      PARAMETER( PP=300 , QQ=400 , KK=8 , PI=3.141592653589793D0 )
0619 C
0620      REAL*8      RHO(0:PP,0:QQ)
0621      REAL*8      RX( 0:PP,0:QQ) , RY(0:PP,0:QQ)
0622      REAL*8      VX( 0:PP,0:QQ) , VY(0:PP,0:QQ)
0623      INTEGER      PX , PY , PXY
0624 C
0625      C1 = XL/DBLE(PX)
0626      C2 = YL/DBLE(PY)
0627      DO 100 J=0, PY
0628      DO 90 I=0, PX
0629          RX(I,J) = DBLE(I)*C1 - XLL
0630          RY(I,J) = DBLE(J)*C1 - YLL
0631      90 CONTINUE
0632      100 CONTINUE
0633
0634
0635 C**** SUB INIDIST *****

```

• The weighting coefficient  $w_\alpha$  is set.

• IINC is used for describing the relationship between the lattice point and the  $\alpha$ -direction. For example, the neighboring site in the  $\alpha$ -direction of  $\alpha=1$  is arrived at by moving  $(+1,0)$  in the  $x$ - and  $y$ -direction from the site of interest. In this case, the movement is described as  $IINC(1,1)=1$  and  $IINC(2,1)=0$ .

• The opposite direction of the  $\alpha$ -direction is saved in ATIALPH(\*).

RETURN  
END

• A subroutine for setting the lattice positions.

•  $(PX+1, PY+1)$  lattice points are set in the  $x$ - and  $y$ -direction.

RETURN  
END

```

0636      SUBROUTINE INIDIST( DNS0 , ALPHAMX )
0637 C
0638      IMPLICIT REAL*8 ( A-H,O-Z ), INTEGER ( I-N )
0639 C
0640      COMMON /BLOCK1/   F , FTILD
0641      COMMON /BLOCK5/   XL , YL , XL1 , YL1 , XL2 , YL2 , PX , PY , PXY
0642      COMMON /BLOCK6/   UVELX , UVELY
0643 C
0644      INTEGER     PP , QQ , KK
0645      PARAMETER( PP=300 , QQ=400 , KK=8 , PI=3.141592653589793D0 )
0646 C
0647      REAL*8      F(0:PP,0:QQ,0:KK) , FTILD(0:PP,0:QQ,0:KK)
0648      INTEGER     PX , PY , PXY , ALPHAMX
0649 C
0650      REAL*8      FEQ, CDNS0
0651 C
0652      CDNS0 = DNS0
0653 C
0654      DO 110 J=0, PY
0655      DO 100 I=0, PX
0656          DO 10  K=0, ALPHAMX
0657              IF( I.EQ.0 ) THEN
0658                  F(I,J,K)= FEQ( UVELX, UVELY, K, CDNS0 )
0659              ELSE
0660 CCC                  F(I,J,K)= FEQ( 0.D0 , 0.D0 , K, CDNS0 )
0661                  F(I,J,K)= FEQ( UVELX, UVELY, K, CDNS0 )
0662          END IF
0663      10  CONTINUE
0664      100 CONTINUE
0665      110 CONTINUE
0666
0667      RETURN
END
0668 **** SUB INICOLOR ****
0669      SUBROUTINE INICOLOR( PX , PY , DCYL2SQ )
0670 C
0671 C
0672 C          0 : USUAL TREATMENT
0673 C          1 : TREATMENT AT Bupstream
0674 C          2 : TREATMENT AT Bdownstream
0675 C          3 : TREATMENT AT Bupper_side
0676 C          4 : TREATMENT AT Blower_side
0677 C          5 : TREATMENT AT Bcyl_surface
0678 C          6 : NO BC TREAT. INSIDE PTCL,
0679 C               BUT INTERACTING OUTER SITES
0680 C          7 : NO BC TREAT. INSIDE PTCL,
0681 C               NOT INTERACTING OUTER SITES
0682      IMPLICIT REAL*8 ( A-H,O-Z ), INTEGER ( I-N )
0683 C
0684      COMMON /BLOCK3/   RHO , RX , RY , VX , VY
0685 C
0686      COMMON /BLOCK14/  RXCYL , RYCYL , ICYL , JCYL , DCYL
0687      COMMON /BLOCK15/  COLOR    , POSINTBL
0688      COMMON /BLOCK18/  TBLNAMIN , NTBLNAMI
0689 C
0690 C
0691      INTEGER     PP , QQ , KK
0692      PARAMETER( PP=300 , QQ=400 , KK=8 , PI=3.141592653589793D0 )
0693 C
0694      REAL*8      RHO(0:PP,0:QQ)
0695      REAL*8      RX( 0:PP,0:QQ) , RY(0:PP,0:QQ)
0696      REAL*8      VX( 0:PP,0:QQ) , VY(0:PP,0:QQ)
0697      INTEGER     PX , PY , PXY
0698 C
0699      INTEGER     PPXY
0700      PARAMETER( PPXY=150000 , NNTBL=2200 , NNTBL2=4400 , NNTBL3=4400 )
0701 C
0702      INTEGER     COLOR(PPXY) , POSINTBL(PPXY)
0703      INTEGER     TBLNAMIN(NNTBL3) , NTBLNAMI
0704 C
0705      REAL*8      RJDG1 , RJDG2 , RJDG2SQ , RXI , RYI , C1
0706      REAL*8      RXIJ , RYIJ , RIJSQ
0707      INTEGER     ISITE , IC1, IS, IE, JS, JE
0708 C
0709      DO 120 J=0, PY
0710      DO 100 I=0, PX
0711          ISITE = (PX+1)*J + (I+1)
0712 C
0713      POSINTBL( ISITE ) = 0
0714 C

```

• A subroutine for setting the initial value of the distribution functions.

• An equilibrium distribution with the uniform velocity  $U$  is used as an initial distribution.

• A subroutine for evaluating the values of the variable *color* explained in Section 7.4.2.

```

0715      IF(      I.EQ.0 ) THEN          COLOR(ISITE) = 1
0716      ELSE IF( I.EQ.PX ) THEN          COLOR(ISITE) = 2
0717      ELSE IF( J.EQ.PY ) THEN          COLOR(ISITE) = 3
0718      ELSE IF( J.EQ.0 ) THEN          COLOR(ISITE) = 4
0719      ELSE                           COLOR(ISITE) = 0
0720
0721      END IF
0722
0723      CONTINUE
0724      CONTINUE
0725
0726      100 CONTINUE
0727      120 CONTINUE
0728 C      --- FOR SPECIAL TREATMENT OF SITES INSIDE CYLINDER ---
0729      DO 150 I=1, PX
0730      IF( RX(I,0) .GE. RXYCYL ) THEN
0731          ICYL = I
0732          GOTO 170
0733      END IF
0734      150 CONTINUE
0735      ICYL = PX
0736 C
0737      170 DO 160 J=1, PY
0738      IF( RY(0,J) .GE. RYCYL ) THEN
0739          JCYL = J
0740          GOTO 180
0741      END IF
0742      160 CONTINUE
0743      JCYL = PY
0744 C
0745      180 C1    = (DCYL/2.D0+0.01D0) / ( RX(2,0)-RX(1,0) )
0746 CCC     IC1    = IDINT(C1)
0747     IC1    = IDINT(C1) + 2
0748     IS     = ICYL - IC1 - 1
0749     IE     = ICYL + IC1
0750     JS     = JCYL - IC1 - 1
0751     JE     = JCYL + IC1
0752     RJDG1   = (DCYL/2.D0) + 3.D0*( RX(2,0)-RX(1,0) )
0753     RJDG2   = RJDG1
0754     RJDG2SQ = RJDG2**2
0755 C
0756     NTBLNAMI = 0
0757     DO 220 J=JS, JE
0758     DO 200 I=IS, IE
0759 C
0760     RXI = RX(I,J)
0761     RYI = RY(I,J)
0762 C
0763     ISITE   = (PX+1)*J + (I+1)
0764     RXIJ   = RXI - RXYCYL
0765     IF( DABS(RXIJ) .GE. RJDG1 ) GOTO 200
0766     RYIJ   = RYI - RYCYL
0767     IF( DABS(RYIJ) .GE. RJDG1 ) GOTO 200
0768     RIJSQ   = RXIJ**2 + RYIJ**2
0769     IF( RIJSQ .GE. RJDG2SQ ) GOTO 200
0770 C
0771     IF( RIJSQ .LE. DCYL2SQ ) THEN
0772         COLOR(ISITE) = 7
0773         NTBLNAMI = NTBLNAMI + 1
0774         TBLNAMIN(NTBLNAMI) = ISITE
0775     END IF
0776 C
0777     200 CONTINUE
0778     220 CONTINUE
0779
0780
0781 C**** SUB MAKETBLE *****
0782     SUBROUTINE MAKETBLE( DCYL2SQ , NTBL , NTBLDW )
0783 C
0784     IMPLICIT REAL*8 ( A-H,O-Z ), INTEGER ( I-N )
0785 C
0786     COMMON /BLOCK3/  RHO , RX , RY , VX , VY
0787     COMMON /BLOCK5/  XL , YL , XLL , YLL , XL2 , YL2 , PX , PY , PXY
0788 C
0789     COMMON /BLOCK14/ RXYCYL , RYCYL , ICYL , JCYL , DCYL
0790     COMMON /BLOCK15/ COLOR , POSINTBL
0791 C
0792     -----
0793     INTEGER PP , QQ , KK
0794     PARAMETER( PP=300 , QQ=400 , KK=8 , PI=3.141592653589793D0 )
0795 C

```

• The values shown in Section 7.4.2 are assigned to the lattice sites next to each boundary surface.

• The treatment concerning the sites related to the cylinder.

• The sites to be checked are limited to the neighboring sites around the cylinder to a certain degree.

• color(\*)=7 is set for the site inside the cylinder.

RETURN  
END

• A subroutine for making a list of the lattice sites interacting with the cylinder.

```

0796      REAL*8      RHO(0:PP,0:QQ)
0797      REAL*8      RX( 0:PP,0:QQ)      , RY(0:PP,0:QQ)
0798      REAL*8      VX( 0:PP,0:QQ)      , VY(0:PP,0:QQ)
0799      INTEGER     PX , PY , PXY
0800 C -----
0801      INTEGER     PXY
0802      PARAMETER( PXY=150000 , NNTBL=2200 , NNTBL2=4400 , NNTBL3=4400 )
0803 C -----
0804      INTEGER     COLOR(PXY)      , POSINTBL(PXY)
0805 C -----
0806      REAL*8      C1 , RXI , RYI
0807      REAL*8      RJDG1 , RJDG2 , RJDG2SQ
0808      INTEGER     IS , IE , JS , JE , IC1 , ISITE
0809 CCC   INTEGER     JJ , JJ2 , II , II2 , IALPHA(0:8) , NIALPHA
0810      INTEGER     IALPHA(0:8) , NIALPHA
0811 C -----
0812 C ----- CYLINDER POSITION IS (ICYL,JCYL) IN LATTICE ---
0813      NTBL = 0
0814      NTBLDW= 0
0815 C ----- CHECK WHETHER OR NOT SITES ARE INSIDE CYL ---
0816 C -----
0817      40 C1    = (DCYL/2.D0+0.01D0) / ( RX(2,0)-RX(1,0) )
0818 CCC   IC1    = IDINT(C1)
0819      IC1    = IDINT(C1) + 2
0820      IS    = ICYL - IC1 - 1
0821      IE    = ICYL + IC1
0822      JS    = JCYL - IC1 - 1
0823      JE    = JCYL + IC1
0824 C -----
0825      RJDG1   = (DCYL/2.D0) + 3.D0*( RX(2,0)-RX(1,0) )
0826      RJDG2   = RJDG1
0827      RJDG2SQ = RJDG2**2
0828 C -----
0829 C -----
0830      DO 220 J=JS, JE
0831      DO 200 I=IS, IE
0832 C -----
0833      RXI = RX(I,J)
0834      RYI = RY(I,J)
0835 C ----- FOR THE MOST OUTER SITES ---
0836      IF( (I.EQ.IS) .AND. (J.EQ.JS) ) THEN
0837 C           +--+AT LEFT-DOWN CORNER+++
0838      IALPHA(1) = 5
0839      NIALPHA = 1
0840      CALL INTERACT( I, J, RXI, RYI, RXCYL, RYCYL, NIALPHA, IALPHA,
0841      &          RJDG2SQ , DCYL2SQ )
0842      & ELSE IF ( (I.EQ.IE) .AND. (J.EQ.JS) ) THEN
0843 C           +--+AT RIGHT-DOWN CORNER+++
0844      IALPHA(1) = 8
0845      NIALPHA = 1
0846      CALL INTERACT( I, J, RXI, RYI, RXCYL, RYCYL, NIALPHA, IALPHA,
0847      &          RJDG2SQ , DCYL2SQ )
0848      & ELSE IF ( (I.EQ.IS) .AND. (J.EQ.JE) ) THEN
0849 C           +--+AT LEFT-UP CORNER+++
0850      IALPHA(1) = 7
0851      NIALPHA = 1
0852      CALL INTERACT( I, J, RXI, RYI, RXCYL, RYCYL, NIALPHA, IALPHA,
0853      &          RJDG2SQ , DCYL2SQ )
0854      & ELSE IF ( (I.EQ.IE) .AND. (J.EQ.JE) ) THEN
0855 C           +--+AT RIGHT-UP CORNER+++
0856      IALPHA(1) = 6
0857      NIALPHA = 1
0858      CALL INTERACT( I, J, RXI, RYI, RXCYL, RYCYL, NIALPHA, IALPHA,
0859      &          RJDG2SQ , DCYL2SQ )
0860 C -----
0861 C ----- FOR OUTER CIRCUMFERENCE SITE
0862 C -----
0863      ELSE IF ( (J.EQ.JS) ) THEN
0864 C           +--+ALONG X-AXIS (DOWN)+++
0865      IALPHA(1) = 3
0866      IALPHA(2) = 5
0867      IALPHA(3) = 8
0868      NIALPHA = 3
0869 C -----
0870      CALL INTERACT( I, J, RXI, RYI, RXCYL, RYCYL, NIALPHA, IALPHA,
0871      &          RJDG2SQ , DCYL2SQ )
0872      & ELSE IF ( (I.EQ.IS) ) THEN
0873 C           +--+ ALONG Y-AXIS (LEFT)  +++

```

• The sites to be checked are limited to the neighboring sites around the cylinder to a certain degree.

• The treatment for the four corner sites of the outermost rectangle.

• For the left-down site.

• For the right-down site.

• For the left-up site.

• For the right-up site.

• The treatment for the sites on the outermost rectangle, except the four corner sites.

• For the sites on the bottom line along the x-axis.

```

0874      IALPHA(1) = 1
0875      IALPHA(2) = 5
0876      IALPHA(3) = 7
0877      NIALPHA = 3
0878 C
0879      CALL INTERACT( I, J, RXI, RYI, RXCYL, RYCYL, NIALPHA, IALPHA,
0880      &          RJDG2SQ , DCYL2SQ )
0881      ELSE IF ( I.EQ.IE ) THEN
0882      &          +++ ALONG Y-AXIS (RIGHT) +++
0883      IALPHA(1) = 2
0884      IALPHA(2) = 6
0885      IALPHA(3) = 8
0886      NIALPHA = 3
0887 C
0888      CALL INTERACT( I, J, RXI, RYI, RXCYL, RYCYL, NIALPHA, IALPHA,
0889      &          RJDG2SQ , DCYL2SQ )
0890      ELSE IF ( J.EQ.JE ) THEN
0891      &          +++ ALONG X-AXIS (UP) +++
0892      IALPHA(1) = 4
0893      IALPHA(2) = 6
0894      IALPHA(3) = 7
0895      NIALPHA = 3
0896 C
0897      CALL INTERACT( I, J, RXI, RYI, RXCYL, RYCYL, NIALPHA, IALPHA,
0898      &          RJDG2SQ , DCYL2SQ )
0899 C
0900 C
0901      ----- FOR INNER SITES OF CHECKING RECTANGLE -----
0902      ELSE
0903      IALPHA(1) = 1
0904      IALPHA(2) = 2
0905      IALPHA(3) = 3
0906      IALPHA(4) = 4
0907      IALPHA(5) = 5
0908      IALPHA(6) = 6
0909      IALPHA(7) = 7
0910      IALPHA(8) = 8
0911      NIALPHA = 8
0912 C
0913      CALL INTERACT( I,J, RXI,RYI, RXCYL, RYCYL, NIALPHA, IALPHA,
0914      &          RJDG2SQ , DCYL2SQ )
0915 C
0916      END IF
0917 C
0918      200 CONTINUE
0919      220 CONTINUE
0920
0921
0922 C**** SUB INTERACT *****
0923      SUBROUTINE INTERACT( I, J, RXI, RYI, RXCYL, RYCYL,
0924      &          NIALPHA, IALPHA, RJDG2SQ, DCYL2SQ )
0925 C
0926      IMPLICIT REAL*8 (A-H,O-Z), INTEGER (I-N)
0927 C
0928      COMMON /BLOCK2/  CVEL, W, IINC, ANTIALPH, ALPHAMX
0929      COMMON /BLOCK3/  RHO, RX, RY, VX, VY
0930      COMMON /BLOCK5/  XL, YL, XLI, YLI, XL2, YL2, PX, PY, PXY
0931 C
0932      COMMON /BLOCK15/ COLOR, POSINTBL
0933      COMMON /BLOCK16/ TBLNAM, TBLNUM, TBLPOS, NTBL
0934      COMMON /BLOCK17/ TBLDW, TBLAL, NTBLDW
0935 C
0936 C
0937      INTEGER PP, QQ, KK
0938      PARAMETER( PP=300, QQ=400, KK=8, PI=3.141592653589793D0 )
0939 C
0940      REAL*8   CVEL(2,0:KK), W(0:KK)
0941      REAL*8   RHO(0:PP,0:QQ)
0942      REAL*8   RX( 0:PP,0:QQ), RY(0:PP,0:QQ)
0943      REAL*8   VX( 0:PP,0:QQ), VY(0:PP,0:QQ)
0944      INTEGER  ALPHAMX, IINC(2,0:KK), ANTIALPH(0:KK)
0945      INTEGER  PX, PY, PXY, NIALPHA, IALPHA(0:8)
0946 C
0947      INTEGER  PPXY
0948      PARAMETER( PPXY=150000, NNTBL=2200, NNTBL2=4400, NNTBL3=4400 )
0949 C
0950      REAL*8   TBLDW(NNTBL2)
0951      INTEGER  COLOR(PPXY), POSINTBL(PPXY)
0952      INTEGER  TBLNAM(NNTBL), TBLNUM(NNTBL), TBLPOS(NNTBL), NTBL
0953      INTEGER  TBLAL(NNTBL2), NTBLDW
0954 C

```

• For the sites on the left line along the y-axis.

• For the sites on the right line along the y-axis.

• For the sites on the top line along the x-axis.

• For the sites inside the outermost rectangle.

• A subroutine for assessing whether or not the neighboring site is inside the cylinder.

```

0955 C
0956      INTEGER  ISITE, ISITE1, IPATH, IALPHA0
0957      INTEGER  IX1 , IY1 , JJJ
0958      REAL*8   RXI , RYI , RXIJ , RYIJ , RIJSQ
0959      REAL*8   RXI1 , RYI1 , RXIJ1 , RYIJ1 , RIJSQ1 , RJDG2SQ
0960      REAL*8   RXCYL, RYCYL, DCYL2SQ
0961      REAL*8   C01 , C1 , C2 , C3 , CDW
0962 C
0963 C
0964      ISITE = (PX+1)*J + (I+1)
0965      RXIJ = RXI - RXCYL
0966      RYIJ = RYI - RYCYL
0967      RIJSQ = RXIJ**2 + RYIJ**2
0968      IF( RIJSQ .GE. RJDG2SQ ) THEN
0969          COLOR(ISITE) = 0
0970          RETURN
0971      END IF
0972      IF( RIJSQ .LE. DCYL2SQ ) RETURN
0973 C
0974      IPATH = 0
0975      DO 200 JJJ = 1, NIALPHA
0976 C
0977 C
0978 C
0979 C
0980 C
0981 C
0982 C
0983      IALPHA0= IALPHA(JJJ)
0984      IX1 = I + IIINC(1,IALPHA0)
0985      IY1 = J + IIINC(2,IALPHA0)
0986      RXI1 = RX(IX1,IY1)
0987      RYI1 = RY(IX1,IY1)
0988      RXIJ1 = RXI1 - RXCYL
0989      RYIJ1 = RYI1 - RYCYL
0990      RIJSQ1 = RXIJ1**2 + RYIJ1**2
0991 C
0992      IF( RIJSQ1 .LE. DCYL2SQ ) THEN
0993          IPATH = IPATH + 1
0994          IF( IPATH .EQ. 1 ) THEN
0995              NTBL = NTBL + 1
0996              TBLNAM(NTBL) = ISITE
0997              COLOR(ISITE) = 5
0998              POSINTBL(ISITE) = NTBL
0999          END IF
1000 C
1001      C01 = RXIJ*RXIJ1 + RYIJ*RYIJ1
1002      C1 = RIJSQ + RIJSQ1 - 2.D0*C01
1003      C2 = -RIJSQ + C01
1004      C3 = RIJSQ - DCYL2SQ
1005      CDW = ( - C2 - DSQRT( C2**2 - C1*C3 ) ) / C1
1006 C
1007      NTBLDW = NTBLDW + 1
1008      TBLDW( NTBLDW ) = CDW
1009      TBLAL( NTBLDW ) = IALPHA0
1010      IF( IPATH .EQ. 1 ) TBLPOS(NTBL) = NTBLDW
1011 C
1012 C
1013      ISITE1 = (PX+1)*IY1 + (IX1+1)
1014      COLOR(ISITE1) = 6
1015      END IF
1016 C
1017      200 CONTINUE
1018 C
1019      IF( IPATH .GE. 1 ) THEN
1020          TBLNUM(NTBL) = IPATH
1021      ELSE
1022          COLOR(ISITE) = 0
1023      END IF
1024
1025
1026 **** SUB VELCAL *****
1027      SUBROUTINE VELCAL( COLOR , ITREESID , ITREEDWN , NTIME )
1028 C
1029      IMPLICIT REAL*8 (A-H,O-Z), INTEGER (I-N)
1030 C
1031      COMMON /BLOCK1/ F , FTILD
1032      COMMON /BLOCK3/ RHO , RX , RY , VX , VY
1033      COMMON /BLOCK4/ DNS0 , TAU , DX , DT , CLAT
1034      COMMON /BLOCK5/ XL , YL , XL1 , YL1 , XL2 , YL2 , PX , PY , PXY
1035      COMMON /BLOCK6/ UVELX , UVELY

```

• The sites being far over the RJDG2SQ distance (note the square) have no interaction with the cylinder.

• If the neighboring site is inside the cylinder, then the variable color is set to be 5 for this site, its site name is saved in TBLNAM, and the order of the site appearing in TBLNAM is saved in POSINTBL.

•  $\Delta_w$ =CDW is calculated from Eq. (7.14). The direction of the neighboring site inside the cylinder is saved in TBLAL, and the value of  $\Delta_w$  is saved in TBLDW.

• The order of the quantities, related to the site of interest, first appearing in TBLAL and TBLDW, is saved in TBLPOS.

• The number of the sites, inside the cylinder, interacting with the site of interest is saved in TBLNUM.

RETURN  
 END

• A subroutine for calculating the velocities and densities at each lattice site.

```

1036 C
1037 C -----+
1038 INTEGER PP , QQ , KK
1039 PARAMETER( PP=300 , QQ=400 , KK=8 , PI=3.141592653589793D0 )
1040 C
1041 REAL*8 F(0:PP,0:QQ,0:KK), FTILD(0:PP,0:QQ,0:KK)
1042 REAL*8 RHO(0:PP,0:QQ)
1043 REAL*8 RX( 0:PP,0:QQ) , RY(0:PP,0:QQ)
1044 REAL*8 VX( 0:PP,0:QQ) , VY(0:PP,0:QQ)
1045 INTEGER PX , PY , PXY
1046 C -----
1047 INTEGER PPXY
1048 PARAMETER( PPXY=150000 , NNTBL2=2200 , NNTBL3=4400 , NNTBL4=4400 )
1049 C
1050 INTEGER COLOR(PPXY)
1051 C -----
1052 REAL*8 VX0, VY0, RH00
1053 INTEGER ITH, ICLR
1054 C
1055 DO 50 J=0, PY
1056   VX( 0, J) = UVELX
1057   VY( 0, J) = UVELY
1058   RHO( 0, J) = DNS0
1059 50 CONTINUE
1060 C
1061 DO 100 I=1, PX
1062 DO 90 J=0, PY
1063   ITH = ( PX+1 )*J + ( I+1 )
1064   ICLR = COLOR(ITH)
1065   IF( (ICLR .EQ. 6) .OR. (ICLR .EQ. 7) ) GOTO 90
1066 C
1067   VX0 = F(I,J,1) - F(I,J,2) + F(I,J,5) - F(I,J,6)
1068   &           + F(I,J,7) - F(I,J,8)
1069   &           VY0 = F(I,J,3) - F(I,J,4) + F(I,J,5) - F(I,J,6)
1070   &           + F(I,J,8) - F(I,J,7)
1071   &           RH00 = F(I,J,0) + F(I,J,1) + F(I,J,2) + F(I,J,3) + F(I,J,4)
1072   &           + F(I,J,5) + F(I,J,6) + F(I,J,7) + F(I,J,8)
1073   VX( I,J) = VX0 /RH00
1074   VY( I,J) = VY0 /RH00
1075   RHO(I,J) = RH00
1076   IF( (ICLR.EQ.1) .OR. (ICLR.EQ.2) .OR. (ICLR.EQ.3) .OR.
1077   &           (ICLR.EQ.4) ) THEN
1078     IF( RHO(I,J) .LT. DNS0 ) RHO(I,J) = DNS0
1079   END IF
1080 90 CONTINUE
1081 100 CONTINUE
1082 C
1083 IF( (ITREESID.EQ.3).OR.(ITREESID.EQ.4).OR.(ITREESID.EQ.5) ) THEN
1084 DO 120 I=1, PX-1
1085   IF( ITREESID.EQ.3 ) THEN
1086     VX( I,PY) = UVELX
1087     VY( I,PY) = UVELY
1088     RHO(I,PY) = DNS0
1089     VX( I, 0) = UVELX
1090     VY( I, 0) = UVELY
1091     RHO(I, 0) = DNS0
1092   ELSE IF( ITREESID.EQ.4 ) THEN
1093     VX( I,PY) = VX( I,PY-1)
1094     VY( I,PY) = VY( I,PY-1)
1095     RHO(I,PY) = RHO(I,PY-1)
1096     IF( RHO(I,PY) .LT. DNS0 ) RHO(I,PY) = DNS0
1097     VX( I, 0) = VX( I,1)
1098     VY( I, 0) = VY( I,1)
1099     RHO(I, 0) = RHO(I,1)
1100   IF( RHO(I, 0) .LT. DNS0 ) RHO(I, 0) = DNS0
1101   ELSE IF( ITREESID.EQ.5 ) THEN
1102     VX( I,PY) = 2.D0*VX( I,PY-1) - VX( I,PY-2)
1103     VY( I,PY) = 2.D0*VY( I,PY-1) - VY( I,PY-2)
1104     RHO(I,PY) = 2.D0*RHO(I,PY-1) - RHO(I,PY-2)
1105     IF( RHO(I,PY) .LT. DNS0 ) RHO(I,PY) = DNS0
1106     VX( I, 0) = 2.D0*VX( I,1) - VX( I,2)
1107     VY( I, 0) = 2.D0*VY( I,1) - VY( I,2)
1108     RHO(I, 0) = 2.D0*RHO(I,1) - RHO(I,2)
1109     IF( RHO(I, 0) .LT. DNS0 ) RHO(I, 0) = DNS0
1110   END IF
1111 120 CONTINUE
1112 END IF
1113 C
1114 IF( (ITREEDWN.EQ.3).OR.(ITREEDWN.EQ.4).OR.(ITREEDWN.EQ.5) ) THEN

```

• A uniform flow is set at the upstream boundary surface.

--- Bupstream ---

• The local velocities and densities are calculated inside the cylinder from Eq. (7.20).

--- INSIDE AREA ---

• The densities are assumed to be not smaller than the given density at the outer boundary surfaces.

• The treatment at the side boundary surfaces.

• (1) The equilibrium distribution.

• (2) The zero-gradient condition (Eq. (7.8)).

• (3) The extrapolation condition (Eq. (7.7)).

• The treatment at the downstream boundary surface.

--- Bdownstream ---

```

1115      DO 140 J=1, PY-1
1116      IF( ITREEDWN.EQ.3 ) THEN
1117          VX( PX,J ) = UVELX
1118          VY( PX,J ) = UVELY
1119          RHO(PX,J) = DNS0
1120      ELSE IF( ITREEDWN.EQ.4 ) THEN
1121          VX( PX,J ) = VX( PX-1,J )
1122          VY( PX,J ) = VY( PX-1,J )
1123          RHO(PX,J) = RHO(PX-1,J )
1124          IF( RHO(PX,J) .LT. DNS0 ) RHO(PX,J) = DNS0
1125      ELSE IF( ITREEDWN.EQ.5 ) THEN
1126          VX( PX,J ) = 2.D0*VX( PX-1,J ) - VX( PX-2,J )
1127          VY( PX,J ) = 2.D0*VY( PX-1,J ) - VY( PX-2,J )
1128          RHO(PX,J) = 2.D0*RHO(PX-1,J ) - RHO(PX-2,J )
1129          IF( RHO(PX,J) .LT. DNS0 ) RHO(PX,J) = DNS0
1130      END IF
1131 140    CONTINUE
1132 C
1133      IF( ITREEDWN.EQ.3 ) THEN
1134          VX( PX,PY ) = UVELX
1135          VY( PX,PY ) = UVELY
1136          RHO(PX,PY) = DNS0
1137          VX( PX, 0 ) = UVELX
1138          VY( PX, 0 ) = UVELY
1139          RHO(PX, 0 ) = DNS0
1140      ELSE IF( ITREEDWN.EQ.4 ) THEN
1141          VX( PX,PY ) = VX( PX-1,PY-1 )
1142          VY( PX,PY ) = VY( PX-1,PY-1 )
1143          RHO(PX,PY) = RHO(PX-1,PY-1 )
1144          IF( RHO(PX,PY) .LT. DNS0 ) RHO(PX,PY) = DNS0
1145          VX( PX, 0 ) = VX( PX-1,1 )
1146          VY( PX, 0 ) = VY( PX-1,1 )
1147          RHO(PX, 0 ) = RHO(PX-1,1 )
1148          IF( RHO(PX, 0 ) .LT. DNS0 ) RHO(PX, 0 ) = DNS0
1149      ELSE IF( ITREEDWN.EQ.5 ) THEN
1150          VX( PX,PY ) = 2.D0*VX( PX-1,PY-1 ) - VX( PX-2,PY-2 )
1151          VY( PX,PY ) = 2.D0*VY( PX-1,PY-1 ) - VY( PX-2,PY-2 )
1152          RHO(PX,PY) = 2.D0*RHO(PX-1,PY-1 ) - RHO(PX-2,PY-2 )
1153          IF( RHO(PX,PY) .LT. DNS0 ) RHO(PX,PY) = DNS0
1154          VX( PX, 0 ) = 2.D0*VX( PX-1,1 ) - VX( PX-2,2 )
1155          VY( PX, 0 ) = 2.D0*VY( PX-1,1 ) - VY( PX-2,2 )
1156          RHO(PX, 0 ) = 2.D0*RHO(PX-1,1 ) - RHO(PX-2,2 )
1157          IF( RHO(PX, 0 ) .LT. DNS0 ) RHO(PX, 0 ) = DNS0
1158      END IF
1159  END IF
1160
1161
1162 **** SUB COLLPROC *****
1163      SUBROUTINE COLLPROC( COLOR , ALPHAMX )
1164 C
1165      IMPLICIT REAL*8 ( A-H,O-Z ), INTEGER ( I-N )
1166      COMMON /BLOCK1/ F   , FTILD
1167      COMMON /BLOCK3/ RHO  , RX  , RY  , VX  , VY
1168      COMMON /BLOCK4/ DNS0 , TAU , DX  , DT  , CLAT
1169      COMMON /BLOCK5/ XL   , YL   , XL1 , YL1 , XL2 , YL2 , PX  , PY  , PXY
1170
1171 C
1172 C
1173      INTEGER     PP , QQ , KK
1174      PARAMETER( PP=300 , QQ=400 , KK=8 , PI=3.141592653589793D0 )
1175 C
1176      REAL*8     F(0:PP,0:QQ,0:KK), FTILD(0:PP,0:QQ,0:KK)
1177      REAL*8     RHO(0:PP,0:QQ)
1178      REAL*8     RX( 0:PP,0:QQ)   , RY(0:PP,0:QQ)
1179      REAL*8     VX( 0:PP,0:QQ)   , VY(0:PP,0:QQ)
1180      INTEGER     ALPHAMX , PX , PY , PXY
1181 C
1182      INTEGER     PPXY
1183      PARAMETER( PPXY=150000 , NNTBL=2200 , NNTBL2=4400 , NNTBL3=4400 )
1184 C
1185      INTEGER     COLOR(PPXY)
1186 C
1187      REAL*8     FEQ, CDNS0, UVELX0, UVELY0
1188      INTEGER     ITH, ICLR
1189 C
1190 CCC      CDNS0 = DNS0
1191 C
1192      DO 210 I=0, PX
1193      DO 200 J=0, PY

```

• (1) The equilibrium distribution.

• (2) The zero-gradient condition (Eq. (7.8)).

• (3) The extrapolation condition (Eq. (7.7)).

++ Corners ++

• (1) The equilibrium distribution.

• (2) The zero-gradient condition (Eq. (7.8)).

• (3) The extrapolation condition (Eq. (7.7)).

• A subroutine for treating the collision at each site.

• The treatment for the sites at the downstream boundary surface and inside the simulation region, and also for the sites interacting with the cylinder according to Eq. (7.17).

```

1195      ITH = (PX+1)*J + (I+1)
1196      ICLR = COLOR(ITH)
1197      IF( (ICLR.EQ.6) .OR. (ICLR.EQ.7) ) GOTO 200
1198 C          --- FOR Busual,Bdownstream,Bcyl_surface ---
1199      IF( (ICLR.EQ.0) .OR. (ICLR.EQ.2) .OR. (ICLR.EQ.5) ) THEN
1200          UVELX0 = VX( I,J )
1201          UVELY0 = VY( I,J )
1202          CDNS0 = RHO(I,J)
1203          DO 100 K=0, ALPHAMX
1204              FTILD(I,J,K) = F(I,J,K) * (TAU-1.D0)/TAU
1205          &             + FEQ( UVELX0, UVELY0, K, CDNS0 ) / TAU
1206          100    CONTINUE
1207 C          --- FOR Bupstream ---
1208      ELSE IF( ICLR.EQ.1 ) THEN
1209          UVELX0 = VX( 0,J )
1210          UVELY0 = VY( 0,J )
1211          CDNS0 = RHO(0,J)
1212          DO 120 K=0, ALPHAMX
1213              FTILD(0,J,K) = FEQ( UVELX0, UVELY0, K, CDNS0 )
1214          120    CONTINUE
1215 C          --- FOR Bupper_side ---
1216      ELSE IF( ICLR.EQ.3 ) THEN
1217          UVELX0 = VX( I,PY )
1218          UVELY0 = VY( I,PY )
1219          CDNS0 = RHO(I,PY)
1220          DO 140 K=0, ALPHAMX
1221              FTILD(I,PY,K) = F(I,PY,K) * (TAU-1.D0)/TAU
1222          &             + FEQ( UVELX0, UVELY0, K, CDNS0 ) / TAU
1223          140    CONTINUE
1224 C          --- FOR Blower_side ---
1225      ELSE IF( ICLR.EQ.4 ) THEN
1226          UVELX0 = VX( I,0 )
1227          UVELY0 = VY( I,0 )
1228          CDNS0 = RHO(I,0)
1229          DO 160 K=0, ALPHAMX
1230              FTILD(I,0,K) = F(I,0,K) * (TAU-1.D0)/TAU
1231          &             + FEQ( UVELX0, UVELY0, K, CDNS0 ) / TAU
1232          160    CONTINUE
1233      END IF
1234 C
1235      200 CONTINUE
1236      210 CONTINUE
1237
1238      RETURN
1239 C**** SUB MOVEPROC *****
1240      SUBROUTINE MOVEPROC( PX , PY , ANTIALPH , RHO , DNS0 , ITREECYL )
1241 C          ----- MOVEMENT PROCEDURE -----
1242      IMPLICIT REAL*8 (A-H,O-Z), INTEGER (I-N)
1243 C
1244      COMMON /BLOCK1/ F , FTILD
1245 C          ----- *
1246      COMMON /BLOCK14/ RXCYL , RYCYL , ICYL , JCYL , DCYL
1247      COMMON /BLOCK15/ COLOR , POSINTBL
1248      COMMON /BLOCK16/ TBLNAM , TBLNUM , TBLPOS , NTBL
1249      COMMON /BLOCK17/ TBLDW , TBLAL , NTBLDW
1250 C
1251      COMMON /BLOCK21/ CD , CDFORCE0 , CDFORCE , RE , NSMPLCD
1252 C
1253 C          ----- *
1254      INTEGER PP , QQ , KK
1255      PARAMETER( PP=300 , QQ=400 , KK=8 , PI=3.141592653589793D0 )
1256 C
1257      REAL*8 F(0:PP,0:QQ,0:KK) , FTILD(0:PP,0:QQ,0:KK)
1258      REAL*8 RHO(0:PP,0:QQ)
1259      INTEGER PX , PY , ANTIALPH(0:KK)
1260 C          ----- *
1261      INTEGER PPXY
1262      PARAMETER( PPXY=150000 , NNTBL=2200 , NNTBL2=4400 , NNTBL3=4400 )
1263 C
1264      REAL*8 TBLDW(NNTBL2)
1265      INTEGER COLOR(PPXY) , POSINTBL(PPXY)
1266      INTEGER TBLNAM(NNTBL) , TBLNUM(NNTBL) , TBLPOS(NNTBL) , NTBL
1267      INTEGER TBLAL(NNTBL2) , NTBLDW
1268 C
1269      INTEGER NNCD
1270      PARAMETER( NNCD=1000000 )
1271 C
1272      REAL*8 CDFORCE(NNCD)
1273 C
1274      INTEGER ITH , ICLR , ITBL , INUM , IPOS , IALPHA , K , KANTI
1275      INTEGER I1 , I2 , ID , J1 , J2 , JD , IOO , JOO

```

• The treatment for the sites at the upstream boundary surface. The equilibrium distribution is used.

• The treatment for the sites at the upper side boundary surface. Eq. (7.17) is treated.

• A subroutine for the transfer process of the particle distribution function.

```

1276      INTEGER   I11, J11, I21, I22, J21, J22
1277      REAL*8    FWALL, CDW , C1   , C2
1278      REAL*8    CA11 , CA12 , CA21 , CA22 , CA23
1279      REAL*8    CB11 , CB12 , CB21 , CB22 , CB23
1280      REAL*8    CD11 , CD12 , CD21 , CD22 , CD23
1281 C      -----
1282 C      ----- 0-DIRECTION ---
1283 DO 3 I=0, PX
1284 DO 1 J=0, PY
1285     F(I,J,0)=FTILD(I,J,0)
1286 1 CONTINUE
1287 3 CONTINUE
1288 C      -----
1289 C      ----- 1,2,3,4,5,6,7,8-DIRECTION ---
1290 C
1291 DO 100 K=1,8
1292 C
1293 IF( K.EQ.1 ) THEN
1294     I1 = PX-1
1295     I2 = 1
1296     ID = -1
1297     J1 = PY-1
1298     J2 = 1
1299     JD = -1
1300 ELSE IF( K.EQ.2 ) THEN
1301     I1 = 1
1302     I2 = PX-1
1303     ID = 1
1304     J1 = PY-1
1305     J2 = 1
1306     JD = -1
1307 ELSE IF( K.EQ.3 ) THEN
1308     I1 = 1
1309     I2 = PX-1
1310     ID = 1
1311     J1 = PY-1
1312     J2 = 1
1313     JD = -1
1314 ELSE IF( K.EQ.4 ) THEN
1315     I1 = 1
1316     I2 = PX-1
1317     ID = 1
1318     J1 = 1
1319     J2 = PY-1
1320     JD = 1
1321 ELSE IF( K.EQ.5 ) THEN
1322     I1 = PX-1
1323     I2 = 1
1324     ID = -1
1325     J1 = PY-1
1326     J2 = 1
1327     JD = -1
1328 ELSE IF( K.EQ.6 ) THEN
1329     I1 = 1
1330     I2 = PX-1
1331     ID = 1
1332     J1 = 1
1333     J2 = PY-1
1334     JD = 1
1335 ELSE IF( K.EQ.7 ) THEN
1336     I1 = PX-1
1337     I2 = 1
1338     ID = -1
1339     J1 = 1
1340     J2 = PY-1
1341     JD = 1
1342 ELSE IF( K.EQ.8 ) THEN
1343     I1 = 1
1344     I2 = PX-1
1345     ID = 1
1346     J1 = PY-1
1347     J2 = 1
1348     JD = -1
1349 END IF
1350 C
1351 C      DO 40 I= I1, I2, ID
1352      DO 20 J= J1, J2, JD
1353
1354      ITH = (PX+1)*J + (I+1)
1355      ICLR = COLOR(ITH)

```

• K means the  $\alpha$ -direction.

• The sites to be treated begin from I1 to I2 at interval ID for the x-direction.

• The sites to be treated begin from J1 to J2 at interval JD for the y-direction.

• The ITH-th site is treated in the following.

```

1357      IF( (ICLR.EQ.6) .OR. (ICLR.EQ.7) ) GOTO 20
1358 C
1359      IF( K.EQ.1 ) THEN
1360          I00 = I-1
1361          J00 = J
1362      ELSE IF( K.EQ.2 ) THEN
1363          I00 = I+1
1364          J00 = J
1365      ELSE IF( K.EQ.3 ) THEN
1366          I00 = I
1367          J00 = J-1
1368      ELSE IF( K.EQ.4 ) THEN
1369          I00 = I
1370          J00 = J+1
1371      ELSE IF( K.EQ.5 ) THEN
1372          I00 = I-1
1373          J00 = J-1
1374      ELSE IF( K.EQ.6 ) THEN
1375          I00 = I+1
1376          J00 = J+1
1377      ELSE IF( K.EQ.7 ) THEN
1378          I00 = I-1
1379          J00 = J+1
1380      ELSE IF( K.EQ.8 ) THEN
1381          I00 = I+1
1382          J00 = J-1
1383  END IF
1384 C
1385 IF( ICLR .EQ. 5 ) THEN
1386 C
1387     ITBL = POSINTBL(ITH)
1388     INUM = TBLNUM(ITBL)
1389     IPOS = TBLPOS(ITBL)
1390 C
1391 DO 10 JJ=0,INUM-1
1392 C
1393     IALPHA = TBLAL( IPOS+JJ )
1394     KANTI = ANTIALPH(K)
1395 C
1396     IF( IALPHA .EQ. KANTI ) THEN
1397
1398     IF( (K.EQ.1) .OR. (K.EQ.5) .OR. (K.EQ.7) ) THEN
1399         CDFFORCE(NSMPLCD)=CDFFORCE(NSMPLCD) - FTILD(I,J,KANTI)
1400     END IF
1401 C
1402     IF( K.EQ.1 ) THEN
1403         I11 = I+1
1404         J11 = J
1405         I21 = I+1
1406         I22 = I+2
1407         J21 = J
1408         J22 = J
1409     ELSE IF( K.EQ.2 ) THEN
1410         I11 = I-1
1411         J11 = J
1412         I21 = I-1
1413         I22 = I-2
1414         J21 = J
1415         J22 = J
1416     ELSE IF( K.EQ.3 ) THEN
1417         I11 = I
1418         J11 = J+1
1419         I21 = I
1420         I22 = I
1421         J21 = J+1
1422         J22 = J+2
1423     ELSE IF( K.EQ.4 ) THEN
1424         I11 = I
1425         J11 = J-1
1426         I21 = I
1427         I22 = I
1428         J21 = J-1
1429         J22 = J-2
1430     ELSE IF( K.EQ.5 ) THEN
1431         I11 = I+1
1432         J11 = J+1
1433         I21 = I+1
1434         I22 = I+2
1435         J21 = J+1
1436         J22 = J+2

```

- The position (name) of the site in the opposite direction to the  $\alpha$ -direction (K) is described as (I00,J00). For example, if  $\alpha=2$  ( $K=2$ ), such a site is I00=I+1 and J00=J, where (I,J) is the position (name) of the site of interest.

- The treatment of the site interacting with the cylinder.

- The order of the ITH-site, in which its information is saved in TBLNUM and TBLPOS, is extracted from POSINTBL. The result is saved in ITBL.

----- FOR CYL\_surface -----

- INUM is the number of the interacting sites inside the cylinder. IPOS is the first position of such sites appearing in the corresponding variables.

- (I) For IALPHA=KANTI.

- IALPHA is the direction of the ITH-th site toward the neighboring site inside the cylinder, and the opposite direction to K is KANTI.

- The variables (I11,J11) are used in the linear interpolation procedure of the BFL and YMLS methods.
- The variables (I21,J21) and (I22,J22) are used in the quadratic interpolation procedure for the BFL and YMLS methods.

```

1437          ELSE IF( K.EQ.6 ) THEN
1438             I11 = I-1
1439             J11 = J-1
1440             I21 = I-1
1441             I22 = I-2
1442             J21 = J-1
1443             J22 = J-2
1444          ELSE IF( K.EQ.7 ) THEN
1445             I11 = I+1
1446             J11 = J-1
1447             I21 = I+1
1448             I22 = I+2
1449             J21 = J-1
1450             J22 = J-2
1451          ELSE IF( K.EQ.8 ) THEN
1452             I11 = I-1
1453             J11 = J+1
1454             I21 = I-1
1455             I22 = I-2
1456             J21 = J+1
1457             J22 = J+2
1458        END IF
1459 C
1460 C
1461 IF( (ITREECYL.EQ.2) .OR. (ITREECYL.EQ.3) ) THEN
1462   CDW = TBLDW(IPOS+JJ)
1463   FWALL = (1.D0-CDW) * FTILD(I11,J11,KANTI)
1464   &           + CDW * FTILD(I11,J21,KANTI)
1465 C
1466   C1      = 1.D0+CDW
1467   C2      = 2.D0+CDW
1468   CA11    = CDW/C1
1469   CA12    = 1.D0/C1
1470   CA21    = 2.D0*CA12/C2
1471   CA22    = 2.D0*CA12*CDW
1472   CA23    = -CDW/C2
1473 END IF
1474 C
1475 IF( (ITREECYL.EQ.4) .OR. (ITREECYL.EQ.5) ) THEN
1476   CDW = TBLDW(IPOS+JJ)
1477   C1  = 1.D0+2.D0*CDW
1478   C2  = 1.D0-2.D0*CDW
1479   CB11 = C2
1480   CB12 = 2.D0*CDW
1481   CB21 = CDW*C1
1482   CB22 = C1*C2
1483   CB23 = -CDW*C2
1484   CD11 = (-C2)/(2.D0*CDW)
1485   CD12 = 1.D0/(2.D0*CDW)
1486   CD21 = 1.D0/CDW
1487   CD22 = (-C2)/CDW
1488   CD23 = C2/C1
1489 END IF
1490 C
1491 C
1492 IF( ITREECYL .EQ. 1 ) THEN
1493   &+++ (1) BOUNCE-BACK ++++++
1494   F(I,J,K) = FTILD(I,J,KANTI)
1495 C
1496 ELSE IF( ITREECYL .EQ. 2 ) THEN
1497   &+++ (2A) YMLS METHOD (Quadratic) +++
1498   F(I,J,K) = CA21*FWALL + CA22*F(I21,J21,K)
1499   &           + CA23*F(I22,J22,K)
1500 C
1501 ELSE IF( ITREECYL .EQ. 3 ) THEN
1502   &+++ (2B) YMLS METHOD (Liner) ++++++
1503   F(I,J,K) = CA11*F(I11,J11,K) + CA12*FWALL
1504 C
1505 ELSE IF( ITREECYL .EQ. 4 ) THEN
1506   &+++ (3A) BFL METHOD (Quadratic) +++
1507   IF( CDW .LE. 0.5D0 ) THEN
1508     F(I,J,K) = CB21*FTILD(I,J,KANTI)
1509     &           + CB22*FTILD(I21,J21,KANTI)
1510     &           + CB23*FTILD(I22,J22,KANTI)
1511   ELSE
1512

```

• CA11 and CA12 are used in the linear interpolation procedure of YMLS expressed in Eq. (7.5), and CA21, CA22, and CA23 are used in the quadratic interpolation procedure of YMLS in Eq. (8.121); in advance, the coefficients are calculated and saved in these variables for the successive procedures.

• CB11 and CB12 are used in the linear interpolation procedure of BFL in Eq. (8.117), and CB21, CB22, and CB23 are used in the quadratic interpolation procedure of BFL in Eq. (8.112); in advance, the coefficients are calculated and saved in these variables for the successive procedures. Similarly, CD11, CD12, ..., CD23 are used in calculating Eqs. (8.118) and (8.116) for  $\Delta_w > 1/2$ .

• The bounce-back rule.

• The quadratic YMLS method.

• The linear YMLS method.

• The quadratic BFL method.

• Eq. (8.112) is evaluated.

• Eq. (8.116) is evaluated.

```

1513 C
1514      F(I,J,K) = CD21*FTILD(I,J,KANTI)
1515      &          + CD22*FTILD(I,J,K)
1516      &          + CD23*FTILD(I21,J21,K)
1517      END IF
1518 C
1519      ELSE IF( ITREECYL .EQ. 5 ) THEN
1520 C          +++ (3B) BFL METHOD (Linear) ++++++
1521      IF( CDW .LE. 0.5D0 ) THEN
1522 C              F(I,J,K) = CB11*FTILD(I11,J11,KANTI)
1523          &          + CB12*FTILD(I,J,KANTI)
1524      ELSE
1525          F(I,J,K) = CD11*FTILD(I,J,K)
1526          &          + CD12*FTILD(I,J,KANTI)
1527      END IF
1528 C
1529      END IF
1530 C
1531      IF( (K.EQ.1) .OR. (K.EQ.5) .OR. (K.EQ.7) ) THEN
1532          CDFORCE(NSMPLCD) = CDFORCE(NSMPLCD) - F(I,J,K)
1533      ELSE IF( (K.EQ.2) .OR. (K.EQ.6) .OR. (K.EQ.8) ) THEN
1534          CDFORCE(NSMPLCD) = CDFORCE(NSMPLCD) + F(I,J,K)
1535      END IF
1536      GOTO 20
1537 C
1538      ELSE IF( IALPHA .EQ. K ) THEN
1539          IF( (K.EQ.1) .OR. (K.EQ.5) .OR. (K.EQ.7) ) THEN
1540              CDFORCE(NSMPLCD) = CDFORCE(NSMPLCD) + FTILD(I,J,K)
1541          END IF
1542          GOTO 20
1543 C
1544      ELSE IF( (K.EQ.1) .OR. (K.EQ.5) .OR. (K.EQ.7) ) THEN
1545          CDFORCE(NSMPLCD) = CDFORCE(NSMPLCD) + FTILD(I,J,K)
1546      END IF
1547 C
1548      F(I,J,K) = FTILD(I00, J00, K)
1549      GOTO 20
1550 C
1551      END IF
1552 C
1553      10    CONTINUE
1554      END IF
1555 C
1556      F(I,J,K) = FTILD(I00, J00, K)
1557 C
1558      20    CONTINUE
1559      40    CONTINUE
1560 C
1561      100   CONTINUE
1562
1563
1564 C**** SUB BCPROC *****
1565      SUBROUTINE BCPROC( PX , PY , DNS0 , ALPHAMX , ITREESID ,
1566      &                      ITREEDWN )
1567 C
1568      IMPLICIT REAL*8 ( A-H,O-Z ), INTEGER ( I-N )
1569 C
1570      COMMON /BLOCK1/ F      , FTILD
1571      COMMON /BLOCK3/ RHO   , RX   , RY   , VX   , VY
1572      COMMON /BLOCK6/ UVELX , UVELY
1573 C
1574      INTEGER     PP , QQ , KK
1575      PARAMETER( PP=300 , QQ=400 , KK=8 , PI=3.141592653589793D0 )
1576 C
1577      REAL*8     F(0:PP,0:QQ,0:KK) , FTILD(0:PP,0:QQ,0:KK)
1578      REAL*8     RHO(0:PP,0:QQ)
1579      REAL*8     RX( 0:PP,0:QQ)   , RY(0:PP,0:QQ)
1580      REAL*8     VX( 0:PP,0:QQ)   , VY(0:PP,0:QQ)
1581      INTEGER     PX , PY , ALPHAMX
1582 C
1583      REAL*8     FEQ , CDNS0 , UVELX0 , UVELY0
1584 C
1585      CDNS0 = DNS0
1586 C
1587 C
1588      DO 100 J=0, PY
1589      DO 80 K=0, ALPHAMX
1590 C
1591      F(0,J,K) = FEQ( UVELX , UVELY , K , CDNS0 )
1592 C

```

• The linear BFL method.

• Eq. (8.117) is evaluated.

• Eq. (8.118) is evaluated.

• (II) For IALPHA=K.

----- FOR USUAL -----

RETURN  
END

• A subroutine for treating the boundary surfaces.

----- BC for Upstream ---

• I. The treatment at the upstream boundary surface.

+++ UNIFORM FLOW +++

• An equilibrium distribution is assigned.

```

1593     80 CONTINUE
1594    100 CONTINUE
1595 C
1596 C ----- BC for Bupper_side & Blower_side ---
1597 DO 300 I=1, PX-1
1598 DO 280 K=0, ALPHAMX
1599 IF( ITREESID .EQ. 1 ) THEN
1600 C
1601      F(I,PY,K) = 2.D0*F(I,PY-1,K) - F(I,PY-2,K)
1602      F(I, 0,K) = 2.D0*F(I,1,K) - F(I,2,K)
1603 C
1604 ELSE IF( ITREESID .EQ. 2 ) THEN
1605 C
1606      F(I,PY,K) = F(I,PY-1,K)
1607      F(I, 0,K) = F(I,1,K)
1608 C
1609 ELSE IF( ITREESID .EQ. 3 ) .OR. (ITREEDWN.EQ.1) .OR.
1610      (ITREEDWN.EQ.5) ) THEN
1611 C
1612      UVELX0 = VX( I,PY)
1613      UVELY0 = VY( I,PY)
1614      CDNS0 = RHO(I,PY)
1615      F(I,PY,K) = FEQ( UVELX0, UVELY0, K, CDNS0 )
1616 C
1617      UVELX0 = VX( I,0)
1618      UVELY0 = VY( I,0)
1619      CDNS0 = RHO(I,0)
1620      F(I, 0,K) = FEQ( UVELX0, UVELY0, K, CDNS0 )
1621 C
1622 END IF
1623 C
1624 280 CONTINUE
1625 300 CONTINUE
1626 C
1627 C ----- BC for Bdownstream ---
1628 DO 500 J=0, PY
1629 DO 480 K=0, ALPHAMX
1630 IF( ITREEDWN .EQ. 1 ) THEN
1631 C
1632      F(PX,J,K) = 2.D0*F(PX-1,J,K) - F(PX-2,J,K)
1633 C
1634 ELSE IF( ITREEDWN .EQ. 2 ) THEN
1635 C
1636      F(PX,J,K) = F(PX-1,J,K)
1637 C
1638 ELSE IF( ITREEDWN .EQ. 3 ) .OR.
1639      (ITREEDWN.EQ.4) .OR.
1640      (ITREEDWN.EQ.5) ) THEN
1641 C
1642      UVELX0 = VX( PX,J)
1643      UVELY0 = VY( PX,J)
1644      CDNS0 = RHO(PX,J)
1645      F(PX,J,K) = FEQ( UVELX0, UVELY0, K, CDNS0 )
1646 C
1647 END IF
1648 480 CONTINUE
1649 C
1650 C ----- TWO Corners for Bdownstream ---
1651 DO 530 K=0, ALPHAMX
1652 IF( ITREEDWN .EQ. 1 ) THEN
1653      F(PX,PY,K) = 2.D0*F(PX-1,PY-1,K) - F(PX-2,PY-2,K)
1654      F(PX, 0,K) = 2.D0*F(PX-1, 1,K) - F(PX-2, 2,K)
1655 ELSE IF( ITREEDWN .EQ. 2 ) THEN
1656      F(PX,PY,K) = F(PX-1,PY-1,K)
1657      F(PX, 0,K) = F(PX-1, 1,K)
1658 END IF
1659 530 CONTINUE
1660
1661
1662 C**** SUB GRAPHVEL *****
1663 SUBROUTINE GRAPHVEL( NANMCTR )
1664 C
1665 CCC IMPLICIT REAL*8 (A-H,O-Z), INTEGER (I-N)
1666 IMPLICIT REAL (A-H,O-Z), INTEGER (I-N)
1667 C
1668 COMMON /BLOCK3/ RHO , RX , RY , VX , VY
1669 COMMON /BLOCK5/ XL , YL , XL1 , YL1 , XL2 , YL2 , PX , PY , PXY
1670 COMMON /BLOCK6/ UVELX , UVELY
1671 COMMON /BLOCK14/ RXCYL , RYCYL , ICYL , JCYL , DCYL
1672 C

```

• II. The treatment at the side boundary surfaces.

• The extrapolation condition in Eq. (7.7) is applied.

• The zero-gradient condition in Eq. (7.8) is applied.

• An equilibrium distribution with each local velocity is assigned.

• III. The treatment at the downstream surface.

• The extrapolation condition in Eq. (7.7) is applied.

• The zero-gradient condition in Eq. (7.8) is applied.

• An equilibrium dist. with each local velocity is assigned.

• IV. The treatment at both corner sites of the downstream surface.

• The extrapolation condition in Eq. (7.7) is applied.

• The zero-gradient condition in Eq. (7.8) is applied.

RETURN  
END

• A subroutine for writing out the data used for making an animation based on the commercial software MicroAVS.

```

1673      INTEGER     PP , QQ , KK
1674      REAL*8     PI
1675      PARAMETER( PP=300 , QQ=400 , KK=8 , PI=3.141592653589793D0 )
1676 C
1677 C-----+
1678      REAL*8     RHO( 0:PP,0:QQ)
1679      REAL*8     RX( 0:PP,0:QQ) , RY( 0:PP,0:QQ)
1680      REAL*8     VX( 0:PP,0:QQ) , VY( 0:PP,0:QQ)
1681      INTEGER    PX , PY , PXY
1682 C-----+
1683      REAL*8     XL , YL , XL1 , YL1 , XL2 , YL2 , UVELX , UVELY
1684      REAL*8     RXCYL , RYCYL , DCYL
1685 C-----+
1686      INTEGER    QQSQ , NNDUM
1687      PARAMETER( QQSQ=150000 , NNDUM=150000 )
1688 C
1689      REAL      DUMRX(NNDUM) , DUMRY(NNDUM) , DUMVX(NNDUM) , DUMVY(NNDUM)
1690      REAL      VEL
1691      INTEGER    NNDUM, ISKIP
1692 C
1693 C-----+ DATA OUTPUT FOR VEL-FIELD MicroAVS ---
1694 C
1695      VEL = REAL( DSQRT( UVELX**2 + UVELY**2 ) )
1696 C
1697      WRITE(42,83) NANMCTR
1698 C
1699      II = 0
1700      DO 100 J=0, PY, 1
1701      DO 90 I=0, PX, 1
1702      II = II + 1
1703      DUMRX(II) = REAL( RX(I,J) )
1704      DUMRY(II) = REAL( RY(I,J) )
1705      DUMVX(II) = REAL( VX(I,J) ) / VEL
1706      DUMVY(II) = REAL( VY(I,J) ) / VEL
1707      WRITE(42,85) DUMRX(II), DUMRY(II), DUMVX(II), DUMVY(II)
1708      90 CONTINUE
1709      100 CONTINUE
1710 C
1711      NNDUM = II
1712 C
1713      IF( NANMCTR .EQ. 1 ) THEN
1714      WRITE(41,181)
1715      WRITE(41,183)
1716      WRITE(41,185) (PX+1), (PY+1)
1717      WRITE(41,187)
1718      END IF
1719 C
1720      ISKIP = (NNDUM+1)*( NANMCTR-1 ) + 1
1721 C
1722      WRITE(41,188) ISKIP-1
1723      WRITE(41,189) ISKIP
1724      WRITE(41,191) ISKIP
1725      WRITE(41,197)
1726 C
1727 C
1728      83 FORMAT( I5 )
1729      85 FORMAT( 4F8.3 )
1730      181 FORMAT('# AVS field file'/'#')
1731      183 FORMAT( 'ndim=2' )
1732      185 FORMAT( 'dim1=',I4,'dim2=',I4)
1733      187 FORMAT( 'nspace= 2'/'veclen= 2'/'data= float'
1734      &   /'fields= uniform'/' )
1735      188 FORMAT(
1736      &   'time file=./avsvell.dat filetype=ascii '
1737      189 FORMAT(
1738      &   'variable 1 file=./avsvell.dat filetype=ascii '
1739      191 FORMAT(
1740      &   'variable 2 file=./avsvell.dat filetype=ascii '
1741      197 FORMAT( 'EOT')

1742
1743      RETURN
END
1744 C#### FUN FEQ ####
1745      DOUBLE PRECISION FUNCTION FEQ( UVELX, UVELY, ALPHA, CDNS0 )
1746 C-----+
1747 C-----+ EQUILIBRIUM DISTRIBUTION FUNCTION F^(eq)
1748 C-----+
1749      IMPLICIT REAL*8 (A-H,O-Z), INTEGER (I-N)
1750 C
1751      COMMON /BLOCK2/ CVEL , W , IINC , ANTIALPH , ALPHAMX
1752 C
1753      INTEGER     PP , QQ , KK

```

• The equilibrium distribution function.

```
1754      PARAMETER( PP=300 , QQ=400 , KK=8 , PI=3.141592653589793D0 )  
1755 C  
1756      REAL*8      CVEL(2,0:KK) , W(0:KK)  
1757      INTEGER     ALPHAMX , IINC(2,0:KK) , ANTIALPH(0:KK)  
1758      INTEGER     ALPHA  
1759 C  
1760      REAL*8      C0, C1, C2, C3  
1761 C  
1762      K      = ALPHA  
1763      C0     = W(K)*CDNS0  
1764      C1     = CVEL(1,K)*UVELX + CVEL(2,K)*UVELY  
1765      C2     = C1*C1  
1766      C3     = UVELX**2 + UVELY**2  
1767      FEQ   = C0*( 1.D0 + 3.D0*C1 + (9.D0/2.D0)*C2 - (3.D0/2.D0)*C3 )  
1768  
1769      RETURN  
      END
```

• An equilibrium distribution is assigned according to Eq. (7.18).

# 8 Theoretical Background of Lattice Boltzmann Method

The lattice Boltzmann method [9–12] is a useful simulation technique for numerically solving flow problems. This method is also feasible as a simulation technique for systems such as a suspension of solid particles or a polymeric liquid. In a multi-component system, the motion of the suspended particles or polymers must be solved together with the flow field of the solvent molecules. In a molecular simulation of a suspension composed of solid particles in a liquid, it is very difficult to treat the multibody hydrodynamic interactions among the suspended particles. Hence, it is usual to model the flow field as a simple shear flow, and under this approach only the motion of the suspended particles will be solved during the simulation. A typical simulation technique employing this concept is the Stokesian dynamics method. On the other hand, the lattice Boltzmann method enables us to solve the motion of suspended particles and the ambient flow field simultaneously, so there is much of interest in this method.

In the present chapter, we turn from the practice of molecular simulations to the theoretical background of the lattice Boltzmann method. The key equations are almost all indicated for the successive derivation procedure such that the reader will be able to derive all the important equations from the key expressions. Understanding the theoretical background is essential if, for example, the reader needs to employ a new boundary condition or develop a new version of the lattice Boltzmann method that can take into account the random motion of the suspended particles. For a clear, logical development, the fundamental equations for the following derivation may be found in Appendix A1. Note that we focus here on the BGK lattice Boltzmann method, which is the simplest and provides a solid foundation for application to various flow problems.

## 8.1 Equilibrium Distribution

The lattice Boltzmann method treats the particle distribution function of virtual fluid particles, which are able to move from site to site on a lattice system. A macroscopic quantity of interest, such as the fluid velocity, can be obtained from the solution of the particle distribution function. In the case of a two-dimensional system, such as the D2Q9 model shown in Figure 8.1, fluid particles at lattice site 0 have a possibility of moving to the neighboring lattice sites 1, . . . , 8. If the quiescent

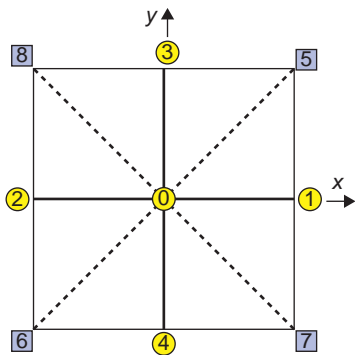


**Figure 8.1** Lattice model for the D2Q9.

state is included, there are nine velocities for the fluid particles moving (or not moving) to a neighboring site; a fluid particle will arrive at its neighboring site with a given microscopic velocity during a given time interval. We use the notation  $\mathbf{c}_\alpha$  for the velocity for the transfer in the  $\alpha$ -direction ( $\alpha = 0, 1, 2, \dots, 8$ ). The particle distribution function  $f_\alpha(\mathbf{r}, t)$  in the  $\alpha$ -direction at the lattice site  $\mathbf{r}$  at time  $t$  can be obtained by treating the collision of the fluid particles at  $\mathbf{r}$  and evaluating the inflow and the outflow of fluid particles from and to the lattice site  $\mathbf{r}$ . In the BGK lattice Boltzmann method, the particle distribution function  $f_\alpha(\mathbf{r} + \mathbf{c}_\alpha \Delta t, t + \Delta t)$  is obtained from the following equation:

$$f_\alpha(\mathbf{r} + \mathbf{c}_\alpha \Delta t, t + \Delta t) = \tilde{f}_\alpha(\mathbf{r}, t) \quad (8.1)$$

$$\tilde{f}_\alpha(\mathbf{r}, t) = f_\alpha(\mathbf{r}, t) + \frac{1}{\tau} \{ f_\alpha^{(0)}(\mathbf{r}, t) - f_\alpha(\mathbf{r}, t) \} \quad (8.2)$$

The  $\tilde{f}_\alpha$  in Eq. (8.2) is the particle distribution function after the collision at the site  $\mathbf{r}$ . Eq. (8.1) implies that this distribution moves to the neighboring site  $(\mathbf{r} + \mathbf{c}_\alpha \Delta t)$  in the  $\alpha$ -direction. The second term on the right-hand side in Eq. (8.2) is the collision term, frequently denoted by the notation  $\Omega_\alpha(\mathbf{r}, t)$ :

$$\Omega_\alpha(\mathbf{r}, t) = \frac{1}{\tau} \{ f_\alpha^{(0)}(\mathbf{r}, t) - f_\alpha(\mathbf{r}, t) \} \quad (8.3)$$

With the above particle distribution, the macroscopic fluid density  $\rho(\mathbf{r}, t)$  and momentum  $\rho(\mathbf{r}, t)\mathbf{u}(\mathbf{r}, t)$  can be evaluated as

$$\rho(\mathbf{r}, t) = \sum_\alpha f_\alpha(\mathbf{r}, t) \quad (8.4)$$

$$\rho(\mathbf{r}, t)\mathbf{u}(\mathbf{r}, t) = \sum_\alpha f_\alpha(\mathbf{r}, t)\mathbf{c}_\alpha \quad (8.5)$$

Additionally, if a system is in thermodynamic equilibrium with constant temperature  $T$ , the following equi-partition law of energies must be satisfied:

$$\frac{D}{2}kT = \sum_\alpha \frac{m}{2}(\mathbf{c}_\alpha - \mathbf{u})^2 \frac{f_\alpha}{\rho} \quad (8.6)$$

in which  $D$  is a constant for describing the dimension with the value 2 or 3 for a two- or three-dimensional space, respectively, and  $m$  is the mass of a fluid particle.

The thermodynamic equilibrium velocity distribution in the lattice Boltzmann method differs from that in the MD method. This is because virtual fluid particles in the lattice Boltzmann method are not allowed to move freely in a simulation region, but are restricted to move only from site to site. The velocity  $\mathbf{c}$  of a molecule (a fluid particle), which moves freely in a three-dimensional space with a uniform flow velocity  $\mathbf{u}$  of the system, is specified by the Maxwellian distribution  $f^{(\text{eq})}(\mathbf{c})$  [25]:

$$f^{(\text{eq})}(\mathbf{c}) = \rho \left( \frac{m}{2\pi kT} \right)^{3/2} \exp \left\{ -\frac{m}{2kT} (\mathbf{c} - \mathbf{u})^2 \right\} \quad (8.7)$$

Note that this definition includes the density  $\rho$ , whereas the usual Maxwellian distribution does not include the density in its expression. The equilibrium distribution in the lattice Boltzmann method  $f_\alpha^{(0)}$  may be expressed by expanding the exponential function in Eq. (8.7) in a Taylor series expansion as

$$f_\alpha^{(0)} = \rho w_\alpha \left\{ 1 + b \frac{\mathbf{c}_\alpha \cdot \mathbf{u}}{c^2} + e \frac{u^2}{c^2} + h \frac{(\mathbf{c}_\alpha \cdot \mathbf{u})^2}{c^4} \right\} \quad (8.8)$$

in which  $w_\alpha$ ,  $b$ ,  $e$ , and  $h$  are unknown constants to be determined later,  $w_\alpha$  is a weighting constant, and  $c$  is the lattice speed for fluid particles moving from site to site, expressed as  $c = \Delta x / \Delta t$ .

In the lattice Boltzmann method, the whole system space is divided into a fine mesh that acts as the lattice system, and the fluid particles are only able to move from lattice site to lattice site. However, any physical phenomenon should not depend on the setting of the lattice system, and Eqs. (8.4)–(8.6) are required to remain valid for an arbitrary rotation of the lattice. This requirement will determine the above-mentioned unknown constants and, because the values of these unknown constants depend on the model used, we discuss the derivation for determining the unknown constants for the D2Q9 and D3Q19 models separately.

### 8.1.1 D2Q9 Model

The  $xy$ -coordinate system and the  $\alpha$ -direction are specified as shown in Figure 8.1. As already pointed out, the equilibrium distribution can be obtained explicitly by determining the unknown constants  $w_\alpha$ ,  $b$ ,  $e$ , and  $h$  such that the terms on the right-hand side in Eqs. (8.4)–(8.6) remain unchanged by a rotation of the whole lattice system by an angle  $\phi$ . Before we start the procedure of determining the unknown constants, we show preliminary expressions that are useful in the following discussion. Note that the relationship of the momentum flux is necessary for determining these constants.

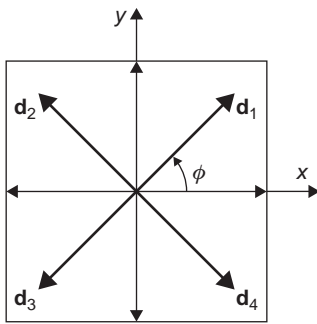


**Figure 8.2** Rotation of the unit vectors.

As shown in Figure 8.2, the four unit vectors, which are along the plus and minus  $x$ - and  $y$ -axes of the orthogonal coordinate system, are rotated about the  $z$ -axis, and the new unit vectors are denoted by  $\mathbf{d}_1$ ,  $\mathbf{d}_2$ ,  $\mathbf{d}_3$ , and  $\mathbf{d}_4$ . These vectors are written in component expressions as

$$\left. \begin{aligned} \mathbf{d}_1 &= (d_{1x}, d_{1y}) = (\cos \phi, \sin \phi) \\ \mathbf{d}_2 &= (d_{2x}, d_{2y}) = \left( \cos \left( \phi + \frac{\pi}{2} \right), \sin \left( \phi + \frac{\pi}{2} \right) \right) \\ \mathbf{d}_3 &= (d_{3x}, d_{3y}) = (\cos(\phi + \pi), \sin(\phi + \pi)) \\ \mathbf{d}_4 &= (d_{4x}, d_{4y}) = \left( \cos \left( \phi + \frac{3\pi}{2} \right), \sin \left( \phi + \frac{3\pi}{2} \right) \right) \end{aligned} \right\} \quad (8.9)$$

Using these expressions, we derive several useful equations for the successive derivation. Although these equations can be derived from a simple transformation, as will be shown in the next subsection for the D3Q19 model, we here show a more sophisticated derivation based on the concept of imaginary numbers.

With the Euler formula  $e^{i\theta} = \cos \theta + i \sin \theta$  for imaginary numbers, the following relationships can be obtained:

$$\sum_{k=1}^4 (d_{kx} + id_{ky})^4 = \sum_{k=0}^3 \left\{ e^{i(k\frac{\pi}{2} + \phi)} \right\}^4 = \sum_{k=0}^3 e^{i(2\pi k + 4\phi)} = e^{i4\phi} \sum_{k=0}^3 e^{i2\pi k} = 4e^{i4\phi} \quad (8.10)$$

Similarly,

$$\left. \begin{aligned} \sum_{k=1}^4 (d_{kx} + id_{ky})^3 (d_{kx} - id_{ky}) &= 0 \\ \sum_{k=1}^4 (d_{kx} + id_{ky})^2 (d_{kx} - id_{ky})^2 &= 4 \end{aligned} \right\} \quad (8.11)$$

The corresponding real and imaginary parts on the left- and right-hand sides in Eq. (8.10) are equal, which leads to the following equation:

$$\left. \begin{aligned} \sum_{k=1}^4 (d_{kx}^4 + d_{ky}^4 - 6d_{kx}^2 d_{ky}^2) &= 4 \cos 4\phi \\ \sum_{k=1}^4 4(d_{kx}^3 d_{ky} - d_{kx} d_{ky}^3) &= 4 \sin 4\phi \end{aligned} \right\} \quad (8.12)$$

These relationships have been derived by expanding the left-hand side in Eq. (8.10). Similarly, from Eq. (8.11),

$$\left. \begin{aligned} \sum_{k=1}^4 (d_{kx}^4 - d_{ky}^4) &= 0 \\ \sum_{k=1}^4 (d_{kx}^3 d_{ky} + d_{kx} d_{ky}^3) &= 0 \\ \sum_{k=1}^4 (d_{kx}^4 + d_{ky}^4 + 2d_{kx}^2 d_{ky}^2) &= 4 \end{aligned} \right\} \quad (8.13)$$

Further preliminary relationships can be derived from Eqs. (8.12) and (8.13). From the first equation in Eq. (8.12) and the third equation in Eq. (8.13),

$$\sum_{k=1}^4 d_{kx}^2 d_{ky}^2 = \frac{1}{2}(1 - \cos 4\phi) \quad (8.14)$$

From the second equation in Eqs. (8.12) and (8.13),

$$\left. \begin{aligned} \sum_{k=1}^4 d_{kx}^3 d_{ky} &= \frac{1}{2} \sin 4\phi \\ \sum_{k=1}^4 d_{kx} d_{ky}^3 &= -\frac{1}{2} \sin 4\phi \end{aligned} \right\} \quad (8.15)$$

From the first and third equations in Eq. (8.13),

$$\sum_{k=1}^4 d_{kx}^4 = \sum_{k=1}^4 d_{ky}^4 = 2 - \sum_{k=1}^4 d_{kx}^2 d_{ky}^2 = \frac{3}{2} + \frac{1}{2} \cos 4\phi \quad (8.16)$$

From a similar derivation procedure, the terms concerning  $d_{kx}$  or  $d_{ky}$  to the first, second, and third powers are obtained as

$$\left. \begin{aligned} \sum_{k=1}^4 d_{kx} &= \sum_{k=1}^4 d_{ky} = 0 \\ \sum_{k=1}^4 d_{kx}^2 &= \sum_{k=1}^4 d_{ky}^2 = 2, \quad \sum_{k=1}^4 d_{kx} d_{ky} = 0 \\ \sum_{k=1}^4 d_{kx}^3 &= \sum_{k=1}^4 d_{ky}^3 = \sum_{k=1}^4 d_{kx}^2 d_{ky} = \sum_{k=1}^4 d_{kx} d_{ky}^2 = 0 \end{aligned} \right\} \quad (8.17)$$

We have now obtained all the preliminary equations and will proceed to the determination procedures for the unknown constants  $w_\alpha$ ,  $b$ ,  $e$ , and  $h$ .

As shown in Figure 8.1, we consider the rotation of the D2Q9 lattice system about the  $z$ -axis by the angle  $\phi$ . We first evaluate the following quantity:

$$\begin{aligned} \sum_{\alpha=0}^8 w_\alpha c_{\alpha x}^2 c_{\alpha y}^2 &= w_1 \sum_{\alpha=1}^4 c_{\alpha x}^2 c_{\alpha y}^2 + w_5 \sum_{\alpha=5}^8 c_{\alpha x}^2 c_{\alpha y}^2 = w_1 c^4 \frac{1}{2} (1 - \cos 4\phi) \\ &\quad + w_5 \left( \sqrt{2}c \right)^4 \frac{1}{2} \left\{ 1 - \cos 4\left(\phi + \frac{\pi}{4}\right) \right\} \end{aligned} \quad (8.18)$$

With the assumption of

$$w_1 = 4w_5 \quad (8.19)$$

Eq. (8.18) comes to be independent of  $\phi$ . That is,

$$\sum_{\alpha=0}^8 w_\alpha c_{\alpha x}^2 c_{\alpha y}^2 = w_1 c^4 \quad (8.20)$$

Similar manipulation gives rise to

$$\left. \begin{aligned} \sum_{\alpha=0}^8 w_\alpha c_{\alpha x}^3 c_{\alpha y} &= \sum_{\alpha=0}^8 w_\alpha c_{\alpha x} c_{\alpha y}^3 = 0 \\ \sum_{\alpha=0}^8 w_\alpha c_{\alpha x}^4 &= \sum_{\alpha=0}^8 w_\alpha c_{\alpha y}^4 = 3w_1 c^4 \end{aligned} \right\} \quad (8.21)$$

The above results can be written in one expression by using the Kronecker delta  $\delta_{ij}$ :

$$\sum_{\alpha=0}^8 w_\alpha c_{\alpha i} c_{\alpha j} c_{\alpha k} c_{\alpha l} = w_1 c^4 (\delta_{ij} \delta_{kl} + \delta_{ik} \delta_{jl} + \delta_{il} \delta_{jk}) \quad (8.22)$$

Similarly,

$$\left. \begin{aligned} \sum_{\alpha=0}^8 w_\alpha c_{\alpha x} &= \sum_{\alpha=0}^8 w_\alpha c_{\alpha y} = 0, & \sum_{\alpha=0}^8 w_\alpha c_{\alpha i} c_{\alpha j} &= 3w_1 c^2 \delta_{ij} \\ \sum_{\alpha=0}^8 w_\alpha c_{\alpha x}^2 &= \sum_{\alpha=0}^8 w_\alpha c_{\alpha y}^2 = 3w_1 c^2, & \sum_{\alpha=0}^8 w_\alpha c_{\alpha x} c_{\alpha y} &= 0 \\ \sum_{\alpha=0}^8 w_\alpha c_{\alpha x}^3 &= \sum_{\alpha=0}^8 w_\alpha c_{\alpha y}^3 = \sum_{\alpha=0}^8 w_\alpha c_{\alpha x}^2 c_{\alpha y} = \sum_{\alpha=0}^8 w_\alpha c_{\alpha x} c_{\alpha y}^2 & &= 0 \end{aligned} \right\} \quad (8.23)$$

We now determine the appropriate values of the constants  $b$ ,  $e$ ,  $h$ , and  $w_\alpha$  for an equilibrium distribution in Eq. (8.8). The relationships that must be satisfied for an equilibrium state are the equation of mass in Eq. (8.4), the equation of momentum in Eq. (8.5), and the equi-partition law of energies in Eq. (8.6). In these equations,  $f_\alpha^{(0)}$  must be used as  $f_\alpha$ . Substitution of Eq. (8.8) into the right-hand side of Eq. (8.4) leads to

$$\sum_{\alpha=0}^8 f_\alpha^{(0)} = \sum_{\alpha=0}^8 \rho w_\alpha \left\{ 1 + b \frac{\mathbf{c}_\alpha \cdot \mathbf{u}}{c^2} + e \frac{u^2}{c^2} + h \frac{(\mathbf{c}_\alpha \cdot \mathbf{u})^2}{c^4} \right\} = \rho \left\{ w_{\text{sum}} + w_{\text{sum}} \frac{u^2}{c^2} e + 3w_1 \frac{u^2}{c^2} h \right\} \quad (8.24)$$

In deriving this equation, the following relationships have been used:

$$\left. \begin{aligned} \sum_{\alpha=0}^8 w_\alpha (\mathbf{c}_\alpha \cdot \mathbf{u}) &= \sum_{\alpha=0}^8 w_\alpha (c_{\alpha x} u_x + c_{\alpha y} u_y) = 0 \\ \sum_{\alpha=0}^8 w_\alpha (\mathbf{c}_\alpha \cdot \mathbf{u})^2 &= \sum_{\alpha=0}^8 w_\alpha (c_{\alpha x}^2 u_x^2 + c_{\alpha y}^2 u_y^2 + 2u_x u_y c_{\alpha x} c_{\alpha y}) = 3w_1 c^2 u^2 \end{aligned} \right\} \quad (8.25)$$

Equation (8.4) says that the quantity in Eq. (8.24) must equal the density  $\rho$ , so that the following relationships are obtained:

$$w_{\text{sum}} = 1, \quad w_{\text{sum}} e + 3w_1 h = 0 \quad (8.26)$$

in which  $w_{\text{sum}} = w_0 + 4w_1 + 4w_5 = w_0 + 5w_1$ .

Similarly, we obtain the following equation:

$$\sum_{\alpha=0}^8 c_{\alpha i} f_\alpha^{(0)} = \sum_{\alpha=0}^8 \rho w_\alpha c_{\alpha i} \left\{ 1 + b \frac{\mathbf{c}_\alpha \cdot \mathbf{u}}{c^2} + e \frac{u^2}{c^2} + h \frac{(\mathbf{c}_\alpha \cdot \mathbf{u})^2}{c^4} \right\} = 3\rho w_1 u_i b \quad (8.27)$$

in which the following relationships have been used for the derivation.

$$\left. \begin{aligned} \sum_{\alpha=0}^8 w_\alpha c_{\alpha x} (\mathbf{c}_\alpha \cdot \mathbf{u}) &= \sum_{\alpha=0}^8 w_\alpha (c_{\alpha x}^2 u_x + c_{\alpha x} c_{\alpha y} u_y) = 3w_1 c^2 u_x \\ \sum_{\alpha=0}^8 w_\alpha c_{\alpha x} (\mathbf{c}_\alpha \cdot \mathbf{u})^2 &= \sum_{\alpha=0}^8 w_\alpha (c_{\alpha x}^3 u_x^2 + 2c_{\alpha x}^2 c_{\alpha y} u_x u_y + c_{\alpha x} c_{\alpha y}^2 u_y^2) = 0 \end{aligned} \right\} \quad (8.28)$$

Since the momentum equation in Eq. (8.5) must be satisfied,  $b$  is obtained as

$$b = \frac{1}{3w_1} \quad (8.29)$$

Then, we evaluate the momentum flux  $\Pi_{ij}^{(0)}$  by substituting the equilibrium distribution  $f_\alpha^{(0)}$  in Eq. (8.8) into this momentum flux expression:

$$\begin{aligned} \Pi_{ij}^{(0)} &= \sum_{\alpha=0}^8 c_{\alpha i} c_{\alpha j} f_\alpha^{(0)} = \sum_{\alpha=0}^8 \rho w_\alpha c_{\alpha i} c_{\alpha j} \left\{ 1 + b \frac{\mathbf{c}_\alpha \cdot \mathbf{u}}{c^2} + e \frac{u^2}{c^2} + h \frac{(\mathbf{c}_\alpha \cdot \mathbf{u})^2}{c^4} \right\} \\ &= \rho w_1 \left\{ 3c^2 \left( 1 + \frac{u^2}{c^2} e \right) \delta_{ij} + u^2 h \delta_{ij} \right\} + 2\rho w_1 u_i u_j h \end{aligned} \quad (8.30)$$

in which the following relationships have been used for deriving this equation:

$$\left. \begin{aligned} \sum_{\alpha=0}^8 w_\alpha c_{\alpha x} c_{\alpha y} (\mathbf{c}_\alpha \cdot \mathbf{u}) &= \sum_{\alpha=0}^8 w_\alpha c_{\alpha x}^2 (\mathbf{c}_\alpha \cdot \mathbf{u}) = \sum_{\alpha=0}^8 w_\alpha c_{\alpha y}^2 (\mathbf{c}_\alpha \cdot \mathbf{u}) = 0 \\ \sum_{\alpha=0}^8 w_\alpha c_{\alpha x} c_{\alpha y} (\mathbf{c}_\alpha \cdot \mathbf{u})^2 &= 2w_1 c^4 u_x u_y \\ \sum_{\alpha=0}^8 w_\alpha c_{\alpha x}^2 (\mathbf{c}_\alpha \cdot \mathbf{u})^2 &= 2w_1 c^4 u_x^2 + w_1 c^4 u^2 \end{aligned} \right\} \quad (8.31)$$

For the case of an equilibrium state,  $\Pi_{ij}^{(0)}$  can be related to the pressure  $p$  as

$$\Pi_{ij}^{(0)} = p \delta_{ij} + \rho u_i u_j \quad (8.32)$$

Hence, the comparison of Eq. (8.30) with Eq. (8.32) yields the following relationships:

$$h = \frac{1}{2w_1}, \quad p = 3\rho w_1 c^2 \quad (8.33)$$

$$3e + h = 0 \quad (8.34)$$

The pressure  $p$  is related to the speed of sound  $c_s$  as  $p = \rho c_s^2$ , so that  $c_s$  can be written as

$$c_s = \sqrt{3w_1c} \quad (8.35)$$

Finally, we evaluate the kinetic energy. Preliminary relationships can be derived from Eq. (8.23) as

$$\left. \begin{aligned} \sum_{\alpha=0}^8 w_\alpha c_\alpha^2 &= 6w_1 c^2 \\ \sum_{\alpha=0}^8 w_\alpha c_{\alpha x}^2 (\mathbf{c}_\alpha \cdot \mathbf{u}) &= \sum_{\alpha=0}^8 w_\alpha c_{\alpha y}^2 (\mathbf{c}_\alpha \cdot \mathbf{u}) = \sum_{\alpha=0}^8 w_\alpha c_\alpha^2 (\mathbf{c}_\alpha \cdot \mathbf{u}) = 0 \\ \sum_{\alpha=0}^8 w_\alpha c_\alpha^2 (\mathbf{c}_\alpha \cdot \mathbf{u})^2 &= 4w_1 c^4 u^2, \quad \sum_{\alpha=0}^8 w_\alpha (\mathbf{c}_\alpha \cdot \mathbf{u})^3 = 0 \end{aligned} \right\} \quad (8.36)$$

Using these relationships, the right-hand side in Eq. (8.6) may be calculated as

$$\begin{aligned} \sum_{\alpha=0}^8 \frac{m}{2} (\mathbf{c}_\alpha - \mathbf{u})^2 \frac{f_\alpha^{(0)}}{\rho} &= \frac{m}{2} \sum_{\alpha=0}^8 w_\alpha (c_\alpha^2 + u^2 - 2\mathbf{c}_\alpha \cdot \mathbf{u}) \\ &\times \left\{ 1 + b \frac{\mathbf{c}_\alpha \cdot \mathbf{u}}{c^2} + e \frac{u^2}{c^2} + h \frac{(\mathbf{c}_\alpha \cdot \mathbf{u})^2}{c^4} \right\} \\ &= \frac{m}{2} \left\{ 6w_1 \left( 1 + e \frac{u^2}{c^2} \right) c^2 + 4w_1 h u^2 + w_{\text{sum}} \left( 1 + e \frac{u^2}{c^2} \right) u^2 + 3w_1 h \frac{u^4}{c^2} - 6w_1 b u^2 \right\} \end{aligned} \quad (8.37)$$

By taking into account Eqs. (8.26), (8.29), and (8.33), the above equation is simplified as

$$\sum_{\alpha=0}^8 \frac{m}{2} (\mathbf{c}_\alpha - \mathbf{u})^2 \frac{f_\alpha^{(0)}}{\rho} = \frac{m}{2} (6w_1 c^2 + 6w_1 u^2 e + w_{\text{sum}} u^2) \quad (8.38)$$

Hence, Eq. (8.6) reduces to

$$\frac{2}{2} kT = \frac{m}{2} (6w_1 c^2 + 6w_1 u^2 e + w_{\text{sum}} u^2) \quad (8.39)$$

Since the temperature  $T$  is independent of the macroscopic velocity  $u$ , this equation yields the final relationships:

$$6w_1 e + w_{\text{sum}} = 0 \quad (8.40)$$

$$3mw_1 c^2 = kT \quad (8.41)$$

We now have the same number of equations as the unknown constants, so that the solutions required can be obtained in a straightforward way as

$$b = 3, \quad e = -\frac{3}{2}, \quad h = \frac{9}{2} \quad (8.42)$$

$$w_{\text{sum}} = 1, \quad w_0 = \frac{4}{9}, \quad w_1 = \frac{1}{9}, \quad w_5 = \frac{1}{36} \quad (8.43)$$

We summarize the final results as

$$f_{\alpha}^{(0)} = \rho w_{\alpha} \left\{ 1 + 3 \frac{\mathbf{c}_{\alpha} \cdot \mathbf{u}}{c^2} - \frac{3}{2} \cdot \frac{u^2}{c^2} + \frac{9}{2} \cdot \frac{(\mathbf{c}_{\alpha} \cdot \mathbf{u})^2}{c^4} \right\} \quad (8.44)$$

$$w_{\alpha} = \begin{cases} 4/9 & \text{for } \alpha = 0 \\ 1/9 & \text{for } \alpha = 1, 2, 3, 4, \\ 1/36 & \text{for } \alpha = 5, 6, 7, 8 \end{cases} \quad |\mathbf{c}_{\alpha}| = \begin{cases} 0 & \text{for } \alpha = 0 \\ c & \text{for } \alpha = 1, 2, 3, 4 \\ \sqrt{2}c & \text{for } \alpha = 5, 6, 7, 8 \end{cases} \quad (8.45)$$

The speed of sound  $c_s$  is expressed as

$$c_s = c / \sqrt{3} \quad (8.46)$$

### 8.1.2 D3Q19 Model

In the case of the D3Q19 lattice model, the thermodynamic equilibrium distribution can be assumed to have the form of Eq. (8.8), and therefore the unknown constants can be derived through similar procedures to the previous D2Q9 model. Only in this present subsection, we use the notation  $\tilde{c}$  ( $= \Delta x / \Delta t$ ) for the lattice speed instead of  $c$ , since the notation  $c$  will be used for the abbreviated symbol of the cosine function.

In order to satisfy the isotropy condition, the lattice system has to be adopted such that it is independent of an arbitrary rotation of the lattice. In Figure 8.3, for a rotation of the lattice system about the  $z$ -axis by an angle  $\phi$  and a rotation about the  $y$ -axis by an angle  $\theta$ , the rotation matrix  $\mathbf{R}$  is written as

$$\mathbf{R} = \begin{pmatrix} \cos \theta & 0 & \sin \theta \\ 0 & 1 & 0 \\ -\sin \theta & 0 & \cos \theta \end{pmatrix} \begin{pmatrix} \cos \phi & -\sin \phi & 0 \\ \sin \phi & \cos \phi & 0 \\ 0 & 0 & 1 \end{pmatrix} = \begin{pmatrix} Cc & -Cs & S \\ s & c & 0 \\ -Sc & Ss & C \end{pmatrix} \quad (8.47)$$

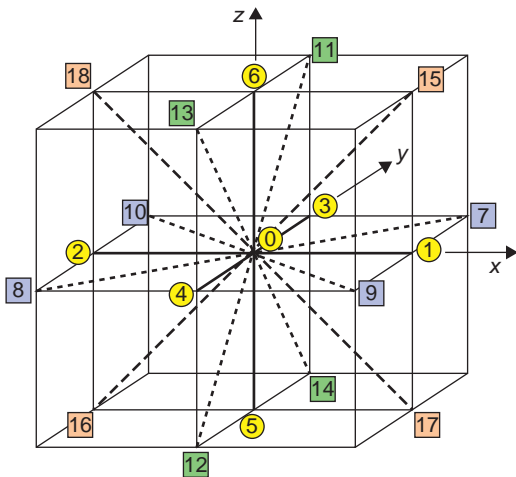


**Figure 8.3** Lattice model for the D3Q19.

in which the abbreviations  $C = \cos \theta$ ,  $S = \sin \theta$ ,  $c = \cos \phi$ , and  $s = \sin \phi$  are used for simplification of the equations. An arbitrary component  $\mathbf{X}$  is related to the corresponding rotated component  $\mathbf{X}'$  by the expression  $\mathbf{X}' = \mathbf{R} \cdot \mathbf{X}$ . The transferred component  $\mathbf{d}_k$  ( $k = 1, 2, \dots, 18$ ) of each lattice point in Figure 8.3 is obtained as

$$\left. \begin{aligned} \mathbf{d}_1 &= \mathbf{R} \begin{pmatrix} 1 \\ 0 \\ 0 \end{pmatrix} = \begin{pmatrix} Cc \\ s \\ -Sc \end{pmatrix}, & \mathbf{d}_3 &= \mathbf{R} \begin{pmatrix} 0 \\ 1 \\ 0 \end{pmatrix} = \begin{pmatrix} -Cs \\ c \\ Ss \end{pmatrix}, & \mathbf{d}_5 &= \begin{pmatrix} -S \\ 0 \\ -C \end{pmatrix} \\ \mathbf{d}_7 &= \begin{pmatrix} C(c-s) \\ s+c \\ -S(c-s) \end{pmatrix}, & \mathbf{d}_9 &= \begin{pmatrix} C(c+s) \\ s-c \\ -S(c+s) \end{pmatrix}, & \mathbf{d}_{11} &= \begin{pmatrix} -Cs+S \\ c \\ Ss+C \end{pmatrix} \\ \mathbf{d}_{13} &= \begin{pmatrix} Cs+S \\ -c \\ -Ss+C \end{pmatrix}, & \mathbf{d}_{15} &= \begin{pmatrix} Cc+S \\ s \\ -Sc+C \end{pmatrix}, & \mathbf{d}_{17} &= \begin{pmatrix} Cc-S \\ s \\ -Sc-C \end{pmatrix} \end{aligned} \right\} \quad (8.48)$$

From symmetric considerations, the following relationship must be satisfied:

$$\mathbf{d}_{2k} = -\mathbf{d}_{2k-1} \quad (k = 1, 2, \dots, 9) \quad (8.49)$$

The final expressions are summarized in Table 8.1.

The results in Table 8.1 give rise to those concerning  $c_{\alpha x}$ ,  $c_{\alpha y}$ , and  $c_{\alpha z}$ , such as  $\sum_{\alpha=0}^{18} w_{\alpha} c_{\alpha i} c_{\alpha j} c_{\alpha k} c_{\alpha l} = w_{\alpha} c_{\alpha i} c_{\alpha j} c_{\alpha k} c_{\alpha l}$  in Table 8.2. As seen from the result of  $\sum_{\alpha=0}^{18} w_{\alpha} c_{\alpha i}^4$ , the

**Table 8.1** Results of Quantities for the Successive Derivation

$\sum_{k=1}^6 d_{kx}^4 = -4(C^2 S^2 + C^4 c^2 s^2) + 2$	$\sum_{k=7}^{18} d_{kx}^4 = 8(C^2 S^2 + C^4 c^2 s^2) + 8$
$\sum_{k=1}^6 d_{ky}^4 = 4(c^4 - c^2) + 2$	$\sum_{k=7}^{18} d_{ky}^4 = -8(c^4 - c^2) + 8$
$\sum_{k=1}^6 d_{kz}^4 = -4(C^2 S^2 + S^4 c^2 s^2) + 2$	$\sum_{k=7}^{18} d_{kz}^4 = 8(C^2 S^2 + S^4 c^2 s^2) + 8$
$\sum_{k=1}^6 d_{kx}^2 d_{ky}^2 = 4C^2 c^2 s^2$	$\sum_{k=7}^{18} d_{kx}^2 d_{ky}^2 = -8C^2 c^2 s^2 + 4$
$\sum_{k=1}^6 d_{kx}^2 d_{kz}^2 = 4C^2 S^2(1 - c^2 s^2)$	$\sum_{k=7}^{18} d_{kx}^2 d_{kz}^2 = -8C^2 S^2(1 - c^2 s^2) + 4$
$\sum_{k=1}^6 d_{ky}^2 d_{kz}^2 = 4S^2 c^2 s^2$	$\sum_{k=7}^{18} d_{ky}^2 d_{kz}^2 = -8S^2 c^2 s^2 + 4$
$\sum_{k=1}^6 d_{kx}^2 d_{ky} d_{kz} = 2C^2 S c s(-c^2 + s^2)$	$\sum_{k=7}^{18} d_{kx}^2 d_{ky} d_{kz} = 4C^2 S(c^2 - s^2) c s$
$\sum_{k=1}^6 d_{kx} d_{ky}^2 d_{kz} = -4C S c^2 s^2$	$\sum_{k=7}^{18} d_{kx} d_{ky}^2 d_{kz} = 8C S c^2 s^2$
$\sum_{k=1}^6 d_{kx} d_{ky} d_{kz}^2 = 2C S^2 c s(c^2 - s^2)$	$\sum_{k=7}^{18} d_{kx} d_{ky} d_{kz}^2 = -4C S^2(c^2 - s^2) c s$
$\sum_{k=1}^6 d_{kx}^3 d_{ky} = 2C^3 c s(c^2 - s^2)$	$\sum_{k=7}^{18} d_{kx}^3 d_{ky} = -4C^3(c^2 - s^2) c s$
$\sum_{k=1}^6 d_{kx}^3 d_{kz} = -2C^3 S(1 - 2c^2 s^2) + 2C S^3$	$\sum_{k=7}^{18} d_{kx}^3 d_{kz} = 4C^3 S(1 - 2c^2 s^2) - 4C S^3$
$\sum_{k=1}^6 d_{ky}^3 d_{kx} = 2C c s(-c^2 + s^2)$	$\sum_{k=7}^{18} d_{ky}^3 d_{kx} = 4C(c^2 - s^2) c s$
$\sum_{k=1}^6 d_{ky}^3 d_{kz} = 2S c s(c^2 - s^2)$	$\sum_{k=7}^{18} d_{ky}^3 d_{kz} = -4S(c^2 - s^2) c s$
$\sum_{k=1}^6 d_{kz}^3 d_{kx} = -2C S^3(1 - 2c^2 s^2) + 2C^3 S$	$\sum_{k=7}^{18} d_{kz}^3 d_{kx} = 4C S^3(1 - 2c^2 s^2) - 4C^3 S$
$\sum_{k=1}^6 d_{kz}^3 d_{ky} = -2S^3 c s(c^2 - s^2)$	$\sum_{k=7}^{18} d_{kz}^3 d_{ky} = 4S^3(c^2 - s^2) c s$
$\sum_{k=1}^6 d_{kx}^2 = \sum_{k=1}^6 d_{ky}^2 = \sum_{k=1}^6 d_{kz}^2 = 2$	$\sum_{k=7}^{18} d_{kx}^2 = \sum_{k=7}^{18} d_{ky}^2 = \sum_{k=7}^{18} d_{kz}^2 = 8$
$\sum_{k=1}^6 d_{kx} d_{ky} = \sum_{k=1}^6 d_{kx} d_{kz} = \sum_{k=1}^6 d_{ky} d_{kz} = 0$	$\sum_{k=7}^{18} d_{kx} d_{ky} = \sum_{k=7}^{18} d_{kx} d_{kz} = \sum_{k=7}^{18} d_{ky} d_{kz} = 0$

**Table 8.2** Final Results of Quantities for the Successive Derivation

$$\sum_{\alpha=0}^{18} w_{\alpha} c_{\alpha x}^4 = \tilde{c}^4 (-4w_1 + 8w_7)(C^2 S^2 + C^4 c^2 s^2) + \tilde{c}^4 (2w_1 + 8w_7)$$

$$\sum_{\alpha=0}^{18} w_{\alpha} c_{\alpha y}^4 = \tilde{c}^4 (4w_1 - 8w_7)(c^4 - c^2) + \tilde{c}^4 (2w_1 + 8w_7)$$

$$\sum_{\alpha=0}^{18} w_{\alpha} c_{\alpha z}^4 = \tilde{c}^4 (-4w_1 + 8w_7)(C^2 S^2 + S^4 c^2 s^2) + \tilde{c}^4 (2w_1 + 8w_7)$$

$$\Downarrow w_1 = 2w_7$$

$$\sum_{\alpha=0}^{18} w_{\alpha} c_{\alpha x}^4 = \sum_{\alpha=0}^{18} w_{\alpha} c_{\alpha y}^4 = \sum_{\alpha=0}^{18} w_{\alpha} c_{\alpha z}^4 = 6w_1 \tilde{c}^4$$

$$\sum_{\alpha=0}^{18} w_{\alpha} c_{\alpha x}^2 c_{\alpha y}^2 = \sum_{\alpha=0}^{18} w_{\alpha} c_{\alpha x}^2 c_{\alpha z}^2 = \sum_{\alpha=0}^{18} w_{\alpha} c_{\alpha y}^2 c_{\alpha z}^2 = 2w_1 \tilde{c}^4$$

$$\sum_{\alpha=0}^{18} w_{\alpha} c_{\alpha x}^3 c_{\alpha y} = \sum_{\alpha=0}^{18} w_{\alpha} c_{\alpha x}^3 c_{\alpha z} = \sum_{\alpha=0}^{18} w_{\alpha} c_{\alpha y}^3 c_{\alpha x} = \sum_{\alpha=0}^{18} w_{\alpha} c_{\alpha y}^3 c_{\alpha z} = \sum_{\alpha=0}^{18} w_{\alpha} c_{\alpha z}^3 c_{\alpha x} = \sum_{\alpha=0}^{18} w_{\alpha} c_{\alpha z}^3 c_{\alpha y} = 0$$

$$\sum_{\alpha=0}^{18} w_{\alpha} c_{\alpha x}^2 c_{\alpha y} c_{\alpha z} = \sum_{\alpha=0}^{18} w_{\alpha} c_{\alpha x} c_{\alpha y}^2 c_{\alpha z} = \sum_{\alpha=0}^{18} w_{\alpha} c_{\alpha x} c_{\alpha y} c_{\alpha z}^2 = 0$$

$$\sum_{\alpha=0}^{18} w_{\alpha} c_{\alpha x}^3 = \sum_{\alpha=0}^{18} w_{\alpha} c_{\alpha y}^3 = \sum_{\alpha=0}^{18} w_{\alpha} c_{\alpha z}^3 = 0$$

$$\sum_{\alpha=0}^{18} w_{\alpha} c_{\alpha x}^2 c_{\alpha y} = \sum_{\alpha=0}^{18} w_{\alpha} c_{\alpha x}^2 c_{\alpha z} = \sum_{\alpha=0}^{18} w_{\alpha} c_{\alpha y}^2 c_{\alpha x} = \sum_{\alpha=0}^{18} w_{\alpha} c_{\alpha y}^2 c_{\alpha z} = \sum_{\alpha=0}^{18} w_{\alpha} c_{\alpha z}^2 c_{\alpha x} = \sum_{\alpha=0}^{18} w_{\alpha} c_{\alpha z}^2 c_{\alpha y} = 0$$

$$\sum_{\alpha=0}^{18} w_{\alpha} c_{\alpha x} c_{\alpha y} c_{\alpha z} = 0$$

$$\sum_{\alpha=0}^{18} w_{\alpha} c_{\alpha x}^2 = \sum_{\alpha=0}^{18} w_{\alpha} c_{\alpha y}^2 = \sum_{\alpha=0}^{18} w_{\alpha} c_{\alpha z}^2 = 6w_1 \tilde{c}^2$$

$$\sum_{\alpha=0}^{18} w_{\alpha} c_{\alpha x} c_{\alpha y} = \sum_{\alpha=0}^{18} w_{\alpha} c_{\alpha x} c_{\alpha z} = \sum_{\alpha=0}^{18} w_{\alpha} c_{\alpha y} c_{\alpha z} = 0$$

$$\sum_{\alpha=0}^{18} w_{\alpha} c_{\alpha x} = \sum_{\alpha=0}^{18} w_{\alpha} c_{\alpha y} = \sum_{\alpha=0}^{18} w_{\alpha} c_{\alpha z} = 0$$

relationship of  $w_1 = 2w_7$  has to be satisfied in order for this result to be independent of the rotational angle. Hence, the results after the arrow in Table 8.2 have taken into account this relationship. The expressions in Table 8.2 are written in simply unified equations as

$$\left. \begin{aligned} \sum_{\alpha=0}^{18} w_{\alpha} c_{\alpha i} c_{\alpha j} c_{\alpha k} c_{\alpha l} &= 2w_1 \tilde{c}^4 (\delta_{ij}\delta_{kl} + \delta_{ik}\delta_{jl} + \delta_{il}\delta_{jk}) \\ \sum_{\alpha=0}^{18} w_{\alpha} c_{\alpha i} c_{\alpha j} c_{\alpha k} &= 0 \\ \sum_{\alpha=0}^{18} w_{\alpha} c_{\alpha i} c_{\alpha j} &= 6w_1 \tilde{c}^2 \delta_{ij}, \quad \sum_{\alpha=0}^{18} w_{\alpha} c_i &= 0 \end{aligned} \right\} \quad (8.50)$$

We are now ready to derive the equilibrium distribution for the D3Q19 lattice model.

As mentioned before, the relationships that the equilibrium distribution  $f_{\alpha}^{(0)}$  shown in Eq. (8.8) must satisfy are the mass, momentum, kinetic energy, and momentum flux equations. The former three equations are written as

$$\sum_{\alpha=0}^{18} f_{\alpha}^{(0)} = \rho \quad (8.51)$$

$$\sum_{\alpha=0}^{18} \mathbf{c}_{\alpha} f_{\alpha}^{(0)} = \rho \mathbf{u} \quad (8.52)$$

$$\sum_{\alpha=0}^{18} \frac{m}{2} (\mathbf{c}_{\alpha} - \mathbf{u})^2 \frac{f_{\alpha}^{(0)}}{\rho} = \frac{3}{2} kT \quad (8.53)$$

With the results shown in Table 8.2, the following equation is obtained:

$$\begin{aligned} \sum_{\alpha=0}^{18} f_{\alpha}^{(0)} &= \sum_{\alpha=0}^{18} w_{\alpha} \rho \left\{ 1 + b \frac{\mathbf{c}_{\alpha} \cdot \mathbf{u}}{\tilde{c}^2} + e \frac{u^2}{\tilde{c}^2} + h \frac{(\mathbf{c}_{\alpha} \cdot \mathbf{u})^2}{\tilde{c}^4} \right\} \\ &= \rho \left\{ w_{\text{sum}} + \frac{u^2}{\tilde{c}^2} (w_{\text{sum}} e + 6w_1 h) \right\} \end{aligned} \quad (8.54)$$

The comparison of this equation with Eq. (8.51) leads to

$$w_{\text{sum}} = 1, \quad w_{\text{sum}} e + 6w_1 h = 0 \quad (8.55)$$

in which  $w_{\text{sum}} = w_0 + 6w_1 + 12w_7 = w_0 + 12w_1$ .

In order to compare this result with the right-hand side of Eq. (8.52), the left-hand side is evaluated using the equilibrium distribution as

$$\sum_{\alpha=0}^{18} c_{\alpha i} f_{\alpha}^{(0)} = \sum_{\alpha=0}^{18} \rho w_{\alpha} c_{\alpha i} \left\{ 1 + b \frac{\mathbf{c}_{\alpha} \cdot \mathbf{u}}{\tilde{c}^2} + e \frac{u^2}{\tilde{c}^2} + h \frac{(\mathbf{c}_{\alpha} \cdot \mathbf{u})^2}{\tilde{c}^4} \right\} = 6bw_1\rho u_i \quad (8.56)$$

Hence, the comparison of the right-hand sides in Eqs. (8.56) and (8.52) gives rise to

$$6w_1 b = 1 \quad (8.57)$$

Similar to the D2Q9 model, the momentum flux  $\Pi_{ij}^{(0)}$  is calculated as

$$\Pi_{ij}^{(0)} = \sum_{\alpha=0}^{18} c_{\alpha i} c_{\alpha j} f_{\alpha}^{(0)} = \left\{ 6\rho w_1 \tilde{c}^2 \left( 1 + e \frac{u^2}{\tilde{c}^2} \right) + 2\rho w_1 u^2 h \right\} \delta_{ij} + 4\rho w_1 u_i u_j h \quad (8.58)$$

In deriving this equation, the following relationships are used:

$$\left. \begin{aligned} \sum_{\alpha=0}^{18} w_{\alpha} c_{\alpha x} c_{\alpha y} \left\{ 1 + b \frac{\mathbf{c}_{\alpha} \cdot \mathbf{u}}{\tilde{c}^2} + e \frac{u^2}{\tilde{c}^2} + h \frac{(\mathbf{c}_{\alpha} \cdot \mathbf{u})^2}{\tilde{c}^4} \right\} &= 4w_1 u_x u_y h \\ \sum_{\alpha=0}^{18} w_{\alpha} c_{\alpha x}^2 \left\{ 1 + b \frac{\mathbf{c}_{\alpha} \cdot \mathbf{u}}{\tilde{c}^2} + e \frac{u^2}{\tilde{c}^2} + h \frac{(\mathbf{c}_{\alpha} \cdot \mathbf{u})^2}{\tilde{c}^4} \right\} \\ &= 6w_1 \tilde{c}^2 \left( 1 + e \frac{u^2}{\tilde{c}^2} \right) + 2w_1 u^2 h + 4w_1 u_x^2 h \end{aligned} \right\} \quad (8.59)$$

The expression for  $\Pi_{ij}^{(0)}$  as defined by Eq. (8.32) is also valid for a three-dimensional system. The following relationships can therefore be obtained by comparison with Eq. (8.58) as

$$p = 6\rho w_1 \tilde{c}^2 \quad (8.60)$$

$$4w_1 h = 1, \quad 3e + h = 0 \quad (8.61)$$

Hence, the speed of sound  $c_s$  is expressed from  $p = \rho c_s^2$  as

$$c_s = \sqrt{6w_1 \cdot \tilde{c}} \quad (8.62)$$

Finally, in order to compare with Eq. (8.53), the following reformation is performed:

$$\begin{aligned}
 \sum_{\alpha=0}^{18} (\mathbf{c}_\alpha - \mathbf{u})^2 \frac{f_\alpha^{(0)}}{\rho} &= \sum_{\alpha=0}^{18} w_\alpha (\mathbf{c}_\alpha - \mathbf{u})^2 \left\{ 1 + b \frac{\mathbf{c}_\alpha \cdot \mathbf{u}}{\tilde{c}^2} + e \frac{u^2}{\tilde{c}^2} + h \frac{(\mathbf{c}_\alpha \cdot \mathbf{u})^2}{\tilde{c}^4} \right\} \\
 &= \sum_{\alpha=0}^{18} w_\alpha (c_\alpha^2 - 2\mathbf{c}_\alpha \cdot \mathbf{u} + u^2) \left\{ 1 + b \frac{\mathbf{c}_\alpha \cdot \mathbf{u}}{\tilde{c}^2} + e \frac{u^2}{\tilde{c}^2} + h \frac{(\mathbf{c}_\alpha \cdot \mathbf{u})^2}{\tilde{c}^4} \right\} \\
 &= \sum_{\alpha=0}^{18} w_\alpha (c_\alpha^2 - 2\mathbf{c}_\alpha \cdot \mathbf{u} + u^2) \left( 1 + e \frac{u^2}{\tilde{c}^2} \right) \\
 &\quad + \sum_{\alpha=0}^{18} w_\alpha (c_\alpha^2 - 2\mathbf{c}_\alpha \cdot \mathbf{u} + u^2) (\mathbf{c}_\alpha \cdot \mathbf{u}) \frac{b}{\tilde{c}^2} \\
 &\quad + \sum_{\alpha=0}^{18} w_\alpha (c_\alpha^2 - 2\mathbf{c}_\alpha \cdot \mathbf{u} + u^2) (\mathbf{c}_\alpha \cdot \mathbf{u})^2 \frac{h}{\tilde{c}^4} \\
 &= \left( 1 + e \frac{u^2}{\tilde{c}^2} \right) (18w_1 \tilde{c}^2 + w_{\text{sum}} u^2) - \frac{2b}{\tilde{c}^2} \sum_{\alpha=0}^{18} w_\alpha (\mathbf{c}_\alpha \cdot \mathbf{u})^2 \\
 &\quad + \frac{h}{\tilde{c}^4} \sum_{\alpha=0}^{18} w_\alpha \left\{ c_\alpha^2 (\mathbf{c}_\alpha \cdot \mathbf{u})^2 + u^2 (\mathbf{c}_\alpha \cdot \mathbf{u})^2 \right\} \\
 &= 18w_1 \tilde{c}^2 + (w_{\text{sum}} - 12w_1 b + 18w_1 e + 10w_1 h) u^2
 \end{aligned} \tag{8.63}$$

in which Eq. (8.55) and the following relationship have been used for the derivation:

$$\left. \begin{aligned}
 \sum_{\alpha=0}^{18} w_\alpha (\mathbf{c}_\alpha \cdot \mathbf{u})^2 &= 6w_1 \tilde{c}^2 u^2 \\
 \sum_{\alpha=0}^{18} w_\alpha c_\alpha^2 (\mathbf{c}_\alpha \cdot \mathbf{u})^2 &= 10w_1 \tilde{c}^4 u^2
 \end{aligned} \right\} \tag{8.64}$$

Since the temperature is independent of the macroscopic velocity  $u$ , the second term on the right-hand side in Eq. (8.63) must vanish:

$$w_{\text{sum}} - 12w_1 b + 18w_1 e + 10w_1 h = 0 \tag{8.65}$$

The comparison of Eq. (8.63) with Eq. (8.6) yields the following equation:

$$\frac{m}{2} 18w_1 \tilde{c}^2 = \frac{3}{2} kT \tag{8.66}$$

We now have the same number of equations as the unknown constants. The final results for the unknown constants can be obtained from Eqs. (8.55), (8.57), (8.61), and (8.65) and the relationships of  $w_1 = 2w_7$  and  $w_{\text{sum}} = w_0 + 12w_1$ , as

$$\left. \begin{aligned} w_0 &= \frac{1}{3}, & w_1 &= \frac{1}{18}, & w_7 &= \frac{1}{36}, & w_{\text{sum}} &= 1 \\ b &= 3, & e &= -\frac{3}{2}, & h &= \frac{9}{2} \end{aligned} \right\} \quad (8.67)$$

With the original notation  $c$  for the lattice velocity, the equilibrium distribution for the D3Q19 model is finally written as

$$f_a^{(0)} = \rho w_\alpha \left\{ 1 + 3 \frac{\mathbf{c}_\alpha \cdot \mathbf{u}}{c^2} - \frac{3}{2} \cdot \frac{u^2}{c^2} + \frac{9}{2} \cdot \frac{(\mathbf{c}_\alpha \cdot \mathbf{u})^2}{c^4} \right\} \quad (8.68)$$

$$w_\alpha = \begin{cases} 1/3 & \text{for } \alpha = 0 \\ 1/18 & \text{for } \alpha = 1, 2, \dots, 6 \\ 1/36 & \text{for } \alpha = 7, 8, \dots, 18 \end{cases}, \quad |\mathbf{c}_\alpha| = \begin{cases} 0 & \text{for } \alpha = 0 \\ c & \text{for } \alpha = 1, 2, \dots, 6 \\ \sqrt{2}c & \text{for } \alpha = 7, 8, \dots, 18 \end{cases} \quad (8.69)$$

## 8.2 Navier–Stokes Equation

In this section, we derive the Navier–Stokes equation from the preliminary equations derived in Appendix A1, which is the basic macroscopic equation for flow problems. The following derivation procedure is valid for both D2Q9 and D3Q19 models, with the exception that  $\alpha$  is taken as  $\alpha = 0, 1, \dots, 8$ , the axis index  $i$  is  $x$  or  $y$  for the former model,  $\alpha$  is taken as  $\alpha = 0, 1, \dots, 18$ , and  $i$  is  $x$ ,  $y$ , or  $z$  for the latter model.

The starting equation for the derivation procedure is Eq. (A1.27), rewritten as

$$\frac{\partial}{\partial t}(\rho u_i) + \sum_j \frac{\partial}{\partial r_j} \Pi_{ij} + \frac{\Delta t}{2} \varepsilon \sum_j \frac{\partial}{\partial r_j} \left\{ \frac{\partial}{\partial t_1} \Pi_{ij}^{(0)} \right\} + \frac{\Delta t}{2} \sum_j \sum_k \frac{\partial}{\partial r_j} \left\{ \frac{\partial}{\partial r_k} S_{ijk}^{(0)} \right\} = 0 \quad (8.70)$$

Another starting equation is Eq. (A1.31), rewritten as

$$-\frac{1}{\tau \Delta t} f_\alpha^{(1)} = -\frac{\partial f_\alpha^{(0)}}{\partial \rho} \cdot \frac{\partial}{\partial \mathbf{r}_1} \cdot (\rho \mathbf{u}) - \sum_i \sum_j \frac{\partial f_\alpha^{(0)}}{\partial (\rho u_i)} \cdot \frac{\partial}{\partial r_{1j}} \Pi_{ij}^{(0)} + \sum_i \frac{\partial}{\partial r_{1i}} (c_{\alpha i} f_\alpha^{(0)}) \quad (8.71)$$

in which

$$f_\alpha = f_\alpha^{(0)} + \varepsilon f_\alpha^{(1)} + \varepsilon^2 f_\alpha^{(2)} + \dots \quad (8.72)$$

$$\Pi_{ij}^{(0)} = \sum_\alpha c_{\alpha i} c_{\alpha j} f_\alpha^{(0)} = p \delta_{ij} + \rho u_i u_j = \frac{\rho}{3} c^2 \delta_{ij} + \rho u_i u_j \quad (8.73)$$

$$S_{ijk}^{(0)} = \sum_\alpha c_{\alpha i} c_{\alpha j} c_{\alpha k} f_\alpha^{(0)} \quad (8.74)$$

$$\frac{\partial}{\partial t} = \varepsilon \frac{\partial}{\partial t_1} + \varepsilon^2 \frac{\partial}{\partial t_2}, \quad \frac{\partial}{\partial r_i} = \varepsilon \frac{\partial}{\partial r_{1i}} \quad (8.75)$$

We now begin the derivation procedure for the Navier–Stokes equation by deriving the solution for  $f_\alpha^{(1)}$  from the basic equation in Eq. (8.71). If the terms higher than the order of  $(u/c)^2$  are neglected, the following relationships are obtained:

$$f_\alpha^{(0)} = \rho w_\alpha \left\{ 1 + 3 \frac{\mathbf{c}_\alpha \cdot \mathbf{u}}{c^2} \right\} \quad (8.76)$$

$$\Pi_{ij}^{(0)} = \frac{\rho}{3} c^2 \delta_{ij} + \rho u_i u_j \quad (8.77)$$

$$\frac{\partial f_\alpha^{(0)}}{\partial \rho} = w_\alpha \quad (8.78)$$

$$\frac{\partial f_\alpha^{(0)}}{\partial (\rho u_i)} = w_\alpha \frac{\partial}{\partial (\rho u_i)} \left\{ \frac{3}{c^2} \sum_j c_{\alpha j} (\rho u_j) \right\} = w_\alpha \frac{3}{c^2} c_{\alpha i} \quad (8.79)$$

$$\frac{\partial}{\partial r_{1j}} \Pi_{ij}^{(0)} = \frac{c^2}{3} \cdot \frac{\partial \rho}{\partial r_{1j}} \delta_{ij} + \frac{\partial}{\partial r_{1j}} (\rho u_i u_j) \quad (8.80)$$

$$\frac{\partial}{\partial r_{1i}} (c_{\alpha i} f_\alpha^{(0)}) = w_\alpha \frac{\partial}{\partial r_{1i}} (\rho c_{\alpha i}) + 3 w_\alpha \frac{1}{c^2} \cdot \frac{\partial}{\partial r_{1i}} \left\{ \sum_j \rho c_{\alpha i} c_{\alpha j} u_j \right\} \quad (8.81)$$

By substituting these relationships into Eq. (8.71), the solution of  $f_\alpha^{(1)}$  can finally be obtained as

$$f_\alpha^{(1)} = -3w_\alpha \Delta t \tau \frac{1}{c^2} \sum_k \sum_l \left( c_{\alpha k} c_{\alpha l} - \frac{1}{3} c^2 \delta_{kl} \right) \frac{\partial}{\partial r_{1l}} (\rho u_k) \quad (8.82)$$

With this solution, the next quantity can be evaluated:

$$\begin{aligned}
 \varepsilon \Pi_{ij}^{(1)} &= \varepsilon \sum_{\alpha} c_{\alpha i} c_{\alpha j} f_{\alpha}^{(1)} \\
 &= -3 \Delta t \tau \frac{1}{c^2} \sum_k \sum_l \left( \sum_{\alpha} w_{\alpha} c_{\alpha i} c_{\alpha j} c_{\alpha k} c_{\alpha l} \right) \frac{\partial}{\partial r_l} (\rho u_k) \\
 &\quad + \Delta t \tau \left( \sum_{\alpha} w_{\alpha} c_{\alpha i} c_{\alpha j} \right) \frac{\partial}{\partial \mathbf{r}} \cdot (\rho \mathbf{u}) \\
 &= -\frac{\Delta t \tau c^2}{3} \left\{ \frac{\partial}{\partial r_j} (\rho u_i) + \frac{\partial}{\partial r_i} \left( \frac{\partial}{\partial \mathbf{r}} \cdot (\rho \mathbf{u}) \right) \right\}
 \end{aligned} \tag{8.83}$$

In deriving this equation, Eqs. (8.50), (8.22), and (8.23) are used. This equation leads to

$$\sum_j \frac{\partial}{\partial r_j} (\varepsilon \Pi_{ij}^{(1)}) = -\frac{\Delta t \tau c^2}{3} \left\{ \frac{\partial^2}{\partial \mathbf{r}^2} (\rho u_i) + \frac{\partial}{\partial r_i} \left( \frac{\partial}{\partial \mathbf{r}} \cdot (\rho \mathbf{u}) \right) \right\} \tag{8.84}$$

On the other hand,  $\Pi_{ij}^{(0)}$  is written as

$$\sum_j \frac{\partial}{\partial r_j} (\Pi_{ij}^{(0)}) = \sum_j \frac{\partial}{\partial r_j} (p \delta_{ij} + \rho u_i u_j) \tag{8.85}$$

With the approximation of  $\Pi_{ij} \approx \Pi_{ij}^{(0)} + \varepsilon \Pi_{ij}^{(1)}$ , the following equation is obtained from Eqs. (8.84) and (8.85):

$$\sum_j \frac{\partial}{\partial r_j} \Pi_{ij} = \sum_j \frac{\partial}{\partial r_j} (p \delta_{ij} + \rho u_i u_j) - \frac{\Delta t \tau c^2}{3} \left\{ \frac{\partial^2}{\partial \mathbf{r}^2} (\rho u_i) + \frac{\partial}{\partial r_i} \left( \frac{\partial}{\partial \mathbf{r}} \cdot (\rho \mathbf{u}) \right) \right\} \tag{8.86}$$

Moreover, Eqs. (A1.11) and (A1.17) give rise to

$$\frac{\Delta t}{2} \varepsilon \frac{\partial}{\partial t_1} \Pi_{ij}^{(0)} = \frac{1}{6} \Delta t c^2 \delta_{ij} \varepsilon \frac{\partial \rho}{\partial t_1} = -\frac{1}{6} \Delta t c^2 \delta_{ij} \frac{\partial}{\partial \mathbf{r}} \cdot (\rho \mathbf{u}) \tag{8.87}$$

From this equation, the following equation can be obtained:

$$\frac{\Delta t}{2} \varepsilon \sum_j \frac{\partial}{\partial r_j} \left( \frac{\partial}{\partial t_1} \Pi_{ij}^{(0)} \right) = -\frac{1}{6} \Delta t c^2 \frac{\partial}{\partial r_i} \left\{ \frac{\partial}{\partial \mathbf{r}} \cdot (\rho \mathbf{u}) \right\} \tag{8.88}$$

We next evaluate the quantity  $S_{ijk}^{(0)}$ . First,

$$S_{ijk}^{(0)} = \sum_{\alpha} c_{\alpha i} c_{\alpha j} c_{\alpha k} f_{\alpha}^{(0)} = \sum_{\alpha} w_{\alpha} c_{\alpha i} c_{\alpha j} c_{\alpha k} \rho \left( 1 + 3 \frac{\mathbf{c}_{\alpha} \cdot \mathbf{u}}{c^2} \right) \tag{8.89}$$

With this equation, the partial derivative in Eq. (8.70) is obtained as

$$\begin{aligned} \sum_j \sum_k \frac{\partial}{\partial r_j} \cdot \frac{\partial}{\partial r_k} (S_{ijk}^{(0)}) &= \frac{1}{3} c^2 \sum_j \sum_k \frac{\partial}{\partial r_j} \cdot \frac{\partial}{\partial r_k} (\rho u_k \delta_{ij} + \rho u_j \delta_{ik} + \rho u_i \delta_{jk}) \\ &= \frac{2}{3} c^2 \left\{ \frac{\partial}{\partial r_i} \left( \frac{\partial}{\partial \mathbf{r}} \cdot (\rho \mathbf{u}) \right) + \frac{1}{2} \cdot \frac{\partial^2}{\partial \mathbf{r}^2} (\rho u_i) \right\} \end{aligned} \quad (8.90)$$

We have now finished the preparation for deriving the Navier–Stokes equation. If the summation of the first and second terms, and the summation of the third and fourth terms on the left-hand side in Eq. (8.70), are denoted by  $A$  and  $B$ , respectively, these quantities are evaluated as

$$\begin{aligned} A &= \frac{\partial}{\partial t} (\rho u_i) + \sum_j \frac{\partial}{\partial r_j} (p \delta_{ij} + \rho u_i u_j) - \frac{\Delta t \tau c^2}{3} \left\{ \frac{\partial^2}{\partial \mathbf{r}^2} (\rho u_i) + \frac{\partial}{\partial r_i} \left( \frac{\partial}{\partial \mathbf{r}} \cdot (\rho \mathbf{u}) \right) \right\} \\ &= \frac{\partial}{\partial t} (\rho u_i) + \sum_j \frac{\partial}{\partial r_j} (\rho u_i u_j) + \frac{\partial p}{\partial r_i} - \frac{\Delta t \tau c^2}{3} \left\{ \frac{\partial^2}{\partial \mathbf{r}^2} (\rho u_i) + \frac{\partial}{\partial r_i} \left( \frac{\partial}{\partial \mathbf{r}} \cdot (\rho \mathbf{u}) \right) \right\} \end{aligned} \quad (8.91)$$

$$\begin{aligned} B &= \frac{\Delta t}{2} \varepsilon \sum_j \frac{\partial}{\partial r_j} \left( \frac{\partial}{\partial t_1} \Pi_{ij}^{(0)} \right) + \frac{\Delta t}{2} \sum_j \sum_k \frac{\partial}{\partial r_j} \left( \frac{\partial}{\partial r_k} S_{ijk}^{(0)} \right) \\ &= \frac{1}{6} \Delta t c^2 \left\{ \frac{\partial^2}{\partial \mathbf{r}^2} (\rho u_i) + \frac{\partial}{\partial r_i} \left( \frac{\partial}{\partial \mathbf{r}} \cdot (\rho \mathbf{u}) \right) \right\} \end{aligned} \quad (8.92)$$

By substituting Eqs. (8.91) and (8.92) into Eq. (8.70), together with the relationship of  $\frac{\partial}{\partial \mathbf{r}} \cdot (\rho \mathbf{u}) = 0$  for noncompressible fluids, the Navier–Stokes equation is finally obtained as

$$\rho \left\{ \frac{\partial \mathbf{u}}{\partial t} + (\mathbf{u} \cdot \nabla) \mathbf{u} \right\} = -\nabla p + \mu^{\text{LB}} \nabla^2 \mathbf{u} \quad (8.93)$$

in which  $\mu^{\text{LB}}$  is the viscosity, expressed as

$$\mu^{\text{LB}} = \frac{\rho \Delta t c^2}{3} \left( \tau - \frac{1}{2} \right), \quad \nu^{\text{LB}} = \frac{\mu^{\text{LB}}}{\rho} = \frac{\Delta t c^2}{3} \left( \tau - \frac{1}{2} \right) \quad (8.94)$$

In this equation  $\nu^{\text{LB}}$  is the kinematic viscosity.

### 8.3 Body Force

If a body force, such as the gravitational force, acts on a fluid, how do we incorporate it into the lattice Boltzmann equation? The method can be seen in the following:

$$\left. \begin{aligned} f_\alpha(\mathbf{r} + \mathbf{c}_\alpha \Delta t, t + \Delta t) &= \tilde{f}_\alpha(\mathbf{r}, t) \\ \tilde{f}_\alpha(\mathbf{r}, t) &= f_\alpha(\mathbf{r}, t) + \Omega_\alpha + g_\alpha \end{aligned} \right\} \quad (8.95)$$

in which

$$\Omega_\alpha = \frac{1}{\tau} \{ f_\alpha^{(0)}(\mathbf{r}, t) - f_\alpha(\mathbf{r}, t) \} \quad (8.96)$$

$$g_\alpha = \begin{cases} 0 & \text{for } \alpha = 0 \\ \frac{3\Delta t}{c^2} w_\alpha \mathbf{c}_\alpha \cdot \mathbf{F} & \text{for } \alpha \neq 0 \end{cases} \quad (8.97)$$

$g_\alpha$  is a quantity that is due to the body force  $\mathbf{F}$  per unit volume and has the following characteristics:

$$\left. \begin{aligned} \sum_\alpha g_\alpha &= 0 \\ \sum_\alpha \mathbf{c}_\alpha g_\alpha &= \sum_\alpha \frac{3\Delta t}{c^2} w_\alpha (\mathbf{c}_\alpha \mathbf{c}_\alpha) \cdot \mathbf{F} = \Delta t \mathbf{F} \end{aligned} \right\} \quad (8.98)$$

In this reformation, the following relationship has been used:

$$\sum_\alpha w_\alpha \mathbf{c}_\alpha \mathbf{c}_\alpha = (c^2/3) \mathbf{I} \quad (8.99)$$

in which  $\mathbf{I}$  is the unit tensor, and Eq. (8.99) is valid for both D2Q9 and D3Q19 models. It is quite clear that the quantity  $g_\alpha$  can be expressed in the form of Eq. (8.97), because the particle distribution tends to move in the direction of the body force  $\mathbf{F}$  acting. Therefore, the relationship of the form  $g_\alpha \propto \mathbf{c}_\alpha \cdot \mathbf{F}$  can be expected.

We will now confirm that the  $g_\alpha$ , expressed in Eq. (8.97), appears in a reasonable form in the Navier–Stokes equation by deriving these equations starting from Eq. (8.95), as conducted in Section 8.2. There is no new concept applied here except for the inclusion of the new term  $g_\alpha$  into the derivation procedure shown in Section 8.2; therefore we show only the important expressions.

From Appendix A1, the relationships of the orders  $\varepsilon$  and  $\varepsilon^2$  are written as

$$\left. \begin{aligned} \frac{\partial \rho}{\partial t_1} + \nabla_1 \cdot (\rho \mathbf{u}) &= 0 \\ \frac{\partial}{\partial t_1} (\rho u_i) + \sum_j \frac{\partial}{\partial r_{1j}} \Pi_{ij}^{(0)} &= \frac{1}{\varepsilon} F_i \\ \frac{\partial \rho}{\partial t_2} + \frac{\Delta t}{2} \cdot \frac{\partial^2 \rho}{\partial t_1^2} + \frac{\Delta t}{2} \sum_i \sum_j \frac{\partial}{\partial r_{1i}} \cdot \frac{\partial}{\partial r_{1j}} \Pi_{ij}^{(0)} + \Delta t \sum_i \frac{\partial}{\partial t_1} \cdot \frac{\partial}{\partial r_{1i}} (\rho u_i) &= 0 \end{aligned} \right\} \quad (8.100)$$

$$\begin{aligned} \frac{\partial}{\partial t_2} (\rho u_i) + \frac{\Delta t}{2} \cdot \frac{\partial^2}{\partial t_1^2} (\rho u_i) + \sum_j \frac{\partial}{\partial r_{1j}} \Pi_{ij}^{(1)} + \frac{\Delta t}{2} \sum_j \sum_k \frac{\partial}{\partial r_{1j}} \cdot \frac{\partial}{\partial r_{1k}} S_{ijk}^{(0)} \\ + \Delta t \sum_j \frac{\partial}{\partial t_1} \cdot \frac{\partial}{\partial r_{1j}} \Pi_{ij}^{(0)} &= 0 \end{aligned} \quad (8.101)$$

These expressions lead to the following basic equations:

$$\frac{\partial \rho}{\partial t} + \nabla \cdot (\rho \mathbf{u}) = 0 \quad (8.102)$$

$$\frac{\partial}{\partial t} (\rho u_i) + \sum_j \frac{\partial}{\partial r_j} \Pi_{ij} + \sum_j \frac{\Delta t}{2} \cdot \frac{\partial}{\partial r_j} \left\{ \varepsilon \frac{\partial}{\partial t_1} \Pi_{ij}^{(0)} + \sum_k \frac{\partial}{\partial r_k} S_{ijk}^{(0)} \right\} = F_i \quad (8.103)$$

Also,  $f_\alpha^{(1)}$  is written as

$$\begin{aligned} f_\alpha^{(1)} &= -t\tau\Delta t \left\{ \frac{\partial f_\alpha^{(0)}}{\partial t_1} + \sum_i \frac{\partial}{\partial r_{1i}} (c_{\alpha i} f_\alpha^{(0)}) \right\} + \frac{\tau}{\varepsilon} g_\alpha \\ &= -3w_\alpha \Delta t \frac{1}{c^2} \sum_k \sum_l \left( c_{\alpha k} c_{\alpha l} - \frac{1}{3} c^2 \delta_{kl} \right) \frac{\partial}{\partial r_{1l}} (\rho u_k) \end{aligned} \quad (8.104)$$

Finally, using these expressions in a derivation procedure similar to that used previously, the Navier–Stokes equation is obtained as

$$\rho \left\{ \frac{\partial \mathbf{u}}{\partial t} + (\mathbf{u} \cdot \nabla) \mathbf{u} \right\} = -\nabla p + \mu^{\text{LB}} \nabla^2 \mathbf{u} + \mathbf{F} \quad (8.105)$$

in which  $\mu^{\text{LB}}$  has already been shown in Eq. (8.94). Eq. (8.105) clearly shows that  $g_\alpha$  defined in Eq. (8.97) gives rise to the body force  $\mathbf{F}$  appearing in the appropriate form in the Navier–Stokes equation.

## 8.4 Boundary Conditions

In simulations by the lattice Boltzmann method, it is very important to treat the boundary conditions in an appropriate manner at all the simulation boundary surfaces. Hence, there is a lot of current interest in developing more accurate boundary conditions, and papers addressing this problem have been appearing in academic journals. For example, if we consider a flow inside a tube or around an obstacle, or a suspension composed of solid particles, the treatment of the boundary condition at the wall or particle surface is very important for obtaining reliable solutions of the flow field. In this section, we first explain the historical bounce-back boundary condition, and then focus on several alternative boundary conditions that have a clearer physical and mathematical background.

### 8.4.1 Bounce-back Rule

We explain the historical bounce-back rule [35,36] using Figure 8.4. The lattice position of interest in a fluid is denoted by  $\mathbf{r}_l$ , its neighboring site inside the material by  $\mathbf{r}_p$ , and the point at the material surface on a straight line between these two points by  $\mathbf{r}_w$ , as shown in Figure 8.4. According to the BGK lattice Boltzmann method, the particle distribution  $\tilde{f}_\alpha$  after the collision at time  $t$  becomes that at the neighboring site in the  $\alpha$ -direction at time  $(t + \Delta t)$ . The bounce-back rule employs the following treatment of the collision at the material surface:

$$f_{\bar{\alpha}}(\mathbf{r}_l, t + \Delta t) = \tilde{f}_\alpha(\mathbf{r}_l, t) - 2\rho w_\alpha \frac{\mathbf{u}_w \cdot \mathbf{c}_\alpha}{c_s^2} \quad (8.106)$$

$$f_\alpha(\mathbf{r}_p, t + \Delta t) = \tilde{f}_{\bar{\alpha}}(\mathbf{r}_p, t) + 2\rho w_\alpha \frac{\mathbf{u}_w \cdot \mathbf{c}_\alpha}{c_s^2} \quad (8.107)$$

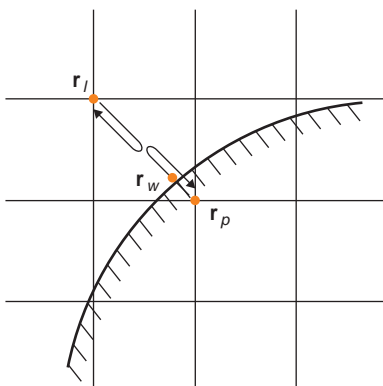


**Figure 8.4** Bounce-back rule for the treatment at the material surface.

in which  $\bar{\alpha}$  implies the opposite direction of  $\alpha$ ;  $\alpha$  is the direction toward the object. Eq. (8.106) means that the fluid particles at  $\mathbf{r} = \mathbf{r}_l$  move in the  $\alpha$ -direction, collide with the obstacle at the middle point of the two lattice points, and return to the original lattice point during  $t$  and  $t + \Delta t$ . In this movement, if the solid surface moves in the  $\alpha$ -direction, the number of the particles returning after the collision decreases, so that the second term on the right-hand side in Eq. (8.106) is necessary to make this modification. The following consideration makes clear that the bounce-back rule does not offer sufficient accuracy. That is, in the treatment of Eq. (8.106), the fluid particles starting from the point  $\mathbf{r}_l$  do not collide with the actual solid surface  $\mathbf{r}_w$ , but at the exact middle point between  $\mathbf{r}_l$  and  $\mathbf{r}_p$ , before returning to the original site. In other words, the collision procedure is conducted under the assumption that the surface of the obstacle is at the middle point between two neighboring lattice sites. In order to improve this approach, various boundary conditions have been developed. Research in this area is still a topic of interest.

Here we consider the validity of the second term on the right-hand side in Eq. (8.106). The consideration of Eqs. (8.82), (8.72), and (A1.11) leads to

$$\tilde{f}_\alpha(\mathbf{r}_l, t) = f_\alpha(\mathbf{r}_l, t) + \frac{1}{\tau} \{ f_\alpha^{(0)}(\mathbf{r}_l, t) - f_\alpha(\mathbf{r}_l, t) \} = f_\alpha(\mathbf{r}_l, t) + \rho \frac{w_\alpha}{c_s^2} \left( \mathbf{c}_\alpha \cdot \frac{\partial \mathbf{u}(\mathbf{r}_l)}{\partial \mathbf{r}} \right) \cdot \mathbf{c}_\alpha \Delta t \quad (8.108)$$

in which a fluid has been assumed to be noncompressive. Substituting this equation into Eq. (8.106) yields

$$\bar{f}_\alpha(\mathbf{r}_l, t + \Delta t) = f_\alpha(\mathbf{r}_l, t) + \rho \frac{w_\alpha}{c_s^2} \left( \mathbf{c}_\alpha \cdot \frac{\partial \mathbf{u}(\mathbf{r}_l)}{\partial \mathbf{r}} \right) \cdot \mathbf{c}_\alpha \Delta t - 2\rho w_\alpha \frac{\mathbf{u}_w \cdot \mathbf{c}_\alpha}{c_s^2} \quad (8.109)$$

If  $f_\alpha(\mathbf{r}_l, t)$  in Eq. (8.109) is assumed to be not far from an equilibrium state, it is approximated from Eq. (8.68) as

$$f_\alpha(\mathbf{r}_l, t) \approx \bar{f}_\alpha(\mathbf{r}_l, t) + 2\rho w_\alpha \frac{\mathbf{u}(\mathbf{r}_l) \cdot \mathbf{c}_\alpha}{c_s^2} \quad (8.110)$$

Substituting this equation into Eq. (8.109) gives rise to

$$\begin{aligned} \bar{f}_\alpha(\mathbf{r}_l, t + \Delta t) &= \bar{f}_\alpha(\mathbf{r}_l, t) + \frac{2\rho w_\alpha}{c_s^2} \left[ \left\{ \mathbf{u}(\mathbf{r}_l) + \frac{\partial \mathbf{u}(\mathbf{r}_l)}{\partial \mathbf{r}} \cdot \frac{\Delta t}{2} \mathbf{c}_\alpha \right\} - \mathbf{u}_w \right] \cdot \mathbf{c}_\alpha \\ &\approx \bar{f}_\alpha(\mathbf{r}_l, t) + \frac{2\rho w_\alpha}{c_s^2} \{ \mathbf{u}(\mathbf{r}_l + (1/2)\mathbf{c}_\alpha \Delta t) - \mathbf{u}_w \} \cdot \mathbf{c}_\alpha \end{aligned} \quad (8.111)$$

It is seen from Eq. (8.111) that  $\mathbf{u}(\mathbf{r}_l + (1/2)\mathbf{c}_\alpha \Delta t)$  is equal to  $\mathbf{u}_w$ , if the medium point  $(\mathbf{r}_l + (1/2)\mathbf{c}_\alpha \Delta t)$  is sufficiently near to the solid surface. Hence, we obtain the result  $\bar{f}_\alpha(\mathbf{r}_l, t + \Delta t) = \bar{f}_\alpha(\mathbf{r}_l, t)$ . That is, the particle distribution in the direction away from

the solid surface approximates to the equilibrium distribution and is independent of time.

### 8.4.2 BFL Method

In this subsection we explain the BFL method [37]. In the bounce-back rule, the solid surface is regarded as being at the middle point of two lattice sites, and virtual fluid particles are reflected at this point. Hence, the exact position of the solid surface is not employed in the bounce-back method. The BFL method attempts to improve this drawback by taking into account the exact position of the solid surface in the procedure of the collision process between virtual fluid particles and the material. As shown in Figure 8.5,  $\mathbf{r}_l$  is the point of interest in a fluid,  $\mathbf{r}_p$  is the neighboring point inside the particle,  $\mathbf{r}_w$  is the point at the solid surface on a line between these two points, and  $\mathbf{r}_l'$  is the next neighboring point in the direction away from the solid surface. The exact position of the solid surface can be expressed using the quantity  $\Delta_w = |\mathbf{r}_l - \mathbf{r}_w|/|\mathbf{r}_l - \mathbf{r}_p|$ ; although the lattice separation is defined to be  $\Delta x$ , we regarded  $\Delta x$  as unity in Sections 8.4.2 and 8.4.3 for simplicity's sake, because the final results derived here are unaffected even if  $\Delta x$  is not unity. The solid surface is at the position which is away from  $\mathbf{r}_l$  in the direction toward  $\mathbf{r}_p$  determined by  $\Delta_w$ , as shown in Figure 8.5. The BFL method is based on an interpolation but, so as not to lose the accuracy of the interpolation, two different procedures are adopted for  $\Delta_w \leq 1/2$  and  $\Delta_w > 1/2$ , although the concept of the treatment is the same for both cases. The fundamental concept is that fluid particles move, collide with the solid material, and return to a certain point during the time interval  $\Delta t$ . Since the unit lattice length is assumed in this analysis, the transportation distance is unity. In this collision process, the exact position of the solid surface is necessary. In the following text, the treatment for  $\Delta_w \leq 1/2$  is discussed first.

As shown in Figure 8.5A, in the case of  $\Delta_w \leq 1/2$ , the particle distribution function  $\tilde{f}_\alpha(\mathbf{r}_m, t)$  at  $\mathbf{r}_m$  becomes that at  $\mathbf{r}_l$ ,  $f_\alpha(\mathbf{r}_l, t + \Delta t)$ , in which the point  $\mathbf{r}_m$  is evaluated such that fluid particles move in the  $\alpha$ -direction, collide with the solid surface, and arrive at the lattice point  $\mathbf{r}_l$ ; the distance of travel for a fluid particle is just unity. The point  $\mathbf{r}_m$  can be obtained straightforwardly as the position away from  $\mathbf{r}_l$

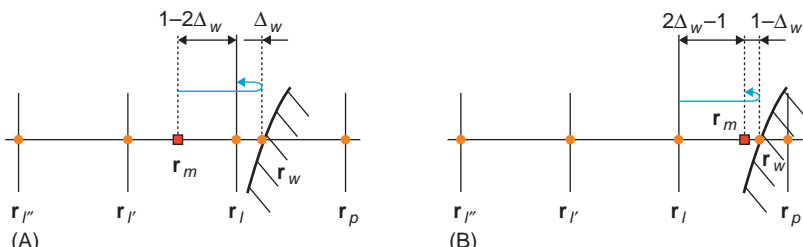


**Figure 8.5** BFL method for the treatment at the material surface.

at the distance of  $(1 - 2\Delta_w)$ , shown in Figure 8.5A. Hence, the particle distribution function  $\tilde{f}_\alpha(\mathbf{r}_m, t)$  is easily obtained from the quadratic extrapolation procedure as

$$\tilde{f}_\alpha(\mathbf{r}_m, t) = \Delta_w(1 + 2\Delta_w)\tilde{f}_\alpha(\mathbf{r}_l, t) + (1 - 4\Delta_w^2)\tilde{f}_\alpha(\mathbf{r}_{l'}, t) - \Delta_w(1 - 2\Delta_w)\tilde{f}_\alpha(\mathbf{r}_{l''}, t) \quad (8.112)$$

Since fluid particles collide with the solid surface,  $f_{\bar{\alpha}}(\mathbf{r}_l, t + \Delta t)$  can finally be obtained as

$$f_{\bar{\alpha}}(\mathbf{r}_l, t + \Delta t) = \tilde{f}_\alpha(\mathbf{r}_m, t) - 2\rho w_\alpha \frac{\mathbf{u}_w \cdot \mathbf{c}_\alpha}{c_s^2} \quad (8.113)$$

Equation (8.112) has been obtained from the following formula of the quadratic interpolation method. If an arbitrary function  $h(x)$  has values  $h(x_1)$ ,  $h(x_2)$ , and  $h(x_3)$  for  $x = x_1$ ,  $x_2$ , and  $x_3$ , respectively,  $h(x)$  at an arbitrary position  $x$  between  $x_1$  and  $x_3$  can be given from the quadratic interpolation as

$$h(x) = \frac{(x - x_2)(x - x_3)}{(x_1 - x_2)(x_1 - x_3)}h(x_1) + \frac{(x - x_1)(x - x_3)}{(x_2 - x_1)(x_2 - x_3)}h(x_2) + \frac{(x - x_1)(x - x_2)}{(x_3 - x_1)(x_3 - x_2)}h(x_3) \quad (8.114)$$

We now consider the treatment for  $\Delta_w > 1/2$ . As shown in Figure 8.5B, fluid particles leaving the lattice point  $\mathbf{r}_l$  collide with the object, and return to the position  $\mathbf{r}_m$  between  $\mathbf{r}_l$  and  $\mathbf{r}_w$ . Hence, the following relationship is satisfied:

$$f_{\bar{\alpha}}(\mathbf{r}_m, t + \Delta t) = \tilde{f}_\alpha(\mathbf{r}_l, t) - 2\rho w_\alpha \frac{\mathbf{u}_w \cdot \mathbf{c}_\alpha}{c_s^2} \quad (8.115)$$

With this expression, the particle distribution function  $f_{\bar{\alpha}}(\mathbf{r}_l, t + \Delta t)$  can be evaluated from the interpolation procedure based on a quadratic curve using values at  $\mathbf{r}_m$ ,  $\mathbf{r}_{l'}$ , and  $\mathbf{r}_{l''}$ :

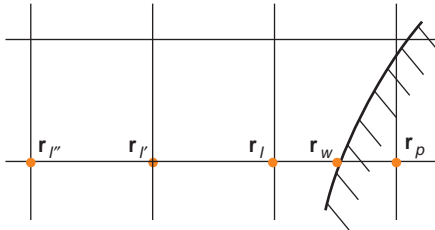
$$\begin{aligned} f_{\bar{\alpha}}(\mathbf{r}_l, t + \Delta t) &= \frac{1}{\Delta_w(2\Delta_w + 1)}\tilde{f}_\alpha(\mathbf{r}_l, t) + \frac{2\Delta_w - 1}{\Delta_w}\tilde{f}_{\bar{\alpha}}(\mathbf{r}_l, t) \\ &\quad + \frac{1 - 2\Delta_w}{1 + 2\Delta_w}\tilde{f}_{\bar{\alpha}}(\mathbf{r}_{l'}, t) - \frac{1}{\Delta_w(2\Delta_w + 1)}2\rho w_\alpha \frac{\mathbf{u}_w \cdot \mathbf{c}_\alpha}{c_s^2} \end{aligned} \quad (8.116)$$

We call the method using Eqs. (8.112), (8.113), (8.115), and (8.116) the “quadratic BFL method.”

Instead of the quadratic interpolation procedure, the linear interpolation method is also applicable, and in this case each procedure for  $\Delta_w \leq 1/2$  and  $\Delta_w > 1/2$  can be expressed as

$$\Delta_w \leq 1/2:$$

$$f_{\bar{\alpha}}(\mathbf{r}_l, t + \Delta t) = (1 - 2\Delta_w)\tilde{f}_\alpha(\mathbf{r}_{l'}, t) + 2\Delta_w\tilde{f}_\alpha(\mathbf{r}_l, t) - 2\rho w_\alpha \frac{\mathbf{u}_w \cdot \mathbf{c}_\alpha}{c_s^2} \quad (8.117)$$

**Figure 8.6** YMLS method.

$$\Delta_w > 1/2:$$

$$f_{\bar{\alpha}}(\mathbf{r}_l, t + \Delta t) = \frac{2\Delta_w - 1}{2\Delta_w} \tilde{f}_{\bar{\alpha}}(\mathbf{r}_l, t) + \frac{1}{2\Delta_w} \tilde{f}_{\alpha}(\mathbf{r}_l, t) - \frac{1}{2\Delta_w} 2\rho w_{\alpha} \frac{\mathbf{u}_w \cdot \mathbf{c}_{\alpha}}{c_s^2} \quad (8.118)$$

We call this scheme the “linear BFL method.”

### 8.4.3 YMLS Method

In this subsection, we explain the YMLS method [34] using Figure 8.6. This method is also based on an interpolation scheme. The distribution function  $\tilde{f}_{\alpha}(\mathbf{r}_m, t)$  at the position  $\mathbf{r}_m$ , from which fluid particles start and arrive at  $\mathbf{r}_w$  after the time interval  $\Delta t$ , is used for the interpolation procedure. The particle distribution  $f_{\bar{\alpha}}(\mathbf{r}_l, t + \Delta t)$  in the  $\bar{\alpha}$ -direction away from the material surface can be obtained from the interpolation using the distribution  $\tilde{f}_{\alpha}(\mathbf{r}_m, t)$ . As shown in Figure 8.6, with the notation of the point  $\mathbf{r}_p$  inside the material, and the points  $\mathbf{r}_l$ ,  $\mathbf{r}_{l'}$ , and  $\mathbf{r}_{l''}$  on the fluid side away from the solid surface, the particle distribution functions at the solid surface in the  $\alpha$ - and  $\bar{\alpha}$ -directions are written, respectively, as

$$f_{\alpha}(\mathbf{r}_w, t + \Delta t) = (1 - \Delta_w) \tilde{f}_{\alpha}(\mathbf{r}_{l'}, t) + \Delta_w \tilde{f}_{\alpha}(\mathbf{r}_l, t) \quad (8.119)$$

$$f_{\bar{\alpha}}(\mathbf{r}_w, t + \Delta t) = f_{\alpha}(\mathbf{r}_w, t + \Delta t) - 2\rho w_{\alpha} \frac{\mathbf{u}_w \cdot \mathbf{c}_{\alpha}}{c_s^2} \quad (8.120)$$

in which  $\Delta_w = |\mathbf{r}_l - \mathbf{r}_w| / |\mathbf{r}_l - \mathbf{r}_p|$ , as previously defined. Eq. (8.119) implies that  $f_{\alpha}(\mathbf{r}_w, t + \Delta t)$  is obtained from the interpolation procedure using  $\tilde{f}_{\alpha}(\mathbf{r}_{l'}, t)$  and  $\tilde{f}_{\alpha}(\mathbf{r}_l, t)$ , and Eq. (8.120) means that fluid particles are reflected at the solid surface. If  $f_{\bar{\alpha}}(\mathbf{r}_w, t + \Delta t)$ ,  $f_{\bar{\alpha}}(\mathbf{r}_{l'}, t + \Delta t)$ , and  $f_{\bar{\alpha}}(\mathbf{r}_{l''}, t + \Delta t)$  are used, then  $f_{\bar{\alpha}}(\mathbf{r}_l, t + \Delta t)$  can be obtained from the quadratic interpolation procedure as

$$f_{\bar{\alpha}}(\mathbf{r}_l, t + \Delta t) = \frac{2}{(1 + \Delta_w)(2 + \Delta_w)} f_{\bar{\alpha}}(\mathbf{r}_w, t + \Delta t) + \frac{2\Delta_w}{1 + \Delta_w} f_{\bar{\alpha}}(\mathbf{r}_{l'}, t + \Delta t) - \frac{\Delta_w}{2 + \Delta_w} f_{\bar{\alpha}}(\mathbf{r}_{l''}, t + \Delta t) \quad (8.121)$$

This is known as the quadratic YMLS method.

The linear interpolation procedure yields the following linear YMLS method instead of Eq. (8.121):

$$f_{\bar{\alpha}}(\mathbf{r}_l, t + \Delta t) = \frac{\Delta_w}{1 + \Delta_w} f_{\bar{\alpha}}(\mathbf{r}_l, t + \Delta t) + \frac{1}{1 + \Delta_w} f_{\bar{\alpha}}(\mathbf{r}_w, t + \Delta t) \quad (8.122)$$

in which  $f_{\bar{\alpha}}(\mathbf{r}_w, t + \Delta t)$  is evaluated from Eq. (8.120). In this method,  $f_{\bar{\alpha}}(\mathbf{r}_l, t + \Delta t)$  can be obtained from the interpolation scheme using  $f_{\bar{\alpha}}(\mathbf{r}_l, t + \Delta t)$  in the fluid region and  $f_{\bar{\alpha}}(\mathbf{r}_w, t + \Delta t)$  at the solid surface. In the linear YMLS method, only two lattice points are used for the interpolation procedure, so that it may be suitable for particle dispersions in which a near-contact situation of dispersed particles frequently arises.

#### 8.4.4 Other Methods

As in the MD or the MC simulations, the periodic boundary condition is applicable for the thermodynamic equilibrium case. For this case, the particle distribution function at the point  $\mathbf{r}_{\text{out}}$  of the fluid particles outgoing from the simulation box,  $f_{\alpha}(\mathbf{r}_{\text{out}}, t + \Delta t)$ , is made to equal to that at the point  $\mathbf{r}_{\text{in}}$  of the incoming fluid particles,  $f_{\alpha}(\mathbf{r}_{\text{in}}, t + \Delta t)$ .

Finally, we explain the extrapolation boundary condition, which is usually used for numerical simulations based on the finite difference or finite element method for a flow past an obstacle. The extrapolation boundary condition is also applicable to lattice Boltzmann simulations, for which the distribution functions at the points  $\mathbf{r}_N$ ,  $\mathbf{r}_{N-1}$ ,  $\mathbf{r}_{N-2}$ , which are taken from the boundary surface into the simulation region, are assumed to be in the linear relationship

$$f_{\bar{\alpha}}(\mathbf{r}_N, t + \Delta t) = 2f_{\bar{\alpha}}(\mathbf{r}_{N-1}, t + \Delta t) - f_{\bar{\alpha}}(\mathbf{r}_{N-2}, t + \Delta t) \quad (8.123)$$

in which  $\bar{\alpha}$  is in the direction leaving the outer boundary toward the simulation region. If the zero-gradient condition is applicable, then the differential away from the boundary is regarded as zero: that is,  $f_{\bar{\alpha}}(\mathbf{r}_N, t + \Delta t) = f_{\bar{\alpha}}(\mathbf{r}_{N-1}, t + \Delta t)$ . This boundary condition can be used for lattice points that are physically symmetric. If a simulation region is taken to be sufficiently large, the zero-gradient condition may be expected to give rise to results that are reasonably accurate.

## 8.5 Force and Torque Acting on Particles

In the case of a suspension composed of spherical or rod-like particles, the forces and torques acting on the suspended particles need to be evaluated in order to solve the particle motion and the flow field around the suspended particles simultaneously. The momentum change of the fluid particles that collide with the particle surface and are reflected during the time interval  $\Delta t$  is equal to the impulse acting

on the particle. Hence, the force  $\mathbf{F}_\alpha$  acting on the particle in the  $\alpha$ -direction is obtained as

$$\mathbf{F}_\alpha(t + \Delta t/2) = \mathbf{c}_\alpha \left\{ f_{\bar{\alpha}}(\mathbf{r}_l^{(\text{int})}, t + \Delta t) + \tilde{f}_\alpha(\mathbf{r}_l^{(\text{int})}, t) \right\} \frac{\Delta V}{\Delta t} \quad (8.124)$$

in which  $\Delta V$  is the volume occupied by one lattice site. Hence, the force  $\mathbf{F}_p$  and torque  $\mathbf{T}_p$  acting on the mass center of the particle are obtained from summing the contributions from the neighboring lattice sites of the particle as

$$\mathbf{F}_p(t + \Delta t/2) = \sum_{\text{all } \mathbf{r}_l^{(\text{int})}} \sum_\alpha \frac{\Delta V}{\Delta t} \left\{ f_{\bar{\alpha}}(\mathbf{r}_l^{(\text{int})}, t + \Delta t) + \tilde{f}_\alpha(\mathbf{r}_l^{(\text{int})}, t) \right\} \mathbf{c}_\alpha \quad (8.125)$$

$$\mathbf{T}_p(t + \Delta t/2) = \sum_{\text{all } \mathbf{r}_l^{(\text{int})}} \sum_\alpha (\mathbf{r}_w - \mathbf{r}_c) \times \frac{\Delta V}{\Delta t} \left\{ f_{\bar{\alpha}}(\mathbf{r}_l^{(\text{int})}, t + \Delta t) + \tilde{f}_\alpha(\mathbf{r}_l^{(\text{int})}, t) \right\} \mathbf{c}_\alpha \quad (8.126)$$

in which  $\mathbf{r}_c$  is the position vector of the particle mass center, and  $\mathbf{r}_w$  is the position vector at the particle surface on a line drawn in the  $\alpha$ -direction from the lattice point  $\mathbf{r}_l^{(\text{int})}$  in the liquid region. The summation concerning  $\alpha$  is only performed for the directions along which the above-mentioned line crosses the particle surface. Given the force and the torque from Eqs. (8.125) and (8.126), the translational and angular velocities  $\mathbf{u}_p$  and  $\boldsymbol{\Omega}_p$  of an arbitrary particle  $p$  with mass  $M_p$  and inertia moment  $I_p$  can be evaluated as

$$\left. \begin{aligned} \mathbf{u}_p(t + \Delta t) &= \mathbf{u}_p(t) + \frac{\Delta t}{M_p} \mathbf{F}_p(t + \Delta t/2) \\ \boldsymbol{\Omega}_p(t + \Delta t) &= \boldsymbol{\Omega}_p(t) + \frac{\Delta t}{I_p} \mathbf{T}_p(t + \Delta t/2) \end{aligned} \right\} \quad (8.127)$$

Note that here we have treated the case of the axisymmetric particle; therefore, only the inertia moment appears in the equation and not the inertia tensor.

## 8.6 Nondimensionalization

Finally, we show the usual nondimensionalization method used in lattice Boltzmann simulations. The following representative quantities are used in nondimensionalizing each quantity:  $\Delta x$  for distances,  $\Delta t$  for time,  $c$  ( $= \Delta x/\Delta t$ ) for velocities,  $\rho_0$  for the particle distribution,  $\rho_0(\Delta x)^2 \Delta x / (\Delta t)^2$  for forces,  $(\Delta x)^2 / \Delta t$  for kinematic viscosity, and  $\rho_0(\Delta x/\Delta t)^2$  for pressures in the case of a two-dimensional system. Nondimensional equations are obtained by expressing a dimensional quantity as the product of the corresponding representative and nondimensional quantity

—for example,  $f_\alpha = \rho_0 \times f_\alpha^*$ —and substituting such quantities into the dimensional equations. Since the derivation procedure is quite straightforward, only the final results are shown in the following equations:

$$f_\alpha^*(\mathbf{r}^* + \mathbf{c}_\alpha^*, t^* + 1) = \tilde{f}_\alpha^*(\mathbf{r}^*, t^*) \quad (8.128)$$

$$\tilde{f}_\alpha^*(\mathbf{r}^*, t^*) = f_\alpha^*(\mathbf{r}^*, t^*) + \frac{1}{\tau} \{ f_\alpha^{(0)*}(\mathbf{r}^*, t^*) - f_\alpha^*(\mathbf{r}^*, t^*) \} \quad (8.129)$$

in which

$$f_\alpha^{(0)*}(\mathbf{r}^*, t^*) = w_\alpha \rho^* \left\{ 1 + 3\mathbf{c}_\alpha^* \cdot \mathbf{u}^* + \frac{9}{2} (\mathbf{c}_\alpha^* \cdot \mathbf{u}^*)^2 - \frac{3}{2} u^{*2} \right\} \quad (8.130)$$

$$c^* = 1, \quad c_s^* = 1/\sqrt{3}, \quad \nu^* = (2\tau - 1)/6, \quad p^* = \rho^* c_s^{*2} \quad (8.131)$$

In these equations, the superscript \* indicates the nondimensional quantities.

# Appendix 1: Chapman–Enskog Expansion

In this appendix, we derive the important equations which are the starting expressions for deriving the Navier–Stokes equation, by means of the Chapman–Enskog expansion [38].

The basic equations required in the derivation are as follows:

$$\rho(\mathbf{r}, t) = \sum_{\alpha} f_{\alpha}(\mathbf{r}, t) \quad (\text{A1.1})$$

$$\rho(\mathbf{r}, t)\mathbf{u}(\mathbf{r}, t) = \sum_{\alpha} \mathbf{c}_{\alpha} f_{\alpha}(\mathbf{r}, t) \quad (\text{A1.2})$$

$$\Pi_{ij} = \sum_{\alpha} c_{\alpha i} c_{\alpha j} f_{\alpha}(\mathbf{r}, t) \quad (\text{A1.3})$$

$$f_{\alpha}(\mathbf{r} + \mathbf{c}_{\alpha} \Delta t, t + \Delta t) = f_{\alpha}(\mathbf{r}, t) + \Omega_{\alpha}(\mathbf{r}, t) \quad (\text{A1.4})$$

$$\Omega_{\alpha}(\mathbf{r}, t) = \frac{1}{\tau} \{ f_{\alpha}^{(0)}(\mathbf{r}, t) - f_{\alpha}(\mathbf{r}, t) \} \quad (\text{A1.5})$$

Note that the following derivation is valid for both D2Q9 and D3Q19 models, except that  $\alpha$  has to be taken as  $\alpha = 0, 1, \dots, 8$  and  $\alpha = 0, 1, \dots, 16$ , respectively.

A Taylor series expansion of the left-hand side of Eq. (A1.4) gives rise to

$$\begin{aligned} \Delta t \frac{\partial f_{\alpha}}{\partial t} + \frac{(\Delta t)^2}{2} \cdot \frac{\partial^2 f_{\alpha}}{\partial t^2} + \Delta t (\mathbf{c}_{\alpha} \cdot \nabla) f_{\alpha} + \frac{(\Delta t)^2}{2} (\mathbf{c}_{\alpha} \cdot \nabla)(\mathbf{c}_{\alpha} \cdot \nabla) f_{\alpha} \\ + (\Delta t)^2 (\mathbf{c}_{\alpha} \cdot \nabla) \frac{\partial f_{\alpha}}{\partial t} = \frac{1}{\tau} (f_{\alpha}^{(0)} - f_{\alpha}) \end{aligned} \quad (\text{A1.6})$$

The particle distribution function is expanded using the infinitesimal small quantity  $\varepsilon$  as

$$f_{\alpha} = f_{\alpha}^{(0)} + \varepsilon f_{\alpha}^{(1)} + \varepsilon^2 f_{\alpha}^{(2)} + \dots \quad (\text{A1.7})$$

By substituting Eq. (A1.7) into Eqs. (A1.1) and (A1.2), the following relationships are obtained:

$$\sum_{\alpha} f_{\alpha}^{(0)} = \rho, \quad \sum_{\alpha} \mathbf{c}_{\alpha} f_{\alpha}^{(0)} = \rho \mathbf{u} \quad (\text{A1.8})$$

$$\sum_{\alpha} f_{\alpha}^{(n)} = 0, \quad \sum_{\alpha} \mathbf{c}_{\alpha} f_{\alpha}^{(n)} = 0 \quad \text{for } n = 1, 2, \dots \quad (\text{A1.9})$$

Next, we consider the Chapman–Enskog expansion. There are two characteristic times employed in characterizing fluid problems:  $T_1$  relating to the fluid velocity, and  $T_2$  relating to the viscous dissipation. It is generally satisfied that  $T_2$  is much longer than  $T_1$  (i.e.,  $T_2 \gg T_1$ ). Hence, if the infinitesimal quantities  $\varepsilon$  and  $\Delta t$  are taken as  $\Delta t/T_1 = O(\varepsilon)$ ,  $T_2$  satisfies the relationship of  $\Delta t/T_2 = O(\varepsilon^2)$ . On the other hand, if the representative distance is denoted by  $L_1$ , the distance  $\Delta x$  is generally taken such that  $\Delta x/L_1 = O(\varepsilon)$ . With these assumptions, the time derivative is regarded as the summation of the time derivations due to the characteristics of  $T_1$  and  $T_2$ . That is,

$$\frac{\partial}{\partial t} = \varepsilon \frac{\partial}{\partial t_1} + \varepsilon^2 \frac{\partial}{\partial t_2} \quad (\text{A1.10})$$

Similarly, the position derivative  $\partial/\partial \mathbf{r}$  is expressed, for the three-dimensional position  $\mathbf{r} = (r_x, r_y, r_z)$ , as

$$\frac{\partial}{\partial r_i} = \varepsilon \frac{\partial}{\partial r_{1i}} \quad (i = x, y, z) \quad (\text{A1.11})$$

The expressions in Eqs. (A1.10) and (A1.11) imply that the original variables  $(t, \mathbf{r})$  can be transformed into the new ones  $(t_1, t_2, \mathbf{r}_1)$ . In the usual approach, the differentiated quantities are used for comparing the magnitudes of all the terms in an equation. That is, the magnitudes of, for example,  $\partial g_1/\partial t$  and  $\partial g_2/\partial t$  are evaluated in such a way that  $\partial g_1/\partial t = O(\varepsilon)$  and  $\partial g_2/\partial t = O(\varepsilon^2)$ , and they are compared with each other to neglect the smaller terms such as  $\partial g_2/\partial t = O(\varepsilon^2)$ . In contrast, according to the Chapman–Enskog expansion,  $\partial g_1/\partial t$  and  $\partial g_2/\partial t$  are of the same order of magnitude but are moderated by the infinitesimal parameter  $\varepsilon$  and written as  $\varepsilon \partial g_1/\partial t$  and  $\varepsilon^2 \partial g_2/\partial t$  in an equation.

We are now ready to proceed to the important equations in the derivation of the Navier–Stokes equation by means of the Chapman–Enskog expansion. The collision term in Eq. (A1.5) has the following characteristics:

$$\sum_{\alpha} \Omega_{\alpha} = 0, \quad \sum_{\alpha} \mathbf{c}_{\alpha} \Omega_{\alpha} = 0 \quad (\text{A1.12})$$

From Eqs. (A1.6), (A1.10) and (A1.11),

$$\begin{aligned} \Delta t \left\{ \varepsilon \frac{\partial f_\alpha}{\partial t_1} + \varepsilon^2 \frac{\partial f_\alpha}{\partial t_2} \right\} + (\Delta t)^2 \frac{\varepsilon^2}{2} \cdot \frac{\partial^2 f_\alpha}{\partial t_1^2} + \Delta t \varepsilon (\mathbf{c}_\alpha \cdot \nabla_1) f_\alpha \\ + (\Delta t)^2 \frac{\varepsilon^2}{2} (\mathbf{c}_\alpha \cdot \nabla_1) (\mathbf{c}_\alpha \cdot \nabla_1) f_\alpha + (\Delta t)^2 \varepsilon^2 (\mathbf{c}_\alpha \cdot \nabla_1) \frac{\partial f_\alpha}{\partial t_1} + O(\varepsilon^3) = \Omega_\alpha \end{aligned} \quad (A1.13)$$

By multiplying  $\mathbf{c}_\alpha$  on both sides of this equation,

$$\begin{aligned} \Delta t \left\{ \varepsilon \mathbf{c}_\alpha \frac{\partial f_\alpha}{\partial t_1} + \varepsilon^2 \mathbf{c}_\alpha \frac{\partial f_\alpha}{\partial t_2} \right\} + (\Delta t)^2 \frac{\varepsilon^2}{2} \mathbf{c}_\alpha \frac{\partial^2 f_\alpha}{\partial t_1^2} + \Delta t \varepsilon \mathbf{c}_\alpha (\mathbf{c}_\alpha \cdot \nabla_1) f_\alpha \\ + (\Delta t)^2 \frac{\varepsilon^2}{2} \mathbf{c}_\alpha (\mathbf{c}_\alpha \cdot \nabla_1) (\mathbf{c}_\alpha \cdot \nabla_1) f_\alpha + (\Delta t)^2 \varepsilon^2 \mathbf{c}_\alpha (\mathbf{c}_\alpha \cdot \nabla_1) \frac{\partial f_\alpha}{\partial t_1} + O(\varepsilon^3) = \mathbf{c}_\alpha \Omega_\alpha \end{aligned} \quad (A1.14)$$

Equation (A1.7) is substituted into Eq. (A1.13), the summation of  $\alpha$  is conducted on the both sides, and the terms of the order  $\varepsilon$  are collected. Then, taking these collected terms equal to zero finally yields

$$\sum_{\alpha} \left\{ \Delta t \frac{\partial f_\alpha^{(0)}}{\partial t_1} + \Delta t (\mathbf{c}_\alpha \cdot \nabla_1) f_\alpha^{(0)} \right\} = 0 \quad (A1.15)$$

Similarly, from Eq. (A1.14),

$$\sum_{\alpha} \left\{ \Delta t \frac{\partial}{\partial t_1} (c_{\alpha i} f_\alpha^{(0)}) + \Delta t \sum_j c_{\alpha i} c_{\alpha j} \frac{\partial}{\partial r_{1j}} f_\alpha^{(0)} \right\} = 0 \quad (A1.16)$$

With Eqs. (A1.8) and (A1.3), Eqs. (A1.15) and (A1.16) become

$$\frac{\partial}{\partial t_1} \rho + \nabla_1 \cdot (\rho \mathbf{u}) = 0 \quad (A1.17)$$

$$\frac{\partial}{\partial t_1} (\rho u_i) + \sum_j \frac{\partial}{\partial r_{1j}} (\Pi_{ij}^{(0)}) = 0 \quad (A1.18)$$

in which  $\Pi_{ij}^{(0)} = \sum_{\alpha} c_{\alpha i} c_{\alpha j} f_\alpha^{(0)}$ .

Returning to the substitution of Eq. (A1.7) into Eq. (A1.13), but now taking the collected terms of the order  $\varepsilon^2$  equal to zero, the following expression is derived:

$$\begin{aligned} \frac{\partial \rho}{\partial t_2} + \frac{\Delta t}{2} \cdot \frac{\partial^2 \rho}{\partial t_1^2} + \frac{\Delta t}{2} \sum_i \sum_j \frac{\partial}{\partial r_{1i}} \cdot \frac{\partial}{\partial r_{1j}} \Pi_{ij}^{(0)} + \Delta t \sum_i \frac{\partial}{\partial t_1} \cdot \frac{\partial}{\partial r_{1i}} (\rho u_i) = 0 \end{aligned} \quad (A1.19)$$

Similarly, returning to the derivation of Eq. (A1.16) and taking the collected terms of the order  $\varepsilon^2$  equal to zero yields

$$\begin{aligned} \frac{\partial}{\partial t_2}(\rho u_i) + \frac{\Delta t}{2} \cdot \frac{\partial^2}{\partial t_1^2}(\rho u_i) + \sum_j \frac{\partial}{\partial r_{1j}} \Pi_{ij}^{(1)} \\ + \frac{\Delta t}{2} \sum_j \sum_k \frac{\partial}{\partial r_{1j}} \cdot \frac{\partial}{\partial r_{1k}} S_{ijk}^{(0)} + \Delta t \sum_j \frac{\partial}{\partial t_1} \cdot \frac{\partial}{\partial r_{1j}} \Pi_{ij}^{(0)} = 0 \end{aligned} \quad (\text{A1.20})$$

in which  $\Pi_{ij}^{(1)} = \sum_\alpha c_{\alpha i} c_{\alpha j} f_\alpha^{(1)}$  and  $S_{ijk}^{(0)} = \sum_\alpha c_{\alpha i} c_{\alpha j} c_{\alpha k} f_\alpha^{(0)}$ .

Next, we reform Eqs. (A1.19) and (A1.20). Differentiating Eq. (A1.17) with respect to  $t_1$  yields

$$\frac{\partial^2 \rho}{\partial t_1^2} = \frac{\partial}{\partial t_1} \left\{ -\nabla_1 \cdot (\rho \mathbf{u}) \right\} = -\frac{\partial}{\partial t_1} \left\{ \sum_i \frac{\partial}{\partial r_{1i}} (\rho u_i) \right\} \quad (\text{A1.21})$$

With this result, Eq. (A1.19) is reformed and finally obtained as

$$\frac{\partial \rho}{\partial t_2} + \frac{\Delta t}{2} \sum_i \frac{\partial}{\partial r_{1i}} \left\{ \frac{\partial}{\partial t_1} (\rho u_i) + \sum_j \frac{\partial}{\partial r_{1j}} \Pi_{ij}^{(0)} \right\} = 0 \quad (\text{A1.22})$$

With Eq. (A1.18), Eq. (A1.22) reduces to

$$\frac{\partial \rho}{\partial t_2} = 0 \quad (\text{A1.23})$$

Differentiating Eq. (A1.18) with respect to  $t_1$  gives rise to

$$\frac{\partial^2}{\partial t_1^2} (\rho u_i) = \frac{\partial}{\partial t_1} \left\{ -\sum_j \frac{\partial}{\partial r_{1j}} \Pi_{ij}^{(0)} \right\} = -\sum_j \frac{\partial}{\partial t_1} \cdot \frac{\partial}{\partial r_{1j}} \Pi_{ij}^{(0)} \quad (\text{A1.24})$$

By substituting this result into Eq. (A1.20), the following equation is obtained:

$$\frac{\partial}{\partial t_2} (\rho u_i) + \sum_j \frac{\partial}{\partial r_{1j}} \left[ \Pi_{ij}^{(1)} + \frac{\Delta t}{2} \left\{ \frac{\partial}{\partial t_1} \Pi_{ij}^{(0)} + \sum_k \frac{\partial}{\partial r_{1k}} S_{ijk}^{(0)} \right\} \right] = 0 \quad (\text{A1.25})$$

If Eqs. (A1.17) and (A1.23) are multiplied by  $\varepsilon$  and  $\varepsilon^2$ , respectively, summing each side of these equations, and taking into account Eq. (A1.10), the following mass conservation law is obtained:

$$\frac{\partial \rho}{\partial t} + \nabla \cdot (\rho \mathbf{u}) = 0 \quad (\text{A1.26})$$

From a similar manipulation of Eqs. (A1.18) and (A1.25), the momentum conservation law is obtained as

$$\frac{\partial}{\partial t}(\rho u_i) + \sum_j \frac{\partial}{\partial r_j} \Pi_{ij} + \sum_j \frac{\Delta t}{2} \cdot \frac{\partial}{\partial r_j} \left\{ \varepsilon \frac{\partial}{\partial t_1} \Pi_{ij}^{(0)} + \sum_k \frac{\partial}{\partial r_k} S_{ijk}^{(0)} \right\} = 0 \quad (\text{A1.27})$$

in which  $\Pi_{ij} \approx \Pi_{ij}^{(0)} + \varepsilon \Pi_{ij}^{(1)}$ .

Finally, we derive another important equation. The variable transformation of Eqs. (A1.10) and (A1.11) is conducted for Eq. (A1.6) to give

$$\begin{aligned} \Delta t \left\{ \varepsilon \frac{\partial f_\alpha}{\partial t_1} + \varepsilon^2 \frac{\partial f_\alpha}{\partial t_2} \right\} + \frac{(\Delta t)^2}{2} \varepsilon^2 \frac{\partial^2 f_\alpha}{\partial t_1^2} + \Delta t \varepsilon (\mathbf{c}_\alpha \cdot \nabla_1) f_\alpha \\ + \frac{(\Delta t)^2}{2} \varepsilon^2 (\mathbf{c}_\alpha \cdot \nabla_1) (\mathbf{c}_\alpha \cdot \nabla_1) f_\alpha + (\Delta t)^2 \varepsilon^2 (\mathbf{c}_\alpha \cdot \nabla_1) \frac{\partial f_\alpha}{\partial t_1} = \frac{1}{\tau} (f_\alpha^{(0)} - f_\alpha) \end{aligned} \quad (\text{A1.28})$$

Substituting Eq. (A1.7) into this equation, collecting the terms of the order  $\varepsilon$ , and taking these collected terms equal to zero then yields

$$-\frac{1}{\tau \Delta t} f_\alpha^{(1)} = \frac{\partial f_\alpha^{(0)}}{\partial t_1} + \sum_i \frac{\partial}{\partial r_{1i}} (c_{\alpha i} f_\alpha^{(0)}) \quad (\text{A1.29})$$

Since  $f_\alpha^{(0)}$  can be regarded as a function of the macroscopic quantities  $\rho$  and  $\rho u_i$ ,  $\partial f_\alpha^{(0)} / \partial t$  can be reformed using Eqs. (A1.17) and (A1.18) as

$$\begin{aligned} \frac{\partial f_\alpha^{(0)}}{\partial t_1} &= \frac{\partial f_\alpha^{(0)}}{\partial \rho} \cdot \frac{\partial \rho}{\partial t_1} + \sum_i \frac{\partial f_\alpha^{(0)}}{\partial (\rho u_i)} \cdot \frac{\partial (\rho u_i)}{\partial t_1} \\ &= -\frac{\partial f_\alpha^{(0)}}{\partial \rho} \cdot \frac{\partial}{\partial \mathbf{r}_1} \cdot (\rho \mathbf{u}) - \sum_i \sum_j \frac{\partial f_\alpha^{(0)}}{\partial (\rho u_i)} \cdot \frac{\partial}{\partial r_{1j}} \Pi_{ij}^{(0)} \end{aligned} \quad (\text{A1.30})$$

Substituting this equation into Eq. (A1.29) yields the required equation:

$$-\frac{1}{\tau \Delta t} f_\alpha^{(1)} = -\frac{\partial f_\alpha^{(0)}}{\partial \rho} \cdot \frac{\partial}{\partial \mathbf{r}_1} \cdot (\rho \mathbf{u}) - \sum_i \sum_j \frac{\partial f_\alpha^{(0)}}{\partial (\rho u_i)} \cdot \frac{\partial}{\partial r_{1j}} \Pi_{ij}^{(0)} + \sum_i \frac{\partial}{\partial r_{1i}} (c_{\alpha i} f_\alpha^{(0)}) \quad (\text{A1.31})$$

Equations (A1.27) and (A1.31) are the basic equations for deriving the important relationships in Chapter 8.

This page intentionally left blank

## Appendix 2: Generation of Random Numbers According to Gaussian Distribution

In order to set the initial velocities of particles in MD simulations, or to generate random displacements in BD and DPD simulations, it is necessary to generate random numbers according to a particular probability distribution. The probability distributions of interest here are the Gaussian distribution (also known as the normal distribution), and the Maxwell–Boltzmann distribution (or Maxwellian distribution). For example, since the velocity of particles theoretically has the Maxwellian velocity distribution for thermodynamic equilibrium, as explained in Section 2.2, the initial velocity of particles in simulations must have such a velocity distribution. We show the method of setting the initial velocity of particles according to the Maxwellian distribution in the following paragraphs.

We assume that the stochastic variable  $x$ , such as the particle velocity or a random displacement, obeys the following normal distribution  $\rho(x)$ :

$$\rho(x) = \frac{1}{(2\pi)^{1/2}\sigma} \exp\left\{-\frac{(x - \bar{x})^2}{2\sigma^2}\right\} \quad (\text{A2.1})$$

in which  $\sigma^2$  is the variance and  $\bar{x}$  is the average of the stochastic variable  $x$ . In order to generate the stochastic variable  $x$  according to this normal distribution, the following equations are used together with a uniform random number sequence ranging from zero to unity:

$$x = \bar{x} + (-2\sigma^2 \ln R_1)^{1/2} \cos(2\pi R_2) \quad \text{or} \quad x = \bar{x} + (-2\sigma^2 \ln R_1)^{1/2} \sin(2\pi R_2) \quad (\text{A2.2})$$

According to either equation of Eq. (A2.2), the required number of values of the stochastic variable are generated using a series of random numbers, such as  $R_1$  and  $R_2$ , taken from a uniform random number sequence. In this way, the initial velocities of particles and random displacements can be assigned. The technique in Eq. (A2.2) is called the Box–Müller method [26].

For generating a uniform random number sequence, there is an arithmetic method and a machine-generated method; the former is shown in the last subroutine of the sample simulation program in Section 3.1.6. The arithmetic method is

reproducible, and the same random number sequence can be obtained at any time in the simulations. In contrast, the machine-generated method is generally not a reproducible sequence, and a different sequence of random numbers is generated each time a simulation is run.

For the case of the Maxwellian velocity distribution, the velocity components of particle  $i$  can be assigned using the random numbers  $R_1, R_2, \dots, R_6$  taken from a uniform random number sequence as

$$\left. \begin{aligned} v_{ix} &= \{-2(kT/m)\ln R_1\}^{1/2} \cos(2\pi R_2) \\ v_{iy} &= \{-2(kT/m)\ln R_3\}^{1/2} \cos(2\pi R_4) \\ v_{iz} &= \{-2(kT/m)\ln R_5\}^{1/2} \cos(2\pi R_6) \end{aligned} \right\} \quad (\text{A2.3})$$

In this way, all the initial velocity components can be assigned using random numbers.

# Appendix 3: Outline of Basic Grammars of FORTRAN and C Languages

We here do not aim to explain the entire grammar of the programming languages; indeed, there is not sufficient space to do so. In each section of programming language, the main structure of a program is first explained in order to understand the logical framework of a program. Then, such important grammar as control statements is explained. Finally, several points of interest that may be outside of the main body of a program will be addressed. This will be followed by a short sample program that demonstrates the essence of a research simulation program and explains the grammar used in the program in detail. This approach is most effective, because the grammar is explained in relation to the logical flow of a simulation program. The skill to develop a simulation program has a strong relationship with the ability for embodying a logical flow using a programming language.

## A3.1 FORTRAN Language

The general structure of a program written in the FORTRAN language is composed of a main program together with subroutine subprograms or function subprograms, as shown below.

123456789...

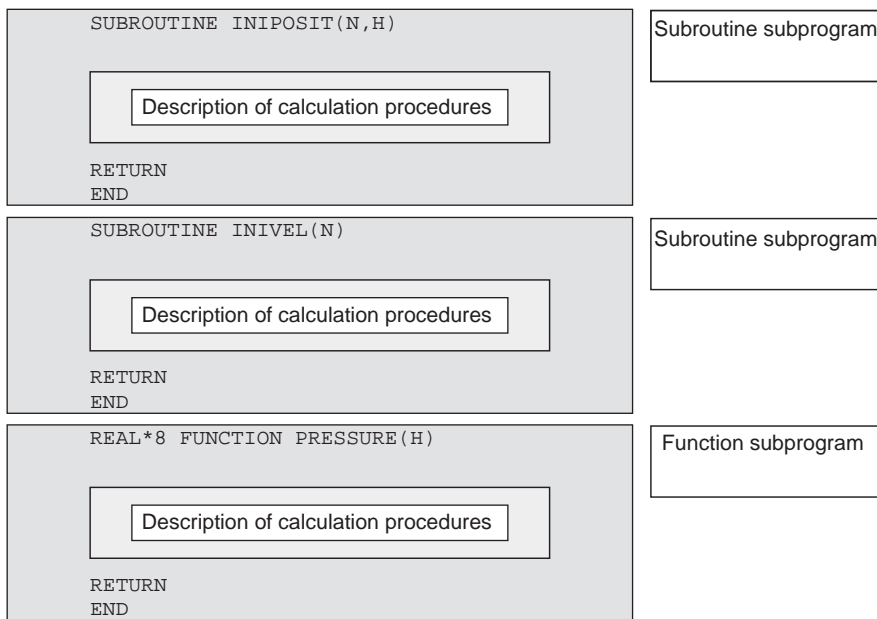
...72

```
IMPLICIT REAL*8 (A-H, O-Z), INTEGER (I-N)
PARAMETER( NN=8)
REAL*8 RX(NN), RY(NN)
REA8 VX(NN), VY(NN)
INTEGER N
```

Main program

Description of calculation procedures

```
STOP
END
```



A main program first needs to be constructed, and then subroutine or/and function subprograms necessarily follow the main program. The main program begins with the definition of the variables and finishes with the STOP and END statements that are placed at the end to halt the execution of the program. A subroutine or function subprogram begins with a SUBROUTINE (name of a subroutine) or (precision) FUNCTION (name of a function) statement, respectively, and finishes with the RETURN and END statements that signal the return to the task of the main program. A main program must be written in such a way that the logical flow is clear, and calculations that disturb this logical flow should be treated in subroutine or function subprograms. In other words, when a program is constructed in such a way that a reader is able to grasp the logical flow in a straightforward manner, it becomes more than a hobby program—it becomes a common useful tool. This is an important consideration for developing a simulation program with contributions from and used by different persons in a successive research project.

In a subroutine subprogram, routine calculations are carried out. The calculation task moves from a main program to a subroutine subprogram by calling the name of the subroutine (the CALL statement) and returns to the main program on meeting the RETURN statement in the subroutine. A function subprogram is quite similar to a subroutine subprogram in that routine calculations are carried out in an area (the subprogram) aside from the main program. The difference between the two is that in a function subprogram the name of the function subprogram itself assumes a calculated value, and this value is passed to the main program by simply referring to the name of the function subprogram in the main program. In other words, the name of a function subprogram is treated as a variable in a main program: the calculation

task moves to a function subprogram at the time of meeting its name, and returns to the main program with a value calculated there on meeting the RETURN statement. Hence, a CALL statement is unnecessary in order to move to a subprogram area. These are the main points of the program structure and flow of the calculation procedures. There is an important point concerning the data transfer between a main program and a subprogram. In the FORTRAN language, information regarding the value of variables cannot be transferred between a main program and a subprogram unless definite descriptions are written for that purpose. There is a significant difference between the FORTRAN and the C language in this respect. We explain the method of transferring data between a main program and a subprogram in detail later.

As shown in the preceding example, main sentences generally have to be written between the 7th and 72nd columns in a FORTRAN77 program. The first column is used for defining whether or not that line is a comment line (that does not influence calculations) by employing a C character or a blank; the sixth column is for defining whether or not the line is regarded as a continuation line from the previous line by the “&” character or blank; and the area between the 2nd and 5th columns is used for writing figures (or labels) of the end statements, such as the CONTINUE statement or of an indication of the destination of the GOTO statement. Various examples of this type of use can be seen in the sample simulation programs, and therefore we omit such explanations here.

```
IF(X.GT.0.D0)A=B+10.D0
```

- This is the simplest IF statement, and THEN is unnecessary in this case.

```
IF(X.GT.0.D0)THEN  
...  
END IF
```

- Execution only for  $X > 0$ .

```
IF(X.GT.0.D0)THEN  
...  
ELSE  
...  
END IF
```

- One of separate procedures is chosen for  $X > 0$  or  $X \leq 0$ .

```
IF(X.GT.0.D0)THEN  
...  
ELSE IF(X.LE.-10.D0) THEN  
...  
ELSE  
...  
END IF
```

- One of three separate procedures is chosen for  $X > 0$  or  $X \leq -10$  or the other cases.

```
IF(X.GT.0.D0)THEN  
...  
ELSE IF(X.LE.-10.D0) THEN  
...  
ELSE IF(X.EQ.-5.D0) THEN  
...  
END IF
```

- One of three separate procedures is chosen for  $X > 0$  or  $X \leq -10$  or  $X = -5$ .

We now explain the IF and DO statements, which are perhaps the most important control statements for developing a calculation program. The IF statement is a control statement to select a calculation procedure by assessing the condition. The DO statement is a control statement to repeat a certain procedure a prescribed number of times. Typical examples of the IF statement are shown above. The IF statement implies the execution of a certain procedure if a condition is satisfied; another procedure is carried out if it is not satisfied. In the above examples, the first IF statement is the simplest and the following examples become more complex. Several IF statements can be combined to make a complex assessment, and such examples may be found in the sample simulation programs. In the IF statement, LT and LE imply  $<$  and  $\leq$ , respectively; GT and GE imply  $>$  and  $\geq$ , respectively; and EQ and NE imply  $=$  and  $\neq$ , respectively. The statement for repeating procedures is the DO statement. Several representative examples of the DO statement are shown in the following.

```
DO 20 I=1,N
...
20 CONTINUE
```

```
DO 30 I=N,1,-2
...
30 CONTINUE
```

```
DO 90 I=-N,N+1,5
...
90 CONTINUE
```

- The procedure starts at  $I=1$ , then is conducted at  $I=2$  and continued until  $I=N$ .
- The procedure starts at  $I=N$ , then is conducted at  $I=N-2$  and continued at  $I=N-4, N-6, \dots$ .
- The procedure starts at  $I=-N$ , then is conducted at  $I=-N+5, I=-N+10, \dots$ , until I becomes over  $N+1$ .

The DO statement implies that the procedure written between DO and CONTINUE is executed until the index arrives at the required end value. In the above example, I is the index and N is the end value of the loop. In the first example, the index I changes in the sequence  $I = 1, 2, \dots, N$ . In the second example, the index I changes in the sequence  $I = N, N - 2, N - 4, \dots$ ; if N is even, the procedures are repeated until  $N = 2$ , and if N is odd, they are repeated until  $N = 1$ . The last example shows that a negative value,  $-N$ , is possible as a starting value of the index I. Either specific numbers or variables are possible for the starting and ending values and the increment interval value of the DO loop statement. Be aware that although REAL variables can be used as an index of the DO loop, INTEGER variables are desirable in order to remove any ambiguity in relation to the assessment concerning the termination of the DO loop. In order to move out of the DO loop at any time before the designed end, the GOTO statement employed with the previous IF statement may be used. A final point to be noted relating to the DO loop is that in the first above example, the index I does not have the figure N but  $(N + 1)$  for the end of the procedure; thus, care should be taken in using the variable I in the next task. Using variables in this way should be avoided in order to prevent causing an unexpected error.

Next, we explain several types of grammar that are relatively difficult to understand when learning the FORTRAN language. First, we explain how to transfer the values of variables between the main program and a subprogram. In FORTRAN, there are two methods for the data transfer: (1) the values of variables are transferred to a subprogram through the arguments of the subprogram, and (2) the variables to be transferred between a main program and a subprogram are declared with the COMMON statements so that they can be accessed from both the main program and the subprograms. An example of the former method is as follows:

```
CALL INIVEL(N, H, T)
...
SUBROUTINE INIVEL(N, H, T)
...
```

In this case, the values of the variables N and H are transferred from a main program to a subprogram, and the procedure returns to the main program with a value of T, which was calculated in the subprogram. A big difference between FORTRAN and the C language is that in the former language new values of N and H, which were changed in the subprogram, are reflected in the main program, but in the latter language this never arises unless a specific direction is given to do so. This will be explained in detail later in the grammar of the C language.

The second method for the data transfer is to use the COMMON statement: the variables declared in the COMMON statements can be accessed from both the main program and all the subprograms without any need for specific statements for the data transfer. An example is as follows:

```
PARAMETER (NN = 100)
COMMON /BLOCK1/ N, RX, RY
REAL*8 RX(NN), RY(NN), H
INTEGER N
...
CALL INIVEL(H)
...
STOP
END
...
SUBROUTINE INIVEL(H)
PARAMETER (NN = 100)
COMMON /BLOCK1/ N, RX, RY
REAL*8 RX(NN), RY(NN), H
INTEGER N
```

```

...
RETURN
END

```

In a main program, the variables, which are used in subprograms, can be defined in the COMMON statements before the definition of other standard variables. By defining the same variables in the COMMON statements in a subprogram, the values saved on the variables can be referred to; also, new values may be saved on these variables. In the above example, the values of N, RX(\*), and RY(\*) are transferred using the COMMON statement, and a value of H is transferred as an argument. Note that the names of the variables in the COMMON statements are not necessarily the same, but we recommend that the beginner use the same names until they obtain a more complete understanding of the language.

Another feature that the beginner may find difficult is the WRITE and FORMAT statements. These statements are used for outputting results to a data file and have no relation to the execution of the calculations. The following example is for outputting the data for the purpose of confirming either the final or intervening results of the calculation:

```

I = 3
XI = 5.D0
YI = 2.D0
PRESS = XI*YI
WRITE(NP,20) I, XI, YI, PRESS
20  FORMAT('I = ',I3,3X,'XI = ',F7.3,2X,'YI = ',F7.3,2X,
          &           'PRESSURE AT (XI,YI) = ', F10.3)

```

The result of the output from this FORMAT statement is as follows:

I= 3 XI= 5.000 YI= 2.000 PRESSURE AT (XI,YI)= 10.000
--

The above example is a part of the program for outputting the data of the variable PRESS, which is obtained by multiplying XI by YI. For the case of NP = 6, the results are output to the display of the computer, and if the OPEN statement relates the device number (or device unit number) NP with a data file, the result is output to the data file. For example, if “OPEN (11, FILE = ‘faa1.data’, STATUS = ‘UNKNOWN’)” is declared and NP is set as NP = 11, the data is output to the file faa1.data. Since the results shown on a display can be seen only once, data is usually output to a data file. Inside the

parentheses of the FORMAT statement, I3 means that the output is an integer and is output up to three spaces (columns) to the right of the space, F7.3 means that the output is a real number and is output using 7 spaces (columns), in which the number is rounded to three decimal places and is written to the right of the space; 3X means that three blank spaces are to be inserted. The reader can see many examples of FORMAT statements in the sample simulation programs in Chapters 3–7.

A long run of the execution of a simulation program is sometimes divided into several short runs. For this case, the intervening results are output to a data file, and the following run is carried out to continue from the previous run using the data saved in the file. This data may also be used for visualizing a particle configuration in a form such as a snapshot. To do so, only numerical data is suitable for the output to a data file—that is, without the specification of the names of the variables. A typical example is as follows:

```

...
      WRITE(NP,50) N
50   FORMAT( I8 )
      WRITE(NP,55) (RX(I),I=1,N), (RY(I),I=1,N)
55   FORMAT( (5E16.8) )

```

In the above example, the data saved in the array-type variables RX(\*) and RY(\*) are output using a simple specification without using the DO statement. The specification of (5E16.8) in the FORMAT statement means that five data are output in one line. The outer bracket ( ) is used for the repetition of the output specification 5E16.8, which means that the output data is real and is output using 16 spaces (columns) in which the data is written to the right of the space with 8 decimal places. In order to continue a separate successive run using the data which is output in the above example, we need to use the following READ statement for reading the necessary data:

```

      READ(NP1,60) N
60   FORMAT( I8 )
      READ(NP1,65) (RX(I),I=1,N), (RY(I),I=1,N)
65   FORMAT( (5E16.8) )

```

An important point is that the same FORMAT statement must be used for the WRITE and READ statements; otherwise, the exact numerical values cannot be read by the READ statement.

Finally, to assist the reader in understanding the grammar in more detail, we have added explanatory remarks to the following sample program, which was made by compressing a full simulation program.

```

0001 C*****diffuse_sample.f*****
0002 C*          diffuse_sample.f
0003 C*
0004 C*      MOLECULAR 1
0005 C*      IMPLICIT REAL*8 (A-H,O-Z), INTEGER (I-N)
0006 C*      and similarly those with one of I~N are regarded to be an integer.
0016 C*****diffuse_sample.f
0033 IMPLICIT REAL*8 (A-H,O-Z), INTEGER (I-N)
0034 C
0035 COMMON /BLOCK1/ RX0 , RY0 , RX , RY
0036 COMMON /BLOCK2/ FX , FY
0040 C
0041 PARAMETER( NN=80, NRANMX=50000 )
0042 PARAMETER( PI=3.141592653589793D0 )
0043 C
0044 REAL*8 RX0(NN), RY0(NN), RX(NN) , RY(NN)
0045 REAL*8 FX(NN) , FY(NN) , VELX(NN), VELY(NN)
0046 REAL*8 H , RC , L , T , K , NDENS
0047 C
0048 REAL
0049 INTEGER
0050 C
0051 REAL*8
0052 INTEGER N, NA, NB

```

• The line number is added for convenience and the first column starts from the position of C character. The C in the first column implies that the line is just a comment.

• IMPLICIT is the implicit data type declaration. In this case, the variables with their name starting with one of A~H and O~Z are regarded to be a double-precision real, and similarly those with one of I~N are regarded to be an integer.

• The variable defined in the COMMON statement can be accessed from everywhere without transferring them into subprograms as arguments. In the case of array variables, the dimension must be defined in the data type statement.

• The PARAMETER statement is frequently used for defining the variables used for specifying the dimensions of array variables; the change of these values in PARAMETER enables us to change the dimensions of the related array variables.

• REAL\*8, REAL, and INTEGER are the data type declaration statements for double-precision reals, single-precision reals, and integers, respectively. Although a computer can usually treat integers only between  $\pm$  several ten billions, the INTEGER\*8 statement enables one to use a much wider range of integers. Double-precision reals may be sufficient in scientific computations, but quad-precision reals are appropriate in some cases.

```

0055 C
0056 OPEN( 9,FILE= '@aa1.data' ,STATUS='UNKNOWN')
0057 OPEN(21,FILE='aaa001.data' ,STATUS='UNKNOWN')
0058 OPEN(22,FILE='aaa011.data' ,STATUS='UNKNOWN')

```

• OPEN statements can relate data files to the input/output devices; CLOSE statements must be used together. The number 5 is the keyboard, 6 is the display, and other numbers are used for data files (numbers larger than 8 may be desirable). OLD in the STATUS statement implies an already-existed file.

```

0062 C
0063 C
0064 T = 5.0D0
0065 K = 10.D0
0066 NA = 20
0072 L = DSQRT( DBLE(N)/NDENS )
0073 HSQ = H*K
0079 C
0080 IX = 0
0081 CALL RANCAL( NRANMX, IX, RAN )
0082 NRAN = 1
0083 C
0084 C
0085 C
0086 C
0087 C
0100 C
0101 CALL POSITR1( N, NA, H, K )
0102 C
0103 C
0104 WRITE(NP,5) T , K , NDENS ,
0105 C
0109 C
0110 C

```

NP=9  
----- PARAMETER (1) -----  
-----  
• Double-precision reals are expressed for example 5.2D0 or 0.052D2; single-precision reals are expressed such as 5.2 or 0.052E2. DSQRT means the square root, and \* means the multiplication.

• The subroutine POSITR1 is called by the CALL statement. The variables necessary in the subroutine are passed as arguments (N, NA, H, K); the description of these variables has to be described in this order in the subroutine subprogram.

PRINT OUT CONSTANTS  
• The data are written out in the format expressed in the 5 FORMAT statement; these statements should be placed before the STOP statement.

```

0111 C -----
0114 C      DO 100 NTIME=1, NTIMEMX
0115 C
0116 C      DO 50 I=1,N
0121 C
0122 C      IF ( I .EQ. NA+1 ) GOTO 50
0123 C      RXI = 2.D0*RX(I)
0124 C      RXO(I) = RX(I)
0128 C      RX(I) = RXI
0130 C
0131 C      50 CONTINUE
0132 C
0133 C      IF ( MOD(NTIME,NPRINT) EQ. 0 ) THEN
0134 C          TIME = H*DBLE(NTIME)
0135 C          CALL PRINTOUT( N, NA,
0136 C          END IF
0141 C
0142 C      DO 60 I =1,N
0143 C          IF( I .LE. NA ) THEN
0144 C              R = 1.D0
0145 C          ELSE
0146 C              R = 1.5D0
0147 C          END IF
0148 C          WRITE(NOPT,58) I, R, R
0149 C      60 CONTINUE
0153 C
0154 C      100 CONTINUE
0155 C
0156 C      ----- END OF MAIN LOOP
0157 C
0158 C      CLOSE(NP, STATUS='KEEP')
0160 C
0161 C      FORMAT
0162 C      5 FORMAT(/1H , '-----'
0163 C      &   /1H , ' MOLECULAR DYNAMICS SIMULATION '
0164 C      &   /1H , 'FOR TWO-DIMENSIONAL MOLECULAR DYNAMICS PROGRAM'
0165 C      &   /1H , 'TEMPERATURE=' ,F6.3
0166 C      &   'NDENS=' ,F6.3
0167 C      &   /1H , 'NUMBER OF MOLECULES=' ,I5
0168 C      &   /1H , 'NUMBER OF MOLECULES=' ,I5
0169 C      &   /1H , 'MAGNITUDE OF CAVEAT=' ,F8.5 ,2X, 'CUTOFF=' ,F8.5 ,2X
0170 C
0171 C      56 FORMAT( 316, 2E13.8 )
0172 C      58 FORMAT( I5, F8.3 , 2E26.18 )
0173 C
0174 C
0175 C
0176 C
0177 C*****
0178 C*****      SUBROUTINE *****
0179 C*****      SUBROUTINE POSITR1 *****
0180 C
0380 C**** SUB POSITR1 *****
0381 C      SUBROUTINE POSITR1( N, NA, H, K )
0382 C
0383 C      IMPLICIT REAL*8 (A-H,O-Z), INTEGER (I-N)
0384 C
0385 C      COMMON /BLOCK1/ RX0 , RY0, RX, RY
0386 C      COMMON /BLOCK2/ FX , FY
0387 C      COMMON /BLOCK3/ VELX, VELY
0388 C
0389 C      PARAMETER( NN=80 )
0390 C
0391 C      REAL*8 RX0(NN), RY0(NN), RX(NN) , RY(NN)
0392 C      REAL*8 FX(NN) , FY(NN) , VELX(NN), VELY(NN)
0393 C      REAL*8 H , K
0394 C      REAL*8 HSQ2, CC0, CC1

```

The DO loop implies the iteration calculation; the statements between DO and CONTINUE are repeatedly carried out. The procedure starts at NTIME=1, and then is conducted at NTIME=2, 3,..., until I=NTIMEMX. DO loops are possible inside the DO loop.

MOD(NTIME, NPRINT) returns the remainder after NTIME is divided by NPRINT. DMOD is used for such an operator of double-precision reals. As in this example, operators have a slightly different name depending on the data type of variables.

--- PRINT OUT DATA ---

EQ. 0 ) THEN

DBLE(\*) is used for transforming an integer into a double-precision real. For developing a universal program, it is desirable that the data types be the same between the left and right-hand sides in the equation. INT(\*) is used for transforming a double-precision real into an integer.

One of the procedures is chosen after assessing the IF statement. In this example, R=1.D0 if I≤NA, and R=1.5D0 if I>NA.

The data file opened by the OPEN statement must be closed using the CLOSE statement. NP is the device number (name) of the I/O device, which is used to open the data file. KEEP is used in the STATUS statement in almost all cases.

The collection of FORMAT statements before the STOP statement makes the logical structure of calculations clearer.

/ on the first line means the insertion of one blank line; / in the later lines mean starting a new line. "1H " means one blank space indent in each line. "56 FORMAT" and "58 FORMAT" are for writing out only numerical data (or figures).

STOP

END

The variables are described in the same order in which they have been written in CALL POSITR1.

IMPLICIT, PARAMETER, and REAL\*8 statements are described in the same way as in the main program. The subroutine can access the variables in the COMMON statements, as well as the arguments of N, NA, H, and K; note that the change in these variables in the subroutine is reflected in the main program. The other variables are valid only in this subroutine, and never affect the main program.

```

0395      INTEGER NA , N
0396 C
0397      HSQ2 = H*H/2.D0
0398      CC0 = 1.D0/K
0399      CC1 = 1.D0
0400 C
0401      DO 10 I=1,N
0402      IF( I .EQ. NA+1 ) CC1 = CC0
0403      RX(I) = RX0(I) + H*VELX(I) + HSQ2*FX(I)*CC1
0404      RY(I) = RY0(I) + H*VELY(I) + HSQ2*FY(I)*CC1
0405 10 CONTINUE
0406
0407

```

RETURN  
END

The use of the RETURN statement arbitrary times is possible in the subroutine. The END statement is necessary for specifying the end of the descriptions of the subroutine.

## A3.2 C Language

We will explain the grammar of the C language in a way similar to our discussion of the FORTRAN language. The main structure of a program written in the C language is made up of the function **main** and a set of functions that correspond to subprograms in FORTRAN. The C language has considerable flexibility in writing a program in comparison to FORTRAN. However, the logical structure concerning the arrangement of **main** and functions has similarities to FORTRAN, and therefore it may be beneficial for the reader to write a simulation program in a similar structure to one in FORTRAN.

We show a typical structure of a C program in the following. Note that there is no requirement that the statements be written between 7th and 72nd columns in the C language.

```

#include <stdio.h>
#include <math.h>
#define PI    3.1415926535
#define NN   20
double RX[NN], RY[NN] ;
main()
{
    double rxi, ryi ;
    int     n, i, j ;
    Description of calculation procedures
}
setiniposit(n,temp)
    double temp ;
    int     n ;
    {
        double rxi, ryi ;
        int i, j ;
    Description of calculation procedures
}

```

The function **main**

Function (setiniposit)

```
setinivel(n,press)
    double press ;
    int      n ;
{
    double vxi, vyi ;
    int i, j ;
}
```

Description of calculation procedures

Function (setinivel)

The function **main** is placed first, and other functions, corresponding to subprograms in FORTRAN, follow **main**. The main body of the statements in each function begins with the notation { and ends with the notation }. Since there is no limit on the number of characters in one line, the notation ; is used for terminating a line of statement—that is, it means the end of the line. Except for special statements, every line must end with such a notation ;. Because mathematical functions such as **sin** and **sqrt** are necessarily used in scientific calculations, the statement of **#include <math.h>** needs to be declared in the first description area. Also, the statement of **#include <stdio.h>** is indispensable to any program to facilitate the input or output of data to a display or data file, and for reading data from a keyboard or data file. The statements of **#define PI 3.14...** and **#define NN 20** correspond to the PARAMETER statement in FORTRAN. A statement beginning with the notation # is a preprocessor directive, which is a command to the compiler's preprocessor that treats instructions before the compilation procedure starts. The preprocessor directive of **#define NN 20** implies that the value of 20 is assigned to the variable **NN**. The next statement, corresponding to the COMMON statement in FORTRAN, is the declaration of the array-type variables **RX[NN]** and **RY[NN]** being used as global variables (which can be used in the other function programs with no further definitions). The C language typically uses lower-case characters, but it may be best that the names of global variables are declared using upper case, so a programmer can be more aware of treating the global variables. In a way similar to FORTRAN, the execution of a program starts with the function **main**; the procedures move to a function when the function name is met and return to the main program (**main**) after completion of the procedures in the function. As seen in this explanation, the C language does not need the CALL statement used in the FORTRAN language for transferring the task to another function. It employs only the name of the function. The function **main** is written in a way to clarify the flow of calculations, whilst any complex calculation procedure is recommended as a separate function.

Next, we explain the most important statements for developing a program: the **if**, **for**, **do while**, and **switch** statements. We first explain the **if** statement, which is

used for choosing tasks according to certain conditions specified by the instructions. Some typical examples are as follows:

```
if(i==3) x=a ;
```

- This is the simplest **if** statement. “ $i=3$ ” is expressed as “ $i==3$ ” in the C language.

```
if( x>=0.) z=b ;
else if( x<-10. ) z=c ;
else z=d ;
```

- If  $x \geq 0$ ,  $z=b$  is set, if  $x < -10$ ,  $z=c$ , and  $z=d$  for the other cases.

```
if( x>=5. ) {
    z=a1 ;
}
```

- This is a block-type **if** statement.

```
if( x>5. ) {
    z=a1 ;
} else if( x<=-10. ) {
    z=b1 ;
} else {
    z=c1 ;
}
```

- This is also a block-type **if** statement. One procedure is chosen depending on the condition; there are three cases  $x > 5$ ,  $x \leq -10$ , and the other cases.

```
if( (x>=-10.) && (x<=10.) ) {
    z=a1 ;
} else if( (x>=50.) || (x<=-50.) ) {
    z=b1 ;
}
```

- This is also a block-type **if** statement. “ $\&\&$ ” means that if both the conditions are satisfied,  $z=a1$  is assigned and “ $| |$ ” means that if one of the conditions at least is satisfied,  $z=b1$  is assigned.

The **if** statement implies that the procedure is carried out if a certain condition specified in the **if** statement is satisfied; otherwise, another assessment or another procedure (including the end of the execution of the **if** directive) is conducted. The specification “ $\leq$ ” in the condition statements represents the mathematical meaning  $\leq$ , “ $\geq$ ” means  $\geq$ , “ $=$ ” means  $=$ , and “ $\neq$ ” means  $\neq$ . We next explain the statements of **for**, **while**, and **do while**, which are used for specifying the repeating procedures. Several typical examples follow.

```
for(i=1; i<=n; i++) {
    ...
}
```

- The procedure starts at  $i=1$ , then is conducted at  $i=2$  and continued until  $i=n$ .

```
for(i=100; i>=0; i-=2) {
    ...
}
```

- The procedure starts at  $i=100$ , and is conducted at  $i=98, 96, \dots$ , while  $i \geq 0$ . “ $i-=2$ ” means “ $i=i-2$ .”

```
i=3 ;
do {
    xnew = xold + xdef ;
    i++ ;
} while( i<=n ) ;
```

- The procedure starts at  $i=3$  and is conducted at  $i=4, 5, \dots$ , while  $i \leq n$ . “ $i++$ ” means “ $i=i+1$ ” and “ $i--$ ” means “ $i=i-1$ .”

```
i=3 ;
while( i<=n ) {
    xnew = xold + xdef ;
    i++ ;
}
```

- The procedure is the same as in the previous case, but terminating the procedure is assessed in a different position.

The above statements correspond to the **DO** statement in FORTRAN. The procedures specified between { and } are repeated, with the value of the index variable i increasing or decreasing after the execution of each cycle step. The way of changing the index value is specified by the statement between ( and ) in the **for** statement, such as “*i++*” or “*i = 2*”. In the case of the **do while** and **while** statements, the way of changing the index value is specified by “*i++*.” If the statement of “*i = 3*” is used, the index *i* will change so that “*i = i + 3*.” A difference between the **do while** and the **while** statements is the position for assessing the termination of the procedures. The procedure specified between { and } is repeatedly carried out, whilst the condition indicated in the **while** statement is satisfied.

A statement with characteristics similar to **if** is the **switch** statement. This statement is quite simple to use; an example follows:

```
switch (itree) {
    case 2 ;
        x = a1 ;
        y = b1 ;
        break ;
    case 3 ;
        x = a2 ;
        y = b2 ;
        break ;
    default ;
        x = a4 ;
        y = b4 ;
        break ;
}
```

- When *itree=2*, a series of statements defined in “case 2” are executed, and **break** means the exit from the **switch** statement. A similar procedure is carried out for “case 3.” In the other cases, a series of statements defined in **default** are executed; the **break** statement is possibly unnecessary in the default area.

As already pointed out, the function **main** and other functions correspond to a main program and subprograms in the FORTRAN language, respectively. There are two types of functions in the C language. That is, the first type of function corresponds to a function subprogram in the FORTRAN language, and therefore a value calculated in the function is transferred through the variable (i.e., the name of the function) in the function **main**. The second type of function corresponds to a subroutine subprogram, and a value calculated there is not transferred through the name of the function. Several examples that explain these two types of functions are shown here:

```
setinivel(n,press)
double press ;
int      n ;
{
    double vxi, vyi ;
    int i, j ;
    ...
}
```

- This is a function that returns no calculated values to the main function. It corresponds to the subroutine subprogram in FORTRAN.

```
double press(x, y)
    double x, y;
{
    double c1, c2, cans ;
    c1=1. ; c2=2. ;
    cans = c1*x + c2*y ;
    return( cans ) ;
}
```

- This corresponds to the function subprogram in FORTRAN; the calculated value "cans" is substituted into the double-precision variable "press," and the value of "press" is returned to **main**.

```
int press(x,y)
    double x, y ;
{
    int ic, jc, ians ;
    ians = ic*(int)x
        + jc*(int)y ;
    return( ians ) ;
}
```

- This also corresponds to the integer function subprogram in FORTRAN; the calculated value "ians" is substituted into the integer variable "press," and the value of "press" is returned to **main**.

In the second and third examples, a value calculated in the function is transferred to the main program **main** through the function name. The descriptor of the function type, such as **double** and **integer**, is, therefore, attached before the function name. In the first example, the function does not return a calculated value to the main program, but certain procedures are carried out in this function, so that the declaration of the function type is unnecessary and not attached to the function name. Note that **int**, **float**, and **double** imply that a variable (or data) is integer-type, single-precision-real-type, and double-precision-real-type, respectively.

Next, we explain several important points that seem to be relatively difficult or may be misunderstood by the beginner who is learning the grammar of the C language. Array-type variables are defined in the declaration statements of the data type in such a way as **double a[100]** or **rx[20][20]**. For example, in the case of a one-dimensional array such as **double a[100]**, it is noted that **a[0], a[1], ..., a[99]** storage spaces are prepared, but **a[100]** is not available. The second example of **double rx[20][20]** means the declaration of a two-dimensional array variable, and **rx[0][0], rx[0][1], rx[0][2], ..., rx[19][19]** storage spaces are prepared.

A significant difference between FORTRAN and the C language concerns the data transfer between the function **main** (main program) and other functions (subprograms). In FORTRAN, when one transfers data to a subprogram as arguments, one does not take the values themselves saved in the variables but rather takes the positions or addresses of the variables in which the data are saved. This means that the values saved in the variables can freely be accessed from the subprogram, and also that new data can be assigned to such variables; these new values are reflected in the main program. This data transfer type is the "call by reference." In the case of the C language, the specification of variables as arguments, as in the FORTRAN language, does not mean the transfer of the address of the variables; rather, the values themselves saved in the variables are transferred to the function; therefore the assignment of new values to the variables in the function is never reflected in the main program. This type of data transfer is the "call by value." This means that in respect to data transfer, the C language is much safer than FORTRAN. If the data transfer is carried out by "call by reference" in a similar way to FORTRAN, then the variables of the "pointer" class must be used in the C language. A pointer variable saves the position or address of a standard variable, and therefore it is important to declare what type of data is saved at the

position. For example, if an integer value is to be saved in a variable, the address of which a pointer variable “pa” saves, then the asterisk \* must be attached to the pointer variable like “\*pa,” and the data type must be declared like “int \*pa.” In the body of the program, the variable “\*pa” is treated as a standard integer variable. If “int \*pb, ix” is declared in the definition statement of the data types, the statement “pb = &ix” is used in order to save the address of the integer variable “ix” in the pointer variable “pb.” If “&” is attached to a standard variable, for example, “&ix,” it will return the value of the address of the variable ix. Therefore, since a pointer variable—for example, “pa”—has the information about the address of a standard variable, a value (data) saved at the address of the standard variable can be extracted using the notation “\*pa.” We are now ready to begin the explanation of “call by reference.”

In order to return from a function with the calculated values, the information of the addresses of the variables, in which the calculated values are saved, need to be transferred to the function by using arguments of the pointer type. For example, consider a sample program in which a calculation is carried out using a value saved in the variable “h” in the function “anscal,” and the calculated data is returned to the main program through the variable “ans.” One has to call the function using the statement “anscal (h, &ans),” in which a value (i.e., not the pointer information) saved in the variable “h” is transferred to the function “anscal,” and the address of the variable “ans” can be transferred to the function using the pointer information “&ans.” It is important that the data type of the variable “\*ans” is declared in the function “anscal,” so that the variable “\*ans” can be treated as a standard variable in the function. Several typical examples (including a bad example) follow.

```
double h, ans ;
...
x = anscal(h, &ans) ;
...
anscal(h, pans)
double h, *pans ;
{
    *pans = h*h ;
}
```

- The address of “ans” is transferred to the function; “&ans” is the address of the variable “ans.” In the function, the pointer variable “pans” is used for receiving the value of “ans” in the main function. Since “ans” is a double-precision real, “pans” has to be defined as a double-precision-real variable.

```
double h, ans ;
...
x = anscal(h, ans) ;
...
anscal(h, ans)
double h, ans ;
{
    ans = h*h ;
}
```

- This is a bad example. In this case the values saved in “h” and “ans” are transferred to the function “anscal,” but the values calculated in the function can never be returned (reflected) to the main function.

```
double h, ans[100] ;
...
x = anscal(h, ans) ;
...
anscal(h, ans)
double h, ans[100] ;
{
    for( i=0, i<=99; i++ ) {
        ans[i] = h*(dble)i ;
    }
}
```

- For array variables, the data transfer to the function is quite similar to FORTRAN; the pointer variables are unnecessary for the data transfer for the case of array variables. The variable name itself is used as an argument in calling the function and also in the definition of the function name.

In the first example, the address of the variable “ans” in the main program is transferred as an argument “&ans.” This value is saved in the pointer variable “pans” in the function; the data type of the variable “ans” is recognized in the function by declaring “double \*pans” there. Through these statements, the original value saved in the variable “ans” in the main program is changed into a new value after this new value is substituted into the variable “\*pans” in the function. Clearly identifying pointer variables from standard variables by attaching the asterisk \* may significantly assist the programmer by removing the danger of mistakes arising from substituting new values to those variables in other functions.

The second example demonstrates a bad example of programming, where new values calculated in the function “anscal” are not transferred to the variables “h” and “ans” in the main program, since the connection of the variables between the main function and the function “anscal” can never be made using a statement of the type “anscal (h, ans).” If the arguments are defined without pointer variables, then a function that returns a calculated value to the main program may be used, as already explained; in this case, “anscal (h, ans)” has to be changed into “double anscal (h, ans);” and “return (ans);” is added to the line after “ans = h\*h;,” which corresponds to a function subprogram in the FORTRAN language.

The third example demonstrates how to transfer values saved in array-type variables such as “ans.” The data transfer of array-type variables can be conducted in the same way as for the FORTRAN language, and therefore pointer variables are unnecessary. That is, calling a function with the arguments that are array-type variables will have a direct type of connection, so that new values assigned to the array-type variables in the function are reflected in **main** without the need for pointer variables.

We have shown the three methods of returning calculated values from a function back to the main function. The first method is to use pointer variables; the second is to use array-type variables; and the third is to use a function that returns a calculated value through the name of the function itself. In addition to these three methods is another method that uses global variables that correspond to variables declared in the COMMON statements in FORTRAN. The global variables have to be declared before the “main( )” statement, and for these variables we recommend the use of capital characters in their names, to help the programmer recognize them. An example of using global variables is in the sample simulation program shown in Section 5.6 as the array-type variables such as RX[NN], RY[NN], and RZ[NN].

Next, we explain the statements for inputting data, **scanf** and **fscanf** statements, and for outputting data, **printf** and **fprintf** statements. The **scanf** and **printf** statements correspond to READ(5,\*) and WRITE(6,\*) statements in FORTRAN; in these statements, data are input from a keyboard and results shown on a display. In the case of the **fscanf** and **fprintf** statements, data files are used for reading and writing the data. If the reader understands the latter reading and writing statements, the former statements are quite straightforward to understand, so we only focus on the explanation of the **fscanf** and **fprintf** statements. In order to use data files, pointer variables must be connected to the data files used in a program. To do so, the **fopen** statement is used, and **fclose** must be used to disconnect the data file used before the end of the main program; this means that a data file connected by the **fopen** statement should always be disconnected in a program. Some examples follow.

```
main()
{
    double a, b, c;
    int i;
    FILE *fopen(), *np1, *np2, *np[4];
    np1 = fopen("aaa0.data", "r");
    np2 = fopen("aaa1.data", "w");
    np[1] = fopen("bbb1.data", "w");
    np[2] = fopen("bbb2.data", "w");
    np[3] = fopen("bbb3.data", "w");
    ...
    fscanf(np1, "%lf", &c);
    fprintf(np2, "a=%10.3f b=%10.3f\n", a, b);
    i = 2;
    fprintf(np[i], "a=%10.3f b=%10.3f c=%10.3f\n",
    a,b,c);
    ...
    fclose(np[1]);
    fclose(np[2]);
    fclose(np[3]);
    fclose(np1);
    fclose(np2);
```

As shown in the above example, a data file must be connected to the file pointer variable, which is declared in the **FILE** statement, by using the **fopen** statement. After a data file is opened (connected), data can be input from the data file by using the **fscanf (np1,...)** statement, and also can be output by the **fprintf (np2,...)** or **fprintf (np[2],...)**. The latter example for **fprintf** is quite useful for outputting the particle positions at given time step intervals, which may be used for making an animation of the particle motion. In this case, the index “i” in “np[i]” is made to change in such a way as  $i=1,2,3,\dots$ , with advancing time for the output. The arguments “r” and “w” in the **fopen** statement indicate the reading and the writing mode, respectively. A data file opened by the **fopen** statement must be closed (disconnected) using the **fclose** statement before the end of the program. If a data is read and saved in a standard variable “c,” the pointer information (address) of “c” is necessary as an argument in the **fscanf** statement. In contrast, when a data saved in the variable “a” is output to a data file, only a value is necessary, so that the name itself is used as an argument in the **fprintf** statement; the pointer information is unnecessary in this case.

Next, we explain how to describe the format to output data, using the following example:

```
i = 3;
xi = 5.;
```

```

yi = 2. ;
press = xi*yi ;
fprintf(np2,"i = %3d  xi = %7.3f  yi = %7.3f  pressure =
%10.3f\n", i, xi, yi, press) ;

```

The output result of the above **fprintf** statement is as follows:

```
i= 3  xi= 5.000  yi= 2.000  pressure= 10.000
```

The C language does not have a statement corresponding to the FORMAT statement in FORTRAN. Instead, the output format for the data is specified in the **fprintf** statement. In the above example, “%3d” is used for integer-type data and is written using 3 columns (spaces) from the right. Similarly, “%7.3f” is for real-type data and is written using 7 columns from the right with three decimal places, and “\n” means the start of a new paragraph. If a data is output in exponential form, for example, using “%10.2e,” this implies that a value is written using 10 columns with 2 decimals. The reader sees many examples in the sample simulation program shown in Section 5.6.

In order to make a visualization, such as an animation or snapshot, using the data of the particle positions, it is necessary to write out only data (figures) in a data file without any characters for explaining the data such as the names of variables. An example for this output is as follows:

```

...
for (i = 1; i < 100; i++) {
    fprintf(np2,"%10.4f%10.4f%10.4f\n", rx[i], ry[i],
    rz[i]);
}
...

```

In this example, the components of the particle position vector, rx[\*], ry[\*], and rz[\*] are output at each time step using the **for** loop statement; the position data of particle 1, particle 2, and particle i are written in the first, second, and ith lines, respectively, of the data file. In order to conduct another run using the data saved in the above-mentioned manner, one needs to read such data from the data file in the following way:

```

...
for (i = 1; i < 100; i++) {
    fscanf(np1,"%lf%lf%lf\n", &rx[i], &ry[i], &rz[i]);
}
...

```

In the above example, “rx[\*], ry[\*], and rz[\*]” are assumed to be defined as double-precision-real-type variables. As this example demonstrates, in the C language, data does not need to be read using the same format description that was used in the **fprintf** statement, but only described as “%lf%lf%lf/n” in the **fscanf** statement; this is in contrast to FORTRAN. As already pointed out, the address of the variables—not the name itself—is necessary in reading the data by the **fscanf** statement.

The C language has several characteristic concepts for using variables, such as structure variables, which are not contained in the FORTRAN77 language. We do not explain them in this book, because these characteristic statements are not used in the sample simulation programs. Since imaginary variables may be useful in certain cases, the reader may find them in a textbook on the C language, if necessary.

Finally, we show some additional features of the grammar using a short sample simulation program.

```

0001 /*-----*
0002 /*-----* alde
0003 /*-----*
0004 /*----- Hard Sphere Molecular Dynamics -----*/
0005 /*----- Simulation of phase transition for a two
0006 /*----- dimensional system. */ */
0021 /*-----*
0042 #include <stdio.h>
0043 #include <math.h>
0044 #define PI      3.141592653589793
0045 #define NN      201
0046 #define NNCOLMX 2001
0047 #define NRANMX 100001
0048     double RX[NN] , RY[NN] ;
0049     double VX[NN] , VY[NN] ;
0050     double XL , YL ;
0051     float   RAN[NRANMX] ;
0052     int     NRAN, IX ;
0053
0054 /*----- main function ---*/
0055 main()
0056 {
0057     int    n, partnr[NN] ;
0058     int    n, partnr[NN] ;
0059     double coltim[NN] , tstep, tij , tim, timbig ;
0060     float  rx0[NN][NNCOLMX], ry0[NN][NNCOLMX] ;
0061     int    i, j, k, ii, ncol, ncolmx , nbump ;
0062     FILE   *fopen(), *np[10], *np1, *np2 ;
0063
0064     np1   = fopen("@baal.data", "w");
0065     np[1] = fopen("baa011.data", "w");
0066     np[2] =
0067
0068
0069
0070
0071
0072
0073
0074
0075
0076
0077
0078
0079
0080
0081     n      = 36 ;
0082     vdens = 0.1 ;
0083     ndens = vdens*(4.0);
0084     dsq   = d*d ;
0085     timbig = 1.e10 ;
0086
0087     IX   = 0 ;
0091
0092

```

- The statements enclosed by “/\*” and “\*/” are regarded as comment lines and therefore have no influence on the calculation. Comment lines are placed at any positions, which is dissimilar to FORTRAN.
- “#include <stdio.h>” is necessary for the input/output of data, and “#include <math.h>” is necessary for the use of mathematical calculations.
- The “define” statement corresponds to the PARAMETER statement in FORTAN, which is useful for defining the size of the array-type variables.
- The variables defined using “double,” “float,” and “int” are regarded as global variables that can be accessed from any functions without any definition in each function.
- In order to output the calculated data on a data file, the file has to be related to the pointer variable (device number) using the “fopen” statement; the opened file has to be closed using the “fclose” statement before the end of the main function. “w” and “r” are used for writing and reading the data, respectively.
- This is calling the function rancal(\*), in which arguments are unnecessary because of the use of the global variables. This is a void function of returning no calculated results, which corresponds to a subroutine subprogram in FORTRAN.





```

0266     c1    = sqrt( -t*log( (double)(RAN[NRAN]) ) ) ;
0267     NRAN += 1 ;
0268     c2    = c0*(double)( RAN[NRAN] ) ;
0269     vxii = c1*cos(c2) ;
0271
0272     if( (vxii*vxii+vyii*vyii) >= c3 )  goto L5 ;
0273     VX[i] = vxii ;
0275   }
0276 }
```

- The “`goto`” statement tends to make the logical flow complex, so this statement should be used limitedly.

In this example, the line numbers are attached for the sake of convenience—they are not necessary in writing a program. In the C language, all variables used in a program must be defined using the data type statement such as **int**, **float**, and **double**.

### A3.3 Execution Procedures of FORTRAN and C Programs

The execution of a program in the FORTRAN or the C language involves two procedures: one to make an executive-type program by compiling the program, and another to conduct a command for running the executive-type program. When error messages appear in compiling a program, one has to modify the program so as to completely remove those errors. Error messages are quite useful for the beginner in the process to learn how to develop a program, so that the reader is recommended to spend sufficient time on tackling such problems. Note that if there are no error messages, it does not mean that there are no bugs in the simulation program, but just implies there are no grammatical errors. Hence, after error messages disappear in compiling, one should check a program another 5 times. Since this kind of careful verification procedure is necessary to remove fatal bugs, programmers have to avoid employing complex logical structures in writing a program.

The sample simulation programs shown in each chapter of this book are almost directly portable to free FORTRAN and C compilers, for example, in a free Linux system. However, if the reader intends to conduct a large-scale simulation, it is desirable to introduce a commercial compiler, which may offer higher performance for the computer.

If a Linux system is installed with GNU family compilers in the FORTRAN and C languages, typical execution procedures are as follows:

```
> f77 sample1.f
> ./a.out
```

```
> cc sample1.c -lm
> ./a.out
```

```
> f77 -o sample1.out sample1.f
> ./sample1.out
```

```
> cc -o sample1.out sample1.c -lm
> ./sample1.out
```

The “`a.out`” is a default name of an executive-type program, but in the second example, the name of an executive-type program is assigned to a chosen name and

the execution is carried out using this name. Since mathematical functions are usually used in a program, the compile option “-lm” is necessary for a C program.

If you use a commercial compiler, offered by Intel or other companies, installed on a Linux system, a typical example for the execution is as follows:

```
> ifort -o sample1.out sample1.f  
> ./sample1.out
```

in which “ifort” is the command for starting the FORTRAN compiler. If the reader is using a freeware, the required command may be “g77,” “f90,” “f95,” “gfortran,” “ifc,” or “fort.”

If the reader wants more information on the compile options, “man ifort” or “man ifc” can be used to access to the manual of the compiler. Note that since the grammar is slightly different among different compilers, one compiler may output error messages in compiling, but another does not. Hence, we recommend that the reader devise a program in a general form, otherwise, a large amount of tuning tasks may be necessary to apply it to a compiler on another computer.

If error messages are output in compiling the same programs in this book, the following data type statement may be a reason; in this case, the reader is advised to replace “REAL\*8” with “DOUBLE PRECISION.” Also, error messages may be resolved by reducing the size of array-type variables.

This page intentionally left blank

# Appendix 4: Unit Systems of Magnetic Materials

The CGS unit system and the SI unit system, which was developed from the MKSA unit system, are generally used in the field of magnetic materials. Although the CGS unit system is commonly used in the commercial world, the SI unit system is invariably used in textbooks on magnetic materials. Using quantities expressed in different unit systems at the same time will lead to wrong expressions for physical quantities, so one must adhere to the same unit system for handling equations or physical values of magnetic materials. Many textbooks on magnetic materials provide tables to transform values from one unit system to another. We here summarize the two unit systems based on the MKSA system. In the first unit system, the magnetization  $\mathbf{M}$  corresponds to the magnetic field  $\mathbf{H}$  in units. In the second unit system,  $\mathbf{M}$  corresponds to the magnetic flux density  $\mathbf{B}$ . Some typical quantities used for magnetic materials are tabulated below.

Note that in this book we use the first unit system of  $\mathbf{M}$  corresponding to  $\mathbf{H}$  in units.

	$\mathbf{B} = \mu_0(\mathbf{H} + \mathbf{M})$	$\mathbf{B} = \mu_0\mathbf{H} + \mathbf{M}$
Magnetic field strength, $\mathbf{H}$	[A/m]	[A/m]
Magnetization strength, $\mathbf{M}$	[A/m]	[Wb/m <sup>2</sup> ]
Magnetic flux density, $\mathbf{B}$	[T] ( $=[\text{Wb}/\text{m}^2]$ )	[T] ( $=[\text{Wb}/\text{m}^2]$ )
Permeability of free space, $\mu_0$	$\mu_0 = 4\pi \times 10^{-7}$ [H/m] $(=[\text{Wb}/(\text{A} \cdot \text{m})]$ )	$\mu_0 = 4\pi \times 10^{-7}$ [H/m] $(=[\text{Wb}/(\text{A} \cdot \text{m})]$ )
Magnetic charge, $q$	[A · m]	[Wb] ( $=[\text{N} \cdot \text{m}/\text{A}]$ )
Magnetic moment, $\mathbf{m}$	[A · m <sup>2</sup> ]	[Wb · m] ( $=[\text{N} \cdot \text{m}^2/\text{A}]$ )
Potential energy, $U$	$U = -\mu_0\mathbf{m} \cdot \mathbf{H}$ [J] $(=[\text{Wb} \cdot \text{A}])$	$U = -\mathbf{m} \cdot \mathbf{H}$ [J] ( $=[\text{Wb} \cdot \text{A}]$ )
Torque, $\mathbf{T}$	$\mathbf{T} = \mu_0\mathbf{m} \times \mathbf{H}$ [N · m] $(=[\text{Wb} \cdot \text{A}])$	$\mathbf{T} = \mathbf{m} \times \mathbf{H}$ [N · m] $(=[\text{Wb} \cdot \text{A}])$
Magnetic field induced by magnetic charge, $\mathbf{H}$	$\mathbf{H} = \frac{q}{4\pi r^2} \cdot \frac{\mathbf{r}}{r}$ [A/m]	$\mathbf{H} = \frac{q}{4\pi\mu_0 r^2} \cdot \frac{\mathbf{r}}{r}$ [A/m]
Magnetic force acting between two magnetic charges, $\mathbf{F}$	$\mathbf{F} = \frac{\mu_0 q q'}{4\pi r^2} \cdot \frac{\mathbf{r}}{r}$ [N] $(=[\text{Wb} \cdot \text{A}/\text{m}])$	$\mathbf{F} = \frac{qq'}{4\pi\mu_0 r^2} \cdot \frac{\mathbf{r}}{r}$ [N] $(=[\text{Wb} \cdot \text{A}/\text{m}])$
Magnetic interaction between two magnetic moments, $U$	$U = \frac{\mu_0}{4\pi} \left\{ \mathbf{m}_1 \cdot \mathbf{m}_2 - \frac{3}{r^2} \times (\mathbf{m}_1 \cdot \mathbf{r})(\mathbf{m}_2 \cdot \mathbf{r}) \right\}$ $[J] (=[\text{Wb} \cdot \text{A}])$	$U = \frac{1}{4\pi\mu_0 r^3} \left\{ \mathbf{m}_1 \cdot \mathbf{m}_2 - \frac{3}{r^2} \times (\mathbf{m}_1 \cdot \mathbf{r})(\mathbf{m}_2 \cdot \mathbf{r}) \right\}$ $[J] (=[\text{Wb} \cdot \text{A}])$
Combined units: $[\mathbf{H}] = [\text{Wb}/\text{A}]$ , $[\mathbf{T}] = [\text{Wb}/\text{m}^2]$ , $[\mathbf{J}] = [\text{N} \cdot \text{m}]$		
Equivalent units: $[\mathbf{N}] = [\text{Wb} \cdot \text{A}/\text{m}]$		

This page intentionally left blank

# How to Acquire Simulation Programs

A copy of the sample simulation programs that are shown in this book can be requested directly from the author via e-mail:

asatoh\_book2010@excite.co.jp

Please note that the following information is required:

1. the purchase date,
2. the number of purchased copies,
3. the profession of the purchaser.

The sample simulation programs in this book can be used free of charge for educational purposes in an academic environment such as a university, but are not permitted to be used for commercial purposes. In addition, the user takes responsibility for all results obtained from using the sample simulation programs.

The author would deeply appreciate the report of any bugs in the programs, but regrets that he is unable to accept any inquiries concerning the content of the simulation programs.

This page intentionally left blank

# References

- [1] M.P. Allen, D.J. Tildesley, Computer Simulation of Liquids, Clarendon Press, Oxford, 1987.
- [2] D.C. Rapaport, The Art of Molecular Dynamics Simulation, Cambridge University Press, Cambridge, 1995.
- [3] J.M. Haile, Molecular Dynamics Simulation, Elementary Methods, John Wiley & Sons, New York, 1992.
- [4] A. Satoh, Introduction to Molecular-Microsimulation of Colloidal Dispersions, Elsevier Science, Amsterdam, 2003.
- [5] P.J. Hoogerbrugge, J.M.V.A. Koelman, Simulating microscopic hydrodynamic phenomena with dissipative particle dynamics, *Europhys. Lett.* 19 (1992) 155–160.
- [6] J.M.V.A. Koelman, P.J. Hoogerbrugge, Dynamic simulations of hard-sphere suspensions under steady shear, *Europhys. Lett.* 21 (1993) 363–368.
- [7] P. Espanol, Hydrodynamics from dissipative particle dynamics, *Phys. Rev. E* 52 (1995) 1734–1742.
- [8] C.A. Marsh, G. Backx, M.H. Ernst, Static and dynamic properties of dissipative particle dynamics, *Phys. Rev. E* 56 (1997) 1676–1691.
- [9] S. Succi, The Lattice Boltzmann Equation for Fluid Dynamics and Beyond, Clarendon Press, Oxford, 2001.
- [10] D.H. Rothman, S. Zaleski, Lattice-Gas Cellular Automata, Simple Models of Complex Hydrodynamics, Cambridge University Press, Cambridge, 1997.
- [11] J.-P. Rivet, J.P. Boon, Lattice Gas Hydrodynamics, Cambridge University Press, Cambridge, 2001.
- [12] B. Chopard, M. Droz, Cellular Automata Modeling of Physical Systems, Cambridge University Press, Cambridge, 1998.
- [13] L. Verlet, Computer experiments on classical fluids. I. Thermodynamical properties of Lennard-Jones molecules, *Phys. Rev.* 159 (1967) 98–103.
- [14] W.C. Swope, H.C. Andersen, P.H. Berens, K.R. Wilson, A computer simulation method for the calculation of equilibrium constants for the formation of physical clusters of molecules: application to small water clusters, *J. Chem. Phys.* 76 (1982) 637–649.
- [15] R.W. Hockney, The potential calculation and some applications, *Methods Comput. Phys.* 9 (1970) 136–211.
- [16] S. Kim, S.J. Karrila, Microhydrodynamics: Principles and Selected Applications, Butterworth-Heinemann, Stoneham, 1991.
- [17] H. Brenner, Rheology of a dilute suspension of axisymmetric Brownian particles, *Int. J. Multiphase Flow* 1 (1974) 195–341.
- [18] S. Kim, R.T. Mifflin, The resistance and mobility functions of two equal spheres in low-Reynolds-number flow, *Phys. Fluids* 28 (1985) 2033–2045.
- [19] D.A. McQuarrie, Statistical Mechanics, Harper & Row, New York, 1976.
- [20] J.P. Hansen, I.R. McDonald, Theory of Simple Liquids, second ed., Academic Press, London, 1986.

- [21] N. Metropolis, A.W. Rosenbluth, M.N. Rosenbluth, A.H. Teller, E. Teller, Equation of state calculations by fast computing machines, *J. Chem. Phys.* 21 (1953) 1087–1092.
- [22] H.C. Tuckwekk, *Elementary Applications of Probability Theory*, second ed., Chapman & Hall, London, 1995.
- [23] A. Jeffrey, *Mathematics for Engineers and Scientists*, fifth ed., Chapman & Hall, London, 1996.
- [24] D.L. Ermak, J.A. McCammon, Brownian dynamics with hydrodynamic interactions, *J. Chem. Phys.* 69 (1978) 1352–1360.
- [25] G.A. Bird, *Molecular Gas Dynamics and the Direct Simulation of Gas Flows*, second ed., Oxford University Press, Oxford, 1994.
- [26] G.E.P Box, M.E. Müller, A note on the generation of random normal deviates, *Ann. Math. Stat.* 29 (1958) 610–611.
- [27] B. Quentrec, C. Brot, New method for searching for neighbors in molecular dynamics computations, *J. Comput. Phys.* 13 (1975) 430–432.
- [28] R.W. Hockney, J.W. Eastwood, *Computer Simulation Using Particles*, McGraw-Hill, New York, 1981.
- [29] S.M. Thompson, Use of neighbor lists in molecular dynamics, *CCP5 Quarterly* 8 (1983) 20–28.
- [30] A.W. Lees, S.F. Edwards, The computer study of transport processes under extreme conditions, *J. Phys. C* 5 (1972) 1921–1929.
- [31] R.E. Rosensweig, *Ferrohydrodynamics*, Cambridge University Press, Cambridge, 1985.
- [32] R.E. Rosensweig, J.W. Nestor, R.S. Timminins, Ferrohydrodynamics fluids for direct conversion of heat energy, *Symp. AIChE-I Chem. Eng.* 5 (1965) 104–118.
- [33] C. Pozrikidis, *Introduction to Theoretical and Computational Fluid Dynamics*, Oxford University Press, Oxford, 1997.
- [34] D. Yu, R. Mei, L.-S. Luo, W. Shyy, Viscous flow computations with the method of lattice Boltzmann equation, *Prog. Aerospace Sci.* 39 (2003) 329–367.
- [35] A.J.C. Ladd, Numerical simulations of particulate suspensions via a discretized Boltzmann equation. Part 1. Theoretical foundation, *J. Fluid Mech.* 271 (1994) 285–309.
- [36] A.J.C. Ladd, Short-time motion of colloidal particles: numerical simulation via a fluctuating lattice-Boltzmann equation, *Phys. Rev. Lett.* 70 (1993) 1339–1342.
- [37] M. Bouzidi, M. Firdauss, P. Lallemand, Momentum transfer of a Boltzmann-lattice fluid with boundaries, *Phys. Fluids* 13 (2001) 3452–3459.
- [38] S. Chapman, T.G. Cowling, *The Mathematical Theory of Non-Uniform Gases*, Cambridge University Press, Cambridge, 1960.